THE MECHANISM OF CYTOKINE SYNERGY INDUCED BY COMBINATORIAL TLR ACTIVATION

LIU QIAN

(B.Sc. (Hons.), Sichuan University, China)

A THESIS SUBMITTED

FOR THE DEGREEE OF DOCTOR OF PHILOSOPHY

DEPARTMENT OF BIOLOGICAL SCIENCES

NATIONAL UNIVERSITY OF SINGAPORE

2015

DECLARATION

I hereby declare that this thesis is my original work and it has been written by me in its entirety. I have duly acknowledged all the sources of information which have been used in the thesis.

This thesis has also not been submitted for any degree in any university previously.

Liu Qian

19 Jan 2015

ACKNOWLEGEMENTS

I would like to thank my supervisor, Prof Ding Jeak Ling, for her support and guidance. She has always been there whenever I have difficulties during the project. Her perseverance and dedication to teaching and research is truly inspiring. Thanks to her, I have gained the skills and confidence to be a researcher.

I would also like to thank my QE examiners and TAC members, Assistant Prof Zhang Yong Liang, Associate Prof Low Boon Chuan and Prof Yu Hao, for their guidance and valuable input.

Several other scientists have also generously shared their resources and time during the project. I would like to thank Associate Prof Tan Nguan Soon from NTU for his helpful suggestions and comments on iTRAQ experiment and on manuscript, and for his generosity of sharing Partek and Ingenuity data analysis software. I'd like to express my special gratitude for our collaborators Assoc Prof Sze Siu Kwan and his lab members Dr. Meng Wei and Qian Jing Ru for their help on iTRAQ and data analysis; and Prof Thiagarajan PS, Dr. Liu Bing and Sucheendra Kumar Palaniappan from School of Computing, NUS for their help on computational modeling of TLR3-TLR7 signaling network.

I am deeply grateful to all my previous and current lab members for their help and encouragement. They make lab a pleasant place to work in. In particular, I would like to thank my PRR crosstalk group members, Zhu Yong (Dr. Zhu invented promoter pull down assay and we worked closely on several experiments), Bin, Becky, Lu Ning, Wai Khang, Yang Lei and Jun Zhi. They helped me a lot on experiment techniques and design, and they are very open to discussion and a lot of interesting ideas sparkled from discussions with them. In addition, I would like to express my special gratitude to Bin, Becky, Lifeng and Susan, who not only helped me on research but also are mentally supportive and gave me great encouragement during my candidature.

I'm deeply grateful to all my friends and loved ones, who have been great encouragement and support during hard time and tiredness. My parents are always so supportive and encouraging and they are my source of strength. I'd like to thank my friends CC, Yier, Su Mei, Shu Jie and all others, who are good accompanies, cheering, and they make my PhD life in Singapore a memorable one.

TABLE OF CONTENTS

SUMMARY

As the sentinel of immune system, macrophages are the first to encounter pathogen invasion. Macrophages sense pathogens through pattern recognition receptors, of which Toll-like receptors (TLR) are the most well characterized ones. Pathogens usually display multiple TLR ligands, which activate a collective of TLRs. Activation of some combination of TLRs could induce synergistic production of cytokines. The level of cytokine expressed is finely tuned and closely related to disease pathology. Insufficient cytokine expression might fail to mount effective immune responses, but overwhelming cytokine expression could also cause damage to the host itself, such as acute and chronic inflammatory diseases. Thus, it is important to understand the molecular basis of cytokine expression, especially cytokine synergy, induced by combinatorial TLR activation. Although it is known that activation of both TLR adaptor MyD88 and TRIF pathways are needed for cytokine synergy, indicating crosstalk between MyD88 and TRIF pathway, the detailed mechanism is not known.

This thesis aimed to unravel the cryptic mechanism of cytokine synergy induced by combinatorial TLR activation. We stimulated mouse macrophages with poly (I:C) and R848, which are ligands, respectively for TLR3 (mediated through TRIF adaptor) and TLR7 (mediated through MyD88 adaptor). We found that synergy in cytokine expression was especially profound for secondary response pro-inflammatory cytokines, IL6 and IL12p40. The time interval and the sequence between poly (I:C) and R848 treatments could affect the magnitude of synergy. To investigate the mechanism of cytokine synergy, and how TLR3-TRIF and TLR7-MyD88 might crosstalk, we utilized both systems biology approach and conventional biology methods.

With systems approach, we built the first calibrated ordinary differential equations (ODE) based kinetic model for TLR-3 and 7 pathways and their crosstalk. The model provided good descriptive and predictive properties. It identified MAPK and type I IFN-JAK-STAT pathways to be critical signaling pathways for cytokine synergy, which was verified by empirical data.

With conventional biology methods, we found TLR3-TRIF and TLR7-MyD88 to directly collaborate at the transcriptional level to synergize cytokine expression. Through proteomic analysis and cytokine *Il6* and *Il12b* promoter affinity assay, we identified three indispensible transcription factors, IRF1, JunB and C/EBPβ, for cytokine synergy. We showed that TLR3-TRIF pathway activates IRF1, while TLR7-MyD88 contributes to the activation of JunB and C/EBPβ. All the three transcription factors are necessary for optimal transcription of *Il6* and *Il12b*, and combinatorial activation of TLR3-TRIF and TLR7-MyD88 pathway synchronize and sustained the activation of IRF1, JunB and C/EBPβ, leading to the synergistic production of cytokine IL6 and IL12p40. Notably, TLR7-MyD88 pathway has an inhibitory effect on IRF1, which controls the timing and magnitude of cytokine expression and prevents immune over-reaction.

Next, through MAPK and JAK inhibitor study, we found that JunB is upregulated by MAPK JNK, ERK and p38, and C/EBPβ is upregulated by ERK and p38. Interestingly, ERK and p38 inhibit IRF1 expression under R848 stimulation, which might explain the inhibitory effect of TLR7-MyD88 pathway on IRF1. In addition, JAK-STAT upregulates IRF1 under poly (I:C) stimulation. The inhibitor study linked the signaling pathway predicted by computational modeling with the transcription factors identified by conventional biology method.

Our results explained how TLR3-TRIF pathway collaborates with TLR7-MyD88 pathway by activating JAK-STAT pathway, which activates IRF1, and MAPK pathway, which in turn induces JunB and C/EBPβ, respectively. Together, they synchronized transcription factors necessary for cytokine expression and facilitate synergy. These results shed light on the crosstalk mechanisms of TLRs with potentials for therapeutics.

PROJECT OVERVIEW

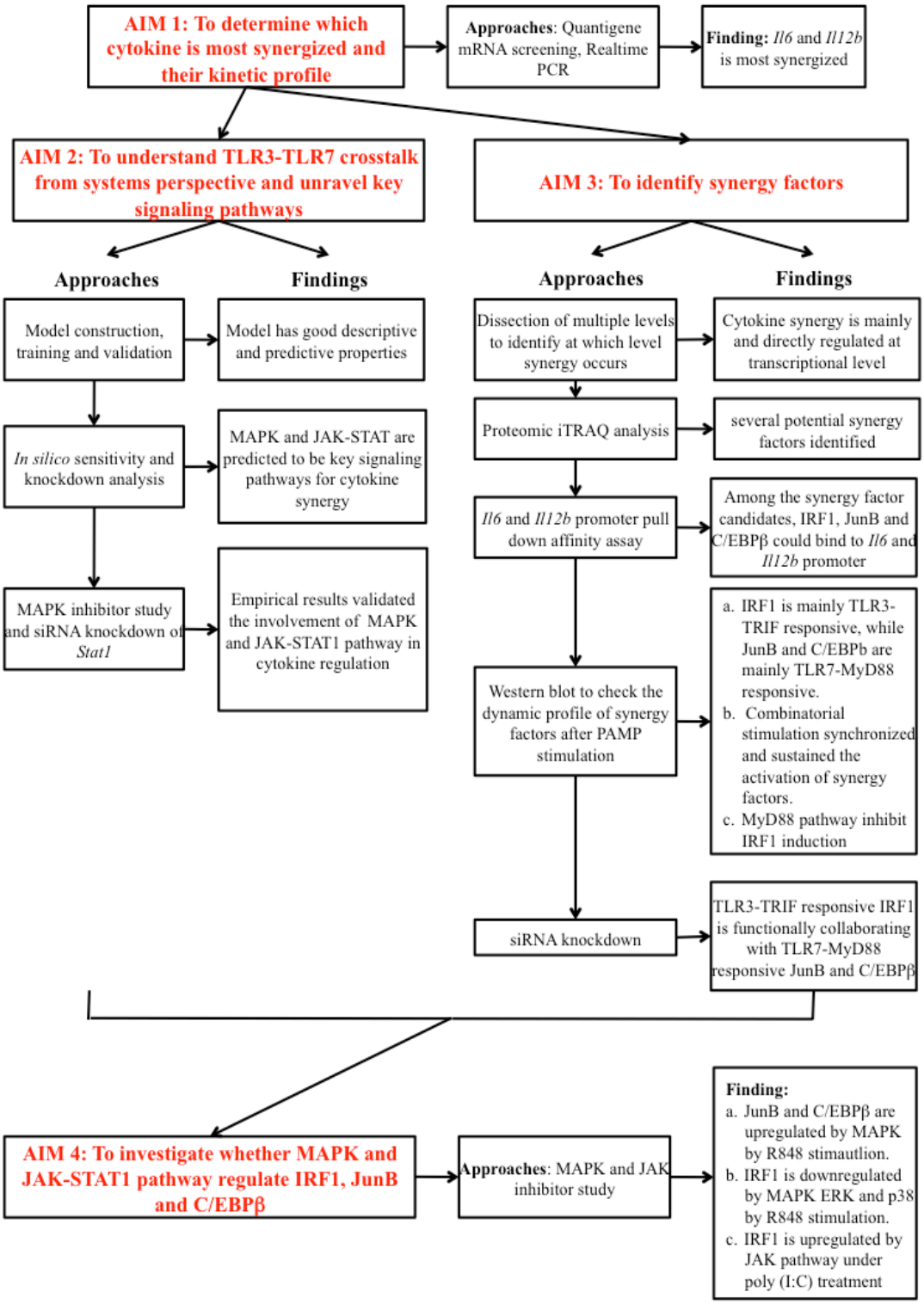

LIST OF TABLES

LIST OF FIGURES

LIST OF ABBREVIATIONS

ACN	Acetonitrile
AKT	Protein kinase B
AP1	Activator protein 1
ATF3	Cyclic AMP-dependent transcription factor
BMDC	Bone marrow derived dendritic cell
BMDM	Bone marrow derived macrophage
C/EBPβ	CCAAT/enhancer-binding protein beta
C1-FFL	Coherent type 1 feed forward loop
CCL	Chemokine (C-C motif) ligand
CLR	C-type lectin receptor
CPV	Cell pellet volume
CSF2	Colony stimulatory factor 2
CST	Cell signaling technology
CXCL	Chemokine (C-X-C motif) ligand
DAMP	Danger associated molecular pattern
DAVID	Database for annotation, visualization and integrated discovery
DC	Dendritic cell
DEPC	Diethylpyrocarbonate
DMEM	Dulbecco's modified Eagle's medium
dsRNA	Double stranded RNA
DTT	Dithiothreitol
ERK	Extracellular signal-regulated kinases

ERLIC	Electrostatic Repulsion-Hydrophilic Interaction Chromatography
FA	Formic acid
FADD	Fas-Associated protein with Death Domain
FBS	Fetal bovine serum
FDR	False discovery rate
GAPDH	Glyceraldehyde 3-phosphate dehydrogenase
GO	Gene ontology
GUSB	Glucuronidase, beta
HPLC	High performance liquid chromatography
HPRT	Hypoxanthine-guanine phosphoribosyltransferase
HRP	Horseradish peroxidase
I	Poly (I:C)
I1-FFL	Incoherent type 1 feedforward loop
I24R	I pretreatment for 24 h followed by R treatment
I8R	I pretreatment for 8 h followed by R treatment
IACUC	Institutional Animal Care and Use
ICSBP	Interferon (IFN) consensus sequence binding protein/IRF8
Ifi204	Interferon-activated protein 204
IFN	Interferon
IFNAR	The interferon-α/β receptor
IKK	IκB kinase
IL12p40	Interleukin 12p40
IL6	Interleukin 6
IR	Simultaneous combinatorial stimulation with I and R

IRAK	IL-1R-associated kinase
IRF	Interferon regulatory factor
IRSE	Interferon-Responsive Sequence Element
ISGF3	IFN-stimulated gene factor 3
iTRAQ	Isobaric tag for relative and absolute quantitation
JAK	Janus kinase
JNK	c-Jun N-terminal kinases
JunB	Transcription factor JunB
KEGG	Kyoto Encyclopedia of Genes and Genomes
LC	Liquid chromatography
LIF	Leukemia inhibitory factor
LPS	Lipopolysaccharide
MAPK	Mitogen-activated protein kinase
MCMV	Murine cytomegalovirus
MCSF	Macrophage colony stimulating factor
MDA5	Melanoma Differentiation-Associated protein 5
MPSA	Multi-parametric sensitivity analysis
MS	Mass spectrometry
MSK1/2	Mitogen- and stress-activated protein kinase-1/2
MyD88	Myeloid differentiation primary response gene 88
NE	Nuclear extract
NEMO	NF-κB essential modulator
NF-κB	Nuclear factor κB
NIK	NF-κB inducing kinase
NLR	NOD-like receptor

NP40	Nonidet P40
NT	No treatment control
ODE	Ordinary differential equation
p38	p38 mitogen-activated protein kinases
PAGE	Polyacrylamide gel electrophoresis
PAMP	Pathogen associated molecular pattern
PANTHER	Protein analysis through evolutionary relationship
PBS	Phosphate buffered saline
PCR	Polymerase chain reaction
PRR	Patten recognition receptor
R	R848
RIG	Retinoic acid-inducible gene
RIP1	Receptor-interacting protein 1
RLR	RIG-I-like receptors
RSV	Respiratory syncytial virus
SAPE	Streptavidin-conjugated R-Phycoerythrin
SARM	Sterile-alpha and Armadillo motif containing protein
SDS	Sodium dodecyl sulfate
SLE	Systemic Lupus Erythematosus
SMC	Statistical model checking
ssRNA	Single stranded RNA
STAT	Signal Transducers and Activators of Transcription
Tab	TAK1-binding protein
TAK1	TGF-β-activated kinase 1
TBK1	TANK-binding kinase 1

TBP	TATA binding protein TBP
TEAB	Triethylammonium bicarbonate
TF	Transcription factors
TIR	Toll–interleukin 1 receptor
TIRAP	TIR-associated protein
TLR	Toll like receptor
TNF	Tumor necrosis factors
TRADD	Tumor necrosis factor receptor type 1-associated DEATH domain protein
TRAF6	TNF receptor-associated factor 6
TRAM	TRIF-related adaptor molecule
TRIF	TIR-domain-containing adapter-inducing interferon-β
TYK2	Tyrosine kinase 2

CHAPTER I

INTRODUCTION

CHAPTER I. INTRODUCTION

1.1 Innate immunity and macrophages

Innate immune system is an evolutionarily ancient arm of the host defense mechanism and the molecular players are well-conserved in both plants and animals. While innate immunity is solely responsible for pathogen surveillance and antimicrobial defense in plants and invertebrates, it makes the front line of host defense in vertebrates [1]. During an infection, pathogenic microorganisms are first encountered by innate immune cells, such as macrophages that reside in the tissue. This is followed by recruitment of neutrophils to the infection site. Both macrophages and neutrophils are known as phagocytes, which could kill pathogens through a process called phagocytosis by producing toxic products such as nitric oxide and antimicrobial peptides. In addition, activated phagocytes, especially macrophages, release small proteins called cytokines and chemokines, which attract and activate more macrophages and neutrophils. More importantly, these cytokines and chemokines could activate co-stimulatory molecules on the macrophages and dendritic cells (DC), another type of phagocyte that reside in the tissue, enabling these antigen-presenting cells to initiate the adaptive immune system [2]. **Figure 1.1** illustrates the innate and adaptive immune response activated by a pathogen infection.

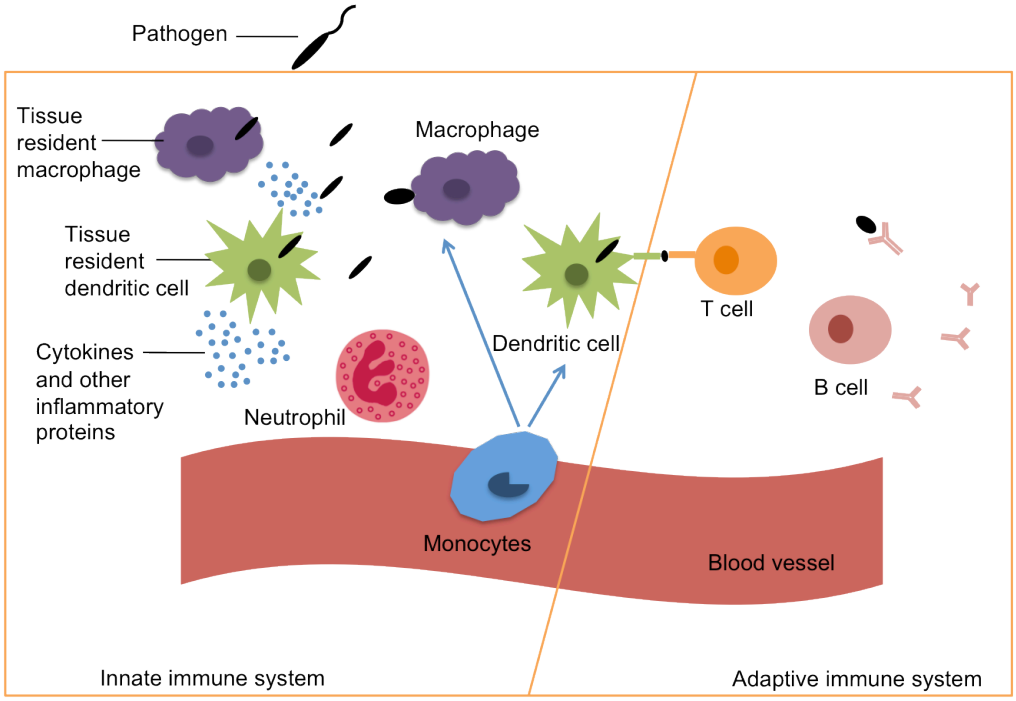

Figure 1.1. Activation of innate and adaptive immune system by pathogens. Upon pathogen infection, innate immune system is first activated. Tissue resident macrophages are the first to sense invading microbes. They produce cytokines and chemokines which recuit neutrophils and monocytes to fight against pathogens. If innate immune system fails to contain a pathogen, adaptive immune system kicks in. The antigen presenting innate immune cells, such as macrophages and dendritic cells, could activate adaptive immune cells, mounting a later but highly targeted attack against the specific invader.

As the sentinel of innate immune system, macrophages mature from monocytes from the circulation system and migrate into the tissues throughout the host. According to their different localization in the body, they are given different names, for examples, microglial cells in neural tissue and Kupffer cells in liver. Macrophages are found in especially large numbers in connective tissues, lung, submucosal layer of gastrointestinal tract and spleen. Not only can they kill pathogens, but also remove senescent cells and maintain homeostasis. They are the first to encounter invading pathogens, making them particular interesting and attractive immune responsive cells for our study.

For the past few decades, the innate immune system was considered to be non-specific in microbial recognition until the discovery of Pattern Recognition Receptors (PRRs) in the mid-1990. With PRRs, macrophages, as well as other innate immune cells, could specifically recognize pathogens and discriminate 'infectious non-self' from 'non-infectious self', and initiate downstream signaling and immune responses.

1.2 Pattern recognition receptors

Germline-encoded PRRs recognize evolutionarily conserved structures on microbes, which are known as pathogen-associated molecular patterns (PAMPs) [3]. Recently, PRRs were also found to recognize endogenous molecules released from damaged cells, which are known as danger-associated molecular patterns (DAMPs). Among PRRs, Toll-like Receptors (TLRs) are the first to be discovered and also the most well-studied [4]. Besides TLRs, three other classes of PRRs have been identified so far, including transmembrane C-type lectin receptors (CLRs), as well as cytoplasmic receptors such as the Retinoic acid-inducible gene (RIG)-I-like receptors (RLRs) and NOD-like receptors (NLRs) [3,5] (**Figure 1.2**). CLRs are transmembrane proteins with carbohydrate-binding domain and can recognize carbohydrates from virus, bacteria and fungi. RLRs are comprised of RIG-1, MDA5 and LGP5, which recognize cytoplasmic viral RNAs. NLRs consist of more than 20 members, which recognize PAMPs, non-PAMP particles and cellular stress effectors, to induce pro-inflammatory responses, particularly inflammasome formation. Expression of these PRRs is not limited to immune cells and some of these PRRs share the same PAMPs with TLRs.

Thus non-TLR PRRs might work in concert with TLRs in innate and adaptive immunity and in maintaining homeostasis. Although this thesis mainly focuses on the crosstalk between TLRs, we should also bear in mind the possible interplay of other PRRs with TLRs under pathogen infection, which warrants future study.

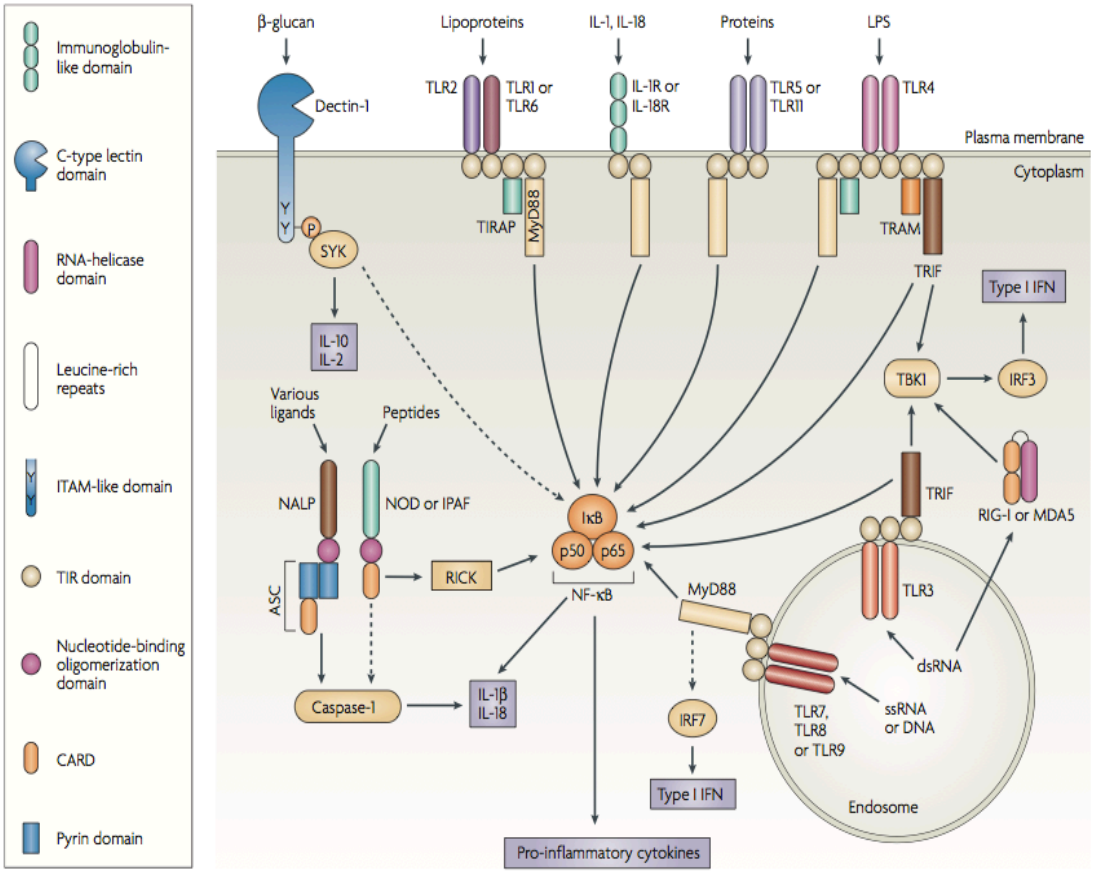

Figure 1.2. Schematic representation of the structure, cellular localization and major components of the PRR families. Four classes of PRRs have been identified so far, including membrane binding recoptors TLRs, CLRs, as well as cytoplasmic receptors such as the RLRs and NLRs. All TLRs use MyD88 as their adaptor, except TLR3, which uses TRIF as its adaptor. TLR4 needs both MyD88 and TRIF to induce downstream signaling. MyD88 pathways mainly induce pro-inflammatory cytokines through activating NF-kB family members, while TRIF pathways mainly induce type I IFN through activating IRF3. The figure is from Giorgio *et al* [6] with copyright permission in Appendices.

1.2.1 Toll-like receptors (TLRs)

Among all the PRRs, the TLRs are the first to be identified and the most well characterized pathogen receptors. Toll was first discovered in drosophila in 1985 by Nüsslein-Volhard [7]; it controls early embryogenesis. A decade later, Jules Hoffmann's lab found its role in the drosophila immune defense [8]. In 1997, Ruslan Medzhitov and Charles Janeway found the toll equivalent in human, which is now known as TLR4 [9]. So far, 10 and 12 functional TLRs have been identified in human and mouse, respectively, with TLR1-9 conserved in both mice and human. Mouse TLR10 is hitherto not known to be functional and TLRs11-13 are missing during the evolution in human.

TLRs are type I transmembrane proteins with ectodomains containing leucine-rich repeats which is required for PAMP recognition, transmembrane domain and intracellular Toll–interleukin 1 (IL-1) receptor (TIR) domains mediating downstream signaling pathways. TLRs are expressed on various immune cells including macrophages, DCs, B cells and even on some atypical cells such as fibroblasts and epithelial cells. TLRs recognize a vast range of PAMPs including proteins, lipids, lipoproteins, nucleic acids from viruses, bacteria, parasites and fungi [10] (Figure 1.2). Some TLRs (TLR1, 2, 4, 5, 6) are expressed on the cell surfaces and they recognize mainly microbial membrane components. For example, subfamily of TLR1, 2 and 6 recognize lipids, TLR5 recognizes flagellin, and TLR4 recognizes lipopolysaccharide (LPS). While certain others (TLRs 3, 7, 8, 9) are expressed exclusively in intracellular vesicles such as endosome, lysosome and endo-lysosomes, where they recognize intracellular microbial nucleic acid and their ligands need to be

internalized into endosomes before signaling occurs [10]. The cellular localization of TLRs is important for the accessibility of their ligands and the maintenance of tolerance to self molecules such as nucleic acid.

1.2.2 TLR-induced signaling pathways

After sensing PAMPs, individual TLRs trigger a distinct response, which is mainly determined by the adaptors with which each of them collaborate (Figure 1.2). The TIR domains of the receptors recruit the TIR domain-containing adaptor proteins to initiate downstream signaling pathways. These TIR domain-containing adaptor proteins include Myeloid differentiation primary response gene (88) (MyD88), TIR-domain-containing adapter-inducing interferon-β (TRIF), TIR-associated protein (TIRAP), TRIF-related adaptor molecule (TRAM) and Sterile-alpha and Armadillo motif containing protein (SARM). The adaptor MyD88, used by all TLRs except TLR3, mainly triggers the activation of NF-κB, a core transcription factor (TF) for pro-inflammatory cytokines and mitogen-activated protein kinase (MAPK). In contrast, the adaptor TRIF used by TLR3 and TLR4 [11], mainly activates interferon regulatory factor 3 (IRF3), a master transcription controller of antiviral responses, as well as NF-κB and MAPK pathways [12]. TRAM and TIRAP function as sorting adaptors that recruit TRIF to TLR4 and MyD88 to TLR2 and TLR4, respectively. SARM, on the contrary, is reported to be a negative regulator of TLR signaling [13]. Thus, TLR signaling pathways can be generally subgrouped into either MyD88-dependent pathways, which drive the induction of inflammatory cytokines, or TRIF-dependent pathways, which are responsible for the induction of type I

interferon as well as inflammatory cytokines. Notably, TLR4 is the only TLR that uses both MyD88 and TRIF for its downstream signaling.

1.3 TLR crosstalk and cytokine synergy

During an infection, each pathogen usually carries with it multiple PAMPs which are likely to interact with multiple TLRs (**Table 1.1**). However, the consequences of combinatorial TLR-activation vary a lot depending on different combinations of TLRs which are activated. For example, the combined activation of TLRs can lead to complementary, synergistic and antagonistic cytokine production, indicating crosstalk amongst the TLRs.

1.3.1 Collaboration and antagonism of TLRs

Initial studies on the collaborations between TLRs expressed by mouse macrophages showed that TLR3 and TLR9 ligands could induce more than additive production of TNF, IL6 and IL12p40 [14], which confirmed that crosstalk between TLRs does exist. Subsequent studies showed both gene expression and protein production of TNF, IL1β, IL10, IL6, IL12 and IL23 which are several fold higher in DCs simulated with combinatorial TLR ligands than single stimulations [15,16]. Some *in vivo* experiments also support the notion that TLRs collaborate. For example, *Tlr*2$^{-/-}$ or *Tlr*9$^{-/-}$ mice are more susceptible to a high dose of *M. tuberculosis* challenge than their wild-type counterparts [17]. In addition, both *Tlr*3$^{-/-}$ or *Tlr*9$^{-/-}$ mice have reduced resistance to murine cytomegalovirus (MCMV) and this decreased resistance is associated with reduced type I IFN and IL12 synthesis [18], which would have been produced by the presence of both TLRs 3 and 9.

Table 1.1. Examples of pathogens expressing multiple TLR ligands.

Pathogen	TLR	TLR ligand
Mycobacterium tuberculosis	TLR2	Lipoarabinomannan
	TLR4	Phosphatidylinositol mannosides
	TLR9	DNA
Salmonella typhimurium	TLR2	Bacterial lipoprotein
	TLR4	Lipopolysaccharide
	TLR5	Flagellin
Neisseria meningitidis	TLR2	Porin
	TLR4	Lipopolysaccharide
	TLR9	DNA
Haemophilus influenzae	TLR2	Lipoprotein
	TLR4	Lipopolysaccharide
Candida albicans	TLR2	Phospholipomannan
	TLR4	Mannan
	TLR9	DNA
Murine cytomegalovirus	TLR2	Viral protein
	TLR3	Double-stranded RNA
	TLR9	DNA
Herpes simplex virus	TLR2	Viral protein
	TLR3	Double-stranded RNA
	TLR9	DNA
Influenza virus	TLR7, 8	Single-stranded RNA
	TLR3	Double-stranded RNA
	TLR5	Not determined
Respiratory syncytial virus	TLR3	Double-stranded RNA
	TLR4	Envelope F protein
Trypanosoma cruzi	TLR2	Glycosylphosphatidylinositol anchor
	TLR4	Glycoinositolphospholipid-ceramides
	TLR9	DNA
Toxoplasma gondii	TLR2	Glycosylphosphatidylinositol anchor?
	TLR11	Profilin

*Adapted from Giorgio et al [6]

On the other hand, cytokine production could also be antagonized by certain combinations of TLRs. IL10 produced by TLR2 ligands was shown to inhibit IL12p35 and IP10 induced by TLR3/4 ligands in human DCs [19]. In addition, TLR9-mediated type I interferon production was shown to be negatively regulated by TLR2 and TLR7 ligands in mouse and human DCs, respectively [20,21].

The positive and negative regulatory role of TLR crosstalk is selective and mainly affects genes, such as cytokine genes, that are important for immune responses to pathogens.

1.3.2 Cytokines and immune-homeostasis

The production of cytokines and chemokines is one of the major events after TLR signaling is activated. Cytokines constitute the central "language" of immune cell communication, interaction and coordination with one another. There are more than 150 "words" in this language system characterized in humans, each with a specific meaning (function). For example, activated macrophages produce chemokines to recruit T-cells and phagocytes to the site of infection, and activate them by producing pro-inflammatory cytokines (e.g. TNFα and IL12). Stimulated phagocytes become phagocytic, and produce more cytokines while stimulated T-cells are involved in the development of antibody-based acquired immunity with memory. TNFα, IL1, IL6, IL10 and IL12 secreted by activated macrophages are key immunomodulators [22,23]. While TNFα, IL1, IL6 and IL12 are pro-inflammatory cytokines, the IL10 is an anti-inflammatory cytokine. Under infection, the magnitude and timing of cytokine production by innate immune

cells usually depends on the coordinated sum of the signals induced by multiple TLRs and this determines the quality and magnitude of subsequent immune response. Effective and coordinated cytokine production results in efficient elimination of infectious agents and tissue repair without compromising homeostasis. However, any imbalance or imprecision in cytokine production could result in either unsuccessful clearance of pathogens or a fatal cytokine storm and chronic inflammatory diseases [24-26].

1.3.3 Physiological significance of cytokine synergy

This thesis focused on studying cytokine synergy induced by TLR collaboration. Cytokine synergy plays a critical role in immune response and understanding of the mechanism underlying cytokine synergy will enlighten us on its close association with immune-related diseases and how to intervene immune over- or under- activation.

On one hand, insufficient cytokine production may hamper immune responses to pathogen infection. This is especially profound in age-dependent dysregulation of immune system. One of the first studies of age-dependent immune deficiency in mouse showed a generalized decrease in *Tlr* gene (*Tlr1-9*) expression and TLR-induced TNF and IL6 production by splenic and peritoneal macrophages from aged mice [27]. An age-dependent impairment of TLR2-induced cytokine expression and signaling was also reported in alveolar macrophages from a *S. pneumoniae* infection of a Balb/c mouse model and a *Porphyromonas gingivalis* infection of a C57BL/6 mouse model [28,29]. In human, decreased TLR-induced cytokine production was also observed in aged monocytes and macrophage as well as DCs [30-35].

On the other hand, uncontrolled cytokine synergy can be lethal and is associated with various diseases. Septic shock is one example that uncontrolled production of pro-inflammatory cytokine in response to pathogen infection may cause dysfunction of organs and lead to death [36]. Cytokine synergy is also involved in chronic inflammatory and autoimmune diseases such as Systemic Lupus Erythematosus (SLE). Elevated levels of IL6, IL12p40 and IL12p19 were observed in SLE patients as well as mouse models [37-41]. MyD88 deficient mouse produces less IFNα, IL6 and IL12, and delays the mortality of SLE and prevents nephritis and immunologic aberrations than wild type mouse [42]. Thus understanding how cytokine synergy occurs during TLR crosstalk will not only contribute to basic research on the understanding of how TLR signaling network is shaped, but also sheds light on disease pathology which may be translated into potential therapeutics.

1.4 Gap of knowledge in cytokine synergy mechanisms

Considering the physiological significance of cytokine synergy induced by combinatorial TLR activation, it is important to unravel the molecular mechanism underlying it. This may help us understand the disease etiology and harness strategies relevant to cytokines production. Although some researches have been carried out to characterize the synergy mechanism from different levels, molecular details are still unclear. The subsections below summarize the known mechanisms and why they are insufficient, especially on how macrophages play a role during TLR crosstalk under multiple PAMP-stimulation.

1.4.1. TLRs synergize cytokine production through crosstalk between MyD88 and TRIF pathways.

Studies have been carried out to systematically examine the pairwise combinations of TLR activation in both macrophages and DCs [16,43-45], and the results showed that two TLR ligands could induce synergistic cytokine production if the stimuli collectively activated both MyD88 and TRIF pathways. Neither MyD88$^{-/-}$ nor TRIF$^{-/-}$ bone marrow derived DCs (BMDC) releases synergetic level of cytokines after combinatorial stimulation [45,46]. These results suggest that TLR synergy might be mediated through certain crosstalks between MyD88 and TRIF pathways. However, the molecular mechanism underlying the MyD88-TRIF crosstalk is still poorly defined.

1.4.2. Role of the autocrine-paracrine loop in synergy is controversial.

Based on the notion that a TRIF-dependent TLR is essential for synergy, one postulation was raised that IFNβ produced by the TRIF pathway might selectively enhance the cytokine production since TRIF pathway is more specialized in type I interferon production than MyD88 pathway. However, controversial views on the involvement of the autocrine-paracrine loop in DC emerged from different research groups. Bagchi and coworkers as well as Napolitani et al [16,43] believed it unlikely because the addition of exogenous IFNβ did not further enhance the cytokine production. On the contrary, Gautier et al [15] found that knockout of IFNβ receptor abolished synergism in cytokine production completely or partially in BMDC). This controversy might be a result of different cell culture conditions and experimental methods. However, it could also imply that endogenous IFNβ might be the "synergy factor," or, that IFNAR might play another role besides

sensing IFNβ in DC. In macrophages, the evidence is consistent among different studies, in that the addition of type I interferon and knockout of IFNAR do not affect the synergistic production of cytokines [15,47].

1.4.3. Multiple signaling pathways might be responsible for synergy

The cytokine production induced by TLR activation is primarily mediated by NFκB and MAPK signaling, thus many research groups have focused their attention on the signaling mechanisms to investigate synergy. However, most of the studies of this kind are in DCs and their results showed association of NFκB, JNK, p38, cJun and ERK signaling [16,45,48,49] with synergy. In macrophages, which are frontline innate immune cells, only sustained ERK phosphorylation has thus far been reported to be concordant with synergy [44]. However, none of the research provided in-depth understanding on the mechanisms on how MyD88 and TRIF might crosstalk to enhance signaling pathways as well as how these signaling pathways synergize in cytokine production.

1.4.4. Transcription regulation of cytokine synergy

Synergistic cytokine production occurs at both the protein and mRNA levels [16,44], suggesting the involvement of transcriptional regulation. Sanna and co-workers [49] studied transcription factor-binding ability to IL12p35 promoter under single- or combinatorial- PAMP stimulation of DCs, and showed that a combinatorial treatment with TLR3+TLR8 agonists accelerated the binding of IRF1 and IRF8 to the IL12p35 gene Interferon-Responsive Sequence Element (IRSE) site, which might have resulted in synergy. Ouyang

et al [50] found the involvement of another IRF family member, IRF5, in synergy, because synergistic production of cytokines (IL12p40, IL12p19 and IL6) was impaired in IRF5 knockout mouse peritoneal macrophages. These results provided hints that the IRF family members might play a critical role in cytokine synergy. However, the role of different transcription factors on synergy seems to be gene- and/or cell- type specific [49], for example IL12p35 is synergistically regulated by IRF1 and IRF8 in DCs but the expression of IL12p35 is very low in macrophage even under combinatorial TLR activation. Thus, findings of transcriptional regulation in DC are not sufficient to explain the synergy phenomenon in macrophages

1.4.5 Limited information is available on TLR signaling network from a global perspective

The study of complex signaling network such as TLR signaling needs more than just searching for specific genes and proteins critical for synergy. It is also necessary to understand the whole TLR signaling crosstalk from a systems perspective. A system, such as TLR signaling network, is not just an assembly of genes and proteins, its properties cannot be fully understood merely by drawing static diagrams. Although such a pathway diagram represents an important first step, what we really seek to know are the dynamics and patterns, why a certain profile emerges, and how we can control them. Lack of a general knowledge of the system may mislead us in interpreting experimental results. This is especially important in drug design. Many drugs are proven to have side effects in clinical trials, although most of them may be favorably effective during *in vitro* experiment. An understanding

of the whole system with computational biology approach might help us gain a more comprehensive overview of the system.

Over the past two decades, intensive research has identified and characterized hundreds of components and interactions involved in TLR signaling, constituting a first step towards understanding TLR signaling on the whole. Systems biology approaches were then extensively applied to enhance our understanding of TLR-mediated innate immune responses [51]. For example, steady-state based flux balance analysis has been carried out on a modified version of the TLR reaction map built by Oda and Kitano [52]. By establishing input-output relationships based on ligand/receptor and transcription/anti-pathogen activities, critical reactions such as MyD88-mediated NFκB/AP-1 activation have been identified [53]. There are also quantitative modeling works to study the dynamics of TLR3 and TLR4 signaling [54-56]. However, these models are either static or over-simplified (no crosstalk was taken into account), which limited the use for an in-depth understanding of TLR pathways. To understand the pattern of TLR crosstalk, an accurate and validated mathematical model of TLR signaling pathways, taking into account of their dynamic interactive behavior need to be derived. This will not only enhance our understanding of TLR crosstalk, but also provide an invaluable platform for designing pharmaceutical strategies.

Given the above rationale, it is important for us to investigate the mechanisms of cytokine synergy in macrophages from both the systems level and detailed molecular level.

1.5 Aims and approaches

1.5.1 The biological question

The major question this thesis seeks to address is how MyD88 and TRIF pathways crosstalk and collaborate to synergize cytokine production when an immune responsive cell encounters more than one TLR agonist.

1.5.2 A proposed model to use- TLR3 and TLR7 combinatorial stimulation

In our lab's previous work [57], Tan *et al* reported that the combination of induction of TLR3 and TLR7 in macrophage induces the most significant cytokine synergy. Thus, we used poly (I:C), a viral dsRNA analogue which activates TLR3-TRIF (Henceforth, Poly (I:C) was denoted **I**), and R848, a viral ssRNA analogue which activates TLR7-MyD88 (R848 was denoted **R**) in our study. Mouse macrophages were stimulated with either I or R or a combination of I and R to study the mechanism of MyD88-TRIF crosstalk. In this thesis, TLR8, which also recognizes single-stranded RNA, was not studied, because it is not functional in mouse. A combination of viral dsRNA- and ssRNA- induced immune cell activation is common in a real infection senario. For example, influenza virus (ssRNA virus) possesses the ligands for both TLR3 and TLR7 [6]. And many other ssRNA viruses also undergo a dsRNA phage during genomic replication in the host cell, and thus contain both TLR3 and TLR7 ligands. Thus, studying the combination of ssRNA and dsRNA bear significance in a real life infection since both dsRNA and ssRNAs of pathogen co-exist in a host cell.

TLR3 pathway The TLR3 pathway is initiated by binding of TLR3 and poly(I:C) (**Figure 1.3**). The activated TLR3 transduces the signal via the

adaptor protein TIR domain containing adapter-inducing interferon-β (TRIF) dependent pathway. The activated TRIF recruits TRAF6, TRADD, FADD and RIP1and forms a complex, which leads to the activation of TAK1:Tab2:Tab3 complex. The activated TAK1 complex, in turn activates the IKK complex (NEMO:IKKb:IKKa). NF-κB is usually associated with IκBα in the cytoplasm. IκBα sequesters with the transcription factor NF-κB, which renders NF-κB inactive. The activated IKK complex, phosphorylates IκBα (that is sequestered to NF-κB), this leads to the dissociation and nuclear translocation of NF-κB. NF-κB then induces the transcription and translation of inflammatory cytokines. TAK1 complex simultaneously activates the MAPKs Erk, p38 and JNK by inducing the phosphorylation of MAPK kinases, which in turn activates the AP-1 transcription factor, which then induces the transcription of inflammatory cytokines. More significantly, the TRIF-dependent pathway leads to IRF3 activation and subsequent Type 1 IFN production. TRIF, along with TRAF3 recruits a signaling complex involving TBK1 and IKKi (IKKε), which catalyze the phosphorylation of IRF3 and induce its nuclear translocation. Phosphorylated IRF3 in the nucleus (a transcription factor) induces the transcription and subsequent translation of Type-1-IFNs. In summary, TLR3 induces antiviral immune response by promoting the production of type 1 IFNs predominantly and cytokines to a lesser extent. The main signaling intermediaries in this pathway are IRF3, NF-κB and AP-1. IRF3 leads to the production of Type 1 IFNs while NF-κB and AP-1 lead to production of inflammatory cytokines [3,5].

TLR7 pathway On the other hand, the TLR7 pathway is initiated by the binding of TLR7 and R848 (Figure 1.3). The activated TLR7 activates

MyD88, which in turn recruits and activates IL-1 receptor associated kinases, IRAK4, IRAK1, IRAK2 and IRAK-M. The activated IRAK complex interacts with TRAF6 and activates TAB2 and TAB3, the regulatory components of the kinase TAK1 complex, to activate TAK1. At this point, the TLR3 and TLR7 pathways merge at the signaling cascade that leads to the activation of AP-1 and NF-κB and the production of cytokines. These form the predominant signaling events of TLR7 pathway. To a lesser extent, the TLR7 cascade activates the transcription factor IRF7, which is usually constitutively expressed in the nucleus and is in inactive form. IRF7 binds to forms a multi-protein signaling complex with IRAK4, TRAF6, TRAF3, IRAK1. This leads to the phosphorylation of IRF7, which then dissociates from the complex and translocates into the nucleus. The nuclear IRF7 plays a role in the transcription of genes for Type I IFNs [3,5].

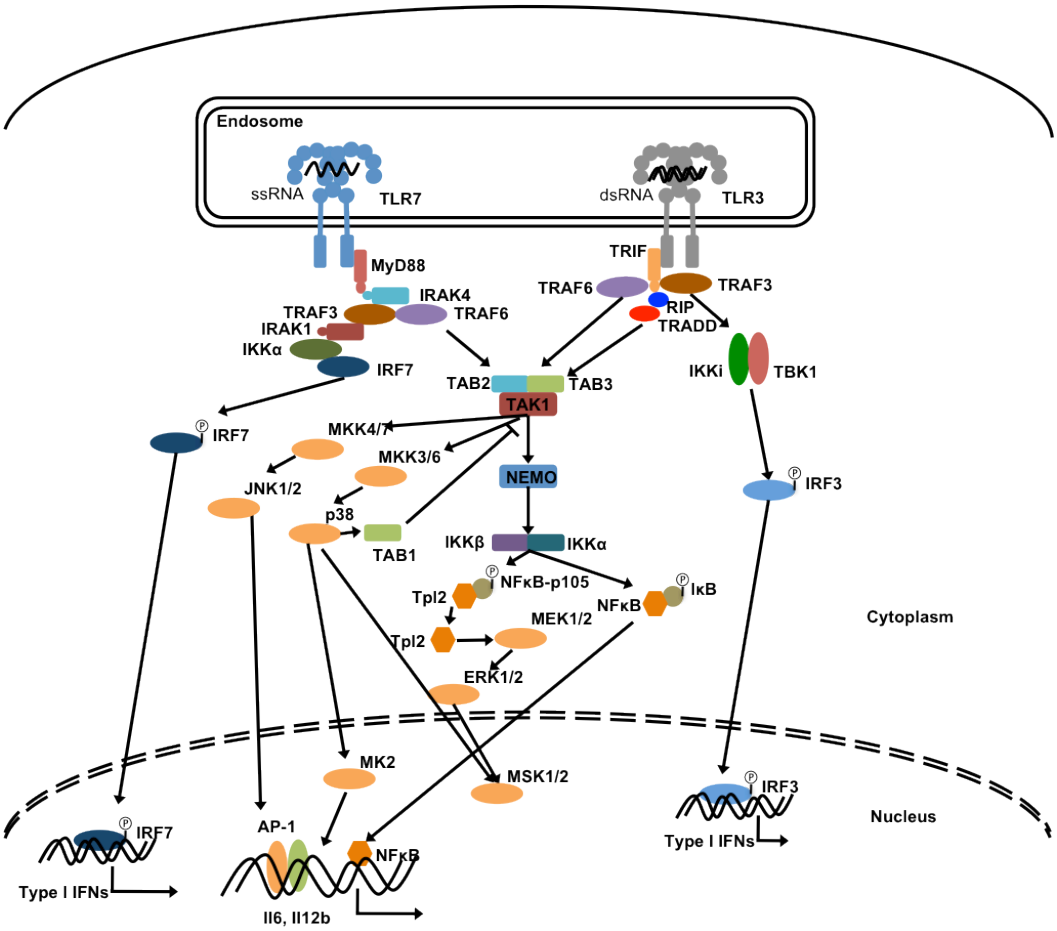

Figure 1.3. A schematic model of TLR3 and TLR7 signaling pathways. TLR7 recognize single stranded RNA and recruits MyD88 as its adaptor. The TLR7 pathway mainly activate inflammatory cytokines such as IL6 and IL12p40 through activating NFκB and MAPKs. On the contrary, TLR3 recoginize double stranded RNA and recruits TRIF as its adaptor. It mainly induces type I IFN through activating IRF3 and mount anti-viral responses. Detailed descriptions are in the text above.

1.5.3 Specific aims

The following 4 specific aims are each provided with an approach:

1.5.3.1 Specific aim 1.

To check whether synergy is a prevalent phenomenon among all the macrophage-secreted cytokines and the kinetic profile of cytokine -

Approach: QuantiGene cytokine mRNA screening and realtime PCR

1.5.3.2 Specific aim 2.

To understand the dynamics of TLR3-TRIF and TLR7-MyD88 pathways from a systems biology perspective and to unravel key signaling pathways of cytokine synergy-

Approach: Computational modeling and empirical validation.

1.5.3.3 Specific aim 3.

To identify the potential synergy factors induced by TLR7-MyD88 and TLR3-TRIF crosstalk.

Approach: proteomic iTRAQ analysis, cytokine gene promoter affinity pulldown and functional knockdown of synergy factors.

1.5.3.4 Specific aim 4.

To understand whether key signaling pathways identified by systems biology regulate transcriptional synergy factors uncovered by conventional molecular biology approach.

Approach: MAPK and JAK-STAT inhibitor study.

The whole project is summarized in the **Project overview** (page ix).

CHAPTER II

MATERIALS AND METHODS

DECLARATION

In Chapter II, the computational modeling was carried out in collaboration with Prof Thiagarajan P.S. and Dr Liu Bing from the School of Computing, National University of Singapore. iTRAQ (including in-gel trypsin digestion and isobaric labeling, fractionation of isobaric tag labeled chromatin protein peptides by HPLC, LC-MS/MS analysis of fractionated peptides using QSTAR and analysis of MS data) was carried out in collaboration with Assoc Prof Sze Siu Kwan and his team from Nanyang Technological University.

CHAPTER II. MATERIALS AND METHODS

All experiments were carried out in compliance with National and Institutional guidelines on ethics and biosafety (Institutional Review Board, Reference codes: NUS-IRB 08-296) and the Institutional Animal Care and Use guidelines (IACUC Protocol Ref: 049/11).

2.1 Materials

2.1.1 Mice

7-8-week old female BALB/c mice were purchased from NUS-CARE, which were used for derivation of bone marrow-derived macrophages (BMDM).

2.1.2 Aseptic tools and pyrogen-free equipment

To minimize endotoxin contamination, scissors and forceps for mice dissection and all glassware for cell culture were baked at 200°C for 2 h.

2.1.3 Cell culture medium

Medium for cell culture: Dulbecco's modified Eagle's medium (DMEM) powder (Gibco, Life Technologies, Carlsbad, CA, USA) was dissolved in pyrogen-free water (Baxter, Deerfield, IL, USA) to make incomplete medium. Complete medium were made with DMEM supplemented with fetal bovine serum (FBS) (Hyclone, Thermo Fischer Scientific, Waltham, MA, USA).

2.1.4 Antibodies

Antibodies for immuno-detection are summarized in **Table 2.1**.

Table 2.1. List of antibodies used

Antibody	Supplier	Cat#	Raised	Dilution
Primary antibodies				
pp38 (Thr180/Tyr182)	CST	4511	Rabbit	1:1000
pERK (Thr202/Tyr204)	CST	4370	Rabbit	1:2000
pJNK (Thr183/Tyr185)	CST	4668	Rabbit	1:1000
pIκBα (Ser32/36)	CST	9246	Mouse	1:1000
STAT1	CST	9172	Rabbit	1:1000
pSTAT1 (Tyr701)	CST	9171	Rabbit	1:1000
NFκB p65	Abcam	ab7970	Rabbit	1:1000
IRF3	Abcam	ab25950	Rabbit	1:1000
TATA binding protein TBP	Abcam	ab818	Mouse	1:2000
C/EBP beta	Thermo	MA1-827	Mouse	1:1000
JunB	Santa Cruz	sc-73	Rabbit	1:1000
RelB	Santa Cruz	sc-226	Rabbit	1:1000
IRF1	Santa Cruz	sc-640	Rabbit	1:1000
ICSBP*	Santa Cruz	sc-6058	Goat	1:1000
GAPDH	Santa Cruz	sc-32233	Mouse	1:3000
NF kappa B p50 and p105	eBiosciences	14-6732-63	Rabbit	1:1000
c-Rel	eBiosciences	14-6111-82	Rat	1:1000
Actin	Sigma	A2066	Rabbit	1:2000
Secondary antibodies				
Goat α-rabbit HRP	Dako	P0448	Goat	1:3000
Goat α-mouse HRP	Dako	P044701	Goat	1:3000
Goat α-rat HRP	Biolegend	405405	Goat	1:3000
Rabbit α-goat HRP	Dako	P0449	Rabbit	1:3000

*ICSBP: Interferon (IFN) consensus sequence-binding protein, or interferon regulatory factor 8 (IRF8).

2.1.5 Primer sequences

The PCR primers used in this thesis are summarized in Table 2.2

Table 2.2 Primer sequences

Primer sequences for restriction enzyme accessibility assay		
Il6 promoter region with AflII restriction site	Forward	5'-cccatcaagacatgctcaagtg-3'
	Reverse	5'-gcacaatgtgacgtcgtttagc-3'
Il12b promoter region with SpeI restriction site	Forward	5'-tctgtatgatagatgcactcagg-3'
	Reverse	5'- ggaaacccaaagtagaaactgac-3'
Il12b enhancer region with SpeI restriction site	Forward	5'- agtttcaccagtgactccagca -3'
	Reverse	5'- acagtctcaaaggaccatggct -3'
Control region	Forward	5'-gaggcagagagccagcattg-3'
	Reverse	5'-aagggaaaaccggcaagtgag-3'
Primer sequences for promoter cloning		
Il6 promoter	Forward	5'-attctcgagattttaatctactctaatcgcctgt-3'
	Reverse	5'-cccaagcttagcggtttctggaattgactat-3'
Il12b promoter	Forward	5'-agttcatgctgctatcaatcca-3'
	Reverse	5'-cacccactgttccttctgct-3'

2.2 Derivation of bone marrow macrophages

Bone marrow derived macrophages (BMDMs) were isolated as described previously [58]. Mice were euthanized with CO_2 and disinfected with 70% ethanol. Using aseptic tools, an excision was made on the skin on the back of the mouse, peeling the skin from the top of each hind leg down and over the foot. The hind legs were broken from the hip joint and the femur and tibia were obtained intact. Excessive muscles were removed from the legs, and the femur and tibia were kept in ice-cold incomplete DMEM. The bones proximal to each joint were carefully severed and flushed with 3 ml ice-cold DMDM twice at both end. The cells were spin down at 500 g for 10 min at room temperature. The cells were resuspended and plated in DMEM supplemented with 10% (v/v) FBS, 100 U/ml recombinant M-CSF (Ebioscience, San Diego, CA, USA), 100 U/ml penicillin and 100 μg/ml streptomycin (Gibco, Life Technologies, Carlsbad, CA, USA) at a density of

$1.5x10^6$ cells/ml. The cells were incubated at 37°C, 5% CO_2 incubator. At day 3 post-harvest, additional (half of the original volume) MCSF conditional medium was added to the bone marrow cells and were incubated for another 4 days before harvesting macrophages for experiments.

2.3 Cell culture

Primary cells (BMDM) and established mouse macrophage cell line (J774) were cultured in DMEM supplemented with 10% (v/v) FBS at 37°C, in an incubator supplied with 5% CO_2, 95% air. One day before PAMP stimulation, cells were plated at a density of $1x10^6$/ml for BMDM and $0.5x10^6$/ml for J774 cells.

2.4 PAMP treatment

R848 and low molecular weight poly (I:C) were purchased from InvivoGen (SD, CA, USA). R848 was used at a final concentration of 25 ng/ml and poly (I:C) was used at a final concentration of 10 μg/ml. The concentration of PAMPs was previously optimized in our lab by Tan *et al* [57]. The concentrations we used here fall in the exponential part of the dose-response curve of each PAMP, and their combinatorial response could induce synergy, and yet not saturated. For combinatorial stimulation with different time intervals and stimulation sequential, the treatment strategies and corresponding controls are summarized in Figure 2.1 and Table 2.3. The number between I and R denotes the time interval between first and second stimulation, and number following second stimulation denotes the treatment time after second stimulation. For example, I8R8 means poly (I:C)

pretreatment for 8 h followed by R848 treatment for another 8 h. The single PAMP stimulation controls for I8R8 are I16 (I stimulation for 16 h) and R8 (R treatment for 8 h).

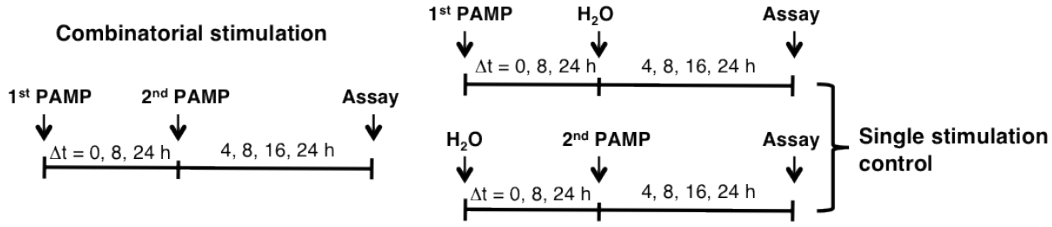

Figure 2.1 Stimulation strategies for combinatorial PAMP stimulation with different time interval between two PAMP treatments. Here the two PAMPs used are poly (I:C) and R848.

Table 2.3 Combinatorial I and R stimulation, and their controls

Simultaneous I and R stimulation for 4, 8, 16 and 24 h			
Combinatorial	Single control	Combinatorial	Single control
IR4	I4 R4	IR16	I16 R16
IR8	I8 R8	IR24	I24 R24
I pretreatment for 8 h followed by R stimulation for 4, 8, 16, 24 h			
Combinatorial	Single control	Combinatorial	Single control
I8R4	I12 R4	I8R16	I24 R16
I8R8	I16 R8	I8R24	I32 R24
I pretreatment for 24 h followed by R stimulation for 4, 8, 16, 24 h			
Combinatorial	Single control	Combinatorial	Single control
I24R4	I28 R4	I24R16	I40 R16
I24R8	I32 R8	I24R24	I48 R24
R pretreatment for 8 h followed by I stimulation for 4, 8, 16, 24 h			
Combinatorial	Single control	Combinatorial	Single control
R8I4	R12 I4	R8I16	R24 I16
R8I8	R16 I8	R8I24	R32 I24
R pretreatment for 24 h followed by I stimulation for 4, 8, 16, 24 h			
Combinatorial	Single control	Combinatorial	Single control
R24I4	R28 I4	R24I16	R40 I16
R24I8	R32 I8	R24I24	R48 I24

2.5 Total RNA extraction

Total RNA from BMDM or J774 was extracted with Trizol (Invitrogen) according to the manufacturer's instruction. Briefly, cells from 1 well of a 24-well plate were resuspended in 500 μl Trizol reagent. Samples were kept in -80°C for long-term storage. Before extraction, cells were kept at room temperature for 10 min to allow for dissociation of nucleoprotein complexes. 100 μl chloroform was added to each sample followed by vigorous shaking for 15 s. After 2-3min incubation at room temperature, samples were centrifuged at 12000 g for 15 min at 4°C. The aqueous phase was carefully aspirated and mixed with 250μl isopropanol without disturbing the interphase and organic phase. The mixture was incubated for another 10 min at room temperature before spinning down at 12000 g for 10 min at 4°C. The RNA pellet was then washed with 75% ethanol and pelleted by centrifugation at 7500 g for 5 min at 4°C. The pellet was air dried and dissolved in 10 μl DEPC treated water. The dissolved RNA was kept in -80°C or used immediately for experiments.

2.6 Reverse-transcription PCR

cDNA was synthesized from RNA with SuperScript® III First-strand Synthesis System (Invitrogen). In each 10 μl reaction, 1-2 μg RNA was mixed with 0.5 μl oligo $(deoxythymidine)_{12-18}$ primers (50μM) and 0.5 μl dNTP mix (10 mM), 2 μl $MgCl_2$ (25 mM), 1 μl DTT(0.1 M), 1 μl RT buffer (10X), 0.5 μl RNase OUT (40 U/μl) and 0.5 μl SuperScript® III RT (200 U/μl) and incubated in PCR machine with following program: 50 min at 50°C, 5 min at 85°C. cDNA can be stored at -20°C.

2.7 Quantification of mRNA

2.7.1 Real-time PCR

Two types of chemistries (TaqMan® chemistry and SYBR® chemistry) were used to detect PCR products using Lightcycler® 480 system (Roche). Their working principles are summarized in **Figure 2.2 and 2.3**.

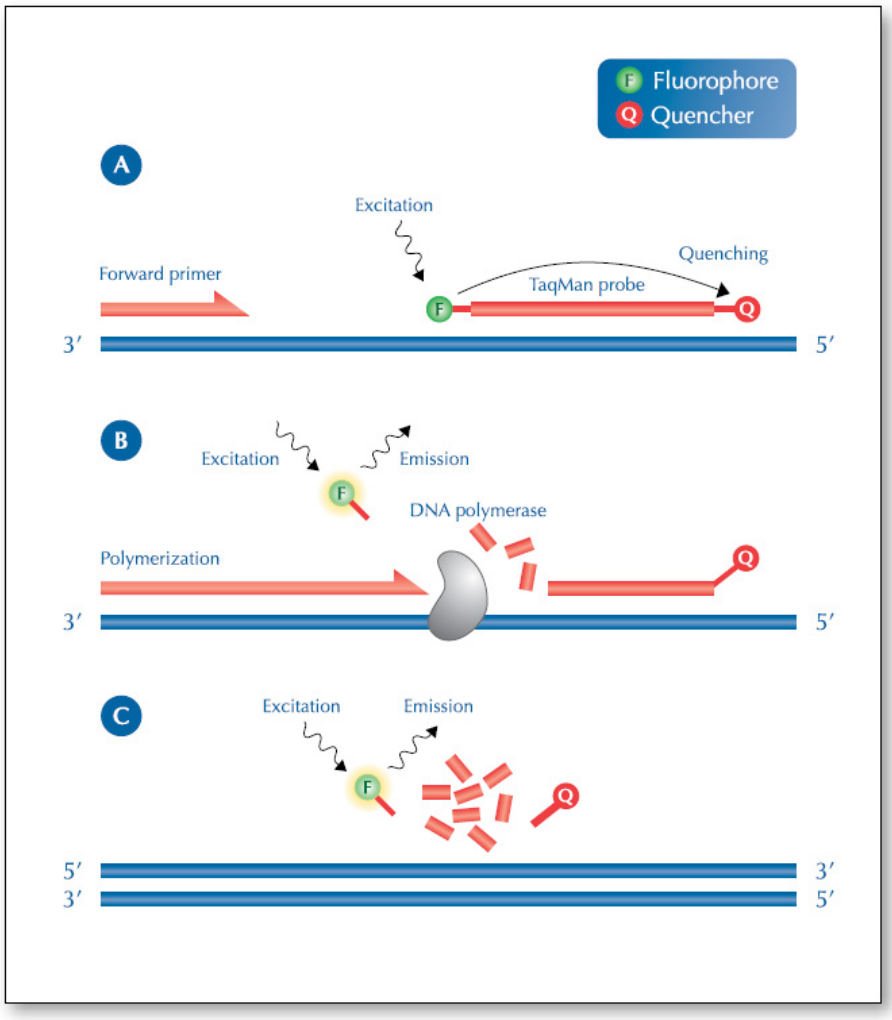

Figure 2.2. TaqMan probe chemistry. A) Primers and probes anneal to the targeted DNA template. Probes are conjugated with fluorophore at 5' end and quencher at 3' end. Fluorophore could be activated by light and pass the energy to quencher so that no fluoresce is detected. B) During polymeriztion, DNA polymerase encounters the probe and hydrolyzes it to release fluorophore, which is no longer quenched when excited by light. C) DNA polymerase hydrolyzes the whole probe from the template and completes strand elongation. Figure from http://www.thermoscientificbio.com/applications/pcr-and-qpcr/introduction-to-qpcr/

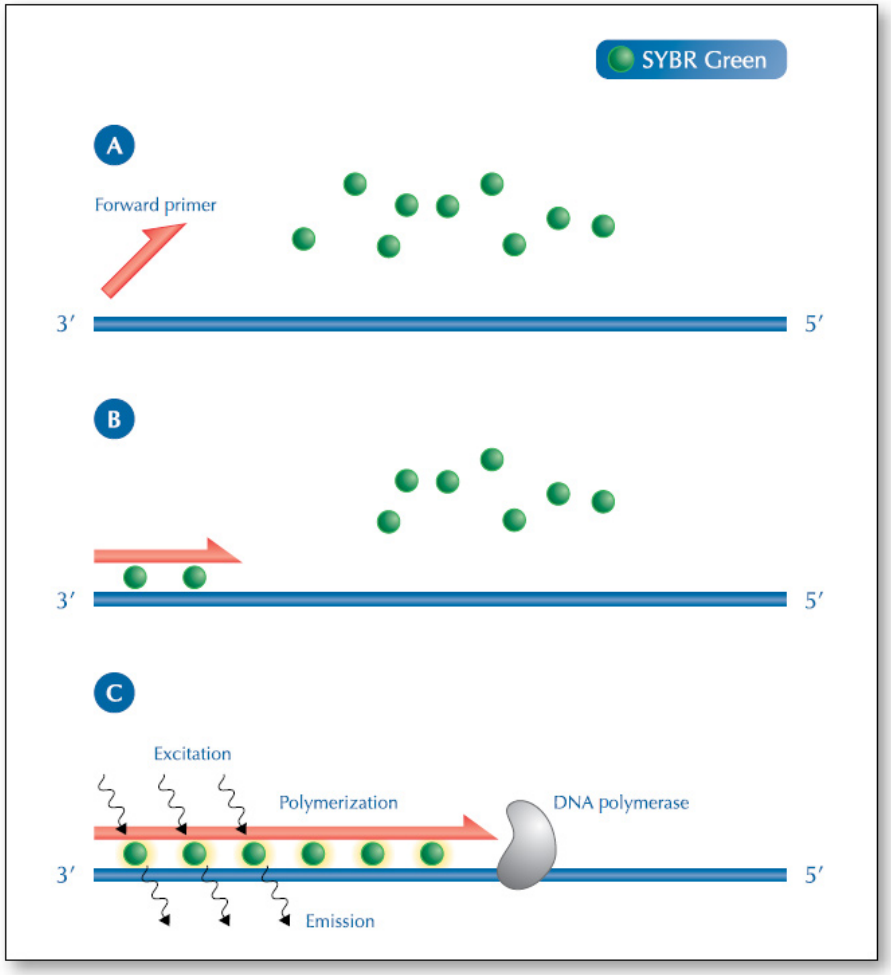

Figure 2.3. SYBR green chemistry. A) DNA template is denatured and SYBR Green molecules are free in the reaction mix. B) Primers anneal with the targeted DNA template and SYBR Green molecules bind to the dsDNA. C) DNA polymerase elongate PCR products and more SYBR GREEN molecules bind to double stranded DNA and they can be detected after light excitation. Figure from http://www.thermoscientificbio.com/applications/pcr-and-qpcr/introduction-to-qpcr/

2.7.1.1 TaqMan realtime PCR

Lightcycler® 480 probes master (Roche) was used for the Taqman assays, and pre-designed TaqMan® Gene Expression Assays (Life Technologies) Mm00446190_m1, Mm00434174_m1, Mm00446968_m1 were used for the detection of *Il6*, *Il12b*, *Hprt* mRNA, respectively. 5 µl of Probe mastermix, 1 µl of the 1:10 diluted cDNA, and 0.5 µl primer and probe

were made up to a final volume of 10 μl reaction system with nuclease-free water. Real-time PCR was carried out with Light cycler® 480 system (Roche). The PCR cycles were: 1 cycle of 95°C for 10 min, 40 cycles of 95°C for 10 s, 60°C for 20 s. The mRNA levels of *Il6* and *Il12b* were normalized to the amount of *Hprt*.

2.7.1.2 SYBR-Green realtime PCR

SYBR Green chemistry was used to determine the percentage of DNA digested at the restriction site in the restriction enzyme accessibility assay. LightCycler® 480 SYBR Green I Master mix (Roche) was used in restriction enzyme accessibility assay. Briefly, 5 μl of SYBR Green I mastermix, 3 μl of the 10 ng/μl DNA, and 2 μl primer mix (2.5 μM) were made up to a final volume of 10 μl reaction system. PCR program was: 1 cycle of 95°C for 7 min 30 s; 45 cycles of 95°C for 10 s, 61°C for 10 s, and 72°C for 15 s.

2.7.2 QuantiGene plex 2.0 assay for profiling of cytokine and chemokine transcription.

The screening of cytokine mRNA expression profile of the primary BMDM was determined using a QuantiGene plex 2.0 assay kit (Panomics/Affymetrix, Freemont, CA, USA). The principle of QuantiGene assay is summarized in **Figure 2.4**.

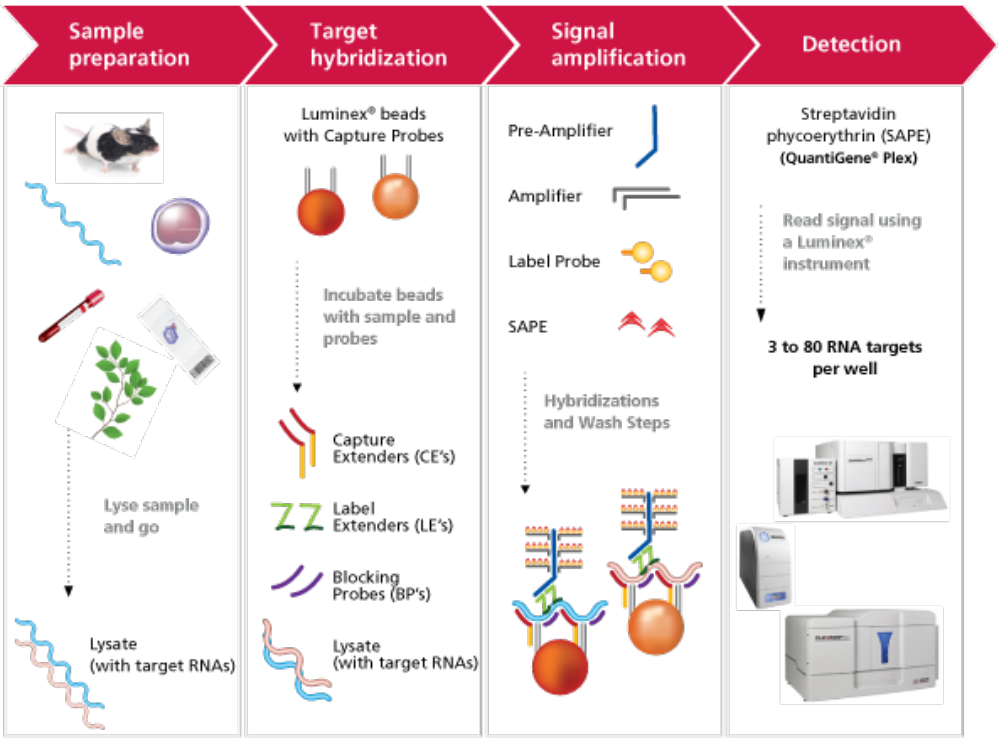

Figure 2.4. Principle of QuantiGene Plex 2.0 assay. The QuantiGene Plex 2.0 Assay is a hybridization-based assay using the xMAP® Luminex® magnetic beads and performed on 96-well plates. The assay is based on direct quantification of the RNA targets using xMAP Luminex beads for multiplexing of 3 to 80 RNA targets and branched DNA (bDNA) signal amplification technology. On the first day, samples are lysed to release target RNAs. Then lysate is incubated with probes that recognize specific sequence on target RNAs. Probes include blocking probes which prevent non-specific binding, label extenders, which bind to target RNA and signal amplifiers, and capture extenders, which bind to target RNA and magenetic beads. On the second day the signal amplification is conducted through adding PreAmplifier, Amplifier and Label Probe. Each amplification unit gives a 400x signal amplification and there are six amplification units per target RNA copy leaning to a 2400x signal amplification per copy RNA. The signal is then detected by adding SAPE substrate and using a Luminex instrument for the read out. The figure is from http://www.panomics.com/products/gene-expression/plex-2.0-assay/how-it-works

A 21-plex panel containing *Il6*, *Il1b*, *Csf2*, *Ccl3*, *Ccl2*, *Actb*, *Cxcl1*, *Ifnb1*, *Il23a*, *Il10*, *Il12b*, *Cxcl10*, *Csf3*, *Tnf*, *Cxcl2*, *Il1a*, *Hprt1*, *Gusb*, *Lif*, *Ccl5*, *Il12a* of mouse 2.0 plex set 21310 was used to analyze the BMDM cell lysates. The assay was carried out according to the manufacturer's instructions. Briefly, 25 µl cell lysate was diluted four times with lysis

mixture (Panomics/Affymetrix, Freemont, CA, USA). Then 80 μl of diluted cell lysate was added into each well of a 96-well hybridization plate and incubated overnight at 54°C with working bead-mixture containing capture beads and 2.0 probe set with shaking. The 2.0 probe set is composed of oligonucleotide probes that target RNA molecules of interest. For each RNA molecule of interest, three types of synthetic probes, capture extenders, label extenders and blockers that hybridize and span contiguous sequences of target RNA, was present in the probe sets. On the next day, the capture beads with bound RNA were washed and incubated with 2.0 pre-amplifier working reagent for 1 h at 50°C with shaking. After brief washing to remove the unbound pro-amplifier, samples were incubated with 2.0 amplifier for another 1 h at 50°C with shaking. Next, samples were washed and incubated with biotinylated probe for 1 h at 50°C with shaking. Subsequently, samples were washed again and incubated with Streptavidin-conjugated R-Phycoerythrin (SAPE), which binds to biotin-labeled probes, for 30 min at room temperature. Then unbound SAPE was washed away and the fluorescence signal of SAPE was detected and analyzed by Bio-Plex system (Bio-rad, Hercules, CA). *Hprt* was chosen as an internal control for each sample.

2.8 Western blot immune-detection

2.8.1 Cell lysis

For whole cell lysate analysis, the culture media were removed and the cells were washed once with ice-cold PBS. Cells were then lysed with RIPA buffer (50 mM Tris-HCl pH7.5, 0.5% deoxycholate, 150 mM NaCl, 1% NP-40, 0.1% SDS, 1 mM EDTA) in the presence of a cocktail of proteinase and

phosphatase inhibitor (Roche). Usually, 40 μl, 60 μl and 100 μl RIPA buffer was added to one well of 24-, 12- and 6- well plate, respectively. Lysis was carried out on ice for 20-30 min and cell lysates were then centrifuged at 16000 g for 15 min at 4°C to remove insoluble pellet. Cell lysates can be stored at -80°C, but freeze and thaw cycles should be minimized.

2.8.2 Bradford protein assay

The protein concentration of the cell lysate was determined by Bradford protein assay according to manufacturer's instruction (Biorad). Briefly, 10 μl samples (1:50 diluted in 50 μl water) were mixed with 200 μl Bradford reagent (1:5 diluted). After 5-min incubation, the absorbance was measured at 595 nm using a BioTek plate reader. To determine the protein concentration of the cell lysate sample, a standard curve of 0, 0.025, 0.05, 0.075, 0.1, 0.125, 0.15, 0.175, 0.2 mg/ml BSA was used. For each sample, triplicate readings were obtained.

2.8.3 SDS-PAGE and immunblotting analyses of cell lysate proteins.

For whole cell lysates, samples containing 15 μg protein were first mixed with SDS loading buffer (62.5 mM Tris-HCl pH 6.8, 2% w/v SDS, 10% glycerol, 50 mM DTT, 0.01% w/v bromophenol blue) and heated at 95°C for 10 min. Protein samples were resolved in a reducing SDS-PAGE (10%) and electrotransferred to polyvinyldifluoride membranes for 1 h at 10V. Blots were subsequently blocked with 5% dry, skimmed milk in TBST (50 mM Tris-base, 150 mM NaCl, 0.01% Tween-20, pH 7.6) and probed with specific antibodies (Table 2.1). Blots were then incubated with HRP-conjugated rabbit,

mouse, goat or rat secondary antibodies (Table 2.1) and were visualized with Western Bright ECL (Advansta, Menlo Park, CA, US) and ImageQuant LAS4000 mini system (GE, Fairfield, CT, US).

2.9 mRNA stability test

BMDMs were stimulated for 4 h with polyI:C (10 μg/ml) and/or R848 (25 ng/ml). The *Il6*, *Il12b* and *Hprt* mRNA levels were determined by Taqman Real-Time PCR in samples collected before (0 min) and 30, 60, 120 min after the addition of actinomycin D (5 μg/ml), which halts synthesis of new mRNAs.

2.10 Restriction enzyme accessibility assay

In order to assess the openness of the chromatin complex, we measured its assessibility to various restriction enzymes. This will provide a clue on how open/competent the chromatin structure is for its functionality when the cells were stimulated by PAMPs.

2.10.1 Nuclei isolation

Cultured cells were collected by scraping, washed twice with ice cold PBS, centrifuged at 800 × g for 5 min 4°C and re-suspended gently. Cell pellets were fully suspended in 10 CPV (cell pellet volume) of lysis buffer (10 mM Tris-HCl, pH 7.4, 60 mM KCl, 1 mM EDTA, 0.075 % Nonidet P-40, 1 mM dithiothreitol, including the Complete^{TM} protease inhibitor cocktail (Roche), and incubated on ice for 3 min. Thereafter, the nuclei were pelleted by a pulse spin (14,000× g for 30 s) at 4 °C.

2.10.2 Restriction enzyme digestion

The pelleted nuclei was washed once with the restriction enzyme buffer (10 mM Tris [pH 7.4], 50 mM NaCl, 10 mM MgCl2, 0.2 mM EDTA, 0.2 mM EGTA, 1 mM β-Mercaptoethanol, 0.15 mM spermine, and 0.5 mM spermidine) [59], and re-suspended in corresponding digestion buffer (New England Biolabs). After the addition of enzymes (New England Biolabs) (AflII for *Il6* promoter analysis, SpeI for both promoter and enhancer of *Il12b*), the digestion mixtures were incubated for 1 h at 37°C.

2.10.3 Accessibility of restriction enzyme to chromatin detected with Real-Time PCR

Genomic DNAs were extracted with TRizol reagent (Invitrogen) following the manufacturer's instruction. The percentage of DNA digested at the restriction site was determined by quantitative real-time PCR, using LightCycler® 480 SYBR Green I Master mix (Roche). A series of diluted genomic DNA, which were not digested with the restriction enzymes, were amplified (together with those test samples mentioned above), to create standard curves for both target region and a control region nearby without targeted restriction site (to be used as internal calibrator for quantification). The percentage of DNA digested was calculated by subtracting the relative ratio of "apparent template" covering the restriction site (amplifiable) to that of non-digested control region.

2.11 Calculation of "fold-synergy" of TLR-ligand stimulations

To quantify the synergistic effect, the level of cytokine produced under combinatorial stimulation was divided by the sum of the respective single stimulations to give a value we termed "fold synergy."

$$\text{Fold synergy of cytokine expression} = \frac{\text{Combinatorial stimulation (IR)}}{\text{I stimulation + R stimulation}}$$

2.12 Proteomic profiling of chromatin binding proteins with Isobaric tag for relative and absolute quantitation (iTRAQ).

2.12.1 Extraction of chromatin binding proteins

Chromatin binding proteins were purified as described previously [60]. Briefly, cells were washed twice with PBS and resuspended in extraction buffer A (10 mM Tris-Cl, pH 7.4, 15 mM NaCl, 60 mM KCl, 150 mM sucrose, 1 mM EDTA, 1% TritonX-100, 0.1% NP40, 1 mM DTT and protease inhibitor) and kept on ice for 10 min. The cell suspension was passed through a 25G needle 3-4 times and spun down at 500 g for 10 min at 4°C to pellet the nuclei. The nuclear pellet was resuspended in 0.5 ml extraction buffer A and gently pipetted onto the surface of a 2-ml ice-cold sucrose cushion (10 mM Tris-Cl, pH 7.4, 15 mM NaCl, 60 mM KCl, 300 mM sucrose, 1 mM EDTA, 1 mM DTT, and protease inhibitor). The sucrose gradient was centrifuged at 230g for 10 min at 4°C to pellet the nuclei, which was washed twice in 1 ml of wash buffer A and once with wash buffer B (10 mM Tris-Cl, pH 7.4, 15 mM NaCl, 60 mM KCl, 1 mM EDTA, 1 mM DTT and Complete^{TM} protease inhibitor cocktail (Roche)). The nuclear pellet was resuspended in extraction buffer B and kept on ice for 10 min to lyse the nuclear membrane. The chromatin pellet was washed twice in 1 ml of wash

buffer A and once with wash buffer B followed by dissolving in 0.5% SDS solution with sonication to aid dissolution. The protein quantified using Bradford protein assay (see section 2.8.2).

2.12.2 In-gel tryptic digestion and isobaric labeling

The chromatin extracts were resolved in denaturing SDS-PAGE to remove the non-protein interfering reagents left from the sample extraction. Briefly, 500 μg of chromatin-binding protein from each treatment condition was electrophoresed on a 3-layer polyacrylamide gel composed of 4% stacking, and 10% and 25% resolving polyacrylamide gels. After migrating into the 10% layer, proteins were detained by the 25% layer, thus they were concentrated in a narrow strip between the 4% stacking and 25% resolving gel. After staining with Coommassie blue, the gel was excised into 1 × 1 mm pieces and completely destained. Next the diced gel was reduced in 5 mM Tris-(2-carboxyethyl) phosphine at 37°C for 3 h and alkylated in 10 mM methyl methanethiosulfonate in isopropanol at room temperature for 1 h before digestion with 10 ng/μl of sequencing-grade modified trypsin (Promega, Madison, WI) overnight at 37 C. Then an equal amount of trypsin was added and the mixture was incubated for another 4 h at 37 °C. The peptides were extracted with 1 ml 50% ACN/5% acetic acid, and the solution was vacuum concentrated. After dissolving in 0.5 M triethylammonium bicarbonate (TEAB) and ethanol, the peptides were labeled with respective isobaric tags using 8-plex iTRAQ reagent Multi-Plex kit (Applied Biosystems, Foster City, CA). Each labeled sample was vortex-mixed for 2 h before combining and drying in a vacuum centrifuge.

2.12.3 Fractionation of isobaric tag-labeled chromatin protein peptides by high performance liquid chromatography (HPLC)

The combined and dried samples were desalted through Sep-Pak C18 SPE cartridges (Waters, Milford, MA) and vacuum-dried again. Then the peptide mixture was reconstituted in mobile phase A buffer (10 mM CH_3COONH_4/85% ACN/1% formic acid [FA]) and fractionated using Electrostatic Repulsion-Hydrophilic Interaction Chromatography (ERLIC) as previously described [61]. Briefly, peptides were loaded into a PolyWAX LP weak anion-exchange column (4.6 x 200 mm; 5 μm, 300 Å; PolyLC) followed by fractionation by the UFLC system with a UV detector at a wavelength of 280 nm. Two solvents (30% ACN/0.1% FA) used to generate composition gradient were used as mobile phase A and mobile phase B. A 50-min elution gradient started from 0-28% mobile buffer B for 40 min followed by 28-100% buffer B for 5 min and 100% buffer B for 5 min at a flow rate of 1 mL/min. Thirty fractions were collected, vacuum dried and combined into 20 fractions for LC-MS/MS analysis.

2.12.4 LC-MS/MS analysis of fractionated peptides using QSTAR

Reverse-phase separation of the peptides was performed on a home-packed nanobore C18 column (15 cm x 75 μm; 5 μm particles) in a Tempo™ nano-MDLC system. The samples were directly injected via a Picofrit nanospray tip (New Objectives, Woburn, MA, USA) at a flow rate of 300 nl/min over a gradient of 90 min, into a QSTAR® Elite Hybrid LC-MS/MS system (Applied Biosystems). Data were acquired with Analyst® QS 2.0 software (Applied Biosystems). The QSTAR system carried out a survey scan of peptides with mass ranging over 300–1600 m/z using positive ion mode.

For each MS spectrum, the three most abundant peptides of above a five-count threshold with +2 to +4 charge states were selected for MS/MS. Once selected, they were placed under dynamic exclusion for 30 s with a mass tolerance of 0.03 Da. Smart information-dependent acquisition was adopted with automatic collision energy and automatic MS/MS accumulation with a 20-time fragment intensity multiplier and 2 s of maximum accumulation time. Peptides from each fraction were analyzed three times on the same platform.

2.12.5 Analysis of MS data

Spectra generated from the three technical replicates were analyzed using ProteinPilot (v3.0.0.0, Applied Biosystems) to generate the peak-list and the identity and quantity of each protein. The ProteinPilot software was used for user-defined parameters of the Paragon algorithm with the following configuration: (1) Sample Type - iTRAQ 8-plex (Peptide Labeled); (2) Cysteine alkylation - MMTS; (3) Digestion - Trypsin; (4) Instrument - QSTAR Elite ESI; (5) Special factors - None; (6) Species- None; (7) Specify Processing - Quantitate & Bias Correction; (8) ID Focus - biological modifications, amino acid substitutions; (9) Database - concatenated Uniprot mouse database (62,604 sequences, and 27,441,367 residues; download on 12 March 2010) and its reverse complement; (10) Search effort - thorough ID; (11) Result quality - Unused ProtScore (Conf) >0.05 (10.0%). The default precursor and MS/MS tolerance for QSTAR ESI MS instrument were automatically employed by the software. A cut off of 1% was adopted for the false discovery rates (FDR) of both peptide and protein identification (FDR = 2.0 × decoy_hits/total_hits).

2.12.6 Bioinformatics analysis of iTRAQ data

The protein classification of total reliably identified and quantified proteins were made with PANTHER (Protein ANalysis THrough Evolutionary Relationships) classification system [62]. Functional annotation cluster analyses of perturbed proteins were made with Database for Annotation, Visualization and Integrated Discovery (DAVID) [63]. Annotation categories used for DAVID analysis are Gene Ontology (GO) biological process, GO molecular function and KEGG pathway.

2.13 Promoter pull down assay

2.13.1 Nuclear extraction preparation

Cell nuclei were isolated from macrophages treated with I, R or IR for 5 h, as described above (2.10.1). The supernatants were removed and the nuclei were washed by re-suspending in lysis buffer without Nonidet P-40, followed by suspending in 4 CPV of nuclear extraction buffer (20 mM Tris-HCl, pH 8.0, 420 mM NaCl, 1.5 mM $MgCl_2$, 0.2 mM EDTA, 25 % (v/v) glycerol and protease inhibitors), and incubated on ice for 1 h with intermittent mixing by vortex for 15 s each. Finally the nuclear extracts were cleared by centrifugation at 20,000× g for 15 min at 4 °C, snap-frozen in liquid nitrogen, and stored at −80 °C. Nuclear extracts (NE), in aliquots, were only thawed once for each experimental use. The protein concentration was determined by Bradford assay (2.8.2).

2.13.2 Promoter cloning

The *Il12b* promoter region, -640 to +17, was amplified using primers: 5'-agttcatgctgctatcaatcca-3' and 5'-cacccactgttccttctgct-3', and cloned into pGEM-T easy vector (Promega). Plasmid construct was double-restriction digested with ApaI/SacI to release the promoter fragment. The *Il6* promoter region -1578 to +31 was amplified by primers: 5'-attctcgagattttaatctactctaatcgcctg-3' and 5' –cccaagcttagcggtttctggaattgactat-3', using genomic DNA as template and cloned into pGL2 promoter vector (Promega). The *IL6* promoter fragment was released from the plasmid DNAs by PstI and *HindIII* double digestion.

2.13.3 DNA 3'-end biotin labeling

The purified promoter DNAs were labeled with biotin using 3' end DNA labeling kit (Thermo Fisher Scientific, Waltham, MA, USA, No. 89818), according to the manufacturer's instructions. Labeled DNAs were further purified using Wizard SV Gel and PCR clean-up kit (Promega).

2.13.4 Pull down assay for *Il12b* and *Il6* promoter-binding nuclear proteins

For promoter pulldown, 100 fmol of biotin-labeled DNA was added to the pre-mixture to make up a 100 μl binding reaction volume using 10 mM Tris-HCl, pH 7.5, 50 mM KCl, 1 mM DTT, 12.5 % glycerol, 0.05 % NP-40, 5 μg polydI:dC (Roche), 25 μl NE (~40 μg protein). The binding mixtures were incubated at 25 °C for 25-30 min, chilled on ice, and transferred to streptavidin-conjugated magnetic Dynabeads M-280 (Life Technologies Inc.) that were pre-washed thoroughly with wash buffer (1x binding buffer with

12.5 % glycerol, 0.05 % NP-40, 2 mM $MgCl_2$). The suspensions were agitated at 4 °C for 3 h. Thereafter a magnetic stand (Life Technologies Inc.) was employed to separate the beads from the supernatants. The beads were immediately washed once by re-suspension in wash buffer, and re-suspended in SDS-PAGE loading buffer and boiled at 100 °C for 5 min. Protein samples derived from 10 µl binding reaction (10 fmol, 4 µg Nucelar extract) were subjected to Western analysis to detect the presence of the transcription factors of interest.

2.14 Gene specific knockdown by siRNA transfection

For RNAi experiments, J774 cells were seeded at $0.4x10^6$/ml and transfected with a scramble control (Darmacon) or ON-TARGETplus SMARTpool siRNA (Darmacon) against mouse *Stat1* (50 nM), *Junb* (50 nM), *Irf1* (50 nM) or/and *Cebpb* (50 nM) using X-tremeGENE HP DNA Transfection Reagent (Roche) for 24 h until subsequent PAMP stimulation. The X-tremeGene HP used per 100 µl transfection mix was 8 µl.

2.15 ELISA

Cell supernatants were collected 12 h after PAMP stimulation and stored at -80°C until assay. The levels of IL6 and IL12p40 were measured using mouse ELISA kits (Beckton Dickinson, BD OptEIA™) according to the manufacturer's protocol.

2.16 Phosphatase treatment

In order to distinguish the two bands of JunB we observed, we treat the nuclear extract sample from J774 stimulated with IR for 5 h with phosphatase. For phosphatase treatment, 5 μg of nuclear extract was incubated with 0, 0.2, 2 and 20 Units of phosphatase (CIAP, Promega) for 1 h at 37 °C and then analyzed by Western blot.

2.17 Chemical inhibition of MAPK and JAK signaling study

The respective inhibitors for JNK (SP600125), ERK (U0126) and p38 (SB203580) were all purchased from Cell Signaling Technology (Boston, MA, USA). Cells were first treated with 10 μM of each of the inhibitors for 50 min, followed by the corresponding PAMP stimulation. The inhibitor for JAK1/2, Ruxolitinib (INCB018424), was purchased from Selleckchem (Boston, MA, USA). 1 μM of the Ruxolitinib was added to the cell for 1 h, followed by PAMP treatment. The cell culture medium was not changed after inhibitor treatment in order to maintain the inhibition throughout the PAMP stimulation.

2.18 Statistical analysis

Data are represented as means and standard error of at least three independent experiments. Statistically significant differences between treatments were analyzed with two-tailed Student's t-test. A value of $p<0.05$ was considered significant (*) and $p<0.01$ very significant (**).

CHAPTER III

RESULTS

CHAPTER III. RESULTS

3.1 Synergy is especially profound for secondary response cytokines, *Il6* and *Il12b*.

Combinatorial stimulations with MyD88-activating and TRIF-activating TLR ligands have been shown to induce synergistic levels of cytokines like IL10, IL6 and IL12 in macrophages [57]. To investigate whether cytokine synergy is a prevalent event in activated macrophages, we compared the mRNA levels of 18 major chemokines and cytokines that are known to be produced by macrophages, in mouse BMDMs under single (poly (I:C), I or R848, R) or combinatorial stimulation(IR) over a time course of 4, 8, 16, 24 h (**Figure 3.1A**).

Csf2, *Ifnb1*, *Lif*, *Il23a* and *Il12a* were barely detected in macrophages. Together with IL12p40 (encoded by gene *Il12b*), IL23p19 (encoded by gene *Il23a*) and IL12p35 (Encoded by gene *Il12a*) form cytokine IL23 and IL12 respectively. Although *Il12a* and *Il23a* are highly expressed in DCs, we did not observe their abundance in macrophages. This appears to be consistent with different roles that DC and macrophage play in the immune system [64]. DC is the key player that bridges innate and adaptive immunity by inducing Th1 response, where IL12 is a major mediator in the process. However, macrophages are known to produce more *Il12b* than *Il12a* or *Il23a*, where *Il12b* probably acts as a macrophage chemoattractant. It has been shown that Il12p40 homodimer, IL12 p80, recruits macrophages to the airways to protect the host from respiratory tract viral infection [65]. Thus macrophages induce high amounts of Il12p40 to enhance innate immune response rather than binding with Il12p35 to drive Th1 response.

On the whole, we found that R848 induced much higher mRNA levels for most of the cytokines and chemokines, except *Ccl5* and *Cxcl10*, which were mainly induced by poly(I:C), and this is in agreement with a previous report [66]. Upon combinatorial PAMP stimulation, most of the cytokine gene expression is enhanced to a certain extent. While chemokine genes exhibit fast temporal responses, the mRNA levels for the majority of other cytokine genes peaked at 8 h. We further checked the fold-synergy of cytokine expression at 8 h by dividing co-stimulation induced cytokine levels by the sum of single stimulation induced-cytokine levels (**Figure 3.1B**). Amongst these, secondary response pro-inflammatory cytokine genes, *Il6* and *Il12b,* which requires newly synthesized protein for their induction [67], and anti-inflammatory cytokine gene, *Il10*, elicited the most significant synergy of above 5-fold. The remaining genes showed only moderate to negligible transcription synergy.

Thus, the observed synergistic induction in macrophages appears confined to pro-inflammatory cytokines, *Il6* and *Il12b*, as well as anti-inflammatory *Il10*. Being anti-inflammatory, IL10 is influenced by other cytokines in a complex feedback manner[68]. Furthermore, a variety of diseases are related to uncontrolled overexpression of pro-inflammatory cytokines. Thus, in this thesis, we focused on investigating the mechanism of synergy of secondary response pro-inflammatory cytokine genes, namely *Il6* and *Il12b*.

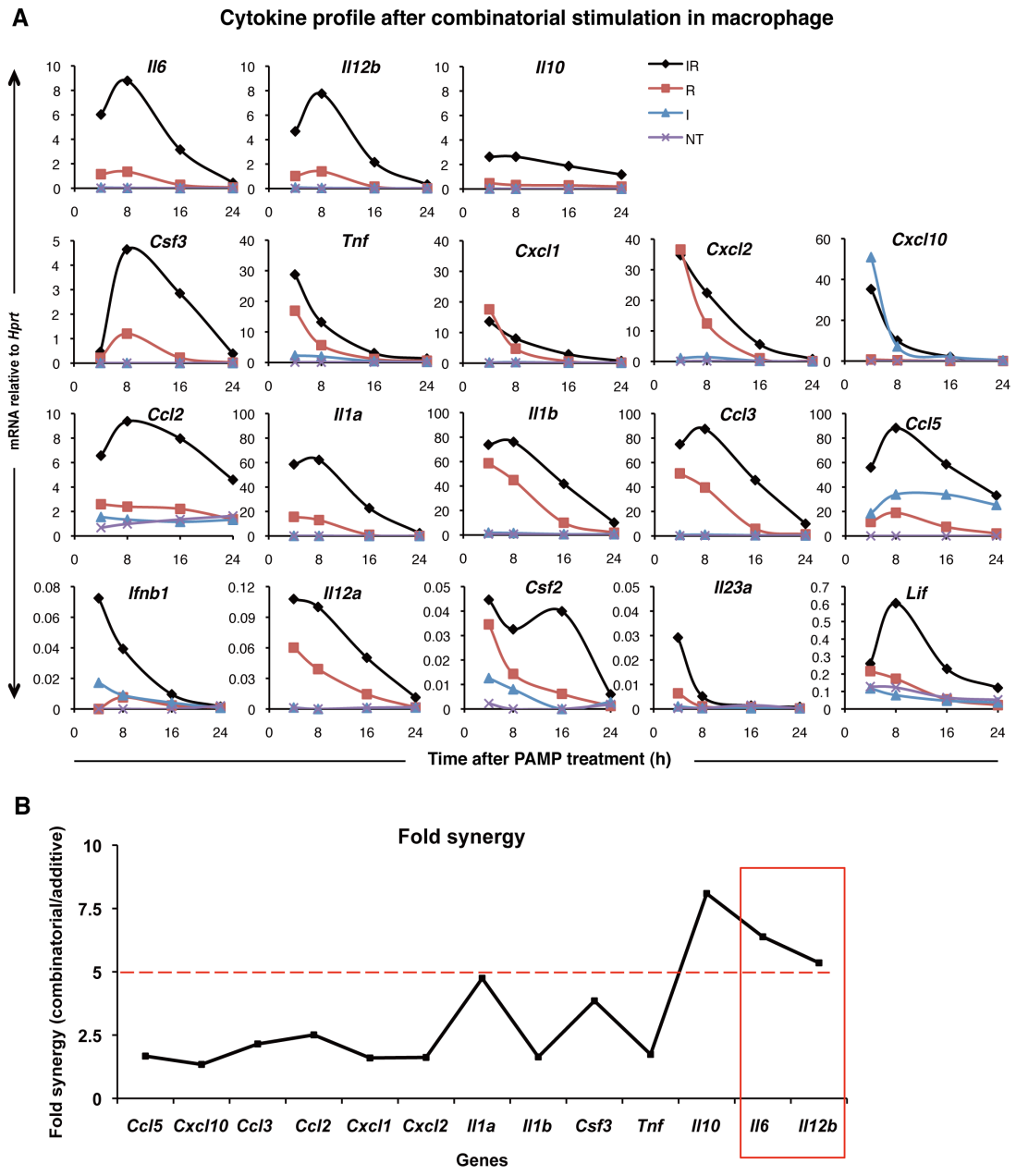

Figure 3.1 Analysis of the cytokine profile after R848 and poly (I:C) stimulation. A. Bone marrow derived macrophages (BMDMs) were stimulated simultaneously by adding poly(I:C) (I, 10 μg/ml) and R848 (R, 25 ng/ml) for 4, 8, 16 and 24 h (indicated as "combinatorial" with black line), control for combinatorial is the levels of cytokine produced by poly(I:C) single treatment (blue line) and R848 single treatment (red line) and no treatment (NT, purple line), each for 4, 8, 16 and 24 h. Cytokine mRNAs were measured by Quantigene plex 2.0 assay. All the values are relative to *Hprt*. **b.** Fold synergy of cytokine expression 8 h after PAMP stimulation was calculated, when majority of the cytokines peaked. Fold synergy was calculated as the ratio of the amount of cytokine mRNA produced by the co-stimulation to the sum of single stimulations by I and R. *Il6* and *Il12b* (red box) above the 5-fold synergy (dashed line) are the two pro-inflammatory cytokines focused in this study.

3.2 The magnitude of synergistic production of *Il6* and *Il12b* induced by combinatorial TLR activation depends on time interval and sequential order of two PAMP stimulations.

We then checked the kinetic profiles of *Il6* and *Il12b* expressions after treatments with either poly(I:C) (I) or R848 (R) or combinatorial stimulation, over different time intervals and orders of stimulations **(Figure 3.2A)**. BMDMs were treated with the first PAMP for 0, 8, 24 h followed by the second PAMP for 4, 8, 16, 24 h before realtime-PCR analysis (**Figure 3.2B** solid lines). The control for combinatorial stimulation was the sum of single PAMP stimulations (Figure 3.2B dashed lines); taking I8R8 (treatment with I for 8 h followed by R for 8 h) for an example, the single stimulation control for it is poly (I:C) single stimulation for 16 h and R848 single stimulation for 8 h, hence annotated as I16 and R8, respectively (Detailed description of experimental strategies could be found in Chapter II section 2.4 at page 25). Compared to single stimulation with either I or R (Figure 3.2B right panel), cytokine expression was greatly upregulated after combinatorial (IR) stimulation, and the enhancement is more than the sum of single stimulations (Figure 3.2B left and middle panel). Co-stimulation with IR was found to enhance both *Il6* and *Il12b* expression by more than 5-folds. Interestingly, cytokine synergy by co-stimulation was further boosted when poly(I:C) was given before R848 treatment. However, enhanced synergy was not observed in the converse treatment regime (R first followed by I), indicating that the order of PAMP treatment has a significant effect on cytokine synergy. Different time intervals between poly(I:C) and R848 treatment would also have an effect on synergy (**Figure 3.2B and C**). We tested 0, 4, 8, 12, 16 and 24 h time intervals between first poly (I:C) and second R848 stimulation in figure

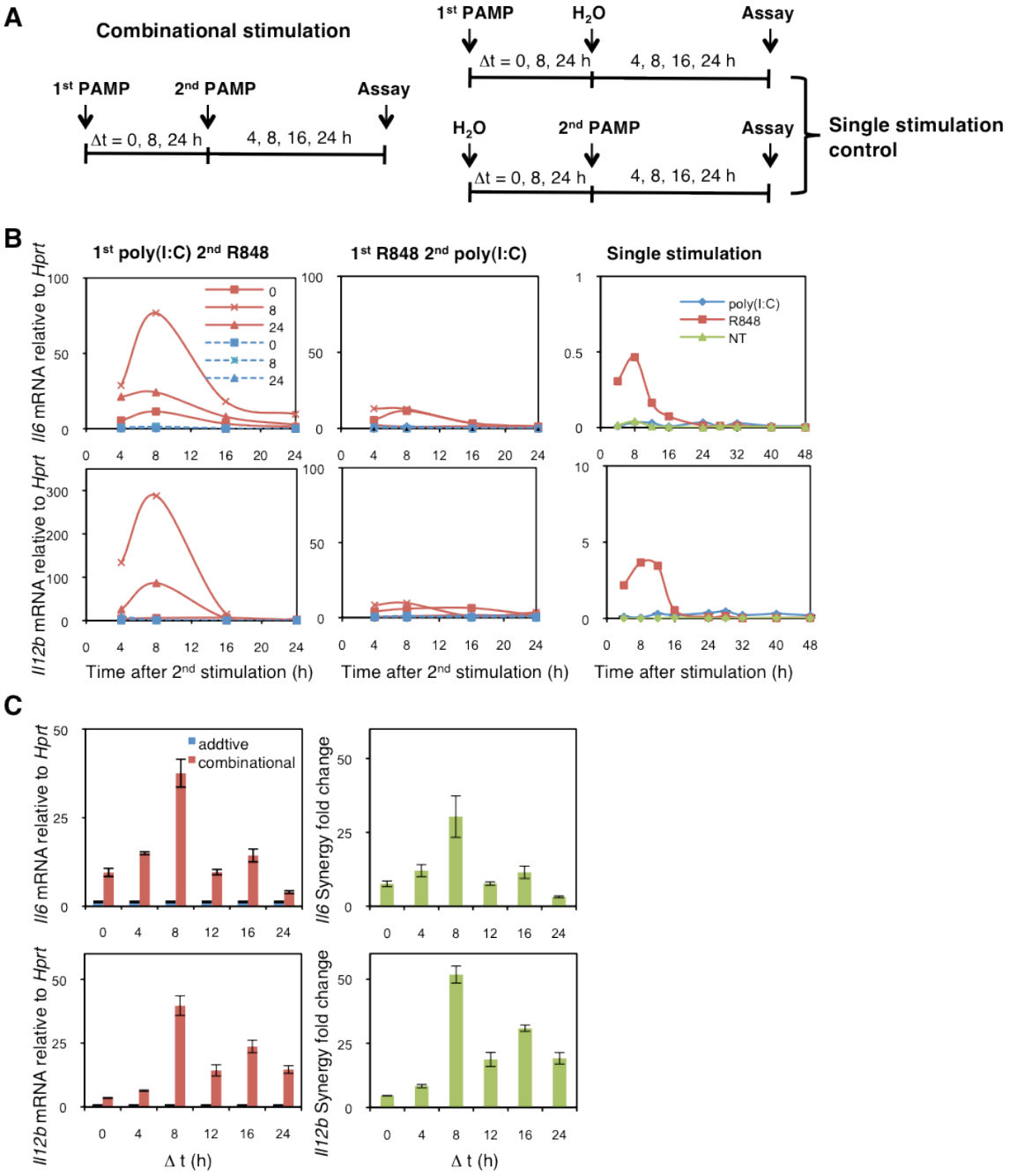

Figure 3.2. Characterization of *Il6* and *Il12b* expression profile after TLR3 and TLR7 co-activation with different time interval and order. A. Experimental design. BMDMs were treated with 1st PAMP for 0, 8, 24 h followed by 2nd PAMP for 4, 8, 16, 24 h. The control for the combinatorial stimulation is the single PAMP stimulation. Take I8R8 for example, the single control for it are poly (I:C) stimulation for 16 h and R848 stimulation for 8 h. **B.** *Il6* and *Il12b* synergy is dependent on the order and time interval between poly (I:C) and R848 treatments. Bone marrow derived macrophages (BMDMs) were treated with 10 μg/ml poly(I:C) followed by 25 ng/ml R848 (left panel) or R848 followed by poly(I:C) (middle panel) for 4, 8, 16, 24 h, or single stimulation for 4, 8, 12, 16, 24, 28, 32, 40, 48 h as control(right panel, NT stands for no treatment). Time intervals between poly(I:C) and R848

treatment are 0(■), 8(×), 24(Δ) h. Solid lines are combinatorial stimulation, dashed lines indicate additive value of single stimulation control for combinatorial stimulation as described in A. *Il6* and *Il12b* mRNA were analyzed with Real-Time PCR and normalized with *Hprt*. Data are representative of three independent experiments. **C.** 8-h pretreatment with poly(I:C) elicited the strongest cytokine synergy. BMDMs were treated with 10 μg/ml poly(I:C) for 0, 4, 8, 12, 16, 24 h followed by 25 ng/ml R848 stimulation for 8 h. *Il6* and *Il12b* mRNA were analyzed with RT-PCR and normalized to *Hprt.* Data are presented as means ± SEM of three individual experiments.

3.3 The computational modeling reveals that MAPK and JAK-STAT pathways are important for cytokine synergy.

The above observation of time interval and order-dependent synergy effect suggests complex dynamic interactions of the various intracellular molecules and pathways of TLR3-TLR7 signaling network. To understand how TLR3-TLR7 crosstalk to regulate cytokine expression from a global and dynamic perspective, we required a systems approach to incorporate the known knowledge of TLR3-TLR7 signaling network with empirical data of kinetics of certain components in the network to construct a dynamic model for the whole network. With such a model, we aimed to (1) understand which part of the network is most critical for the signaling outcome (in our case the outcome is cytokine expression), (2) predict potential mechanisms of TLR3-TLR7 crosstalk at the signaling level, (3) explain why synergy is dependent on time interval and order of treatment, and (4) how the dynamic network controls its behavior.

We therefore collaborated with Prof P. S. Thiagarajan from the School of Computing, NUS, to build a model to better understand the global dynamics of TLR3-TLR7 crosstalk and how cytokine synergy might occur at the signaling level.

3.3.1 Model construction – computational modeling of conjectured signaling crosstalk between TLR3-TLR7 pathways

The computational model construction was based on the known signaling pathways downstream of TLR3 and TLR7 receptors (see Figure 1.3) and our own conjectured crosstalk signaling mechanisms between TLR3-TLR7 pathways. The description of the main features of TLR3 and TLR7 pathways can be found in the Introduction section 1.5.2.

Our hypothesized mechanisms were based on the observation in Figure 3.1 and 3.2 that R848 mediated TLR7-MyD88 pathway activation induces cytokine production mildly. TLR3-TRIF pathway alone produces only negligible level of cytokines, but it greatly enhances TLR7-MyD88 induced cytokine expression. This indicated that factors activated specifically by TLR3-TRIF might collaborate with the TLR7-MyD88 pathway [57]. The key features of the TRIF pathway, which distinguishes it from the MyD88 pathway, involve the activation of IRF3 and production of type I IFN [5,69]. Based on this, we postulated the following IRF3- and type I IFN- related mechanisms that might explain cytokine synergy: **(i)** Activated IRF3 is known to bind to NF-κB and AP-1 to form an enhanceosome in the nucleus [70]. Hence the coordinated activation of the three transcription factors after poly(I:C) and R848 co-stimulation might enhance the transcription of *Il6* and *Il12b*. In addition, IRF3 could bind to the Interferon-Stimulated Response Element (ISRE) of the gene promoter and might induce other yet-to-be determined cytokine regulatory genes, which might be involved in cytokine expression (indicated as IRF3 target genes in **Figure 3.3**) [69]. **(ii)** Among the IRF3-induced genes, type I interferon (*Ifn*) is the most functionally prominent.

Secreted type I IFN protein binds to type I IFN receptor on the cell surface and activates its associated Janus activated kinases (JAKs) tyrosine kinase 2 (TYK2) and JAK1. Activation of JAKs leads to tyrosine phosphorylation of STAT2 and STAT1, inducing the formation of STAT1–STAT2–IRF9 complexes, which are known as ISGF3 (IFN-stimulated gene factor 3) complexes. These complexes translocate to the nucleus and initiate transcription of genes with ISREs (indicated as ISGF3 target genes in Figure 3.3). Genes activated by ISGF3, such as IRF1, might be involved in cytokine synergy [71]. **(iii)** In addition, type I IFN could activate NF-κB p52 through NF-κB inducing kinase (NIK) and the tumor necrosis factor receptor-associated factor-2 (TRAF2), which might regulate cytokine expression [72]. **(iv)** Furthermore, type I IFN could activate PI-3K-Akt pathway, leading to the activation of NF-κB [73]. **(v)** Finally, we also modeled the anti-inflammatory cytokine IL-10 mediated feedback. Activated ERK1/2 and p38 phosphorylate mitogen- and stress-activated protein kinase-1/2 (MSK1/2), which promotes the transcription of *Il10*[74]. ISGF3 target genes might also upregulate IL10 production [75]. Secreted IL10 then binds to the IL-10R, which promotes the activation of JAK1 and Tyk2, resulting in the phosphorylation of STAT3. STAT3 is required for the repressive effects of IL-10 on TLR-mediated cytokine[76,77].

A complete TLR3-TLR7 signaling network structure with both the known signaling pathways and conjectured crosstalk mechanisms is schematically summarized in **Figure 3.3**. The network was then converted into a system of ordinary differential equations (ODEs) by our collaborators (**Figure 3.4**). Briefly, biological processes including protein association,

degradation and translocation were modeled with mass action kinetics and processes such as activation and inhibition were modeled with Michaelis-Menten kinetics. Gene transcription is modeled using the equation proposed by Kuttykrishnan et al (2010) [78]. The resulting model consists of 97 species (molecules), 128 equations and 147 parameters (rate constants of the equations) with 120 unknowns.

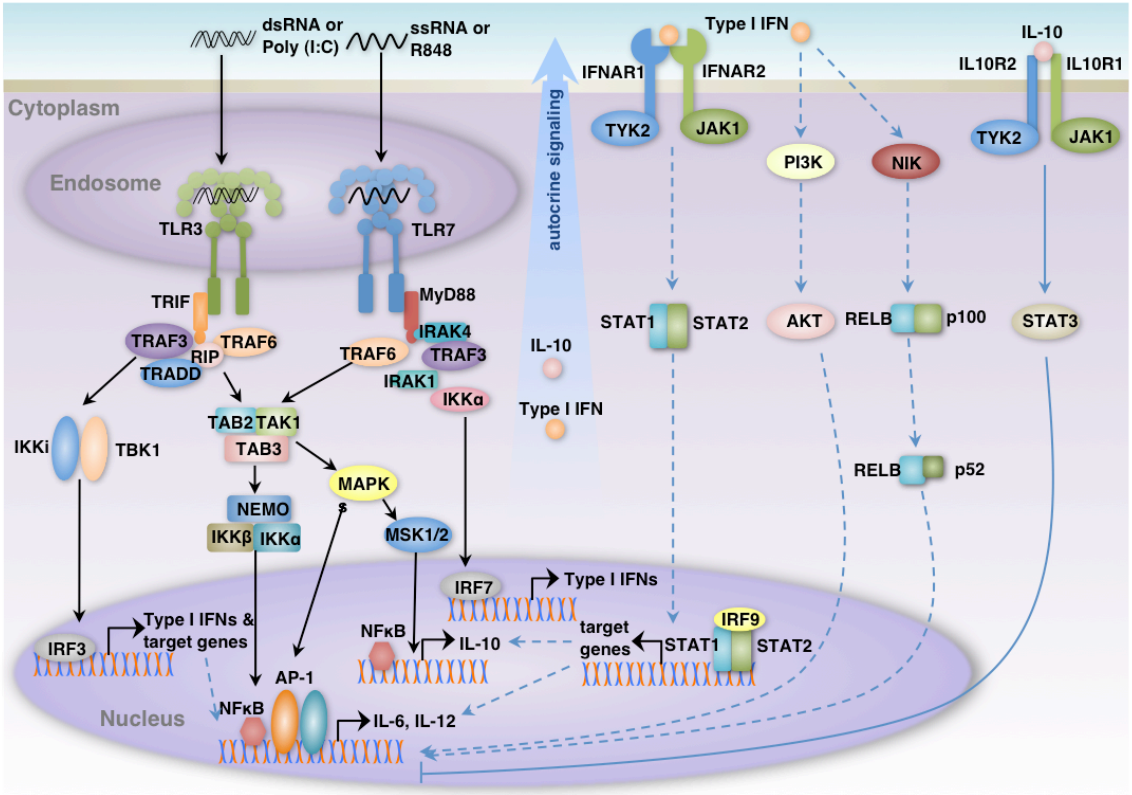

Figure 3.3. Schematic representation of TLR3 and TLR7 signaling pathways. TLR3 recognizes dsRNA (and analogues such as poly(I:C)) derived from viruses or virus-infected cells and induces antiviral immune response by promoting the expression of type I IFNs and inflammatory cytokines (e.g. IL-6 and IL-12p40), via the TRIF-dependent pathway. TLR7 recognizes ssRNA (and analogues such as R848) and induces the production of type I IFNs and cytokines via the MyD88-dependent pathway. IRF3 and IRF7 activated by TLR3 and TLR7 pathways respectively lead to the production of type I IFNs. NF-kB and AP-1 activated by both pathways lead to the production of inflammatory cytokines. In this model, the known signaling pathways downstream of TLR3 and TLR7 are indicated with solid black lines. The conjectured crosstalk mechanisms were indicated with dashed blue lines.

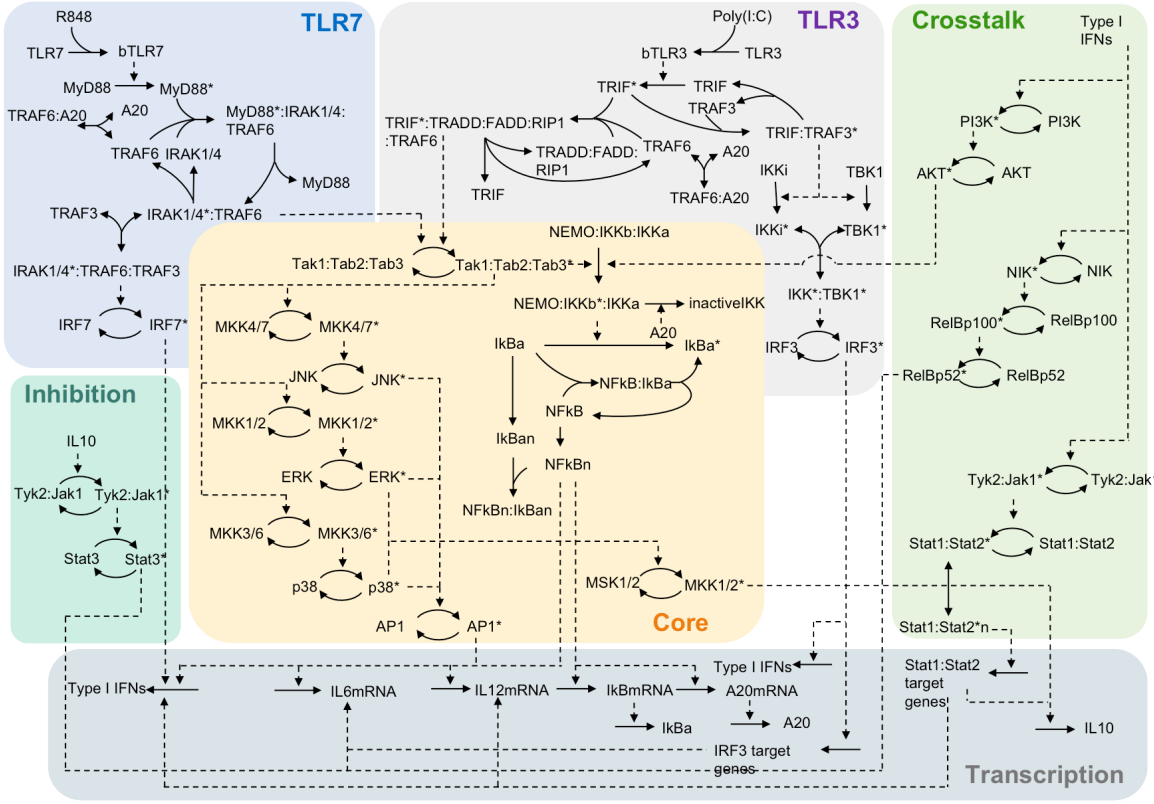

Figure 3.4. Reaction network diagram of the mathematical model. Complexes are denoted by the names of their components, separated by a ‘‘:’’. Single-headed solid arrows denote irreversible reactions and double-headed arrows denote reversible reactions. Dotted arrows indicate enzymatic reactions.

3.3.2. Model training and validation – the calibrated model has excellent descriptive and predictive properties

Using our empirical data, the computational model training and *in silico* validation were performed (Prof Thiagu’s team; Bing L & Qian L et al., manuscript in preparation). The values of 27 rate constants which correspond to the NFκB pathway were adapted from Lipniacki et al. (2004) [79]. To estimate the remaining 120 unknown parameters, empirical time course data for *Il6* mRNA and *Il12b* mRNA (Figure 3.2) and several major players in cytokine regulation including phosphorylated ERK, p38, JNK and IκBα (this was measured in collaboration with our previous lab member and published in

[57]) were used. The following empirical data were used as training data: (1) The expression level of *Il6* mRNA and *Il12b* mRNA measured at 10 time points (0, 4, 8, 12, 16, 24, 28, 32, 40, 48 h) under conditions of I, R single stimulation, and at 4 h, 8 h, 16 h and 24 h after second stimulation of IR (simultaneous poly(I:C) and R848 stimulation) and I8R(poly(I:C) stimulation with 8 hour interval followed by R848 stimulation); (2) The concentrations of activated ERK, activated p38, phosphorylated JNK, phosphorylated IκBα measured at 7 time points (5, 15, 30 min, 1, 4, 8, 12 h) after the stimulation with I, R, IR and I8R. We used the *Il6* and *Il12b* time course after I24R (poly(I:C) pretreatment for 24 h followed by R848 stimulation), R8I (R848 stimulation for 8 h followed by poly (I:C) stimulation) and R24I (R848 stimautlion for 8 h followed by poly(I:C) stimulation) stimulation as the test data for model validation. A statistical model checking (SMC)-based framework developed earlier [80] by our collaborator was used for parameter estimation.

Figure 3.5 A shows that the model simulation profiles generated using the estimated parameters (blue lines) fit well with the experimental time course data (red dots) for most of the cases. Although data fitting for the active IκBα in Figure 3.5A fourth panel (I8R) is not as tight as others, the simulation curve still captured the correct qualitative trend and reproduced the two rounds of activation behaviors. **Figure 3.5B** shows the comparison of the *Il12b* and *Il6* expression data with the simulated profiles. The model successfully reproduced the time- and order- dependent synergy of cytokine production and its prediction matches not only the training data (R, I, IR, I8R) but also the test data (I24R, R8I, R24I). This shows that our model is not over-fitted and thus

enabled us to perform subsequent *in silico* experiments using the calibrated model.

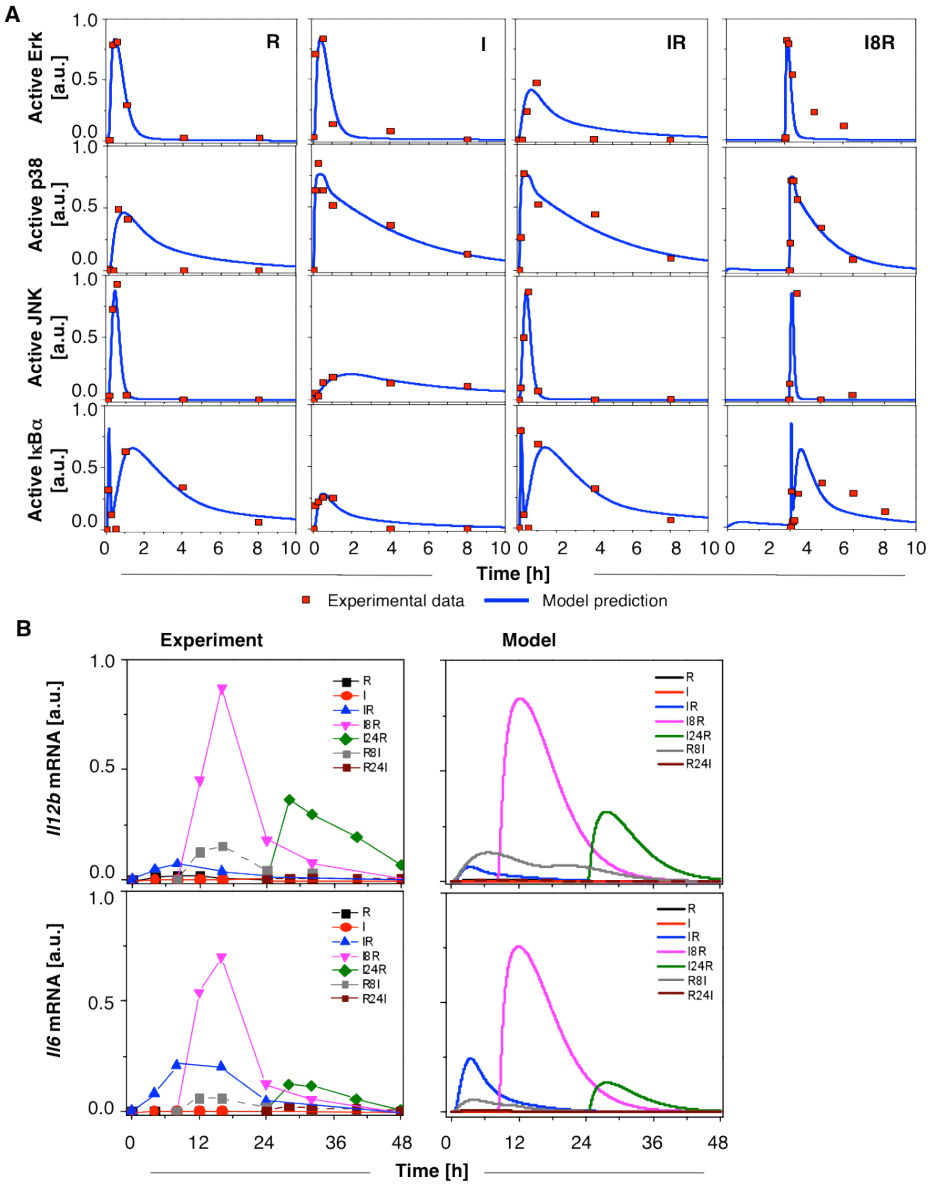

Figure 3.5. Model training and validation. A. Experimental and simulated protein dynamics of the TLR3-TLR7 pathway. The time profiles of activated ERK, p38, JNK, and IkBa under the following four conditions were simulated using estimated parameters and compared against the experimental data: R848 single stimulation, poly(I:C) single stimulation, poly(I:C) and R848 combinatorial stimulation with 0 h time interval, poly(I:C) and R848 combinatorial stimulation with 8 h time interval. Blue curves depict the model simulation results and red dots display experimental data. **B.** Model predictions and experimental validation of the synergistic cytokine production. The simulated time profiles of *Il6* and *Il12b* expression levels under various conditions (right panels) reconcile the observed (left panel) time-dependent synergistic effect induced by the combinatorial TLR3-TLR7 activation. On the left panels, the experimental data are connected by lines to guide the eye.

3.3.3 Parameter sensitivities identified crucial species and reactions for cytokine synergy.

To pinpoint molecules and reactions that are crucial in determining the synergistic cytokine production, we conducted the sensitivity analysis, which is a commonly used analysis technique for assessing the relative importance of model parameters with respect to the model behavior. Here again we used our logic based statistical (SMC) technique [80].

We first carried out the control coefficients-based local sensitivity analysis. In local sensitivity analysis, parameters are varied one at a time to see the effects on model output. We defined the model output as the integrated *Il12b* and *Il6* expression in response to the five stimulation conditions (R, I, IR, I8R, I24R). The computed normalized local sensitivities are summarized in **Figure 3.6A**. The results for single stimulation conditions (R or I) show that TLR7 pathway is more sensitive than TLR3 pathway. TLR3-mediated cytokine production is mainly regulated by IκBα-NFκB, which possesses high sensitivities under all five conditions. In contrast, AP-1, another key transcription factor regulating cytokine production, is sensitive only under conditions that involve TLR7 activation (R, IR, I8R, and I24R). Mkk1/2, Mkk3/6, Mkk/4/7, ERK, p38, and JNK have the similar sensitivity pattern as their downstream AP-1, suggesting that MAPK pathways play a crucial role in coupling the upstream TLR3 and TLR7 regulatory modules to the downstream nuclear module, especially under the combinatorial stimulation conditions. Although three MAPK pathways can activate AP-1 in parallel, the sensitivities of species on the JNK pathway are positive while the sensitivities of species on the ERK and p38 pathways are negative. This implies the distinct roles of JNK, ERK and p38 in regulating cytokine synergy. Together with the highly

negative sensitivities that MSK1/2 and Stat3 display, it also suggests the importance of STAT3 pathway in inhibiting cytokine production and maintaining homeostasis. Interestingly, TYK2-JAK1 and STAT1-STAT2 expressed very strong controls over the system response while the sensitivities of species from other conjectured mechanisms, the AKT pathway and NIK pathway, are low, which implies the importance of JAK-STAT pathway among all the potential crosstalk mechanisms.

We next computed global sensitivities for kinetic parameters using a multi-parametric sensitivity analysis (MPSA) method based on our SMC method. In global sensitivity analysis, all parameters are varied simultaneously, and the effects on output are assessed. The model output for global sensitivity analysis is defined as integrated *Il12b* and *Il6* expression under I8R stimulation. The results are shown in **Figure 3.6B**. A set of 32 kinetic parameters with high sensitivities (> 0.1) are colored in blue and their functions are classified in **Figure 3.6C**. Strong controls over the cytokine production are distributed among the parameters associated with the production of *Il12b, Il16* and type I IFN, MAPKs signaling cascade, JAK-STAT signaling cascade, and IL10-STAT3 signaling cascade. The two parameters (k_{72} and k_{73}) with the highest sensitivities are associated with the transcription of *Il12b* and degradation of *Il12b* and *Il16* mRNA. This is not surprising as these two parameters directly determine the production rate of *Il12b* and *Il16* mRNA. Eleven sensitive parameters are associated with reactions along the MAPK pathway, which leads to the activation of AP-1. This result is consistent with the local sensitivity analysis, which suggests the important role of MAPK pathways in cytokine expression. In addition, the

sensitive reactions associated with IL10-STAT3 pathway highlights its important inhibitory role, compared to other inhibitors in the system, such as A20. More importantly, many critical reactions are involved in Type I IFN transcription and the activation of JAK1-STAT1/2 pathway, which can be connected together by our hypothesized pathway type I IFN→JAK1-STAT1/2→cytokines. Thus, a crucial insight that emerges from these findings is that the time-dependent cytokine synergy we observed experimentally is most likely induced by the JAK1-STAT1/2 mediated crosstalk mechanism

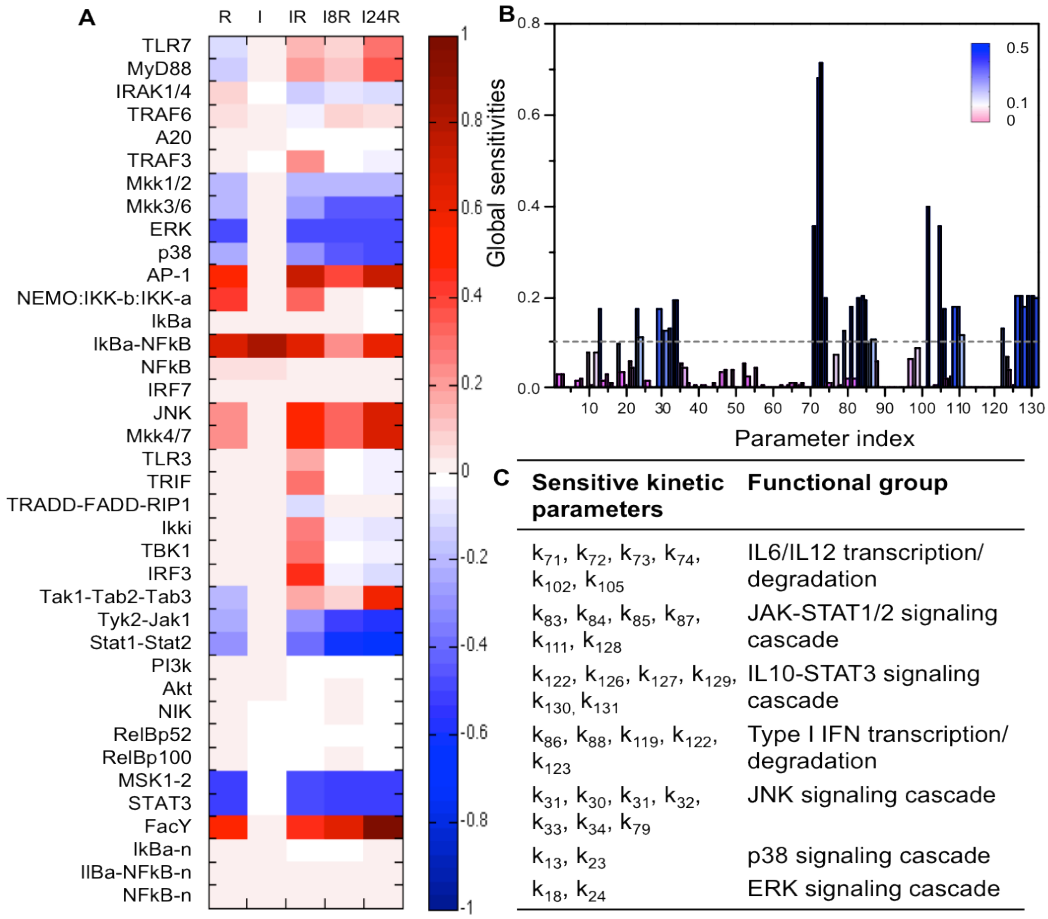

Sensitive kinetic parameters	Functional group
k_{71}, k_{72}, k_{73}, k_{74}, k_{102}, k_{105}	IL6/IL12 transcription/ degradation
k_{83}, k_{84}, k_{85}, k_{87}, k_{111}, k_{128}	JAK-STAT1/2 signaling cascade
k_{122}, k_{126}, k_{127}, k_{129}, k_{130}, k_{131}	IL10-STAT3 signaling cascade
k_{86}, k_{88}, k_{119}, k_{122}, k_{123}	Type I IFN transcription/ degradation
k_{31}, k_{30}, k_{31}, k_{32}, k_{33}, k_{34}, k_{79}	JNK signaling cascade
k_{13}, k_{23}	p38 signaling cascade
k_{18}, k_{24}	ERK signaling cascade

Figure 3.6. Parameter sensitivities. A. Local sensitivities (control coefficients) of the initial protein concentrations (listed along the ordinate) to the integrated response of the *Il12b* production under R, I, IR, I8R and I24R conditions. Dark colors (*blue* or *red*) refer to components that strongly influence the model outcome, in opposite directions (see *color code* on the right). **B.** Global sensitivities calculated according to the SMC-MPSA method. Sensitive parameters (that strongly influence the observed behavior) are shown by the peaks, colored *dark blue*. Robust parameters (the variations of

which have little effect of the model dynamics) are colored *purple*. The highest peaks refer to *Il6* and *Il12b* transcription or degradation rate constants. **C.** Functional classification of 33 kinetic parameters that led to the highest sensitivity peaks (above the *dotted* threshold line in panel **B**).

3.3.4 The time interval between TLR3- and TLR7- activation coordinates cytokine synergy but not type I IFN production.

In addition to the crucial species and reactions we identified in the previous section, the overall expression of both *Il6* and *Il12b* genes are also highly sensitive to the time interval (Δt) between the two PAMP stimulations as illustrated in Figure 3.2C. Here, we simulated the model by increasing Δt from 0 h to 48 h to understand the dependency of the immune response with respect to the time interval (Δt) between TLR3 and TLR7 activations. The predicted effects of Δt on the immune response in terms of *Il6* and *Il12b* expression levels are shown in **Figure 3.7A**. We calculated the peak amplitudes and peak time (starting from R stimulation) of each response curve in Figure 3.7A and plotted them as functions of time (**Figure 3.7B**). With increasing Δt, the peak amplitudes of *Il6* and *Il12b* were raised until the maximal values were reached, and then the expression levels started to drop. The optimal Δt corresponding to the peak amplitude was predicted to be around 7 h for both *Il6* and *Il12b* production. This is consistent with our experimental data shown in Figure 3.2C, which indicates that the optimal Δt is around 8 h. On the other hand, the duration needed to reach the response peaks is relatively robust. The average peak time is around 4 h for *Il12b* and *Il6*.

We also simulated the time profile of type I IFN for different values of Δt under sequential treatments: poly(I:C) followed by R848 (I→R) and R848 followed by poly(I:C) R→I (**Figure 3.7C**). For I→R stimulation, the effects of Δt on type I IFN production is negligible (**Figure 3.7C**, left panel). In contrast,

for R→I stimulation, the type I IFN production curve shifted along with the starting time point of I stimulation and maintained a constant peak amplitude (Figure 3.7C, right panel).

Taken together, these results imply that the type I IFN production is predominantly governed by the TLR3 pathway, while the cytokine production is regulated by a subtle coordination of the TLR3 and TLR7 pathways. Although type I IFN mediates most of the hypothetical crosstalk between TLR3 and TLR7 pathways, it is not sufficient *per se* to explain the dependency of cytokine production to the time interval, Δt alone.

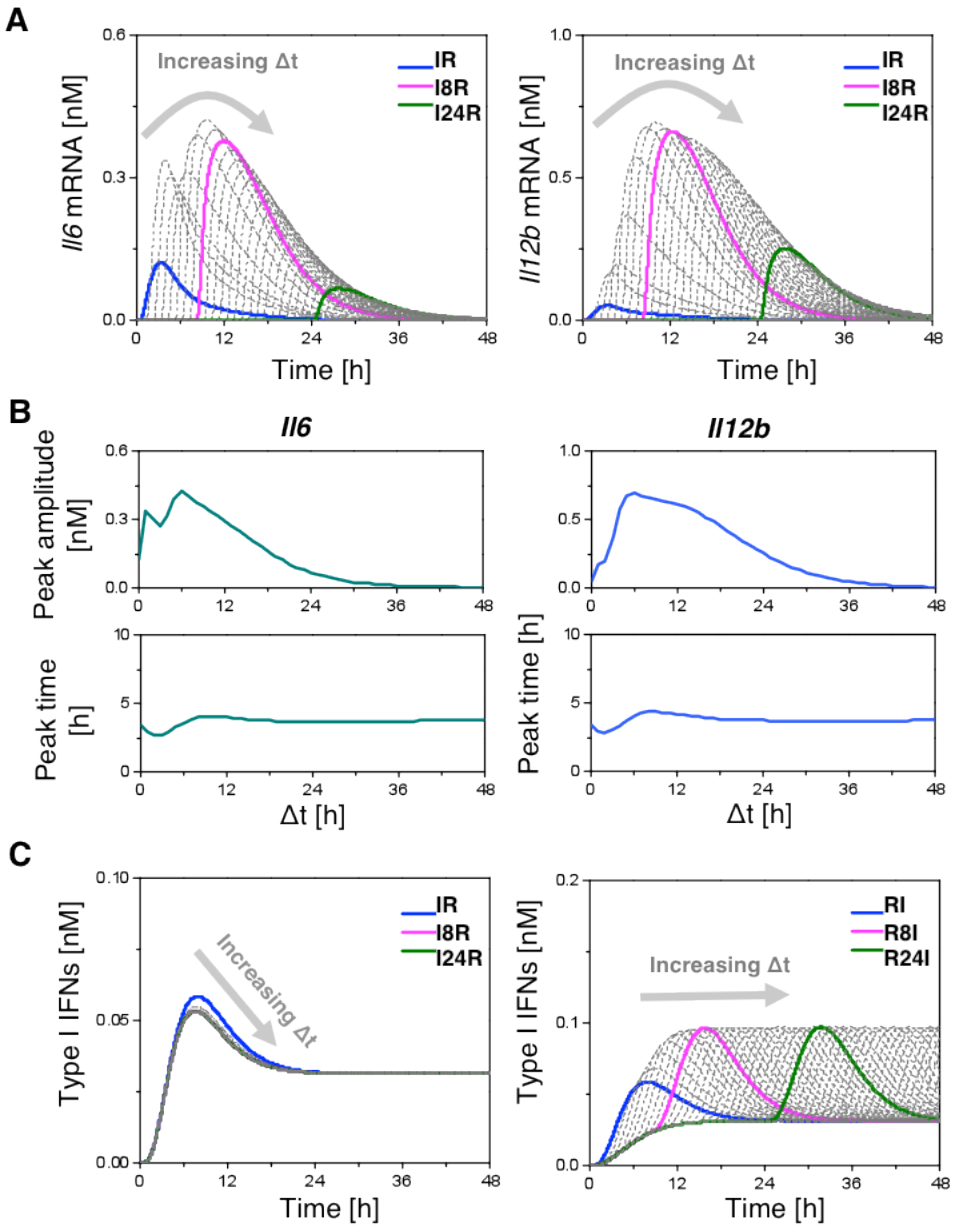

Figure 3.7. Dependency of the immune response on the time interval Δt between the two stimuli. A. Predicted time evolutions of the *Il6* and *Il12b* mRNA expression levels in response to various combinatorial stimulations with a time interval Δt (between the first (I) and second (R) stimulus) varying from 0 h to 48 h. The series of dotted curves represent results for successive Δt values, the ordinate referring to the time elapsed with respect to the application of the first stimulus. Highest cytokine production occurs when the time interval between the two stimuli is Δt ≈ 7 h. The results for Δt = 0 (*blue*), 8 h (*magenta*), and 24 h (*dark green*) are shown by the *thick colored* curves. **B**. Peak amplitude and peak time derived from curves in (**A**). **C**. Predicted expression profiles for type I IFN produced in response to the combinatorial I→R (*left* panel) or R→I (*right* panel) stimuli with Δt ranging from 0 h to 48 h.

3.3.5 *In silico* and empirical knockdown MAPKs revealed distinct roles of JNK, ERK and p38 in regulating cytokine synergy.

The sensitivity analysis highlights the significant role of MAPKs in modulating cytokine synergy. As shown in Figure 3.4, TAK1 complex activates ERK, JNK and p38 pathways in parallel, any of which is capable of triggering the activation of AP-1 and promoting the production of *Il12b* and *Il16* mRNA. At the same time, ERK and p38 also induce the production of the anti-inflammatory cytokine, *Il10*, which leads to the suppression of *Il12b* and *Il16* production through the STAT3-dependent pathway. This forms incoherent type 1 feed-forward loops (I1-FFL), which complicates the roles of ERK and p38. To assess the relative contributions of different MAPK pathways to elicit cytokine synergy, we performed *in silico* knockout of the phosphorylation reaction for each pathway. The predicted time profile of *Il12b* and *Il16* mRNA for Δt ranging from 0 to 48 h are shown in **Figure 3.8A-C**. The results indicate that knocking down 90% activated JNK significantly decreased the cytokine production, indicating its dominant upregulating role amongst the three pathways. In contrast, the knockdown of activated ERK increased cytokine production under various conditions (e.g. IR, I8R, I24R), which might be due to that its inhibitory branch mediated by IL10 and STAT3 are stronger than the strength of the enhancing branch mediated by AP-1. Hence ERK is overall a negative modulator of cytokine synergy. p38 also down-regulated cytokine production under IR condition. However, the negative effect is anticipated to decay when Δt increases. In other words, knocking down p38 did not significantly influence cytokine synergy under conditions such as I8R and I24R.

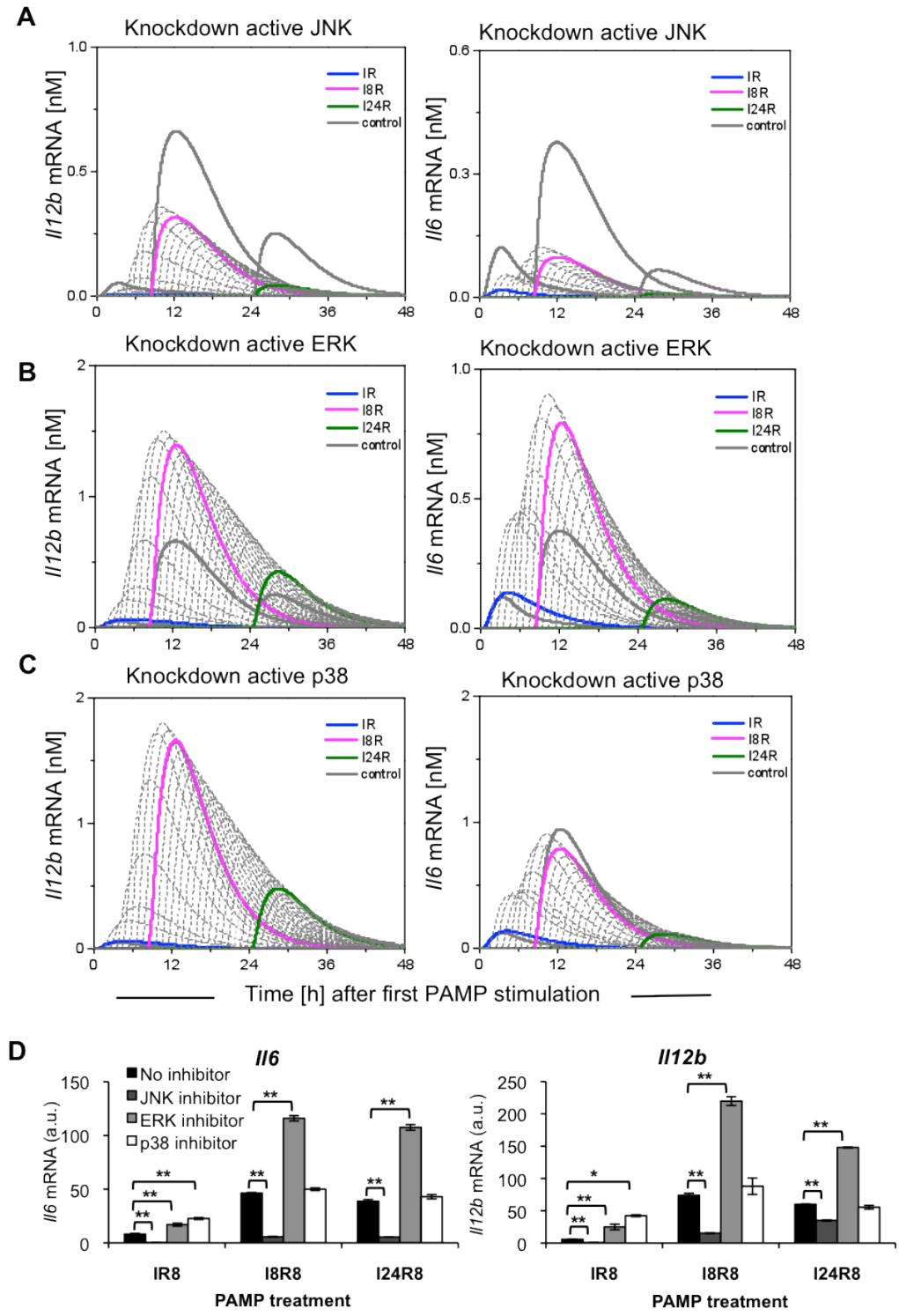

Figure 3.8. Effect of JNK, ERK and p38 inhibition on cytokine production. A-C Time evolution of *Il12b* mRNA (*left*) and *Il6* mRNA (*right*) levels in the absence of JNK (**A**), ERK (**B**) and p38 (**C**) activation. The series of curves refer to different time intervals between the two stimuli. JNK and ERK have opposite effects, i.e. upregulation and downregulation of cytokines, as can be seen from the comparison of the computationally predicted curves for Δt = 0, 8 and 24 (*colored, thick*) with those deduced from control simulations (*thick, gray curves*). The inhibition of p38 has relatively small

effects, if any, on cytokine production. **D**. Experimental verification of computational predictions. BMDMs were treated with 10μM MAPK inhibitors for 50 min followed by IR, I8R or I24R stimulation. After 8 h of R848 stimulation, *Il6* and *Il12b* mRNA were then measured with RT-PCR normalized with *Hprt*. Data are presented as mean values and SEMs obtained from three independent experiments.

To experimentally verify the model predictions, we perturbed the initial amount of JNK, ERK or p38 by incubating the BMDM cells with inhibitors SP600125, U0126 or SB203580 for 50 min. BMDMs were then treated first with poly (I:C) for 0, 8, 24 h followed by R848 for 8 h before realtime-PCR analysis of the mRNA levels. As can be seen in **Figure 3.8D**, for all the three conditions, low JNK decreased cytokine production, while low ERK increased cytokine production. Furthermore, low p38 mediated increase in cytokine production under IR stimulation condition, but did not affect cytokine levels under I8R and I24R condition. These observations are consistent with the simulation results shown in Figure 3.8A-C and confirmed the distinct roles of MAPKs in cytokine synergy.

3.3.6 *In silico* knockdown revealed the role of JAK1-STAT1/2 pathway in cytokine synergy.

The sensitivity analysis results (Figure 3.6) also implied that JAK1-STAT1/2 pathway is the major determinant of cytokine synergy. To confirm this, we carried out *in silico* knockout of the reactions involved in each of the four hypothetical mechanisms discussed earlier, namely the: (i) IRF3 mechanism, (ii) AKT mechanism, (iii) NIK mechanism, and (iv) JAK1-STAT1/2 mechanism. The simulation profiles of *Il12b* mRNA in response to the knockout shows that only the knockout of STAT1-STAT2 was able to

significantly reduce the cytokine synergy (**Figure 3.9**). Taken together, these results demonstrated the essential role of JAK1-STAT1/2 pathway in mediating the cytokine synergy, which is consistent with the parameter sensitivity results.

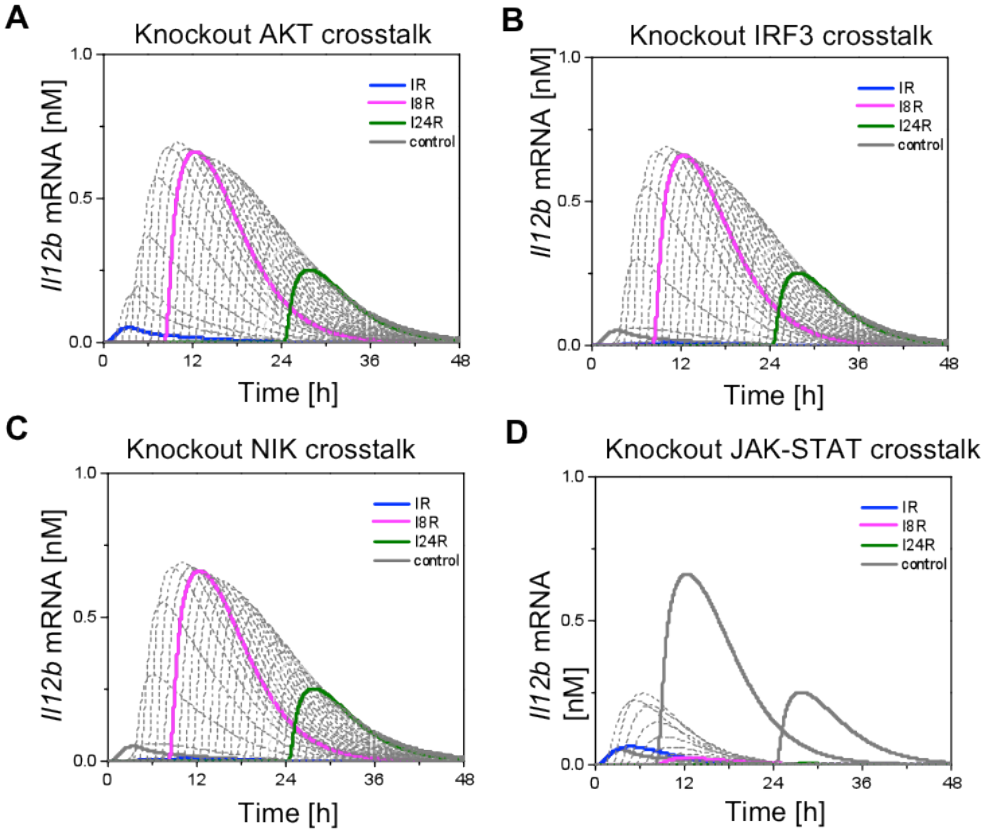

Figure 3.9. Knockout simulations highlight the significance of JAK-STAT pathway in triggering synergistic cytokine production. Simulation profiles of *Il12b* mRNA (**A**) in the absence of Akt activation reaction, **(B)** without crosstalk mechanism induced by IRF3, **(C)** in the absence of NIK activation, and **(D)** in the absence of STAT1-STAT2 activation.

3.3.7 *In silico* and Empirical knockdown of STAT1 revealed a complex regulatory role of JAK-STAT pathway and an incoherent feed-forward loop.

Similar to ERK and p38, JAK-STAT1/2 pathway mediates an I1-FFL since its target genes not only directly regulate the production of *Il12b* and *Il16* but also enhance the production of *Il10,* which inhibit the production of

Il12b and *Il16*. In previous section, we showed that knockout STAT1 would lead to a significant decrease of cytokine synergy (Figure 3.9D). However, the negative local sensitivity values of STAT1-STAT2 complex (Figure 3.6A) suggest that a mild decrease of STAT1 initial concentration will induce an increase of cytokine production. The opposite roles of STAT1 in cytokine synergy imply that the STAT1-mediated I1-FFL (**Figure 3.10A**) might lead to the generation of non-monotonic input-output relations, i.e. *biphasic response* [81,82]. To verify this, we simulated *Il12b* levels 8 h after the second PAMP challenge under IR, I8R and I24R conditions with the initial concentration of STAT1 ranging from 0.01 to 10 nM. The results summarized in **Figure 3.10B** show that under IR stimulation, knocking down of *Stat1* increases cytokine expression. Biphasic responses could be observed under I8R and I24R stimulation. Reducing STAT1 concentration around normal concentration will first lead to an increase and then a decrease of the cytokine production.

To confirm the role of STAT1 predicted by our model, we performed *in vitro Stat1* knockdown experiments with mouse macrophage cell line, J744 cells. Cells were transfected with *Stat1* sequence-specific siRNA or non-target control siRNA. **Figure 3.11A** shows that the effect of knocking down *Stat1* was substantial. 24 h after *Stat1* knockdown, cells were stimulated with (i) IR simultaneously for 8 h (IR), (ii) I for 8 h followed by R for 8 h, or (iii) I for 24 h followed by R for 8 h. *Stat1* knockdown enhanced *Il6* and *Il12b* mRNA expression in cells stimulated with IR, I8R and I24R (**Figure 11B**). These observations agree well with model predictions, which confirmed the biphasic response induced by STAT1-mediated I1-FFL.

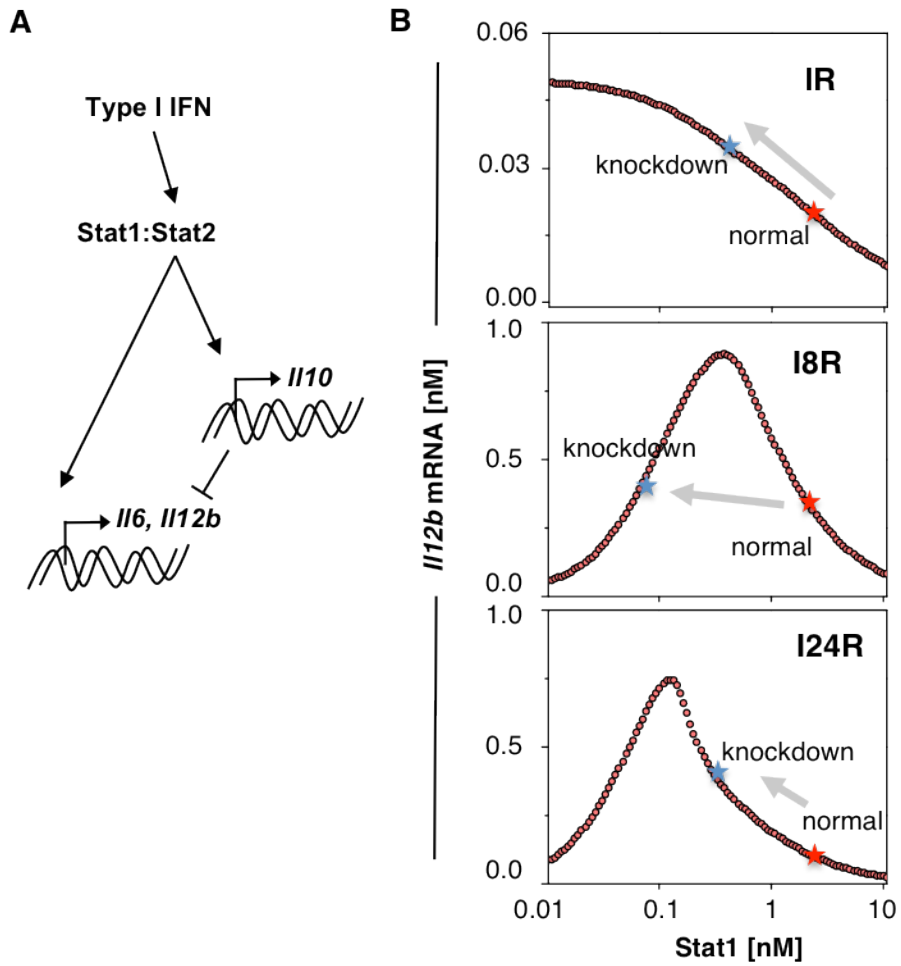

Figure 3.10. ***In silico*** **knockdown of STAT1 revealed a complex regulatory role of an incoherent feedforward loop.** A. STAT1-mediated incoherent type 1 feedforward loop. B. Simulated STAT1 initial concentration-cytokine production response curves under IR, I8R, and I24R conditions.

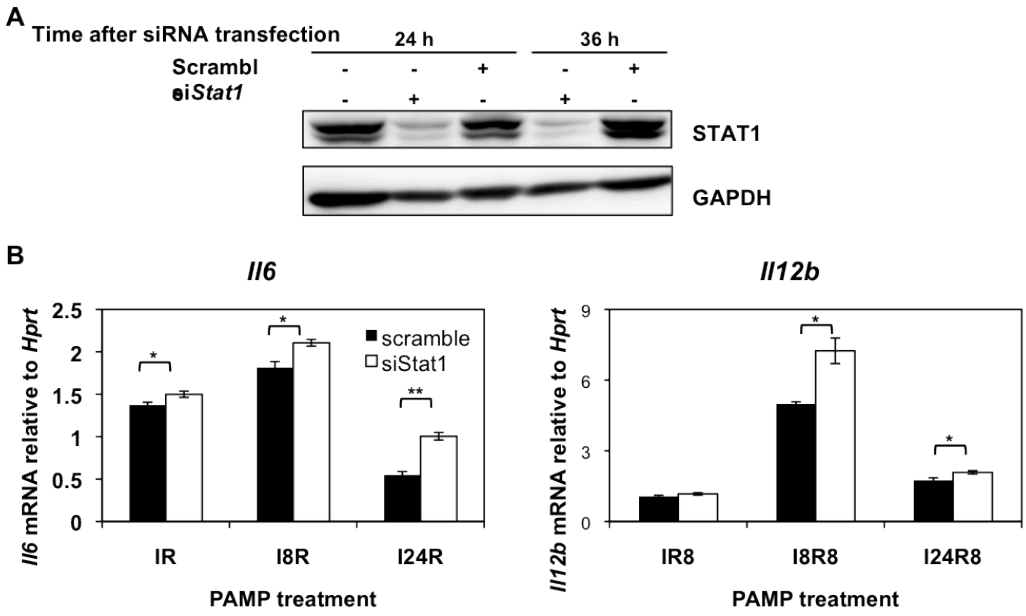

Figure 3.11. *In silico* and empirical knockdown of STAT1 revealed a complex regulatory role of an incoherent feedforward loop. A. Knockdown efficiency of *Stat1*. J774 cells were transfected with either anti-*Stat1* siRNA or control scramble siRNA for 24. Cell lysates were collected for Western analysis. Data are representative of two independent experiments. **B.** *Stat1* knockdown enhanced cytokine production. 24 h after either anti-*Stat1* siRNA or control siRNA transfection, cells were stimulated with IR, I8R, I24R for 8 h. Then expression of *Il6* and *Il12b* mRNAs were analyzed by real-time PCR. Data are presented as means ± SEM of three individual experiments.

3.4 Synchronization of transcription factors, IRF1, JunB and C/EBPβ orchestrated timely cytokine synergy during TLR3-TLR7 crosstalk.

Although systems biology method showed us a big picture of the TLR signaling network and predicted key signaling pathways that contribute to synergy, it could not specifically identify unknown molecules, especially transcription regulators which directly regulate cytokine synergy. Thus, conventional cell and molecular biology approach is still needed to enhance and fully validate the computational predictions and search for potential synergy regulatory molecules.

3.4.1 Dissection of possible mechanisms at multiple levels indicated that cytokine synergy was mainly and directly regulated at transcription level.

To solve the molecular mechanism of cytokine synergy, we first checked the level at which synergy occurs. Although we observed synergy at the cytokine mRNA level, synergy might not necessarily happen at the transcription level. It is possible that under combinatorial stimulation, a synergistic activation of signaling molecules upstream of cytokine transcription, or enhanced openness of the cytokine gene promoter structure, or a more stabilized mRNA (post-transcriptional regulation) occurs (**Figure 3.12**). Thus, we checked each possibility systematically, one at a time.

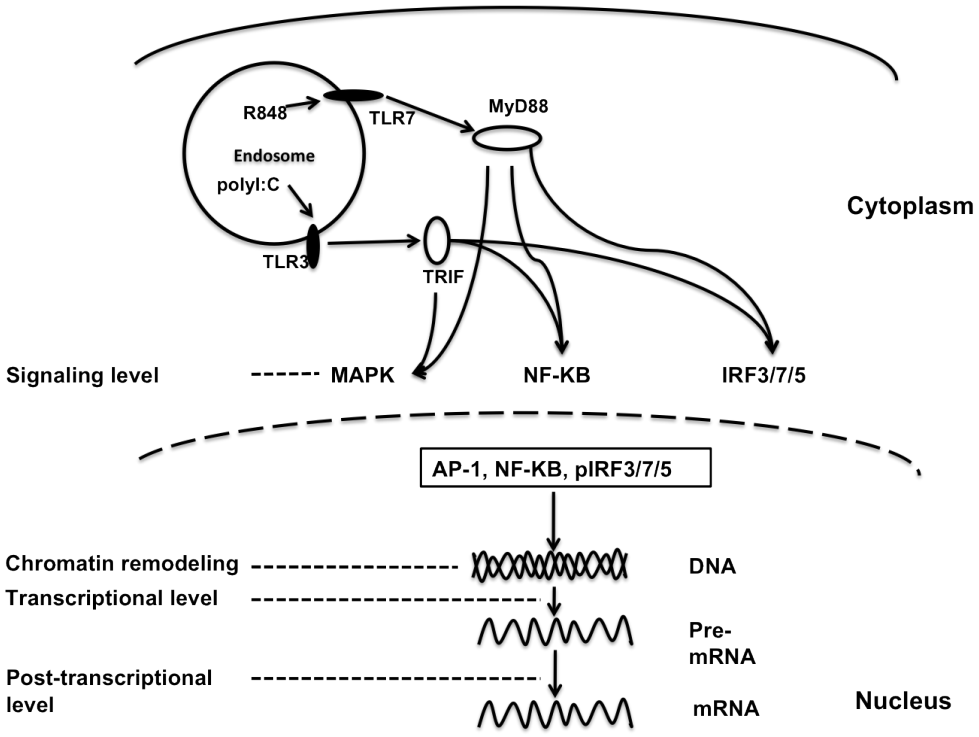

Figure 3.12. A schematic representation of possible regulatory levels where synergy might occur. Although in section 3.1, we observed synergy at the cytokine transcriptional level, it might not be the original level where synergy occurs. Synergy might occur at signaling level, where signaling molecules might be synergistically activated under combinatorial stimulation. Synergy could also happen at chromatin remodeling level by enhancing the cytokine gene promoter openness after combinatorial stimulation. Post-transcriptional level is also possible by regulating the stability of the cytokine mRNA.

3.4.1.1 Signaling molecules are not synergized by combinatorial stimulation.

To check whether synergy occurs, before cytokine production, at the signaling level, we measured the profiles of MAPK and NFκB, which are two major signaling families that regulate cytokine expression (this was done in collaboration with our lab member, Rebecca Tan). This work was published [57]). BMDMs were stimulated with either 10 μg/ml poly(I:C) or 25 ng/ml R848 alone, or poly(I:C) and R848 simultaneously (IR). The cells were harvested at 5, 15 and 30 min, 1, 4, 8, 12 and 24 h time points. Cell lysates were resolved on SDS-PAGE gel and probed with anti-phospho-JNK, anti-phospho-ERK, anti-phospho-p38, anti-phospho-IκB antibody and loading control anti-actin.

In general, both the MAPK and NFκB signals are more responsive to the R848 stimulation (**Figure 3.13**). Notably, poly(I:C) seemed to inhibit the R848 induced p-JNK, indicating a negative regulation of the TRIF pathway on the MyD88 pathway. Phosphorylation of ERK by poly(I:C) stimulation was weak and late compared to R848, and so is the poly(I:C) induced phospho-p38 signaling. None of the signaling tested was enhanced after combinatorial stimulation except pERK. However, the enhancement of pERK was only additive, not synergistic. The enhancement of pERK by combinatorial stimulation might contribute to cytokine synergy, but this may occur in an indirect way possibly by activating certain transcription factors [57]. Thus, here we draw the conclusion that synergy does not directly happen at the signaling level *per se*, but enhanced ERK signaling might contribute to cytokine synergy in an indirect manner.

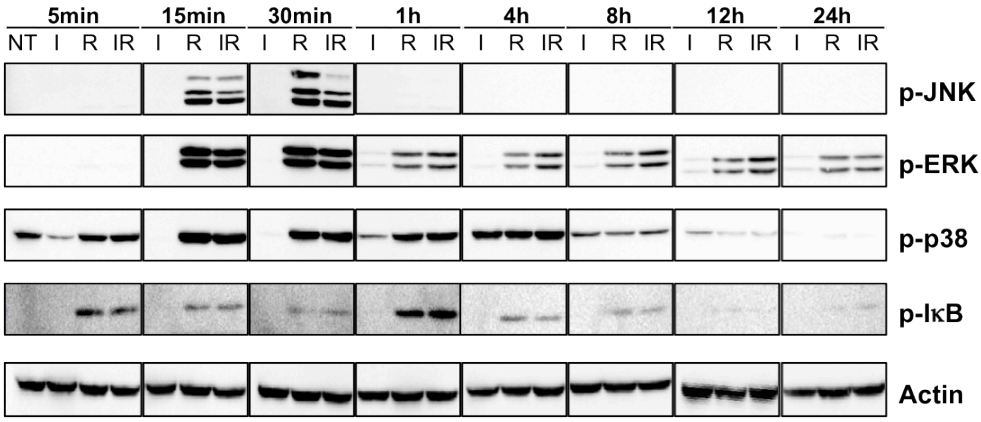

Figure 3.13. Synergy does not happen directly at signaling levels. A. BMDMs were treated with either poly(I:C) or R848 alone, or poly(I:C) and R848 together. Cells were collected after 5, 15, 30 min, or 1, 4, 8, 12, 24 h later to measure the levels of phospho JNK, phospho-ERK, phospho-p38, phospho-IκB and actin by western blot. Data is representative of three independent experiments. (Experiments for this figure were done in collaboration with a previous lab member, Rebecca Tan, and published on [57]).

3.4.1.2 DNA accessibility is not affected by combinatorial stimulation compared with single stimulation.

Transcriptional synergy may occur through different mechanisms, including chromatin remodeling, a crucial event for the transcriptional activation of pro-inflammatory cytokine genes [16,83,84]. Topologically closed promoter and enhancer of murine *Il6* and *Il12b* were shown to become significantly opened and accessible to TFs when the macrophages were treated with LPS [47,57,85,86]. Thus we speculated that the synergistic action of TLR3-TRIF and TLR7-MyD88 activation pathways might occur through chromatin remodeling. To test this hypothesis, we carried out restriction enzyme accessibility assay as described for the study of LPS response [85], to examine whether poly(I:C)- and R848- activated pathways cooperate during the chromatin remodeling stage. Surprisingly, although poly(I:C) by itself is a very weak inducer of *Il6* and *Il12b* expression, it strongly stimulated an open

chromatin in the *Il12b* enhancer, similar to the effect of R848 (**Figure 3.14**). Both poly(I:C) and R848 significantly induced an open chromatin in *Il6* and *Il12b* promoters. Compared to single stimulation, combinatorial stimulations did not significantly enhance *Il6* promoter remodeling, but it considerably remodeled the *Il12b* promoter (possibly an additive effect), which is even higher than the level induced by LPS stimulation. Arguably PAMP-induced chromatin remodeling of pro-inflammatory cytokine genes in macrophages could be a global primary event that may not involve the synergistic action of distinct TLR-signaling pathways.

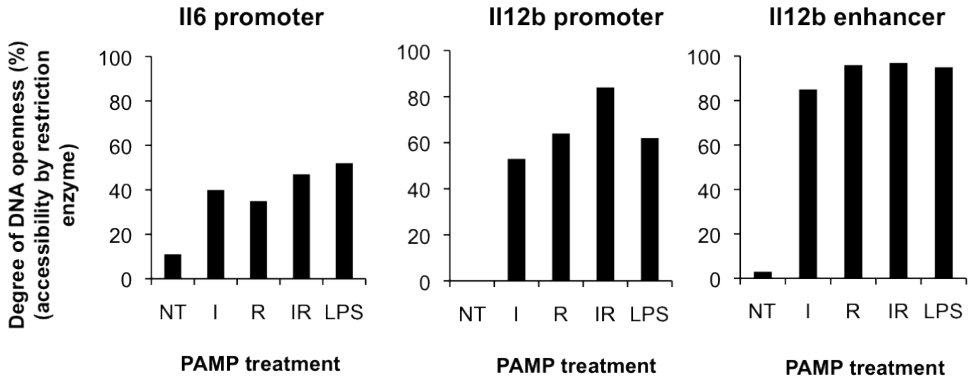

Figure 3.14. Chromatin remodeling might not contribute to cytokine synergy. Macrophages were treated with poly(I:C) (10 μg/ml, I), R848(25 ng/ml, R) or LPS(100 ng/ml), or co-stimulated with both poly(I:C) and R848 (IR), for 5 h before collection for restriction enzyme accessibility assay as described in the Material and Method 2.10. Data are representative of two independent experiments.

3.4.1.3 mRNA stability is not enhanced by combinatorial stimulation.

Next, we tested whether cytokine synergy was attributable to enhanced mRNA stability. After a 4 h stimulation with poly(I:C) and/or R848, BMDMs were treated with actinomycin D to halt further mRNA synthesis. We found that over 2 h, the *Il12b* mRNA remained highly stable under all treatment conditions (**Figure 3.15)**. In contrast, *Il6* mRNA underwent rapid

degradation, especially under combinatorial stimulation, with a $T_{½}$ of ~25 min. While *Il6* and *Il12b* mRNAs exhibited different stability profiles, combinatorial stimulation consistently reduced the mRNA stability.

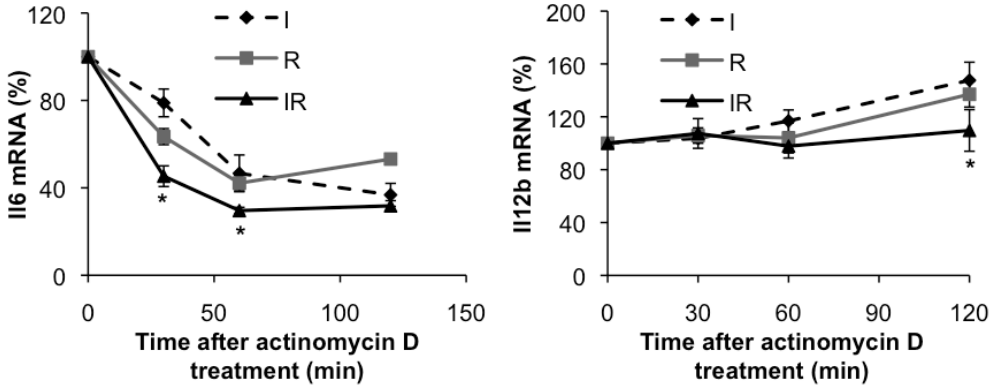

Figure 3.15. Cytokine synergy is not due to enhanced mRNA stability. BMDMs were incubated for 4 h with poly(I:C) (10 μg/ml, I, dashed line) or R848 (25 ng/ml, R, solid grey line) or poly(I:C)+R848 (IR, solid black line). The *Il6*, *Il12b* and *Hprt* mRNA levels were determined by real-time PCR in samples collected before (0 min) and 30, 60, 120 min after the addition of actinomycin D (5 μg/ml), which halts synthesis of new mRNAs. The amounts of *Il6* and *Il12b* mRNAs after actinomycin D treatment are shown as a percentage of the levels in the cells at the start, time 0. Data are presented as means ± SEM of three independent experiments. * P <0.05 (Student's t-test).

3.4.2 Proteomic analysis revealed candidate synergy factors.

Evidence from both the chromatin remodeling and mRNA stability experiments support that synergistic expression of *Il6* and *Il12b* is attributable to their elevated transcriptional activity when under co-stimulation. Evidence shown above, together with the notion that newly synthesized protein(s) are required for the induction of both IL6 and IL12p40 [67], prompted us to look for the newly synthesized/ activated transcriptional regulators, which may regulate the crosstalk of MyD88- and TRIF- mediated pathways. To define such "transcriptional synergy factors", we performed functional proteome profiling of chromatin binding proteins purified from stimulated macrophages, using iTRAQ (Isobaric Tag for Relative and Absolute Quantitation). We

compared their profiles on the basis that transcriptional synergy might be facilitated by collaboration between the R848-specific and poly(I:C)-specific TFs, or by co-stimulation (IR)-activated TFs.

3.4.2.1 iTRAQ experiment shows reliable protein identification.

To obtain sufficient amount of proteins, we used J774 macrophage cell line instead of the primary BMDM cells, which were limited. We first confirmed whether J774 cells exhibit cytokine synergy consistent with that of the primary cells by stimulating J774 cells with 10 μg/ml poly (I:C), 25 ng/ml R848 separately or together. Consistent with BMDM, the J774 cells produced negligible amount of cytokines under I single stimulation and produced moderate amount of cytokines under R single stimulation. But when I and R were given together (IR), the cytokine expressions were synergized (**Figure 3.16A)**. Thus henceforth, we used J774 cells to study the proteome profile of chromatin binding proteins after different treatments.

J774 cells were stimulated with poly(I:C) (I), or R848 (R), or both (IR) for 1 or 5 h, as this duration of stimulation falls within the peak range of mRNA production (Figure 3.1). Chromatin-binding proteins of two biological replicates were extracted. The quality of chromatin binding proteins were examined by Western blot for both cytosolic and nuclear markers, GAPDH and TBP. As shown in **Figure 3.16B,** the chromatin binding proteins acquired were free of cytosol protein contamination. The proteins were then digested in-gel, labeled with isobaric tag (8-plex iTRAQ labeling kit), pooled, fractionated by HPLC. Each of the 30 fractions acquired from HPLC was analyzed by LC-MS/MS three times (technical triplicates) (**Figure 3.16C**).

Based on the LC-MS/MS data, we identified 1163 proteins from both replicates (see Appendices for detailed information of proteins reliably identified by iTRAQ), with false discovery rates (FDR) of <1%. We then calculated the geometric mean of the two replicates and analyze the data using the geometric mean of iTRAQ ratio from biological duplicates.

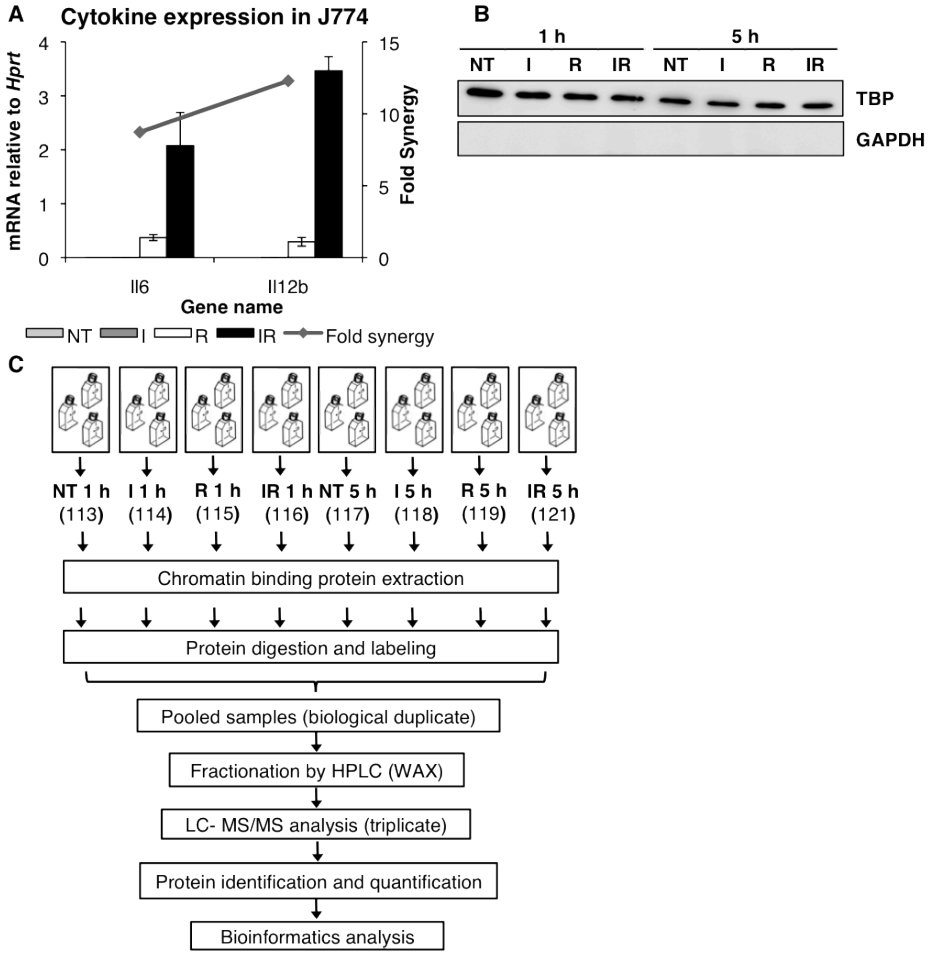

Figure 3.16. iTRAQ analysis of chromatin binding proteins under different PAMP treatments. A. J774 showed synergy effect under combinatorial stimulation, consistent with primary cells. J774 cells were stimulated with polyI:C (10 μg/ml), R848 (25 ng/ml) alone or combinatorially for 8 h followed by mRNA analysis. **B**. Western blot analysis of the purity of chromatin binding protein samples (10 μg) from different treatments with nuclear marker, TBP and cytosolic marker, GAPDH. NT, non-treated control; treatment with polyI:C (I) or R848 (R) or polyI:C+R848 (IR) for 1 h or 5 h. **C.** Experimental strategy. Chromatin proteins were extracted from two biological replicates of J774 cells, which were stimulated with I, R, IR, or no treatment (NT) for 1 h or 5 h. Data are presented as means ± SEM of three independent experiments (A) or representative of two biological replicates (B).

3.4.2.2 iTRAQ data analysis revealed several potential transcriptional synergy factors

To gain an overview of chromatin-binding proteins, we first analyzed all the reliably identified proteins with PANTHER (**Figure 3.17A**) according to their protein classification. As anticipated, the majority of the proteins are nucleic acid binding proteins, and the next abundant protein classes are transcription factors. Next, we checked the proteins downregulated or upregulated under different treatment with a threshold of ≥1.5 used for iTRAQ ratios (**Figure 3.17B**). The thresholds set for the ratios, which were derived from quantification of isobaric tags, are generally considered significant due to the intrinsic tendency of ratio under-estimation by compression in iTRAQ [87]. More proteins were perturbed 5 h after treatment. Furthermore, IR treatment tended to make more changes to the protein profile. Interestingly, at 1 h post-stimulation, more proteins are upregulated by R and IR stimulation than I alone. However, fewer proteins were observed to be upregulated at 5 h after IR stimulation while more were downregulated, indicating the existence of certain immune regulatory mechanisms, which may protect against overwhelming immune responses.

Then we looked into protein groups that are up- or down- regulated by different PAMP treatments using DAVID. With DAVID analysis, we could reveal what GO molecular function, biological processes and KEGG pathways are enriched in the perturbed protein group (**Figure 3.18A, B**). Interestingly, the GO functions of the "transcription regulation" group were enriched only in proteins upregulated by IR combinatorial stimulation for 5 h (Figure 3.18B box).

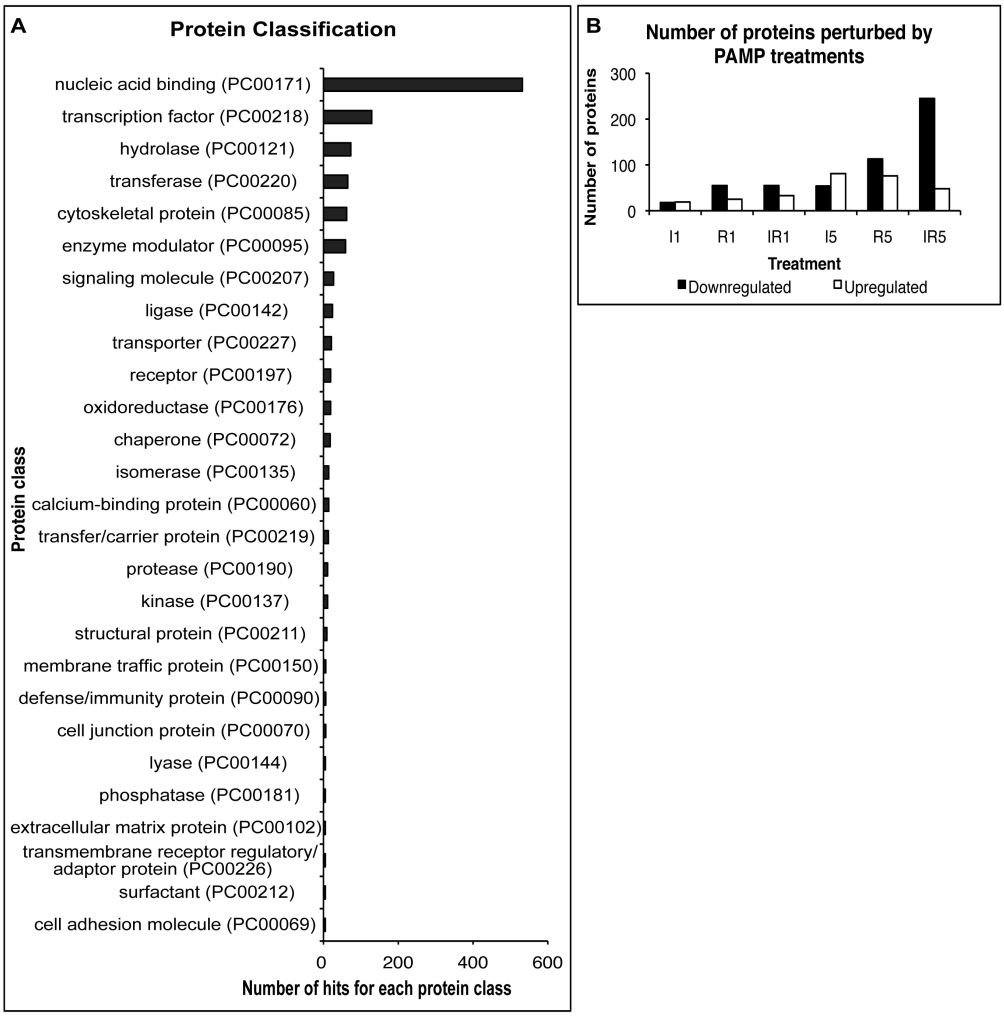

Figure 3.17. Preliminary iTRAQ data analysis. A. PANTHER-classification of proteins identified by iTRAQ. **B.** Numbers of differentially regulated proteins (fold difference ≤0.67 or ≥1.5) under different treatments.

Next, we checked the iTRAQ ratios of proteins, which are upregulated by IR5 and belong to the cluster of transcription regulatory function (**Table 3.1**). Proteins were earmarked with "b" as candidate synergy factors if they are (1) significantly upregulated in the presence of R848 or poly (I:C), but not further enhanced by combinatorial stimulation, which indicates they are either I responsive or R responsive and might collaborate when both pathways are activated. (2) more enhanced after combinatorial stimulation compared with single treatments. C/EBPβ and NFκB-p105 were more responsive to R stimulation, while interferon activated protein 204 (Ifi204) responded to I

only. JunB and ATF3 are more upregulated after co-stimulation than single stimulation, indicating synergistic actions of two distinct pathways.

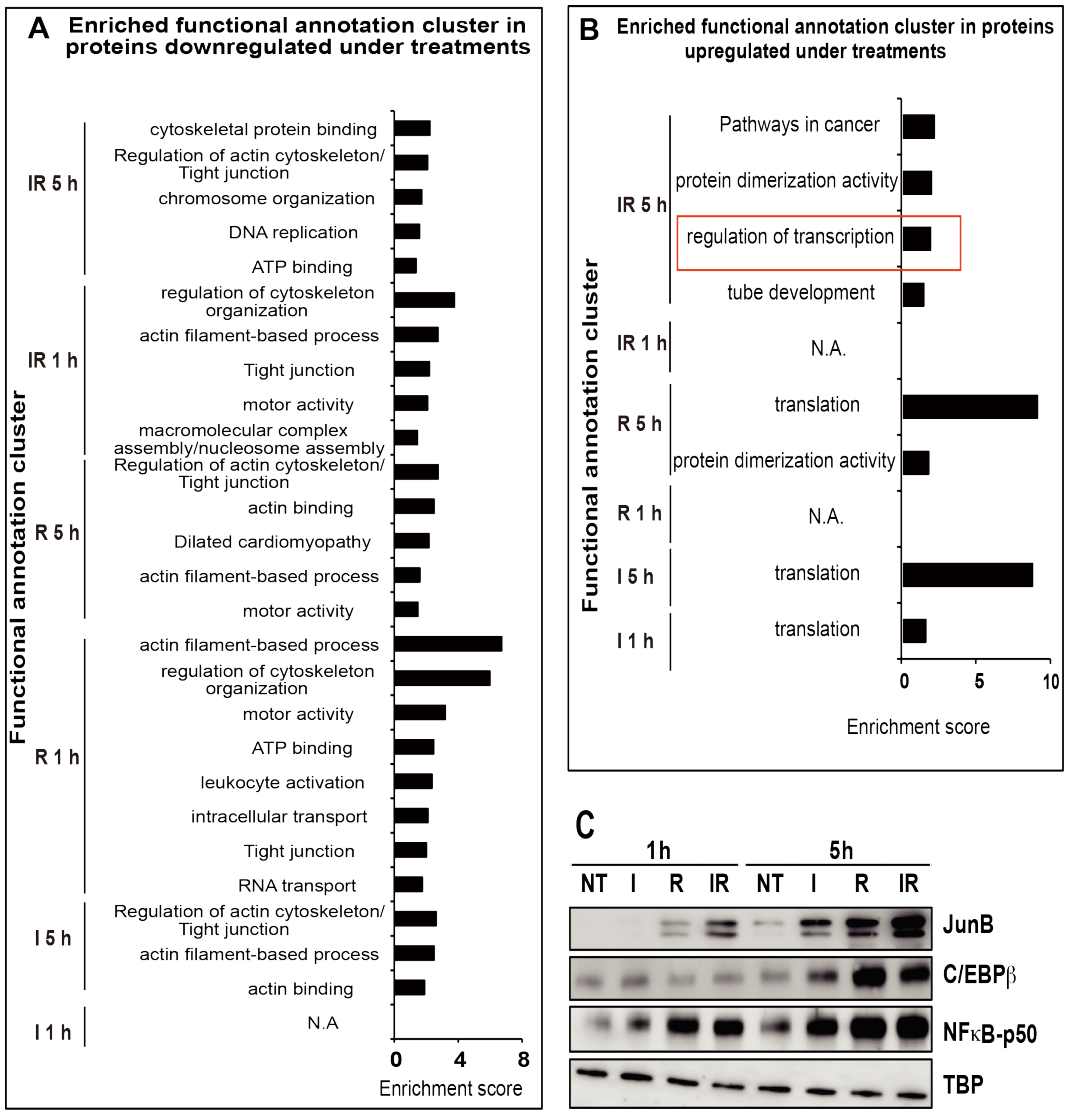

Figure 3.18 Functional analysis of proteins perturbed under different treatment. A. Functional annotation clusters enriched in proteins down regulated (with arbitrary threshold of fold difference ≤0.67) under different treatment (analysis using the DAVID v6.7). There was no functional annotation cluster enriched in proteins down-regulated, by I for 5 h and I for 1h (indicated as N.A, not applicable). **B.** Functional annotation clusters enriched in proteins up regulated (with arbitrary threshold of fold difference ≥1.5) under different treatments. Annotation cluster of "regulation of trasncription" (indicated in box) was exclusively enriched in 5 h combinatorial stimulation. **C.** Validation of iTRAQ ratio of potential synergy factors with Western blot. Same chromatin binding protein samples used for iTRAQ were dissolved in SDS page to check whether the profile of JunB, C/EBPβ, NFκB-p50 and TBP is consistent with iTRAQ results. Data are representative of two biological replicates.

As a negative regulator of cytokines [88], ATF3 was not further studied here. Being relatively uncharacterized, Ifi204 was also excluded. Western blot of NFκBp105, JunB and C/EBPβ (**Figure 3.18C)** validated their changes in expression detected by iTRAQ. Thus, these three transcription factors are shortlisted as candidate synergy factors and further examined.

Table 3.1. Transcriptional regulatory proteins upregulated after IR combinatorial stimulation for 5 h

Gene name (accession number)	I1/NT1[a] (114:113)	R1/NT1[a] (115:113)	IR1/NT1[a] (116:113)	I5/NT5[a] (118:117)	R5/NT5[a] (119:117)	IR5/NT5[a] (121:117)
Interferon regulatory factor 5 (P56477)	1.08	1.20	1.24	1.66	1.54	1.53
ETS translocation variant 3 (Q8R4Z4)	0.87	1.17	1.10	1.42	1.12	1.69
Zinc finger E-box-binding homeobox 2 (Q9R0G7)	1.03	1.12	1.15	1.28	1.60	1.61
Poly [ADP-ribose] polymerase 14 (Q2EMV9)	1.35	1.36	1.16	2.70	1.28	1.80
Forkhead box protein P1 (P58462)	1.03	1.00	1.24	0.91	1.35	1.52
Bromodomain adjacent to zinc finger domain protein 1A (O88379)	1.06	1.15	1.09	1.23	1.29	1.55
CCAAT/enhancer-binding protein beta (P28033)[b]	1.05	1.10	1.16	1.58	3.65	2.73
C-terminal-binding protein 2 (P56546)	0.87	1.01	0.91	1.34	1.33	1.57
DEAD (Asp-Glu-Ala-Asp) box polypeptide 5 (Q8BTS0)	1.37	1.36	1.21	4.27	4.47	2.83
Transcription factor jun-B (P09450)[b]	1.54	2.81	2.91	3.48	6.49	11.27
Cyclic AMP-dependent transcription factor ATF-3 (Q60765)[b]	1.23	1.02	0.90	0.97	1.16	2.42
Mothers against decapentaplegic homolog 4 (P97471)	0.65	1.07	1.06	1.56	1.35	1.53
Transcriptional repressor p66 alpha (Q8CHY6)	0.68	0.93	0.94	1.72	1.71	1.70
Nuclear factor NF-kappa-B p105 subunit (P25799)[b]	1.92	3.45	3.93	1.35	2.70	3.58
Interferon-activated protein 204 (P15092)[b]	1.06	1.32	1.17	3.61	0.99	3.08
C-terminal-binding protein 1 (O88712)	0.87	1.00	0.95	1.61	1.49	1.58

Ear mark a are iTRAQ ratio indicating fold change of proteins perturbed by I, R, IR treatments compared to untreated control (NT). Potential synergy factors are earmarked with b.

3.4.3 JunB, C/EBPβ and IRF1 are the core transcription factors which interact with *Il6* and *Il12b* promoters.

While proteome profiling has identified candidate TFs that might regulate cytokine synergy, an examination of gene-specific association is required to demonstrate their direct or indirect involvement in the regulation of *Il6* and *Il12b* transcription. Thus, we performed *in vitro* promoter affinity pulldown assay, in a comparative manner using nuclear extracts prepared from macrophages, which were challenged with poly (I:C) or R848 alone or together. We analyzed the promoter association of shortlisted candidates and other core cytokine regulatory factors, which might have been missed in iTRAQ analysis due to their scarcity in absolute abundance or their hydrophilic properties. In total, we examined: (1) JunB, (2) C/EBPβ, (3) NFκB family members (RelA, RelB and c-Rel, NFκBp50), and (4) IRF members (IRF1, IRF3, and IRF8), which have been documented to be downstream of the TRIF signaling pathway and are involved in the production of type I interferon. The proteins associated with either of the 3' end-biotin labelled *Il6* or *Il12b* promoter that were pulled down using streptavidin-conjugated magnetic beads from the nuclear extracts, were immunoblotted and probed using antibodies against the selected targets (**Figure 3.19A**). We observed consistent association of JunB, IRF1 and C/EBPβ with both promoters. To make sure the binding we observed is specific, and not due to non-specific binding by beads, we also pulled down with empty beads as negative control. Although there was a band for IRF1 in the empty beads in the presence of polydI:dC, it is negligible compared to specific bands in the presence of promoters (**Figure 3.19B**). Notably, the intensities of the

detection signal appeared roughly proportional to their respective levels in the nuclear extract, suggesting that the association of these TFs to the respective promoter is independent of one another.

The IRF1 and C/EBPβ were strongly induced by poly(I:C) and R848, respectively, as seen in the nuclear extracts, and no additive effect was observed with co-stimulation. This suggests that IRF1 and C/EBPβ are regulated under distinct pathways; TRIF- and MyD88- signaling, respectively. In contrast, JunB, which was induced only weakly by poly (I:C) but strongly by R848, showed a higher expression in co-stimulation, indicating that crosstalk between the TRIF- and MyD88- pathways might regulate JunB expression. Surprisingly, Rel proteins were not significantly associated with either of the *Il12b* or *Il6* promoters, although NFκB is functionally important for pro-inflammatory responses, and there is a characterized NFκB binding element in *Il12b* [89] and *Il6* promoters [90].

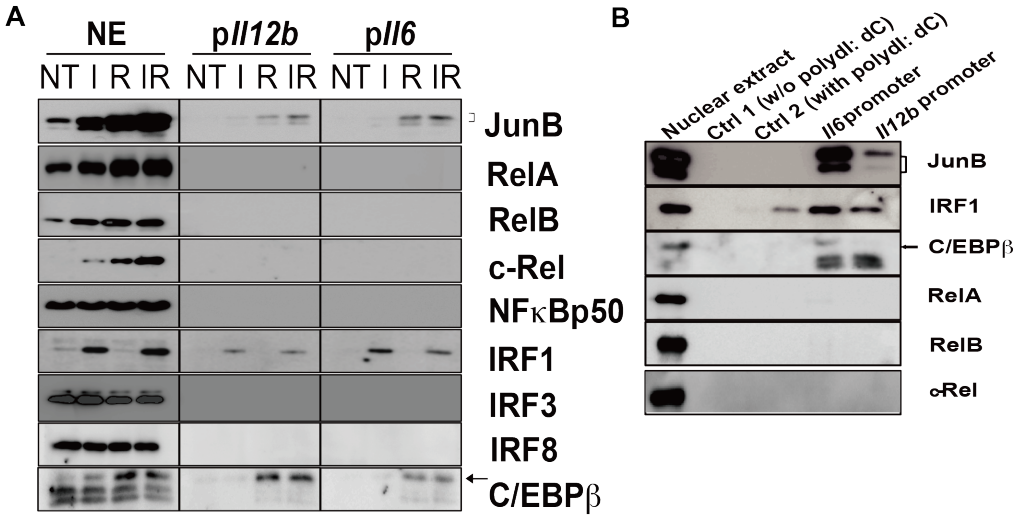

Figure 3.19. ***In vitro*** **promoter-affinity pulldown revealed transcription factor C/EBPβ, IRF1 and JunB bind to** ***Il6*** **and** ***Il12b*** **promoter. A.** For promoter pulldown, nuclear extracts were prepared from J774 cells stimulated with poly(I:C) (I), R848 (R) and both (IR) or left untreated (NT) for 5h. Aliquots of 100 fmol of biotin- labeled DNA were incubated with different nuclear extracts (as indicated in Materials and Methods) in a 100 µl binding reaction. DNA-protein complexes were affinity-absorbed to streptavidin-conjugated beads, and released by boiling in SDS-PAGE sample buffer. Nuclear extracts (NE) and protein samples derived from 10 µl binding reaction (10 fmol DNA: 4µg nuclear proteins) each were resolved on a 10 % gel, transferred to PVDF membrane, and probed using antibody against interested target. **B.** Nuclear extracts from macrophages stimulated simultaneously (combinatorially) by IR for 5 h were incubated with empty beads (ctrl 1 and ctrl 2), beads with Il6 promoter or beads with Il12b promoter in a 100 µl binding reaction. In the binding reaction, polydI:dC was added for all conditions except ctrl 1. DNA-protein complexes were affinity-absorbed to streptavidin-conjugated beads, and released by boiling in SDS-PAGE sample buffer. Protein samples derived from 10 µl binding reaction (10 fmol DNA: 4 µg nuclear proteins) each were resolved on a 10 % SDS reducing gel, and probed using respective antibody against interested target. All the targets, except IRF1, showed only specific binding to the promoters. The non-specific binding of IRF1 to empty beads was not significant compared to that bound to the promoters, especially when blocking DNA poly (dI:dC) was included. Data are representative of three independent experiments.

3.4.4 Combinatorial stimulation synchronizes IRF1, JunB and C/EBPβ activities, and MyD88 pathway inhibits IRF1 activity.

Next, we examined the dynamic profile of IRF1, C/EBPβ and JunB under different treatments with different time points (**Figure 3.20A**). C/EBPβ responded mainly to R stimulation. IRF1 was upregulated and sustained by I,

but marginally and transiently upregulated for 1 h by R. This is likely due to the rapid primary activation of NFκB, which is known to be required for IRF1 expression [91]. However, R-induced MyD88 pathway activation apparently represses the I-induced expression of IRF1. The IRF1 returned to a low basal level at 12 h post co-stimulation, correlating with subdued cytokine gene transcriptions. In contrast, JunB was rapidly upregulated within 1 h, by all stimulations. Notably, over 4-8 h, R induced a stronger JunB response than I. By 12 h, both I and R separately induced comparable levels of JunB, indicating equally limited potentials in single stimulations. Nevertheless, in co-stimulated macrophages, JunB expression was sustained and accumulated over 8-24 h. As we consistently observed two bands of JunB, we further tested whether they were differently modified forms of JunB proteins. Treatment with phosphatase showed a dose-dependent conversion of the upper to lower band (**Figure 3.20B**), indicating that JunB was extensively phosphorylated upon induction.

Taken together, the coincidence /synchronization of the levels of IRF1, C/EBPβ and JunB in the 4-8 h post-combinatorial stimulation and the obvious correlation with the mRNA peaks of *Il6* and *Il12b* (Figure 3.1), strongly indicate their co-operation in synergistic transcription.

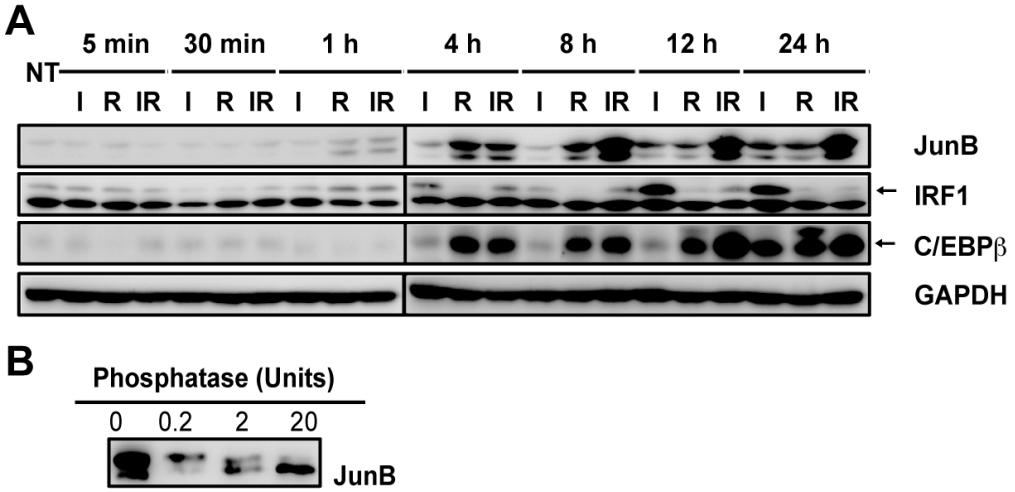

Figure 3.20. Combinatorial stimulation synchronizes C/EBPβ, IRF1 and JunB. A. J774 cells were treated with either 10 μg/ml poly(I:C) or 25 ng/ml R848 alone, or poly(I:C) and R848 in combination (IR) for 5 and 30 min, 1, 5, 8, 12 and 24 h or no treatment (NT). Cells were harvested and analyzed by Western blot and probed with anti-JunB, IRF1, C/EBPβ and GAPDH antibody. **B.** J774 cells were harvested after 5 h treatment with R848. 5 μg of the nuclear extracts were treated with 0, 0.2, 2 and 20 Units of phosphatase for 1 h at 37°C and were analyzed by Western blot probed with anti-JunB antibody. The upper band of JunB is a phosphorylated form. Data are representative of three independent experiments.

3.4.5 IRF1, JunB and C/EBPb functionally collaborate with each other to facilitate cytokine expression.

Although we observed synchronized induction of IRF1, Junb and C/EBPβ under combinatorial stimulation and confirmed their binding with *Il6* and *Il12b* promoter, it is not clear whether they are functionally required for cytokine production and whether they functionally collaborate with each other. Thus, we then checked their functional role with siRNA knockdown.

3.4.5.1 TRIF- and MyD88- signaling pathways collaborate to synergize IL6 and IL12p40 expression through synchronized activities of IRF1 and C/EBPβ.

We next examined the functional cooperation between TRIF-responsive IRF1 and MyD88-responsive C/EBPβ, in macrophages using single and double knockdown with gene-specific siRNAs of *Irf1* and *Cebpb*.

At 24 h post-transfection with *Irf1*-specific siRNA (si*Irf1*), or *Cebpb*-specific siRNA (si*Cebpb*) or scramble (control) siRNA, macrophages were co-stimulated with poly(I:C) and R848, and the expression levels of IRF1 and C/EBPβ were monitored for up to another 24 h. C/EBPβ and IRF1 expression was suppressed over the 24-h time course (**Figure 3.21A**). However, no significant difference in efficiencies was observed between single and double knockdown conditions for either IRF1 or C/EBPβ, indicating that the expressions of IRF1 and C/EBPβ are regulated independently of each other.

Subsequently, we compared mRNA (**Figure 3.21B**) and protein (**Figure 3.21C**) levels of *Il6* and *Il12b* in the single (*Irf1* or *Cebpb*) or double (*Irf1* and *Cebpb*) knockdown cells. Significant attenuation of both the mRNA and protein levels was observed in R848 and co-stimulated cells (Figure 3.21B, C). In poly(I:C)-stimulated cells, *Il6* and *Il12b* mRNAs remained at their basal levels. In the co-stimulated cells, the effects of single knockdown appeared only incremental, while double knockdown achieved the greatest reduction of *Il6* and *Il12b* (IL12p40: ~50% by si*Irf1*+si*Cebpb*; IL6: ~75% by si*Irf1*+si*Cebpb)*. Interestingly, C/EBPβ exerts a stronger influence on the *Il6* expression than *Il12b* expression. The knockdown results clearly indicate that significant expression of *Il6* and *Il12b* can only be induced by co-stimulation of TLR3 and TLR7, and the presence of a certain level of both IRF1 and C/EBPβ is necessary and sufficient for the optimal transcription activity of *Il6* and *Il12b*.

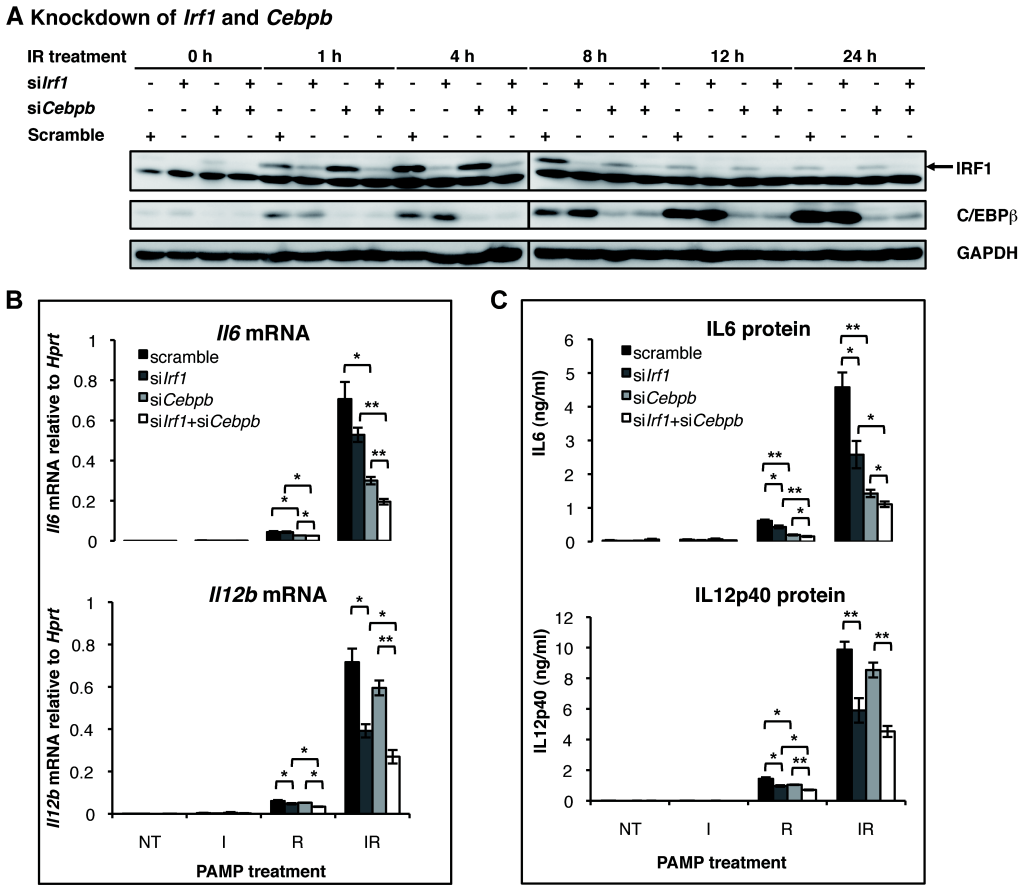

Figure 3.21. Collaboration of IRF1 with C/EBPβ is required for synergistic production of cytokines. A. *Irf1* and *Cebpb* were successfully knocked down by siRNA. Cells were transfected with either siRNA targeted on *Irf1* or *Cebpb* alone or together, or scramble control for 24 h, followed by 0, 1, 4, 8, 12 and 24 h stimulation with IR. Cell lysates were immunodetected for IRF1 and C/EBPβ, and with GAPDH as control. **B.** 24 h after *Irf1* and *Cebpb* siRNA transfection alone or together, cells were stimulated with I and/or R for 8 h or were not treated with any PAMP as negative control (NT). Then expression of *Il6* and *Il12b* mRNA were analyzed by real-time PCR. **C.** 24 h after *Irf1* and *Cebpb* siRNA transfection alone or together, cells were stimulated with I and/or R for 12h or were not treated with any PAMP as negative control (NT). IL6 and IL12p40 were quantified by ELISA. Data are representative of three independent experiments (A) or presented as means ± SEM of three individual experiments (B, C). * P <0.05, ** P < 0.01 (Student's t-test).

3.4.5.2 TRIF- and MyD88- signaling pathways collaborate to synergize cytokine expression through enhancing JunB production and synchronizing IRF-JunB activation.

To functionally characterize JunB-mediated regulation of expression of *Il6* and *Il12b* and its potential cooperation with IRF1, we knocked down *Junb* alone or both *Junb and Irf1* (**Figure 3.22A**). The efficiencies of knockdown were verified to be approximately 80% and this was consistent between single and double knockdown, indicating that the expressions of *Irf1* and *Junb* are regulated independently of each other. Significant reduction in R- or IR- induced *Il6* and *Il12b* was observed in *Junb* knockdown cells (**Figure 3.22B, C**) at both the mRNA and protein levels. With I-stimulation, both *Il6* or *Il12b* mRNAs remained extremely low, similar to non-treated cells (Figure 3.21B, C), thus the impact of *JunB* knockdown on I-induced cytokine expression was not further assessed. The drastic difference in the induction of cytokines between single and co-stimulation, compared to the smaller difference caused by *Junb* knockdown, clearly indicates the involvement of additional critical cofactors induced by the TRIF-pathway, which is necessary for the synergistic transactivation of *Il6* and *Il12b* promoters. This is supported by the double knockdown of *Junb* and *Irf1,* which yielded more pronounced attenuation of *Il6* and *Il12b* (IL12p40: ~75% by si*Junb*+si*Irf1*; IL6: ~80% by si*Irf1*+si*Junb*) at both mRNA and protein levels (Figure 3.22B, C) compared to single knockdown. Thus co-stimulation-mediated enhancement of JunB itself promoted cytokine expression and at the same time, Junb collaborates with TRIF-responsive IRF1 to augment cytokine production.

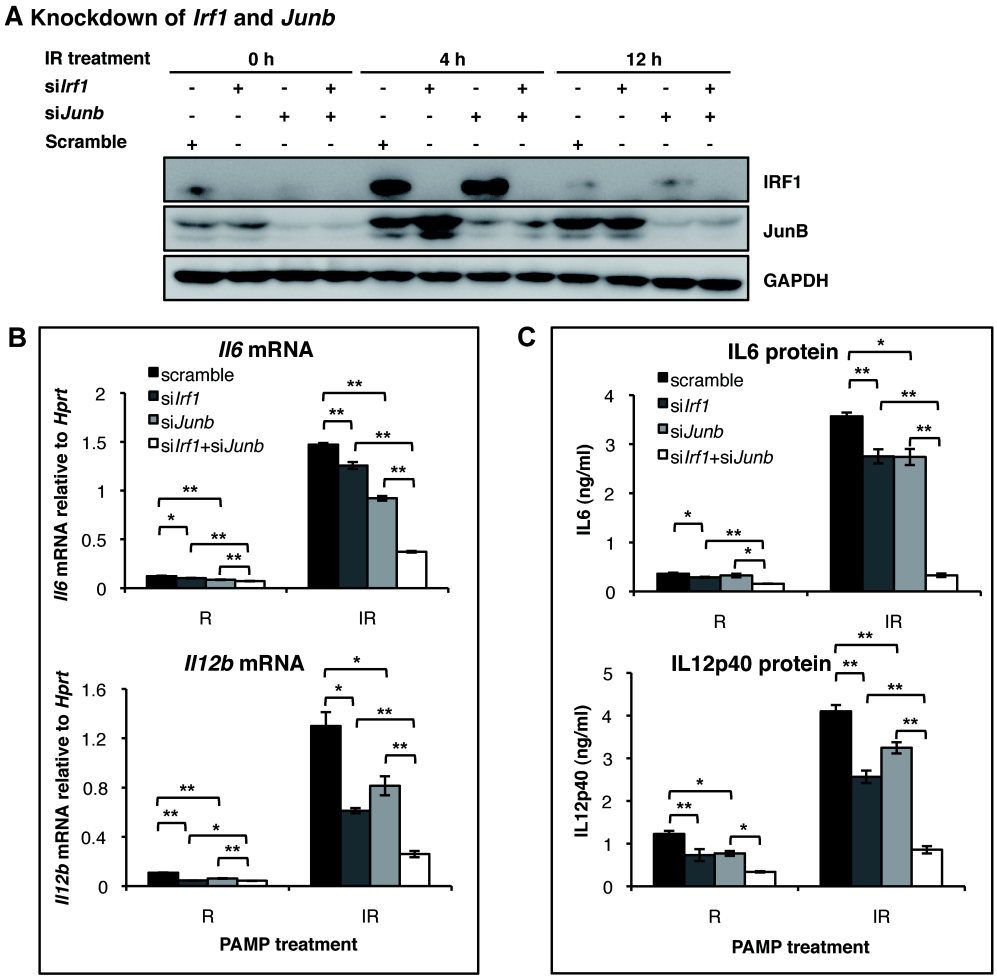

Figure 3.22. IRF1 works together with JunB to synergize cytokine production under combinatorial stimulation. A. *Irf1* and/or *Junb* was successfully knocked down by siRNA. J774 cells were transfected with either siRNA targeted on *Irf1* or *Junb* alone or together, or scramble control for 24 h, followed by 0, 4 and 12 h stimulation with IR. Cell lysates were immunodetected for IRF1 and JunB, and with GAPDH as control. **B and C.** 24 h after *Irf1* and *Junb* siRNA transfection alone or together, cells were stimulated with R alone or IR for 8 h. Then cells were collected for *Il6* and *Il12b* mRNA expression analysis by real-time PCR. (**B**) and supernatant were subject to IL6 and IL12p40 proteins measurement by ELISA(**C**). Data are representative of two independent experiments (A), or presented as means ± SEM of three individual experiments (B, C). * P <0.05, ** P < 0.01 (Student's t-test).

Taken together, R strongly upregulates and sustains MyD88-responsive JunB and C/EBPβ but R only transiently activates IRF1, resulting in mild transcription activation of *Il6* and *Il12b*. In contrast, I induces a high level of TRIF-responsive IRF1 but only minimally, of JunB and C/EBPβ. On

its own, IRF1 appeared insufficient to drive the basal transcription. However, combinatorial stimulation synchronized the activation of IRF1, JunB and C/EBPβ for up to 8-12 h, where these TFs probably worked in concert to achieve optimal cytokine expression.

3.5 MAPK pathway activates synergy factors JunB and C/EBPβ, but ERK and p38 inhibits IRF1 induction under R848 stimulation.

Although we have identified JunB, C/EBPβ and IRF1 to be required for optimal cytokine production, it is still unclear what upstream pathways lead to their activation. As MAPK pathway was predicted to be critical for cytokine expression in computational modeling, we checked whether MAPK could regulate the induction of synergy factors: JunB, C/EBPβ and IRF1. BMDMs were treated with JNK, ERK or p38 inhibitors as described in 3.3.5 followed by I or R single stimulation or IR combinatorial stimulation or no PAMP treatment (NT). Cells were then lysed and dissolved in SDS page to check for JunB, C/EBPβ and IRF1 expression with Western blot (JunB expression level measurement was done in collaboration with our lab member, Lu Ning).

As can be seen in **Figure 3.23**, poly (I:C) induced JunB could be inhibited by p38 inhibitor. But under R or IR stimulation, inhibition of all three MAPKs could reduce the production of JunB. Induction of the other MyD88 responsive synergy factor, C/EBPβ, was not affected by JNK pathway, but regulated by ERK and p38 under R and IR stimulation. C/EBPβ was barely induced by poly (I:C) stimulation and this was not altered by MAPK inhibitor.

Notably, the IRF1 induction was greatly enhanced by ERK and p38 inhibitors under R and IR stimulations. However, inhibition of ERK and p38 did not further enhance IRF1 expression after single stimulation by I. This is very interesting because we observed enhancement of cytokine expression after ERK and p38 inhibition under R and IR stimulation. And the upregulation of IRF1 expression by the same condition might be responsible for the enhancement of cytokine production. In addition, we have also previously observed an inhibitory role of R848-induced MyD88 pathway on IRF1 expression (Figure 3.20A). This might also be explained by Figure 3.23 that MAPK activated by R848 might inhibit IRF1 expression through some unknown mechanism and inhibition of MAPK thus increase IRF1 expression.

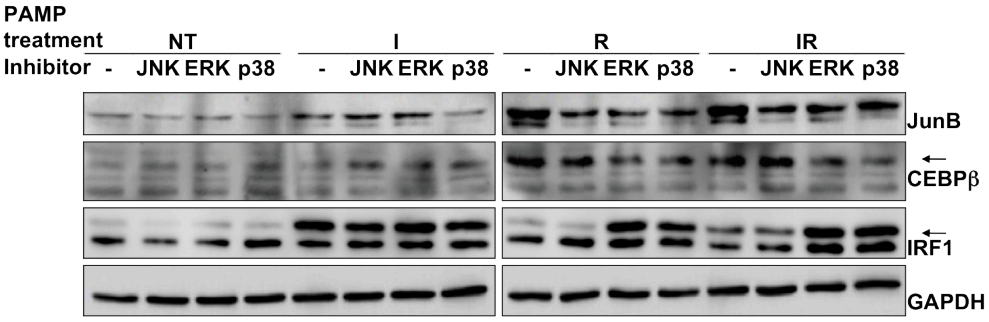

Figure 3.23. MAPK's role on JunB, C/EBPβ and IRF1 expression. BMDMs were treated with 10mM JNK, ERK or p38 inhibitor for 50 min, followed by I, R, IR or no treatment (NT) for 5 h. Cells were then lysed and analyzed with western blot against JunB, C/EBPβ, IRF1 and GAPDH antibody. Data are representative of three independent experiments. (Western blot for JunB and GAPDH were done in collaboration with lab mate Lu Ning)

3.6 JAK-STAT pathways upregulate synergy factor IRF1 induction under poly (I:C) stimulation.

Computational modeling predicted that JAK-STAT1 pathway to be important for cytokine expression. To check whether JAK-STAT1 pathway is involved in the regulation of synergy factors IRF1, JunB and C/EBPβ, we inhibited JAK1/2 with inhibitor Ruxolitinib. BMDMs were treated with 1 μM

Ruxolitinib for 1 h followed by I, R or IR treatment or no treatment (NT) control for 4 h before collected with RIPA buffer and analyzed with Western blot. As can be seen in **Figure 3.24**, the inhibition of JAK1/2 is successful because the phosphorylation of STAT1 at Tyr 701 was reduced when the inhibitor was added. JAK1/2 is known to phosphorylate STAT1 at Tyr 701 site after IFN activation [92]. In Figure 3.24, we observed reduced expression levels of IRF1 when cells were treated with poly (I:C) alone as well as the IR combinatorial stimulation. Under R stimulation, the expression level of IRF1 was very low and barely affected by the JAK1/2 inhibitor. This is not surprising, as poly (I:C) induced TLR3-TRIF pathway could induce type I IFN expression. Secreted type I IFN activates JAK-STAT1, which further activates its downstream signaling molecules, IRF1. However, the JAK1/2 inhibitor barely has any effect on the induction of JunB and C/EBPβ under all conditions, indicating the JAK-STAT1/2 pathway is not involved in the regulation of JunB and C/EBPβ.

This results indicate that the TLR3-TRIF pathway contributes to the induction of IRF1 through activating JAK-STAT1/2 signaling, and activated IRF1 could cooperate with TLR7-MyD88 induced JunB and C/EBPβ to regulate cytokine synergy. However, as shown previously in section 3.3.7, inhibition of JAK-STAT1/2 signaling by *Stat1* siRNA knockdown increased cytokine expression. Similar results have also been observed by other group, where inhibition of JAK1/2 increases LPS induced cytokine expression in macrophages [75]. This could be explained by the JAK-STAT1 induced I1-FFL loop as mentioned earlier in section 3.3.7. On one hand, JAK-STAT1/2 pathway could induce the cytokine regulatory transcription factor IRF1 which

upregulates cytokine expression. On the other hand the JAK-STAT1/2 pathway also induces anti-inflammatory cytokine IL10, which inhibits cytokine expression. Thus inhibition of JAK-STAT pathway might lead to biphasic responses.

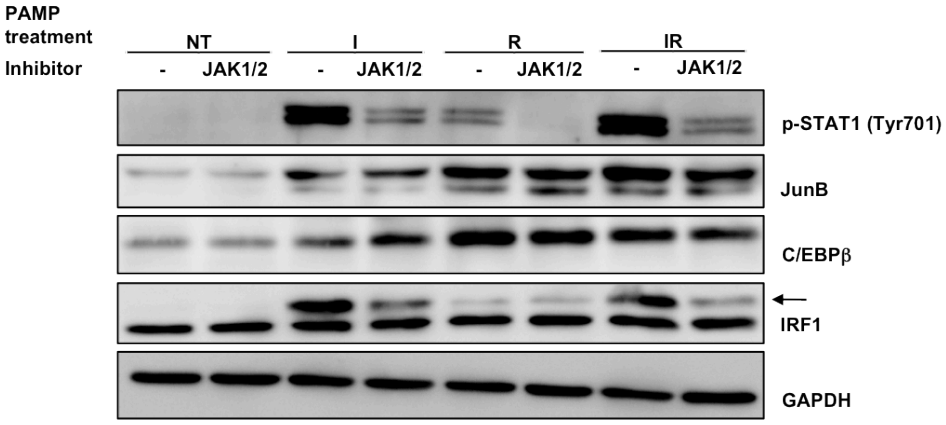

Figure 3.24. The JAK-STAT1 pathway upregulates IRF1 expression under I stimulation. BMDMs were incubated with JAK1/2 inhibitor Ruxolitinib (1mM) for 1 h before I or/ and R treatment for 4 h, or no PAMP treatment (NT). Cells were then dissolved in SDS PAGE and detected with Tyr701 phospho-STAT1, JunB, C/EBPβ, IRF1 and GAPDH. Data are representative of three independent experiments.

CHAPTER IV

DISCUSSION

CHAPTER IV. DISCUSSION

During an infection, innate immune cells such as tissue resident macrophages are the first to sense the foreign invasion through their PRRs. Activation of macrophages leads to production of cytokines and chemokines, which recruit more immune cells and initiate adaptive immune response. The amount of cytokines produced could vary a lot depending on the type of PRRs activated by the pathogen. Some combinations of TLRs, which activate both MyD88 and TRIF pathways, could induce cytokine synergy. The timing and magnitude of production of each cytokine in the immune system is finely tuned in response to infection. Loss of the balance and precision in cytokine production results in insufficient immune response or acute and/or chronic inflammatory diseases. However, the precise molecular mechanisms governing the expression of individual cytokine genes are only poorly investigated.

In our study, we identified key transcription factors, that regulate the expression of cytokine genes and we also found their upstream signaling pathways by computational modeling and empirical validation. Our results unravel the collaboration mechanism of TLR3-TLR7 signaling network to synergize cytokine expression.

4.1 Cooperation of transcription factors in the cytokine gene regulation.

Most of the proinflammatory cytokines are regulated by a collective of transcription factors, which bind to their promoters. After pathogen infection, numerous transcription factors are activated. And the activation of a given gene depends on a defined set of transcription factors activated by a defined

set of signaling pathways. By binding cooperatively to the control regions and forming a three-dimensional structural architecture for the recruitment of other coactivators, the factors will activate the transcription of the given gene synergistically. A classic example of cooperative binding and synergy between multiple transcription factors is the selective activation of human *IFNB* gene upon Sendai virus infection [93,94]. In Sendai virus-infected cells, a highly stable protein complex composed of NFκB, IRF3/IRF7 and ATF-2/cJun binds cooperatively on the promoter region of *IFNB*, maximizeing the production of *IFNB*.

Similar to the human *IFNB* promoter, we found that transcription factors cooperation also occurs during the activation of mouse *Il6* and *Il12b* genes after PAMP stimulation. By promoter pulldown, we demonstrated that IRF1, C/EBPβ and JunB are the critical components of the active transcription initiation complex of *Il6* and *Il12b*. siRNA knockdown further demonstrated that all these TFs are critical for optimal transcription of *Il6 and Il12b*. Additionally, we showed that IRF1 and C/EBPβ are responsive respectively, to TLR3/TRIF- and TLR7/MyD88-activation, while JunB is preferentially responsive to and sustained by TLR7-MyD88 under co-stimulation. Thus, under combinatorial stimulation, TLR3/TRIF responsive IRF1 and TLR/MyD88 responsive C/EBPβ and JunB collaborate and activate transcription of *Il6* and *Il12b* synergistically (**Figure 4.1**). However, we cannot rule out other yet-to-be defined "transcriptional synergy factor(s)," indicated as the X factor in Figure 4.1, which may be the product(s) of the cooperation of distinct pathways responsive to co-stimulation [85] or just TRIF/MyD88 responsive transcription factors.

Figure 4.1. A schematic representation of IRF1, JunB and C/EBPβ cooperation in cytokine *Il6* and *Il12b* regulation. Factor X is other unidentified TFs that might be involved in cytokine regulation.

Of the three transcription synergy factors we identified, IRF1 is of particular interest. Although known to be strongly induced in macrophages by IFN-γ, the detailed functional role and the mechanisms of IRF1 in regulating immune-responses are poorly documented [95]. An IRF1-binding element (-72 to -58) was characterized in the *Il12b* promoter [96] but not in the mouse *Il6* promoter. IRF1 was shown to play a major role in the transcriptional activation of the *Il12a* gene but not *Il12b* previously [97]. Current investigation revealed that IRF1 is the principle TF induced by the TLR3-TRIF signaling pathway and it binds both *Il6* and *Il12b* promoters. We also showed that C/EBPβ is necessary for cytokine synergy under combinatorial stimulation. C/EBPs recruit co-activators such as CBP and p300 [98,99], which in turn recruit basal TFs. An earlier investigation using *Il12b*-promoter reporter assay demonstrated that a proper distance and orientation of AP1 binding site (−79 to −74) and the adjacent C/EBP binding sites (−96 to −88) [100] are important for the promoter activation [101]. This correlates with our observation of the functional co-operation between C/EBPβ and AP1 member, JunB. On *Il6* promoter, binding sites of C/EBPβ and JunB have also been identified at -178~ -168 and -78~ -72, respectively [102]. JunB and C/EBPβ collaboratively form the core-transcriptional complex for the transcription of pro-inflammatory genes. However, to achieve a full transcriptional activity, IRF1 is required, prompting us to speculate that IRF1

functions as a bridging factor in the transcriptional regulation of *Il6* and *Il12b*, a hypothesis, which warrants further study.

Surprisingly, in the promoter pull-down analysis, we could not detect significant association of well-recognized master regulators such as NFκB and IRF3, to either *Il6* or *Il12b* promoter. NFκB-binding element has been characterized in the murine *Il12b* (−132 to −122) [89] and *Il6* (−75 to −63) [90]. However, as a primary response regulator, NFκB members likely function at the outset of the assembly of transcriptional initiation complex of pro-inflammatory cytokine gene *Il6* and *Il12b* [88]. The promoter-binding activity of NFκB could thus be transient and highly dynamic, and therefore not captured by pulldown assay. This is consistent with the observation of extremely weak signals of Rel members (Figure 3.19B), compared to the strong signals of IRF1, C/EBPβ and JunB. As for IRF3, which is deemed a master regulator of response to viral stimulations, it may simply function in upstream events (e.g. induce/activate other IRF members), but may not be physically involved in the transcription of pro-inflammatory cytokine genes.

4.2 Selective transcription of cytokine gene and immune homeostasis – an important role of R848-induced suppression of IRF1.

An inflammatory response is initiated by finely tuned activation of transcription factors. A central goal of immune system is to selectively modulate proinflammatory genes to maintain a robust host defense while suppressing genes responsible for inflammation-associated pathologies to avoid overwhelming inflammatory response.

In support of the above-mentioned notion, we found that the regulation of IRF1 during combinatorial stimulation might play a role to control the

magnitude and timing of cytokine expression. It is clear from Figure 3.20 that R848-induced MyD88 pathway is suppressing the expression of IRF1. Under single stimulation with poly(I:C), the up-regulated production of IRF1 is sustained and accumulated in the cells. In contrast, under co-stimulation, the expression level of IRF1 is curtailed. It falls back to a low basal level at 12 h post-stimulation. This inhibition of IRF1 expression correlates with the waning of Il6 and Il12b transcription over time, thus controlling the timing and magnitude of cytokine production.

Interestingly, the MAPK inhibitor study (Figure 3.24) revealed that R848-induced suppression of IRF1 might be through MAPK pathways. We observed enhanced IRF1 expression as well as increased cytokine expression when ERK and p38 are inhibited. IRF1 is known to be a target gene of STAT1. According to previous reports, activation of STAT1 requires phosphorylation at both the Tyr701 and Ser727 sites by JAK1/2 and p38, respectively [92]. However, when STAT1 is only phosphorylated at Ser727 site, it is retained in the cytoplasm and functions as a cytoplasmic inhibitor of TLR signaling. It is known that mice with mutation at Ser727 site of STAT1, has altered gene expression profile, with Il12p40 higher than wildtype mice [103]. In our study, it is possible that under R848 stimulation, IFNβ was barely produced, thus autocrine IFNβ-induced JAK1 is unlikely to be activated. But R848 could activate p38, which phosphorylates Ser727, but not Tyr701, leading to the altered STAT1 activity, and subsequently STAT1 target gene IRF1. The inhibition of IRF1 reduced the overwhelming production of pro-inflammatory cytokines and maintained immune homeostasis. However, it

is unclear why ERK also inhibited the expression of IRF1. This prompts a future study to check the phosphorylation site of STAT1 after ERK activation.

4.3 Cooperation of PRR signaling pathways in innate immune defense.

In our study, we demonstrated that TLR3 and TLR7 activate different combinations of transcription factors, which are collectively required for optimal transcription of cytokine gens, through activating distinct signaling pathways. TLR3 and TLR7 have been shown previously to be the most "cooperative" pair to induce cytokine synergy [57]. Although, theoretically, a combination of MyD88 and TRIF activating TLRs could induce cytokine synergy, some combinations are much weaker in inducing synergy. Only a low level of TNF, IL6 and IL12p40 synergy was observed when TLR2 was activated together with TLR3 and TLR4 [15,104]. In addition, TLRs with different subcellular localization might have distinct downstream signaling. An example is provided that TLR9 could activate different signaling pathways when they are located on different stage of endosome (early or late endosome) [105]. Thus the different cellular localizations of TLRs and the accessory molecules used that govern their signaling properties might affect their ability to interact "synergistically". It is possible that our findings on the interactive mechanism of TLR3-TLR7 is not a universal one for all combinations of TLRs that induces synergy.

Apart from TLRs, other PPRs including RLRs, CLRs and NLRs also contribute to PAMP recognition and the regulation of innate immunity [106]. As pathogens often contain various PAMPs which activate multiple PRRs, crosstalk of TLRs with other PRRs will be expected [106]. One example of

the crosstalk is between NLR and TLR, as bacterial peptidoglycans (TLR2 ligands) can be degraded into compounds that activate NOD1 and NOD2 [107-109]. In addition, double stranded RNA, poly(I:C), could activate both TLR3 (membrane binding receptor) and RLRs, MDA5 and RIG-I, in cytoplasm. Thus the synergy between TLR- and other PRRs can amplify the response not only to a single pathogen but also to a single component of a pathogen. Therefore, it is also important to reveal how immune responses are coordinated and regulated by different PRRs.

4.4 Computational modeling of signaling network crosstalk

Conventional cell and molecular biology look at genes, proteins and pathways separately at individual level. However, the molecules in a living cell work as a system and needs to be studied at global level, which make the collaboration of conventional research approach and computational biology an urgent need.

Our combined experimental and model-based computational analysis identified MAPK and JAK1-STAT1/2 to be critical signaling pathways for cytokine synergy. We elucidated the kinetic role of AP-1 and NFκB in determining cytokine production, and showed different roles of JNK, ERK and p38 in cytokine expression regulation, which are verified by empirical data. Notably, one of our key findings is that STAT1 level induces a biphasic response of cytokine production through an incoherent type 1 feedforward loop (I1-FFL). I1-FFL is one of the most frequently observed network motifs in biological networks. It appears hundreds of times in bacteria [110], yeast [111], and animals [111,112]. It has been reported that the roles of I1-FFL

include (see a recent review [81]): (i) shortening gene-circuit response time, (ii) generating of gene expression pulses, [81](iii) distinguishing time-varying inputs, (iv) filtering out noise, (v) detecting fold change of input signal, and (vi) generating non-monotonic input-output relations [81]. There exists several I1-FFLs in our model, mediated by ERK, p38 and STAT1 respectively. We found that the STAT1-dependent I1-FFL, exhibiting biphasic response, is crucial to both amplifying antiviral response and avoiding excessive inflammatory response. This is a case study that further demonstrated the importance of I1-FFL in innate immune system.

Notably, I1-FFL might be a good explanation for the controversial effect of type I IFN autocrine loop (Details in section 1.4.2). Some groups added exogenous IFNβ, but did not further enhance the cytokine production [16,43]. On the contrary, knockout of IFNβ receptor abolished synergism in cytokine production completely or partially [15]. This controversy might be a result of biphasic response of STAT1-dependent I1-FFL. On one hand, STAT1 induces IRF1, which is needed for cytokine expression. On the other hand, JAK-STAT pathway increases the level of anti-inflammatory cytokine IL10, which inhibits cytokine expression. The blockage of JAK-STAT pathway through manipulating the upstream inducer IFN might affect the two arms of JAK-STAT pathway. And the outcome is difficult to predict depending on the level of pathway blockage. Such kind of biphasic response is difficult to control through experiment, but can be predictable with computational modeling.

In the past two decades, intense research has identified and characterized hundreds of components and interactions for TLR signaling.

Various systems biology approaches have been used for enhancing our understanding of TLR-mediated innate immune responses [51]. However, an accurate and validated mathematical model of TLR signaling pathways, taking into account of their dynamic crosstalk has not yet been derived [52,53,56,113-121]. In our project, we developed the first calibrated ODE based kinetic model for two specific TLR pathways and their crosstalk. This is an important step towards a comprehensive mathematical model for all TLR pathways. But in the mean time, we cannot overlook some of the limitations of our model. As we have adopted most of the protein-protein interaction information from literature, some of the interaction information is achieved by overexpression experiments in HEK cells, which might not be reproducible in immune cells. In addition, the TLR signaling is a very complex network with a lot of cell type specific regulatory mechanisms, feedback loops, which are not considered in our model. Most importantly, our model didn't incorporate the synergy factors identified with conventional biological methods and their presumable upstream signaling. Thus, as new knowledge becomes available, our present model should be refined and extended exhaustively to reveal the TLR signaling network more accurately.

CHAPTER V

CONCLUSIONS AND FUTURE PERSPECTIVES

CHAPTER IV. CONCLUSIONS AND FUTURE PERSPECTIVES

5.1 Conclusion

During pathogen infection, host innate immune cells encounter multiple PAMPs, which activate multiple TLRs. Ligands that activate both MyD88 and TRIF pathways could induce synergistic expression of cytokines, but the underlying mechanism is still an enigma. In this study, we clarified that activation of NFκB members, chromatin remodeling (unpacking and DNA modification) and post-transcriptional regulation may be redundantly and/or additively induced by PAMP stimulations, and showed that the TLR3-TRIF- and TLR7-MyD88- signaling pathways synergize directly at the transcription of *Il6* and *Il12b*. TRIF pathway activates JAK1-STAT1 pathway which induces activation of IRF1, while MyD88 pathway induces JunB and C/EBPβ through activating MAPK pathways. Activated IRF1, JunB and C/EBPβ are required for optimal cytokine expression. Thus, TLR3-TRIF and TLR7-MyD88 combinatorial activation synchronized and sustained the activation of transcription factors that are necessary for cytokine expression.

Under single stimulation with poly(I:C), there is only mild expression of JunB, plausibly induced by p38 (In Figure 3.24, p38 inhibitor could inhibit the expression of JunB under I single stimulation), and barely any C/EBPβ production. IRF1 is mainly produced under TRIF pathway through JAK1/2-STAT1 pathway, which was activated by autocrine type I IFN (**Figure 5.1**). Thus, only IRF1 and a small amount of JunB is present, which is not sufficient for the expression of cytokines and only a negligible level of *Il6* and *Il12b* can be detected under I stimulation.

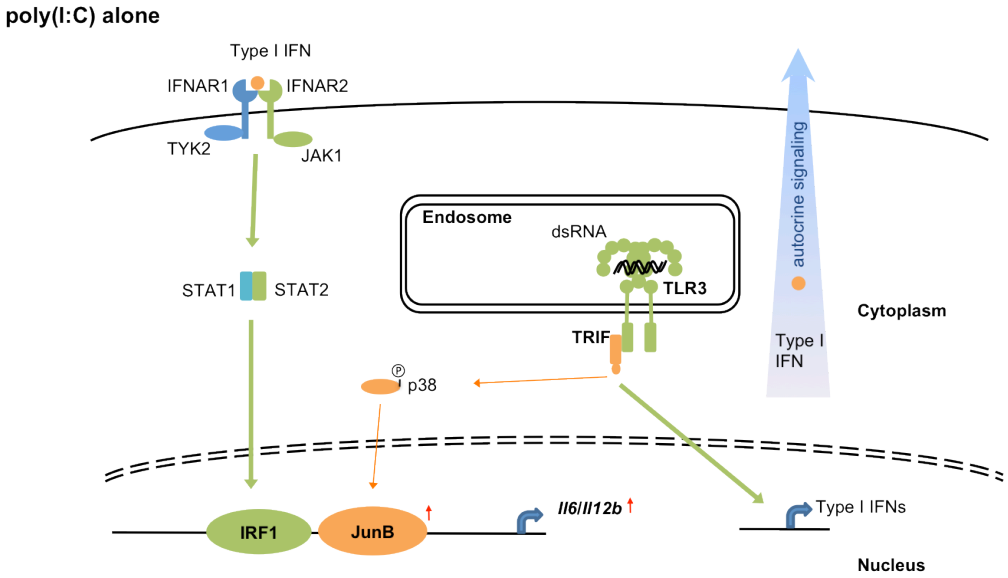

Figure 5.1. The signaling and transcriptional events occur after poly (I:C) single stimulation. Under poly (I:C) (dsRNA analogue) single stimulation, TLR3-TRIF gets activated, which mainly induces the expression of type I IFN. The autocrined type I IFN binds to its receptor and activate TYK2-JAK1, which activates STAT1 and its target genes including IRF1. TRIF pathway could also activate a marginal amount of JunB, plausibly through p38 MAPK. Both IRF1 and JunB are required for cytokine expression, however another necessary TF, C/EBPβ could not be induced under TRIF alone pathway, which results in negligible amount of cytokine *Il6* and *Il12b* production.

Under single stimulation with R848, C/EBPβ and more JunB are activated through MAPK pathways. However, MyD88 pathway is not the major activator of type I IFN, which activates IRF1 through an autocrine loop. Furthermore, MAPK p38 and ERK activated by MyD88 pathway inhibit the expression of IRF1. Thus, there is only transient induction of IRF1 (**Figure 5.2**). The optimal condition for cytokine expression, where all of the three transcription factors are present, is transient and thereafter, only mild expressions of cytokine *Il6* and *Il12b* were detected under R848 single stimulation.

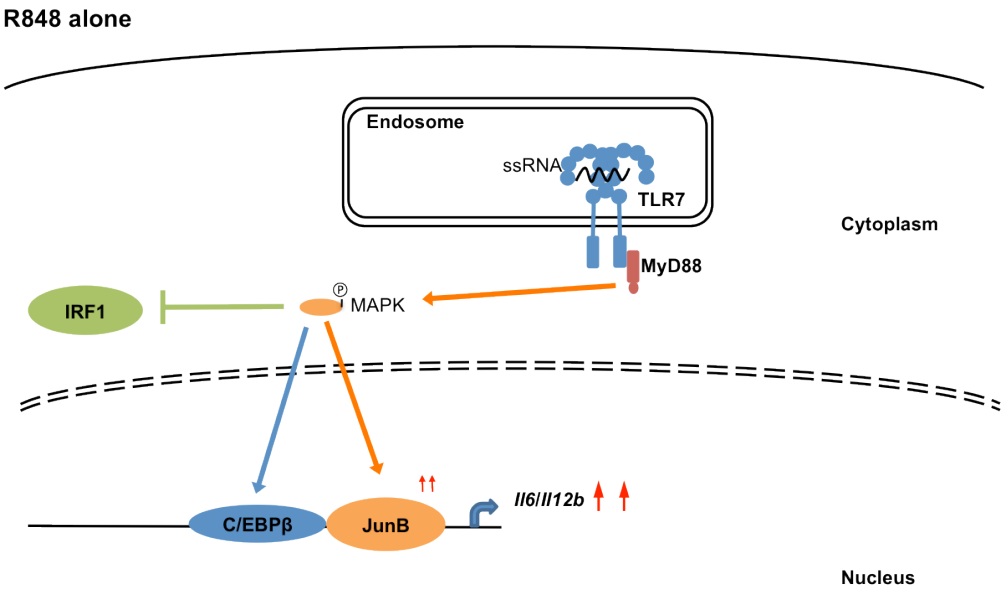

Figure 5.2. The signaling and transcriptional events occur after R848 single stimulation. Under R848 (ssRNA analogue) single stimulation, TLR7-MyD88 is activated, which could activate JunB and C/EBPβ through MAPK pathways. However, TLR7-MyD88 pathway is not the main inducer of type I IFN, and it activates p38 and ERK, which inhibits IRF1 expression. Thus only transient and little amount of IRF1 is induced under R848 stimulation. A mild amount of cytokine level could be detected under this condition, but cytokine synergy is not observed due to insufficient amount of IRF1.

Under combinatorial stimulation, C/EBPβ and JunB are activated through MyD88-MAPK pathways, providing sufficient amounts of these two transcription factors for cytokine expression. Although the MyD88 induced p38 and ERK MAPK inhibited IRF1, the autocrine type I IFN, which is significantly induced by TLR3-TRIF pathway, sustained the IRF1 activation longer than R848 single stimulation (**Figure 5.3**). Thus, under combinatorial stimulation, TLR3-TRIF and TLR7-MyD88 pathway collaborate to synchronize and sustain the activation of IRF1, JunB and C/EBPβ, which provides optimal condition for cytokine transcription and make cytokine synergy occur. Notably, the inhibitory role of R848 on IRF1 controls the magnitude of immune responses and maintains immune homeostasis. However, we cannot rule out other possible transcriptional synergy factors

(factor X), which might be induced only after combinatorial stimulation or favorably induced by either MyD88 or TRIF pathway, and are needed for cytokine synergy.

In addition, by turning to computational methods, our study demonstrated that the SMC-based framework [80] was able to obtain good estimates for hundreds of unknown parameters by fitting noisy cell-population data and qualitative knowledge. We developed the first calibrated ODE based kinetic model for two specific TLR pathways and their crosstalk. Furthermore, we also showed that this framework enables the computation of local and global sensitivities of parameters for a large signaling network and has excellent descriptive and predictive properties. This is an important step towards a comprehensive mathematical model for all TLR pathways. The model also provides an invaluable platform for designing pharmaceutical strategies on regulating the immune priming of host cells, which could improve the immunotherapy efficacy.

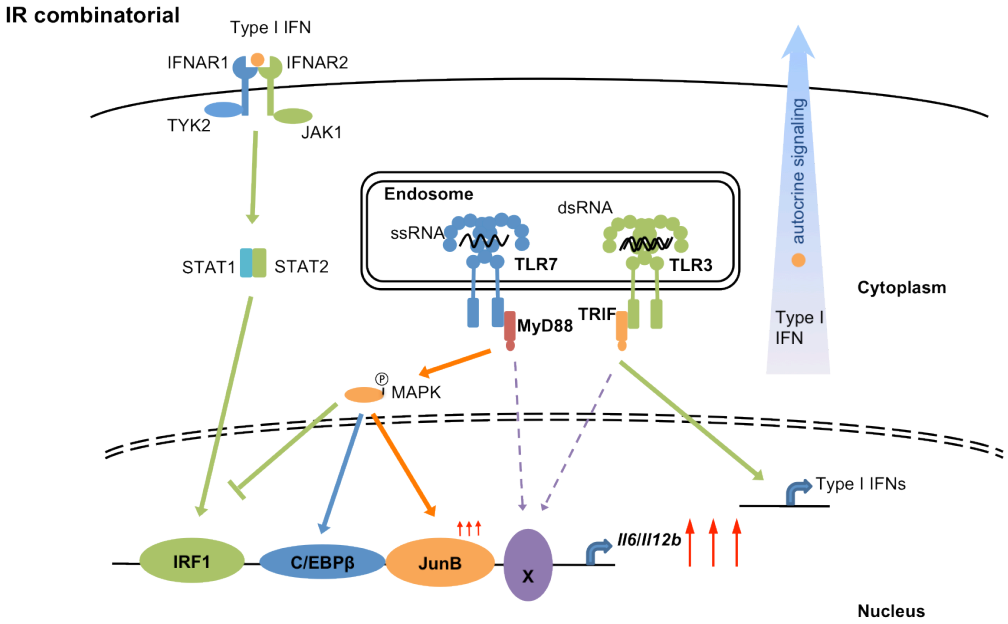

Figure 5.3. The signaling and transcriptional events occur after poly (I:C) and R848 combinatorial stimulation. Under combinatorial stimulation, both MyD88 and TRIF pathway are activated. MyD88 induces activation of JunB and C/EBPβ through activating MAPKs. Although the MyD88 induced p38 and ERK MAPK inhibit IRF1, the autocined type I IFN, which is significantly induced by TLR3-TRIF pathway, sustained the IRF1 activation longer than R848 single stimulation. Thus all of the three transcription factors are present for sufficient time to maximize cytokine expression. But other potential synergy factors which might be produced only under combinatorial stimulation or favorably induced by either MyD88 or TRIF pathway could also exist, which might be necessary for cytokine synergy.

5.2 Future perspectives

Based on this thesis work, there are several interesting directions for future study to shed more light on the signaling mechanism of TLR pathways.

5.2.1 The regulatory mechanism on IRF1 expression

From this thesis work, we observed an interesting inhibitory effect of R848 on IRF1 expression. We also demonstrated that R848 might be inhibiting IRF1 expression through p38 and ERK pathway. However, the detailed mechanism of how p38 and ERK pathway inhibit IRF1 expression needs to be elucidated. In addition, MyD88 pathway is not known to be a major inducer of type I IFN. Thus, the autocrine type I IFN is not sufficient to induce IRF1 expression under R848 stimulation. Nevertheless, we did observe decent amount of IRF1 expression in the presence of p38 and ERK inhibitor under R848 single stimulation, and these IRF1 might be induced through mechanisms other than type I IFN induced autocrine signaling. Thus it would be interesting to further investigate the upstream signal of IRF1 under R848 stimulation and the detailed mechanism of how MAPK inhibit IRF1 expression.

5.2.2 The upstream signal of JunB and C/EBPβ

Although we have found that MAPK plays a role in JunB and C/EBPβ expression through MAPK inhibitor study, there might be other upstream signaling pathways responsible for the induction of JunB and C/EBPβ. As both JunB and C/EBPβ are closely related to cytokine expression, it's necessary to find out more about their regulatory mechanism.

5.2.3 The function of IL12p40 produced by macrophages

IL12p40 is known to be a subunit of IL12 and IL23. It could form heterodimer with IL12p35 to make IL12, and with IL12p19 to make IL23, respectively. However, we detected high level of IL12p40 expression in macrophages but not IL12p35 and IL12p19, indicating that IL12p40 might have other roles besides functioning as a subunit of IL12 and IL23. One previous research on IL12p40 suggest that it could form a homodimer of IL12-p80 to serve as pro-inflammatory cytokine to recruit more innate immune cells [65]. However, other researches indicate it as an inherently agonistic cytokine [122]. Thus the precise role of IL12p40 produced by macrophages need to be verified.

5.2.4 TLR crosstalk with other PRRs

Apart from TLRs, other PPRs including RIG-I-like receptors (RLRs), C-type lectin receptors, NOD-like receptors, also contribute to PAMP recognition and the regulation of innate immunity [106]. As pathogens often contain various PAMPs activating multiple PRRs, TLRs in crosstalk with other PRRs, orchestrate both host innate and adaptive immune responses to combat the infections [106]. For instance, hepatitis C virus (HCV) can be recognized by both TLR3 and retinoic acid-inducible gene 1 (RIG-I). The HCV RNA delivered from infected hepatocytes can also trigger TLR7 pathway [123]. PRR crosstalk can either positively or negatively regulate the eventual immune responses. For example, combinatorial stimulation of NOD2 and TLR2 attenuates IL12 production in human DCs, whereas NOD2 activation significantly enhanced IL12 induction in response to activation of

other TLRs such as TLR7 and 8 [6]. Interestingly, the production of cytokines induced by TLR2 ligands, but not by other TLR ligands, was shown to be higher in mice deficient for NOD2 compared with wild-type mice [124]. Different types of collaborative responses have been reviewed by Tan et al [125]. Thus, it is important to reveal how immune responses are coordinated and regulated by different PRRs.

5.2.5 Cell type-specific TLR crosstalk

Different cells behave differently to PAMP stimulation. For example, macrophages produce high level of IL12p40 but marginal level of IL12p35 after PAMP stimulation, whereas DCs produce more IL12p35. In this thesis work, our main focus is on macrophages. However, same synergy mechanism might not apply to other cell types such dendritic cells, as they produce different sets of cytokines, plausibly through activation of different downstream pathways of MyD88 and TRIF. In this context, an intriguing future direction will be to extend our study on TLR crosstalk in different cell types.

5.2.6 The mechanism of synergistic IL10 production under combinatorial TLR3-TLR7 activation.

In the cytokine screening, IL10 also showed high synergy fold. As an anti-inflammatory cytokine, the regulatory mechanism of IL10 is very different from IL6 and IL12p40. Since IL10 is anti-inflammatory, it can regulate the crosstalk between TLR3 and TLR7, although not at the transcriptional level. Many autocrine cytokines would feed back and

upregulate the production of IL10. In addition, as a primary response gene, *Il10* might also be regulated at post-transcriptional level instead of transcriptional level. Thus the mechanisms of synergistic production of *Il10* would be interesting to further study.

5.2.7 TLR3-TLR7 crosstalk in human system

Our study was carried out in mouse model. Translation of our findings in mouse system may be performed using human cells such as PBMC (Peripheral Blood Mononuclear Cell) derived macrophages.

5.2.8 The regulation of synergy factors in human patient with auto-immune diseases

Patients with autoimmune diseases tend to have uncontrolled production of cytokine. As mentioned in Introduction 1.3.3, elevated levels of IL6, IL12p40 and IL12p19 were observed in SLE patients as well as mouse models. MyD88 deficient mouse produces less IFNα, IL6 and IL12, and delays the mortality of SLE and prevents nephritis and immunologic aberrations than wild type mouse. Thus it would be interesting to examine the expression level of synergy factors IRF1, CEBPβ and JunB in autoimmune disease patient samples.

BIBLIOGRAPHY

BIBLIOGRAPHY

1. Janeway CA, Jr., Medzhitov R (2002) Innate immune recognition. Annu Rev Immunol 20: 197-216.
2. Murphy KP, Travers P, Walport M, Janeway C (2008) Janeway's Immunobiology: Garland Science.
3. Takeuchi O, Akira S (2010) Pattern recognition receptors and inflammation. Cell 140: 805-820.
4. Rubartelli A, Lotze MT (2007) Inside, outside, upside down: damage-associated molecular-pattern molecules (DAMPs) and redox. Trends Immunol 28: 429-436.
5. Kawai T, Akira S (2010) The role of pattern-recognition receptors in innate immunity: update on Toll-like receptors. Nat Immunol 11: 373-384.
6. Trinchieri G, Sher A (2007) Cooperation of Toll-like receptor signals in innate immune defence. Nat Rev Immunol 7: 179-190.
7. Hansson GK, Edfeldt K (2005) Toll to be paid at the gateway to the vessel wall. Arterioscler Thromb Vasc Biol 25: 1085-1087.
8. Lemaitre B, Nicolas E, Michaut L, Reichhart JM, Hoffmann JA (1996) The dorsoventral regulatory gene cassette spatzle/Toll/cactus controls the potent antifungal response in Drosophila adults. Cell 86: 973-983.
9. Medzhitov R, Preston-Hurlburt P, Janeway CA, Jr. (1997) A human homologue of the Drosophila Toll protein signals activation of adaptive immunity. Nature 388: 394-397.
10. Birbach A, Gold P, Binder BR, Hofer E, de Martin R, et al. (2002) Signaling molecules of the NF-kappa B pathway shuttle constitutively between cytoplasm and nucleus. J Biol Chem 277: 10842-10851.
11. Ishii KJ, Koyama S, Nakagawa A, Coban C, Akira S (2008) Host innate immune receptors and beyond: making sense of microbial infections. Cell Host Microbe 3: 352-363.
12. Honda K, Taniguchi T (2006) IRFs: master regulators of signalling by Toll-like receptors and cytosolic pattern-recognition receptors. Nat Rev Immunol 6: 644-658.
13. Panneerselvam P, Singh LP, Selvarajan V, Chng WJ, Ng SB, et al. (2013) T-cell death following immune activation is mediated by mitochondria-localized SARM. Cell Death Differ 20: 478-489.
14. Whitmore MM, DeVeer MJ, Edling A, Oates RK, Simons B, et al. (2004) Synergistic activation of innate immunity by double-stranded RNA and CpG DNA promotes enhanced antitumor activity. Cancer Res 64: 5850-5860.
15. Gautier G, Humbert M, Deauvieau F, Scuiller M, Hiscott J, et al. (2005) A type I interferon autocrine-paracrine loop is involved in Toll-like receptor-induced interleukin-12p70 secretion by dendritic cells. J Exp Med 201: 1435-1446.
16. Napolitani G, Rinaldi A, Bertoni F, Sallusto F, Lanzavecchia A (2005) Selected Toll-like receptor agonist combinations synergistically

trigger a T helper type 1-polarizing program in dendritic cells. Nat Immunol 6: 769-776.
17. Bafica A, Scanga CA, Feng CG, Leifer C, Cheever A, et al. (2005) TLR9 regulates Th1 responses and cooperates with TLR2 in mediating optimal resistance to Mycobacterium tuberculosis. J Exp Med 202: 1715-1724.
18. Tabeta K, Georgel P, Janssen E, Du X, Hoebe K, et al. (2004) Toll-like receptors 9 and 3 as essential components of innate immune defense against mouse cytomegalovirus infection. Proc Natl Acad Sci U S A 101: 3516-3521.
19. Re F, Strominger JL (2004) IL-10 released by concomitant TLR2 stimulation blocks the induction of a subset of Th1 cytokines that are specifically induced by TLR4 or TLR3 in human dendritic cells. J Immunol 173: 7548-7555.
20. Liu YC, Simmons DP, Li X, Abbott DW, Boom WH, et al. (2012) TLR2 signaling depletes IRAK1 and inhibits induction of type I IFN by TLR7/9. J Immunol 188: 1019-1026.
21. Marshall JD, Heeke DS, Gesner ML, Livingston B, Van Nest G (2007) Negative regulation of TLR9-mediated IFN-alpha induction by a small-molecule, synthetic TLR7 ligand. J Leukoc Biol 82: 497-508.
22. Mosser DM (2003) The many faces of macrophage activation. J Leukoc Biol 73: 209-212.
23. Bjorkbacka H, Fitzgerald KA, Huet F, Li X, Gregory JA, et al. (2004) The induction of macrophage gene expression by LPS predominantly utilizes Myd88-independent signaling cascades. Physiol Genomics 19: 319-330.
24. Berg DJ, Davidson N, Kuhn R, Muller W, Menon S, et al. (1996) Enterocolitis and colon cancer in interleukin-10-deficient mice are associated with aberrant cytokine production and CD4(+) TH1-like responses. J Clin Invest 98: 1010-1020.
25. Parrillo JE (1993) Pathogenetic mechanisms of septic shock. N Engl J Med 328: 1471-1477.
26. Medzhitov R (2008) Origin and physiological roles of inflammation. Nature 454: 428-435.
27. Renshaw M, Rockwell J, Engleman C, Gewirtz A, Katz J, et al. (2002) Cutting edge: impaired Toll-like receptor expression and function in aging. J Immunol 169: 4697-4701.
28. Boyd AR, Shivshankar P, Jiang S, Berton MT, Orihuela CJ (2012) Age-related defects in TLR2 signaling diminish the cytokine response by alveolar macrophages during murine pneumococcal pneumonia. Exp Gerontol 47: 507-518.
29. Liang S, Domon H, Hosur KB, Wang M, Hajishengallis G (2009) Age-related alterations in innate immune receptor expression and ability of macrophages to respond to pathogen challenge in vitro. Mech Ageing Dev 130: 538-546.
30. Nyugen J, Agrawal S, Gollapudi S, Gupta S (2010) Impaired functions of peripheral blood monocyte subpopulations in aged humans. J Clin Immunol 30: 806-813.

31. van Duin D, Mohanty S, Thomas V, Ginter S, Montgomery RR, et al. (2007) Age-associated defect in human TLR-1/2 function. J Immunol 178: 970-975.
32. Agius E, Lacy KE, Vukmanovic-Stejic M, Jagger AL, Papageorgiou AP, et al. (2009) Decreased TNF-alpha synthesis by macrophages restricts cutaneous immunosurveillance by memory CD4+ T cells during aging. J Exp Med 206: 1929-1940.
33. Panda A, Qian F, Mohanty S, van Duin D, Newman FK, et al. (2010) Age-associated decrease in TLR function in primary human dendritic cells predicts influenza vaccine response. J Immunol 184: 2518-2527.
34. Della Bella S, Bierti L, Presicce P, Arienti R, Valenti M, et al. (2007) Peripheral blood dendritic cells and monocytes are differently regulated in the elderly. Clin Immunol 122: 220-228.
35. Qian F, Wang X, Zhang L, Lin A, Zhao H, et al. (2011) Impaired interferon signaling in dendritic cells from older donors infected in vitro with West Nile virus. J Infect Dis 203: 1415-1424.
36. Nimah M, Brilli RJ (2003) Coagulation dysfunction in sepsis and multiple organ system failure. Crit Care Clin 19: 441-458.
37. Huang X, Hua J, Shen N, Chen S (2007) Dysregulated expression of interleukin-23 and interleukin-12 subunits in systemic lupus erythematosus patients. Mod Rheumatol 17: 220-223.
38. Linker-Israeli M (1992) Cytokine abnormalities in human lupus. Clin Immunol Immunopathol 63: 10-12.
39. Metsarinne KP, Nordstrom DC, Konttinen YT, Teppo AM, Fyhrquist FY (1992) Plasma interleukin-6 and renin substrate in reactive arthritis, rheumatoid arthritis, and systemic lupus erythematosus. Rheumatol Int 12: 93-96.
40. Linker-Israeli M, Deans RJ, Wallace DJ, Prehn J, Ozeri-Chen T, et al. (1991) Elevated levels of endogenous IL-6 in systemic lupus erythematosus. A putative role in pathogenesis. J Immunol 147: 117-123.
41. Spronk PE, ter Borg EJ, Limburg PC, Kallenberg CG (1992) Plasma concentration of IL-6 in systemic lupus erythematosus; an indicator of disease activity? Clin Exp Immunol 90: 106-110.
42. Adachi O, Kawai T, Takeda K, Matsumoto M, Tsutsui H, et al. (1998) Targeted disruption of the MyD88 gene results in loss of IL-1- and IL-18-mediated function. Immunity 9: 143-150.
43. Bagchi A, Herrup EA, Warren HS, Trigilio J, Shin HS, et al. (2007) MyD88-dependent and MyD88-independent pathways in synergy, priming, and tolerance between TLR agonists. J Immunol 178: 1164-1171.
44. Zhou L, Nazarian AA, Xu J, Tantin D, Corcoran LM, et al. (2007) An inducible enhancer required for Il12b promoter activity in an insulated chromatin environment. Mol Cell Biol 27: 2698-2712.
45. Zhu Q, Egelston C, Vivekanandhan A, Uematsu S, Akira S, et al. (2008) Toll-like receptor ligands synergize through distinct dendritic cell pathways to induce T cell responses: implications for vaccines. Proc Natl Acad Sci U S A 105: 16260-16265.

46. Krummen M, Balkow S, Shen L, Heinz S, Loquai C, et al. (2010) Release of IL-12 by dendritic cells activated by TLR ligation is dependent on MyD88 signaling, whereas TRIF signaling is indispensable for TLR synergy. J Leukoc Biol 88: 189-199.
47. Weinmann AS, Mitchell DM, Sanjabi S, Bradley MN, Hoffmann A, et al. (2001) Nucleosome remodeling at the IL-12 p40 promoter is a TLR-dependent, Rel-independent event. Nat Immunol 2: 51-57.
48. Bohnenkamp HR, Papazisis KT, Burchell JM, Taylor-Papadimitriou J (2007) Synergism of Toll-like receptor-induced interleukin-12p70 secretion by monocyte-derived dendritic cells is mediated through p38 MAPK and lowers the threshold of T-helper cell type 1 responses. Cell Immunol 247: 72-84.
49. Makela SM, Strengell M, Pietila TE, Osterlund P, Julkunen I (2009) Multiple signaling pathways contribute to synergistic TLR ligand-dependent cytokine gene expression in human monocyte-derived macrophages and dendritic cells. J Leukoc Biol 85: 664-672.
50. Ouyang X, Negishi H, Takeda R, Fujita Y, Taniguchi T, et al. (2007) Cooperation between MyD88 and TRIF pathways in TLR synergy via IRF5 activation. Biochem Biophys Res Commun 354: 1045-1051.
51. Vandenbon A, Teraguchi S, Akira S, Takeda K, Standley DM (2012) Systems biology approaches to toll-like receptor signaling. Wiley Interdiscip Rev Syst Biol Med 4: 497-507.
52. Oda K, Kitano H (2006) A comprehensive map of the toll-like receptor signaling network. Mol Syst Biol 2: 2006 0015.
53. Li S, Wang L, Berman M, Kong YY, Dorf ME (2011) Mapping a dynamic innate immunity protein interaction network regulating type I interferon production. Immunity 35: 426-440.
54. Helmy M, Gohda J, Inoue J, Tomita M, Tsuchiya M, et al. (2009) Predicting novel features of toll-like receptor 3 signaling in macrophages. PLoS One 4: e4661.
55. Krishnan J, Selvarajoo K, Tsuchiya M, Lee G, Choi S (2007) Toll-like receptor signal transduction. Exp Mol Med 39: 421-438.
56. Covert MW, Leung TH, Gaston JE, Baltimore D (2005) Achieving stability of lipopolysaccharide-induced NF-kappaB activation. Science 309: 1854-1857.
57. Suet Ting Tan R, Lin B, Liu Q, Tucker-Kellogg L, Ho B, et al. (2013) The synergy in cytokine production through MyD88-TRIF pathways is co-ordinated with ERK phosphorylation in macrophages. Immunol Cell Biol 91: 377-387.
58. Lee C, Huang CH (2013) LASAGNA: a novel algorithm for transcription factor binding site alignment. BMC Bioinformatics 14: 108.
59. Weinmann AS, Plevy SE, Smale ST (1999) Rapid and selective remodeling of a positioned nucleosome during the induction of IL-12 p40 transcription. Immunity 11: 665-675.
60. Dutta B, Adav SS, Koh CG, Lim SK, Meshorer E, et al. (2012) Elucidating the temporal dynamics of chromatin-associated protein release upon DNA digestion by quantitative proteomic approach. J Proteomics 75: 5493-5506.

61. Hao P, Qian J, Ren Y, Sze SK (2011) Electrostatic repulsion-hydrophilic interaction chromatography (ERLIC) versus strong cation exchange (SCX) for fractionation of iTRAQ-labeled peptides. J Proteome Res 10: 5568-5574.
62. Mi H, Muruganujan A, Thomas PD (2013) PANTHER in 2013: modeling the evolution of gene function, and other gene attributes, in the context of phylogenetic trees. Nucleic Acids Res 41: D377-386.
63. Huang da W, Sherman BT, Lempicki RA (2009) Systematic and integrative analysis of large gene lists using DAVID bioinformatics resources. Nat Protoc 4: 44-57.
64. D'Andrea A, Rengaraju M, Valiante NM, Chehimi J, Kubin M, et al. (1992) Production of natural killer cell stimulatory factor (interleukin 12) by peripheral blood mononuclear cells. J Exp Med 176: 1387-1398.
65. Gunsten S, Mikols CL, Grayson MH, Schwendener RA, Agapov E, et al. (2009) IL-12 p80-dependent macrophage recruitment primes the host for increased survival following a lethal respiratory viral infection. Immunology 126: 500-513.
66. Li K, Li NL, Wei D, Pfeffer SR, Fan M, et al. (2012) Activation of chemokine and inflammatory cytokine response in hepatitis C virus-infected hepatocytes depends on Toll-like receptor 3 sensing of hepatitis C virus double-stranded RNA intermediates. Hepatology 55: 666-675.
67. Ramirez-Carrozzi VR, Braas D, Bhatt DM, Cheng CS, Hong C, et al. (2009) A unifying model for the selective regulation of inducible transcription by CpG islands and nucleosome remodeling. Cell 138: 114-128.
68. Ouyang W, Rutz S, Crellin NK, Valdez PA, Hymowitz SG (2011) Regulation and functions of the IL-10 family of cytokines in inflammation and disease. Annu Rev Immunol 29: 71-109.
69. Doyle S, Vaidya S, O'Connell R, Dadgostar H, Dempsey P, et al. (2002) IRF3 mediates a TLR3/TLR4-specific antiviral gene program. Immunity 17: 251-263.
70. Oeckinghaus A, Hayden MS, Ghosh S (2011) Crosstalk in NF-kappaB signaling pathways. Nat Immunol 12: 695-708.
71. Platanias LC (2005) Mechanisms of type-I- and type-II-interferon-mediated signalling. Nat Rev Immunol 5: 375-386.
72. Yang CH, Murti A, Pfeffer LM (2005) Interferon induces NF-kappa B-inducing kinase/tumor necrosis factor receptor-associated factor-dependent NF-kappa B activation to promote cell survival. J Biol Chem 280: 31530-31536.
73. Yang CH, Murti A, Pfeffer SR, Kim JG, Donner DB, et al. (2001) Interferon alpha /beta promotes cell survival by activating nuclear factor kappa B through phosphatidylinositol 3-kinase and Akt. J Biol Chem 276: 13756-13761.
74. Arthur JS, Ley SC (2013) Mitogen-activated protein kinases in innate immunity. Nat Rev Immunol 13: 679-692.

75. Pattison MJ, Mackenzie KF, Arthur JS (2012) Inhibition of JAKs in macrophages increases lipopolysaccharide-induced cytokine production by blocking IL-10-mediated feedback. J Immunol 189: 2784-2792.
76. Murray PJ (2006) Understanding and exploiting the endogenous interleukin-10/STAT3-mediated anti-inflammatory response. Curr Opin Pharmacol 6: 379-386.
77. Takeda K, Clausen BE, Kaisho T, Tsujimura T, Terada N, et al. (1999) Enhanced Th1 activity and development of chronic enterocolitis in mice devoid of Stat3 in macrophages and neutrophils. Immunity 10: 39-49.
78. Kuttykrishnan S, Sabina J, Langton LL, Johnston M, Brent MR (2010) A quantitative model of glucose signaling in yeast reveals an incoherent feed forward loop leading to a specific, transient pulse of transcription. Proc Natl Acad Sci U S A 107: 16743-16748.
79. Lipniacki T, Paszek P, Brasier AR, Luxon B, Kimmel M (2004) Mathematical model of NF-kappaB regulatory module. J Theor Biol 228: 195-215.
80. Palaniappan S, Gyori B, Liu B, Hsu D, Thiagarajan PS (2013) Statistical model checking based calibration and analysis of bio-pathway models. Lecture Notes in Computer Science 8130: 120-134.
81. Hart Y, Alon U (2013) The utility of paradoxical components in biological circuits. Mol Cell 49: 213-221.
82. Kim D, Kwon YK, Cho KH (2008) The biphasic behavior of incoherent feed-forward loops in biomolecular regulatory networks. Bioessays 30: 1204-1211.
83. Iglesias MJ, Reilly SJ, Emanuelsson O, Sennblad B, Pirmoradian Najafabadi M, et al. Combined chromatin and expression analysis reveals specific regulatory mechanisms within cytokine genes in the macrophage early immune response. PLoS One 7: e32306.
84. Aung HT, Schroder K, Himes SR, Brion K, van Zuylen W, et al. (2006) LPS regulates proinflammatory gene expression in macrophages by altering histone deacetylase expression. FASEB J 20: 1315-1327.
85. Kayama H, Ramirez-Carrozzi VR, Yamamoto M, Mizutani T, Kuwata H, et al. (2008) Class-specific regulation of pro-inflammatory genes by MyD88 pathways and IkappaBzeta. J Biol Chem 283: 12468-12477.
86. Armenante F, Merola M, Furia A, Tovey M, Palmieri M (1999) Interleukin-6 repression is associated with a distinctive chromatin structure of the gene. Nucleic Acids Res 27: 4483-4490.
87. Ow SY, Salim M, Noirel J, Evans C, Wright PC (2011) Minimising iTRAQ ratio compression through understanding LC-MS elution dependence and high-resolution HILIC fractionation. Proteomics 11: 2341-2346.
88. Gilchrist M, Thorsson V, Li B, Rust AG, Korb M, et al. (2006) Systems biology approaches identify ATF3 as a negative regulator of Toll-like receptor 4. Nature 441: 173-178.

89. Murphy TL, Cleveland MG, Kulesza P, Magram J, Murphy KM (1995) Regulation of interleukin 12 p40 expression through an NF-kappa B half-site. Mol Cell Biol 15: 5258-5267.
90. Libermann TA, Baltimore D (1990) Activation of interleukin-6 gene expression through the NF-kappa B transcription factor. Mol Cell Biol 10: 2327-2334.
91. Su RC, Sivro A, Kimani J, Jaoko W, Plummer FA, et al. (2011) Epigenetic control of IRF1 responses in HIV-exposed seronegative versus HIV-susceptible individuals. Blood 117: 2649-2657.
92. Decker T, Stockinger S, Karaghiosoff M, Muller M, Kovarik P (2002) IFNs and STATs in innate immunity to microorganisms. J Clin Invest 109: 1271-1277.
93. Thanos D, Maniatis T (1995) Virus induction of human IFN beta gene expression requires the assembly of an enhanceosome. Cell 83: 1091-1100.
94. Agalioti T, Lomvardas S, Parekh B, Yie J, Maniatis T, et al. (2000) Ordered recruitment of chromatin modifying and general transcription factors to the IFN-beta promoter. Cell 103: 667-678.
95. Ikushima H, Negishi H, Taniguchi T The IRF Family Transcription Factors at the Interface of Innate and Adaptive Immune Responses. Cold Spring Harb Symp Quant Biol.
96. Maruyama S, Sumita K, Shen H, Kanoh M, Xu X, et al. (2003) Identification of IFN regulatory factor-1 binding site in IL-12 p40 gene promoter. J Immunol 170: 997-1001.
97. Liu J, Cao S, Herman LM, Ma X (2003) Differential regulation of interleukin (IL)-12 p35 and p40 gene expression and interferon (IFN)-gamma-primed IL-12 production by IFN regulatory factor 1. J Exp Med 198: 1265-1276.
98. Kovacs KA, Steinmann M, Magistretti PJ, Halfon O, Cardinaux JR (2003) CCAAT/enhancer-binding protein family members recruit the coactivator CREB-binding protein and trigger its phosphorylation. J Biol Chem 278: 36959-36965.
99. Ramji DP, Foka P (2002) CCAAT/enhancer-binding proteins: structure, function and regulation. Biochem J 365: 561-575.
100. Plevy SE, Gemberling JH, Hsu S, Dorner AJ, Smale ST (1997) Multiple control elements mediate activation of the murine and human interleukin 12 p40 promoters: evidence of functional synergy between C/EBP and Rel proteins. Mol Cell Biol 17: 4572-4588.
101. Zhu C, Gagnidze K, Gemberling JH, Plevy SE (2001) Characterization of an activation protein-1-binding site in the murine interleukin-12 p40 promoter. Demonstration of novel functional elements by a reductionist approach. J Biol Chem 276: 18519-18528.
102. Baccam M, Woo SY, Vinson C, Bishop GA (2003) CD40-mediated transcriptional regulation of the IL-6 gene in B lymphocytes: involvement of NF-kappa B, AP-1, and C/EBP. J Immunol 170: 3099-3108.
103. Schroder K, Spille M, Pilz A, Lattin J, Bode KA, et al. (2007) Differential effects of CpG DNA on IFN-beta induction and STAT1 activation in murine macrophages versus dendritic cells:

alternatively activated STAT1 negatively regulates TLR signaling in macrophages. J Immunol 179: 3495-3503.
104. Rhee SH, Jones BW, Toshchakov V, Vogel SN, Fenton MJ (2003) Toll-like receptors 2 and 4 activate STAT1 serine phosphorylation by distinct mechanisms in macrophages. J Biol Chem 278: 22506-22512.
105. Honda K, Ohba Y, Yanai H, Negishi H, Mizutani T, et al. (2005) Spatiotemporal regulation of MyD88-IRF-7 signalling for robust type-I interferon induction. Nature 434: 1035-1040.
106. Kawai T, Akira S (2011) Toll-like receptors and their crosstalk with other innate receptors in infection and immunity. Immunity 34: 637-650.
107. Fritz JH, Girardin SE, Fitting C, Werts C, Mengin-Lecreulx D, et al. (2005) Synergistic stimulation of human monocytes and dendritic cells by Toll-like receptor 4 and NOD1- and NOD2-activating agonists. Eur J Immunol 35: 2459-2470.
108. van Heel DA, Ghosh S, Butler M, Hunt K, Foxwell BM, et al. (2005) Synergistic enhancement of Toll-like receptor responses by NOD1 activation. Eur J Immunol 35: 2471-2476.
109. Uehara A, Yang S, Fujimoto Y, Fukase K, Kusumoto S, et al. (2005) Muramyldipeptide and diaminopimelic acid-containing desmuramylpeptides in combination with chemically synthesized Toll-like receptor agonists synergistically induced production of interleukin-8 in a NOD2- and NOD1-dependent manner, respectively, in human monocytic cells in culture. Cell Microbiol 7: 53-61.
110. Alon U (2007) Network motifs: theory and experimental approaches. Nat Rev Genet 8: 450-461.
111. Milo R, Shen-Orr S, Itzkovitz S, Kashtan N, Chklovskii D, et al. (2002) Network motifs: simple building blocks of complex networks. Science 298: 824-827.
112. Boyer LA, Lee TI, Cole MF, Johnstone SE, Levine SS, et al. (2005) Core transcriptional regulatory circuitry in human embryonic stem cells. Cell 122: 947-956.
113. Hoffmann A, Levchenko A, Scott ML, Baltimore D (2002) The IkappaB-NF-kappaB signaling module: temporal control and selective gene activation. Science 298: 1241-1245.
114. Werner SL, Barken D, Hoffmann A (2005) Stimulus specificity of gene expression programs determined by temporal control of IKK activity. Science 309: 1857-1861.
115. Basak S, Kim H, Kearns JD, Tergaonkar V, O'Dea E, et al. (2007) A fourth IkappaB protein within the NF-kappaB signaling module. Cell 128: 369-381.
116. O'Dea EL, Barken D, Peralta RQ, Tran KT, Werner SL, et al. (2007) A homeostatic model of IkappaB metabolism to control constitutive NF-kappaB activity. Mol Syst Biol 3: 111.
117. Cheong R, Hoffmann A, Levchenko A (2008) Understanding NF-kappaB signaling via mathematical modeling. Mol Syst Biol 4: 192.

118. Shih VF, Kearns JD, Basak S, Savinova OV, Ghosh G, et al. (2009) Kinetic control of negative feedback regulators of NF-kappaB/RelA determines their pathogen- and cytokine-receptor signaling specificity. Proc Natl Acad Sci U S A 106: 9619-9624.
119. Longo DM, Selimkhanov J, Kearns JD, Hasty J, Hoffmann A, et al. (2013) Dual delayed feedback provides sensitivity and robustness to the NF-kappaB signaling module. PLoS Comput Biol 9: e1003112.
120. Shinohara H, Behar M, Inoue K, Hiroshima M, Yasuda T, et al. (2014) Positive feedback within a kinase signaling complex functions as a switch mechanism for NF-kappaB activation. Science 344: 760-764.
121. Tay S, Hughey JJ, Lee TK, Lipniacki T, Quake SR, et al. (2010) Single-cell NF-kappaB dynamics reveal digital activation and analogue information processing. Nature 466: 267-271.
122. Cooper AM, Khader SA (2007) IL-12p40: an inherently agonistic cytokine. Trends Immunol 28: 33-38.
123. Takahashi K, Asabe S, Wieland S, Garaigorta U, Gastaminza P, et al. (2010) Plasmacytoid dendritic cells sense hepatitis C virus-infected cells, produce interferon, and inhibit infection. Proc Natl Acad Sci U S A 107: 7431-7436.
124. Watanabe T, Kitani A, Murray PJ, Strober W (2004) NOD2 is a negative regulator of Toll-like receptor 2-mediated T helper type 1 responses. Nat Immunol 5: 800-808.
125. Tan RS, Ho B, Leung BP, Ding JL (2014) TLR Cross-talk Confers Specificity to Innate Immunity. Int Rev Immunol.

APPENDICES

APPENDICES

TABLE

Protein identification and quantitation results from ProteinPilot for all the analyzed samples.

PUBLICATIONS

Tan, R*., Lin, B*., **Liu, Q.**, Tucker-Kellogg, L., Ho, B., Leung, P.L. & Ding, J.L., *The synergy in cytokine production through MyD88-TRIF pathways is co-ordinated with ERK phosphorlation in macrophages.* Immunol Cell Biol. 2013, 91 (377-387).

Liu, Q*., Zhu, Y*., Yong, W.K., Sze, S.K., Tan, N.S., & Ding, J.L., *Synchronization of IRF1, JunB and C/EBPβ activities during TLR3-TLR7 crosstalk orchestrates timely cytokine synergy in proinflammatory response.* Under revision.

Liu, B*., **Liu, Q*.,** Palaniappan, S.K., Bahar, I., Thiagaraja, P.S., Ding, J.L., *Toll-like receptors crosstalk reveals innate immune memory and homeostasis.* Manuscript in preparation.

*Equal first author

CONFERENCE

15th International Congress of Immunology, Aug 22-27, 2013, Milan, Italy. Poster presentation

COPYRIGHT PERMISSION

Figure 1.2. Schematic representation of the structure, cellular localization and major components of the PRR families

Trinchieri G, Sher A (2007) Cooperation of Toll-like receptor signals in innate immune defence. Nat Rev Immunol 7: 179-190.

Protein identification and quantitation results from ProteinPilot for all the analyzed samples

		Batch 1										batch 2										Geometric mean					
Name	Accession number	% FDR	Unused	Total	%Cov	114:113	115:113	116:113	118:117	119:117	121:117	% FDR	Unused	Total	%Cov	114:113	115:113	116:113	118:117	119:117	121:117	114:113	115:113	116:113	118:117	119:117	121:117
Plectin OS=Mus musculus GN=Plec PE=1 SV=2	Q9QXS1	0.00	0.00	425.91	72.69	1.10	0.93	1.03	1.27	1.14	1.25	0.00	428.91	428.91	76.74	0.98	0.93	0.96	1.37	1.58	1.58	1.04	0.93	1.00	1.32	1.34	1.41
Protein Snrnp200 OS=Mus musculus GN=Snrnp200 PE=2 SV=1	Q6P4T2	0.00	135.74	135.76	55.01	1.26	1.21	1.18	0.89	1.22	1.28	0.00	120.36	120.36	58.66	1.20	1.25	1.06	0.76	0.64	0.45	1.23	1.23	1.12	0.82	0.89	0.76
Prelamin-A/C OS=Mus musculus GN=Lmna PE=1 SV=2	P48678	0.00	134.99	134.99	89.02	0.95	1.13	1.09	0.65	0.70	0.82	0.00	111.06	111.06	88.42	1.34	1.47	1.43	0.90	0.39	0.47	1.13	1.29	1.25	0.76	0.52	0.62
Pre-mRNA-processing-splicing factor 8 OS=Mus musculus GN=Prpf8 PE=1 SV=2	Q99PV0	0.00	130.85	130.85	54.00	0.96	1.12	0.97	0.96	1.36	1.29	0.00	116.87	116.87	56.45	0.99	1.01	0.64	0.70	0.80	0.52	0.98	1.06	0.79	0.82	1.04	0.82
Protein Mki67 OS=Mus musculus GN=Mki67 PE=4 SV=1	E9PVX6	0.00	127.83	127.83	47.47	1.43	1.49	1.33	1.31	0.95	0.82	0.00	123.50	123.50	54.20	1.61	1.67	1.60	1.10	0.60	0.47	1.52	1.58	1.46	1.20	0.76	0.62
DNA topoisomerase 2-alpha OS=Mus musculus GN=Top2a PE=1 SV=2	Q01320	0.00	116.10	116.11	57.85	1.32	1.45	1.34	1.51	1.39	1.14	0.00	102.75	102.75	61.85	1.53	1.67	1.31	1.53	0.75	0.61	1.42	1.56	1.32	1.52	1.02	0.84
Myb-binding protein 1A OS=Mus musculus GN=Mybbp1a PE=1 SV=2	Q7TPV4	0.00	0.00	114.28	61.38	1.22	1.64	1.33	0.98	1.94	1.53	0.00	88.27	88.28	64.29	1.46	1.39	0.92	0.89	0.95	1.01	1.34	1.51	1.11	0.93	1.36	1.24
Structural maintenance of chromosomes flexible hinge domain-containing protein 1 OS=Mus musculus GN=Smchd1 PE=1 SV=2	Q6P5D8	0.00	102.38	103.39	50.12	0.98	1.26	1.08	0.95	0.89	0.82	0.00	94.66	94.66	56.65	0.95	1.21	0.91	0.86	0.70	0.51	0.96	1.24	0.99	0.91	0.79	0.65
Structural maintenance of chromosomes protein 3 OS=Mus musculus GN=Smc3 PE=1 SV=2	Q9CW03	0.00	0.00	94.30	64.75	1.25	1.36	1.31	0.81	0.83	0.86	0.00	85.59	85.60	67.71	1.54	1.41	1.31	0.69	0.53	0.39	1.39	1.38	1.31	0.75	0.66	0.58
ATP-dependent RNA helicase A OS=Mus musculus GN=Dhx9 PE=4 SV=1	E9QNN1	0.00	92.45	92.45	57.95	0.87	1.27	1.19	0.88	1.12	1.13	0.00	98.21	98.21	64.23	0.83	0.98	0.77	0.62	0.47	0.55	0.85	1.12	0.95	0.74	0.73	0.79
Protein Tpr OS=Mus musculus GN=Tpr PE=4 SV=1	F6ZDS4	0.00	91.62	91.81	52.86	1.13	0.96	0.99	0.70	0.68	0.70	0.00	80.25	80.30	50.27	1.04	0.97	1.01	0.68	0.64	0.68	1.08	0.97	1.00	0.69	0.66	0.69
Heterogeneous nuclear ribonucleoproteins A2/B1 OS=Mus musculus GN=Hnrnpa2b1 PE=1 SV=2	O88569	0.00	83.79	83.79	79.04	0.82	0.86	1.39	0.79	0.94	1.12	0.00	0.00	94.74	87.25	0.52	1.06	0.99	1.34	1.85	1.46	0.66	0.95	1.17	1.03	1.32	1.28
Nucleolar RNA helicase 2 OS=Mus musculus GN=Ddx21 PE=1 SV=3	Q9JIK5	0.00	82.01	82.03	71.92	1.31	1.20	1.25	1.41	1.72	1.75	0.00	85.97	85.98	76.62	1.64	1.94	2.00	1.32	1.18	1.12	1.47	1.53	1.58	1.36	1.43	1.40
Heterogeneous nuclear ribonucleoprotein U OS=Mus musculus GN=Hnrnpu PE=1 SV=1	Q8VEK3	0.00	80.07	80.07	61.87	1.26	1.37	1.42	1.20	0.88	0.90	0.00	82.80	82.80	63.63	1.28	1.27	1.36	0.98	0.34	0.41	1.27	1.32	1.39	1.09	0.55	0.61
Chromodomain-helicase-DNA-binding protein 4 OS=Mus musculus GN=Chd4 PE=1 SV=1	Q6PDQ2	0.00	0.00	79.96	51.38	1.19	1.26	1.12	1.09	1.09	0.95	0.00	0.00	77.60	50.50	1.33	1.16	1.14	0.86	0.39	0.75	1.26	1.21	1.13	0.97	0.65	0.85
Heterogeneous nuclear ribonucleoprotein A3 OS=Mus musculus GN=Hnrnpa3 PE=1 SV=1	Q8BG05	0.00	0.00	81.94	73.88	0.94	1.14	1.50	0.77	0.69	0.70	0.00	72.42	81.10	74.93	1.00	0.90	0.94	0.90	0.49	0.11	0.97	1.01	1.19	0.83	0.58	0.28
Lamin-B1 OS=Mus musculus GN=Lmnb1 PE=1 SV=3	P14733	0.00	75.54	79.54	72.11	1.16	1.17	1.43	0.94	0.72	0.87	0.00	69.29	73.16	79.25	1.20	1.45	1.31	0.70	0.32	0.52	1.18	1.30	1.37	0.81	0.48	0.67
Histone H4 OS=Mus musculus GN=Hist1h4a PE=1 SV=2	P62806	0.00	0.00	74.99	74.76	1.01	1.03	1.06	0.94	0.97	0.93	0.00	69.60	69.60	94.17	0.70	0.63	0.91	0.94	0.54	0.19	0.84	0.80	0.98	0.94	0.73	0.42
SWI/SNF-related matrix-associated actin-dependent regulator of chromatin subfamily A member 5 OS=Mus musculus GN=Smarca5 PE=1 SV=1	Q91ZW3	0.00	74.41	74.41	64.13	1.02	1.60	1.28	1.27	1.28	1.20	0.00	66.80	67.07	70.79	1.17	1.17	1.13	1.03	0.80	0.83	1.09	1.37	1.20	1.14	1.01	1.00
Splicing factor 3B subunit 1 OS=Mus musculus GN=Sf3b1 PE=1 SV=1	Q99NB9	0.00	0.00	73.45	56.29	0.90	1.07	0.93	1.06	1.28	1.28	0.00	0.00	67.63	54.37	1.00	1.00	0.88	0.96	0.72	0.68	0.95	1.03	0.90	1.01	0.96	0.93
HEAT repeat containing 1 OS=Mus musculus GN=Heatr1 PE=4 SV=1	G3X9B1	0.00	73.19	73.22	39.43	0.96	1.02	0.99	1.08	1.57	1.46	0.00	71.31	71.49	43.07	1.09	1.11	0.84	1.24	1.29	0.70	1.02	1.06	0.91	1.15	1.43	1.01
Protein RRP5 homolog OS=Mus musculus GN=Pdcd11 PE=2 SV=2	Q6NS46	0.00	71.90	71.92	45.27	1.06	1.21	1.04	0.95	1.57	1.38	0.00	81.11	81.13	53.01	0.91	0.97	1.06	0.96	1.32	0.77	0.98	1.09	1.05	0.95	1.44	1.03
Structural maintenance of chromosomes protein 1A OS=Mus musculus GN=Smc1a PE=1 SV=4	Q9CU62	0.00	70.28	70.30	59.04	1.22	1.19	1.22	0.87	0.90	0.79	0.00	80.36	80.36	61.96	1.20	1.02	0.95	0.64	0.53	0.16	1.21	1.10	1.08	0.75	0.70	0.35
Protein Ahnak OS=Mus musculus GN=Ahnak PE=4 SV=1	E9Q616	0.00	69.55	69.55	44.98	1.32	0.87	1.02	1.91	1.04	0.68	0.00	74.08	74.08	51.34	1.51	0.95	1.11	1.57	0.73	0.46	1.41	0.91	1.06	1.73	0.87	0.56
Histone H2A.x OS=Mus musculus GN=H2afx PE=1 SV=2	P27661	0.00	67.20	67.20	91.61	0.94	1.05	1.19	1.02	1.10	0.93	0.00	63.72	63.72	81.82	0.92	0.69	0.51	0.88	1.06	0.58	0.93	0.85	0.78	0.95	1.08	0.73
Heterogeneous nuclear ribonucleoprotein M OS=Mus musculus GN=Hnrnpm PE=1 SV=3	Q9D0E1	0.00	0.00	63.55	75.99	1.00	1.15	1.13	0.82	0.82	0.79	0.00	66.99	66.99	80.11	1.05	0.87	0.77	0.54	0.20	0.31	1.02	1.00	0.93	0.67	0.41	0.49
Splicing factor 3B subunit 3 OS=Mus musculus GN=Sf3b3 PE=2 SV=1	Q921M3	0.00	0.00	61.36	49.06	1.00	1.22	1.12	0.95	1.25	1.36	0.00	56.62	56.62	48.56	1.02	1.18	0.98	1.06	1.00	1.31	1.01	1.20	1.05	1.00	1.12	1.33
116 kDa U5 small nuclear ribonucleoprotein component OS=Mus musculus GN=Eftud2 PE=2 SV=1	O08810	0.00	0.00	60.90	51.18	1.10	1.08	1.06	1.03	1.06	1.18	0.00	0.00	49.10	57.78	1.17	1.13	0.99	1.09	0.90	0.89	1.13	1.10	1.02	1.06	0.97	1.02
Tyrosine-protein kinase BAZ1B OS=Mus musculus GN=Baz1b PE=1 SV=2	Q9Z277	0.00	59.66	59.72	45.23	0.82	1.28	1.05	1.00	1.00	0.89	0.00	48.03	48.04	46.38	0.94	1.28	0.96	0.72	0.94	0.83	0.88	1.28	1.00	0.85	0.97	0.86
DEAD (Asp-Glu-Ala-Asp) box polypeptide 5 OS=Mus musculus GN=Ddx5 PE=2 SV=1	Q8BTS0	0.00	0.00	58.75	61.30	1.43	1.38	1.42	5.20	7.24	4.88	0.00	53.40	53.40	62.44	1.32	1.33	1.04	3.50	2.75	1.64	1.37	1.36	1.21	4.27	4.47	2.83
Nucleolin OS=Mus musculus GN=Ncl PE=1 SV=2	P09405	0.00	0.00	56.30	59.83	1.61	1.39	1.67	2.99	3.08	1.75	0.00	60.91	61.07	61.95	1.57	1.13	1.20	3.50	2.96	0.72	1.59	1.25	1.42	3.24	3.02	1.12
Myosin-9 OS=Mus musculus GN=Myh9 PE=1 SV=4	Q8VDD5	0.00	54.86	54.89	42.45	1.11	0.42	0.52	0.39	0.22	0.10	0.00	45.43	45.46	48.06	1.05	0.54	0.72	0.44	0.26	0.13	1.08	0.47	0.61	0.41	0.24	0.12
Heterogeneous nuclear ribonucleoprotein K OS=Mus musculus GN=Hnrnpk PE=2 SV=1	B2M1R6	0.00	54.43	54.43	86.59	0.83	1.03	1.02	0.82	0.77	0.79	0.00	58.60	58.60	92.05	1.03	1.29	0.95	0.79	0.55	0.63	0.92	1.15	0.99	0.81	0.65	0.70
Nucleolar protein 56 OS=Mus musculus GN=Nop56 PE=1 SV=2	Q9D6Z1	0.00	54.05	54.05	67.93	0.70	0.97	0.96	0.92	1.17	1.25	0.00	55.50	55.50	66.72	1.01	1.45	0.93	0.99	0.80	0.63	0.84	1.19	0.95	0.95	0.97	0.89
Actin, cytoplasmic 1 OS=Mus musculus GN=Actb PE=1 SV=1	P60710	0.00	0.00	53.91	75.73	1.10	0.25	0.41	0.86	0.27	0.52	0.00	49.90	49.91	74.67	1.13	0.18	0.35	0.51	0.08	0.41	1.11	0.21	0.38	0.66	0.15	0.47

Protien identification and qunatitation results from ProteinPilot for all the analyzed samples

Name	Accession number	% FDR	Unused	Total	%Cov	114:113	115:113	116:113	118:117	119:117	121:117	% FDR	Unused	Total	%Cov	114:113	115:113	116:113	118:117	119:117	121:117	114:113	115:113	116:113	118:117	119:117	121:117
Actin, cytoplasmic 2 OS=Mus musculus GN=Actg1 PE=1 SV=1	P63260	0.00	0.00	53.76	75.20	1.10	0.25	0.41	0.86	0.27	0.52	0.00	0.00	49.02	70.13	1.13	0.18	0.35	0.51	0.08	0.41	1.11	0.21	0.38	0.66	0.15	0.47
Histone H1.2 OS=Mus musculus GN=Hist1h1c PE=1 SV=2	P15864	0.00	0.00	53.38	64.15	0.92	0.95	1.03	0.95	0.95	0.97	0.00	12.79	46.30	64.15	0.96	1.00	0.59	0.73	0.79	0.61	0.94	0.97	0.78	0.84	0.87	0.77
MCG13402, isoform CRA_c OS=Mus musculus GN=Ptbp1 PE=2 SV=1	Q922I7	0.00	52.34	52.34	59.28	0.83	0.95	0.95	0.63	0.64	0.61	0.00	0.00	63.49	77.66	0.85	1.01	0.51	0.65	0.60	0.55	0.84	0.98	0.70	0.64	0.62	0.58
Heterogeneous nuclear ribonucleoprotein L (Fragment) OS=Mus musculus GN=Hnrnpl PE=4 SV=1	G5E924	0.00	52.22	52.22	67.64	0.99	1.17	1.17	0.95	1.03	0.99	0.00	56.34	56.34	70.08	1.21	1.39	1.02	0.64	0.20	0.52	1.10	1.28	1.09	0.78	0.45	0.72
Matrin-3 OS=Mus musculus GN=Matr3 PE=1 SV=1	Q8K310	0.00	0.00	52.02	56.86	0.88	1.34	1.19	1.05	1.34	1.33	0.00	0.00	34.25	50.35	1.09	1.45	0.95	1.11	1.07	1.18	0.98	1.39	1.07	1.08	1.20	1.25
Histone H2B type 1-P OS=Mus musculus GN=Hist1h2bp PE=1 SV=3	Q8CGP2	0.00	0.00	50.90	81.75	1.74	1.37	2.19	0.70	0.79	0.35	0.00	56.70	56.74	85.71	0.90	0.40	0.35	0.71	0.84	0.45	1.25	0.74	0.87	0.70	0.82	0.40
Histone H2B type 1-B OS=Mus musculus GN=Hist1h2bb PE=1 SV=3	Q64475	0.00	0.00	50.76	80.95	1.74	1.37	2.19	0.70	0.79	0.35	0.00	0.00	56.73	82.54	0.90	0.40	0.35	0.71	0.84	0.45	1.25	0.74	0.87	0.70	0.82	0.40
Histone H2B type 1-F/J/L OS=Mus musculus GN=Hist1h2bf PE=1 SV=2	P10853	0.00	0.00	50.76	82.54	1.74	1.37	2.19	0.70	0.79	0.35	0.00	0.00	56.72	85.71	0.90	0.40	0.35	0.71	0.84	0.45	1.25	0.74	0.87	0.70	0.82	0.40
Histone H2B type 1-C/E/G OS=Mus musculus GN=Hist1h2bc PE=1 SV=3	Q6ZWY9	0.00	0.00	51.20	82.54	1.74	1.37	2.19	0.70	0.79	0.35	0.00	0.00	56.72	80.95	0.90	0.40	0.35	0.71	0.84	0.45	1.25	0.74	0.87	0.70	0.82	0.40
Histone H2B type 2-B OS=Mus musculus GN=Hist2h2bb PE=1 SV=3	Q64525	0.00	0.00	51.20	82.54	1.74	1.37	2.19	0.70	0.79	0.35	0.00	0.00	56.72	80.16	0.90	0.40	0.35	0.71	0.84	0.45	1.25	0.74	0.87	0.70	0.82	0.40
Histone H2B type 1-H OS=Mus musculus GN=Hist1h2bh PE=1 SV=3	Q64478	0.00	0.00	51.20	78.57	1.74	1.37	2.19	0.70	0.79	0.35	0.00	0.00	56.72	77.78	0.90	0.40	0.35	0.71	0.84	0.45	1.25	0.74	0.87	0.70	0.82	0.40
Histone H2B type 1-M OS=Mus musculus GN=Hist1h2bm PE=1 SV=2	P10854	0.00	0.00	51.20	82.54	1.74	1.37	2.19	0.70	0.79	0.35	0.00	0.00	56.72	80.95	0.90	0.40	0.35	0.71	0.84	0.45	1.25	0.74	0.87	0.70	0.82	0.40
Small subunit processome component 20 homolog OS=Mus musculus GN=Utp20 PE=2 SV=2	Q5XG71	0.00	49.76	49.82	33.86	1.01	1.00	0.99	0.82	1.19	0.96	0.00	0.00	51.24	41.75	1.14	1.14	1.06	0.65	0.97	0.32	1.07	1.07	1.02	0.73	1.08	0.56
Heat shock cognate 71 kDa protein OS=Mus musculus GN=Hspa8 PE=1 SV=1	P63017	0.00	0.00	49.15	57.89	0.92	0.65	0.82	1.49	0.74	0.81	0.00	57.59	57.59	63.93	0.90	0.65	0.70	1.57	0.29	0.26	0.91	0.65	0.76	1.53	0.47	0.46
Nestin OS=Mus musculus GN=Nes PE=1 SV=1	Q6P5H2	0.00	49.08	49.19	34.92	1.33	0.95	1.04	1.09	1.09	0.90	0.00	40.81	40.90	39.11	1.05	0.72	0.96	1.42	1.29	1.45	1.18	0.83	1.00	1.24	1.19	1.14
Transcription activator BRG1 OS=Mus musculus GN=Smarca4 PE=1 SV=1	Q3TKT4	0.00	48.29	48.30	41.35	1.00	0.95	1.04	1.05	1.02	1.03	0.00	48.37	48.37	42.53	1.42	1.33	1.20	0.82	1.06	1.15	1.19	1.13	1.12	0.93	1.04	1.09
N-acetyltransferase 10 OS=Mus musculus GN=Nat10 PE=2 SV=1	Q8K224	0.00	48.13	48.16	40.63	0.87	0.95	0.83	0.69	1.04	0.94	0.00	47.48	47.49	50.78	0.86	0.94	0.82	0.90	0.93	0.77	0.87	0.95	0.82	0.78	0.98	0.85
Non-POU domain-containing octamer-binding protein OS=Mus musculus GN=Nono PE=1 SV=3	Q99K48	0.00	0.00	47.95	78.01	0.36	1.24	0.99	1.32	1.54	1.67	0.00	0.00	34.70	78.65	0.82	1.15	0.87	0.91	0.22	0.92	0.55	1.19	0.93	1.10	0.58	1.24
E3 SUMO-protein ligase RanBP2 OS=Mus musculus GN=Ranbp2 PE=1 SV=2	Q9ERU9	0.00	47.33	47.36	29.09	1.26	1.17	1.07	1.19	1.00	1.31	0.00	45.45	45.48	34.13	1.21	1.11	1.26	1.06	0.90	0.46	1.24	1.14	1.16	1.12	0.95	0.78
Heterogeneous nuclear ribonucleoprotein H OS=Mus musculus GN=Hnrnph1 PE=1 SV=3	O35737	0.00	0.00	46.52	65.26	0.62	0.87	0.65	0.77	1.06	0.39	0.00	0.00	41.92	78.40	0.95	1.04	0.83	0.96	0.92	0.17	0.77	0.95	0.74	0.86	0.99	0.26
Cytoskeleton-associated protein 5 OS=Mus musculus GN=Ckap5 PE=2 SV=1	A2AGT5	0.00	0.00	46.42	31.64	1.18	1.27	1.33	1.54	1.54	1.36	0.00	47.51	47.55	42.67	1.77	1.32	1.82	1.28	1.15	0.51	1.45	1.29	1.56	1.41	1.33	0.83
Putative pre-mRNA-splicing factor ATP-dependent RNA helicase DHX15 OS=Mus musculus GN=Dhx15 PE=2 SV=2	O35286	0.00	0.00	46.39	51.19	1.03	1.01	0.89	0.95	0.91	1.08	0.00	42.00	42.00	57.11	1.00	0.86	0.90	0.98	0.53	0.85	1.01	0.93	0.89	0.97	0.70	0.95
Poly (ADP-ribose) polymerase family, member 1 OS=Mus musculus GN=Parp1 PE=2 SV=1	Q921K2	0.00	46.26	46.26	47.24	1.08	0.98	0.91	1.61	1.20	1.27	0.00	53.23	53.23	51.18	1.79	1.32	1.36	1.46	0.79	0.39	1.39	1.14	1.11	1.53	0.98	0.70
Nucleolar protein 58 OS=Mus musculus GN=Nop58 PE=1 SV=1	Q6DFW4	0.00	46.11	46.72	61.01	0.94	1.05	1.09	1.04	1.20	1.32	0.00	39.92	39.94	58.96	0.80	1.22	0.91	0.93	0.67	0.93	0.87	1.13	1.00	0.98	0.90	1.11
Lamina-associated polypeptide 2, isoforms alpha/zeta OS=Mus musculus GN=Tmpo PE=1 SV=4	Q61033	0.00	45.07	45.07	52.96	0.72	0.82	1.08	1.04	0.98	1.17	0.00	36.76	36.76	61.33	0.85	0.95	0.97	1.11	1.18	1.25	0.78	0.88	1.02	1.07	1.08	1.21
Sister chromatid cohesion protein PDS5 homolog A OS=Mus musculus GN=Pds5a PE=3 SV=3	Q6A026	0.00	0.00	44.64	39.34	0.90	1.00	0.83	0.64	0.71	0.77	0.00	0.00	45.52	47.60	0.97	1.12	0.96	0.64	0.67	0.37	0.94	1.06	0.90	0.64	0.69	0.53
FACT complex subunit SPT16 OS=Mus musculus GN=Supt16h PE=1 SV=2	Q920B9	0.00	0.00	43.93	42.88	1.03	1.12	0.94	1.34	1.10	0.88	0.00	0.00	50.56	48.23	0.95	1.07	0.88	1.24	0.83	0.63	0.99	1.09	0.91	1.29	0.95	0.74
Splicing factor, proline- and glutamine-rich OS=Mus musculus GN=Sfpq PE=1 SV=1	Q8VIJ6	0.00	43.54	44.74	57.51	1.06	1.20	1.26	1.19	1.27	1.33	0.00	48.06	48.06	58.66	0.72	1.08	0.88	0.82	0.40	0.40	0.87	1.14	1.05	0.99	0.71	0.73
Elongation factor 1-alpha 1 OS=Mus musculus GN=Eef1a1 PE=1 SV=3	P10126	0.00	0.00	43.08	64.07	1.04	1.20	1.16	1.08	1.28	1.22	0.00	35.50	35.50	58.87	1.14	1.21	0.84	1.49	1.19	1.09	1.09	1.21	0.99	1.26	1.24	1.15
Targeting protein for Xklp2 OS=Mus musculus GN=Tpx2 PE=1 SV=1	A2APB8	0.00	42.47	42.48	50.07	1.17	1.19	1.31	1.07	1.15	1.22	0.00	40.06	40.07	55.97	1.32	1.32	1.39	1.17	1.21	0.92	1.24	1.25	1.35	1.12	1.18	1.06
SWI/SNF complex subunit SMARCC1 OS=Mus musculus GN=Smarcc1 PE=1 SV=2	P97496	0.00	0.00	42.17	41.30	0.91	1.16	1.19	1.46	1.32	1.27	0.00	53.29	53.29	50.09	0.77	1.21	0.70	1.10	0.70	0.54	0.84	1.19	0.92	1.26	0.96	0.83
Heterogeneous nuclear ribonucleoprotein U-like protein 2 OS=Mus musculus GN=Hnrnpul2 PE=1 SV=2	Q00PI9	0.00	42.11	42.11	50.87	1.01	1.08	0.95	0.94	0.72	0.82	0.00	0.00	33.65	51.54	1.08	1.13	1.18	0.61	0.34	0.48	1.04	1.10	1.06	0.76	0.50	0.63
Far upstream element-binding protein 2 OS=Mus musculus GN=Khsrp PE=1 SV=2	Q3U0V1	0.00	41.90	41.91	62.97	0.80	0.98	1.13	1.02	0.89	0.95	0.00	41.00	41.01	61.76	0.73	1.16	1.14	0.80	0.59	0.90	0.77	1.07	1.13	0.90	0.72	0.92
ATPase family AAA domain-containing protein 2 OS=Mus musculus GN=Atad2 PE=3 SV=1	G3X963	0.00	41.35	41.38	39.66	1.13	1.08	1.08	0.72	0.62	0.63	0.00	47.44	47.48	48.31	1.02	1.05	1.03	0.55	0.28	0.22	1.07	1.06	1.05	0.63	0.42	0.37
Transformation/transcription domain-associated protein OS=Mus musculus GN=Trrap PE=4 SV=1	E9PWT1	0.00	0.00	41.33	26.44	0.95	1.12	0.77	1.17	1.37	1.22	0.00	33.27	33.30	36.94	1.31	1.26	1.75	1.19	1.32	0.27	1.11	1.19	1.16	1.18	1.34	0.58
78 kDa glucose-regulated protein OS=Mus musculus GN=Hspa5 PE=1 SV=3	P20029	0.00	0.00	47.02	60.15	1.47	1.20	1.46	2.09	1.79	1.75	0.00	34.96	42.57	57.25	1.66	1.36	1.89	1.96	1.63	0.74	1.56	1.28	1.66	2.02	1.71	1.14

Protien identification and qunatitation results from ProteinPilot for all the analyzed samples

Name	Accession number	% FDR	Unused	Total	%Cov	114:113	115:113	116:113	118:117	119:117	121:117	% FDR	Unused	Total	%Cov	114:113	115:113	116:113	118:117	119:117	121:117	114:113	115:113	116:113	118:117	119:117	121:117
DNA topoisomerase 1 OS=Mus musculus GN=Top1 PE=1 SV=2	Q04750	0.00	40.57	40.58	52.80	1.02	1.07	1.08	0.87	1.07	0.95	0.00	41.02	41.02	48.76	0.80	0.95	1.13	0.65	0.47	0.47	0.90	1.00	1.10	0.75	0.70	0.67
Eukaryotic initiation factor 4A-III OS=Mus musculus GN=Eif4a3 PE=2 SV=3	Q91VC3	0.00	40.34	40.35	70.07	1.09	1.15	1.25	0.81	0.99	1.09	0.00	35.52	35.53	59.12	1.28	0.98	0.54	0.91	0.55	0.82	1.18	1.06	0.82	0.86	0.74	0.94
Heterochromatin protein 1-binding protein 3 OS=Mus musculus GN=Hp1bp3 PE=1 SV=1	Q3TEA8	0.00	39.65	39.66	60.29	0.90	1.09	1.12	0.97	0.81	0.87	0.00	28.74	28.74	60.11	0.87	0.70	0.61	0.99	0.52	0.49	0.89	0.87	0.83	0.98	0.65	0.65
Heterogeneous nuclear ribonucleoprotein A1 OS=Mus musculus GN=Hnrnpa1 PE=1 SV=2	P49312	0.00	0.00	61.85	71.56	0.82	0.78	0.89	0.96	1.13	1.15	0.00	0.00	64.90	92.81	1.06	0.86	0.77	1.00	1.16	0.39	0.93	0.82	0.83	0.98	1.14	0.67
ATP-dependent RNA helicase DDX18 OS=Mus musculus GN=Ddx18 PE=2 SV=1	Q8K363	0.00	0.00	39.22	51.52	1.36	1.28	1.20	1.22	1.63	1.50	0.00	40.04	40.32	65.00	1.19	0.84	1.00	1.63	1.47	0.67	1.27	1.04	1.10	1.41	1.55	1.00
MCG21756, isoform CRA_a (Fragment) OS=Mus musculus GN=Nup205 PE=2 SV=1	Q6ZQG1	0.00	38.89	38.91	35.22	0.99	0.97	0.85	0.91	0.88	0.96	0.00	36.42	36.46	34.06	1.19	0.92	0.91	0.73	0.86	0.61	1.09	0.95	0.88	0.82	0.87	0.77
Metastasis-associated protein MTA2 OS=Mus musculus GN=Mta2 PE=1 SV=1	Q9R190	0.00	38.85	38.85	60.33	0.86	1.01	1.06	1.04	1.12	0.85	0.00	41.01	41.01	68.56	0.55	1.11	0.77	1.08	0.64	0.59	0.69	1.06	0.90	1.06	0.84	0.71
rRNA 2'-O-methyltransferase fibrillarin OS=Mus musculus GN=Fbl PE=1 SV=2	P35550	0.00	0.00	38.21	77.68	1.03	0.83	1.32	0.90	1.12	1.06	0.00	39.00	39.22	79.51	0.93	0.93	0.82	1.00	0.96	0.58	0.98	0.88	1.04	0.95	1.04	0.78
Core histone macro-H2A.1 OS=Mus musculus GN=H2afy PE=1 SV=3	Q9QZQ8	0.00	38.04	46.15	66.40	1.12	1.21	1.27	0.79	0.85	0.83	0.00	32.30	36.33	63.71	1.02	1.11	0.93	1.06	1.12	0.82	1.07	1.16	1.09	0.92	0.97	0.83
Pre-mRNA-processing factor 6 OS=Mus musculus GN=Prpf6 PE=2 SV=1	Q91YR7	0.00	37.58	37.61	48.88	0.95	1.09	1.12	1.13	1.06	1.28	0.00	35.22	35.24	53.35	0.79	1.01	0.98	1.06	0.64	1.04	0.87	1.05	1.05	1.09	0.82	1.15
Sister chromatid cohesion protein PDS5 homolog B OS=Mus musculus GN=Pds5b PE=1 SV=1	Q4VA53	0.00	37.35	42.00	36.45	1.20	1.08	1.13	0.70	0.73	0.61	0.00	0.00	49.58	40.32	1.12	1.45	1.08	0.69	0.70	0.13	1.16	1.25	1.10	0.70	0.72	0.28
RRP12-like protein OS=Mus musculus GN=Rrp12 PE=1 SV=1	Q6P5B0	0.00	0.00	37.29	46.41	0.86	0.91	0.85	0.90	1.06	1.02	0.00	28.78	28.89	42.93	0.81	0.87	0.91	0.77	0.77	0.90	0.84	0.89	0.88	0.84	0.90	0.95
Spliceosome RNA helicase Ddx39b OS=Mus musculus GN=Ddx39b PE=1 SV=1	Q9Z1N5	0.00	36.94	36.94	71.26	1.18	1.25	0.98	0.95	0.36	0.17	0.00	31.05	31.06	53.97	1.08	1.07	1.08	0.98	0.42	0.19	1.13	1.15	1.03	0.96	0.39	0.18
Tyrosine-protein phosphatase non-receptor type 6 OS=Mus musculus GN=Ptpn6 PE=1 SV=2	P29351	0.00	0.00	36.66	51.76	0.81	0.94	0.90	0.89	1.02	0.82	0.00	35.17	35.17	57.31	0.78	0.96	0.90	0.99	0.90	0.80	0.79	0.95	0.90	0.94	0.95	0.81
Interleukin enhancer-binding factor 3 OS=Mus musculus GN=Ilf3 PE=1 SV=2	Q9Z1X4	0.00	36.35	36.53	42.76	1.21	1.24	1.20	0.78	0.92	0.86	0.00	38.75	38.77	49.55	1.14	1.15	1.06	0.67	0.74	0.63	1.17	1.19	1.13	0.72	0.82	0.73
Nuclear valosin-containing protein-like OS=Mus musculus GN=Nvl PE=1 SV=1	Q9DBY8	0.00	36.21	36.26	51.35	1.28	1.18	1.36	1.22	1.03	1.33	0.00	35.69	35.74	53.22	0.90	1.02	0.97	1.11	1.15	1.12	1.08	1.10	1.15	1.16	1.09	1.22
Protein Rsl1d1 OS=Mus musculus GN=Rsl1d1 PE=2 SV=1	Q8BVY0	0.00	0.00	36.02	67.48	0.97	1.13	1.14	1.14	1.56	1.80	0.00	0.00	37.25	64.16	1.24	1.51	0.76	1.22	1.24	1.01	1.10	1.31	0.93	1.18	1.39	1.35
WD repeat-containing protein 3 OS=Mus musculus GN=Wdr3 PE=2 SV=1	Q8BHB4	0.00	35.98	35.98	46.18	1.38	1.43	1.58	1.19	2.13	1.46	0.00	35.82	35.83	44.69	0.93	0.94	0.99	0.97	1.01	0.91	1.13	1.16	1.25	1.08	1.47	1.15
Transcription elongation factor SPT6 OS=Mus musculus GN=Supt6h PE=1 SV=2	Q62383	0.00	35.97	36.01	30.65	1.36	1.32	1.21	0.96	1.09	0.98	0.00	22.80	22.82	30.94	1.12	1.19	1.11	0.86	1.01	0.79	1.23	1.25	1.16	0.91	1.05	0.88
Nucleolar GTP-binding protein 1 OS=Mus musculus GN=Gtpbp4 PE=2 SV=3	Q99ME9	0.00	35.71	35.77	52.05	1.84	1.63	1.74	1.41	1.74	1.51	0.00	34.29	34.31	61.36	1.98	1.58	1.87	1.24	1.45	1.19	1.91	1.61	1.80	1.32	1.58	1.34
Interferon-activable protein 204 OS=Mus musculus GN=Ifi204 PE=1 SV=2	P15092	0.00	0.00	33.54	58.91	0.83	1.27	1.22	3.34	0.99	3.47	0.00	0.00	25.05	53.44	1.36	1.37	1.12	3.91	0.98	2.73	1.06	1.32	1.17	3.61	0.99	3.08
Splicing factor 3A subunit 1 OS=Mus musculus GN=Sf3a1 PE=1 SV=1	Q8K4Z5	0.00	35.42	35.44	48.55	1.04	0.98	0.86	0.90	0.79	0.97	0.00	41.12	41.12	53.48	1.17	1.10	0.93	0.77	0.29	0.47	1.10	1.04	0.89	0.83	0.47	0.68
AT-rich interactive domain-containing protein 1A OS=Mus musculus GN=Arid1a PE=1 SV=1	A2BH40	0.00	0.00	35.24	26.76	1.24	1.38	1.22	1.32	1.16	0.85	0.00	0.00	29.43	27.03	1.01	0.98	1.01	0.96	0.99	0.95	1.12	1.16	1.11	1.13	1.07	0.90
DNA-directed RNA polymerase II subunit RPB2 OS=Mus musculus GN=Polr2b PE=2 SV=2	Q8CFI7	0.00	35.12	35.13	46.68	1.01	1.20	0.87	0.59	0.95	0.74	0.00	36.86	36.89	44.55	1.17	1.32	0.77	0.74	1.82	1.17	1.09	1.26	0.82	0.66	1.32	0.93
Cell division cycle 5-like protein OS=Mus musculus GN=Cdc5l PE=1 SV=2	Q6A068	0.00	0.00	35.11	55.86	0.98	1.00	0.95	1.06	0.97	1.14	0.00	34.48	34.52	55.61	0.98	0.98	0.90	0.71	0.58	0.61	0.98	0.99	0.92	0.87	0.75	0.84
RNA-binding protein 14 OS=Mus musculus GN=Rbm14 PE=1 SV=1	Q8C2Q3	0.00	34.98	34.98	47.09	0.89	1.00	1.16	1.00	1.14	1.16	0.00	44.92	44.93	58.00	0.74	0.84	0.75	1.08	1.18	1.26	0.81	0.92	0.93	1.04	1.16	1.21
SUN domain-containing protein 2 OS=Mus musculus GN=Sun2 PE=1 SV=3	Q8BJS4	0.00	34.95	35.00	53.49	0.97	1.01	0.92	0.74	0.88	0.86	0.00	31.81	31.83	49.66	0.94	0.67	0.83	0.75	0.92	1.03	0.95	0.82	0.87	0.74	0.90	0.94
Nipped-B-like protein OS=Mus musculus GN=Nipbl PE=1 SV=1	Q6KCD5	0.00	34.91	34.95	27.45	0.94	1.16	1.08	0.75	0.97	1.00	0.00	31.15	31.18	28.66	0.79	1.02	0.81	0.90	1.26	0.96	0.86	1.09	0.93	0.82	1.11	0.98
Homeobox protein cut-like 1 OS=Mus musculus GN=Cux1 PE=3 SV=1	H3BKF6	0.00	34.88	34.95	35.90	0.90	0.97	0.95	1.04	1.08	1.03	0.00	30.81	30.83	40.56	1.09	1.02	0.94	0.84	0.82	0.77	0.99	1.00	0.94	0.93	0.94	0.89
Host cell factor 1 OS=Mus musculus GN=Hcfc1 PE=1 SV=2	Q61191	0.00	0.00	34.53	27.78	0.82	0.98	0.91	0.99	0.88	1.00	0.00	33.56	33.56	31.20	0.69	0.88	0.73	0.86	0.77	0.64	0.75	0.93	0.82	0.92	0.82	0.80
Paired amphipathic helix protein Sin3a OS=Mus musculus GN=Sin3a PE=1 SV=3	Q60520	0.00	34.35	34.35	32.26	1.04	0.82	1.06	0.77	0.61	0.64	0.00	0.00	21.10	37.05	0.96	0.99	0.90	0.69	0.72	0.36	1.00	0.90	0.98	0.73	0.67	0.48
Unconventional myosin-Ic OS=Mus musculus GN=Myo1c PE=1 SV=2	Q9WTI7	0.00	34.23	34.25	44.97	0.89	0.30	0.41	0.50	0.34	0.31	0.00	33.73	33.76	51.36	0.85	0.33	0.48	0.51	0.41	0.61	0.87	0.31	0.44	0.50	0.37	0.44
Protein RCC2 OS=Mus musculus GN=Rcc2 PE=2 SV=1	Q8BK67	0.00	34.05	34.05	60.96	0.70	0.98	0.80	0.91	0.92	0.81	0.00	36.14	36.15	65.96	0.75	1.08	0.86	0.90	0.76	0.56	0.73	1.03	0.83	0.90	0.84	0.67
Heterogeneous nuclear ribonucleoprotein F OS=Mus musculus GN=Hnrnpf PE=1 SV=3	Q9Z2X1	0.00	33.97	41.64	66.02	1.08	1.36	1.14	0.69	0.72	0.33	0.00	31.64	35.67	71.33	1.21	1.21	1.10	1.34	0.47	0.44	1.14	1.28	1.12	0.96	0.58	0.38
Heterogeneous nuclear ribonucleoprotein R OS=Mus musculus GN=Hnrnpr PE=2 SV=1	Q8VHM5	0.00	33.97	33.98	52.69	1.03	1.28	1.19	0.84	0.76	0.30	0.00	39.20	39.21	54.11	1.26	0.82	1.01	0.68	0.47	0.09	1.14	1.03	1.10	0.76	0.60	0.16
RuvB-like 2 OS=Mus musculus GN=Ruvbl2 PE=2 SV=3	Q9WTM5	0.00	0.00	33.91	56.80	0.74	0.99	0.65	0.68	0.90	0.89	0.00	35.36	35.36	63.93	0.86	1.05	0.86	2.27	1.25	2.49	0.80	1.02	0.75	1.24	1.06	1.49
Transcription intermediary factor 1-beta OS=Mus musculus GN=Trim28 PE=1 SV=3	Q62318	0.00	0.00	33.84	39.57	1.14	1.01	1.09	0.77	0.59	0.47	0.00	29.97	29.97	47.12	0.90	0.89	0.74	0.82	0.26	0.47	1.01	0.95	0.90	0.79	0.39	0.47

Protien identification and qunatitation results from ProteinPilot for all the analyzed samples

Name	Accession number	% FDR	Unused	Total	%Cov	114:113	115:113	116:113	118:117	119:117	121:117	% FDR	Unused	Total	%Cov	114:113	115:113	116:113	118:117	119:117	121:117	114:113	115:113	116:113	118:117	119:117	121:117
Poly(U)-binding-splicing factor PUF60 OS=Mus musculus GN=Puf60 PE=2 SV=2	Q3UEB3	0.00	33.17	33.17	55.67	1.10	1.08	1.16	1.17	1.13	0.89	0.00	0.00	30.12	50.71	1.27	1.43	1.43	1.53	1.38	1.12	1.18	1.24	1.29	1.34	1.25	1.00
Histone H3.2 OS=Mus musculus GN=Hist1h3b PE=1 SV=2	P84228	0.00	0.00	33.08	92.65	1.07	0.98	1.29	0.79	0.86	0.83	0.00	28.54	28.54	88.97	0.81	0.67	0.64	0.83	0.83	0.71	0.93	0.81	0.91	0.81	0.85	0.77
Nuclear pore complex protein Nup93 OS=Mus musculus GN=Nup93 PE=2 SV=1	Q8BJ71	0.00	32.89	32.91	42.49	0.99	1.00	0.94	0.92	0.79	1.04	0.00	37.33	37.34	58.36	0.87	0.91	0.82	0.83	0.56	1.02	0.93	0.95	0.88	0.87	0.67	1.03
Dedicator of cytokinesis protein 10 OS=Mus musculus GN=Dock10 PE=1 SV=3	Q8BZN6	0.00	0.00	32.78	25.49	1.00	0.78	0.79	0.84	0.84	0.79	0.00	0.00	24.23	32.19	1.02	0.96	1.01	0.95	1.06	0.91	1.01	0.87	0.90	0.90	0.94	0.85
E3 ubiquitin-protein ligase UHRF1 OS=Mus musculus GN=Uhrf1 PE=1 SV=2	Q8VDF2	0.00	32.36	32.36	47.31	1.27	1.18	1.08	1.56	0.97	0.70	0.00	31.57	31.57	46.04	2.13	1.89	2.61	1.61	0.82	0.40	1.64	1.49	1.67	1.58	0.89	0.53
Nuclear pore complex protein Nup107 OS=Mus musculus GN=Nup107 PE=2 SV=1	Q8BH74	0.00	32.31	32.33	42.01	0.96	1.02	0.97	1.09	1.02	1.18	0.00	29.39	29.39	50.54	0.89	1.03	0.93	0.97	0.79	1.06	0.92	1.02	0.95	1.03	0.90	1.12
DNA topoisomerase 2-beta OS=Mus musculus GN=Top2b PE=1 SV=2	Q64511	0.00	32.10	60.15	41.00	0.99	1.04	1.01	1.01	1.02	1.02	0.00	39.29	60.90	44.35	1.15	0.95	1.20	0.79	0.66	0.60	1.07	0.99	1.10	0.89	0.82	0.78
Pumilio domain-containing protein KIAA0020 OS=Mus musculus GN=Kiaa0020 PE=2 SV=2	Q8BKS9	0.00	32.03	32.06	53.17	0.95	1.07	1.19	1.21	1.50	1.39	0.00	25.38	25.39	50.39	1.37	1.27	1.34	1.00	1.29	0.74	1.14	1.16	1.26	1.10	1.39	1.02
Probable ATP-dependent RNA helicase DDX27 OS=Mus musculus GN=Ddx27 PE=1 SV=3	Q921N6	0.00	31.85	31.87	51.45	0.92	0.94	1.02	1.14	1.45	1.37	0.00	28.90	28.91	50.00	0.72	1.04	0.95	1.29	1.94	0.91	0.82	0.99	0.99	1.21	1.67	1.12
RNA-binding protein Raly OS=Mus musculus GN=Raly PE=1 SV=3	Q64012	0.00	0.00	31.23	64.42	0.99	1.01	1.21	1.19	1.21	1.27	0.00	0.00	30.04	62.82	0.72	0.88	0.53	2.13	1.80	1.08	0.84	0.94	0.80	1.59	1.48	1.17
RNA-binding protein 39 OS=Mus musculus GN=Rbm39 PE=1 SV=2	Q8VH51	0.00	0.00	30.89	63.21	1.05	1.41	1.27	1.28	1.47	1.14	0.00	0.00	28.68	59.81	1.09	1.15	0.81	1.36	1.26	0.55	1.07	1.27	1.01	1.32	1.36	0.79
Double-strand-break repair protein rad21 homolog OS=Mus musculus GN=Rad21 PE=1 SV=3	Q61550	0.00	0.00	30.63	41.57	1.05	1.25	1.20	1.25	1.03	1.24	0.00	26.78	26.79	53.39	1.21	1.33	1.05	0.71	0.64	0.79	1.13	1.29	1.12	0.94	0.81	0.99
Histone H1.5 OS=Mus musculus GN=Hist1h1b PE=1 SV=2	P43276	0.00	0.00	36.73	50.22	0.86	0.67	0.81	1.10	1.02	0.90	0.00	25.54	32.84	64.13	1.03	0.87	0.65	0.81	0.90	0.65	0.94	0.76	0.73	0.94	0.95	0.77
Lamin-B2 OS=Mus musculus GN=Lmnb2 PE=1 SV=2	P21619	0.00	30.26	38.76	58.39	1.18	1.04	1.06	0.39	0.56	0.64	0.00	41.49	49.12	72.32	1.00	1.04	1.06	0.78	0.71	0.95	1.09	1.04	1.06	0.55	0.63	0.78
Mitochondrial inner membrane protein OS=Mus musculus GN=Immt PE=1 SV=1	Q8CAQ8	0.00	30.18	30.27	50.99	1.02	0.76	0.87	1.63	1.42	1.22	0.00	0.00	28.46	57.99	0.95	0.82	1.01	1.50	1.33	1.25	0.98	0.79	0.94	1.56	1.37	1.24
Importin subunit beta-1 OS=Mus musculus GN=Kpnb1 PE=1 SV=2	P70168	0.00	0.00	30.16	36.76	0.93	0.93	1.12	1.38	0.90	1.02	0.00	26.76	26.77	44.98	0.94	0.91	0.82	1.05	0.39	0.84	0.93	0.92	0.96	1.20	0.59	0.92
Heterogeneous nuclear ribonucleoproteins C1/C2 OS=Mus musculus GN=Hnrnpc PE=1 SV=1	Q9Z204	0.00	0.00	30.28	75.72	1.67	1.77	2.25	1.01	1.24	1.28	0.00	0.00	31.42	70.93	1.50	1.05	1.46	0.90	0.29	0.56	1.58	1.36	1.81	0.95	0.59	0.85
Protein polybromo-1 OS=Mus musculus GN=Pbrm1 PE=1 SV=4	Q8BSQ9	0.00	0.00	29.71	32.25	1.02	1.02	0.99	1.00	0.97	0.96	0.00	0.00	35.17	40.09	1.25	1.14	1.24	0.88	0.72	0.56	1.13	1.08	1.11	0.94	0.84	0.73
RNA binding motif protein, X-linked-like-1 OS=Mus musculus GN=Rbmxl1 PE=1 SV=1	Q91VM5	0.00	29.60	29.71	72.42	1.36	1.56	1.71	0.76	0.96	0.98	0.00	23.06	23.40	77.32	0.93	1.13	0.91	1.15	1.25	1.10	1.12	1.32	1.25	0.93	1.10	1.04
Unconventional myosin-Va OS=Mus musculus GN=Myo5a PE=1 SV=2	Q99104	0.00	29.49	29.98	34.92	0.98	0.42	0.61	0.63	0.28	0.34	0.00	31.69	31.95	38.59	1.03	0.42	0.72	0.54	0.17	0.15	1.00	0.42	0.66	0.58	0.22	0.22
Protein Sf3b2 OS=Mus musculus GN=Sf3b2 PE=2 SV=1	Q3UJB0	0.00	0.00	29.42	53.99	1.16	1.03	1.13	0.95	0.86	0.96	0.00	32.99	33.01	50.11	1.42	1.15	1.03	0.84	0.35	0.62	1.28	1.09	1.08	0.89	0.54	0.77
Telomere-associated protein RIF1 OS=Mus musculus GN=Rif1 PE=1 SV=2	Q6PR54	0.00	29.37	29.49	26.37	0.92	0.85	0.77	1.14	0.95	0.89	0.00	0.00	19.50	29.76	1.07	0.78	0.89	0.93	0.84	0.79	0.99	0.81	0.82	1.03	0.90	0.84
Recombining binding protein suppressor of hairless OS=Mus musculus GN=Rbpj PE=1 SV=1	P31266	0.00	29.12	29.12	45.82	0.77	0.97	0.72	0.93	1.34	1.11	0.00	0.00	31.70	55.32	0.90	0.95	0.62	0.77	0.47	0.54	0.84	0.96	0.67	0.85	0.79	0.77
Transducin beta-like protein 3 OS=Mus musculus GN=Tbl3 PE=2 SV=1	Q8C4J7	0.00	0.00	29.06	42.07	0.85	0.91	0.62	0.72	1.16	0.86	0.00	0.00	21.64	36.20	0.72	0.90	0.61	1.17	2.00	1.58	0.78	0.91	0.62	0.92	1.52	1.16
Histone H1.1 OS=Mus musculus GN=Hist1h1a PE=1 SV=2	P43275	0.00	28.89	38.74	53.05	0.90	0.84	0.94	0.96	0.68	0.63	0.00	30.45	38.60	59.15	0.99	1.01	0.29	0.70	0.58	0.24	0.94	0.92	0.52	0.82	0.63	0.39
Protein Rbm15 OS=Mus musculus GN=Rbm15 PE=2 SV=1	Q0VBL3	0.00	0.00	28.78	40.02	0.96	1.00	1.03	0.95	0.97	0.95	0.00	20.05	20.07	47.19	0.74	1.07	0.70	1.25	1.57	0.96	0.85	1.03	0.85	1.09	1.24	0.96
DNA-directed RNA polymerase II subunit RPB1 OS=Mus musculus GN=Polr2a PE=1 SV=3	P08775	0.00	0.00	28.45	38.12	1.50	1.20	1.16	0.77	0.77	0.72	0.00	30.29	30.41	38.32	1.26	1.15	1.00	0.99	1.06	0.49	1.37	1.17	1.08	0.87	0.90	0.60
DNA repair protein RAD50 OS=Mus musculus GN=Rad50 PE=1 SV=1	P70388	0.00	0.00	28.35	30.26	1.03	1.03	0.87	0.90	0.88	1.02	0.00	0.00	23.99	41.23	0.85	0.85	0.93	0.79	0.79	0.61	0.93	0.93	0.90	0.85	0.84	0.79
Protein Wdr36 OS=Mus musculus GN=Wdr36 PE=2 SV=1	Q3TA68	0.00	0.00	28.24	36.81	0.74	0.79	0.94	1.20	1.84	1.50	0.00	0.00	34.83	45.07	0.81	0.81	0.78	1.66	2.96	1.22	0.77	0.80	0.86	1.41	2.33	1.36
Pleiotropic regulator 1 OS=Mus musculus GN=Plrg1 PE=2 SV=1	Q922V4	0.00	28.03	28.03	62.18	0.71	1.05	0.66	1.02	1.08	1.06	0.00	28.29	28.29	53.61	0.90	1.03	0.49	0.87	0.28	0.42	0.80	1.04	0.57	0.94	0.55	0.67
BMS1 homolog, ribosome assembly protein (Yeast) OS=Mus musculus GN=Bms1 PE=2 SV=1	Q6PGF5	0.00	0.00	27.75	27.88	0.64	0.99	0.86	1.02	2.13	1.74	0.00	20.11	20.13	33.33	0.76	0.87	0.79	0.95	0.93	0.68	0.70	0.93	0.82	0.98	1.41	1.09
Putative ribosomal RNA methyltransferase NOP2 OS=Mus musculus GN=Nop2 PE=4 SV=1	E9QN31	0.00	27.68	27.70	49.12	0.95	0.95	0.96	0.96	1.03	1.06	0.00	36.74	36.75	49.75	0.93	0.96	0.86	0.88	1.24	1.56	0.94	0.96	0.91	0.92	1.13	1.28
Sp110 nuclear body protein OS=Mus musculus GN=Sp110 PE=1 SV=1	Q8BVK9	0.00	27.68	27.68	50.34	0.88	0.91	1.00	1.69	0.87	1.64	0.00	19.12	19.12	42.92	1.25	1.26	1.12	3.34	0.55	1.34	1.05	1.07	1.06	2.38	0.69	1.49
Interleukin enhancer-binding factor 2 OS=Mus musculus GN=Ilf2 PE=1 SV=1	Q9CXY6	0.00	0.00	27.45	51.03	1.06	1.42	1.39	0.78	0.81	0.98	0.00	26.99	27.01	65.13	1.17	1.22	1.20	0.86	0.86	0.79	1.11	1.32	1.29	0.82	0.84	0.88
60S ribosomal protein L4 OS=Mus musculus GN=Rpl4 PE=1 SV=3	Q9D8E6	0.00	0.00	27.17	64.44	1.71	1.58	1.72	1.38	1.67	1.47	0.00	19.90	19.91	57.52	1.67	1.27	1.12	1.87	1.66	1.46	1.69	1.42	1.39	1.61	1.67	1.47
RuvB-like 1 OS=Mus musculus GN=Ruvbl1 PE=1 SV=1	P60122	0.00	0.00	26.88	64.91	1.06	1.05	0.88	0.89	0.79	0.70	0.00	33.41	33.48	61.40	1.11	1.06	0.33	0.95	0.84	0.39	1.08	1.05	0.53	0.92	0.81	0.52
Pre-mRNA-processing factor 19 OS=Mus musculus GN=Prpf19 PE=2 SV=1	Q99KP6	0.00	26.83	26.86	47.62	1.08	1.05	0.74	0.66	0.50	0.58	0.00	26.59	26.61	51.98	1.39	1.08	1.14	1.02	0.75	0.49	1.22	1.06	0.92	0.82	0.61	0.53

Protien identification and qunatitation results from ProteinPilot for all the analyzed samples

Name	Accession number	% FDR	Unused	Total	%Cov	114:113	115:113	116:113	118:117	119:117	121:117	% FDR	Unused	Total	%Cov	114:113	115:113	116:113	118:117	119:117	121:117	114:113	115:113	116:113	118:117	119:117	121:117
Protein Mdn1 OS=Mus musculus GN=Mdn1 PE=4 SV=1	A2ANY6	0.00	26.77	26.94	21.04	1.29	1.27	1.29	1.09	1.31	1.01	0.00	28.73	28.99	27.14	1.09	1.08	1.37	1.10	1.34	1.17	1.19	1.17	1.33	1.09	1.32	1.09
Cohesin subunit SA-1 OS=Mus musculus GN=Stag1 PE=1 SV=3	Q9D3E6	0.00	26.66	26.95	35.29	0.90	1.06	0.98	0.72	0.97	0.81	0.00	33.09	33.29	38.55	1.07	1.84	1.37	0.69	0.64	0.49	0.98	1.39	1.16	0.71	0.79	0.63
Kinesin-like protein KIF20A OS=Mus musculus GN=Kif20a PE=2 SV=1	P97329	0.00	26.58	26.61	41.94	1.34	1.36	1.37	1.34	1.72	1.75	0.00	25.66	25.69	50.96	1.21	1.43	1.18	1.24	1.66	1.53	1.28	1.39	1.27	1.29	1.69	1.64
Transcriptional repressor p66 alpha OS=Mus musculus GN=Gatad2a PE=1 SV=2	Q8CHY6	0.00	0.00	26.52	50.08	0.91	0.97	1.02	1.45	1.41	1.50	0.00	0.00	17.62	58.35	0.50	0.90	0.86	2.05	2.07	1.92	0.68	0.93	0.94	1.72	1.71	1.70
U4/U6.U5 tri-snRNP-associated protein 1 OS=Mus musculus GN=Sart1 PE=2 SV=1	Q9Z315	0.00	26.47	26.51	44.54	0.88	0.87	0.94	0.87	0.77	0.86	0.00	20.46	20.57	51.61	1.28	1.00	1.17	0.79	0.86	0.70	1.06	0.93	1.05	0.83	0.81	0.78
MCG18410, isoform CRA_a OS=Mus musculus GN=Ddx23 PE=3 SV=1	D3Z0M9	0.00	26.36	26.37	45.05	1.01	0.87	0.95	0.98	0.79	0.86	0.00	22.99	23.00	50.92	0.90	0.54	1.19	1.03	1.34	0.54	0.95	0.69	1.06	1.00	1.03	0.68
Myelin expression factor 2 OS=Mus musculus GN=Myef2 PE=1 SV=1	Q8C854	0.00	26.27	26.31	46.70	0.98	1.08	0.94	0.65	0.89	0.93	0.00	25.29	25.30	50.25	0.99	1.01	0.97	0.70	0.30	0.29	0.99	1.04	0.95	0.68	0.52	0.52
Histone-binding protein RBBP4 OS=Mus musculus GN=Rbbp4 PE=1 SV=5	Q60972	0.00	26.25	26.26	48.47	1.09	1.02	0.94	0.92	0.76	0.77	0.00	0.00	24.50	44.71	0.95	0.94	0.70	0.86	0.52	0.73	1.02	0.98	0.81	0.89	0.63	0.75
Nesprin-3 OS=Mus musculus GN=Syne3 PE=1 SV=1	Q4FZC9	0.00	26.13	26.17	41.23	1.02	1.05	0.99	0.90	0.83	0.79	0.00	31.19	31.21	49.74	0.80	0.95	1.04	0.95	0.72	1.01	0.90	1.00	1.01	0.92	0.77	0.89
THO complex subunit 2 OS=Mus musculus GN=Thoc2 PE=3 SV=1	B1AZI6	0.00	25.96	26.31	31.62	0.98	1.01	0.98	0.97	1.01	1.01	0.00	31.35	31.37	33.00	0.86	1.08	0.92	1.00	1.27	0.52	0.92	1.04	0.95	0.99	1.13	0.72
Heterogeneous nuclear ribonucleoprotein D0 OS=Mus musculus GN=Hnrnpd PE=1 SV=2	Q60668	0.00	0.00	25.96	47.61	1.08	1.16	1.27	0.89	0.77	0.75	0.00	17.17	19.17	51.55	1.26	0.88	1.22	0.86	0.16	0.18	1.16	1.01	1.25	0.87	0.36	0.37
Chromosome-associated kinesin KIF4 OS=Mus musculus GN=Kif4 PE=2 SV=3	P33174	0.00	25.95	25.99	33.63	0.98	1.18	1.12	1.04	1.08	0.89	0.00	37.80	37.80	41.59	1.24	1.27	0.95	0.97	0.51	0.37	1.10	1.22	1.03	1.00	0.74	0.57
Splicing factor U2AF 65 kDa subunit OS=Mus musculus GN=U2af2 PE=1 SV=3	P26369	0.00	0.00	25.89	56.42	0.92	1.13	1.06	0.88	1.18	1.12	0.00	18.71	18.98	57.05	1.05	1.46	0.98	1.31	0.91	0.82	0.98	1.28	1.02	1.07	1.04	0.96
60S ribosomal protein L3 OS=Mus musculus GN=Rpl3 PE=2 SV=3	P27659	0.00	0.00	25.82	48.39	1.57	1.63	1.67	1.36	1.77	1.51	0.00	24.89	24.92	53.35	1.74	1.49	1.50	1.51	1.63	0.92	1.65	1.56	1.58	1.43	1.70	1.18
Moesin OS=Mus musculus GN=Msn PE=1 SV=3	P26041	0.00	0.00	25.83	49.22	1.31	1.47	1.45	1.37	0.75	0.50	0.00	23.97	23.98	50.43	1.41	1.31	1.66	1.32	0.64	0.43	1.36	1.39	1.55	1.34	0.69	0.46
Serine/arginine-rich splicing factor 1 OS=Mus musculus GN=Srsf1 PE=1 SV=3	Q6PDM2	0.00	0.00	25.78	79.03	0.85	0.77	0.71	1.18	1.13	0.89	0.00	24.14	24.15	89.92	0.85	1.06	1.04	1.57	1.20	0.61	0.85	0.90	0.86	1.36	1.16	0.74
Crooked neck-like protein 1 OS=Mus musculus GN=Crnkl1 PE=2 SV=1	P63154	0.00	25.60	25.61	48.26	1.08	1.04	1.25	1.18	1.25	1.29	0.00	19.07	19.08	36.38	1.04	1.13	1.16	0.99	1.08	1.06	1.06	1.08	1.20	1.08	1.16	1.17
Fermitin family homolog 3 OS=Mus musculus GN=Fermt3 PE=1 SV=1	Q8K1B8	0.00	0.00	25.71	47.67	0.98	1.11	1.15	1.12	0.95	0.72	0.00	26.51	26.54	51.28	0.92	1.12	1.18	1.18	0.87	0.81	0.95	1.11	1.16	1.15	0.91	0.77
Epidermal growth factor receptor kinase substrate 8 OS=Mus musculus GN=Eps8 PE=1 SV=2	Q08509	0.00	0.00	25.51	41.66	0.95	0.79	0.97	0.84	0.61	0.58	0.00	14.44	14.52	30.09	1.15	1.01	1.10	0.82	0.73	0.54	1.05	0.89	1.03	0.83	0.67	0.56
Peptidyl-prolyl cis-trans isomerase B OS=Mus musculus GN=Ppib PE=2 SV=2	P24369	0.00	0.00	25.41	73.15	0.98	0.78	1.08	0.96	0.96	0.82	0.00	23.68	23.68	75.93	1.06	0.74	0.86	1.13	0.53	0.10	1.02	0.76	0.96	1.04	0.72	0.29
Heterogeneous nuclear ribonucleoprotein L-like OS=Mus musculus GN=Hnrpll PE=1 SV=3	Q921F4	0.00	0.00	25.32	37.56	0.95	0.92	1.00	0.72	0.91	0.88	0.00	0.00	19.69	44.67	1.28	1.18	1.06	0.55	0.54	0.71	1.10	1.04	1.03	0.63	0.70	0.79
ATP-dependent RNA helicase DDX54 OS=Mus musculus GN=Ddx54 PE=1 SV=1	Q8K4L0	0.00	25.08	25.09	44.39	1.05	1.00	1.11	1.22	1.47	1.36	0.00	21.44	21.45	50.46	0.82	0.98	0.95	1.15	1.61	1.37	0.92	0.99	1.03	1.19	1.54	1.36
Intron-binding protein aquarius OS=Mus musculus GN=Aqr PE=2 SV=2	Q8CFQ3	0.00	25.01	25.42	31.26	0.88	1.14	1.07	1.21	1.31	1.43	0.00	25.53	25.56	38.08	0.92	1.21	0.69	1.17	1.16	0.46	0.90	1.17	0.86	1.19	1.23	0.81
Pescadillo homolog OS=Mus musculus GN=Pes1 PE=1 SV=1	Q9EQ61	0.00	24.99	25.01	43.66	1.22	1.15	1.38	1.33	1.61	1.47	0.00	0.00	25.87	43.66	1.18	1.46	1.13	1.82	1.49	1.80	1.20	1.29	1.25	1.56	1.55	1.63
ATP-dependent RNA helicase DDX3X OS=Mus musculus GN=Ddx3x PE=1 SV=3	Q62167	0.00	0.00	28.94	43.05	0.92	0.98	1.11	1.56	1.37	1.27	0.00	28.42	32.54	54.83	1.10	0.84	1.00	1.24	1.37	0.93	1.00	0.91	1.05	1.39	1.37	1.09
RNA-binding protein 28 OS=Mus musculus GN=Rbm28 PE=1 SV=4	Q8CGC6	0.00	24.72	24.72	35.87	1.02	1.01	1.08	0.94	0.98	1.07	0.00	27.40	27.40	40.67	1.09	1.24	0.89	0.72	1.60	0.47	1.05	1.12	0.98	0.82	1.25	0.71
Protein ELYS OS=Mus musculus GN=Ahctf1 PE=1 SV=1	Q8CJF7	0.00	24.54	24.71	28.58	1.01	1.00	0.99	1.00	1.05	1.05	0.00	27.68	28.02	38.34	1.10	0.99	1.07	0.96	1.13	0.96	1.05	1.00	1.03	0.98	1.09	1.00
Probable ATP-dependent RNA helicase DDX46 OS=Mus musculus GN=Ddx46 PE=1 SV=2	Q569Z5	0.00	0.00	24.57	37.11	0.90	0.97	0.95	1.11	1.06	0.94	0.00	15.57	15.59	37.31	0.80	0.91	1.22	1.25	1.21	1.15	0.85	0.94	1.08	1.17	1.13	1.04
CCAAT/enhancer-binding protein zeta OS=Mus musculus GN=Cebpz PE=2 SV=2	P53569	0.00	24.43	24.46	26.43	0.89	0.88	0.93	1.05	1.18	1.08	0.00	23.93	23.94	37.55	0.69	0.63	0.64	0.83	1.24	0.38	0.78	0.74	0.77	0.93	1.21	0.64
Probable rRNA-processing protein EBP2 OS=Mus musculus GN=Ebna1bp2 PE=2 SV=1	Q9D903	0.00	24.22	24.23	54.90	1.94	1.57	1.63	0.41	0.86	0.65	0.00	18.34	18.35	59.15	1.72	1.06	0.88	0.91	0.55	0.16	1.83	1.29	1.20	0.61	0.69	0.32
Cirhin OS=Mus musculus GN=Cirh1a PE=2 SV=3	Q8R2N2	0.00	0.00	24.36	41.84	1.09	1.14	1.02	1.12	1.31	1.28	0.00	18.92	19.05	39.21	1.19	1.32	1.06	1.04	1.12	0.68	1.14	1.22	1.04	1.08	1.21	0.93
U4/U6.U5 tri-snRNP-associated protein 2 OS=Mus musculus GN=Usp39 PE=2 SV=2	Q3TIX9	0.00	24.09	24.09	53.37	0.74	0.86	0.90	0.92	0.84	1.08	0.00	21.78	21.78	53.55	1.12	1.03	1.14	1.28	1.00	0.13	0.91	0.94	1.01	1.09	0.92	0.37
5'-3' exoribonuclease 2 OS=Mus musculus GN=Xrn2 PE=1 SV=1	Q9DBR1	0.00	23.98	23.98	36.38	0.98	0.98	0.99	0.97	0.96	1.01	0.00	25.86	26.13	39.96	0.75	1.09	0.82	0.86	0.80	0.45	0.86	1.03	0.90	0.92	0.88	0.67
U2 small nuclear ribonucleoprotein A' OS=Mus musculus GN=Snrpa1 PE=1 SV=2	P57784	0.00	23.96	23.97	71.37	1.03	1.16	1.22	0.95	1.06	1.25	0.00	15.68	15.70	61.96	0.72	0.99	0.66	0.90	1.29	1.02	0.86	1.07	0.90	0.92	1.17	1.13
Inner centromere protein OS=Mus musculus GN=Incenp PE=1 SV=2	Q9WU62	0.00	23.84	23.87	44.43	1.46	1.42	1.46	0.69	0.66	0.71	0.00	20.99	21.01	38.52	1.45	1.34	1.11	0.86	0.90	0.88	1.45	1.38	1.27	0.77	0.77	0.79
Bromodomain-containing protein 4 OS=Mus musculus GN=Brd4 PE=1 SV=1	Q9ESU6	0.00	0.00	23.83	34.50	1.22	1.33	1.16	0.76	0.82	0.65	0.00	0.00	14.15	27.43	1.05	1.00	1.08	0.85	0.83	0.88	1.13	1.15	1.12	0.80	0.83	0.76
Thyroid hormone receptor-associated protein 3 OS=Mus musculus GN=Thrap3 PE=1 SV=1	Q569Z6	0.00	23.78	23.80	41.32	0.99	0.98	1.02	1.28	1.01	1.09	0.00	20.29	20.30	47.21	0.87	0.83	0.71	1.22	0.80	0.95	0.93	0.90	0.85	1.25	0.90	1.02

Protien identification and qunatitation results from ProteinPilot for all the analyzed samples

Name	Accession number	% FDR	Unused	Total	%Cov	114:113	115:113	116:113	118:117	119:117	121:117	% FDR	Unused	Total	%Cov	114:113	115:113	116:113	118:117	119:117	121:117	114:113	115:113	116:113	118:117	119:117	121:117
Heterogeneous nuclear ribonucleoprotein A0 OS=Mus musculus GN=Hnrnpa0 PE=1 SV=1	Q9CX86	0.00	23.69	26.84	59.34	0.78	0.70	0.76	0.98	1.25	1.06	0.00	15.41	18.67	71.48	1.05	1.11	1.08	0.83	0.34	0.28	0.90	0.88	0.90	0.90	0.65	0.54
ADP/ATP translocase 2 OS=Mus musculus GN=Slc25a5 PE=1 SV=3	P51881	0.00	0.00	23.64	65.44	1.24	1.60	1.47	0.67	0.84	0.58	0.00	21.40	21.40	63.76	1.02	0.92	0.84	0.82	0.70	0.08	1.12	1.21	1.11	0.74	0.77	0.22
U5 small nuclear ribonucleoprotein 40 kDa protein OS=Mus musculus GN=Snrnp40 PE=2 SV=1	Q6PE01	0.00	23.50	23.51	53.35	0.90	1.02	1.15	0.86	1.07	1.13	0.00	25.86	25.87	82.40	0.92	1.07	0.74	1.32	0.94	0.98	0.91	1.04	0.92	1.07	1.00	1.05
DBIRD complex subunit KIAA1967 homolog OS=Mus musculus PE=1 SV=2	Q8VDP4	0.00	23.47	23.50	30.69	1.00	1.15	0.98	0.82	0.86	0.88	0.00	13.42	13.44	37.74	0.83	1.32	1.01	0.60	1.09	0.91	0.91	1.23	1.00	0.70	0.96	0.90
Protein Fubp3 OS=Mus musculus GN=Fubp3 PE=2 SV=1	Q3TIX6	0.00	23.31	23.33	54.78	1.10	1.26	1.50	1.17	1.21	1.38	0.00	22.43	22.44	66.96	1.16	1.49	1.38	1.00	1.18	0.23	1.13	1.37	1.44	1.08	1.20	0.57
Apoptosis inhibitor 5 OS=Mus musculus GN=Api5 PE=2 SV=2	O35841	0.00	0.00	23.27	50.60	1.05	1.04	0.96	0.74	0.72	0.82	0.00	28.09	28.09	62.70	1.20	1.28	1.05	0.63	0.61	0.40	1.12	1.15	1.00	0.68	0.67	0.57
WD40 repeat-containing protein SMU1 OS=Mus musculus GN=Smu1 PE=2 SV=2	Q3UKJ7	0.00	23.25	23.25	51.85	0.99	1.10	0.71	0.69	0.79	0.90	0.00	18.99	19.00	52.44	0.86	0.89	0.66	1.14	0.95	0.81	0.92	0.99	0.69	0.88	0.87	0.86
60S ribosomal protein L7a OS=Mus musculus GN=Rpl7a PE=2 SV=2	P12970	0.00	0.00	23.25	67.29	1.46	1.38	1.45	1.56	1.72	1.49	0.00	0.00	22.39	66.17	1.50	1.10	1.13	1.41	1.39	0.68	1.48	1.23	1.28	1.48	1.55	1.00
Pinin OS=Mus musculus GN=Pnn PE=1 SV=4	O35691	0.00	0.00	23.19	41.52	1.04	1.00	1.04	1.02	1.02	0.99	0.00	0.00	21.44	34.76	1.31	1.21	1.46	0.91	0.90	0.85	1.16	1.10	1.23	0.96	0.95	0.92
Structural maintenance of chromosomes protein 4 OS=Mus musculus GN=Smc4 PE=1 SV=1	Q8CG47	0.00	22.78	22.81	30.17	1.15	1.12	1.09	1.17	1.11	0.73	0.00	0.00	30.43	36.08	1.32	0.95	1.18	1.10	1.04	0.63	1.23	1.03	1.13	1.13	1.07	0.68
H/ACA ribonucleoprotein complex subunit 4 OS=Mus musculus GN=Dkc1 PE=1 SV=4	Q9ESX5	0.00	0.00	22.78	50.69	0.82	1.04	0.82	0.74	0.92	0.96	0.00	24.65	24.66	56.58	1.02	1.09	0.72	0.94	0.65	0.77	0.92	1.06	0.77	0.84	0.78	0.86
Nucleolar protein 6 OS=Mus musculus GN=Nol6 PE=2 SV=2	Q8R5K4	0.00	22.68	22.82	34.20	0.90	1.08	1.05	0.94	1.71	1.56	0.00	22.93	22.95	37.76	0.81	0.85	1.29	0.66	0.76	0.41	0.86	0.95	1.16	0.79	1.14	0.79
ELAV-like protein 1 OS=Mus musculus GN=Elavl1 PE=1 SV=2	P70372	0.00	0.00	22.66	58.59	0.90	0.64	0.83	0.74	0.86	0.86	0.00	26.34	26.34	70.86	1.00	0.96	0.79	0.76	0.68	0.36	0.95	0.78	0.81	0.75	0.77	0.55
Guanine nucleotide-binding protein-like 3 OS=Mus musculus GN=Gnl3 PE=1 SV=2	Q8CI11	0.00	0.00	22.60	53.72	1.63	1.47	1.57	1.45	1.61	1.45	0.00	20.66	20.69	53.53	2.61	2.61	2.09	1.84	1.80	0.87	2.06	1.96	1.81	1.63	1.71	1.12
FACT complex subunit SSRP1 OS=Mus musculus GN=Ssrp1 PE=1 SV=2	Q08943	0.00	22.55	22.56	37.71	1.04	0.93	0.99	1.36	1.03	0.80	0.00	0.00	26.02	36.86	0.82	0.94	0.84	1.27	0.86	0.49	0.92	0.93	0.91	1.31	0.94	0.63
U1 small nuclear ribonucleoprotein 70 kDa OS=Mus musculus GN=Snrnp70 PE=1 SV=2	Q62376	0.00	0.00	22.39	57.37	1.29	1.14	1.00	1.42	1.46	0.87	0.00	16.80	16.80	54.46	1.28	1.16	1.24	1.11	0.86	0.82	1.29	1.15	1.11	1.25	1.12	0.84
U3 small nucleolar RNA-associated protein 14 homolog A OS=Mus musculus GN=Utp14a PE=2 SV=1	Q640M1	0.00	22.35	22.37	39.11	0.77	0.69	0.81	1.05	1.04	0.80	0.00	21.42	21.44	38.59	0.95	0.94	0.98	0.95	0.92	1.01	0.86	0.80	0.89	1.00	0.98	0.90
Splicing factor 3A subunit 3 OS=Mus musculus GN=Sf3a3 PE=2 SV=2	Q9D554	0.00	0.00	22.28	49.30	0.98	0.95	0.92	0.88	0.82	0.90	0.00	26.99	26.99	53.29	1.10	0.95	0.95	0.89	0.48	0.39	1.04	0.95	0.94	0.88	0.63	0.59
DNA damage-binding protein 1 OS=Mus musculus GN=Ddb1 PE=1 SV=2	Q3U1J4	0.00	22.19	22.21	29.56	1.08	1.02	1.08	1.07	0.87	1.02	0.00	33.16	33.18	41.23	0.98	1.22	1.04	1.03	0.71	0.67	1.03	1.12	1.06	1.05	0.79	0.83
Transcriptional repressor p66-beta OS=Mus musculus GN=Gatad2b PE=1 SV=1	Q8VHR5	0.00	0.00	24.14	51.18	0.99	0.93	0.91	1.04	0.96	1.02	0.00	25.85	25.87	53.03	0.88	1.03	0.95	0.99	0.81	0.87	0.93	0.98	0.93	1.01	0.88	0.94
Nuclear pore complex protein Nup133 OS=Mus musculus GN=Nup133 PE=1 SV=2	Q8R0G9	0.00	21.99	22.02	29.18	1.00	1.06	0.98	0.84	0.91	0.92	0.00	23.15	23.17	33.68	0.90	0.99	1.02	0.74	0.86	0.51	0.95	1.02	1.00	0.79	0.89	0.68
Cleavage and polyadenylation specificity factor subunit 1 OS=Mus musculus GN=Cpsf1 PE=1 SV=1	Q9EPU4	0.00	21.95	22.11	29.29	0.82	0.95	0.96	1.03	1.24	1.47	0.00	16.34	16.59	33.52	0.78	0.88	0.78	0.94	1.17	1.47	0.80	0.92	0.87	0.98	1.20	1.47
Transcription elongation regulator 1 OS=Mus musculus GN=Tcerg1 PE=1 SV=2	Q8CGF7	0.00	0.00	23.40	34.18	1.01	1.01	0.90	0.77	0.93	0.78	0.00	17.05	18.80	33.36	1.26	1.05	0.95	0.70	0.61	0.57	1.13	1.03	0.92	0.73	0.75	0.67
Growth arrest-specific protein 7 OS=Mus musculus GN=Gas7 PE=1 SV=1	Q60780	0.00	0.00	19.63	52.02	1.17	1.41	1.34	1.51	1.58	1.31	0.00	0.00	20.65	54.16	1.56	1.53	1.66	1.42	1.03	0.70	1.35	1.47	1.49	1.47	1.28	0.96
40S ribosomal protein S3 OS=Mus musculus GN=Rps3 PE=1 SV=1	P62908	0.00	0.00	21.45	72.84	0.89	0.86	0.95	1.46	1.41	1.24	0.00	23.02	23.02	77.37	0.74	0.86	0.73	1.72	1.47	0.39	0.81	0.86	0.83	1.58	1.44	0.70
Hepatoma-derived growth factor OS=Mus musculus GN=Hdgf PE=1 SV=2	P51859	0.00	21.45	21.45	66.24	1.51	1.38	1.38	0.96	0.79	0.73	0.00	14.49	15.93	66.24	1.20	0.86	0.88	0.76	0.34	0.19	1.35	1.09	1.10	0.86	0.52	0.37
U3 small nucleolar RNA-associated protein 15 homolog OS=Mus musculus GN=Utp15 PE=2 SV=1	Q8C7V3	0.00	21.41	21.44	40.72	0.72	0.84	0.76	0.96	1.33	1.32	0.00	19.72	19.73	49.24	0.99	1.12	0.86	1.29	1.51	1.46	0.84	0.97	0.81	1.12	1.42	1.39
Cytoplasmic FMR1-interacting protein 1 OS=Mus musculus GN=Cyfip1 PE=1 SV=1	Q7TMB8	0.00	21.32	21.51	28.33	0.98	1.06	0.97	1.15	1.18	0.77	0.00	13.36	13.44	33.28	0.81	1.07	0.93	1.39	1.12	0.92	0.89	1.06	0.95	1.26	1.15	0.84
40S ribosomal protein S4, X isoform OS=Mus musculus GN=Rps4x PE=2 SV=2	P62702	0.00	0.00	21.26	68.82	1.12	1.32	1.36	1.69	1.79	1.43	0.00	0.00	19.92	74.14	1.01	0.95	0.91	1.27	1.17	0.69	1.06	1.12	1.11	1.47	1.45	1.00
SWI/SNF-related matrix-associated actin-dependent regulator of chromatin subfamily D member 2 OS=Mus musculus GN=Smarcd2 PE=2 SV=2	Q99JR8	0.00	21.18	21.18	51.04	1.03	1.11	1.07	0.84	0.89	0.92	0.00	23.83	23.83	57.63	1.13	1.27	0.95	1.13	0.92	1.12	1.08	1.19	1.01	0.97	0.90	1.01
SWI/SNF complex subunit SMARCC2 OS=Mus musculus GN=Smarcc2 PE=1 SV=2	Q6PDG5	0.00	21.04	35.17	33.06	0.96	0.95	0.98	1.01	0.97	0.96	0.00	0.00	34.38	36.77	0.94	0.80	0.95	0.82	0.32	0.35	0.95	0.87	0.97	0.91	0.56	0.58
Bromodomain adjacent to zinc finger domain protein 1A OS=Mus musculus GN=Baz1a PE=1 SV=3	O88379	0.00	21.03	21.11	30.48	1.08	1.16	1.09	1.29	1.45	1.66	0.00	0.00	28.57	35.69	1.04	1.14	1.10	1.17	1.15	1.45	1.06	1.15	1.09	1.23	1.29	1.55
Integrator complex subunit 1 OS=Mus musculus GN=Ints1 PE=1 SV=2	Q6P4S8	0.00	0.00	21.05	26.29	0.85	0.77	0.79	0.90	0.79	0.94	0.00	14.51	14.52	29.20	0.87	0.94	0.81	0.88	0.90	1.10	0.86	0.85	0.80	0.89	0.84	1.01
Nucleolar transcription factor 1 OS=Mus musculus GN=Ubtf PE=1 SV=1	P25976	0.00	0.00	20.98	30.33	0.65	0.49	0.75	0.95	0.63	0.72	0.00	0.00	17.90	38.04	0.78	0.86	0.82	1.08	0.90	0.62	0.71	0.65	0.78	1.01	0.75	0.67
Protein Kifc5b OS=Mus musculus GN=Kifc5b PE=3 SV=1	E9PUA5	0.00	20.86	20.90	43.45	0.87	1.05	0.83	0.86	0.82	0.86	0.00	12.30	12.31	50.89	0.96	0.91	0.99	0.85	0.93	0.93	0.92	0.98	0.91	0.86	0.87	0.90
Zinc finger RNA-binding protein OS=Mus musculus GN=Zfr PE=1 SV=2	O88532	0.00	20.65	20.76	34.36	1.08	1.21	1.18	0.98	1.07	1.03	0.00	20.72	20.77	46.46	0.90	0.92	0.97	0.60	1.34	0.72	0.99	1.06	1.07	0.77	1.20	0.86

Protien identification and qunatitation results from ProteinPilot for all the analyzed samples

Name	Accession number	% FDR	Unused	Total	%Cov	114:113	115:113	116:113	118:117	119:117	121:117	% FDR	Unused	Total	%Cov	114:113	115:113	116:113	118:117	119:117	121:117	114:113	115:113	116:113	118:117	119:117	121:117
Testis-expressed sequence 10 protein OS=Mus musculus GN=Tex10 PE=1 SV=1	Q3URQ0	0.00	20.63	20.68	29.42	1.34	1.31	1.37	1.18	1.28	1.42	0.00	14.29	14.38	27.80	1.02	1.12	1.06	1.11	1.32	1.46	1.17	1.21	1.20	1.14	1.30	1.44
Actin-binding protein anillin OS=Mus musculus GN=Anln PE=1 SV=2	Q8K298	0.00	20.54	20.55	33.81	1.06	1.18	1.03	1.03	0.92	0.83	0.00	20.03	20.04	33.01	1.02	1.06	1.12	0.93	0.82	0.51	1.04	1.12	1.07	0.98	0.87	0.65
Serine/threonine-protein phosphatase PP1-alpha catalytic subunit OS=Mus musculus GN=Ppp1ca PE=1 SV=1	P62137	0.00	0.00	20.92	45.15	1.13	0.95	1.04	1.03	0.98	1.06	0.00	22.19	22.19	50.00	0.91	0.31	0.35	1.74	1.32	2.29	1.01	0.54	0.61	1.34	1.14	1.56
Coronin-1A OS=Mus musculus GN=Coro1a PE=1 SV=5	O89053	0.00	0.00	20.45	36.01	1.21	0.09	0.26	0.53	0.18	0.17	0.00	19.41	19.41	49.02	1.27	0.17	0.35	0.63	0.39	0.68	1.24	0.12	0.30	0.58	0.26	0.34
THO complex subunit 1 OS=Mus musculus GN=Thoc1 PE=1 SV=1	Q8R3N6	0.00	20.33	20.48	26.48	0.89	0.79	1.01	1.20	0.86	1.27	0.00	26.28	26.28	45.05	0.74	0.56	0.74	1.03	1.04	0.34	0.81	0.67	0.87	1.11	0.95	0.65
N-acylneuraminate cytidylyltransferase OS=Mus musculus GN=Cmas PE=1 SV=2	Q99KK2	0.00	20.30	20.32	52.08	1.12	1.16	0.98	0.61	0.69	0.69	0.00	20.29	20.30	65.97	1.08	1.08	0.85	0.77	0.90	0.31	1.10	1.12	0.91	0.68	0.79	0.46
U3 small nucleolar RNA-associated protein 6 homolog OS=Mus musculus GN=Utp6 PE=2 SV=1	Q8VCY6	0.00	20.30	20.31	40.54	0.98	1.02	1.05	1.07	1.32	1.28	0.00	21.43	21.45	48.41	1.03	1.21	1.25	1.18	0.98	1.03	1.00	1.11	1.14	1.12	1.14	1.15
High mobility group protein B2 OS=Mus musculus GN=Hmgb2 PE=1 SV=3	P30681	0.00	20.29	20.29	71.43	1.14	1.31	1.41	1.08	0.95	0.77	0.00	15.53	15.53	71.90	1.60	1.18	1.20	0.95	0.32	0.15	1.35	1.24	1.30	1.01	0.55	0.34
PH-interacting protein OS=Mus musculus GN=Phip PE=1 SV=2	Q8VDD9	0.00	0.00	19.50	29.98	0.86	0.98	0.83	0.97	0.93	0.97	0.00	0.00	17.51	30.75	0.90	0.91	0.87	0.90	0.88	0.55	0.88	0.95	0.85	0.94	0.90	0.73
Protein DEK OS=Mus musculus GN=Dek PE=1 SV=1	Q7TNV0	0.00	20.03	20.04	37.89	0.90	1.13	0.86	0.78	0.61	0.54	0.00	20.30	20.31	42.37	0.81	1.10	0.69	0.92	0.34	0.23	0.86	1.11	0.77	0.85	0.46	0.35
RNA 3'-terminal phosphate cyclase-like protein OS=Mus musculus GN=Rcl1 PE=2 SV=1	Q9JJT0	0.00	0.00	20.03	37.53	0.72	0.86	0.95	0.75	1.28	1.29	0.00	18.74	18.77	49.60	0.92	0.92	0.95	0.98	1.04	1.04	0.81	0.89	0.95	0.86	1.15	1.16
Superkiller viralicidic activity 2-like 2 OS=Mus musculus GN=Skiv2l2 PE=2 SV=1	Q9CZU3	0.00	0.00	19.99	34.71	1.11	1.07	0.94	1.75	1.79	2.03	0.00	32.39	32.55	46.06	1.01	1.01	1.06	1.31	1.15	1.07	1.06	1.04	1.00	1.51	1.43	1.47
MKI67 FHA domain-interacting nucleolar phosphoprotein OS=Mus musculus GN=Mki67ip PE=2 SV=1	Q91VE6	0.00	19.84	19.84	65.30	1.29	1.20	1.42	1.49	1.94	1.72	0.00	20.92	20.92	63.72	0.97	1.07	1.24	1.29	1.39	0.27	1.12	1.13	1.32	1.39	1.64	0.68
Kinesin-like protein KIF22 OS=Mus musculus GN=Kif22 PE=2 SV=2	Q3V300	0.00	19.70	19.73	50.45	1.31	1.38	1.33	1.08	0.95	0.70	0.00	9.62	9.64	53.94	1.20	1.20	1.22	1.15	1.11	0.88	1.25	1.29	1.28	1.11	1.03	0.78
Regulator of chromosome condensation OS=Mus musculus GN=Rcc1 PE=1 SV=1	Q8VE37	0.00	0.00	19.46	50.59	0.99	1.32	1.14	0.74	1.06	0.95	0.00	0.00	26.75	62.71	0.84	0.93	0.86	1.19	0.93	1.27	0.91	1.11	0.99	0.94	0.99	1.10
Proliferation-associated protein 2G4 OS=Mus musculus GN=Pa2g4 PE=1 SV=3	P50580	0.00	0.00	19.38	54.31	1.75	1.74	1.77	1.25	1.72	1.36	0.00	12.26	12.26	39.09	1.45	1.17	1.28	1.46	1.69	0.75	1.59	1.43	1.51	1.35	1.71	1.01
Myeloid cell nuclear differentiation antigen-like protein OS=Mus musculus GN=Mndal PE=2 SV=1	D0QMC3	0.00	19.33	26.75	48.14	0.87	1.11	0.99	1.34	0.70	1.21	0.00	21.00	26.18	37.55	0.83	0.97	1.06	1.02	0.14	0.77	0.85	1.04	1.02	1.17	0.32	0.96
Scaffold attachment factor B1 OS=Mus musculus GN=Safb PE=1 SV=2	D3YXK2	0.00	19.31	19.67	41.84	1.01	1.01	1.05	1.00	1.00	0.98	0.00	15.23	15.37	37.99	0.93	0.96	0.40	0.95	0.58	0.34	0.97	0.99	0.65	0.97	0.76	0.58
Serine/arginine-rich splicing factor 3 OS=Mus musculus GN=Srsf3 PE=1 SV=1	P84104	0.00	0.00	19.14	82.32	0.77	1.08	1.12	1.37	1.21	1.26	0.00	21.10	21.10	80.49	1.08	0.98	1.06	1.22	1.10	1.02	0.91	1.03	1.09	1.29	1.15	1.13
WD repeat-containing protein 43 OS=Mus musculus GN=Wdr43 PE=1 SV=2	Q6ZQL4	0.00	19.08	19.10	38.40	0.73	0.74	0.86	1.54	1.87	1.71	0.00	26.95	26.96	53.47	0.60	0.45	0.60	1.16	1.21	1.06	0.66	0.58	0.71	1.34	1.51	1.34
Cell division cycle and apoptosis regulator protein 1 OS=Mus musculus GN=Ccar1 PE=1 SV=1	Q8CH18	0.00	18.88	19.09	24.35	0.99	0.92	0.95	0.97	0.95	0.96	0.00	18.33	18.35	29.58	0.80	0.72	0.81	0.81	0.82	0.61	0.89	0.81	0.87	0.89	0.89	0.77
60S ribosomal protein L7 OS=Mus musculus GN=Rpl7 PE=2 SV=2	P14148	0.00	0.00	19.00	60.74	1.58	1.50	1.63	1.53	1.85	1.49	0.00	15.52	15.63	56.30	2.49	1.77	1.87	1.91	1.91	0.18	1.99	1.63	1.75	1.71	1.88	0.52
Probable ATP-dependent RNA helicase DDX17 OS=Mus musculus GN=Ddx17 PE=2 SV=1	Q501J6	0.00	18.84	42.52	55.69	1.16	1.17	1.10	1.25	0.90	0.91	0.00	23.03	45.00	51.08	1.26	1.09	1.10	0.98	0.38	0.13	1.21	1.13	1.10	1.11	0.58	0.35
Dedicator of cytokinesis protein 8 OS=Mus musculus GN=Dock8 PE=1 SV=4	Q8C147	0.00	0.00	18.88	22.33	1.16	0.72	0.76	0.93	0.74	0.70	0.00	23.61	23.63	30.71	1.08	0.68	0.82	0.88	0.76	0.61	1.12	0.70	0.79	0.90	0.75	0.65
Putative oxidoreductase GLYR1 OS=Mus musculus GN=Glyr1 PE=2 SV=1	Q922P9	0.00	0.00	16.76	36.45	1.02	1.05	1.07	0.96	0.98	0.95	0.00	0.00	17.68	49.45	1.14	1.38	1.07	1.03	0.41	0.32	1.08	1.20	1.07	1.00	0.64	0.55
Actin-like protein 6A OS=Mus musculus GN=Actl6a PE=1 SV=2	Q9Z2N8	0.00	0.00	18.55	53.15	0.82	1.01	0.79	0.79	0.79	0.87	0.00	19.51	19.51	50.82	0.81	0.87	0.79	1.03	0.63	0.80	0.82	0.94	0.79	0.90	0.71	0.84
Bifunctional polynucleotide phosphatase/kinase OS=Mus musculus GN=Pnkp PE=1 SV=2	Q9JLV6	0.00	0.00	18.43	46.17	0.75	1.06	0.84	0.93	0.86	0.97	0.00	0.00	13.66	41.57	0.97	1.03	0.96	0.96	0.93	1.02	0.86	1.04	0.90	0.95	0.90	1.00
Lamina-associated polypeptide 2, isoforms beta/delta/epsilon/gamma OS=Mus musculus GN=Tmpo PE=1 SV=4	Q61029	0.00	0.00	35.20	67.70	0.85	1.29	1.11	1.21	1.11	0.82	0.00	20.47	36.51	66.37	1.15	0.95	1.06	1.04	0.48	0.52	0.99	1.11	1.08	1.12	0.73	0.65
Histone deacetylase 1 OS=Mus musculus GN=Hdac1 PE=1 SV=1	O09106	0.00	0.00	18.36	46.47	0.96	1.02	1.07	1.08	1.02	1.09	0.00	19.59	19.59	43.15	0.86	1.05	0.67	0.91	0.93	0.72	0.91	1.03	0.84	0.99	0.97	0.89
CUGBP Elav-like family member 2 OS=Mus musculus GN=Celf2 PE=1 SV=1	Q9Z0H4	0.00	18.34	18.35	37.01	0.96	1.09	0.92	0.84	0.75	0.67	0.00	0.00	12.06	34.84	0.91	1.00	0.81	0.94	0.43	0.62	0.94	1.04	0.86	0.89	0.57	0.64
Polycomb protein Suz12 OS=Mus musculus GN=Suz12 PE=1 SV=2	Q80U70	0.00	0.00	18.24	36.57	0.93	0.95	0.99	1.00	0.99	0.99	0.00	21.54	21.55	45.88	0.82	1.05	0.88	0.95	1.01	1.08	0.87	1.00	0.93	0.97	1.00	1.03
Serrate RNA effector molecule homolog OS=Mus musculus GN=Srrt PE=1 SV=1	Q99MR6	0.00	18.19	18.21	42.40	1.07	1.13	0.95	1.26	1.29	1.34	0.00	23.67	23.68	41.83	0.93	0.89	1.00	0.75	0.76	0.95	1.00	1.00	0.98	0.97	0.99	1.13
Pre-mRNA-splicing factor SYF1 OS=Mus musculus GN=Xab2 PE=2 SV=1	Q9DCD2	0.00	0.00	18.19	45.38	0.95	0.95	1.34	1.27	1.21	1.47	0.00	16.67	16.68	43.51	0.97	1.16	1.08	1.02	1.12	1.42	0.96	1.05	1.20	1.14	1.16	1.45
Condensin complex subunit 1 OS=Mus musculus GN=Ncapd2 PE=1 SV=2	Q8K2Z4	0.00	18.11	18.19	27.16	1.02	0.99	0.82	1.24	1.06	0.82	0.00	10.04	10.11	38.15	0.96	0.99	0.98	1.11	1.08	0.65	0.99	0.99	0.90	1.17	1.07	0.73
KH domain-containing, RNA-binding, signal transduction-associated protein 1 OS=Mus musculus GN=Khdrbs1 PE=1 SV=2	Q60749	0.00	18.11	18.12	56.66	1.38	1.12	1.29	1.18	1.03	0.96	0.00	20.88	20.90	52.82	1.27	1.25	0.90	0.88	0.87	0.52	1.32	1.18	1.08	1.02	0.95	0.71

Protien identification and qunatitation results from ProteinPilot for all the analyzed samples

Name	Accession number	% FDR	Unused	Total	%Cov	114:113	115:113	116:113	118:117	119:117	121:117	% FDR	Unused	Total	%Cov	114:113	115:113	116:113	118:117	119:117	121:117	114:113	115:113	116:113	118:117	119:117	121:117
Nucleophosmin OS=Mus musculus GN=Npm1 PE=1 SV=1	Q61937	0.00	0.00	18.02	55.14	0.95	0.52	0.84	1.00	0.82	1.10	0.00	17.88	17.88	55.14	0.70	0.31	0.47	1.10	0.49	0.79	0.82	0.40	0.63	1.05	0.63	0.93
PC4 and SFRS1-interacting protein OS=Mus musculus GN=Psip1 PE=1 SV=1	Q99JF8	0.00	17.99	19.13	44.32	1.14	1.00	1.08	0.94	0.64	0.64	0.00	25.90	25.90	54.55	2.27	0.95	0.91	0.75	0.33	0.16	1.61	0.98	0.99	0.84	0.46	0.33
Ribosome biogenesis protein BOP1 OS=Mus musculus GN=Bop1 PE=1 SV=1	P97452	0.00	0.00	17.99	33.88	1.02	1.18	1.25	1.28	1.61	1.61	0.00	17.65	17.65	42.76	1.06	2.42	1.82	1.41	1.27	1.09	1.04	1.69	1.51	1.34	1.43	1.32
Exosome component 10 OS=Mus musculus GN=Exosc10 PE=1 SV=2	P56960	0.00	0.00	17.99	37.09	1.41	1.42	1.45	1.56	1.71	1.71	0.00	23.88	23.89	49.27	2.09	2.03	2.03	1.64	1.41	1.34	1.71	1.70	1.71	1.60	1.55	1.51
Nuclear pore complex protein Nup160 OS=Mus musculus GN=Nup160 PE=1 SV=2	Q9Z0W3	0.00	17.90	17.94	27.39	0.87	0.99	0.91	1.08	1.21	1.53	0.00	18.08	18.13	36.45	0.82	1.01	0.77	0.94	1.04	1.05	0.84	1.00	0.84	1.00	1.12	1.26
Heterogeneous nuclear ribonucleoprotein Q OS=Mus musculus GN=Syncrip PE=1 SV=2	Q7TMK9	0.00	17.85	27.57	49.44	1.22	1.04	1.14	0.99	0.89	0.70	0.00	22.02	32.50	63.24	1.33	1.03	1.29	0.97	0.63	0.06	1.28	1.03	1.21	0.98	0.75	0.20
Structural maintenance of chromosomes protein 2 OS=Mus musculus GN=Smc2 PE=1 SV=2	Q8CG48	0.00	17.85	18.20	37.36	0.95	0.94	0.94	1.19	1.06	0.85	0.00	0.00	36.91	42.23	1.17	0.78	0.86	1.26	1.01	0.48	1.05	0.86	0.90	1.22	1.03	0.64
Pre-mRNA-processing factor 40 homolog A OS=Mus musculus GN=Prpf40a PE=1 SV=1	Q9R1C7	0.00	17.81	17.84	24.66	0.94	1.00	0.86	1.45	1.75	1.64	0.00	20.21	20.24	29.59	1.15	1.04	1.00	1.07	1.25	0.78	1.04	1.02	0.92	1.24	1.48	1.13
Proliferating cell nuclear antigen OS=Mus musculus GN=Pcna PE=1 SV=2	P17918	0.00	0.00	17.63	54.02	1.60	1.02	0.91	0.67	0.63	0.39	0.00	21.60	21.60	69.73	1.66	1.16	1.07	0.74	0.39	0.20	1.63	1.09	0.99	0.70	0.50	0.28
Cleavage and polyadenylation specificity factor subunit 3 OS=Mus musculus GN=Cpsf3 PE=1 SV=2	Q9QXK7	0.00	0.00	17.63	28.51	0.78	0.79	0.77	1.07	0.91	1.24	0.00	13.19	13.29	29.39	0.91	0.90	0.94	0.86	0.82	0.96	0.84	0.84	0.85	0.96	0.87	1.09
Protein SON OS=Mus musculus GN=Son PE=1 SV=2	Q9QX47	0.00	17.54	17.57	27.58	1.17	1.08	0.95	1.15	1.26	1.15	0.00	13.64	13.68	28.89	1.12	1.08	1.43	0.95	1.33	0.37	1.14	1.08	1.17	1.05	1.29	0.65
Lymphocyte-specific helicase OS=Mus musculus GN=Hells PE=1 SV=2	Q60848	0.00	17.48	17.49	30.33	1.17	0.91	0.88	0.94	0.78	0.44	0.00	15.06	15.07	41.90	0.39	0.96	0.58	0.77	0.92	0.38	0.68	0.94	0.71	0.85	0.85	0.41
RNA-binding protein 25 OS=Mus musculus GN=Rbm25 PE=1 SV=2	B2RY56	0.00	17.38	17.42	40.93	0.90	1.00	1.10	1.19	1.07	1.08	0.00	20.74	20.83	44.59	1.00	1.04	1.10	1.04	1.02	0.95	0.95	1.02	1.10	1.11	1.04	1.01
mRNA turnover protein 4 homolog OS=Mus musculus GN=Mrto4 PE=2 SV=1	Q9D0I8	0.00	0.00	17.37	58.16	1.63	1.72	1.85	1.47	1.91	1.50	0.00	0.00	17.24	58.58	1.36	1.22	1.25	1.79	1.01	1.75	1.49	1.45	1.52	1.62	1.39	1.62
Cleavage and polyadenylation specificity factor subunit 5 OS=Mus musculus GN=Nudt21 PE=2 SV=1	Q9CQF3	0.00	17.32	17.34	45.81	0.83	1.03	1.27	1.25	1.24	1.16	0.00	13.62	13.64	65.20	0.76	0.90	0.59	1.17	0.56	0.61	0.79	0.96	0.87	1.21	0.83	0.84
U3 small nucleolar ribonucleoprotein protein IMP4 OS=Mus musculus GN=Imp4 PE=2 SV=1	Q8VHZ7	0.00	17.29	17.29	70.45	1.03	0.99	1.13	0.87	1.19	1.22	0.00	8.23	8.23	49.83	0.77	0.93	1.03	1.02	1.72	1.10	0.89	0.96	1.08	0.94	1.43	1.16
Mitotic spindle assembly checkpoint protein MAD1 OS=Mus musculus GN=Mad1l1 PE=2 SV=1	Q9WTX8	0.00	17.18	17.34	39.19	0.86	0.88	0.90	0.93	0.78	0.94	0.00	16.57	16.64	46.58	0.99	0.90	0.98	1.24	1.38	1.36	0.92	0.89	0.94	1.07	1.04	1.13
U4/U6 small nuclear ribonucleoprotein Prp4 OS=Mus musculus GN=Prpf4 PE=2 SV=1	Q9DAW6	0.00	0.00	17.11	33.97	0.69	0.87	0.81	0.81	0.95	1.06	0.00	20.83	20.83	42.99	0.87	0.91	0.86	0.86	0.80	0.72	0.78	0.89	0.84	0.83	0.87	0.87
Nucleolar protein 14 OS=Mus musculus GN=Nop14 PE=1 SV=2	Q8R3N1	0.00	17.10	17.10	32.79	0.96	1.00	0.96	0.96	1.03	1.01	0.00	19.00	19.02	32.67	0.94	0.93	1.00	0.95	0.94	1.01	0.95	0.96	0.98	0.96	0.98	1.01
Probable ATP-dependent RNA helicase DDX47 OS=Mus musculus GN=Ddx47 PE=2 SV=2	Q9CWX9	0.00	0.00	17.18	45.27	1.01	0.99	0.99	0.99	1.12	1.08	0.00	20.36	20.45	55.16	0.72	1.15	0.85	2.86	3.31	0.92	0.85	1.07	0.92	1.68	1.92	1.00
Suppressor of SWI4 1 homolog OS=Mus musculus GN=Ppan PE=2 SV=2	Q91YU8	0.00	17.06	17.07	48.30	0.89	1.07	0.92	1.33	1.94	1.64	0.00	14.97	14.97	51.28	1.03	1.25	1.02	0.95	0.93	0.73	0.95	1.15	0.97	1.13	1.34	1.10
TAR DNA-binding protein 43 OS=Mus musculus GN=Tardbp PE=1 SV=1	Q921F2	0.00	0.00	17.06	50.00	0.78	1.15	1.39	0.75	0.98	0.92	0.00	17.16	17.16	65.94	0.51	1.18	0.70	0.39	1.69	0.20	0.63	1.16	0.99	0.54	1.29	0.42
U4/U6 small nuclear ribonucleoprotein Prp3 OS=Mus musculus GN=Prpf3 PE=1 SV=1	Q922U1	0.00	17.04	17.07	33.67	1.26	1.07	1.14	0.96	0.90	0.92	0.00	15.22	15.23	43.63	1.09	0.82	1.07	0.86	0.90	0.83	1.17	0.93	1.10	0.91	0.90	0.87
Borealin OS=Mus musculus GN=Cdca8 PE=2 SV=2	Q8BHX3	0.00	17.02	17.18	55.71	1.38	1.12	1.02	0.85	0.94	0.87	0.00	22.89	23.31	68.17	2.56	2.40	2.86	1.01	1.10	0.86	1.88	1.64	1.71	0.92	1.01	0.87
Transcription elongation factor SPT5 OS=Mus musculus GN=Supt5h PE=1 SV=1	O55201	0.00	17.00	17.03	34.20	1.41	1.17	1.14	0.82	0.89	0.79	0.00	15.85	15.87	44.92	1.54	1.19	1.08	0.88	0.95	1.17	1.47	1.18	1.11	0.85	0.92	0.96
mRNA export factor OS=Mus musculus GN=Rae1 PE=1 SV=1	Q8C570	0.00	16.98	16.98	53.53	0.94	1.06	1.02	0.85	1.06	1.12	0.00	13.74	13.74	51.63	0.98	0.97	0.91	1.03	1.02	1.08	0.96	1.01	0.96	0.93	1.04	1.10
Lysine-specific histone demethylase 1A OS=Mus musculus GN=Kdm1a PE=1 SV=2	Q6ZQ88	0.00	0.00	16.98	29.31	1.04	1.01	1.03	1.03	0.91	0.93	0.00	0.00	16.86	49.00	1.25	1.61	1.50	1.63	1.58	0.28	1.14	1.28	1.24	1.29	1.20	0.51
THO complex subunit 4 OS=Mus musculus GN=Alyref PE=1 SV=3	O08583	0.00	16.94	16.94	64.31	0.59	0.76	0.54	0.45	0.40	0.34	0.00	18.49	18.49	81.57	1.31	0.95	0.88	0.85	0.24	0.54	0.88	0.85	0.69	0.62	0.31	0.43
Asparagine--tRNA ligase, cytoplasmic OS=Mus musculus GN=Nars PE=1 SV=2	Q8BP47	0.00	16.88	16.91	33.09	1.33	1.09	1.15	0.84	0.88	0.41	0.00	22.17	22.17	44.90	2.09	1.63	2.29	1.16	0.55	0.19	1.67	1.33	1.62	0.99	0.70	0.28
Heterogeneous nuclear ribonucleoprotein D-like OS=Mus musculus GN=Hnrpdl PE=1 SV=1	Q9Z130	0.00	0.00	19.74	58.47	0.99	1.02	1.05	1.00	1.01	1.08	0.00	0.00	15.24	47.84	0.96	0.87	0.95	1.43	0.91	0.77	0.98	0.94	1.00	1.20	0.96	0.91
DNA (cytosine-5)-methyltransferase 3A OS=Mus musculus GN=Dnmt3a PE=1 SV=2	O88508	0.00	16.67	16.67	40.97	0.95	1.00	0.96	1.04	1.03	0.99	0.00	24.36	24.36	49.45	0.69	1.01	0.73	1.17	0.55	0.79	0.81	1.00	0.84	1.10	0.75	0.89
Chromobox protein homolog 3 OS=Mus musculus GN=Cbx3 PE=1 SV=2	P23198	0.00	0.00	16.63	55.19	0.79	0.79	1.10	1.00	0.75	0.64	0.00	0.00	12.06	51.91	0.84	0.82	0.64	1.00	0.58	0.06	0.82	0.81	0.84	1.00	0.66	0.20
Lamin-B receptor OS=Mus musculus GN=Lbr PE=1 SV=2	Q3U9G9	0.00	16.55	16.57	38.18	0.90	0.98	0.88	0.88	0.77	0.77	0.00	17.72	17.74	39.94	0.75	1.15	0.70	0.84	0.67	0.41	0.82	1.06	0.79	0.86	0.72	0.56
SNW domain-containing protein 1 OS=Mus musculus GN=Snw1 PE=1 SV=3	Q9CSN1	0.00	16.55	16.57	43.10	1.01	1.03	0.97	0.90	1.06	1.15	0.00	17.76	17.78	53.92	1.22	1.26	1.09	1.04	0.97	1.31	1.11	1.14	1.03	0.97	1.01	1.22
La-related protein 7 OS=Mus musculus GN=Larp7 PE=1 SV=2	Q05CL8	0.00	0.00	16.57	32.28	0.97	0.99	1.00	0.99	0.95	0.97	0.00	11.63	11.63	27.89	0.70	0.54	0.79	0.94	0.77	0.46	0.83	0.73	0.89	0.96	0.86	0.67
Probable ATP-dependent RNA helicase DDX56 OS=Mus musculus GN=Ddx56 PE=2 SV=1	Q9D0R4	0.00	0.00	16.67	42.67	0.76	0.89	0.75	0.71	1.11	1.04	0.00	19.69	19.80	43.41	0.88	0.93	0.80	0.86	0.98	0.87	0.82	0.91	0.78	0.78	1.04	0.95
Zinc finger CCCH domain-containing protein 11A OS=Mus musculus GN=Zc3h11a PE=1 SV=1	Q6NZF1	0.00	0.00	16.56	40.15	0.95	0.95	1.04	1.27	1.22	1.46	0.00	21.65	21.93	47.73	0.89	0.96	0.97	1.25	1.20	1.28	0.92	0.96	1.00	1.26	1.21	1.37

Protien identification and qunatitation results from ProteinPilot for all the analyzed samples

Name	Accession number	% FDR	Unused	Total	%Cov	114:113	115:113	116:113	118:117	119:117	121:117	% FDR	Unused	Total	%Cov	114:113	115:113	116:113	118:117	119:117	121:117	114:113	115:113	116:113	118:117	119:117	121:117
Nucleolar pre-ribosomal-associated protein 1 OS=Mus musculus GN=Urb1 PE=2 SV=2	Q571H0	0.00	0.00	16.91	25.68	1.01	1.01	1.00	0.93	0.99	0.96	0.00	0.00	17.77	28.06	0.90	0.95	0.92	0.92	1.01	0.97	0.95	0.98	0.96	0.92	1.00	0.97
Transcription initiation factor TFIID subunit 6 OS=Mus musculus GN=Taf6 PE=2 SV=1	Q62311	0.00	16.41	16.42	46.02	0.89	0.92	0.93	0.95	0.99	1.02	0.00	0.00	10.31	35.69	0.72	0.95	0.77	0.96	1.11	0.97	0.80	0.94	0.84	0.95	1.05	1.00
60S ribosomal protein L10a OS=Mus musculus GN=Rpl10a PE=1 SV=3	P53026	0.00	0.00	14.42	41.01	1.37	1.32	1.45	1.32	1.28	1.19	0.00	0.00	12.96	40.55	1.71	1.53	1.42	1.27	0.86	0.71	1.53	1.42	1.43	1.29	1.05	0.92
60S ribosomal protein L7-like 1 OS=Mus musculus GN=Rpl7l1 PE=2 SV=1	Q9D8M4	0.00	16.36	16.55	58.94	1.47	1.67	1.64	1.47	1.91	1.85	0.00	10.43	10.68	52.85	1.28	1.25	1.32	2.31	2.31	0.26	1.37	1.45	1.47	1.85	2.10	0.70
Tubulin alpha-1B chain OS=Mus musculus GN=Tuba1b PE=1 SV=2	P05213	0.00	0.00	16.32	40.35	1.49	1.39	1.11	0.87	0.88	0.70	0.00	16.21	16.23	41.69	1.10	1.02	1.00	1.10	1.05	0.90	1.28	1.19	1.05	0.98	0.96	0.79
Tubulin alpha-1C chain OS=Mus musculus GN=Tuba1c PE=1 SV=1	P68373	0.00	0.00	16.32	40.53	1.49	1.39	1.11	0.87	0.88	0.70	0.00	0.00	16.23	36.53	1.10	1.02	1.00	1.10	1.05	0.90	1.28	1.19	1.05	0.98	0.96	0.79
Tubulin alpha-1A chain OS=Mus musculus GN=Tuba1a PE=1 SV=1	P68369	0.00	0.00	14.32	32.59	1.49	1.39	1.11	0.87	0.88	0.70	0.00	0.00	14.23	39.47	1.10	1.02	1.00	1.10	1.05	0.90	1.28	1.19	1.05	0.98	0.96	0.79
40S ribosomal protein S3a OS=Mus musculus GN=Rps3a PE=1 SV=3	P97351	0.00	0.00	16.24	51.52	1.19	1.06	1.12	1.43	1.33	1.24	0.00	13.22	13.22	68.56	1.26	0.90	0.87	1.94	1.03	0.43	1.22	0.98	0.99	1.67	1.17	0.73
60S ribosome subunit biogenesis protein NIP7 homolog OS=Mus musculus GN=Nip7 PE=2 SV=1	Q9CXK8	0.00	16.23	16.23	68.33	0.62	0.73	1.46	0.81	1.32	1.67	0.00	17.71	17.71	72.78	0.73	0.87	0.41	1.25	1.06	0.32	0.67	0.80	0.78	1.00	1.18	0.73
Protein Wiz OS=Mus musculus GN=Wiz PE=1 SV=2	O88286	0.00	0.00	14.25	24.11	0.80	1.11	0.90	1.10	1.46	1.45	0.00	0.00	10.43	26.90	1.06	0.97	1.00	0.99	1.01	0.95	0.92	1.04	0.95	1.04	1.21	1.17
Protein Nup153 OS=Mus musculus GN=Nup153 PE=4 SV=1	E9Q3G8	0.00	0.00	16.19	20.11	1.03	1.16	1.06	1.05	0.90	1.06	0.00	23.27	23.27	30.51	1.03	1.16	0.94	0.92	0.92	0.96	1.03	1.16	1.00	0.98	0.91	1.01
Methionine aminopeptidase 1 OS=Mus musculus GN=Metap1 PE=2 SV=1	Q8BP48	0.00	0.00	16.17	47.41	1.22	1.46	1.61	1.07	1.29	1.18	0.00	14.48	14.48	39.90	1.46	1.82	1.53	1.28	0.72	1.25	1.34	1.63	1.57	1.17	0.96	1.21
Ribosome biogenesis regulatory protein homolog OS=Mus musculus GN=Rrs1 PE=2 SV=1	Q9CYH6	0.00	0.00	16.08	60.27	1.17	1.17	1.25	1.01	1.39	1.22	0.00	12.92	12.94	54.25	1.21	0.98	1.32	1.94	1.64	0.47	1.19	1.07	1.28	1.40	1.51	0.76
ATP-dependent RNA helicase DHX8 OS=Mus musculus GN=Dhx8 PE=2 SV=1	A2A4P0	0.00	0.00	16.18	35.77	0.91	1.14	1.12	0.99	1.18	1.28	0.00	0.00	19.59	34.08	1.07	1.11	1.11	0.96	1.02	1.01	0.99	1.12	1.11	0.98	1.10	1.14
Periodic tryptophan protein 2 homolog OS=Mus musculus GN=Pwp2 PE=1 SV=1	Q8BU03	0.00	0.00	16.04	22.52	0.97	0.90	0.96	1.11	1.53	1.50	0.00	0.00	18.33	34.28	0.64	0.90	0.89	0.99	1.69	0.54	0.79	0.90	0.92	1.05	1.61	0.90
Probable global transcription activator SNF2L2 OS=Mus musculus GN=Smarca2 PE=1 SV=1	Q6DIC0	0.00	0.00	37.43	35.64	1.51	1.37	1.16	0.86	0.82	0.69	0.00	0.00	36.62	44.20	1.21	1.31	1.19	0.92	0.77	0.46	1.36	1.34	1.17	0.89	0.79	0.56
Calcium homeostasis endoplasmic reticulum protein OS=Mus musculus GN=Cherp PE=1 SV=1	Q8CGZ0	0.00	0.00	16.15	28.42	0.69	0.72	0.77	1.10	0.84	0.83	0.00	0.00	14.40	33.97	0.98	0.86	0.96	1.13	0.71	0.50	0.82	0.79	0.86	1.11	0.77	0.65
Histone H2A.V OS=Mus musculus GN=H2afv PE=1 SV=3	Q3THW5	0.00	0.00	21.60	65.63	1.21	1.05	1.27	0.83	0.81	0.77	0.00	12.69	17.54	73.44	1.19	0.73	1.02	0.83	0.68	0.70	1.20	0.87	1.14	0.83	0.74	0.74
Histone H2A.Z OS=Mus musculus GN=H2afz PE=1 SV=2	P0C0S6	0.00	0.00	21.60	60.16	1.21	1.05	1.27	0.83	0.81	0.77	0.00	0.00	17.53	68.75	1.19	0.73	1.02	0.83	0.68	0.70	1.20	0.87	1.14	0.83	0.74	0.74
Serine/threonine-protein kinase VRK1 OS=Mus musculus GN=Vrk1 PE=1 SV=2	Q80X41	0.00	0.00	15.91	42.95	0.93	1.10	0.88	0.79	0.72	0.71	0.00	0.00	15.14	43.86	1.26	1.32	0.97	0.97	0.54	0.34	1.08	1.20	0.92	0.87	0.63	0.49
Nucleolar complex protein 2 homolog OS=Mus musculus GN=Noc2l PE=1 SV=2	Q9WV70	0.00	0.00	15.87	34.94	0.90	0.81	0.98	0.98	1.24	1.36	0.00	23.71	23.73	41.63	0.71	1.00	0.99	0.80	1.16	0.72	0.80	0.90	0.99	0.89	1.20	0.99
40S ribosomal protein S16 OS=Mus musculus GN=Rps16 PE=2 SV=4	P14131	0.00	0.00	15.77	71.23	0.97	0.89	1.10	1.19	1.28	1.19	0.00	12.42	12.42	63.70	0.87	0.78	0.81	1.18	1.15	1.11	0.92	0.83	0.94	1.19	1.21	1.15
Rho guanine nucleotide exchange factor 1 OS=Mus musculus GN=Arhgef1 PE=1 SV=2	Q61210	0.00	0.00	15.70	39.78	0.79	0.94	0.73	0.87	0.82	0.86	0.00	0.00	16.49	48.59	1.14	1.00	1.05	1.01	0.92	0.64	0.95	0.97	0.87	0.94	0.87	0.74
Pre-mRNA-processing factor 17 OS=Mus musculus GN=Cdc40 PE=1 SV=1	Q9DC48	0.00	15.66	15.66	34.20	1.04	0.99	1.05	0.98	1.00	1.05	0.00	10.76	10.76	35.75	0.93	1.00	0.96	1.00	0.98	1.01	0.98	1.00	1.00	0.99	0.99	1.03
Nucleoporin NUP188 homolog OS=Mus musculus GN=Nup188 PE=1 SV=2	Q6ZQH8	0.00	15.60	15.82	24.16	0.97	0.84	0.90	1.08	1.01	0.97	0.00	13.96	14.20	33.03	0.68	1.13	0.76	0.99	1.02	0.86	0.81	0.97	0.83	1.03	1.01	0.91
Nuclear RNA export factor 1 OS=Mus musculus GN=Nxf1 PE=1 SV=3	Q99JX7	0.00	0.00	15.58	33.01	1.03	0.98	1.06	1.00	1.06	1.06	0.00	16.87	16.87	36.41	1.00	0.99	0.97	1.03	1.03	0.99	1.01	0.99	1.01	1.01	1.04	1.02
Flap endonuclease 1 OS=Mus musculus GN=Fen1 PE=2 SV=1	Q91Z50	0.00	0.00	15.57	40.00	1.01	1.10	1.07	0.69	0.65	0.54	0.00	0.00	14.78	46.58	0.99	1.13	0.75	0.72	0.33	0.24	1.00	1.11	0.90	0.71	0.46	0.36
Cleavage stimulation factor subunit 3 OS=Mus musculus GN=Cstf3 PE=1 SV=1	Q99LI7	0.00	15.49	15.52	45.19	0.90	0.89	0.97	1.07	1.09	1.33	0.00	17.09	17.10	48.54	1.01	0.79	0.87	1.20	1.42	1.58	0.95	0.84	0.92	1.13	1.24	1.45
Parafibromin OS=Mus musculus GN=Cdc73 PE=2 SV=1	Q8JZM7	0.00	15.48	15.51	51.22	1.20	1.04	1.02	0.90	0.89	1.00	0.00	11.95	11.97	52.35	1.32	1.29	1.25	1.19	0.89	0.58	1.26	1.16	1.13	1.04	0.89	0.76
Serine/threonine-protein kinase PRP4 homolog OS=Mus musculus GN=Prpf4b PE=1 SV=3	Q61136	0.00	0.00	15.58	35.05	1.17	0.97	0.93	1.11	0.93	0.71	0.00	0.00	13.28	43.89	1.16	0.97	1.07	1.08	0.86	0.36	1.16	0.97	1.00	1.09	0.90	0.51
Nucleolar protein 10 OS=Mus musculus GN=Nol10 PE=2 SV=1	Q5RJG1	0.00	0.00	15.40	35.66	0.67	0.77	0.86	0.96	1.28	1.28	0.00	11.94	11.95	36.39	0.93	0.93	0.96	0.94	1.05	1.02	0.79	0.85	0.91	0.95	1.16	1.14
Structural maintenance of chromosomes protein 5 OS=Mus musculus GN=Smc5 PE=2 SV=1	Q8CG46	0.00	15.37	15.44	28.52	0.98	1.04	0.89	0.81	0.82	0.65	0.00	14.87	14.93	36.97	0.95	0.98	1.00	0.92	0.95	0.92	0.96	1.01	0.94	0.86	0.89	0.77
Protein Srsf6 OS=Mus musculus GN=Srsf6 PE=2 SV=1	Q3TWW8	0.00	0.00	15.34	65.78	1.15	1.19	1.05	1.57	1.26	0.96	0.00	14.24	14.24	64.90	1.21	1.07	1.10	1.84	1.46	1.17	1.18	1.13	1.07	1.70	1.36	1.06
Probable RNA-binding protein 19 OS=Mus musculus GN=Rbm19 PE=1 SV=1	Q8R3C6	0.00	15.30	15.32	32.77	1.08	1.06	0.99	1.24	1.47	1.34	0.00	15.31	15.31	40.97	1.01	1.03	0.87	1.50	2.05	0.32	1.04	1.04	0.93	1.36	1.74	0.66
Ribosome production factor 2 homolog OS=Mus musculus GN=Rpf2 PE=2 SV=2	Q9JJ80	0.00	15.28	15.28	55.88	0.86	0.62	0.82	1.50	2.40	2.25	0.00	13.35	13.35	63.73	1.01	1.09	0.84	1.53	2.42	0.56	0.93	0.82	0.83	1.51	2.41	1.13
Nucleolar complex protein 3 homolog OS=Mus musculus GN=Noc3l PE=2 SV=2	Q8VI84	0.00	15.21	15.23	24.29	1.06	0.99	1.05	1.06	1.10	1.13	0.00	12.77	12.79	36.80	1.20	0.82	0.90	0.67	0.98	0.77	1.13	0.90	0.97	0.84	1.04	0.93
Nuclear autoantigen Sp-100 OS=Mus musculus GN=Sp100 PE=2 SV=1	Q8C405	0.00	15.16	16.13	37.39	0.86	0.95	0.99	2.01	0.86	2.01	0.00	18.23	19.25	43.49	0.95	1.01	1.02	2.33	0.83	2.29	0.90	0.98	1.00	2.17	0.84	2.15

Protien identification and qunatitation results from ProteinPilot for all the analyzed samples

Name	Accession number	% FDR	Unused	Total	%Cov	114:113	115:113	116:113	118:117	119:117	121:117	% FDR	Unused	Total	%Cov	114:113	115:113	116:113	118:117	119:117	121:117	114:113	115:113	116:113	118:117	119:117	121:117
ATP-dependent RNA helicase DDX24 OS=Mus musculus GN=Ddx24 PE=1 SV=2	Q9ESV0	0.00	0.00	17.15	38.16	1.02	0.97	0.98	1.07	1.18	1.25	0.00	0.00	18.03	40.96	0.79	1.05	0.93	2.47	2.44	1.38	0.90	1.01	0.95	1.62	1.70	1.31
Nuclear cap-binding protein subunit 1 OS=Mus musculus GN=Ncbp1 PE=1 SV=2	Q3UYV9	0.00	15.06	15.07	26.71	1.05	0.93	0.99	1.06	0.92	1.00	0.00	15.56	15.58	31.39	1.05	0.88	0.84	1.10	0.92	0.53	1.05	0.90	0.91	1.08	0.92	0.73
Double-strand break repair protein MRE11A OS=Mus musculus GN=Mre11a PE=2 SV=1	Q61216	0.00	0.00	15.02	39.80	1.10	1.04	1.07	0.99	0.98	0.95	0.00	13.27	13.28	42.21	0.79	0.76	0.95	1.08	0.61	1.11	0.93	0.89	1.00	1.03	0.77	1.02
MKIAA0136 protein (Fragment) OS=Mus musculus GN=Morc3 PE=2 SV=1	Q6A0C2	0.00	14.98	15.01	21.65	0.69	0.93	0.79	0.97	0.82	0.98	0.00	16.25	16.36	40.65	0.82	1.07	0.95	1.36	0.83	1.34	0.75	1.00	0.87	1.15	0.82	1.15
DEAH (Asp-Glu-Ala-His) box polypeptide 37 OS=Mus musculus GN=Dhx37 PE=2 SV=1	Q6NZL1	0.00	14.95	15.02	29.65	0.98	1.05	1.01	1.03	1.05	1.06	0.00	10.27	10.29	33.48	0.95	0.95	0.98	1.02	1.00	0.93	0.96	1.00	1.00	1.02	1.02	0.99
Ribosomal RNA-processing protein 8 OS=Mus musculus GN=Rrp8 PE=1 SV=1	Q9DB85	0.00	0.00	14.87	41.36	0.80	0.79	0.87	0.70	1.06	1.05	0.00	0.00	14.22	48.36	0.64	1.07	1.01	0.61	1.19	0.40	0.72	0.92	0.94	0.65	1.12	0.65
Deoxynucleotidyltransferase terminal-interacting protein 2 OS=Mus musculus GN=Dnttip2 PE=1 SV=1	Q8R2M2	0.00	14.87	14.90	27.97	0.98	0.95	0.98	0.97	1.10	1.14	0.00	13.79	13.82	32.45	0.91	0.93	0.90	1.01	1.12	1.22	0.95	0.94	0.94	0.99	1.11	1.18
U3 small nucleolar RNA-interacting protein 2 OS=Mus musculus GN=Rrp9 PE=1 SV=1	Q91WM3	0.00	14.86	14.88	30.95	0.70	0.87	0.78	0.96	1.24	1.03	0.00	10.03	10.04	41.26	1.06	1.25	1.24	0.99	1.51	0.49	0.86	1.04	0.98	0.98	1.37	0.71
Cleavage and polyadenylation specificity factor subunit 2 OS=Mus musculus GN=Cpsf2 PE=1 SV=1	O35218	0.00	14.79	14.83	35.42	0.95	0.92	0.93	0.94	0.96	0.98	0.00	8.13	8.15	34.91	0.86	1.08	0.95	0.79	1.09	1.39	0.91	1.00	0.94	0.86	1.02	1.17
SWI/SNF-related matrix-associated actin-dependent regulator of chromatin subfamily E member 1 OS=Mus musculus GN=Smarce1 PE=1 SV=1	O54941	0.00	14.71	14.71	43.80	0.74	1.07	0.85	0.90	0.82	0.86	0.00	14.09	14.09	43.07	0.45	1.34	0.77	1.28	1.01	0.54	0.58	1.20	0.81	1.07	0.91	0.69
Metastasis-associated protein MTA1 OS=Mus musculus GN=Mta1 PE=1 SV=1	Q8K4B0	0.00	0.00	18.90	44.06	0.99	0.91	0.96	1.08	1.02	1.18	0.00	0.00	24.69	53.29	1.17	0.85	1.25	1.07	0.83	0.79	1.08	0.88	1.10	1.07	0.92	0.96
Polymerase delta-interacting protein 3 OS=Mus musculus GN=Poldip3 PE=2 SV=1	Q8BG81	0.00	0.00	14.60	47.86	1.12	1.18	0.99	0.72	1.02	0.99	0.00	15.07	15.07	65.48	0.92	1.12	0.95	0.98	1.21	1.10	1.01	1.15	0.97	0.84	1.11	1.04
Nuclear pore complex protein Nup214 OS=Mus musculus GN=Nup214 PE=1 SV=2	Q80U93	0.00	14.50	14.80	15.54	1.07	1.07	1.02	0.96	0.95	0.94	0.00	11.13	11.17	25.28	0.92	1.41	1.17	1.16	1.19	1.60	0.99	1.22	1.09	1.06	1.06	1.22
Pogo transposable element with ZNF domain OS=Mus musculus GN=Pogz PE=1 SV=2	Q8BZH4	0.00	0.00	14.52	24.98	0.99	1.00	0.99	1.00	1.04	1.01	0.00	0.00	21.31	25.41	1.08	1.04	0.97	1.16	1.13	0.51	1.03	1.02	0.98	1.08	1.08	0.71
Lupus La protein homolog OS=Mus musculus GN=Ssb PE=2 SV=1	P32067	0.00	0.00	14.47	42.41	0.96	1.09	1.09	0.67	0.76	0.72	0.00	20.31	20.36	53.98	1.10	1.04	0.98	0.90	0.75	0.67	1.03	1.06	1.03	0.77	0.76	0.70
Dolichyl-diphosphooligosaccharide--protein glycosyltransferase subunit 2 OS=Mus musculus GN=Rpn2 PE=2 SV=1	Q9DBG6	0.00	0.00	14.33	28.68	0.71	0.88	0.88	0.95	0.92	0.65	0.00	0.00	8.11	18.23	1.08	1.11	1.06	0.95	0.91	0.79	0.87	0.99	0.96	0.95	0.92	0.72
Guanine nucleotide-binding protein G(i) subunit alpha-2 OS=Mus musculus GN=Gnai2 PE=1 SV=5	P08752	0.00	14.32	14.34	41.41	0.93	0.29	0.59	0.38	0.20	0.30	0.00	17.37	17.37	54.65	0.84	0.30	0.54	0.58	0.19	0.25	0.88	0.29	0.56	0.47	0.20	0.28
Probable ATP-dependent RNA helicase DDX10 OS=Mus musculus GN=Ddx10 PE=1 SV=2	Q80Y44	0.00	14.30	14.48	35.66	0.90	0.95	0.88	1.10	1.75	1.66	0.00	21.44	21.66	39.09	1.04	0.88	0.90	1.28	1.63	1.20	0.96	0.91	0.89	1.19	1.69	1.41
Nuclear pore complex protein Nup155 OS=Mus musculus GN=Nup155 PE=2 SV=1	Q99P88	0.00	0.00	14.35	32.71	1.01	0.95	0.95	0.87	0.89	0.95	0.00	0.00	10.86	36.02	0.86	0.86	0.74	0.98	1.15	0.87	0.93	0.90	0.84	0.92	1.01	0.91
Protein Wdr75 OS=Mus musculus GN=Wdr75 PE=2 SV=1	Q3U821	0.00	14.26	14.33	31.57	1.01	0.95	1.01	1.21	1.47	1.53	0.00	0.00	17.07	42.89	0.85	0.90	1.34	0.78	1.33	0.23	0.92	0.92	1.16	0.97	1.40	0.60
Heterogeneous nuclear ribonucleoprotein A/B OS=Mus musculus GN=Hnrnpab PE=1 SV=1	Q99020	0.00	0.00	16.24	50.53	0.91	1.05	1.31	0.94	0.89	1.10	0.00	0.00	23.67	53.68	1.15	1.09	1.00	0.86	0.55	0.08	1.02	1.07	1.14	0.90	0.70	0.30
40S ribosomal protein S2 OS=Mus musculus GN=Rps2 PE=1 SV=3	P25444	0.00	0.00	14.21	60.07	1.00	0.88	1.03	1.53	1.37	1.25	0.00	9.86	9.88	71.67	1.01	0.87	0.87	1.27	1.04	0.95	1.00	0.87	0.95	1.39	1.19	1.09
Phenylalanine--tRNA ligase beta subunit OS=Mus musculus GN=Farsb PE=2 SV=2	Q9WUA2	0.00	0.00	14.23	30.39	1.42	1.64	1.57	1.39	1.77	1.41	0.00	8.39	8.48	31.41	1.36	1.47	1.91	1.85	2.61	1.60	1.39	1.56	1.73	1.61	2.15	1.50
60S ribosomal protein L6 OS=Mus musculus GN=Rpl6 PE=1 SV=3	P47911	0.00	0.00	14.08	63.85	1.42	1.09	1.41	1.43	1.50	1.38	0.00	9.76	9.77	55.07	1.53	1.26	1.34	1.85	1.71	1.36	1.47	1.17	1.37	1.63	1.60	1.37
Serine/threonine-protein kinase TAO3 OS=Mus musculus GN=Taok3 PE=1 SV=2	Q8BYC6	0.00	0.00	14.35	36.86	1.19	1.15	1.10	1.13	0.95	0.82	0.00	17.20	17.51	31.74	0.65	1.02	1.12	1.34	1.02	0.11	0.88	1.08	1.11	1.23	0.99	0.30
General transcription factor II-I OS=Mus musculus GN=Gtf2i PE=1 SV=3	Q9ESZ8	0.00	14.00	14.02	34.27	0.77	0.86	0.79	0.67	0.78	0.70	0.00	14.16	14.30	41.48	1.04	0.98	0.91	0.77	0.95	0.21	0.89	0.92	0.85	0.72	0.86	0.39
U1 small nuclear ribonucleoprotein A OS=Mus musculus GN=Snrpa PE=2 SV=3	Q62189	0.00	13.97	13.98	49.48	1.42	0.95	1.26	0.95	1.33	0.72	0.00	13.41	13.41	52.96	1.05	1.01	0.99	1.08	1.36	1.08	1.22	0.98	1.12	1.01	1.34	0.88
Protein MAK16 homolog OS=Mus musculus GN=Mak16 PE=2 SV=1	Q8BGS0	0.00	13.93	13.95	49.66	0.87	1.04	1.06	1.03	1.33	1.34	0.00	9.03	9.16	43.58	1.03	1.06	1.01	0.96	1.08	1.05	0.95	1.05	1.03	1.00	1.20	1.19
Splicing factor 1 OS=Mus musculus GN=Sf1 PE=4 SV=1	D3YZC9	0.00	13.91	13.95	39.93	0.96	1.05	1.10	1.02	1.05	1.22	0.00	9.21	9.22	35.73	0.94	1.25	1.19	0.79	0.24	1.07	0.95	1.14	1.14	0.90	0.51	1.14
EH domain-containing protein 4 OS=Mus musculus GN=Ehd4 PE=1 SV=1	Q9EQP2	0.00	0.00	13.89	33.46	1.10	1.09	1.02	1.34	0.82	0.67	0.00	11.01	11.01	41.04	1.26	1.21	1.15	1.47	0.82	0.34	1.17	1.15	1.08	1.41	0.82	0.48
Tubulin beta-5 chain OS=Mus musculus GN=Tubb5 PE=1 SV=1	P99024	0.00	13.85	13.87	42.12	0.76	0.89	0.69	0.99	1.18	1.10	0.00	18.68	18.69	39.86	1.07	0.95	1.02	0.98	1.00	0.87	0.90	0.92	0.84	0.99	1.09	0.98
Protein Rsf1 OS=Mus musculus GN=Rsf1 PE=4 SV=1	E9Q4Y2	0.00	13.83	13.86	23.32	1.01	1.01	1.03	0.97	0.94	0.95	0.00	11.84	11.85	21.30	1.10	1.01	1.04	0.67	0.83	0.91	1.05	1.01	1.03	0.81	0.88	0.93
U2 snRNP-associated SURP motif-containing protein OS=Mus musculus GN=U2surp PE=1 SV=3	Q6NV83	0.00	13.82	13.91	27.21	0.92	0.96	0.88	1.10	1.08	1.06	0.00	13.45	13.63	36.25	1.19	1.08	1.10	1.07	0.67	0.68	1.05	1.02	0.98	1.08	0.85	0.85
Aurora kinase B OS=Mus musculus GN=Aurkb PE=1 SV=2	O70126	0.00	13.78	13.89	46.67	1.18	1.03	1.39	0.89	0.72	0.85	0.00	11.16	11.17	54.20	0.90	0.90	0.87	0.98	0.65	0.65	1.03	0.96	1.10	0.93	0.69	0.74
Nuclear pore complex protein Nup85 OS=Mus musculus GN=Nup85 PE=1 SV=1	Q8R480	0.00	13.71	13.73	35.52	1.07	1.02	1.07	1.05	1.08	1.03	0.00	16.88	16.90	45.73	1.56	1.43	1.32	0.99	0.43	0.35	1.29	1.21	1.19	1.02	0.68	0.60
Bcl-2-associated transcription factor 1 OS=Mus musculus GN=Bclaf1 PE=1 SV=2	Q8K019	0.00	13.71	13.72	45.38	0.95	0.76	0.87	1.43	1.14	1.03	0.00	9.47	9.48	38.63	0.87	0.84	0.66	1.31	1.21	0.73	0.91	0.80	0.76	1.37	1.17	0.87

Protien identification and qunatitation results from ProteinPilot for all the analyzed samples

Name	Accession number	% FDR	Unused	Total	%Cov	114:113	115:113	116:113	118:117	119:117	121:117	% FDR	Unused	Total	%Cov	114:113	115:113	116:113	118:117	119:117	121:117	114:113	115:113	116:113	118:117	119:117	121:117
SAFB-like transcription modulator OS=Mus musculus GN=Sltm PE=1 SV=1	Q8CH25	0.00	0.00	13.75	28.71	0.93	0.98	0.95	1.00	0.95	0.98	0.00	7.27	7.29	40.54	0.74	1.05	0.84	1.15	1.69	1.43	0.83	1.01	0.89	1.07	1.26	1.19
Surfeit locus protein 6 OS=Mus musculus GN=Surf6 PE=2 SV=1	P70279	0.00	0.00	13.73	47.89	1.06	1.06	1.10	0.92	0.95	0.95	0.00	9.06	9.08	49.58	1.04	0.98	1.02	0.90	0.94	0.86	1.05	1.02	1.06	0.91	0.95	0.90
Structural maintenance of chromosomes protein 6 OS=Mus musculus GN=Smc6 PE=2 SV=1	Q924W5	0.00	13.68	13.72	33.64	0.96	0.96	0.95	0.98	1.03	0.98	0.00	7.37	7.39	32.27	1.16	1.12	1.20	0.95	1.09	1.05	1.06	1.04	1.07	0.96	1.06	1.01
Protein Nolc1 OS=Mus musculus GN=Nolc1 PE=4 SV=1	E9Q5C9	0.00	0.00	13.68	27.64	0.87	0.81	0.73	0.96	0.79	0.90	0.00	13.85	13.85	25.64	1.06	0.77	0.56	0.86	0.86	0.95	0.96	0.79	0.64	0.91	0.83	0.92
Protein AATF OS=Mus musculus GN=Aatf PE=1 SV=1	Q9JKX4	0.00	0.00	13.67	36.31	1.01	0.96	1.01	0.96	1.01	1.00	0.00	8.30	8.32	28.71	0.82	0.69	0.94	1.04	1.26	1.45	0.91	0.81	0.97	1.00	1.13	1.20
Histone H1.4 OS=Mus musculus GN=Hist1h1e PE=1 SV=2	P43274	0.00	13.63	42.96	51.60	1.08	0.90	0.99	1.14	1.03	0.90	0.00	9.08	31.70	54.34	1.11	0.92	0.87	0.76	0.87	0.56	1.09	0.91	0.93	0.93	0.95	0.71
Small nuclear ribonucleoprotein Sm D2 OS=Mus musculus GN=Snrpd2 PE=2 SV=1	P62317	0.00	0.00	13.62	66.10	1.02	0.87	0.99	1.02	1.03	1.14	0.00	14.74	14.76	83.05	1.08	0.63	1.06	0.84	0.88	0.70	1.05	0.74	1.02	0.92	0.95	0.90
Coiled-coil domain-containing protein 86 OS=Mus musculus GN=Ccdc86 PE=1 SV=2	Q9JJ89	0.00	13.60	13.62	40.38	1.06	0.96	1.28	1.61	1.54	1.72	0.00	7.09	7.09	41.55	1.11	0.95	1.19	1.05	0.92	1.10	1.08	0.96	1.24	1.30	1.19	1.37
Protein Ncapg OS=Mus musculus GN=Ncapg PE=4 SV=1	E9PWG6	0.00	13.57	13.61	28.29	0.70	0.77	0.66	1.32	1.13	0.67	0.00	12.84	13.00	25.90	0.80	0.90	0.78	1.21	1.17	0.97	0.75	0.84	0.72	1.26	1.15	0.81
Nucleolar protein 11 OS=Mus musculus GN=Nol11 PE=2 SV=1	Q8BJW5	0.00	13.55	13.58	22.27	0.94	0.92	1.04	1.13	1.50	1.31	0.00	23.48	23.50	30.43	1.25	0.99	0.95	0.99	1.11	0.93	1.08	0.95	1.00	1.06	1.29	1.10
Double-stranded RNA-specific adenosine deaminase OS=Mus musculus GN=Adar PE=1 SV=2	Q99MU3	0.00	13.51	13.94	25.98	0.90	1.09	0.98	1.39	1.28	1.64	0.00	17.60	17.63	42.61	0.96	1.13	1.21	1.01	1.32	1.00	0.93	1.11	1.09	1.19	1.30	1.28
Three prime repair exonuclease 1 OS=Mus musculus GN=Trex1 PE=1 SV=2	Q91XB0	0.00	13.42	13.46	38.85	0.83	0.74	1.63	5.25	2.31	5.40	0.72	1.54	1.57	31.53	0.97	0.69	1.18	2.42	1.77	0.60	0.90	0.71	1.39	3.56	2.02	1.79
Nuclear pore glycoprotein p62 OS=Mus musculus GN=Nup62 PE=1 SV=2	Q63850	0.00	0.00	13.37	30.80	1.05	0.95	0.99	1.11	0.94	0.92	0.00	10.41	10.41	29.09	1.26	0.91	1.08	1.37	0.20	0.17	1.15	0.93	1.03	1.23	0.43	0.39
Sphingomyelin phosphodiesterase 4 OS=Mus musculus GN=Smpd4 PE=2 SV=2	Q6ZPR5	0.00	13.32	13.34	30.01	0.54	0.63	0.90	2.05	1.27	0.98	0.00	10.65	10.67	29.65	0.55	0.58	0.56	1.54	1.77	0.31	0.55	0.60	0.71	1.78	1.50	0.55
Polyadenylate-binding protein 2 OS=Mus musculus GN=Pabpn1 PE=2 SV=3	Q8CCS6	0.00	0.00	13.32	62.58	0.93	1.02	0.97	0.99	0.92	0.95	0.00	0.00	11.53	73.18	0.83	0.77	0.67	0.80	0.74	0.39	0.88	0.88	0.81	0.89	0.82	0.61
Eukaryotic translation initiation factor 2 subunit 1 OS=Mus musculus GN=Eif2s1 PE=1 SV=3	Q6ZWX6	0.00	13.31	13.31	53.33	1.06	0.98	1.01	0.92	0.96	0.95	0.00	8.30	8.30	48.25	1.05	1.06	1.07	1.02	0.92	0.96	1.05	1.02	1.04	0.97	0.94	0.95
Zinc finger protein ubi-d4 OS=Mus musculus GN=Dpf2 PE=1 SV=1	Q61103	0.00	0.00	13.33	34.78	1.08	1.14	1.03	0.95	1.03	1.13	0.00	16.06	16.07	32.74	1.01	1.01	1.02	1.05	1.02	1.01	1.04	1.07	1.02	1.00	1.02	1.07
Zinc finger E-box-binding homeobox 2 OS=Mus musculus GN=Zeb2 PE=1 SV=2	Q9R0G7	0.00	0.00	13.19	21.73	1.09	1.17	1.04	1.37	1.63	1.92	0.00	0.00	14.80	27.08	0.98	1.08	1.27	1.20	1.57	1.36	1.03	1.12	1.15	1.28	1.60	1.61
40S ribosomal protein S19 OS=Mus musculus GN=Rps19 PE=1 SV=3	Q9CZX8	0.00	0.00	13.19	68.97	1.07	1.04	1.19	1.41	1.49	1.06	0.00	0.00	13.31	62.76	1.38	0.75	1.15	1.33	1.24	0.15	1.21	0.88	1.17	1.37	1.36	0.40
THO complex subunit 5 homolog OS=Mus musculus GN=Thoc5 PE=1 SV=2	Q8BKT7	0.00	13.10	13.12	30.75	1.04	1.03	1.08	1.14	1.08	0.68	0.00	14.40	14.40	35.14	1.25	1.04	1.14	0.98	0.60	0.54	1.14	1.03	1.11	1.06	0.80	0.61
Ribosome biogenesis protein BRX1 homolog OS=Mus musculus GN=Brix1 PE=2 SV=3	Q9DCA5	0.00	13.10	13.12	48.44	0.78	0.94	1.15	0.82	1.05	1.36	0.00	11.21	11.23	69.12	0.82	1.01	0.76	0.82	0.94	0.20	0.80	0.97	0.93	0.82	0.99	0.52
Importin subunit alpha-2 OS=Mus musculus GN=Kpna2 PE=1 SV=2	P52293	0.00	0.00	13.09	35.16	1.11	1.17	0.87	3.05	3.02	2.61	0.00	7.76	7.76	35.35	1.57	1.80	1.84	2.07	2.05	0.91	1.32	1.45	1.26	2.51	2.49	1.54
KRR1 small subunit processome component homolog OS=Mus musculus GN=Krr1 PE=2 SV=1	Q8BGA5	0.00	13.07	13.08	47.37	1.05	1.06	1.08	0.99	1.11	1.08	0.00	11.29	11.30	43.95	1.10	1.00	1.05	1.02	1.01	0.99	1.07	1.03	1.06	1.00	1.06	1.03
Polycomb protein EED OS=Mus musculus GN=Eed PE=1 SV=1	Q921E6	0.00	13.05	13.08	29.25	1.29	1.46	1.51	1.43	0.97	0.69	0.00	0.00	13.15	41.72	1.36	1.29	1.16	1.03	0.45	0.48	1.32	1.37	1.32	1.21	0.66	0.57
Ribosome production factor 1 OS=Mus musculus GN=Rpf1 PE=2 SV=2	Q7TND5	0.00	12.99	13.00	39.83	1.46	1.39	1.34	1.02	1.04	0.95	0.00	16.14	16.15	42.41	1.08	1.05	1.10	1.05	1.08	0.99	1.25	1.21	1.21	1.03	1.06	0.97
Mortality factor 4-like protein 1 OS=Mus musculus GN=Morf4l1 PE=2 SV=2	P60762	0.00	12.94	12.95	41.44	1.37	1.34	1.17	1.98	1.58	1.29	0.00	0.00	15.25	59.67	1.24	1.51	1.63	2.01	1.28	0.24	1.30	1.43	1.38	2.00	1.43	0.56
Glyceraldehyde-3-phosphate dehydrogenase OS=Mus musculus GN=Gapdh PE=1 SV=2	P16858	0.00	0.00	12.86	46.85	1.25	1.21	1.19	0.86	0.99	1.20	0.00	0.00	13.86	48.95	1.20	1.36	0.91	0.91	0.99	1.04	1.22	1.28	1.04	0.89	0.99	1.12
Protein Arid2 OS=Mus musculus GN=Arid2 PE=4 SV=1	E9Q7E2	0.00	12.78	12.81	22.59	0.93	0.98	0.99	1.05	1.04	1.10	0.00	11.25	11.28	24.02	0.95	1.00	0.97	0.97	1.00	1.00	0.94	0.99	0.98	1.01	1.02	1.05
Phenylalanine--tRNA ligase alpha subunit OS=Mus musculus GN=Farsa PE=2 SV=1	Q8C0C7	0.00	12.78	12.79	34.45	1.45	1.66	1.31	1.15	1.38	1.15	0.00	0.00	5.26	28.54	1.01	1.10	1.17	0.87	1.11	0.92	1.21	1.35	1.24	1.00	1.24	1.03
ATP-dependent RNA helicase DDX42 OS=Mus musculus GN=Ddx42 PE=1 SV=3	Q810A7	0.00	12.77	12.81	27.23	1.02	1.08	0.99	1.11	0.88	0.87	0.00	10.73	10.74	33.48	0.89	0.84	1.39	0.96	0.98	0.90	0.95	0.95	1.17	1.03	0.93	0.89
40S ribosomal protein S9 OS=Mus musculus GN=Rps9 PE=2 SV=3	Q6ZWN5	0.00	12.76	12.80	72.16	0.93	1.01	1.09	1.13	1.18	0.88	0.00	16.24	16.26	60.82	0.99	0.82	0.89	1.26	1.24	0.95	0.96	0.91	0.98	1.19	1.21	0.92
40S ribosomal protein S18 OS=Mus musculus GN=Rps18 PE=1 SV=3	P62270	0.00	0.00	12.76	73.03	1.00	0.86	1.09	1.25	1.21	1.19	0.00	0.00	10.03	74.34	0.94	0.70	0.72	1.32	0.77	1.12	0.97	0.78	0.88	1.28	0.96	1.15
ATP-dependent RNA helicase DDX51 OS=Mus musculus GN=Ddx51 PE=2 SV=1	Q6P9R1	0.00	12.75	12.77	36.15	0.91	0.97	0.98	1.01	1.02	1.02	0.00	9.58	9.64	43.51	0.91	1.00	1.00	0.97	1.12	1.04	0.91	0.99	0.99	0.99	1.07	1.03
Cleavage stimulation factor subunit 1 OS=Mus musculus GN=Cstf1 PE=2 SV=1	Q99LC2	0.00	12.73	12.77	47.10	0.65	1.17	0.67	0.80	1.09	0.90	0.00	13.32	13.33	45.01	0.97	1.21	1.14	1.02	0.67	0.59	0.79	1.19	0.87	0.90	0.85	0.73
Coronin-1C OS=Mus musculus GN=Coro1c PE=1 SV=2	Q9WUM4	0.00	0.00	12.91	36.71	1.00	0.44	0.47	0.52	0.44	0.42	0.00	12.72	12.76	38.61	1.03	0.38	0.61	0.44	0.58	0.70	1.01	0.41	0.53	0.48	0.51	0.54
Methyl-CpG-binding domain protein 2 OS=Mus musculus GN=Mbd2 PE=2 SV=2	Q9Z2E1	0.00	12.68	12.71	33.82	0.95	0.98	0.95	0.95	0.95	0.99	0.00	12.41	12.41	56.76	0.88	0.94	0.65	0.97	0.85	0.55	0.91	0.96	0.79	0.96	0.90	0.74
Tyrosine-protein kinase Lyn OS=Mus musculus GN=Lyn PE=1 SV=4	P25911	0.00	0.00	12.69	27.73	1.03	0.37	0.45	0.45	0.22	0.37	0.00	0.00	10.65	36.52	0.94	0.26	0.65	0.80	0.45	0.36	0.98	0.31	0.54	0.60	0.32	0.36

Protien identification and qunatitation results from ProteinPilot for all the analyzed samples

Name	Accession number	% FDR	Unused	Total	%Cov	114:113	115:113	116:113	118:117	119:117	121:117	% FDR	Unused	Total	%Cov	114:113	115:113	116:113	118:117	119:117	121:117	114:113	115:113	116:113	118:117	119:117	121:117
Pre-mRNA 3'-end-processing factor FIP1 OS=Mus musculus GN=Fip1l1 PE=1 SV=1	Q9D824	0.00	0.00	12.64	28.74	0.94	1.06	1.04	0.93	0.90	0.98	0.00	0.00	6.31	32.70	0.87	0.89	0.94	1.02	0.91	1.12	0.90	0.97	0.99	0.97	0.90	1.05
Threonine--tRNA ligase, cytoplasmic OS=Mus musculus GN=Tars PE=1 SV=2	Q9D0R2	0.00	0.00	12.63	30.19	0.74	0.96	0.95	1.15	1.12	0.70	0.00	19.06	19.07	34.63	0.40	0.91	0.80	1.02	0.94	0.46	0.54	0.94	0.87	1.08	1.02	0.57
pre-mRNA 3' end processing protein WDR33 OS=Mus musculus GN=Wdr33 PE=2 SV=1	Q8K4P0	0.00	12.59	12.61	30.38	0.90	0.75	0.89	1.03	1.07	1.29	0.00	9.13	9.15	27.97	0.76	1.18	0.61	0.85	1.07	1.10	0.82	0.94	0.74	0.93	1.07	1.19
RNA-binding protein FUS OS=Mus musculus GN=Fus PE=2 SV=1	P56959	0.00	0.00	12.58	37.84	0.97	1.00	1.02	1.60	1.36	1.34	0.00	0.00	17.06	50.97	1.13	0.86	1.06	0.90	0.16	0.27	1.05	0.93	1.04	1.20	0.47	0.60
Nuclear factor of activated T-cells, cytoplasmic 2 OS=Mus musculus GN=Nfatc2 PE=1 SV=3	Q60591	0.00	0.00	12.58	29.99	0.86	0.95	0.74	1.14	1.22	1.15	0.00	14.97	14.98	31.39	1.10	0.79	0.81	1.19	1.10	0.95	0.97	0.87	0.78	1.16	1.16	1.04
NF-kappa-B-repressing factor OS=Mus musculus GN=Nkrf PE=2 SV=3	Q8BY02	0.00	12.54	12.57	28.84	1.05	0.98	1.02	0.98	1.01	1.02	0.00	6.22	6.23	30.29	0.75	0.41	1.10	0.63	0.98	1.01	0.89	0.63	1.06	0.79	1.00	1.01
Cohesin subunit SA-2 OS=Mus musculus GN=Stag2 PE=1 SV=3	O35638	0.00	0.00	20.60	28.68	0.97	1.13	1.07	0.85	0.92	0.90	0.00	0.00	29.58	42.40	1.09	0.95	0.95	0.80	0.66	0.51	1.03	1.03	1.00	0.82	0.78	0.67
40S ribosomal protein S8 OS=Mus musculus GN=Rps8 PE=1 SV=2	P62242	0.00	0.00	12.49	56.73	1.26	1.17	1.25	1.57	1.37	1.16	0.00	13.19	13.19	54.81	0.87	0.96	0.70	1.89	1.91	1.37	1.05	1.06	0.93	1.72	1.61	1.26
Splicing factor 45 OS=Mus musculus GN=Rbm17 PE=1 SV=1	Q8JZX4	0.00	12.44	12.44	40.25	1.03	0.95	0.91	1.05	0.96	0.98	0.00	14.49	14.50	33.58	1.06	0.86	1.03	1.21	0.66	0.90	1.04	0.90	0.97	1.13	0.80	0.94
Protein Bptf OS=Mus musculus GN=Bptf PE=4 SV=1	A2A654	0.00	12.36	12.46	22.13	1.14	0.96	0.99	1.03	1.11	1.03	0.00	0.00	7.20	24.97	0.87	1.03	0.95	1.17	1.07	1.75	1.00	1.00	0.97	1.10	1.09	1.34
LEM domain-containing protein 2 OS=Mus musculus GN=Lemd2 PE=1 SV=1	Q6DVA0	0.00	12.36	12.38	39.92	0.86	1.01	0.92	1.00	1.08	1.13	0.00	11.60	11.60	53.23	1.12	1.21	1.10	1.13	0.90	0.44	0.98	1.11	1.00	1.06	0.98	0.71
MCG7283 OS=Mus musculus GN=Brd1 PE=4 SV=1	G5E8P1	0.00	0.00	10.46	31.47	0.61	0.93	0.89	0.90	0.92	0.99	0.00	15.16	15.22	34.22	0.99	1.07	1.03	1.02	1.02	0.96	0.78	1.00	0.95	0.96	0.97	0.98
Wings apart-like protein homolog OS=Mus musculus GN=Wapal PE=1 SV=2	Q65Z40	0.00	0.00	12.37	20.58	1.05	1.00	1.04	0.95	0.90	0.92	0.00	0.00	13.31	28.25	1.06	1.11	0.95	0.92	0.83	0.89	1.05	1.05	1.00	0.93	0.86	0.90
Serine/arginine-rich splicing factor 9 OS=Mus musculus GN=Srsf9 PE=1 SV=1	Q9D0B0	0.00	12.29	12.98	59.46	1.17	1.11	1.37	1.21	1.14	1.09	0.00	10.39	12.80	74.77	0.92	1.04	0.89	0.89	0.67	0.08	1.04	1.07	1.10	1.04	0.87	0.29
Transformer-2 protein homolog beta OS=Mus musculus GN=Tra2b PE=1 SV=1	P62996	0.00	12.27	12.31	60.07	0.71	1.24	1.36	1.12	1.10	0.77	0.00	5.24	5.24	67.36	0.59	0.52	0.79	2.75	2.51	1.29	0.65	0.80	1.04	1.75	1.66	1.00
Histone H1.0 OS=Mus musculus GN=H1f0 PE=2 SV=4	P10922	0.00	0.00	12.29	43.81	1.07	1.22	1.22	1.01	0.86	0.78	0.00	12.01	12.02	50.00	0.86	1.06	0.46	0.78	0.38	0.42	0.95	1.14	0.75	0.89	0.57	0.57
Ribosomal RNA small subunit methyltransferase NEP1 OS=Mus musculus GN=Emg1 PE=1 SV=1	O35130	0.00	0.00	12.25	56.56	0.95	0.95	0.90	0.98	1.08	1.06	0.00	15.10	15.11	68.44	0.78	0.85	0.86	0.99	1.14	1.07	0.86	0.90	0.87	0.99	1.11	1.06
Bifunctional lysine-specific demethylase and histidyl-hydroxylase NO66 OS=Mus musculus GN=No66 PE=1 SV=2	Q9JJF3	0.00	12.22	12.24	39.30	0.99	1.02	1.00	0.86	0.98	0.86	0.00	6.73	6.80	39.30	1.08	1.18	1.09	1.25	1.16	0.71	1.03	1.10	1.04	1.04	1.07	0.78
GTP-binding nuclear protein Ran OS=Mus musculus GN=Ran PE=1 SV=3	P62827	0.00	0.00	12.19	48.15	1.16	1.15	1.27	1.14	0.97	0.87	0.00	11.71	11.71	50.00	0.95	0.98	0.87	0.98	0.78	0.69	1.05	1.06	1.05	1.06	0.87	0.78
Septin-2 OS=Mus musculus GN=Sept2 PE=1 SV=2	P42208	0.00	12.18	12.21	42.38	1.07	0.96	1.29	1.27	1.27	0.86	0.00	10.89	10.90	45.71	0.85	0.91	1.15	1.69	1.49	0.79	0.95	0.94	1.22	1.47	1.37	0.83
DDB1- and CUL4-associated factor 13 OS=Mus musculus GN=Dcaf13 PE=2 SV=2	Q6PAC3	0.00	12.13	12.15	39.10	0.89	0.95	0.82	1.01	1.11	1.16	0.00	10.40	10.40	36.85	0.82	0.85	0.82	1.49	2.01	0.24	0.86	0.90	0.82	1.22	1.49	0.52
Metastasis-associated protein MTA3 OS=Mus musculus GN=Mta3 PE=1 SV=1	Q924K8	0.00	0.00	18.89	48.73	1.06	1.07	1.12	0.97	1.04	0.82	0.00	0.00	22.03	57.53	0.91	1.02	0.96	0.96	0.47	0.59	0.98	1.04	1.04	0.97	0.70	0.70
Lymphocyte-specific protein 1 OS=Mus musculus GN=Lsp1 PE=1 SV=2	P19973	0.00	12.05	12.05	38.18	0.97	0.08	0.10	0.25	0.07	0.24	0.00	13.45	13.45	63.03	1.06	0.08	0.31	0.27	0.06	0.12	1.01	0.08	0.17	0.26	0.06	0.17
Lysine-specific demethylase 5A OS=Mus musculus GN=Kdm5a PE=1 SV=2	Q3UXZ9	0.00	12.03	12.32	26.57	1.03	1.06	1.00	0.95	0.99	0.95	0.00	4.16	4.20	21.36	1.00	1.09	1.15	0.88	1.06	0.90	1.01	1.07	1.07	0.92	1.02	0.92
Histone-binding protein RBBP7 OS=Mus musculus GN=Rbbp7 PE=1 SV=1	Q60973	0.00	12.01	26.19	50.59	1.05	1.09	0.87	1.16	0.84	0.91	0.00	27.45	27.47	46.35	1.13	1.10	1.33	1.01	0.41	1.06	1.09	1.09	1.08	1.08	0.59	0.98
Cell division cycle protein 16 homolog OS=Mus musculus GN=Cdc16 PE=2 SV=1	Q8R349	0.00	0.00	12.03	22.74	1.11	1.16	1.00	0.90	0.97	0.92	0.00	4.18	4.19	23.06	1.41	1.29	1.11	0.89	0.85	0.71	1.25	1.22	1.05	0.89	0.91	0.81
Mitotic checkpoint protein BUB3 OS=Mus musculus GN=Bub3 PE=2 SV=2	Q9WVA3	0.00	11.99	11.99	41.72	0.62	0.94	1.01	0.79	1.16	1.15	0.00	16.34	16.35	45.71	0.95	0.97	1.00	0.98	0.97	0.98	0.77	0.95	1.00	0.88	1.06	1.06
Serine-protein kinase ATM OS=Mus musculus GN=Atm PE=1 SV=2	Q62388	0.00	11.90	12.08	20.12	0.90	1.03	0.95	0.91	0.99	0.97	0.00	0.00	5.77	24.72	1.01	1.03	0.95	1.05	1.11	1.15	0.95	1.03	0.95	0.98	1.05	1.06
DEAH (Asp-Glu-Ala-His) box polypeptide 16, isoform CRA a OS=Mus musculus GN=Dhx16 PE=4 SV=1	G3X8X0	0.00	11.86	11.93	37.36	0.90	1.11	1.02	0.90	1.15	1.22	0.00	16.35	18.38	40.71	1.03	1.07	1.08	1.06	1.10	1.08	0.96	1.09	1.05	0.98	1.12	1.15
Transcriptional regulator ATRX OS=Mus musculus GN=Atrx PE=1 SV=3	Q61687	0.00	11.86	11.92	21.28	1.05	1.02	0.77	1.03	1.08	0.95	0.00	18.69	18.71	24.96	0.77	0.87	1.00	1.33	0.91	0.63	0.90	0.94	0.88	1.17	0.99	0.77
Ubiquitin carboxyl-terminal hydrolase 48 OS=Mus musculus GN=Usp48 PE=1 SV=2	Q3V0C5	0.00	0.00	11.87	22.72	1.02	1.00	1.03	0.97	0.95	0.93	0.00	0.00	6.09	25.57	0.73	1.22	0.63	0.80	0.86	0.15	0.86	1.11	0.81	0.88	0.90	0.38
Protein Red OS=Mus musculus GN=Ik PE=2 SV=2	Q9Z1M8	0.00	0.00	11.84	43.45	1.03	0.86	0.94	0.80	1.02	1.00	0.00	13.24	13.27	45.24	1.18	0.72	0.85	1.06	0.71	0.30	1.10	0.79	0.89	0.92	0.85	0.55
40S ribosomal protein S13 OS=Mus musculus GN=Rps13 PE=1 SV=2	P62301	0.00	0.00	11.76	73.51	0.91	0.67	1.20	1.41	1.79	1.89	0.00	11.53	11.54	59.60	0.82	0.81	0.72	1.38	1.63	1.77	0.86	0.74	0.93	1.39	1.71	1.83
Activity-dependent neuroprotector homeobox protein OS=Mus musculus GN=Adnp PE=3 SV=1	A2BDX0	0.00	0.00	12.84	27.26	0.95	0.93	0.99	0.84	0.85	0.99	0.00	8.77	8.77	22.65	0.86	0.98	0.90	0.65	0.59	0.48	0.90	0.95	0.95	0.74	0.71	0.69
Ribosome biogenesis protein WDR12 OS=Mus musculus GN=Wdr12 PE=2 SV=1	Q9JJA4	0.00	0.00	11.71	33.81	1.33	1.41	1.12	1.11	1.37	1.11	0.00	16.05	16.05	34.75	1.13	1.02	1.06	1.07	0.65	0.84	1.22	1.20	1.09	1.09	0.94	0.96
Histone-lysine N-methyltransferase NSD2 OS=Mus musculus GN=Whsc1 PE=1 SV=2	Q8BVE8	0.00	11.69	11.69	15.60	1.03	1.05	1.02	1.02	0.98	1.00	0.00	5.35	6.66	24.25	1.03	1.08	1.03	1.05	0.88	0.85	1.03	1.06	1.02	1.03	0.93	0.92
Nuclear factor related to kappa-B-binding protein OS=Mus musculus GN=Nfrkb PE=2 SV=1	Q6PIJ4	0.00	11.66	11.69	26.77	1.01	1.05	0.95	0.99	0.96	0.99	0.00	8.44	8.46	28.40	1.04	0.99	1.15	1.15	1.13	0.97	1.02	1.02	1.05	1.07	1.04	0.98
Procollagen galactosyltransferase 1 OS=Mus musculus GN=Glt25d1 PE=1 SV=2	Q8K297	0.00	11.60	11.64	31.44	1.27	1.16	1.42	0.91	0.74	0.68	0.00	15.25	15.27	42.63	1.13	1.11	1.20	0.85	0.67	0.80	1.20	1.13	1.31	0.88	0.70	0.74

Protien identification and qunatitation results from ProteinPilot for all the analyzed samples

Name	Accession number	% FDR	Unused	Total	%Cov	114:113	115:113	116:113	118:117	119:117	121:117	% FDR	Unused	Total	%Cov	114:113	115:113	116:113	118:117	119:117	121:117	114:113	115:113	116:113	118:117	119:117	121:117
Heat shock protein HSP 90-beta OS=Mus musculus GN=Hsp90ab1 PE=1 SV=3	P11499	0.00	0.00	11.63	28.31	0.86	0.75	0.79	0.98	1.21	1.22	0.00	13.51	13.69	38.81	1.03	0.69	0.88	0.94	1.08	1.28	0.94	0.72	0.83	0.96	1.14	1.25
Putative RNA-binding protein Luc7-like 2 OS=Mus musculus GN=Luc7l2 PE=1 SV=1	Q7TNC4	0.00	0.00	11.57	42.35	1.60	1.63	1.45	1.28	1.15	0.97	0.00	12.77	12.78	55.87	1.32	1.14	0.63	0.94	1.00	0.95	1.45	1.36	0.95	1.10	1.07	0.96
Histone-lysine N-methyltransferase NSD3 OS=Mus musculus GN=Whsc1l1 PE=1 SV=2	Q6P2L6	0.00	0.00	11.64	22.65	1.06	1.06	0.72	1.20	0.89	1.02	0.00	8.19	8.20	23.77	1.02	1.17	1.21	0.92	0.72	0.47	1.04	1.11	0.94	1.05	0.80	0.70
Nuclear receptor coactivator 5 OS=Mus musculus GN=Ncoa5 PE=1 SV=1	Q91W39	0.00	11.55	11.57	50.26	1.07	1.02	1.02	1.08	1.07	1.14	0.00	17.75	17.78	54.23	1.20	1.14	1.31	0.92	0.90	0.79	1.13	1.08	1.15	1.00	0.98	0.95
Integrator complex subunit 10 OS=Mus musculus GN=Ints10 PE=1 SV=3	Q8K2A7	0.00	11.50	11.67	34.08	0.97	1.08	1.04	1.15	1.04	1.09	0.00	9.10	9.29	30.14	0.86	0.96	0.92	1.16	1.24	1.15	0.91	1.02	0.98	1.15	1.13	1.12
H/ACA ribonucleoprotein complex subunit 1 OS=Mus musculus GN=Gar1 PE=2 SV=1	Q9CY66	0.00	0.00	11.49	69.70	1.34	1.18	1.28	0.86	0.93	0.94	0.00	10.86	10.92	90.91	0.82	0.73	0.76	1.09	0.84	0.19	1.05	0.93	0.99	0.97	0.88	0.43
SWI/SNF-related matrix-associated actin-dependent regulator of chromatin subfamily D member 1 OS=Mus musculus GN=Smarcd1 PE=1 SV=3	Q61466	0.00	0.00	12.76	35.73	0.82	1.03	0.70	0.91	0.93	1.25	0.00	14.49	15.76	57.48	0.93	1.37	1.16	1.12	0.85	0.42	0.87	1.19	0.90	1.01	0.89	0.73
Protein Zfp207 OS=Mus musculus GN=Zfp207 PE=2 SV=1	Q9JMD0	0.00	11.40	11.41	22.22	0.76	0.91	0.90	0.74	0.88	0.97	0.00	7.86	7.87	28.69	0.93	1.09	0.91	1.01	0.95	1.20	0.84	1.00	0.91	0.86	0.92	1.08
Bystin OS=Mus musculus GN=Bysl PE=1 SV=3	O54825	0.00	11.39	11.61	43.81	0.97	1.00	0.85	0.95	0.96	1.00	0.00	10.36	10.39	40.37	0.69	0.74	0.63	1.01	1.25	1.37	0.82	0.86	0.73	0.98	1.10	1.17
60S ribosomal protein L18 OS=Mus musculus GN=Rpl18 PE=2 SV=3	P35980	0.00	0.00	11.42	57.98	1.13	1.27	1.45	1.39	1.89	1.63	0.00	10.11	10.14	54.26	0.89	1.06	0.78	1.94	2.70	2.01	1.00	1.16	1.06	1.64	2.26	1.81
Bromodomain-containing protein 3 OS=Mus musculus GN=Brd3 PE=1 SV=2	Q8K2F0	0.00	0.00	16.96	34.57	1.24	1.05	0.97	0.82	0.70	0.63	0.00	6.76	10.77	35.54	1.89	1.28	1.54	0.73	0.64	0.72	1.53	1.16	1.22	0.78	0.67	0.67
Histone-lysine N-methyltransferase EHMT2 OS=Mus musculus GN=Ehmt2 PE=1 SV=2	Q9Z148	0.00	0.00	11.37	27.79	1.02	1.06	1.01	0.95	0.94	0.90	0.00	0.00	13.24	30.80	0.95	1.24	1.37	0.96	0.65	0.82	0.99	1.14	1.17	0.96	0.78	0.86
WD repeat-containing protein 5 OS=Mus musculus GN=Wdr5 PE=1 SV=1	P61965	0.00	11.32	11.59	30.24	1.04	1.01	1.00	1.00	0.95	0.92	0.00	9.35	9.48	41.02	1.01	0.60	0.74	0.91	0.89	0.57	1.02	0.78	0.86	0.95	0.92	0.72
Bifunctional methylenetetrahydrofolate dehydrogenase/cyclohydrolase, mitochondrial OS=Mus musculus GN=Mthfd2 PE=1 SV=1	P18155	0.00	0.00	11.38	41.43	1.31	0.89	1.67	0.82	0.74	0.58	0.00	13.74	13.75	47.43	1.24	0.71	1.10	0.65	0.45	0.11	1.27	0.79	1.36	0.73	0.58	0.25
Fanconi anemia group D2 protein homolog OS=Mus musculus GN=Fancd2 PE=1 SV=2	Q80V62	0.00	0.00	11.34	22.00	1.08	1.08	0.98	0.42	0.48	0.48	0.00	0.00	7.18	29.24	0.91	1.13	0.77	0.67	0.72	0.71	0.99	1.10	0.87	0.53	0.59	0.58
U3 small nucleolar RNA-associated protein 18 homolog OS=Mus musculus GN=Utp18 PE=1 SV=1	Q5SSI6	0.00	0.00	11.29	37.32	0.91	0.95	0.91	1.12	1.26	1.17	0.00	7.41	7.41	38.22	0.98	0.95	0.94	1.01	1.02	0.97	0.95	0.95	0.92	1.06	1.13	1.07
60S ribosomal protein L27 OS=Mus musculus GN=Rpl27 PE=2 SV=2	P61358	0.00	0.00	11.29	69.85	1.01	0.88	1.33	1.16	1.77	1.53	0.00	10.35	10.35	64.71	1.18	0.81	0.90	1.04	1.29	1.01	1.09	0.84	1.10	1.10	1.51	1.24
Putative ATP-dependent RNA helicase DHX33 OS=Mus musculus GN=Dhx33 PE=1 SV=1	Q80VY9	0.00	11.24	11.25	38.97	1.08	1.06	0.92	1.10	1.32	1.22	0.00	11.80	11.83	39.83	0.90	0.95	0.98	1.12	1.34	1.50	0.98	1.00	0.95	1.11	1.33	1.36
Zinc finger protein 512 OS=Mus musculus GN=Znf512 PE=2 SV=2	Q69Z99	0.00	11.24	11.24	27.76	1.01	1.03	1.02	0.95	0.90	0.90	0.00	8.58	8.59	40.57	0.80	1.03	0.97	0.85	0.90	0.82	0.90	1.03	1.00	0.90	0.90	0.86
Major centromere autoantigen B OS=Mus musculus GN=Cenpb PE=2 SV=2	P27790	0.00	11.23	11.25	26.04	0.98	0.96	0.98	0.91	0.95	0.90	0.00	6.45	6.48	30.55	0.75	1.07	0.78	0.89	0.90	0.76	0.86	1.01	0.87	0.90	0.93	0.82
Nuclear factor NF-kappa-B p105 subunit OS=Mus musculus GN=Nfkb1 PE=1 SV=2	P25799	0.00	11.20	11.28	28.12	2.40	5.06	4.92	1.69	3.66	5.92	0.00	10.42	10.50	33.06	1.54	2.36	3.13	1.08	2.00	2.17	1.92	3.45	3.93	1.35	2.70	3.58
Cullin-4B OS=Mus musculus GN=Cul4b PE=1 SV=1	A2A432	0.00	11.19	11.24	30.00	0.99	1.04	0.96	1.02	1.00	0.98	0.00	10.78	10.82	27.42	0.99	1.03	0.98	1.06	1.07	0.92	0.99	1.03	0.97	1.04	1.03	0.95
Serine/arginine-rich splicing factor 10 OS=Mus musculus GN=Srsf10 PE=1 SV=2	Q9R0U0	0.00	0.00	11.19	52.67	1.12	1.18	1.03	0.98	0.98	1.02	0.00	0.00	12.51	49.24	1.13	0.69	0.83	1.16	1.18	0.82	1.12	0.90	0.92	1.07	1.08	0.91
High mobility group nucleosome-binding domain-containing protein 5 OS=Mus musculus GN=Hmgn5 PE=1 SV=2	Q9JL35	0.00	11.18	11.19	33.00	1.05	0.78	1.42	1.11	0.79	0.63	0.00	7.11	7.12	26.85	1.67	1.13	1.47	1.04	0.43	0.88	1.32	0.94	1.45	1.07	0.58	0.74
DNA-(apurinic or apyrimidinic site) lyase OS=Mus musculus GN=Apex1 PE=1 SV=2	P28352	0.00	0.00	11.06	36.28	0.96	1.05	1.14	0.74	1.06	0.67	0.00	11.24	11.25	47.32	0.68	0.90	1.04	0.93	0.93	0.81	0.81	0.97	1.09	0.83	0.99	0.74
ATP-dependent RNA helicase DDX39A OS=Mus musculus GN=Ddx39a PE=2 SV=1	Q8VDW0	0.00	0.00	30.62	59.48	0.64	1.10	0.88	1.17	0.90	0.92	0.00	13.17	30.23	60.66	1.11	0.87	1.03	0.95	0.54	0.20	0.84	0.98	0.95	1.05	0.70	0.43
Origin recognition complex subunit 5 OS=Mus musculus GN=Orc5 PE=2 SV=1	Q9WUV0	0.00	10.97	11.07	30.57	0.94	1.02	1.01	0.90	0.95	0.89	0.00	2.38	2.38	27.59	1.21	1.10	1.10	0.91	0.92	0.95	1.07	1.06	1.05	0.91	0.93	0.92
RNA exonuclease 4 OS=Mus musculus GN=Rexo4 PE=2 SV=2	Q6PAQ4	0.00	0.00	11.02	28.94	1.08	1.02	0.94	0.74	0.86	0.81	0.00	0.00	7.54	49.77	0.96	0.97	0.90	0.95	1.07	0.96	1.02	1.00	0.92	0.84	0.95	0.88
Replication factor C subunit 2 OS=Mus musculus GN=Rfc2 PE=2 SV=1	Q9WUK4	0.00	0.00	10.97	38.68	1.02	1.26	1.39	1.18	0.52	0.47	0.00	4.73	4.73	34.96	1.12	1.07	1.06	1.02	0.95	0.87	1.07	1.16	1.21	1.10	0.71	0.64
Anaphase-promoting complex subunit 7 OS=Mus musculus GN=Anapc7 PE=2 SV=3	Q9WVM3	0.00	0.00	10.93	22.30	0.97	1.00	0.99	0.90	0.92	0.87	0.00	0.00	4.34	33.98	0.99	1.02	1.11	1.03	0.92	0.96	0.98	1.01	1.05	0.96	0.92	0.92
RNA-binding protein 34 OS=Mus musculus GN=Rbm34 PE=1 SV=1	Q8C5L7	0.00	0.00	10.68	43.73	1.01	1.04	1.01	0.95	1.07	1.03	0.00	0.00	15.32	49.33	0.92	1.16	0.93	1.31	1.69	1.46	0.96	1.10	0.97	1.12	1.34	1.22
E1A-binding protein p400 OS=Mus musculus GN=Ep400 PE=1 SV=3	Q8CHI8	0.00	10.89	10.93	22.40	0.92	0.96	0.94	0.93	1.02	1.02	0.00	14.51	14.56	26.40	0.88	0.90	0.91	1.00	0.97	1.03	0.90	0.93	0.92	0.96	1.00	1.02
Chromodomain-helicase-DNA-binding protein 1-like OS=Mus musculus GN=Chd1l PE=2 SV=1	Q9CXF7	0.00	10.88	10.89	30.11	1.00	1.12	1.11	1.24	1.49	1.58	0.00	7.14	7.41	31.33	0.69	0.91	0.95	1.50	1.94	2.21	0.83	1.01	1.03	1.36	1.70	1.87
Chromodomain-helicase-DNA-binding protein 1 OS=Mus musculus GN=Chd1 PE=1 SV=3	P40201	0.00	10.87	11.54	21.04	1.11	1.00	1.02	1.05	0.95	0.93	0.00	2.26	7.19	25.13	0.99	0.98	1.01	0.93	1.01	0.76	1.05	0.99	1.01	0.99	0.98	0.84
Elongation factor 1-gamma OS=Mus musculus GN=Eef1g PE=1 SV=3	Q9D8N0	0.00	0.00	10.85	36.38	1.21	1.18	1.17	1.67	1.75	1.01	0.00	14.31	14.31	45.31	1.09	1.17	1.00	1.85	1.87	0.46	1.15	1.17	1.08	1.76	1.81	0.68

Protien identification and qunatitation results from ProteinPilot for all the analyzed samples

Name	Accession number	% FDR	Unused	Total	%Cov	114:113	115:113	116:113	118:117	119:117	121:117	% FDR	Unused	Total	%Cov	114:113	115:113	116:113	118:117	119:117	121:117	114:113	115:113	116:113	118:117	119:117	121:117
Regulation of nuclear pre-mRNA domain-containing protein 1B OS=Mus musculus GN=Rprd1b PE=1 SV=2	Q9CSU0	0.00	10.81	10.87	42.94	0.94	0.60	1.00	0.89	0.69	0.64	0.00	11.32	11.34	43.25	0.80	1.08	0.95	0.88	0.61	0.59	0.87	0.81	0.97	0.88	0.65	0.61
60S ribosomal protein L12 OS=Mus musculus GN=Rpl12 PE=1 SV=2	P35979	0.00	0.00	10.82	73.94	1.92	1.31	1.94	1.33	1.79	1.49	0.00	11.52	11.53	86.06	1.47	1.11	1.32	1.36	1.37	1.32	1.68	1.20	1.60	1.34	1.56	1.40
Microtubule-actin cross-linking factor 1 OS=Mus musculus GN=Macf1 PE=1 SV=2	Q9QXZ0	0.00	0.00	13.40	20.86	0.91	0.85	0.87	0.97	1.03	0.97	0.00	0.00	16.37	30.35	1.82	0.37	1.63	0.75	0.95	0.84	1.29	0.56	1.19	0.86	0.99	0.90
SWI/SNF-related matrix-associated actin-dependent regulator of chromatin subfamily B member 1 OS=Mus musculus GN=Smarcb1 PE=1 SV=1	Q9Z0H3	0.00	0.00	10.95	45.71	0.60	0.94	1.08	0.26	0.76	0.78	0.00	12.24	12.56	55.32	1.08	0.69	1.36	1.15	0.96	1.18	0.81	0.81	1.21	0.54	0.86	0.96
Torsin-1A-interacting protein 1 OS=Mus musculus GN=Tor1aip1 PE=1 SV=3	Q921T2	0.00	10.79	10.80	49.24	1.18	1.10	1.14	1.28	0.83	0.94	0.00	0.00	8.14	37.82	0.92	0.74	0.60	1.18	0.70	0.52	1.04	0.90	0.82	1.23	0.77	0.70
von Willebrand factor A domain-containing protein 5A OS=Mus musculus GN=Vwa5a PE=1 SV=2	Q99KC8	0.00	10.77	10.81	22.57	0.87	0.85	1.00	1.60	1.14	1.01	0.00	7.04	7.06	27.36	1.24	2.68	2.56	1.96	1.42	0.24	1.04	1.51	1.60	1.77	1.27	0.49
Origin recognition complex subunit 3 OS=Mus musculus GN=Orc3 PE=1 SV=1	Q9JK30	0.00	10.72	10.77	28.95	1.09	1.04	1.02	0.99	1.01	1.04	0.00	10.71	10.77	33.57	1.12	1.18	1.20	0.93	0.78	0.70	1.10	1.11	1.11	0.96	0.89	0.86
Probable U3 small nucleolar RNA-associated protein 11 OS=Mus musculus GN=Utp11l PE=2 SV=1	Q9CZJ1	0.00	10.71	10.78	52.17	0.78	0.96	0.89	0.76	1.15	0.95	0.00	7.49	7.50	50.99	0.98	0.95	0.97	0.98	1.13	1.07	0.87	0.96	0.93	0.86	1.14	1.00
60S ribosomal protein L5 OS=Mus musculus GN=Rpl5 PE=1 SV=3	P47962	0.00	0.00	10.66	47.47	1.31	0.95	1.16	1.57	2.03	1.74	0.00	11.47	11.47	48.48	1.46	1.38	1.11	1.39	1.51	0.94	1.38	1.14	1.13	1.48	1.75	1.28
Protein Srsf11 OS=Mus musculus GN=Srsf11 PE=4 SV=1	E9Q6E5	0.00	10.63	10.65	51.08	0.96	1.11	1.15	1.51	1.29	1.25	0.00	10.35	10.36	53.62	1.50	1.32	1.08	1.17	0.94	0.44	1.20	1.21	1.11	1.33	1.10	0.74
REST corepressor 1 OS=Mus musculus GN=Rcor1 PE=1 SV=2	Q8CFE3	0.00	0.00	10.63	39.62	1.01	1.18	1.15	1.22	0.94	0.94	0.00	0.00	14.62	44.86	1.13	1.24	1.46	0.96	0.74	0.44	1.07	1.21	1.29	1.09	0.84	0.65
Importin subunit alpha-4 OS=Mus musculus GN=Kpna4 PE=2 SV=1	O35343	0.00	0.00	10.57	24.57	1.19	1.11	1.04	0.96	0.81	0.82	0.00	0.00	9.70	33.97	0.97	1.16	1.05	1.11	0.96	1.05	1.08	1.13	1.04	1.03	0.88	0.93
tRNA (cytosine(34)-C(5))-methyltransferase OS=Mus musculus GN=Nsun2 PE=1 SV=2	Q1HFZ0	0.00	10.53	10.54	26.16	0.92	1.15	1.11	0.60	1.46	1.33	0.00	8.43	8.44	32.76	0.95	1.12	1.05	0.84	1.28	1.21	0.94	1.13	1.08	0.71	1.37	1.27
60S ribosomal protein L23a OS=Mus musculus GN=Rpl23a PE=1 SV=1	P62751	0.00	0.00	10.50	48.72	1.22	1.04	1.28	1.03	1.17	1.05	0.00	0.00	9.31	52.56	1.53	0.95	1.22	1.18	1.05	1.03	1.37	0.99	1.25	1.10	1.11	1.04
Histone-lysine N-methyltransferase EHMT1 OS=Mus musculus GN=Ehmt1 PE=1 SV=2	Q5DW34	0.00	10.48	10.63	20.52	0.60	1.15	1.47	0.55	0.91	0.80	0.00	0.00	7.06	27.01	0.96	1.11	0.95	1.05	1.06	1.06	0.76	1.13	1.18	0.76	0.98	0.92
Polyadenylate-binding protein 1 OS=Mus musculus GN=Pabpc1 PE=1 SV=2	P29341	0.00	0.00	10.51	35.06	0.95	0.52	1.00	2.78	1.54	1.38	0.00	0.01	5.27	42.30	1.05	0.97	0.89	1.50	0.95	1.00	1.00	0.71	0.94	2.04	1.21	1.17
Rho GTPase-activating protein 11A OS=Mus musculus GN=Arhgap11a PE=1 SV=2	Q80Y19	0.00	10.41	10.59	20.26	1.54	1.39	1.24	1.03	0.86	0.90	0.00	4.18	4.19	30.70	1.27	1.21	1.25	1.02	0.98	0.82	1.40	1.30	1.24	1.02	0.92	0.86
Nuclear pore complex protein Nup54 OS=Mus musculus GN=Nup54 PE=1 SV=1	Q8BTS4	0.00	10.39	10.41	31.76	0.77	0.79	0.77	0.82	0.68	0.83	0.00	15.72	15.74	34.51	0.99	0.90	0.91	1.02	0.57	0.81	0.87	0.85	0.84	0.92	0.62	0.82
Sentrin-specific protease 7 OS=Mus musculus GN=Senp7 PE=2 SV=1	Q8BUH8	0.00	10.33	10.38	17.65	0.56	0.85	0.82	0.88	0.85	0.92	0.00	6.09	6.12	21.60	0.88	0.91	1.02	0.99	1.06	1.14	0.70	0.88	0.91	0.93	0.95	1.02
DEAH (Asp-Glu-Ala-His) box polypeptide 38 OS=Mus musculus GN=Dhx38 PE=2 SV=1	Q80X98	0.00	10.32	10.34	23.37	0.98	1.02	1.11	0.95	0.91	1.04	0.00	2.91	3.78	28.18	0.93	1.00	1.05	0.97	0.99	1.04	0.95	1.01	1.08	0.96	0.95	1.04
Retinoblastoma-binding protein 5 OS=Mus musculus GN=Rbbp5 PE=1 SV=2	Q8BX09	0.00	10.32	10.34	24.16	1.53	0.91	1.51	1.37	1.34	1.22	0.00	8.93	8.95	29.55	1.05	0.98	1.04	1.00	0.95	0.98	1.26	0.95	1.25	1.17	1.13	1.10
Something about silencing protein 10 OS=Mus musculus GN=Utp3 PE=1 SV=1	Q9JI13	0.00	10.32	10.33	45.63	1.03	0.95	1.04	0.95	0.98	1.01	0.00	5.53	5.54	32.84	1.17	0.61	0.79	1.00	1.24	1.18	1.10	0.76	0.90	0.97	1.10	1.09
Nucleoporin SEH1 OS=Mus musculus GN=Seh1l PE=2 SV=1	Q8R2U0	0.00	10.31	10.31	24.44	0.93	0.80	1.08	0.91	1.03	1.01	0.00	12.03	12.03	34.17	0.96	1.21	0.91	1.19	1.66	0.25	0.95	0.99	0.99	1.04	1.31	0.50
DNA ligase 1 OS=Mus musculus GN=Lig1 PE=1 SV=2	P37913	0.00	0.00	10.31	29.69	1.53	1.54	1.22	1.28	1.18	0.65	0.00	0.00	18.39	44.65	1.25	1.31	1.12	0.95	0.83	0.58	1.38	1.42	1.17	1.10	0.99	0.62
60S ribosomal protein L13a OS=Mus musculus GN=Rpl13a PE=1 SV=4	P19253	0.00	0.00	10.30	56.65	1.32	1.45	1.60	2.17	2.03	2.01	0.00	0.00	8.71	58.13	1.60	1.39	1.41	1.75	1.53	1.50	1.45	1.42	1.50	1.95	1.76	1.74
60S ribosomal protein L18a OS=Mus musculus GN=Rpl18a PE=1 SV=1	P62717	0.00	10.30	10.30	50.57	1.31	1.15	1.47	1.69	1.89	1.77	0.00	10.92	10.93	57.39	1.34	1.11	1.11	1.69	1.58	1.18	1.32	1.13	1.28	1.69	1.73	1.45
Far upstream element-binding protein 1 OS=Mus musculus GN=Fubp1 PE=1 SV=1	Q91WJ8	0.00	0.00	17.04	44.39	1.03	1.07	1.05	0.89	0.98	0.90	0.00	0.00	9.05	44.85	1.00	1.02	1.10	0.88	0.94	0.92	1.01	1.04	1.07	0.88	0.96	0.91
UDP-N-acetylglucosamine--peptide N-acetylglucosaminyltransferase 110 kDa subunit OS=Mus musculus GN=Ogt PE=1 SV=2	Q8CGY8	0.00	10.25	10.27	19.89	0.98	0.94	0.95	1.12	1.14	1.14	0.00	16.65	16.65	36.14	1.06	1.03	1.01	1.33	1.27	1.11	1.02	0.98	0.98	1.22	1.20	1.12
Probable ATP-dependent RNA helicase DDX52 OS=Mus musculus GN=Ddx52 PE=2 SV=2	Q8K301	0.00	0.00	10.24	29.60	0.91	0.90	0.86	0.93	0.98	0.98	0.00	9.56	9.57	39.46	0.84	1.13	0.98	0.71	1.01	0.46	0.87	1.00	0.92	0.81	1.00	0.67
Actin-related protein 2/3 complex subunit 2 OS=Mus musculus GN=Arpc2 PE=1 SV=3	Q9CVB6	0.00	0.00	10.07	38.67	1.31	0.50	0.59	0.96	0.78	0.81	0.00	7.80	7.80	40.33	1.38	0.24	0.52	1.43	0.42	0.69	1.34	0.35	0.56	1.17	0.57	0.74
SURP and G-patch domain-containing protein 1 OS=Mus musculus GN=Sugp1 PE=1 SV=1	Q8CH02	0.00	10.12	10.17	33.59	1.02	0.84	0.88	0.77	0.99	0.82	0.00	6.53	6.54	33.28	1.02	0.97	1.05	0.90	0.95	0.91	1.02	0.90	0.96	0.83	0.97	0.86
GC-rich sequence DNA-binding factor 1 OS=Mus musculus GN=Gcfc1 PE=1 SV=2	P58501	0.00	0.00	10.15	31.84	0.96	0.77	0.86	0.81	1.06	1.06	0.00	0.00	7.16	29.88	0.84	1.01	0.89	1.06	1.21	1.45	0.90	0.88	0.87	0.92	1.13	1.24
Protein Urb2 OS=Mus musculus GN=Urb2 PE=4 SV=1	E9Q7L1	0.00	0.00	9.12	18.18	1.00	1.01	0.97	0.95	1.02	1.04	0.00	2.73	2.87	20.93	0.88	0.87	1.01	0.93	1.04	1.03	0.94	0.94	0.99	0.94	1.03	1.03
RNA-binding protein 5 OS=Mus musculus GN=Rbm5 PE=1 SV=1	Q91YE7	0.00	10.07	10.08	23.31	1.09	1.06	1.03	1.03	0.98	1.06	0.00	11.83	11.84	28.47	1.14	1.08	1.28	1.11	1.57	0.16	1.11	1.07	1.15	1.07	1.24	0.41
Exosome complex component RRP41 OS=Mus musculus GN=Exosc4 PE=2 SV=3	Q921I9	0.00	0.00	10.05	51.84	1.04	1.09	1.04	1.06	1.00	1.14	0.00	6.00	6.00	45.71	0.99	1.57	1.11	1.82	1.91	1.53	1.01	1.31	1.07	1.39	1.38	1.32
SAP domain-containing ribonucleoprotein OS=Mus musculus GN=Sarnp PE=1 SV=3	Q9D1J3	0.00	0.00	10.03	43.81	0.90	0.85	1.09	0.91	0.90	1.08	0.00	10.96	10.96	53.81	0.95	0.95	0.95	0.92	0.91	0.97	0.92	0.90	1.02	0.92	0.91	1.02

Protien identification and qunatitation results from ProteinPilot for all the analyzed samples

Name	Accession number	% FDR	Unused	Total	%Cov	114:113	115:113	116:113	118:117	119:117	121:117	% FDR	Unused	Total	%Cov	114:113	115:113	116:113	118:117	119:117	121:117	114:113	115:113	116:113	118:117	119:117	121:117
Exosome complex exonuclease RRP44 OS=Mus musculus GN=Dis3 PE=2 SV=4	Q9CSH3	0.00	10.01	10.09	32.46	1.10	1.07	1.02	1.03	1.07	0.90	0.00	8.22	8.25	39.98	1.17	1.34	1.31	1.22	1.61	0.77	1.13	1.20	1.15	1.12	1.31	0.84
Ribosomal biogenesis protein LAS1L OS=Mus musculus GN=Las1l PE=1 SV=1	A2BE28	0.00	10.01	10.02	17.78	0.90	1.02	1.10	1.38	1.82	1.66	0.00	6.02	6.04	27.32	1.01	1.01	1.06	1.04	1.10	0.95	0.95	1.01	1.08	1.20	1.41	1.26
Protein mago nashi homolog OS=Mus musculus GN=Magoh PE=2 SV=1	P61327	0.00	0.00	10.02	62.33	1.15	0.85	1.15	0.82	0.95	0.92	0.00	0.00	12.16	61.64	1.22	0.32	0.95	0.85	0.47	0.36	1.19	0.52	1.04	0.83	0.67	0.58
Serine/arginine-rich splicing factor 7 OS=Mus musculus GN=Srsf7 PE=1 SV=1	Q8BL97	0.00	0.00	13.80	69.66	0.89	0.72	0.90	1.24	1.34	1.27	0.00	0.00	15.95	63.30	0.85	1.14	0.86	1.24	1.09	0.86	0.87	0.90	0.87	1.24	1.21	1.05
DNA replication licensing factor MCM3 OS=Mus musculus GN=Mcm3 PE=1 SV=2	P25206	0.00	0.00	9.98	27.34	0.89	1.03	1.08	1.00	0.79	0.56	0.00	9.62	9.62	33.62	1.01	1.18	0.99	1.29	1.14	0.93	0.95	1.10	1.03	1.14	0.95	0.72
Ribosome-binding protein 1 OS=Mus musculus GN=Rrbp1 PE=2 SV=2	Q99PL5	0.00	0.00	10.11	34.83	1.20	1.19	1.13	1.15	1.77	1.32	0.00	0.00	15.33	36.95	1.09	0.95	1.29	1.54	2.29	1.91	1.14	1.06	1.21	1.33	2.01	1.58
IgE-binding protein OS=Mus musculus GN=Iap PE=2 SV=1	P03975	0.00	9.91	9.91	42.19	1.22	0.61	0.81	1.69	0.82	0.95	0.00	10.44	10.44	44.34	1.11	0.59	0.75	1.80	0.97	0.74	1.16	0.60	0.78	1.75	0.90	0.84
Luc7-like protein 3 OS=Mus musculus GN=Luc7l3 PE=1 SV=1	Q5SUF2	0.00	9.88	9.90	41.44	0.91	1.11	0.86	1.13	1.02	0.70	0.00	0.00	6.92	41.90	1.31	1.22	0.90	1.06	0.69	0.07	1.09	1.16	0.87	1.09	0.84	0.21
Tumor suppressor p53-binding protein 1 OS=Mus musculus GN=Tp53bp1 PE=1 SV=2	P70399	0.00	9.87	9.87	16.04	0.96	1.00	1.00	0.93	0.96	0.96	0.00	6.67	6.67	18.80	1.03	1.05	0.95	0.95	1.04	1.04	1.00	1.02	0.98	0.94	1.00	1.00
THO complex subunit 7 homolog OS=Mus musculus GN=Thoc7 PE=1 SV=2	Q7TMY4	0.00	9.84	9.84	36.27	0.95	0.99	1.00	0.95	0.95	0.97	0.00	12.13	12.13	52.94	1.15	0.88	1.12	1.07	0.65	0.74	1.05	0.93	1.06	1.00	0.78	0.85
RNA polymerase-associated protein CTR9 homolog OS=Mus musculus GN=Ctr9 PE=1 SV=2	Q62018	0.00	9.82	10.53	27.79	1.41	1.02	1.08	1.05	0.94	1.06	0.00	13.16	13.17	31.63	1.06	1.21	1.04	1.20	0.79	1.43	1.22	1.11	1.06	1.12	0.86	1.23
Integrator complex subunit 3 OS=Mus musculus GN=Ints3 PE=1 SV=2	Q7TPD0	0.00	9.82	9.85	25.84	0.76	1.12	0.88	0.99	0.80	0.79	0.00	12.13	12.18	32.18	0.53	0.86	0.50	0.90	0.57	0.33	0.63	0.98	0.66	0.95	0.68	0.51
Tuftelin-interacting protein 11 OS=Mus musculus GN=Tfip11 PE=1 SV=1	Q9ERA6	0.00	0.00	9.81	25.89	1.03	0.97	0.95	1.00	1.06	1.00	0.00	7.10	7.10	36.99	0.94	0.98	0.98	0.92	0.92	1.02	0.98	0.98	0.97	0.96	0.99	1.01
60S ribosomal protein L36 OS=Mus musculus GN=Rpl36 PE=3 SV=1	Q6ZWZ4	0.00	0.00	9.73	67.62	1.32	1.14	1.20	1.37	1.58	1.18	0.00	0.00	6.89	42.86	1.22	1.09	1.07	2.31	0.79	1.89	1.27	1.11	1.13	1.78	1.12	1.49
Runt-related transcription factor 1 OS=Mus musculus GN=Runx1 PE=1 SV=1	Q03347	0.00	0.00	9.73	41.69	0.98	1.04	0.98	0.99	0.96	0.95	0.00	0.00	13.62	47.67	0.98	1.06	1.06	1.10	1.01	1.03	0.98	1.05	1.02	1.04	0.99	0.99
WD repeat-containing protein 74 OS=Mus musculus GN=Wdr74 PE=2 SV=1	Q8VCG3	0.00	9.65	9.71	35.94	0.95	1.26	1.34	1.13	1.56	1.33	0.00	16.03	16.03	52.34	1.01	1.25	1.14	1.85	2.44	1.89	0.98	1.25	1.24	1.45	1.95	1.58
Notchless protein homolog 1 OS=Mus musculus GN=Nle1 PE=2 SV=4	Q8VEJ4	0.00	0.00	9.70	44.12	1.56	1.74	1.19	1.19	1.54	1.31	0.00	10.31	10.32	29.28	2.33	1.84	2.61	2.13	2.51	1.18	1.91	1.79	1.76	1.59	1.97	1.24
Integrator complex subunit 2 OS=Mus musculus GN=Ints2 PE=2 SV=2	Q80UK8	0.00	9.63	9.64	24.04	1.06	0.92	0.69	0.90	0.63	0.79	0.00	4.10	4.14	28.30	0.76	0.82	0.77	1.00	1.09	1.09	0.90	0.87	0.73	0.95	0.82	0.92
Origin recognition complex subunit 1 OS=Mus musculus GN=Orc1 PE=1 SV=2	Q9Z1N2	0.00	0.00	9.61	29.40	1.04	1.06	1.03	1.03	1.07	1.04	0.00	0.00	14.13	32.98	0.95	1.45	1.27	1.25	1.27	0.29	0.99	1.24	1.14	1.13	1.16	0.55
Ran GTPase-activating protein 1 OS=Mus musculus GN=Rangap1 PE=1 SV=2	P46061	0.00	0.00	9.59	37.69	0.87	0.78	0.84	1.29	1.07	1.25	0.00	0.00	18.72	37.35	0.70	0.72	0.44	0.94	0.73	0.21	0.78	0.75	0.61	1.10	0.88	0.52
Bromodomain-containing protein 2 OS=Mus musculus GN=Brd2 PE=1 SV=1	Q7JJ13	0.00	0.00	9.46	27.07	0.78	0.81	0.83	1.07	1.05	0.95	0.00	16.96	16.97	43.48	0.90	0.93	0.95	1.03	1.04	0.96	0.84	0.87	0.89	1.05	1.04	0.95
DNA replication licensing factor MCM7 OS=Mus musculus GN=Mcm7 PE=2 SV=1	Q61881	0.00	0.00	9.37	28.65	0.90	1.05	1.09	0.82	0.64	0.47	0.00	6.91	6.92	35.47	0.95	1.22	1.16	1.09	0.96	0.98	0.93	1.13	1.12	0.94	0.78	0.68
60S ribosomal protein L13 OS=Mus musculus GN=Rpl13 PE=2 SV=3	P47963	0.00	9.35	10.14	65.40	1.28	1.43	1.33	1.36	1.54	1.28	0.00	13.49	13.50	72.99	1.15	1.16	1.09	1.45	1.19	1.47	1.21	1.29	1.20	1.40	1.36	1.37
Unconventional myosin-Ig OS=Mus musculus GN=Myo1g PE=2 SV=1	Q5SUA5	0.00	9.33	9.38	30.86	0.94	0.49	0.64	0.63	0.26	0.25	0.00	12.70	12.74	37.99	0.79	0.44	0.49	0.61	0.27	0.26	0.86	0.47	0.56	0.62	0.26	0.25
Beta-arrestin-2 OS=Mus musculus GN=Arrb2 PE=1 SV=1	Q91YI4	0.00	0.00	9.26	25.37	0.76	0.91	0.82	0.93	0.77	0.86	0.00	0.00	12.64	34.39	0.99	0.92	1.15	1.05	0.86	0.90	0.87	0.92	0.97	0.99	0.82	0.88
RNA-binding protein 10 OS=Mus musculus GN=Rbm10 PE=1 SV=1	Q99KG3	0.00	9.24	9.27	23.33	0.90	0.96	0.99	0.81	0.87	0.71	0.00	0.00	7.95	36.34	0.98	0.91	0.95	0.94	0.97	0.98	0.94	0.94	0.97	0.87	0.92	0.84
Pyrroline-5-carboxylate reductase 2 OS=Mus musculus GN=Pycr2 PE=2 SV=1	Q922Q4	0.00	0.00	9.48	36.88	0.69	0.64	0.62	0.82	0.79	0.67	0.00	8.98	8.99	54.69	1.01	0.85	0.88	0.92	0.79	0.80	0.83	0.73	0.74	0.87	0.79	0.73
DNA-directed RNA polymerase I subunit RPA34 OS=Mus musculus GN=Cd3eap PE=1 SV=2	Q76KJ5	0.00	9.22	9.23	27.82	0.95	1.06	0.95	0.95	0.91	0.93	0.00	6.72	6.72	43.11	0.41	1.42	0.77	0.79	0.75	1.17	0.62	1.22	0.86	0.87	0.83	1.04
Aspartate--tRNA ligase, cytoplasmic OS=Mus musculus GN=Dars PE=2 SV=2	Q922B2	0.00	0.00	9.27	54.89	0.90	0.99	1.00	1.08	1.08	0.92	0.00	3.78	3.80	32.73	0.95	1.10	0.93	1.13	1.16	0.98	0.92	1.04	0.96	1.10	1.12	0.95
Cyclic AMP-responsive element-binding protein 1 OS=Mus musculus GN=Creb1 PE=1 SV=1	Q01147	0.00	0.00	9.21	24.63	1.00	1.05	1.03	0.99	0.96	0.96	0.00	0.00	8.41	23.75	1.12	1.15	1.12	1.26	1.02	0.85	1.06	1.10	1.07	1.12	0.99	0.90
RNA-binding protein with serine-rich domain 1 OS=Mus musculus GN=Rnps1 PE=2 SV=1	Q99M28	0.00	9.19	9.19	46.23	1.03	1.06	1.02	1.04	1.00	1.05	0.00	0.00	8.69	45.90	0.99	0.95	0.85	1.03	0.15	0.08	1.01	1.00	0.93	1.03	0.39	0.29
Chromobox protein homolog 5 OS=Mus musculus GN=Cbx5 PE=1 SV=1	Q61686	0.00	9.13	11.14	56.02	0.92	0.87	1.01	1.02	0.73	0.82	0.00	11.98	11.98	53.93	1.11	0.67	0.87	0.81	0.47	0.53	1.01	0.76	0.94	0.91	0.59	0.66
Transcription factor jun-B OS=Mus musculus GN=Junb PE=1 SV=1	P09450	0.00	0.00	9.13	45.06	1.20	1.51	2.15	3.02	5.65	10.76	0.00	13.40	13.40	46.80	1.98	5.20	3.94	4.02	7.45	11.80	1.54	2.81	2.91	3.48	6.49	11.27
General transcription factor 3C polypeptide 4 OS=Mus musculus GN=Gtf3c4 PE=1 SV=2	Q8BMQ2	0.00	0.00	9.11	20.69	0.99	0.84	1.02	0.68	0.70	0.82	0.15	2.06	2.09	27.54	0.54	0.76	1.03	1.01	0.61	0.82	0.73	0.80	1.02	0.83	0.65	0.82
ATP-binding cassette sub-family F member 2 OS=Mus musculus GN=Abcf2 PE=2 SV=1	Q99LE6	0.00	0.00	9.15	24.20	0.90	0.91	0.90	0.95	0.85	0.84	0.00	10.16	10.17	38.38	1.16	1.02	1.28	1.20	0.70	0.14	1.02	0.96	1.07	1.07	0.77	0.35
Ribosomal RNA processing protein 1 homolog B OS=Mus musculus GN=Rrp1b PE=2 SV=2	Q91YK2	0.00	9.06	9.13	23.62	0.90	0.59	0.92	0.88	0.97	0.69	0.00	17.94	17.95	37.43	1.09	0.98	1.09	0.87	0.95	0.88	0.99	0.76	1.00	0.87	0.96	0.78

Protien identification and qunatitation results from ProteinPilot for all the analyzed samples

Name	Accession number	% FDR	Unused	Total	%Cov	114:113	115:113	116:113	118:117	119:117	121:117	% FDR	Unused	Total	%Cov	114:113	115:113	116:113	118:117	119:117	121:117	114:113	115:113	116:113	118:117	119:117	121:117
60S ribosomal protein L9 OS=Mus musculus GN=Rpl9 PE=2 SV=2	P51410	0.00	0.00	9.08	49.48	1.67	2.03	2.13	1.66	1.58	1.31	0.00	0.00	7.86	51.04	1.22	1.10	1.09	1.54	1.53	1.32	1.43	1.49	1.52	1.60	1.56	1.31
60S acidic ribosomal protein P0 OS=Mus musculus GN=Rplp0 PE=1 SV=3	P14869	0.00	0.00	9.01	29.34	1.02	0.80	0.95	1.17	0.91	0.76	0.00	11.12	11.13	48.26	0.95	0.61	0.67	1.29	0.65	0.24	0.98	0.70	0.80	1.23	0.77	0.43
Phospholipase D4 OS=Mus musculus GN=Pld4 PE=2 SV=1	Q8BG07	0.00	8.97	9.01	24.06	0.88	0.92	0.82	1.13	1.10	0.89	0.00	5.38	5.48	33.40	0.80	0.91	0.80	1.08	0.96	0.99	0.84	0.92	0.81	1.10	1.03	0.94
Histone-lysine N-methyltransferase EZH2 OS=Mus musculus GN=Ezh2 PE=1 SV=2	Q61188	0.00	0.00	8.93	28.82	1.82	1.31	1.38	0.73	0.61	0.79	0.00	3.98	4.00	27.61	0.97	0.96	0.95	0.94	1.04	1.01	1.33	1.12	1.14	0.83	0.79	0.90
Protein Arid1b OS=Mus musculus GN=Arid1b PE=4 SV=1	E9Q6R4	0.00	8.91	13.31	18.28	0.99	1.01	0.95	0.97	0.98	0.98	0.00	0.00	4.71	19.26	1.05	1.02	1.07	1.07	0.94	0.95	1.02	1.01	1.01	1.02	0.96	0.96
Protein virilizer homolog OS=Mus musculus GN=Kiaa1429 PE=1 SV=1	A2AIV2	0.00	0.00	9.21	19.66	0.96	0.93	0.92	0.99	0.92	0.95	0.00	0.00	6.41	25.01	0.89	0.90	1.01	1.05	0.97	1.16	0.92	0.92	0.96	1.02	0.95	1.05
THO complex subunit 3 OS=Mus musculus GN=Thoc3 PE=2 SV=1	Q8VE80	0.00	8.84	8.87	23.08	1.03	1.03	1.07	0.92	0.93	1.02	0.00	10.15	10.16	18.23	0.91	0.96	0.87	1.46	0.90	0.38	0.97	1.00	0.96	1.16	0.91	0.62
DNA-directed RNA polymerase I subunit RPA1 OS=Mus musculus GN=Polr1a PE=1 SV=2	O35134	0.00	0.00	9.43	24.17	1.14	1.25	0.99	1.07	0.90	0.97	0.00	9.42	9.50	26.50	0.68	1.12	1.26	0.87	0.71	0.36	0.88	1.18	1.12	0.96	0.80	0.59
Pre-mRNA-splicing factor SYF2 OS=Mus musculus GN=Syf2 PE=2 SV=1	Q9D198	0.00	0.00	8.83	47.11	0.95	0.86	1.04	1.07	1.05	1.17	0.00	6.80	6.80	30.58	0.74	1.29	1.53	1.49	1.46	0.66	0.84	1.05	1.26	1.26	1.24	0.88
Dolichyl-diphosphooligosaccharide--protein glycosyltransferase subunit 1 OS=Mus musculus GN=Rpn1 PE=2 SV=1	Q91YQ5	0.00	0.00	8.84	27.14	0.94	0.91	0.86	0.95	0.91	0.81	0.00	17.07	17.09	25.33	0.90	0.98	0.86	0.95	0.71	0.78	0.92	0.95	0.86	0.95	0.81	0.79
Forkhead box protein K1 OS=Mus musculus GN=Foxk1 PE=1 SV=2	P42128	0.00	8.81	8.82	28.93	2.09	2.00	2.33	1.03	1.06	1.29	0.00	4.69	4.69	27.26	1.04	1.08	0.98	1.10	1.12	1.07	1.47	1.47	1.51	1.06	1.09	1.17
NHP2-like protein 1 OS=Mus musculus GN=Nhp2l1 PE=2 SV=4	Q9D0T1	0.00	8.81	8.81	48.44	0.66	0.82	0.82	0.19	1.27	1.05	0.00	9.87	9.88	42.97	0.64	0.57	0.49	0.67	1.04	0.56	0.65	0.69	0.63	0.36	1.15	0.77
Chromatin assembly factor 1 subunit B OS=Mus musculus GN=Chaf1b PE=2 SV=1	Q9D0N7	0.00	8.77	8.78	23.43	1.12	1.13	1.06	0.88	0.82	0.70	0.00	6.19	6.19	21.85	0.96	1.01	0.87	1.00	0.95	0.88	1.04	1.07	0.96	0.94	0.88	0.79
Cytoplasmic dynein 1 heavy chain 1 OS=Mus musculus GN=Dync1h1 PE=1 SV=2	Q9JHU4	0.00	8.74	9.11	21.92	1.02	0.90	0.69	1.33	1.09	0.70	0.00	9.07	9.26	24.42	1.02	1.12	1.20	0.99	0.95	0.86	1.02	1.00	0.91	1.15	1.02	0.78
60S ribosomal protein L38 OS=Mus musculus GN=Rpl38 PE=2 SV=3	Q9JJI8	0.00	0.00	8.72	57.14	0.90	1.02	0.99	0.96	1.14	1.19	0.00	4.35	4.37	50.00	1.02	0.92	1.18	0.98	1.00	0.67	0.96	0.97	1.08	0.97	1.07	0.89
60S ribosomal protein L17 OS=Mus musculus GN=Rpl17 PE=2 SV=3	Q9CPR4	0.00	0.00	8.70	46.74	1.37	1.36	1.58	1.63	1.58	1.15	0.00	0.00	9.77	64.13	1.49	1.13	1.11	1.64	0.96	0.92	1.43	1.24	1.32	1.64	1.24	1.03
General transcription factor 3C polypeptide 1 OS=Mus musculus GN=Gtf3c1 PE=2 SV=2	Q8K284	0.00	8.67	9.12	22.42	0.92	1.03	1.03	0.95	0.93	0.95	0.00	10.16	10.20	28.18	0.64	0.90	1.19	0.86	1.19	0.19	0.77	0.96	1.11	0.91	1.05	0.43
Regulation of nuclear pre-mRNA domain-containing protein 2 OS=Mus musculus GN=Rprd2 PE=1 SV=1	Q6NXI6	0.00	8.64	8.68	24.37	1.00	1.07	1.01	1.12	1.08	1.03	0.00	5.87	5.88	20.63	0.95	1.11	1.24	1.69	1.72	0.37	0.98	1.09	1.12	1.37	1.36	0.62
40S ribosomal protein S11 OS=Mus musculus GN=Rps11 PE=2 SV=3	P62281	0.00	0.00	8.65	61.39	1.11	0.72	1.19	1.17	1.46	1.36	0.00	0.00	10.99	67.72	0.89	0.73	0.74	1.20	1.31	1.20	0.99	0.72	0.94	1.19	1.38	1.28
Pre-mRNA-splicing factor SPF27 OS=Mus musculus GN=Bcas2 PE=2 SV=1	Q9D287	0.00	0.00	8.65	47.56	0.90	1.10	1.07	1.07	1.12	1.15	0.00	13.93	13.96	49.78	1.01	1.08	0.90	0.90	0.88	0.90	0.95	1.09	0.98	0.98	0.99	1.01
Aminopeptidase N OS=Mus musculus GN=Anpep PE=1 SV=4	P97449	0.00	0.00	8.67	21.12	0.91	0.40	0.60	0.67	0.53	0.54	0.00	6.20	6.30	24.64	0.90	0.46	0.59	0.59	0.42	0.35	0.90	0.43	0.59	0.63	0.47	0.43
DNA replication licensing factor MCM5 OS=Mus musculus GN=Mcm5 PE=2 SV=1	P49718	0.00	0.00	8.64	41.20	0.97	1.10	1.03	1.04	0.80	0.44	0.00	7.82	8.07	44.47	0.82	1.01	0.94	1.17	1.01	0.74	0.90	1.05	0.98	1.10	0.90	0.57
Nucleolar GTP-binding protein 2 OS=Mus musculus GN=Gnl2 PE=2 SV=2	Q99LH1	0.00	0.00	8.62	33.10	2.70	2.42	2.49	1.64	2.27	1.87	0.00	10.86	10.89	34.07	2.13	2.17	2.17	2.25	2.58	0.59	2.40	2.29	2.32	1.92	2.42	1.05
Heterogeneous nuclear ribonucleoprotein H2 OS=Mus musculus GN=Hnrnph2 PE=1 SV=1	P70333	0.00	8.59	35.00	57.91	0.67	1.02	0.81	1.50	1.41	1.45	0.00	16.63	40.33	76.39	1.02	1.22	0.98	1.18	0.08	1.15	0.83	1.12	0.89	1.33	0.33	1.29
Eukaryotic translation initiation factor 2 subunit 2 OS=Mus musculus GN=Eif2s2 PE=1 SV=1	Q99L45	0.00	0.00	8.59	34.14	0.95	0.77	0.74	0.79	0.86	0.65	0.00	6.72	6.73	27.79	0.96	1.04	0.98	1.03	1.10	0.99	0.96	0.89	0.85	0.90	0.97	0.80
Leucine-rich repeat and calponin homology domain-containing protein 4 OS=Mus musculus GN=Lrch4 PE=2 SV=1	Q921G6	0.00	0.00	8.58	41.03	0.89	0.42	0.53	0.87	0.63	0.63	0.00	0.00	7.36	39.71	0.95	0.58	0.74	0.85	0.82	0.86	0.92	0.49	0.63	0.86	0.72	0.73
Ribonucleoprotein PTB-binding 1 OS=Mus musculus GN=Raver1 PE=1 SV=2	Q9CW46	0.00	8.58	8.58	34.22	0.91	0.94	0.95	0.96	0.91	1.06	0.00	13.66	13.66	32.62	0.86	0.84	0.79	0.64	0.66	0.61	0.88	0.89	0.86	0.78	0.78	0.81
SUN domain-containing protein 1 OS=Mus musculus GN=Sun1 PE=1 SV=2	Q9D666	0.00	8.54	9.17	32.20	0.96	0.97	1.03	0.96	0.96	0.95	0.00	13.28	13.41	36.04	0.93	1.00	1.22	1.20	1.77	1.74	0.95	0.99	1.12	1.08	1.31	1.28
Protein Ythdc1 OS=Mus musculus GN=Ythdc1 PE=4 SV=1	E9PW44	0.00	8.54	8.54	23.23	0.98	1.00	1.03	1.11	0.99	1.04	0.00	4.67	4.68	29.35	0.81	0.90	1.10	1.27	0.45	0.80	0.89	0.95	1.06	1.19	0.67	0.91
Atherin OS=Mus musculus GN=Samd1 PE=3 SV=1	D3YXK1	0.00	8.51	8.53	41.62	0.90	1.08	0.93	0.90	0.67	0.58	0.00	8.34	8.35	42.20	0.90	1.02	1.00	0.95	0.90	1.05	0.90	1.05	0.96	0.92	0.77	0.78
Kinesin-like protein KIF20B OS=Mus musculus GN=Kif20b PE=1 SV=3	Q80WE4	0.00	0.00	8.83	20.69	0.97	1.01	0.97	1.10	1.10	1.00	0.00	0.00	10.79	28.24	1.22	1.25	1.22	1.19	1.27	1.02	1.09	1.12	1.09	1.14	1.18	1.01
RIKEN cDNA E330016A19, isoform CRA_e OS=Mus musculus GN=Mb21d1 PE=4 SV=1	D3Z5R0	0.00	0.00	8.24	48.48	0.92	0.86	0.94	1.80	1.53	2.07	0.00	0.00	7.45	41.88	1.22	1.17	1.09	1.47	0.72	0.59	1.06	1.00	1.01	1.63	1.05	1.11
Protein quaking OS=Mus musculus GN=Qki PE=1 SV=1	Q9QYS9	0.00	8.44	8.46	35.48	0.91	0.95	1.06	0.59	0.72	0.67	0.00	0.00	10.08	40.18	1.08	1.06	1.22	0.86	0.82	0.70	0.99	1.00	1.14	0.71	0.77	0.69
Protein Scaf4 OS=Mus musculus GN=Scaf4 PE=2 SV=1	Q6PFF0	0.00	8.41	8.48	22.08	1.04	1.04	1.07	1.00	1.02	0.98	0.00	6.51	6.52	23.74	1.19	1.21	1.28	0.79	0.54	0.72	1.11	1.12	1.17	0.89	0.74	0.84
Protein FAM207A OS=Mus musculus GN=Fam207a PE=1 SV=1	P58468	0.00	0.00	8.48	62.56	0.63	0.70	0.74	0.63	1.14	0.61	0.00	4.12	4.12	41.10	0.82	0.86	0.93	0.97	1.12	1.05	0.72	0.78	0.83	0.78	1.13	0.80
DNA methyltransferase 1-associated protein 1 OS=Mus musculus GN=Dmap1 PE=1 SV=1	Q9JI44	0.00	8.38	8.39	36.97	0.93	0.93	0.93	0.89	0.91	0.95	0.00	11.99	12.00	36.97	0.96	1.01	0.95	1.05	1.04	1.03	0.95	0.97	0.94	0.96	0.97	0.99

Protien identification and qunatitation results from ProteinPilot for all the analyzed samples

Name	Accession number	% FDR	Unused	Total	%Cov	114:113	115:113	116:113	118:117	119:117	121:117	% FDR	Unused	Total	%Cov	114:113	115:113	116:113	118:117	119:117	121:117	114:113	115:113	116:113	118:117	119:117	121:117
Activator of basal transcription 1 OS=Mus musculus GN=Abt1 PE=2 SV=1	Q9QYL7	0.00	0.00	8.37	61.71	0.86	0.75	1.04	1.26	1.82	1.61	0.00	4.53	4.53	46.84	1.00	0.92	1.16	1.19	1.20	1.21	0.93	0.83	1.10	1.22	1.48	1.40
Plasminogen activator inhibitor 1 RNA-binding protein OS=Mus musculus GN=Serbp1 PE=1 SV=2	Q9CY58	0.00	8.36	8.36	35.38	0.89	0.95	1.06	0.91	1.01	0.89	0.00	12.08	12.08	47.17	1.37	1.18	1.46	1.21	0.64	0.92	1.10	1.06	1.24	1.05	0.81	0.90
Cleavage and polyadenylation specificity factor subunit 6 OS=Mus musculus GN=Cpsf6 PE=1 SV=1	Q6NVF9	0.00	0.00	8.25	37.75	0.95	0.92	0.98	1.24	1.06	1.28	0.00	0.00	6.02	35.75	0.91	0.77	0.71	1.06	0.27	0.81	0.93	0.84	0.84	1.14	0.53	1.02
Treacle protein OS=Mus musculus GN=Tcof1 PE=1 SV=1	O08784	0.00	0.00	8.45	26.29	0.65	0.48	0.47	0.70	0.32	0.46	0.00	4.52	4.53	22.73	0.84	0.82	0.72	0.79	0.63	0.64	0.74	0.63	0.58	0.74	0.45	0.54
Lon protease homolog, mitochondrial OS=Mus musculus GN=Lonp1 PE=1 SV=2	Q8CGK3	0.00	0.00	8.40	30.87	1.09	1.07	0.99	0.91	0.96	0.89	0.00	0.00	10.57	28.13	0.69	1.06	1.00	1.36	0.95	0.56	0.87	1.06	1.00	1.11	0.95	0.71
Histone H1.3 OS=Mus musculus GN=Hist1h1d PE=1 SV=2	P43277	0.00	0.00	52.71	61.09	0.92	0.85	0.81	1.07	1.15	1.00	0.00	48.08	48.08	57.01	1.25	1.13	1.01	0.90	1.43	1.00	1.07	0.98	0.90	0.98	1.28	1.00
DEAD/H (Asp-Glu-Ala-Asp/His) box polypeptide 31 OS=Mus musculus GN=Ddx31 PE=2 SV=2	Q6NZQ2	0.00	8.15	8.16	30.28	1.04	0.97	1.06	0.93	0.98	0.95	0.00	6.20	6.21	28.38	1.18	1.25	1.31	0.77	0.94	0.08	1.11	1.10	1.17	0.85	0.96	0.28
WD repeat-containing protein 18 OS=Mus musculus GN=Wdr18 PE=1 SV=1	Q4VBE8	0.00	8.15	8.15	25.29	1.67	1.58	1.66	1.08	1.16	1.22	0.00	13.10	13.10	30.63	1.28	1.25	1.49	1.14	1.25	1.29	1.47	1.41	1.57	1.11	1.20	1.26
Poly [ADP-ribose] polymerase 9 OS=Mus musculus GN=Parp9 PE=1 SV=2	Q8CAS9	0.00	8.14	8.58	24.94	0.99	1.07	1.11	2.73	1.50	2.15	0.00	9.65	9.65	25.52	0.94	0.96	1.19	1.87	1.32	1.09	0.96	1.01	1.15	2.26	1.41	1.53
Glutamate-rich WD repeat-containing protein 1 OS=Mus musculus GN=Grwd1 PE=2 SV=2	Q810D6	0.00	0.00	8.17	26.23	1.24	1.43	1.34	1.34	1.74	1.85	0.00	0.00	9.24	41.93	1.37	1.49	1.34	1.39	1.61	1.96	1.30	1.46	1.34	1.37	1.67	1.91
Sulfide:quinone oxidoreductase, mitochondrial OS=Mus musculus GN=Sqrdl PE=2 SV=3	Q9R112	0.00	0.00	8.14	25.56	1.04	1.03	0.99	0.90	0.95	0.87	0.13	0.00	2.00	21.11	0.89	0.90	0.98	0.98	1.04	0.96	0.96	0.96	0.99	0.94	0.99	0.92
Polyhomeotic-like protein 2 OS=Mus musculus GN=Phc2 PE=1 SV=1	Q9QWH1	0.00	0.00	8.14	16.94	1.00	0.99	1.02	0.99	0.92	0.96	0.00	3.21	3.22	18.00	1.00	1.02	1.07	0.94	1.09	1.01	1.00	1.00	1.04	0.96	1.00	0.99
Probable ATP-dependent RNA helicase DDX6 OS=Mus musculus GN=Ddx6 PE=2 SV=1	P54823	0.00	8.10	8.15	31.47	1.13	0.96	1.11	1.15	1.13	1.09	0.00	8.08	8.08	38.51	1.03	0.94	0.97	1.51	1.47	2.01	1.08	0.95	1.04	1.32	1.29	1.48
Uncharacterized protein OS=Mus musculus GN=Chtop PE=4 SV=1	E9PW20	0.00	0.00	8.07	75.37	0.67	0.83	1.24	1.29	1.05	1.10	0.00	0.00	8.87	87.19	1.10	0.91	0.90	1.12	0.41	0.87	0.86	0.87	1.05	1.20	0.65	0.98
YLP motif-containing protein 1 OS=Mus musculus GN=Ylpm1 PE=2 SV=2	Q9R0I7	0.00	0.00	7.84	18.61	1.05	0.99	1.06	1.00	0.96	0.99	0.00	0.00	3.35	19.19	0.95	1.04	1.03	1.08	0.92	1.07	1.00	1.01	1.04	1.04	0.94	1.03
Serine/threonine-protein phosphatase 2A 65 kDa regulatory subunit A alpha isoform OS=Mus musculus GN=Ppp2r1a PE=1 SV=3	Q76MZ3	0.00	0.00	8.08	39.22	0.95	1.01	0.93	0.91	0.90	0.96	0.00	14.65	14.67	43.80	1.47	1.17	1.53	1.10	0.74	0.78	1.18	1.09	1.19	1.00	0.82	0.87
FYN-binding protein OS=Mus musculus GN=Fyb PE=1 SV=2	O35601	0.00	0.00	8.06	27.59	0.99	0.71	0.85	1.22	1.17	1.11	0.00	13.33	13.35	36.51	1.10	0.62	0.80	1.18	0.97	1.05	1.04	0.66	0.82	1.20	1.07	1.08
Clathrin heavy chain 1 OS=Mus musculus GN=Cltc PE=4 SV=1	Q5SXR6	0.00	0.00	8.12	24.90	0.99	0.63	0.65	0.91	0.82	0.75	0.00	8.27	8.31	25.19	1.07	0.77	0.82	3.08	1.51	1.32	1.03	0.70	0.73	1.67	1.11	1.00
Friend leukemia integration 1 transcription factor OS=Mus musculus GN=Fli1 PE=1 SV=1	P26323	0.00	0.00	8.04	21.02	0.93	1.00	0.86	0.89	0.87	0.84	0.00	6.80	6.80	34.51	0.54	0.65	0.69	1.27	1.11	1.27	0.71	0.81	0.77	1.06	0.98	1.03
Protein FAM111A OS=Mus musculus GN=Fam111a PE=2 SV=1	Q9D2L9	0.00	8.02	8.03	21.53	1.17	0.84	0.91	0.66	0.61	0.60	0.00	5.55	5.56	19.41	1.02	1.09	0.90	0.40	0.44	0.26	1.09	0.95	0.91	0.52	0.52	0.39
Pre-mRNA-splicing factor 38A OS=Mus musculus GN=Prpf38a PE=1 SV=1	Q4FK66	0.00	0.00	8.03	36.22	0.98	1.05	0.96	0.91	1.21	1.17	0.00	9.82	9.83	54.81	1.10	1.09	1.06	1.11	1.27	0.97	1.04	1.07	1.01	1.00	1.24	1.07
Methyl-CpG-binding protein 2 OS=Mus musculus GN=Mecp2 PE=1 SV=1	Q9Z2D6	0.00	8.01	8.02	36.78	1.08	0.99	1.07	1.01	0.90	0.86	0.00	0.00	4.07	29.55	1.14	1.05	1.18	0.87	0.90	0.77	1.11	1.02	1.12	0.94	0.90	0.81
Splicing factor 3A subunit 2 OS=Mus musculus GN=Sf3a2 PE=2 SV=2	Q62203	0.00	0.00	8.01	28.21	0.75	0.98	0.79	1.72	1.84	1.94	0.00	0.00	5.12	22.95	0.96	0.90	1.03	0.87	0.89	0.89	0.85	0.94	0.90	1.22	1.28	1.31
U4/U6 small nuclear ribonucleoprotein Prp31 OS=Mus musculus GN=Prpf31 PE=2 SV=3	Q8CCF0	0.00	8.00	8.96	25.85	1.03	1.04	1.03	0.95	0.96	0.92	0.00	13.53	13.55	37.88	1.15	1.21	1.45	1.16	0.89	0.97	1.09	1.12	1.22	1.05	0.92	0.95
THO complex subunit 6 homolog OS=Mus musculus GN=Thoc6 PE=2 SV=1	Q5U4D9	0.00	0.00	8.01	27.57	0.97	0.90	1.03	0.91	0.95	0.99	0.00	9.67	9.68	50.15	0.65	0.80	0.70	1.08	1.32	0.93	0.80	0.85	0.85	0.99	1.12	0.96
Interferon regulatory factor 8 OS=Mus musculus GN=Irf8 PE=1 SV=1	P23611	0.00	0.00	8.00	25.00	1.08	1.21	1.00	0.97	1.41	1.20	0.00	11.04	11.07	35.85	0.94	1.24	1.15	1.27	1.51	1.49	1.00	1.22	1.07	1.11	1.46	1.34
Histone deacetylase complex subunit SAP18 OS=Mus musculus GN=Sap18 PE=1 SV=1	O55128	0.00	0.00	8.00	57.52	1.09	0.96	1.12	0.94	1.03	1.02	0.00	0.00	7.72	63.40	0.93	0.95	0.87	1.02	1.03	1.03	1.00	0.96	0.99	0.98	1.03	1.02
Survival of motor neuron-related-splicing factor 30 OS=Mus musculus GN=Smndc1 PE=2 SV=1	Q8BGT7	0.00	8.00	8.00	36.97	0.98	0.94	0.86	0.90	0.90	0.97	0.00	8.00	8.00	44.12	1.67	0.94	1.29	0.47	0.34	0.34	1.28	0.94	1.05	0.65	0.55	0.57
Sorting and assembly machinery component 50 homolog OS=Mus musculus GN=Samm50 PE=1 SV=1	Q8BGH2	0.00	7.99	7.99	40.94	0.90	0.85	0.85	1.28	1.12	0.99	0.00	3.93	3.94	38.59	1.12	1.15	0.90	1.50	1.46	1.22	1.00	0.99	0.87	1.39	1.28	1.10
Transcription elongation factor A protein 1 OS=Mus musculus GN=Tcea1 PE=1 SV=2	P10711	0.00	0.00	8.00	39.20	1.04	0.99	1.02	1.02	1.05	1.03	0.00	12.13	12.13	43.52	0.98	0.94	1.05	1.01	0.92	0.93	1.01	0.96	1.03	1.01	0.98	0.98
Proline-, glutamic acid- and leucine-rich protein 1 OS=Mus musculus GN=Pelp1 PE=1 SV=2	Q9DBD5	0.00	7.94	7.97	20.75	1.07	1.15	1.13	1.16	1.54	1.50	0.00	17.11	17.11	33.21	1.28	1.19	1.09	1.58	2.19	1.15	1.17	1.17	1.11	1.36	1.84	1.31
Peptidylprolyl isomerase domain and WD repeat-containing protein 1 OS=Mus musculus GN=Ppwd1 PE=2 SV=2	Q8CEC6	0.00	7.94	7.94	26.78	1.04	1.08	1.11	1.00	0.95	1.03	0.00	15.99	16.00	34.21	1.01	0.79	0.68	0.95	0.60	0.18	1.02	0.92	0.87	0.98	0.76	0.43
Leucine-rich repeat-containing protein 59 OS=Mus musculus GN=Lrrc59 PE=2 SV=1	Q922Q8	0.00	7.94	7.94	35.50	0.97	0.92	0.89	1.05	1.27	1.08	0.00	12.06	12.07	43.32	0.87	0.96	0.65	0.86	1.36	0.32	0.92	0.94	0.76	0.95	1.31	0.58
SH3 domain-binding protein 1 OS=Mus musculus GN=Sh3bp1 PE=1 SV=2	P55194	0.00	0.00	7.93	28.29	0.93	0.91	0.93	0.98	0.94	0.88	0.00	0.00	7.78	44.26	0.99	0.73	0.77	0.89	0.66	0.70	0.96	0.82	0.85	0.93	0.79	0.78
Periodic tryptophan protein 1 homolog OS=Mus musculus GN=Pwp1 PE=1 SV=1	Q99LL5	0.00	7.88	7.90	31.94	1.41	1.34	1.43	1.67	1.72	1.72	0.00	5.53	5.53	17.56	1.24	1.22	1.29	1.53	1.89	0.90	1.32	1.28	1.36	1.60	1.80	1.24

Protien identification and qunatitation results from ProteinPilot for all the analyzed samples

Name	Accession number	% FDR	Unused	Total	%Cov	114:113	115:113	116:113	118:117	119:117	121:117	% FDR	Unused	Total	%Cov	114:113	115:113	116:113	118:117	119:117	121:117	114:113	115:113	116:113	118:117	119:117	121:117
40S ribosomal protein S6 OS=Mus musculus GN=Rps6 PE=1 SV=1	P62754	0.00	0.00	7.90	42.57	1.07	1.10	1.14	1.29	1.27	1.05	0.00	6.57	6.60	47.79	1.53	1.24	1.47	1.26	0.90	0.36	1.28	1.16	1.29	1.28	1.07	0.61
Serine/threonine-protein kinase VRK2 OS=Mus musculus GN=Vrk2 PE=1 SV=2	Q8BN21	0.00	7.80	7.81	23.26	0.87	0.94	0.86	0.96	0.93	0.94	0.15	2.09	2.09	21.67	1.34	1.28	1.24	0.83	0.81	0.43	1.08	1.10	1.03	0.90	0.87	0.63
Origin recognition complex subunit 2 OS=Mus musculus GN=Orc2 PE=1 SV=1	Q60862	0.00	0.00	7.79	31.60	0.99	0.99	0.91	0.93	0.92	0.86	0.00	9.13	9.19	31.60	1.04	1.03	1.01	0.95	1.00	1.03	1.01	1.01	0.96	0.94	0.96	0.94
Splicing factor U2AF 35 kDa subunit OS=Mus musculus GN=U2af1 PE=1 SV=4	Q9D883	0.00	0.00	7.75	67.36	0.78	0.79	1.06	1.26	1.38	1.32	0.00	0.00	8.00	61.51	0.88	0.95	0.82	1.13	0.58	1.29	0.83	0.87	0.93	1.19	0.90	1.31
Histone H2A OS=Mus musculus GN=Hist1h2al PE=3 SV=1	F8WIX8	0.00	0.00	59.07	89.60	1.14	1.06	1.26	1.01	0.72	0.58	0.00	12.26	60.55	92.00	0.93	0.93	0.82	0.94	0.94	0.74	1.03	0.99	1.01	0.97	0.82	0.65
Histone H2A type 2-A OS=Mus musculus GN=Hist2h2aa1 PE=1 SV=3	Q6GSS7	0.00	0.00	59.07	88.46	1.14	1.06	1.26	1.01	0.72	0.58	0.00	0.00	60.55	88.46	0.93	0.93	0.82	0.94	0.94	0.74	1.03	0.99	1.01	0.97	0.82	0.65
C-terminal-binding protein 1 OS=Mus musculus GN=Ctbp1 PE=1 SV=2	O88712	0.00	7.74	7.74	30.39	0.91	0.96	0.95	1.22	1.24	1.27	0.00	0.00	9.91	30.39	0.83	1.05	0.95	2.11	1.80	1.96	0.87	1.00	0.95	1.61	1.49	1.58
LIM domain and actin-binding protein 1 OS=Mus musculus GN=Lima1 PE=1 SV=3	Q9ERG0	0.00	0.00	7.73	24.04	0.98	0.42	0.63	0.63	0.45	0.47	0.00	10.06	10.08	34.26	1.01	0.33	0.64	0.63	0.52	0.61	1.00	0.37	0.63	0.63	0.48	0.54
Nucleolysin TIAR OS=Mus musculus GN=Tial1 PE=2 SV=1	P70318	0.00	0.00	7.72	34.69	0.97	1.05	1.13	0.99	1.16	1.12	0.00	8.71	8.71	40.56	0.72	0.95	1.19	1.15	0.99	1.56	0.84	1.00	1.16	1.07	1.07	1.32
E3 ubiquitin-protein ligase DTX3L OS=Mus musculus GN=Dtx3l PE=2 SV=1	Q3UIR3	0.00	7.70	7.72	21.26	2.61	2.31	2.40	2.33	1.03	1.50	0.00	4.58	4.59	33.56	1.25	0.82	1.00	1.89	1.10	0.20	1.80	1.37	1.55	2.10	1.06	0.54
Src kinase-associated phosphoprotein 2 OS=Mus musculus GN=Skap2 PE=1 SV=2	Q3UND0	0.00	7.70	7.71	24.02	0.91	0.50	0.47	1.17	1.21	1.06	0.00	12.07	12.10	50.00	1.27	0.74	0.82	1.21	0.97	0.90	1.08	0.61	0.62	1.19	1.09	0.97
Wiskott-Aldrich syndrome protein family member 2 OS=Mus musculus GN=Wasf2 PE=1 SV=1	Q8BH43	0.00	7.70	7.70	27.77	0.93	0.91	0.92	1.13	0.91	0.74	0.00	6.28	6.28	37.63	0.77	0.72	0.94	1.37	1.02	0.94	0.84	0.81	0.93	1.24	0.96	0.83
Nucleoporin Nup37 OS=Mus musculus GN=Nup37 PE=2 SV=2	Q9CWU9	0.00	7.70	7.70	22.70	1.03	0.93	0.90	0.90	0.89	0.73	0.00	8.50	8.50	29.14	1.07	0.91	0.85	0.89	0.75	0.38	1.05	0.92	0.87	0.90	0.82	0.52
Procollagen-lysine,2-oxoglutarate 5-dioxygenase 3 OS=Mus musculus GN=Plod3 PE=1 SV=1	Q9R0E1	0.00	7.68	7.68	24.02	1.19	1.08	1.28	0.88	0.69	0.73	0.00	4.09	4.10	21.46	1.18	1.14	1.19	0.95	0.94	0.90	1.19	1.11	1.24	0.91	0.80	0.81
Cofilin-1 OS=Mus musculus GN=Cfl1 PE=1 SV=3	P18760	0.00	0.00	7.67	50.60	1.11	0.19	0.37	0.36	0.22	0.35	0.00	0.00	4.26	69.88	1.33	0.31	0.59	0.39	0.31	0.22	1.21	0.24	0.47	0.37	0.26	0.28
Leucine-rich repeat and WD repeat-containing protein 1 OS=Mus musculus GN=LRWD1 PE=2 SV=1	Q8BUI3	0.00	7.65	7.67	20.68	1.39	1.26	1.14	1.33	1.37	1.14	0.00	7.98	8.00	40.28	1.12	1.85	1.74	0.92	0.95	1.10	1.25	1.53	1.41	1.11	1.14	1.12
17beta-hydroxysteroid dehydrogenase type 10/short chain L-3-hydroxyacyl-CoA dehydrogenase OS=Mus musculus GN=Hsd17b10 PE=2 SV=1	Q99N15	0.00	7.64	7.65	68.97	1.21	1.09	1.11	0.98	0.87	0.90	0.00	15.70	15.70	58.62	1.42	1.53	0.64	0.79	0.59	0.46	1.31	1.29	0.84	0.88	0.72	0.64
Mesencephalic astrocyte-derived neurotrophic factor OS=Mus musculus GN=Manf PE=1 SV=1	Q9CXI5	0.00	0.00	7.61	58.66	0.91	0.77	1.19	1.43	1.05	0.97	0.00	0.00	10.24	73.74	1.37	0.65	1.54	1.32	0.91	0.87	1.12	0.71	1.36	1.37	0.98	0.92
Microspherule protein 1 OS=Mus musculus GN=Mcrs1 PE=1 SV=1	Q99L90	0.00	7.60	7.61	40.48	0.92	0.95	0.97	0.90	0.91	0.93	0.00	5.48	5.74	36.58	1.03	1.13	1.19	1.37	1.50	1.47	0.97	1.03	1.08	1.11	1.17	1.17
Barrier-to-autointegration factor OS=Mus musculus GN=Banf1 PE=1 SV=1	O54962	0.00	7.58	7.60	69.66	1.75	1.51	1.18	1.34	1.42	1.14	0.00	5.42	5.43	60.67	0.82	1.04	1.67	1.28	0.53	0.60	1.20	1.25	1.41	1.31	0.87	0.82
Zinc finger protein 638 OS=Mus musculus GN=Znf638 PE=1 SV=2	Q61464	0.00	0.00	7.62	17.76	1.05	1.04	1.03	1.07	0.99	1.00	0.00	0.00	11.72	21.63	0.99	1.02	0.99	1.03	0.97	1.01	1.02	1.03	1.01	1.05	0.98	1.00
40S ribosomal protein S25 OS=Mus musculus GN=Rps25 PE=2 SV=1	P62852	0.00	0.00	7.51	42.40	1.17	0.99	1.15	1.24	1.33	1.13	0.00	6.06	6.06	44.00	1.16	0.82	0.47	1.58	1.71	0.96	1.16	0.90	0.73	1.40	1.51	1.04
Uncharacterized protein C17orf85 homolog OS=Mus musculus PE=1 SV=1	Q8BZR9	0.00	7.50	7.50	32.20	1.13	1.20	1.29	0.89	0.67	0.69	0.00	8.13	8.15	36.10	0.95	0.98	1.00	0.87	0.92	0.88	1.03	1.09	1.14	0.88	0.78	0.78
Serine/threonine-protein kinase 10 OS=Mus musculus GN=Stk10 PE=1 SV=2	O55098	0.00	0.00	7.51	23.71	1.05	0.96	0.91	0.93	0.90	0.86	0.00	0.00	3.33	23.81	0.93	1.03	0.95	0.97	1.00	0.87	0.99	1.00	0.93	0.95	0.95	0.86
CCAAT/enhancer-binding protein epsilon OS=Mus musculus GN=Cebpe PE=2 SV=1	Q6PZD9	0.00	0.00	7.48	35.59	1.06	0.99	0.98	1.04	1.01	1.00	0.00	5.49	5.50	27.40	0.95	1.00	1.02	1.02	0.97	0.99	1.00	1.00	1.00	1.03	0.99	1.00
Ubiquitin carboxyl-terminal hydrolase 36 OS=Mus musculus GN=Usp36 PE=2 SV=1	B1AQJ2	0.00	7.45	7.51	26.78	0.96	0.97	0.97	0.99	1.02	1.08	0.00	3.92	3.93	33.70	1.11	0.95	1.50	0.96	1.56	0.41	1.03	0.96	1.21	0.98	1.26	0.66
Digestive organ expansion factor homolog OS=Mus musculus GN=Diexf PE=2 SV=2	Q8BTT6	0.00	7.45	7.46	29.02	0.64	0.79	0.67	0.64	0.90	0.86	0.00	3.93	3.93	27.98	0.64	0.76	0.64	0.82	1.06	1.11	0.64	0.77	0.65	0.73	0.97	0.98
Neuroguidin OS=Mus musculus GN=Ngdn PE=1 SV=1	Q9DB96	0.00	7.41	7.44	33.65	0.92	0.93	0.98	0.95	1.02	1.10	0.00	6.42	6.45	36.51	0.95	0.95	0.89	0.93	0.97	0.94	0.93	0.94	0.93	0.94	1.00	1.01
MHC class II regulatory factor RFX1 OS=Mus musculus GN=Rfx1 PE=2 SV=2	P48377	0.00	0.00	7.41	19.42	0.95	0.96	1.06	0.79	0.88	0.83	0.00	11.52	11.53	26.38	1.26	1.02	0.96	0.64	0.58	0.07	1.09	0.99	1.01	0.71	0.71	0.24
Calmodulin OS=Mus musculus GN=Calm1 PE=1 SV=2	P62204	0.00	0.00	7.41	47.65	1.10	0.30	0.60	0.50	0.29	0.33	0.00	0.00	6.06	40.27	1.28	0.33	0.58	0.47	0.23	0.09	1.19	0.31	0.59	0.48	0.26	0.17
Ribosomal RNA processing protein 1 homolog A OS=Mus musculus GN=Rrp1 PE=2 SV=2	P56183	0.00	7.39	7.39	28.14	1.15	1.01	1.20	0.95	1.04	1.11	0.00	0.00	9.01	42.51	1.18	1.21	1.42	1.14	0.94	1.31	1.16	1.11	1.31	1.04	0.99	1.20
Ezrin OS=Mus musculus GN=Ezr PE=1 SV=3	P26040	0.00	0.00	17.39	34.81	1.04	1.15	1.15	1.05	0.97	0.73	0.00	7.50	22.51	39.08	1.37	1.58	1.84	1.14	0.72	0.42	1.19	1.35	1.45	1.09	0.84	0.56
Protein Scaf11 OS=Mus musculus GN=Scaf11 PE=4 SV=1	E9PZM7	0.00	7.38	7.38	23.70	0.97	0.98	0.96	1.00	1.05	1.12	0.00	0.00	7.89	21.22	0.94	0.90	0.92	0.99	0.98	0.92	0.95	0.94	0.94	1.00	1.01	1.01
Deoxynucleotidyltransferase terminal-interacting protein 1 OS=Mus musculus GN=Dnttip1 PE=2 SV=1	Q99LB0	0.00	0.00	7.37	30.49	1.12	0.87	1.03	0.86	0.89	0.78	0.00	5.22	5.24	42.07	0.80	0.66	1.43	0.67	0.93	0.06	0.95	0.76	1.21	0.76	0.91	0.22
Pre-mRNA-splicing factor CWC22 homolog OS=Mus musculus GN=Cwc22 PE=1 SV=1	Q8C5N3	0.00	0.00	7.39	26.43	1.02	1.09	1.09	1.01	1.12	1.11	0.00	0.00	5.03	32.05	0.94	1.24	0.99	1.09	1.49	1.47	0.98	1.16	1.04	1.05	1.29	1.28
Replication factor C subunit 4 OS=Mus musculus GN=Rfc4 PE=1 SV=1	Q99J62	0.00	0.00	7.35	35.16	1.09	1.05	1.07	0.91	0.83	0.70	0.00	13.69	13.70	48.08	0.92	1.01	0.77	1.16	0.86	0.56	1.00	1.03	0.91	1.03	0.84	0.63
40S ribosomal protein S14 OS=Mus musculus GN=Rps14 PE=2 SV=3	P62264	0.00	0.00	7.32	52.32	1.31	0.93	1.18	1.33	1.75	1.33	0.00	6.30	6.30	50.99	1.53	0.64	0.80	1.01	0.55	1.18	1.41	0.77	0.97	1.16	0.98	1.25

Protien identification and qunatitation results from ProteinPilot for all the analyzed samples

Name	Accession number	% FDR	Unused	Total	%Cov	114:113	115:113	116:113	118:117	119:117	121:117	% FDR	Unused	Total	%Cov	114:113	115:113	116:113	118:117	119:117	121:117	114:113	115:113	116:113	118:117	119:117	121:117
U2 small nuclear ribonucleoprotein B" OS=Mus musculus GN=Snrpb2 PE=2 SV=1	Q9CQI7	0.00	0.00	10.53	51.56	1.17	1.04	1.07	0.99	1.02	0.95	0.00	8.91	10.59	47.56	0.90	1.21	0.90	0.86	0.55	0.69	1.02	1.12	0.98	0.92	0.75	0.81
60S ribosomal protein L11 OS=Mus musculus GN=Rpl11 PE=1 SV=4	Q9CXW4	0.00	0.00	7.30	39.89	1.08	0.91	1.33	1.17	1.42	1.24	0.00	0.00	3.36	50.00	1.47	1.06	1.32	1.60	1.41	1.09	1.26	0.98	1.32	1.37	1.41	1.16
Uncharacterized protein OS=Mus musculus GN=Gm10036 PE=3 SV=1	E9PYL9	0.00	0.00	7.29	37.08	1.08	0.91	1.33	1.17	1.42	1.24	0.00	0.00	3.36	47.19	1.47	1.06	1.32	1.60	1.41	1.09	1.26	0.98	1.32	1.37	1.41	1.16
Actin-related protein 2 OS=Mus musculus GN=Actr2 PE=1 SV=1	P61161	0.00	0.00	7.40	37.82	1.12	0.41	0.55	0.94	0.76	0.80	0.00	6.91	6.97	35.28	1.39	0.24	0.55	0.81	0.43	0.86	1.25	0.31	0.55	0.87	0.57	0.83
Protein KRI1 homolog OS=Mus musculus GN=Kri1 PE=1 SV=2	Q8VDQ9	0.00	0.00	7.13	24.23	1.19	1.43	0.99	1.16	1.20	1.29	0.00	0.00	9.65	28.59	0.97	0.98	0.95	1.02	1.04	1.01	1.08	1.19	0.97	1.09	1.12	1.14
60S ribosomal protein L15 OS=Mus musculus GN=Rpl15 PE=2 SV=4	Q9CZM2	0.00	0.00	7.24	60.78	1.08	1.15	1.26	1.45	1.57	1.36	0.00	0.00	7.01	55.88	1.08	1.09	1.07	1.60	1.41	1.87	1.08	1.12	1.16	1.52	1.49	1.59
Ribosomal protein L15 OS=Mus musculus GN=Gm10020 PE=3 SV=1	E9QAZ2	0.00	0.00	7.24	60.78	1.08	1.15	1.26	1.45	1.57	1.36	0.00	0.00	7.01	53.43	1.08	1.09	1.07	1.60	1.41	1.87	1.08	1.12	1.16	1.52	1.49	1.59
Ribosomal protein L15 OS=Mus musculus GN=Gm8420 PE=3 SV=1	E9Q1X1	0.00	0.00	5.27	46.08	1.08	1.15	1.26	1.45	1.57	1.36	0.00	0.00	5.31	59.31	1.08	1.09	1.07	1.60	1.41	1.87	1.08	1.12	1.16	1.52	1.49	1.59
Pre-mRNA-splicing regulator WTAP OS=Mus musculus GN=Wtap PE=2 SV=3	Q9ER69	0.00	0.00	7.25	27.78	0.97	0.90	0.94	0.94	0.93	0.89	0.00	0.00	10.16	42.93	1.39	1.17	1.26	0.95	0.63	0.58	1.16	1.02	1.09	0.95	0.77	0.71
RNA-binding protein 8A OS=Mus musculus GN=Rbm8a PE=1 SV=3	Q9CWZ3	0.00	7.23	7.23	51.72	0.81	0.80	1.04	0.73	0.86	1.16	0.00	8.30	8.30	51.72	0.95	0.90	0.92	1.04	1.00	1.02	0.88	0.85	0.98	0.87	0.92	1.09
Chromobox protein homolog 1 OS=Mus musculus GN=Cbx1 PE=1 SV=1	P83917	0.00	7.22	10.82	40.54	0.82	0.98	1.07	1.01	0.74	0.65	0.00	4.65	6.99	45.41	0.79	0.99	0.84	1.00	0.45	0.34	0.81	0.99	0.95	1.00	0.58	0.47
Monocyte differentiation antigen CD14 OS=Mus musculus GN=Cd14 PE=1 SV=1	P10810	0.00	0.00	7.23	25.14	0.81	0.28	0.47	0.19	0.16	0.12	0.00	9.40	9.41	37.98	0.95	0.35	0.56	0.53	0.30	0.12	0.87	0.31	0.52	0.32	0.22	0.12
40S ribosomal protein S7 OS=Mus musculus GN=Rps7 PE=2 SV=1	P62082	0.00	0.00	7.22	44.33	1.07	0.99	1.11	1.04	1.24	1.17	0.00	7.71	7.71	54.12	0.95	0.93	0.72	1.22	1.39	0.77	1.01	0.96	0.90	1.13	1.31	0.95
Protein Gm9493 OS=Mus musculus GN=Gm9493 PE=4 SV=1	F6SVV1	0.00	0.00	7.08	48.44	1.07	0.99	1.11	1.04	1.24	1.17	0.00	0.00	7.63	53.13	0.95	0.93	0.72	1.22	1.39	0.77	1.01	0.96	0.90	1.13	1.31	0.95
Nucleoporin NUP53 OS=Mus musculus GN=Nup35 PE=1 SV=2	Q8R4R6	0.00	7.21	7.22	36.62	0.74	0.83	0.91	1.07	1.04	1.61	0.00	6.05	6.05	35.38	0.69	0.88	0.85	0.85	0.79	1.37	0.71	0.86	0.88	0.95	0.91	1.49
U3 small nucleolar ribonucleoprotein protein MPP10 OS=Mus musculus GN=Mphosph10 PE=1 SV=2	Q810V0	0.00	7.19	7.22	25.11	0.91	0.95	0.97	0.98	1.06	1.06	0.00	9.44	9.45	22.03	0.83	0.67	0.74	0.94	0.95	0.12	0.87	0.80	0.85	0.96	1.00	0.35
Transcriptional repressor CTCF OS=Mus musculus GN=Ctcf PE=1 SV=2	Q61164	0.00	7.18	7.21	28.53	1.03	1.42	1.10	1.04	1.12	0.84	0.00	11.92	11.93	25.14	0.90	1.12	0.73	0.98	0.86	0.37	0.96	1.26	0.90	1.01	0.98	0.55
Integrator complex subunit 4 OS=Mus musculus GN=Ints4 PE=2 SV=1	Q8CIM8	0.00	7.18	7.20	24.79	0.96	0.91	0.99	0.95	0.89	0.93	0.00	9.32	9.34	31.64	0.90	0.96	0.90	0.89	0.99	0.74	0.93	0.94	0.94	0.92	0.94	0.83
Calcium-binding mitochondrial carrier protein Aralar1 OS=Mus musculus GN=Slc25a12 PE=1 SV=1	Q8BH59	0.00	7.17	7.20	22.60	1.22	1.27	1.26	1.01	1.12	1.06	0.00	0.01	4.10	35.60	1.05	1.11	1.12	0.99	0.90	1.10	1.13	1.19	1.19	1.00	1.00	1.08
Acetyl-CoA acetyltransferase, mitochondrial OS=Mus musculus GN=Acat1 PE=1 SV=1	Q8QZT1	0.00	0.00	7.17	27.59	1.04	0.97	0.98	1.04	0.74	0.87	0.00	8.40	8.41	50.00	1.14	0.79	1.02	1.00	0.58	0.51	1.09	0.87	1.00	1.02	0.65	0.67
p21-activated protein kinase-interacting protein 1 OS=Mus musculus GN=Pak1ip1 PE=2 SV=2	Q9DCE5	0.00	0.00	7.15	31.68	0.91	1.10	0.97	0.88	1.13	1.12	0.00	5.74	5.74	40.05	1.01	1.10	1.03	1.01	1.07	1.05	0.96	1.10	1.00	0.94	1.10	1.08
Zinc finger CCCH domain-containing protein 14 OS=Mus musculus GN=Zc3h14 PE=1 SV=1	Q8BJ05	0.00	7.14	7.15	20.00	0.93	0.89	0.91	0.97	0.86	0.93	0.00	6.02	6.04	27.89	0.96	0.95	0.97	1.05	0.76	0.91	0.95	0.92	0.94	1.01	0.81	0.92
Anaphase-promoting complex subunit 5 OS=Mus musculus GN=Anapc5 PE=2 SV=1	Q8BTZ4	0.00	0.00	7.18	23.11	0.94	1.05	0.98	0.95	0.97	1.07	0.00	0.00	3.09	25.41	0.79	0.95	0.99	1.05	1.00	0.92	0.86	1.00	0.99	1.00	0.99	0.99
Actin-related protein 3 OS=Mus musculus GN=Actr3 PE=1 SV=3	Q99JY9	0.00	0.00	7.16	32.06	1.31	0.28	0.39	0.97	0.44	0.77	0.00	5.89	5.90	41.63	1.29	0.25	0.35	0.95	0.47	0.05	1.30	0.27	0.37	0.96	0.45	0.19
UPF0609 protein C4orf27 homolog OS=Mus musculus PE=2 SV=1	Q8CFE2	0.00	7.13	7.16	24.86	1.13	1.03	1.13	1.02	1.01	0.91	0.00	8.07	8.10	37.57	1.03	1.07	1.14	1.15	1.01	0.79	1.08	1.05	1.13	1.08	1.01	0.85
CTD small phosphatase-like protein 2 OS=Mus musculus GN=Ctdspl2 PE=1 SV=1	Q8BG15	0.00	7.13	7.13	28.39	1.06	1.04	1.05	0.96	0.92	0.94	0.00	13.22	13.22	40.43	1.25	1.10	1.08	1.03	0.89	0.95	1.15	1.07	1.06	1.00	0.90	0.95
Polypyrimidine tract-binding protein 3 OS=Mus musculus GN=Ptbp3 PE=2 SV=1	Q8BHD7	0.00	0.00	12.28	38.43	1.16	1.18	1.00	0.97	0.98	0.79	0.00	0.00	18.29	57.93	1.09	1.03	1.09	0.73	0.47	0.18	1.12	1.10	1.04	0.84	0.68	0.38
High mobility group protein 20A OS=Mus musculus GN=Hmg20a PE=2 SV=1	Q9DC33	0.00	7.10	7.10	22.83	0.96	1.10	1.07	0.96	1.08	1.12	0.00	0.00	3.05	13.87	0.93	1.00	0.95	1.03	1.17	1.18	0.95	1.05	1.00	1.00	1.12	1.15
Histone deacetylase 2 OS=Mus musculus GN=Hdac2 PE=1 SV=1	P70288	0.00	7.04	13.32	37.09	0.95	1.05	0.99	1.04	0.98	0.95	0.00	9.52	14.88	42.01	0.96	0.91	0.81	0.98	0.63	0.68	0.95	0.98	0.90	1.01	0.78	0.81
Mediator of DNA damage checkpoint protein 1 OS=Mus musculus GN=Mdc1 PE=1 SV=1	Q5PSV9	0.00	0.00	7.03	23.61	0.96	1.00	1.00	1.10	1.05	1.08	0.00	0.00	18.43	30.17	1.01	1.15	1.06	0.95	0.97	0.89	0.99	1.07	1.03	1.02	1.01	0.98
DnaJ homolog subfamily C member 8 OS=Mus musculus GN=Dnajc8 PE=2 SV=2	Q6NZB0	0.00	0.00	7.01	39.13	1.00	0.93	0.97	1.03	0.97	0.93	0.00	0.00	2.66	25.69	1.10	0.99	1.14	1.00	0.92	0.95	1.05	0.96	1.05	1.01	0.95	0.94
Paraspeckle component 1 OS=Mus musculus GN=Pspc1 PE=1 SV=1	Q8R326	0.00	6.99	8.54	40.92	0.95	0.97	0.99	0.99	1.01	1.02	0.00	14.09	15.49	47.42	1.17	1.19	1.11	0.67	0.89	1.11	1.06	1.08	1.05	0.82	0.95	1.06
Poly(A)-specific ribonuclease PARN OS=Mus musculus GN=Parn PE=1 SV=1	Q8VDG3	0.00	0.00	6.85	18.27	0.94	0.92	0.95	0.99	0.94	0.97	0.00	6.29	6.31	23.72	0.85	0.77	0.91	0.95	0.87	0.82	0.89	0.84	0.93	0.97	0.90	0.90
Transcription termination factor 2 OS=Mus musculus GN=Ttf2 PE=1 SV=2	Q5NC05	0.00	6.96	7.07	23.11	1.11	1.20	1.10	1.08	1.12	1.14	0.00	8.08	8.14	24.43	1.03	1.09	1.18	1.19	1.17	1.19	1.07	1.14	1.14	1.13	1.14	1.16
Nucleolar complex protein 4 homolog OS=Mus musculus GN=Noc4l PE=2 SV=1	Q8BHY2	0.00	0.00	6.99	25.19	0.99	0.98	0.96	0.95	1.05	1.08	0.00	8.16	8.17	32.95	1.00	0.97	1.06	0.95	1.14	1.22	1.00	0.98	1.01	0.95	1.09	1.15
Putative uncharacterized protein OS=Mus musculus GN=Rpl14 PE=2 SV=1	Q9CWK0	0.00	0.00	6.93	57.27	1.58	1.49	1.64	1.80	1.85	1.82	0.00	8.05	8.06	48.02	1.67	1.72	1.28	2.27	2.49	1.82	1.63	1.60	1.45	2.02	2.15	1.82

Protien identification and qunatitation results from ProteinPilot for all the analyzed samples

Name	Accession number	% FDR	Unused	Total	%Cov	114:113	115:113	116:113	118:117	119:117	121:117	% FDR	Unused	Total	%Cov	114:113	115:113	116:113	118:117	119:117	121:117	114:113	115:113	116:113	118:117	119:117	121:117
60S ribosomal protein L14 OS=Mus musculus GN=Rpl14 PE=2 SV=3	Q9CR57	0.00	6.94	6.95	49.77	1.58	1.49	1.64	1.80	1.85	1.82	0.00	0.00	8.06	46.08	1.67	1.72	1.28	2.27	2.49	1.82	1.63	1.60	1.45	2.02	2.15	1.82
Plastin-2 OS=Mus musculus GN=Lcp1 PE=1 SV=4	Q61233	0.00	0.00	6.95	29.51	1.17	0.38	0.67	0.60	0.62	0.85	0.00	2.43	2.49	34.93	1.41	0.95	1.28	1.03	1.11	0.66	1.28	0.60	0.93	0.79	0.83	0.75
40S ribosomal protein S17 OS=Mus musculus GN=Rps17 PE=1 SV=2	P63276	0.00	0.00	6.93	74.07	0.99	0.95	1.00	1.05	1.13	1.07	0.00	0.00	4.29	36.30	1.07	1.04	1.03	1.05	0.80	0.92	1.03	1.00	1.01	1.05	0.95	0.99
PHD finger protein 3 OS=Mus musculus GN=Phf3 PE=2 SV=1	B2RQG2	0.00	6.91	6.95	22.67	1.09	0.94	0.86	0.98	0.72	0.70	0.00	4.91	4.91	23.85	0.95	1.04	1.10	0.98	1.01	0.99	1.01	0.99	0.97	0.98	0.86	0.84
Eukaryotic translation initiation factor 2 subunit 3, Y-linked OS=Mus musculus GN=Eif2s3y PE=2 SV=2	Q9Z0N2	0.00	6.90	6.92	38.35	1.02	1.07	0.72	0.84	0.77	0.70	0.00	12.32	12.35	41.53	0.91	0.98	0.95	1.12	0.73	1.01	0.96	1.02	0.82	0.97	0.75	0.84
Cyclin-dependent kinase 1 OS=Mus musculus GN=Cdk1 PE=1 SV=3	P11440	0.00	6.87	8.88	33.00	1.11	1.16	1.26	1.25	1.53	1.25	0.00	7.11	9.12	42.42	0.95	1.11	0.96	1.08	1.25	1.28	1.02	1.13	1.10	1.16	1.38	1.26
Nibrin OS=Mus musculus GN=Nbn PE=1 SV=1	Q9R207	0.00	6.86	6.92	20.64	0.99	0.91	1.11	0.75	0.82	0.82	0.00	6.72	6.90	22.37	0.86	1.03	0.99	0.97	1.04	0.96	0.92	0.97	1.05	0.86	0.92	0.89
Cell division cycle protein 27 homolog OS=Mus musculus GN=Cdc27 PE=1 SV=1	A2A6Q5	0.00	6.81	7.12	28.48	1.07	1.04	1.07	1.10	1.05	1.12	0.00	16.70	16.74	31.03	1.69	1.49	1.89	0.81	0.65	0.33	1.34	1.24	1.42	0.94	0.82	0.61
Ras GTPase-activating-like protein IQGAP1 OS=Mus musculus GN=Iqgap1 PE=1 SV=2	Q9JKF1	0.00	0.00	6.85	23.42	1.15	0.69	0.74	1.41	1.58	1.64	0.00	0.00	4.99	32.05	1.36	0.82	0.96	0.83	0.90	0.92	1.25	0.75	0.85	1.08	1.20	1.23
Protein asunder homolog OS=Mus musculus GN=Asun PE=2 SV=2	Q8QZV7	0.00	6.81	6.81	25.68	1.04	1.03	0.96	1.08	0.97	0.98	0.00	4.56	4.56	22.81	1.04	0.96	1.02	1.05	0.97	0.95	1.04	1.00	0.99	1.06	0.97	0.96
Casein kinase II subunit alpha OS=Mus musculus GN=Csnk2a1 PE=1 SV=2	Q60737	0.00	0.00	7.21	36.57	0.97	0.89	0.98	1.13	0.98	0.93	0.00	6.58	6.74	29.67	0.79	0.89	1.25	1.96	1.33	0.40	0.88	0.89	1.11	1.49	1.14	0.61
tRNA-splicing ligase RtcB homolog OS=Mus musculus GN=D10Wsu52e PE=2 SV=1	Q99LF4	0.00	0.00	6.74	20.00	0.96	0.93	0.97	0.99	1.01	0.89	0.00	10.24	10.24	34.46	1.45	1.14	1.29	1.08	0.44	0.52	1.18	1.03	1.12	1.03	0.67	0.68
Nucleoporin 98 OS=Mus musculus GN=Nup98 PE=1 SV=1	Q6PFD9	0.00	6.72	19.69	23.08	0.93	0.93	1.04	0.98	1.00	1.16	0.00	6.21	19.24	31.09	1.00	0.90	0.96	0.93	0.95	0.92	0.96	0.92	1.00	0.95	0.98	1.03
Chromatin assembly factor 1 subunit A OS=Mus musculus GN=Chaf1a PE=1 SV=1	Q9QWF0	0.00	6.72	6.75	19.32	1.18	1.24	1.15	0.86	0.90	0.52	0.00	6.60	6.64	18.77	0.95	1.25	0.98	0.79	0.59	0.15	1.06	1.24	1.06	0.83	0.73	0.28
Ribosome biogenesis protein NSA2 homolog OS=Mus musculus GN=Nsa2 PE=2 SV=1	Q9CR47	0.00	6.72	6.72	45.38	1.56	1.41	1.43	1.36	1.74	1.61	0.00	6.66	6.66	45.00	1.39	1.45	1.15	1.54	1.75	1.66	1.47	1.43	1.28	1.45	1.75	1.64
Mitochondrial 2-oxoglutarate/malate carrier protein OS=Mus musculus GN=Slc25a11 PE=1 SV=3	Q9CR62	0.00	0.00	6.72	33.12	1.50	1.79	1.60	1.09	0.89	1.26	0.00	3.15	3.16	35.99	1.13	1.08	1.16	0.95	0.97	0.87	1.30	1.39	1.36	1.01	0.93	1.05
Poly [ADP-ribose] polymerase 14 OS=Mus musculus GN=Parp14 PE=1 SV=3	Q2EMV9	0.00	0.00	6.73	27.19	1.17	1.21	0.95	2.13	1.05	1.89	0.00	12.39	12.42	27.30	1.56	1.51	1.42	3.44	1.56	1.72	1.35	1.36	1.16	2.70	1.28	1.80
Guanine nucleotide-binding protein G(I)/G(S)/G(T) subunit beta-2 OS=Mus musculus GN=Gnb2 PE=1 SV=3	P62880	0.00	0.00	6.72	31.76	0.81	0.28	0.56	0.49	0.47	0.46	0.00	0.00	5.29	35.00	1.29	0.69	0.95	0.82	1.07	0.88	1.02	0.44	0.73	0.63	0.70	0.64
Aladin OS=Mus musculus GN=Aaas PE=1 SV=1	P58742	0.00	6.67	6.67	28.75	0.93	0.86	0.85	0.90	0.95	1.07	0.00	12.75	12.76	35.71	0.53	1.02	0.67	1.91	1.98	0.88	0.70	0.93	0.76	1.31	1.37	0.97
60S ribosomal protein L21 OS=Mus musculus GN=Rpl21 PE=2 SV=3	O09167	0.00	0.00	6.67	36.88	1.37	1.07	1.25	1.19	1.12	1.09	0.00	0.00	8.48	60.62	1.43	1.13	1.11	1.26	1.13	1.19	1.40	1.10	1.17	1.22	1.12	1.14
Histone acetyltransferase KAT7 OS=Mus musculus GN=Kat7 PE=2 SV=1	Q5SVQ0	0.00	0.00	6.66	33.28	0.94	0.95	0.97	0.99	0.95	0.93	0.00	0.00	5.43	33.93	0.97	0.97	0.89	0.94	1.16	0.95	0.95	0.96	0.93	0.96	1.05	0.94
Muscleblind-like protein 1 OS=Mus musculus GN=Mbnl1 PE=1 SV=1	Q9JKP5	0.00	0.00	6.64	29.62	0.84	1.17	1.12	0.82	0.94	0.86	0.00	0.00	6.64	30.21	0.94	0.95	0.88	0.77	0.89	0.82	0.89	1.05	0.99	0.79	0.91	0.84
Zinc finger protein 22 OS=Mus musculus GN=Znf22 PE=1 SV=2	Q9ERU3	0.00	0.00	6.64	25.74	1.02	0.88	0.97	0.89	0.88	0.76	0.00	2.41	2.41	35.02	0.93	0.90	0.93	0.95	0.88	0.72	0.97	0.89	0.95	0.92	0.88	0.74
Kinesin-like protein KIF2C OS=Mus musculus GN=Kif2c PE=1 SV=1	Q922S8	0.00	0.00	6.75	27.32	0.98	1.09	0.74	1.45	1.04	1.25	0.00	4.16	4.19	28.43	0.97	1.03	1.10	1.19	1.06	0.91	0.98	1.06	0.90	1.31	1.05	1.07
Lysine-specific demethylase 2A OS=Mus musculus GN=Kdm2a PE=1 SV=2	P59997	0.00	6.63	6.71	22.65	0.96	1.01	0.97	1.15	1.22	1.05	0.00	0.00	7.80	25.06	0.99	0.92	1.37	1.16	1.17	0.97	0.98	0.96	1.15	1.15	1.20	1.01
Sentrin-specific protease 1 OS=Mus musculus GN=Senp1 PE=2 SV=1	P59110	0.00	6.60	6.61	21.25	1.01	0.99	1.06	1.04	0.96	1.00	0.00	4.10	4.21	28.91	1.13	1.22	1.24	1.07	0.88	0.96	1.07	1.10	1.14	1.05	0.92	0.98
U3 small nucleolar ribonucleoprotein protein IMP3 OS=Mus musculus GN=Imp3 PE=2 SV=1	Q921Y2	0.00	6.59	6.61	49.46	0.99	0.74	1.13	0.85	1.32	1.16	0.00	9.95	9.99	60.33	1.05	0.68	0.79	1.08	0.89	1.11	1.02	0.71	0.94	0.95	1.08	1.13
Ubiquitin carboxyl-terminal hydrolase isozyme L5 OS=Mus musculus GN=Uchl5 PE=2 SV=2	Q9WUP7	0.00	6.59	6.61	29.79	1.04	0.52	1.43	1.19	1.47	0.93	0.00	4.06	4.07	26.75	0.97	1.06	1.19	1.25	0.98	1.17	1.00	0.74	1.31	1.22	1.20	1.04
Elongation factor 1-beta OS=Mus musculus GN=Eef1b PE=1 SV=5	O70251	0.00	6.57	6.57	28.44	1.21	1.12	1.15	1.75	1.49	1.09	0.00	3.85	3.85	30.22	1.15	1.47	1.27	1.60	1.18	0.88	1.18	1.28	1.21	1.67	1.32	0.98
Protein Taf4a OS=Mus musculus GN=Taf4a PE=4 SV=1	E9QAP7	0.00	6.54	6.56	34.07	0.94	0.97	0.98	0.98	1.01	1.00	0.00	9.79	9.80	37.43	1.07	0.95	1.09	0.97	0.92	0.93	1.00	0.96	1.03	0.98	0.96	0.96
G2/mitotic-specific cyclin-B1 OS=Mus musculus GN=Ccnb1 PE=2 SV=3	P24860	0.00	0.00	6.54	20.70	1.07	1.63	1.45	1.60	2.03	1.75	0.00	0.00	4.53	29.77	0.97	1.07	0.96	1.19	1.32	1.32	1.02	1.32	1.18	1.38	1.64	1.52
N-alpha-acetyltransferase 25, NatB auxiliary subunit OS=Mus musculus GN=Naa25 PE=1 SV=1	Q8BWZ3	0.00	0.00	6.71	22.12	0.79	0.90	0.74	0.95	0.95	1.03	0.32	1.79	1.85	25.21	1.09	1.10	1.29	1.09	0.95	1.21	0.93	1.00	0.98	1.01	0.95	1.12
40S ribosomal protein S15a OS=Mus musculus GN=Rps15a PE=2 SV=2	P62245	0.00	0.00	6.53	57.69	1.11	1.05	1.17	1.14	1.20	1.18	0.00	9.59	9.59	80.00	0.94	0.95	0.99	1.09	1.10	0.99	1.02	1.00	1.08	1.11	1.15	1.08
General transcription factor 3C polypeptide 5 OS=Mus musculus GN=Gtf3c5 PE=2 SV=2	Q8R2T8	0.00	0.00	6.52	22.88	0.72	0.99	0.76	0.76	0.96	0.95	0.00	4.56	4.58	27.12	0.96	1.02	0.94	0.98	0.98	1.00	0.83	1.00	0.84	0.86	0.97	0.97
Uncharacterized protein C9orf114 homolog OS=Mus musculus GN=D2Wsu81e PE=2 SV=1	Q3UHX9	0.00	0.00	6.49	39.74	0.89	0.99	1.11	0.86	1.05	1.13	0.00	4.34	4.34	30.39	0.82	1.05	0.86	1.22	1.28	1.31	0.86	1.02	0.98	1.02	1.16	1.21
DNA-binding protein Ikaros OS=Mus musculus GN=Ikzf1 PE=1 SV=2	Q03267	0.00	0.00	6.56	23.60	0.77	0.65	0.68	1.11	0.90	1.26	0.00	0.00	10.95	25.73	1.16	0.88	1.37	1.72	1.64	1.27	0.95	0.76	0.96	1.38	1.22	1.26
Small nuclear ribonucleoprotein-associated protein B OS=Mus musculus GN=Snrpb PE=1 SV=1	P27048	0.00	6.44	6.44	50.65	0.90	1.27	1.36	1.85	1.49	1.98	0.00	9.16	9.18	41.56	0.87	1.18	0.93	0.95	1.03	0.13	0.89	1.22	1.12	1.33	1.24	0.50

Protien identification and qunatitation results from ProteinPilot for all the analyzed samples

Name	Accession number	% FDR	Unused	Total	%Cov	114:113	115:113	116:113	118:117	119:117	121:117	% FDR	Unused	Total	%Cov	114:113	115:113	116:113	118:117	119:117	121:117	114:113	115:113	116:113	118:117	119:117	121:117
Small nuclear ribonucleoprotein-associated protein N OS=Mus musculus GN=Snrpn PE=2 SV=1	P63163	0.00	0.00	6.38	43.75	0.90	1.27	1.36	1.85	1.49	1.98	0.00	0.00	8.62	72.08	0.87	1.18	0.93	0.95	1.03	0.13	0.89	1.22	1.12	1.33	1.24	0.50
DBIRD complex subunit ZNF326 OS=Mus musculus GN=Znf326 PE=1 SV=1	O88291	0.00	6.43	6.49	23.45	1.09	1.03	0.97	0.97	0.90	0.92	0.00	9.97	10.01	32.41	0.81	0.47	0.96	0.92	1.26	1.53	0.94	0.70	0.97	0.95	1.06	1.19
Eukaryotic translation initiation factor 5B OS=Mus musculus GN=Eif5b PE=1 SV=2	Q05D44	0.00	6.42	6.61	19.41	1.12	1.15	1.06	0.85	0.90	0.74	0.15	2.09	2.14	26.15	1.01	0.88	1.09	1.05	1.24	1.45	1.06	1.00	1.07	0.94	1.06	1.04
Voltage-gated potassium channel subunit beta-2 OS=Mus musculus GN=Kcnab2 PE=1 SV=1	P62482	0.00	0.00	6.45	33.24	0.92	1.01	1.07	1.18	1.08	1.10	0.00	4.17	4.17	21.80	0.88	0.95	0.99	1.19	1.06	1.00	0.90	0.98	1.03	1.19	1.07	1.05
WW domain-binding protein 11 OS=Mus musculus GN=Wbp11 PE=1 SV=2	Q923D5	0.00	0.00	6.42	23.71	0.94	0.71	0.82	0.64	0.84	1.10	0.00	4.08	4.10	29.49	0.82	0.95	0.80	0.79	0.97	0.63	0.87	0.82	0.81	0.71	0.90	0.83
E3 ubiquitin-protein ligase RNF213 OS=Mus musculus GN=Rnf213 PE=2 SV=1	E9Q555	0.00	6.41	6.53	16.95	1.37	1.36	0.95	1.56	1.10	1.38	0.00	2.61	2.75	19.55	1.10	1.10	1.31	1.72	1.56	1.69	1.22	1.22	1.11	1.64	1.31	1.53
Transformer-2 protein homolog alpha OS=Mus musculus GN=Tra2a PE=1 SV=1	Q6PFR5	0.00	0.00	7.70	43.77	0.84	0.82	1.08	1.29	1.47	1.79	0.00	0.00	6.57	59.79	0.67	0.81	0.81	1.29	1.50	1.56	0.75	0.81	0.93	1.29	1.49	1.67
Protein kinase C and casein kinase substrate in neurons protein 2 OS=Mus musculus GN=Pacsin2 PE=1 SV=1	Q9WVE8	0.00	0.00	6.36	25.31	1.10	1.31	1.32	1.13	1.16	0.90	0.00	3.05	3.05	17.28	0.99	1.15	1.00	1.22	1.01	1.11	1.04	1.22	1.15	1.17	1.08	1.00
Macrophage-expressed gene 1 protein OS=Mus musculus GN=Mpeg1 PE=2 SV=1	A1L314	0.00	0.00	6.33	13.60	0.99	0.60	0.81	1.64	1.39	1.38	0.00	0.00	11.68	27.21	0.94	0.76	0.79	1.17	1.10	0.72	0.96	0.68	0.80	1.39	1.24	1.00
Protein BUD31 homolog OS=Mus musculus GN=Bud31 PE=4 SV=1	E0CX20	0.00	6.31	6.31	40.97	0.82	0.83	0.91	0.88	1.14	1.32	0.00	2.72	2.72	38.89	1.00	1.01	1.13	0.96	0.90	0.97	0.91	0.92	1.01	0.92	1.01	1.13
Nucleoporin Nup43 OS=Mus musculus GN=Nup43 PE=2 SV=2	P59235	0.00	6.29	6.31	30.00	0.94	0.92	0.90	0.82	0.90	0.89	0.00	8.25	8.26	27.11	0.92	1.05	1.00	1.09	1.21	1.11	0.93	0.98	0.95	0.94	1.04	0.99
40S ribosomal protein S23 OS=Mus musculus GN=Rps23 PE=2 SV=3	P62267	0.00	0.00	6.31	39.16	0.96	0.92	1.12	1.14	1.28	1.46	0.00	8.21	8.22	50.35	1.02	0.88	0.86	1.10	1.10	1.05	0.99	0.90	0.98	1.12	1.19	1.24
H/ACA ribonucleoprotein complex subunit 2 OS=Mus musculus GN=Nhp2 PE=2 SV=1	Q9CRB2	0.00	6.29	6.29	43.79	0.96	0.87	1.05	0.91	0.96	0.99	0.00	4.00	4.00	28.76	0.52	0.83	0.69	1.00	1.63	1.31	0.70	0.85	0.85	0.95	1.25	1.14
RNA-binding protein 26 OS=Mus musculus GN=Rbm26 PE=1 SV=2	Q6NZN0	0.00	0.00	6.29	23.91	0.94	0.96	1.00	0.95	1.00	1.09	0.00	6.50	6.53	26.88	0.80	0.98	1.09	0.94	1.06	0.91	0.87	0.97	1.04	0.95	1.03	1.00
Menin OS=Mus musculus GN=Men1 PE=1 SV=2	O88559	0.00	0.00	6.28	25.70	1.07	1.01	1.08	1.00	1.07	1.04	0.00	0.00	6.43	34.21	1.10	1.13	1.57	1.15	1.17	1.37	1.08	1.07	1.30	1.07	1.12	1.19
CpG-binding protein OS=Mus musculus GN=Cxxc1 PE=2 SV=1	Q9CWW7	0.00	0.00	6.28	28.03	1.15	0.96	0.96	0.83	0.77	0.77	0.00	3.20	3.21	21.06	1.03	0.84	1.12	0.95	0.81	0.78	1.09	0.90	1.04	0.89	0.79	0.77
Poly(rC)-binding protein 1 OS=Mus musculus GN=Pcbp1 PE=1 SV=1	P60335	0.00	6.23	12.50	47.75	1.01	1.08	0.89	1.01	1.02	1.05	0.00	11.45	18.80	67.70	0.81	1.10	0.79	1.14	1.27	0.88	0.90	1.09	0.84	1.07	1.14	0.96
Chromobox protein homolog 8 OS=Mus musculus GN=Cbx8 PE=1 SV=1	Q9QXV1	0.00	6.23	6.25	46.69	0.56	0.90	1.02	0.86	1.05	0.38	0.00	5.37	5.38	35.64	0.91	1.05	1.06	0.90	0.92	0.81	0.72	0.97	1.04	0.88	0.98	0.55
Actin-related protein 2/3 complex subunit 4 OS=Mus musculus GN=Arpc4 PE=1 SV=3	P59999	0.00	0.00	6.23	42.86	1.13	0.22	0.46	0.83	0.51	0.48	0.00	8.02	8.02	47.02	1.09	0.17	0.37	1.09	0.67	0.40	1.11	0.19	0.41	0.95	0.58	0.44
Bromodomain-containing protein 7 OS=Mus musculus GN=Brd7 PE=1 SV=1	O88665	0.00	6.19	6.19	25.04	0.98	1.00	1.01	0.92	0.94	0.90	0.00	5.83	5.83	37.02	0.97	1.01	1.05	1.01	1.09	1.11	0.98	1.00	1.03	0.96	1.01	1.00
Probable ATP-dependent RNA helicase DHX36 OS=Mus musculus GN=Dhx36 PE=2 SV=2	Q8VHK9	0.00	0.00	6.50	27.27	1.01	0.82	1.18	0.71	1.06	0.67	0.00	0.00	4.08	29.37	0.90	1.21	0.95	0.96	0.93	0.80	0.95	1.00	1.06	0.83	0.99	0.73
Interferon-activable protein 203 OS=Mus musculus GN=Ifi203 PE=1 SV=1	O35368	0.00	0.00	14.23	44.61	0.77	0.95	0.74	1.66	0.60	1.63	0.00	0.00	21.31	56.86	0.94	1.01	0.83	1.28	0.31	0.70	0.85	0.98	0.79	1.46	0.43	1.07
NCK associated protein 1 like OS=Mus musculus GN=Nckap1l PE=2 SV=1	Q8K1X4	0.00	6.15	6.26	21.78	1.12	1.08	0.89	1.18	1.06	0.79	0.00	9.26	9.33	32.80	0.86	0.81	1.05	0.93	0.80	0.12	0.98	0.93	0.96	1.05	0.92	0.31
Dedicator of cytokinesis protein 11 OS=Mus musculus GN=Dock11 PE=1 SV=1	A2AF47	0.00	6.13	8.39	17.17	1.01	0.93	0.99	0.91	0.97	0.94	0.00	4.63	4.78	24.65	0.98	0.96	1.03	0.94	1.00	0.95	1.00	0.95	1.01	0.92	0.99	0.95
60S ribosomal protein L23 OS=Mus musculus GN=Rpl23 PE=1 SV=1	P62830	0.00	6.12	6.12	44.29	1.02	0.95	1.09	1.17	1.47	1.25	0.00	6.34	6.34	47.86	1.21	0.96	0.82	1.20	1.36	1.36	1.11	0.96	0.95	1.19	1.41	1.30
Pre-mRNA-splicing factor 38B OS=Mus musculus GN=Prpf38b PE=1 SV=1	Q80SY5	0.00	6.11	6.14	39.85	0.93	1.08	0.95	0.94	1.15	1.03	0.00	4.68	4.70	35.06	1.03	0.98	0.98	0.96	0.81	1.18	0.98	1.03	0.97	0.95	0.96	1.10
Integrator complex subunit 5 OS=Mus musculus GN=Ints5 PE=2 SV=1	Q8CHT3	0.00	6.10	6.15	22.69	0.92	0.91	0.83	0.89	0.77	0.80	0.00	7.68	7.73	22.10	0.98	0.90	0.84	0.77	0.97	1.04	0.95	0.90	0.84	0.83	0.87	0.91
Exosome complex component RRP45 OS=Mus musculus GN=Exosc9 PE=2 SV=1	Q9JHI7	0.00	6.09	6.11	26.94	1.14	1.15	1.18	1.10	1.12	1.13	0.00	5.10	5.12	31.74	1.45	1.41	2.01	1.74	1.53	1.75	1.28	1.27	1.54	1.38	1.31	1.41
60 kDa heat shock protein, mitochondrial OS=Mus musculus GN=Hspd1 PE=1 SV=1	P63038	0.00	6.07	6.09	29.14	0.49	0.48	0.49	0.51	0.35	0.50	0.00	8.42	8.43	32.11	0.77	0.64	0.64	0.61	0.61	0.67	0.61	0.55	0.56	0.56	0.46	0.58
S-phase kinase-associated protein 1 OS=Mus musculus GN=Skp1 PE=1 SV=3	Q9WTX5	0.00	0.00	6.08	33.13	1.09	0.95	1.01	1.00	1.18	1.04	0.00	6.15	6.16	40.49	1.08	0.74	1.84	0.68	0.82	0.20	1.08	0.84	1.36	0.82	0.99	0.46
Small nuclear ribonucleoprotein Sm D3 OS=Mus musculus GN=Snrpd3 PE=1 SV=1	P62320	0.00	0.00	6.07	69.84	1.01	0.97	1.00	1.02	1.25	1.10	0.00	8.01	8.02	83.33	0.65	0.67	0.61	1.09	1.72	1.53	0.81	0.81	0.78	1.05	1.47	1.29
N-myc-interactor OS=Mus musculus GN=Nmi PE=2 SV=1	O35309	0.00	0.00	6.06	32.80	0.79	0.84	1.38	6.79	2.54	5.11	0.00	4.03	4.03	34.39	1.03	0.24	1.36	2.47	1.29	0.58	0.90	0.44	1.37	4.09	1.81	1.71
Stress-70 protein, mitochondrial OS=Mus musculus GN=Hspa9 PE=1 SV=3	P38647	0.00	6.04	6.22	31.52	0.76	0.68	0.80	0.94	0.92	0.79	0.00	0.00	10.32	44.18	0.65	0.56	0.24	0.54	0.71	0.28	0.70	0.62	0.44	0.71	0.81	0.47
Metal-response element-binding transcription factor 2 OS=Mus musculus GN=Mtf2 PE=1 SV=2	Q02395	0.00	6.03	6.08	20.74	0.96	0.95	0.99	0.90	0.96	0.96	0.00	7.40	7.44	25.80	1.21	1.29	1.25	0.89	0.97	0.94	1.08	1.11	1.11	0.89	0.97	0.95
Protein IWS1 homolog OS=Mus musculus GN=Iws1 PE=1 SV=1	Q8C1D8	0.00	6.03	6.07	14.49	1.18	1.12	1.08	0.90	0.90	0.89	0.00	6.59	6.63	23.24	1.36	1.26	1.53	1.04	0.82	0.92	1.26	1.19	1.28	0.96	0.86	0.90
60S ribosomal protein L32 OS=Mus musculus GN=Rpl32 PE=2 SV=2	P62911	0.00	6.03	6.04	62.22	1.08	0.95	0.97	1.21	1.34	1.28	0.00	5.74	5.75	67.41	1.03	1.04	0.84	2.65	2.47	1.38	1.05	0.99	0.90	1.79	1.82	1.33
MCG124046 OS=Mus musculus GN=Prss1 PE=2 SV=1	Q9Z1R9	0.00	6.03	6.03	13.41	1.34	0.92	1.06	1.00	0.88	0.93	0.00	11.31	11.31	25.61	1.89	1.58	2.58	0.81	0.82	0.20	1.59	1.21	1.65	0.90	0.85	0.43

Protien identification and qunatitation results from ProteinPilot for all the analyzed samples

Name	Accession number	% FDR	Unused	Total	%Cov	114:113	115:113	116:113	118:117	119:117	121:117	% FDR	Unused	Total	%Cov	114:113	115:113	116:113	118:117	119:117	121:117	114:113	115:113	116:113	118:117	119:117	121:117
Signal recognition particle receptor subunit alpha OS=Mus musculus GN=Srpr PE=1 SV=1	Q9DBG7	0.00	6.02	6.10	25.63	1.04	0.92	0.94	1.11	1.07	0.93	0.00	4.83	4.85	27.67	1.01	0.96	0.95	1.16	1.17	1.05	1.02	0.94	0.95	1.13	1.12	0.99
Transmembrane protein 214 OS=Mus musculus GN=Tmem214 PE=2 SV=1	Q8BM55	0.00	6.02	6.02	25.76	1.19	1.14	1.03	0.89	0.65	0.72	0.00	0.00	3.72	34.35	0.96	0.95	0.95	1.07	0.93	0.92	1.07	1.04	0.99	0.97	0.78	0.82
Actin-related protein 2/3 complex subunit 1B OS=Mus musculus GN=Arpc1b PE=1 SV=4	Q9WV32	0.00	0.00	6.02	32.26	1.26	0.33	0.53	0.85	0.63	0.56	0.00	3.07	3.08	19.89	1.14	0.37	0.28	1.11	0.28	0.53	1.20	0.35	0.39	0.97	0.42	0.55
MCG5400 OS=Mus musculus GN=Myl12a PE=2 SV=1	Q6ZWQ9	0.00	0.00	6.02	43.60	0.86	0.41	0.55	0.37	0.25	0.17	0.00	6.05	6.05	48.26	0.76	0.35	0.38	0.39	0.27	0.27	0.81	0.38	0.46	0.38	0.26	0.21
Myosin regulatory light chain 12B OS=Mus musculus GN=Myl12b PE=1 SV=2	Q3THE2	0.00	0.00	6.02	36.63	0.86	0.41	0.55	0.37	0.25	0.17	0.00	0.00	6.05	48.26	0.76	0.35	0.38	0.39	0.27	0.27	0.81	0.38	0.46	0.38	0.26	0.21
Ribosomal RNA-processing protein 7 homolog A OS=Mus musculus GN=Rrp7a PE=2 SV=1	Q9D1C9	0.00	0.00	6.20	38.21	1.10	0.93	1.06	1.05	1.07	1.03	0.00	8.33	8.52	55.71	0.88	0.52	1.12	0.75	0.88	0.18	0.98	0.70	1.09	0.89	0.97	0.43
PCI domain-containing protein 2 OS=Mus musculus GN=Pcid2 PE=2 SV=1	Q8BFV2	0.00	0.00	6.08	32.08	1.10	1.12	1.12	1.02	1.04	0.95	0.00	0.00	3.62	29.57	1.06	0.95	0.97	1.06	0.97	0.99	1.08	1.03	1.04	1.04	1.00	0.97
Leukocyte receptor cluster member 8 homolog OS=Mus musculus GN=Leng8 PE=1 SV=1	Q8CBY3	0.00	0.00	6.01	32.36	1.09	1.03	1.10	0.98	0.99	1.01	0.00	3.41	3.42	32.99	0.83	1.00	0.98	1.07	1.02	1.12	0.95	1.01	1.04	1.02	1.00	1.06
Eukaryotic initiation factor 4A-I OS=Mus musculus GN=Eif4a1 PE=2 SV=1	P60843	0.00	0.00	12.62	37.68	0.95	0.90	0.96	0.88	0.85	0.92	0.00	10.42	15.42	54.43	0.81	0.73	0.77	2.15	1.21	0.56	0.87	0.81	0.86	1.37	1.01	0.72
Protein Zc3h13 OS=Mus musculus GN=Zc3h13 PE=4 SV=1	E9Q784	0.00	6.00	6.06	29.90	1.03	1.02	0.96	1.07	0.95	1.06	0.00	4.47	4.51	41.30	0.87	0.99	0.97	1.14	1.10	1.04	0.95	1.00	0.97	1.10	1.02	1.05
Actin-related protein 5 OS=Mus musculus GN=Actr5 PE=2 SV=3	Q80US4	0.00	6.00	6.05	19.50	0.90	0.98	1.01	1.08	0.98	1.11	0.00	0.00	4.18	26.78	1.07	1.16	1.06	0.95	1.18	1.31	0.98	1.07	1.03	1.01	1.08	1.20
Protein Zfp384 OS=Mus musculus GN=Zfp384 PE=4 SV=1	E9Q1A5	0.00	0.00	6.00	22.60	0.94	0.95	0.84	1.05	0.94	0.93	0.00	0.00	8.01	29.28	1.02	1.08	1.06	0.86	0.92	0.85	0.98	1.01	0.94	0.95	0.93	0.89
Active regulator of SIRT1 OS=Mus musculus GN=Rps19bp1 PE=1 SV=1	Q8C6B9	0.00	6.00	6.00	49.65	1.00	0.96	0.92	0.93	0.97	0.91	0.00	4.74	4.74	54.55	0.92	0.85	0.82	0.89	1.02	0.95	0.96	0.90	0.87	0.91	1.00	0.93
Exosome complex exonuclease RRP42 OS=Mus musculus GN=Exosc7 PE=2 SV=2	Q9D0M0	0.00	0.00	6.00	45.70	1.04	1.10	1.11	1.00	1.11	1.15	0.00	0.00	2.08	28.52	1.13	1.09	1.17	1.08	1.15	1.00	1.08	1.09	1.14	1.04	1.13	1.07
Nucleolar protein 7 OS=Mus musculus GN=Nol7 PE=1 SV=1	Q9D7Z3	0.00	0.00	6.00	27.95	1.02	0.99	1.09	0.95	1.04	1.02	0.00	8.01	8.02	45.28	1.00	1.05	1.05	0.95	0.90	0.98	1.01	1.02	1.07	0.95	0.96	1.00
40S ribosomal protein S27 OS=Mus musculus GN=Rps27 PE=1 SV=3	Q6ZWU9	0.00	6.00	6.00	64.29	1.16	0.99	0.93	1.20	1.63	1.34	0.00	3.37	3.37	42.86	1.06	1.02	1.13	1.16	1.26	1.12	1.11	1.00	1.02	1.18	1.43	1.22
40S ribosomal protein S27-like OS=Mus musculus GN=Rps27l PE=2 SV=3	Q6ZWY3	0.00	0.00	4.00	51.19	1.16	0.99	0.93	1.20	1.63	1.34	0.00	0.00	3.05	29.76	1.06	1.02	1.13	1.16	1.26	1.12	1.11	1.00	1.02	1.18	1.43	1.22
60S ribosomal protein L24 OS=Mus musculus GN=Rpl24 PE=2 SV=2	Q8BP67	0.00	0.00	6.00	29.94	1.08	0.92	0.93	0.96	0.99	0.81	0.00	3.71	3.71	45.86	1.34	1.33	0.70	0.94	1.06	0.04	1.20	1.11	0.81	0.95	1.02	0.18
High mobility group protein HMG-I/HMG-Y OS=Mus musculus GN=Hmga1 PE=1 SV=4	P17095	0.00	0.00	6.00	56.07	1.03	1.09	0.95	1.00	0.90	0.79	0.00	4.00	4.00	43.93	1.05	0.79	0.82	0.93	0.98	0.88	1.04	0.93	0.88	0.96	0.94	0.83
60S ribosomal protein L22 OS=Mus musculus GN=Rpl22 PE=2 SV=2	P67984	0.00	0.00	6.00	30.47	1.27	1.13	1.50	1.02	1.25	1.12	0.00	6.22	6.22	38.28	1.06	0.95	1.08	1.12	1.37	1.07	1.16	1.04	1.27	1.07	1.31	1.09
Ankycorbin OS=Mus musculus GN=Rai14 PE=1 SV=1	Q9EP71	0.00	5.98	6.25	24.62	0.86	0.45	0.48	0.52	0.52	0.50	0.00	5.44	5.47	29.93	1.10	0.83	1.03	0.77	0.64	0.10	0.97	0.61	0.70	0.63	0.58	0.22
Fibronectin OS=Mus musculus GN=Fn1 PE=1 SV=4	P11276	0.00	0.00	5.98	14.29	1.33	1.67	1.85	3.50	3.25	3.08	0.00	0.00	9.12	16.43	1.60	1.64	1.61	3.13	2.40	1.92	1.46	1.66	1.73	3.31	2.79	2.43
Serine/threonine-protein phosphatase 1 regulatory subunit 10 OS=Mus musculus GN=Ppp1r10 PE=1 SV=1	Q80W00	0.00	0.00	6.04	32.43	1.11	1.08	1.02	1.24	1.04	1.07	0.00	8.13	8.18	32.77	1.07	1.08	1.05	1.08	1.04	1.08	1.09	1.08	1.03	1.15	1.04	1.07
60S ribosomal protein L10 OS=Mus musculus GN=Rpl10 PE=2 SV=3	Q6ZWV3	0.00	0.00	5.98	35.98	0.93	0.99	0.94	1.12	1.12	1.01	0.00	6.18	6.19	39.72	0.83	0.93	0.50	1.02	1.11	0.54	0.88	0.96	0.68	1.07	1.11	0.74
60S ribosomal protein L10-like OS=Mus musculus GN=Rpl10l PE=2 SV=1	P86048	0.00	0.00	3.98	27.57	0.93	0.99	0.94	1.12	1.12	1.01	0.00	0.00	4.19	37.85	0.83	0.93	0.50	1.02	1.11	0.54	0.88	0.96	0.68	1.07	1.11	0.74
Mothers against decapentaplegic homolog 4 OS=Mus musculus GN=Smad4 PE=1 SV=2	P97471	0.00	0.00	5.96	22.14	0.55	1.32	1.39	2.25	1.58	1.92	0.00	2.37	2.38	24.32	0.77	0.86	0.80	1.09	1.15	1.21	0.65	1.07	1.06	1.56	1.35	1.53
ADP/ATP translocase 1 OS=Mus musculus GN=Slc25a4 PE=1 SV=4	P48962	0.00	5.95	17.58	58.05	0.92	1.01	0.90	0.84	0.93	0.90	0.00	8.62	18.45	54.03	1.08	0.97	0.88	0.87	0.84	0.69	1.00	0.99	0.89	0.86	0.88	0.79
Interferon-induced 35 kDa protein homolog OS=Mus musculus GN=Ifi35 PE=2 SV=3	Q9D8C4	0.00	5.87	5.89	50.35	0.90	0.79	1.13	1.84	1.00	1.42	0.00	3.01	3.12	27.97	0.96	1.15	1.24	3.70	1.77	2.56	0.93	0.95	1.18	2.61	1.33	1.91
60S ribosomal protein L8 OS=Mus musculus GN=Rpl8 PE=2 SV=2	P62918	0.00	5.85	5.86	34.63	1.24	1.32	1.34	1.53	1.53	1.49	0.00	3.87	3.87	37.35	1.20	1.21	1.09	1.49	1.45	1.36	1.22	1.26	1.21	1.51	1.49	1.42
MCG11326, isoform CRA_a OS=Mus musculus GN=Hnrnph3 PE=4 SV=1	D3Z3N4	0.00	5.84	7.84	25.72	0.98	0.92	1.01	0.95	0.98	0.97	0.00	3.87	6.18	25.72	0.65	1.00	0.77	0.74	0.88	0.04	0.80	0.96	0.88	0.84	0.93	0.20
WD repeat-containing protein 82 OS=Mus musculus GN=Wdr82 PE=1 SV=1	Q8BFQ4	0.00	0.00	5.81	23.64	0.98	0.80	0.81	1.12	1.06	1.14	0.00	6.55	6.56	40.58	0.97	0.98	0.96	1.05	0.99	0.98	0.98	0.89	0.88	1.08	1.02	1.06
Serine--tRNA ligase, cytoplasmic OS=Mus musculus GN=Sars PE=2 SV=3	P26638	0.00	0.00	5.80	29.88	1.14	0.93	0.92	1.11	0.90	0.68	0.88	0.00	1.44	23.63	1.10	0.75	1.10	1.36	1.27	2.70	1.12	0.84	1.00	1.22	1.07	1.36
Exosome complex component RRP4 OS=Mus musculus GN=Exosc2 PE=2 SV=1	Q8VBV3	0.00	0.00	5.80	39.93	1.12	1.32	1.08	1.24	1.27	1.49	0.00	6.41	6.44	51.19	1.28	1.66	2.00	2.75	3.25	3.63	1.20	1.48	1.47	1.85	2.03	2.32
Zinc finger protein 687 OS=Mus musculus GN=Znf687 PE=2 SV=1	Q9D2D7	0.00	5.75	5.80	20.45	1.00	1.04	1.03	1.00	1.00	0.91	0.00	3.21	3.23	20.05	1.02	1.07	0.95	0.97	1.04	0.76	1.01	1.05	0.99	0.99	1.02	0.83
E3 ubiquitin-protein ligase RAD18 OS=Mus musculus GN=Rad18 PE=1 SV=2	Q9QXK2	0.00	0.00	6.31	25.15	1.03	0.92	0.90	0.97	1.04	0.87	0.00	0.00	3.26	32.22	1.01	1.00	1.08	0.94	0.99	0.99	1.02	0.96	0.98	0.95	1.01	0.93
Peptidyl-prolyl cis-trans isomerase H OS=Mus musculus GN=Ppih PE=2 SV=1	Q9D868	0.00	0.00	5.73	34.57	1.20	1.17	1.27	0.98	0.82	0.99	0.00	4.91	4.92	44.68	1.00	0.98	1.14	1.04	0.74	0.37	1.10	1.07	1.20	1.01	0.78	0.60
Exosome complex component RRP43 OS=Mus musculus GN=Exosc8 PE=2 SV=1	Q9D753	0.00	0.00	5.74	30.43	0.98	1.02	1.06	1.04	1.09	1.11	0.00	6.27	6.28	36.59	0.96	0.97	0.99	1.09	1.11	1.16	0.97	1.00	1.02	1.06	1.10	1.13

Protien identification and qunatitation results from ProteinPilot for all the analyzed samples

Name	Accession number	% FDR	Unused	Total	%Cov	114:113	115:113	116:113	118:117	119:117	121:117	% FDR	Unused	Total	%Cov	114:113	115:113	116:113	118:117	119:117	121:117	114:113	115:113	116:113	118:117	119:117	121:117
Nuclear inhibitor of protein phosphatase 1 OS=Mus musculus GN=Ppp1r8 PE=1 SV=1	Q8R3G1	0.00	0.00	5.74	27.92	1.06	1.06	1.01	0.90	0.91	0.98	0.00	0.00	2.35	35.90	1.12	0.96	0.93	0.92	1.03	0.90	1.09	1.01	0.97	0.91	0.97	0.94
CUGBP Elav-like family member 1 OS=Mus musculus GN=Celf1 PE=1 SV=2	P28659	0.00	5.70	7.41	17.49	0.84	0.95	0.81	0.99	1.10	1.11	0.00	0.00	4.09	20.99	0.92	0.96	0.90	0.94	0.90	1.12	0.88	0.95	0.85	0.96	1.00	1.11
Casein kinase II subunit alpha' OS=Mus musculus GN=Csnk2a2 PE=2 SV=1	O54833	0.00	0.00	5.73	26.00	0.91	0.82	0.83	1.05	0.93	0.92	0.15	2.05	2.10	26.57	1.07	0.95	1.22	1.11	1.34	1.15	0.99	0.88	1.01	1.08	1.12	1.03
CD44 antigen OS=Mus musculus GN=Cd44 PE=1 SV=3	P15379	0.00	0.00	5.71	13.75	0.99	0.25	0.57	0.35	0.11	0.10	0.00	0.00	5.20	16.32	0.90	0.24	0.43	0.55	0.27	0.25	0.94	0.24	0.50	0.44	0.17	0.16
Histone acetyltransferase p300 OS=Mus musculus GN=Ep300 PE=1 SV=1	B2RWS6	0.00	5.66	6.03	14.58	1.07	1.09	1.09	0.97	0.96	0.91	0.15	0.00	2.39	15.24	1.08	1.10	1.14	0.97	0.95	0.92	1.07	1.09	1.11	0.97	0.95	0.92
ATP synthase subunit beta, mitochondrial OS=Mus musculus GN=Atp5b PE=1 SV=2	P56480	0.00	5.61	5.62	26.84	0.75	0.81	0.73	1.03	1.15	1.04	0.00	7.53	7.63	41.02	0.88	0.95	0.85	1.00	1.14	0.90	0.81	0.87	0.79	1.01	1.14	0.96
Transcription factor A, mitochondrial OS=Mus musculus GN=Tfam PE=1 SV=2	P40630	0.00	0.00	5.71	30.86	0.72	0.83	0.96	1.14	1.05	1.00	0.00	5.94	6.11	34.57	1.45	1.28	1.28	1.64	1.21	0.33	1.02	1.03	1.11	1.37	1.13	0.57
T-complex protein 1 subunit alpha OS=Mus musculus GN=Tcp1 PE=1 SV=3	P11983	0.00	5.54	6.03	25.72	0.95	0.99	0.95	1.07	1.04	0.95	0.00	5.40	5.46	22.48	1.19	1.08	1.04	1.12	1.20	1.19	1.07	1.03	0.99	1.09	1.12	1.06
CDKN2A-interacting protein OS=Mus musculus GN=Cdkn2aip PE=2 SV=1	Q8BI72	0.00	5.54	5.72	19.01	0.94	0.93	0.86	0.94	0.86	0.84	0.00	2.23	2.35	29.84	0.70	0.72	0.82	0.93	0.64	0.85	0.81	0.82	0.84	0.93	0.74	0.84
RRP15-like protein OS=Mus musculus GN=Rrp15 PE=2 SV=2	Q9CYX7	0.00	5.53	5.56	26.69	1.10	1.12	1.43	0.77	1.57	1.34	0.00	4.53	4.54	25.62	0.73	0.67	0.86	0.70	0.98	0.43	0.90	0.87	1.11	0.73	1.24	0.76
Staphylococcal nuclease domain-containing protein 1 OS=Mus musculus GN=Snd1 PE=1 SV=1	Q78PY7	0.00	0.00	6.18	32.42	0.97	1.05	1.05	1.45	1.67	1.60	0.00	5.31	5.37	28.24	0.94	0.98	0.95	1.00	1.14	1.21	0.95	1.01	1.00	1.20	1.38	1.39
TOX high mobility group box family member 4 OS=Mus musculus GN=Tox4 PE=1 SV=3	Q8BU11	0.00	0.00	5.50	17.45	0.79	0.78	0.78	1.11	1.21	1.28	0.14	2.01	2.02	10.50	1.09	0.91	1.09	0.76	0.90	0.64	0.93	0.84	0.92	0.92	1.04	0.91
Cleavage and polyadenylation specificity factor subunit 7 OS=Mus musculus GN=Cpsf7 PE=1 SV=2	Q8BTV2	0.00	5.48	5.48	31.00	0.95	1.02	0.95	0.96	1.03	1.00	0.00	7.09	7.10	43.74	2.13	1.11	1.36	0.72	0.63	0.51	1.43	1.06	1.14	0.84	0.81	0.71
Chromosome alignment-maintaining phosphoprotein 1 OS=Mus musculus GN=Champ1 PE=1 SV=1	Q8K327	0.00	5.43	5.44	20.82	1.01	1.09	1.05	0.96	1.15	1.06	0.00	8.51	8.53	26.18	1.01	1.13	1.28	0.90	1.15	0.62	1.01	1.11	1.16	0.93	1.15	0.81
Rho guanine nucleotide exchange factor 2 OS=Mus musculus GN=Arhgef2 PE=1 SV=4	Q60875	0.00	0.00	5.48	26.80	0.98	0.94	1.02	1.08	1.05	0.91	0.00	0.00	8.18	35.84	0.97	0.86	0.93	1.02	0.97	0.93	0.98	0.90	0.97	1.05	1.01	0.92
Transcription factor 20 OS=Mus musculus GN=Tcf20 PE=1 SV=2	Q9EPQ8	0.00	0.00	5.43	15.18	1.03	1.02	1.05	1.07	1.05	1.13	0.14	0.00	2.02	20.52	1.09	1.13	1.22	1.08	1.17	1.34	1.06	1.07	1.13	1.07	1.11	1.23
Protein regulator of cytokinesis 1 OS=Mus musculus GN=Prc1 PE=2 SV=2	Q99K43	0.00	0.00	7.09	30.51	1.36	1.27	1.42	0.74	0.85	0.71	0.00	0.00	6.13	38.14	2.17	2.23	2.21	1.16	0.77	0.65	1.71	1.68	1.77	0.93	0.81	0.68
Regulation of nuclear pre-mRNA domain-containing protein 1A OS=Mus musculus GN=Rprd1a PE=2 SV=1	Q8VDS4	0.00	5.41	5.43	37.18	0.99	0.96	1.01	0.95	0.86	0.91	0.00	5.55	5.84	33.97	1.03	0.99	0.95	0.97	0.94	1.00	1.01	0.98	0.98	0.96	0.90	0.95
Peptidyl-prolyl cis-trans isomerase G OS=Mus musculus GN=Ppig PE=1 SV=1	A2AR02	0.00	5.40	5.56	30.19	1.08	1.08	1.03	1.20	1.08	1.05	0.00	2.81	2.82	36.17	0.90	1.02	0.79	1.09	0.76	1.19	0.98	1.05	0.90	1.14	0.90	1.12
Peptidyl-prolyl cis-trans isomerase G (Fragment) OS=Mus musculus GN=Ppig PE=4 SV=1	A2AR01	0.00	0.00	5.53	55.91	1.08	1.08	1.03	1.20	1.08	1.05	0.00	0.00	2.80	49.61	0.90	1.02	0.79	1.09	0.76	1.19	0.98	1.05	0.90	1.14	0.90	1.12
Cell division cycle-associated 7-like protein OS=Mus musculus GN=Cdca7l PE=2 SV=1	Q922M5	0.00	5.40	5.43	24.89	1.16	1.17	1.12	0.95	0.94	0.91	0.00	3.83	3.85	30.14	0.98	1.06	1.06	1.12	1.06	0.98	1.07	1.11	1.09	1.03	1.00	0.95
Vacuolar protein sorting-associated protein 72 homolog OS=Mus musculus GN=Vps72 PE=2 SV=2	Q62481	0.00	5.40	5.42	30.98	1.02	1.02	0.95	0.96	0.99	0.98	0.00	4.89	4.90	38.86	1.00	0.97	1.01	0.90	0.97	0.95	1.01	1.00	0.98	0.93	0.98	0.96
Transcription factor ETV6 OS=Mus musculus GN=Etv6 PE=1 SV=1	P97360	0.00	0.00	5.39	32.16	1.10	1.06	0.97	1.32	1.29	1.47	0.00	5.42	5.44	36.70	1.27	1.14	1.41	1.34	1.00	0.89	1.18	1.10	1.17	1.33	1.14	1.14
Polypyrimidine tract-binding protein 2 OS=Mus musculus GN=Ptbp2 PE=1 SV=2	Q91Z31	0.00	5.33	7.57	27.87	0.61	0.87	0.62	0.64	0.68	0.69	0.00	7.40	9.66	34.84	1.00	1.14	0.78	0.72	0.68	0.57	0.78	1.00	0.70	0.68	0.68	0.63
T-complex protein 1 subunit beta OS=Mus musculus GN=Cct2 PE=1 SV=4	P80314	0.00	0.00	5.37	22.80	1.03	1.03	0.96	1.08	1.10	1.03	0.00	4.05	4.11	31.40	0.93	1.00	0.94	1.10	1.16	1.25	0.98	1.01	0.95	1.09	1.13	1.13
60S ribosomal protein L19 OS=Mus musculus GN=Rpl19 PE=1 SV=1	P84099	0.00	0.00	5.34	35.71	1.29	1.26	1.37	1.27	1.22	1.05	0.00	0.00	5.56	39.80	1.61	1.79	1.57	2.63	2.88	2.00	1.45	1.50	1.47	1.83	1.88	1.45
Splicing factor 3B subunit 4 OS=Mus musculus GN=Sf3b4 PE=2 SV=1	Q8QZY9	0.00	5.32	5.33	31.60	0.96	1.01	0.95	0.94	0.94	1.01	0.00	2.70	2.71	23.58	0.99	0.89	0.95	0.99	0.95	1.04	0.98	0.95	0.95	0.96	0.95	1.02
Transmembrane protein 209 OS=Mus musculus GN=Tmem209 PE=2 SV=1	Q8BRG8	0.00	5.31	5.33	37.97	0.90	0.95	0.80	0.23	0.55	0.68	0.00	6.56	6.57	25.85	0.94	1.11	0.96	0.86	0.95	0.88	0.92	1.02	0.88	0.45	0.73	0.77
TATA-box-binding protein OS=Mus musculus GN=Tbp PE=1 SV=1	P29037	0.00	0.00	5.31	33.54	1.07	0.96	1.08	0.94	0.96	1.03	0.00	2.45	2.45	39.87	0.90	0.95	0.90	1.16	1.05	1.04	0.98	0.96	0.98	1.04	1.00	1.03
TATA box-binding protein-like protein 2 OS=Mus musculus GN=Tbpl2 PE=1 SV=1	Q6SJ95	0.00	0.00	5.30	29.14	1.07	0.96	1.08	0.94	0.96	1.03	0.00	0.00	2.45	22.57	0.90	0.95	0.90	1.16	1.05	1.04	0.98	0.96	0.98	1.04	1.00	1.03
Peptidyl-prolyl cis-trans isomerase-like 1 OS=Mus musculus GN=Ppil1 PE=2 SV=1	Q9D0W5	0.00	0.00	5.44	46.99	1.22	1.03	1.07	0.95	0.98	0.97	0.00	4.13	4.13	42.17	1.02	0.98	1.05	0.87	1.07	0.92	1.12	1.00	1.06	0.91	1.02	0.95
60S ribosomal protein L34 OS=Mus musculus GN=Rpl34 PE=3 SV=2	Q9D1R9	0.00	5.30	5.33	34.19	1.22	1.02	1.18	1.03	1.15	1.12	0.00	4.93	4.93	35.90	1.47	0.96	1.11	1.18	1.14	0.95	1.34	0.99	1.14	1.10	1.14	1.03
Sororin OS=Mus musculus GN=Cdca5 PE=1 SV=1	Q9CPY3	0.00	5.28	5.31	27.65	0.97	0.96	1.02	0.86	0.86	0.87	0.14	2.02	2.04	55.30	1.04	0.86	0.95	0.91	0.91	0.85	1.00	0.91	0.99	0.89	0.88	0.86
Tyrosine--tRNA ligase, cytoplasmic OS=Mus musculus GN=Yars PE=2 SV=3	Q91WQ3	0.00	0.00	5.55	30.49	1.05	0.99	1.05	0.87	0.92	0.92	0.00	0.00	5.24	31.44	0.64	1.13	0.90	0.44	0.86	0.11	0.82	1.06	0.97	0.62	0.89	0.32
Nuclear receptor subfamily 2 group C member 2 OS=Mus musculus GN=Nr2c2 PE=1 SV=1	P49117	0.00	0.00	5.26	20.97	0.95	1.00	0.98	0.95	0.93	0.93	0.00	0.00	9.43	41.11	1.34	1.08	1.64	0.79	0.75	0.29	1.13	1.04	1.27	0.87	0.84	0.52
Chromodomain Y-like protein OS=Mus musculus GN=Cdyl PE=1 SV=1	Q9WTK2	0.00	5.24	5.25	21.42	0.86	0.91	0.98	0.89	0.89	0.91	0.00	3.17	3.18	34.91	0.99	0.97	0.98	1.33	1.58	0.92	0.92	0.94	0.98	1.09	1.19	0.92
Zinc finger CCHC domain-containing protein 8 OS=Mus musculus GN=Zcchc8 PE=2 SV=3	Q9CYA6	0.00	0.00	5.24	17.77	1.11	0.84	0.93	0.79	0.88	0.80	0.00	2.64	2.64	19.61	1.09	0.89	0.90	0.86	1.02	1.13	1.10	0.86	0.91	0.82	0.95	0.95

Protien identification and qunatitation results from ProteinPilot for all the analyzed samples

Name	Accession number	% FDR	Unused	Total	%Cov	114:113	115:113	116:113	118:117	119:117	121:117	% FDR	Unused	Total	%Cov	114:113	115:113	116:113	118:117	119:117	121:117	114:113	115:113	116:113	118:117	119:117	121:117
14-3-3 protein gamma OS=Mus musculus GN=Ywhag PE=1 SV=2	P61982	0.00	0.00	5.23	20.24	0.79	0.87	1.06	1.33	1.50	1.67	0.00	5.70	5.70	24.29	0.95	0.94	1.00	1.00	1.07	1.11	0.87	0.90	1.03	1.15	1.26	1.36
14-3-3 protein beta/alpha OS=Mus musculus GN=Ywhab PE=1 SV=3	Q9CQV8	0.00	0.00	3.23	14.63	0.79	0.87	1.06	1.33	1.50	1.67	0.00	0.00	3.70	34.15	0.95	0.94	1.00	1.00	1.07	1.11	0.87	0.90	1.03	1.15	1.26	1.36
14-3-3 protein theta OS=Mus musculus GN=Ywhaq PE=1 SV=1	P68254	0.00	0.00	3.25	17.96	0.79	0.87	1.06	1.33	1.50	1.67	0.00	0.00	3.70	24.08	0.95	0.94	1.00	1.00	1.07	1.11	0.87	0.90	1.03	1.15	1.26	1.36
14-3-3 protein sigma OS=Mus musculus GN=Sfn PE=1 SV=2	O70456	0.00	0.02	3.25	27.42	0.79	0.87	1.06	1.33	1.50	1.67	0.00	0.00	3.70	16.94	0.95	0.94	1.00	1.00	1.07	1.11	0.87	0.90	1.03	1.15	1.26	1.36
14-3-3 protein zeta/delta OS=Mus musculus GN=Ywhaz PE=1 SV=1	P63101	0.00	0.00	3.24	13.88	0.79	0.87	1.06	1.33	1.50	1.67	0.13	2.00	3.70	21.22	1.28	0.76	1.10	0.95	1.05	0.01	1.00	0.81	1.08	1.12	1.25	0.14
T-complex protein 1 subunit gamma OS=Mus musculus GN=Cct3 PE=1 SV=1	P80318	0.00	0.00	5.25	30.46	1.08	1.00	1.05	1.14	1.11	1.14	0.00	5.87	5.87	34.50	1.03	0.99	0.98	1.13	1.03	1.07	1.05	1.00	1.01	1.13	1.07	1.10
Telomeric repeat-binding factor 2-interacting protein 1 OS=Mus musculus GN=Terf2ip PE=1 SV=1	Q91VL8	0.00	5.22	5.24	27.74	0.87	0.95	0.89	0.83	0.84	0.87	0.00	4.14	4.15	23.16	1.00	0.98	1.02	0.96	1.03	1.09	0.93	0.96	0.95	0.90	0.93	0.97
GA-binding protein alpha chain OS=Mus musculus GN=Gabpa PE=1 SV=2	Q00422	0.00	0.00	5.23	13.44	0.87	0.93	0.90	0.89	0.93	0.89	0.00	3.10	3.11	24.45	1.45	1.12	1.07	1.29	0.94	0.82	1.12	1.02	0.98	1.07	0.93	0.86
Pre-mRNA-splicing factor RBM22 OS=Mus musculus GN=Rbm22 PE=2 SV=1	Q8BHS3	0.00	5.18	5.18	27.86	1.10	0.97	0.92	0.86	0.87	0.88	0.00	9.05	9.05	45.95	1.03	0.96	0.94	1.00	1.07	0.96	1.06	0.97	0.93	0.92	0.96	0.92
DNA/RNA-binding protein KIN17 OS=Mus musculus GN=Kin PE=2 SV=1	Q8K339	0.00	5.18	5.18	24.04	1.29	1.22	1.15	0.89	1.02	1.07	0.00	2.67	2.77	38.62	1.05	1.29	1.47	1.28	2.09	1.45	1.16	1.26	1.30	1.07	1.46	1.24
Peptidyl-prolyl cis-trans isomerase-like 3 OS=Mus musculus GN=Ppil3 PE=2 SV=1	Q9D6L8	0.00	5.16	5.16	30.43	0.91	0.89	1.01	0.97	1.01	1.13	0.14	2.03	2.03	23.60	1.13	1.12	1.06	1.15	1.31	1.29	1.01	1.00	1.03	1.06	1.15	1.21
High mobility group protein B1 OS=Mus musculus GN=Hmgb1 PE=1 SV=2	P63158	0.00	0.00	7.21	44.65	0.97	1.00	0.95	1.07	1.04	0.88	0.00	4.06	6.27	44.19	1.56	1.16	1.53	1.05	0.70	0.21	1.23	1.08	1.20	1.06	0.86	0.42
Zinc finger protein 280C OS=Mus musculus GN=Znf280c PE=2 SV=1	Q6P3Y5	0.00	5.15	5.17	19.81	1.10	1.09	1.05	1.15	1.14	0.98	0.00	4.41	4.49	19.81	0.89	0.94	0.90	1.00	0.94	0.68	0.99	1.01	0.97	1.07	1.03	0.82
Small nuclear ribonucleoprotein Sm D1 OS=Mus musculus GN=Snrpd1 PE=2 SV=1	P62315	0.00	5.15	5.15	72.27	1.01	1.00	1.04	0.95	0.96	1.01	0.00	8.00	8.00	63.87	0.86	0.83	0.77	0.90	1.10	1.03	0.93	0.91	0.89	0.92	1.03	1.02
40S ribosomal protein S12 OS=Mus musculus GN=Rps12 PE=2 SV=1	Q6ZWZ6	0.00	5.15	5.15	28.79	1.09	1.02	1.10	1.01	1.02	0.99	0.00	4.11	4.11	43.18	1.04	0.86	0.95	0.89	0.97	0.63	1.06	0.93	1.02	0.95	1.00	0.79
Eukaryotic translation initiation factor 6 OS=Mus musculus GN=Eif6 PE=1 SV=2	O55135	0.00	0.00	5.14	49.39	1.14	1.12	1.09	1.09	1.08	1.06	0.00	7.31	7.31	42.86	1.38	1.27	1.08	1.08	1.34	0.56	1.25	1.19	1.08	1.08	1.20	0.77
Protein Taf15 OS=Mus musculus GN=Taf15 PE=2 SV=1	Q8BQ46	0.00	5.13	9.32	36.27	1.19	1.20	1.00	1.49	1.09	1.16	0.00	6.18	10.46	41.83	1.46	1.21	1.63	0.54	0.35	0.25	1.32	1.21	1.28	0.90	0.61	0.54
Nucleolar MIF4G domain-containing protein 1 OS=Mus musculus GN=Nom1 PE=2 SV=2	Q3UFM5	0.00	5.12	5.15	31.26	0.88	0.79	0.77	0.89	0.96	0.90	0.00	6.27	6.38	34.66	0.86	0.95	1.05	0.92	1.05	1.06	0.87	0.87	0.90	0.90	1.00	0.98
Cytochrome c, somatic OS=Mus musculus GN=Cycs PE=1 SV=2	P62897	0.00	0.00	5.12	29.52	0.92	0.95	0.98	1.21	1.05	0.74	0.00	6.95	6.95	63.81	0.90	0.99	0.86	0.98	0.92	0.45	0.91	0.97	0.92	1.09	0.98	0.58
POU domain, class 2, transcription factor 1 OS=Mus musculus GN=Pou2f1 PE=2 SV=3	P25425	0.00	0.00	5.11	15.58	1.05	1.15	1.09	0.90	1.74	1.60	0.00	0.00	7.69	21.69	1.07	1.87	0.85	1.12	1.66	1.16	1.06	1.47	0.96	1.00	1.70	1.36
POU domain, class 2, transcription factor 2 OS=Mus musculus GN=Pou2f2 PE=3 SV=1	H3BKB7	0.00	0.00	5.10	21.63	1.05	1.15	1.09	0.90	1.74	1.60	0.00	0.00	5.68	29.98	1.07	1.87	0.85	1.12	1.66	1.16	1.06	1.47	0.96	1.00	1.70	1.36
POU domain, class 2, transcription factor 3 OS=Mus musculus GN=Pou2f3 PE=2 SV=2	P31362	0.00	0.00	5.10	22.27	1.05	1.15	1.09	0.90	1.74	1.60	0.00	0.00	5.68	18.56	1.07	1.87	0.85	1.12	1.66	1.16	1.06	1.47	0.96	1.00	1.70	1.36
Transcription factor MafG OS=Mus musculus GN=Mafg PE=1 SV=1	O54790	0.00	5.09	5.09	25.31	0.79	0.65	1.29	0.87	1.67	1.66	0.00	4.47	4.48	56.79	0.98	1.03	0.90	0.98	0.99	0.99	0.88	0.82	1.08	0.92	1.29	1.28
Keratin, type II cytoskeletal 1b OS=Mus musculus GN=Krt77 PE=1 SV=1	Q6IFZ6	0.00	0.00	6.79	26.75	0.49	0.51	0.39	0.60	0.46	0.43	0.00	4.12	6.12	38.64	0.77	1.28	0.56	0.66	0.43	0.68	0.61	0.81	0.47	0.63	0.44	0.54
Disks large-associated protein 5 OS=Mus musculus GN=Dlgap5 PE=1 SV=2	Q8K4R9	0.00	5.07	5.14	25.37	0.95	1.09	1.05	0.97	0.90	0.98	0.00	3.82	3.84	28.22	0.99	1.01	0.93	0.95	1.19	1.01	0.97	1.05	0.99	0.96	1.04	1.00
Ras-responsive element-binding protein 1 OS=Mus musculus GN=Rreb1 PE=1 SV=2	Q3UH06	0.00	5.07	5.13	16.06	1.12	1.17	1.15	0.93	0.90	1.15	0.00	0.00	3.81	24.06	1.11	1.03	0.90	0.98	0.95	0.86	1.11	1.10	1.01	0.95	0.92	0.99
Cleavage stimulation factor subunit 2 OS=Mus musculus GN=Cstf2 PE=1 SV=2	Q8BIQ5	0.00	0.00	5.07	40.69	0.76	0.86	0.92	0.98	1.13	1.36	0.00	0.00	13.71	53.45	0.87	1.29	1.09	0.89	0.66	0.87	0.81	1.06	1.00	0.93	0.86	1.09
Eukaryotic peptide chain release factor subunit 1 OS=Mus musculus GN=Etf1 PE=1 SV=4	Q8BWY3	0.00	0.00	5.06	22.88	0.65	0.91	0.73	0.82	1.05	1.27	0.00	12.12	12.12	40.73	1.05	1.18	1.22	1.39	1.17	1.51	0.82	1.04	0.95	1.07	1.11	1.39
Cell division cycle protein 23 homolog OS=Mus musculus GN=Cdc23 PE=1 SV=2	Q8BGZ4	0.00	0.00	5.05	26.47	1.01	0.99	0.95	0.89	0.95	0.99	0.00	3.54	3.62	27.47	0.77	1.00	0.90	1.14	1.25	1.19	0.88	1.00	0.92	1.00	1.09	1.09
Interferon-inducible protein AIM2 OS=Mus musculus GN=Aim2 PE=1 SV=2	Q91VJ1	0.00	5.00	5.01	22.60	1.00	1.03	0.93	1.01	0.91	0.95	0.00	4.57	4.58	37.57	0.80	0.68	0.96	0.99	0.83	1.04	0.90	0.84	0.95	1.00	0.87	1.00
60S ribosomal protein L35a OS=Mus musculus GN=Rpl35a PE=2 SV=2	O55142	0.00	0.00	4.99	49.09	1.63	1.38	1.63	1.41	1.61	1.50	0.00	4.81	4.81	78.18	1.38	1.14	1.17	1.67	1.36	1.27	1.50	1.25	1.38	1.53	1.48	1.38
Centromere protein C 1 OS=Mus musculus GN=Cenpc1 PE=1 SV=2	P49452	0.00	4.96	4.98	22.74	1.03	0.98	0.98	1.00	0.95	0.95	0.00	4.26	4.28	26.71	1.46	1.26	1.66	0.96	1.06	0.59	1.22	1.11	1.28	0.98	1.00	0.75
WD repeat-containing protein 1 OS=Mus musculus GN=Wdr1 PE=1 SV=3	O88342	0.00	0.00	4.98	20.46	1.04	0.33	0.45	0.65	0.55	0.62	0.00	8.03	8.06	15.51	0.99	0.21	0.42	0.48	0.26	0.51	1.01	0.26	0.43	0.56	0.38	0.56
Rac GTPase-activating protein 1 OS=Mus musculus GN=Racgap1 PE=2 SV=1	Q9WVM1	0.00	4.92	4.94	30.25	1.21	1.06	1.06	1.18	1.20	1.19	0.00	4.81	4.82	32.48	1.09	1.01	1.01	1.19	1.16	1.15	1.15	1.03	1.03	1.19	1.18	1.17
Nuclear cap-binding protein subunit 2 OS=Mus musculus GN=Ncbp2 PE=1 SV=1	Q9CQ49	0.00	4.92	4.92	25.00	0.99	0.91	1.01	0.98	0.98	0.98	0.00	2.80	2.80	32.05	0.97	0.90	0.95	1.20	1.05	1.27	0.98	0.90	0.98	1.09	1.01	1.12
Glycylpeptide N-tetradecanoyltransferase 1 OS=Mus musculus GN=Nmt1 PE=1 SV=1	O70310	0.00	0.00	4.90	23.99	0.83	0.94	0.80	0.72	0.84	0.36	0.00	5.05	5.06	31.85	1.00	1.02	1.04	1.08	0.92	0.79	0.91	0.98	0.91	0.88	0.88	0.54
Transcription initiation factor TFIID subunit 5 OS=Mus musculus GN=Taf5 PE=2 SV=1	Q8C092	0.00	0.00	4.91	25.34	1.33	1.41	0.96	1.10	0.88	0.91	0.00	0.00	4.91	20.35	0.94	0.96	0.93	0.96	1.07	0.98	1.12	1.16	0.95	1.03	0.97	0.95

Protien identification and qunatitation results from ProteinPilot for all the analyzed samples

Name	Accession number	% FDR	Unused	Total	%Cov	114:113	115:113	116:113	118:117	119:117	121:117	% FDR	Unused	Total	%Cov	114:113	115:113	116:113	118:117	119:117	121:117	114:113	115:113	116:113	118:117	119:117	121:117
DNA polymerase delta catalytic subunit OS=Mus musculus GN=Pold1 PE=1 SV=2	P52431	0.00	0.00	4.87	20.18	1.21	1.18	1.02	0.99	0.93	0.82	0.00	3.28	3.47	22.71	1.42	1.46	1.08	1.12	0.79	0.51	1.31	1.31	1.05	1.05	0.86	0.65
Probable ATP-dependent RNA helicase DDX41 OS=Mus musculus GN=Ddx41 PE=1 SV=2	Q91VN6	0.00	0.00	4.86	28.14	1.00	1.08	1.12	0.98	0.97	1.08	0.00	6.23	6.24	36.50	1.13	1.06	1.11	0.90	0.90	0.72	1.06	1.07	1.11	0.94	0.94	0.88
Condensin-2 complex subunit G2 OS=Mus musculus GN=Ncapg2 PE=2 SV=2	Q6DFV1	0.00	4.81	5.17	20.47	1.06	1.64	0.92	1.10	1.00	1.04	0.00	3.55	4.02	25.92	1.10	0.95	1.22	1.01	1.11	0.95	1.08	1.25	1.06	1.05	1.05	0.99
ESF1 homolog OS=Mus musculus GN=Esf1 PE=1 SV=1	Q3V1V3	0.00	0.00	4.83	15.50	0.93	0.96	0.95	1.06	1.12	1.13	0.00	7.72	7.73	24.62	0.95	0.91	0.90	1.20	1.63	0.49	0.94	0.94	0.92	1.13	1.35	0.74
General transcription factor IIIC, polypeptide 3 OS=Mus musculus GN=Gtf3c3 PE=2 SV=1	Q3TMP1	0.00	4.81	4.82	19.50	0.91	0.93	0.95	0.90	0.90	0.92	0.00	5.85	5.87	20.41	0.83	0.97	1.01	0.94	1.11	1.04	0.87	0.95	0.98	0.92	1.00	0.98
RNA-binding protein 4B OS=Mus musculus GN=Rbm4b PE=1 SV=1	Q8VE92	0.00	0.00	4.75	24.09	1.00	1.06	1.12	1.14	1.12	1.25	0.00	3.24	3.24	29.13	1.00	1.03	0.97	1.17	1.10	1.16	1.00	1.04	1.04	1.15	1.11	1.20
RNA-binding protein 4 OS=Mus musculus GN=Rbm4 PE=1 SV=1	Q8C7Q4	0.00	0.00	4.76	28.25	1.00	1.06	1.12	1.14	1.12	1.25	0.00	0.00	3.24	27.70	1.00	1.03	0.97	1.17	1.10	1.16	1.00	1.04	1.04	1.15	1.11	1.20
RNA-binding protein 4 (Fragment) OS=Mus musculus GN=Rbm4b PE=4 SV=2	F6TBN8	0.00	0.00	4.75	45.35	1.00	1.06	1.12	1.14	1.12	1.25	0.00	0.00	3.23	58.04	1.00	1.03	0.97	1.17	1.10	1.16	1.00	1.04	1.04	1.15	1.11	1.20
MCG8382, isoform CRA_b OS=Mus musculus GN=Rbm4 PE=2 SV=1	Q5CZX8	0.00	0.00	4.75	34.97	1.00	1.06	1.12	1.14	1.12	1.25	0.00	0.00	3.23	41.96	1.00	1.03	0.97	1.17	1.10	1.16	1.00	1.04	1.04	1.15	1.11	1.20
Serine/threonine-protein kinase PLK1 OS=Mus musculus GN=Plk1 PE=1 SV=2	Q07832	0.00	0.00	4.78	14.93	0.94	0.99	1.09	1.13	1.11	0.99	0.00	6.78	6.79	32.34	1.25	1.14	1.03	1.57	1.58	0.77	1.08	1.06	1.06	1.33	1.32	0.87
Dolichyl-diphosphooligosaccharide--protein glycosyltransferase 48 kDa subunit OS=Mus musculus GN=Ddost PE=1 SV=2	O54734	0.00	0.00	4.76	16.10	0.95	0.98	1.00	0.92	0.90	0.86	0.00	9.57	9.57	31.29	0.88	0.92	1.04	0.96	0.99	1.03	0.92	0.95	1.02	0.94	0.95	0.94
Zinc finger and BTB domain-containing protein 7B OS=Mus musculus GN=Zbtb7b PE=1 SV=2	Q64321	0.00	0.00	4.74	18.38	0.89	0.96	0.82	0.79	0.82	0.84	0.00	0.00	5.70	18.01	0.81	0.75	0.73	1.04	0.92	1.02	0.85	0.85	0.77	0.90	0.87	0.92
Serine/arginine repetitive matrix protein 1 OS=Mus musculus GN=Srrm1 PE=1 SV=2	Q52KI8	0.00	0.00	4.75	36.15	1.19	0.91	0.99	0.67	0.77	0.75	0.00	0.00	6.03	45.45	0.92	0.90	0.74	0.99	0.93	0.83	1.05	0.90	0.86	0.82	0.84	0.79
Nucleolar protein 8 OS=Mus musculus GN=Nol8 PE=1 SV=2	Q3UHX0	0.00	0.00	4.73	24.32	1.07	1.06	1.03	1.00	1.02	1.05	0.00	0.00	5.27	21.97	1.10	1.33	1.12	0.85	0.83	0.93	1.08	1.19	1.07	0.92	0.92	0.99
Prohibitin-2 OS=Mus musculus GN=Phb2 PE=1 SV=1	O35129	0.00	0.00	4.74	32.44	0.89	0.71	1.10	0.92	1.08	0.92	0.00	3.28	3.28	29.10	0.87	0.90	1.02	0.95	1.04	1.17	0.88	0.80	1.06	0.93	1.06	1.04
Death domain-associated protein 6 OS=Mus musculus GN=Daxx PE=1 SV=1	O35613	0.00	0.00	4.72	21.24	1.20	1.03	1.03	1.45	1.02	1.21	0.00	4.11	4.11	23.68	1.08	1.01	0.97	0.97	1.21	0.77	1.14	1.02	1.00	1.19	1.11	0.97
Protein Gm20425 OS=Mus musculus GN=Gm20425 PE=4 SV=1	E9Q035	0.00	4.69	4.72	22.49	0.86	0.97	1.00	0.92	0.87	0.85	0.00	6.05	6.07	26.58	0.66	0.64	0.67	0.82	0.90	0.10	0.75	0.79	0.82	0.87	0.88	0.29
Signal recognition particle receptor subunit beta OS=Mus musculus GN=Srprb PE=1 SV=1	P47758	0.00	0.00	4.69	34.94	0.86	0.97	1.00	0.92	0.87	0.85	0.00	0.00	6.05	39.03	0.66	0.64	0.67	0.82	0.90	0.10	0.75	0.79	0.82	0.87	0.88	0.29
Heterogeneous nuclear ribonucleoprotein U-like protein 1 OS=Mus musculus GN=Hnrnpul1 PE=1 SV=1	Q8VDM6	0.00	4.65	4.85	32.83	1.01	1.01	1.01	1.22	1.11	0.89	0.00	3.05	3.20	28.29	1.06	1.06	0.81	0.99	1.08	1.03	1.03	1.03	0.90	1.10	1.09	0.95
Replication factor C subunit 3 OS=Mus musculus GN=Rfc3 PE=2 SV=1	Q8R323	0.00	0.00	4.65	36.52	1.01	0.95	0.94	1.05	1.03	0.99	0.00	7.03	7.04	34.55	1.46	1.07	0.94	0.84	0.78	0.10	1.21	1.00	0.94	0.94	0.90	0.31
DAZ-associated protein 1 OS=Mus musculus GN=Dazap1 PE=2 SV=2	Q9JII5	0.00	0.00	4.64	29.31	0.81	1.06	1.12	0.98	1.08	1.39	0.00	0.00	9.11	41.63	0.84	1.46	1.24	1.20	1.36	2.00	0.82	1.24	1.17	1.09	1.21	1.67
Transcription factor jun-D OS=Mus musculus GN=Jund PE=1 SV=1	P15066	0.00	4.63	4.66	35.78	0.95	0.90	1.03	0.93	0.95	0.90	0.00	2.29	3.47	27.57	0.86	0.91	0.90	1.09	1.12	1.10	0.90	0.91	0.96	1.00	1.03	0.99
Scaffold attachment factor B2 OS=Mus musculus GN=Safb2 PE=1 SV=2	Q80YR5	0.00	4.61	11.67	38.14	2.36	1.80	1.21	0.86	0.90	0.93	0.00	4.22	11.04	38.65	1.01	1.00	1.05	0.94	0.88	1.01	1.54	1.34	1.13	0.90	0.89	0.97
Metastasis suppressor protein 1 OS=Mus musculus GN=Mtss1 PE=1 SV=1	Q8R1S4	0.00	0.00	4.60	14.76	0.97	0.99	0.91	0.88	0.83	0.82	0.00	0.00	5.86	28.46	1.09	1.41	1.26	0.80	0.61	0.38	1.03	1.18	1.07	0.84	0.71	0.56
Protein Kif23 OS=Mus musculus GN=Kif23 PE=3 SV=1	E9Q5G3	0.00	0.00	4.59	25.60	1.09	0.96	1.11	1.15	1.07	1.04	0.00	4.82	4.85	29.59	1.29	1.04	1.12	1.00	1.33	0.99	1.19	1.00	1.11	1.07	1.19	1.01
Transcription factor Sp3 OS=Mus musculus GN=Sp3 PE=1 SV=2	O70494	0.00	0.00	4.57	15.71	1.04	1.13	0.97	0.92	0.89	0.97	0.00	0.00	7.52	20.05	0.95	0.95	0.53	0.90	0.38	0.27	1.00	1.03	0.72	0.91	0.58	0.51
Importin subunit alpha-1 OS=Mus musculus GN=Kpna1 PE=1 SV=2	Q60960	0.00	4.53	4.55	24.72	0.93	0.96	0.95	1.12	0.96	0.95	0.00	2.30	2.31	25.09	1.00	0.97	0.99	1.12	1.10	1.21	0.96	0.97	0.97	1.12	1.03	1.08
Exosome complex component RRP46 OS=Mus musculus GN=Exosc5 PE=1 SV=1	Q9CRA8	0.00	0.00	4.53	21.70	1.14	1.16	1.14	1.10	1.13	1.14	0.00	7.54	7.55	31.91	1.17	1.18	1.11	1.04	1.07	0.95	1.15	1.17	1.12	1.07	1.10	1.04
ATP synthase subunit alpha, mitochondrial OS=Mus musculus GN=Atp5a1 PE=1 SV=1	Q03265	0.00	4.48	4.51	32.91	0.95	1.03	0.94	0.90	1.03	0.90	0.00	6.00	6.03	37.61	0.82	0.87	0.96	0.91	1.09	0.91	0.89	0.95	0.95	0.91	1.06	0.90
EF-hand domain-containing protein D2 OS=Mus musculus GN=Efhd2 PE=1 SV=1	Q9D8Y0	0.00	0.00	4.49	22.92	0.99	0.29	0.32	0.91	0.63	0.64	0.00	0.00	9.32	31.67	1.36	0.26	0.33	0.74	0.32	0.19	1.16	0.28	0.32	0.82	0.45	0.35
Condensin complex subunit 2 OS=Mus musculus GN=Ncaph PE=2 SV=1	Q8C156	0.00	4.47	4.70	16.42	0.68	0.55	0.43	1.31	0.86	0.37	0.00	2.72	2.72	22.30	1.42	1.18	1.20	1.12	0.90	0.88	0.98	0.81	0.72	1.21	0.88	0.57
40S ribosomal protein S10 OS=Mus musculus GN=Rps10 PE=1 SV=1	P63325	0.00	0.00	4.47	40.00	0.96	0.96	0.95	1.01	1.01	0.95	0.00	2.30	2.30	61.82	1.50	0.20	0.93	0.90	0.86	0.83	1.20	0.44	0.94	0.95	0.93	0.89
PHD finger-like domain-containing protein 5A OS=Mus musculus GN=Phf5a PE=1 SV=1	P83870	0.00	4.47	4.47	45.45	1.32	1.24	0.70	1.12	1.53	1.67	0.00	8.85	8.85	62.73	0.92	0.95	1.06	0.85	1.18	1.05	1.10	1.08	0.86	0.97	1.34	1.32
Transcriptional repressor protein YY1 OS=Mus musculus GN=Yy1 PE=1 SV=1	Q00899	0.00	4.45	4.46	25.85	0.78	0.90	0.86	0.93	0.95	1.12	0.00	5.31	5.31	34.06	0.27	0.55	0.82	1.11	1.32	0.46	0.45	0.70	0.84	1.01	1.12	0.71
Nucleoporin NDC1 OS=Mus musculus GN=Tmem48 PE=2 SV=1	Q8VCB1	0.00	4.41	4.42	23.33	1.04	1.07	1.06	1.05	1.22	1.06	0.00	2.29	2.30	17.38	0.95	1.01	0.90	1.04	1.16	1.06	1.00	1.04	0.98	1.04	1.19	1.06
DNA replication licensing factor MCM4 OS=Mus musculus GN=Mcm4 PE=2 SV=1	P49717	0.00	0.00	4.49	21.69	1.03	1.03	0.95	0.95	0.72	0.78	1.00	1.36	1.37	35.38	1.03	0.95	1.07	1.01	0.93	0.91	1.03	0.99	1.00	0.98	0.82	0.84

Protien identification and qunatitation results from ProteinPilot for all the analyzed samples

Name	Accession number	% FDR	Unused	Total	%Cov	114:113	115:113	116:113	118:117	119:117	121:117	% FDR	Unused	Total	%Cov	114:113	115:113	116:113	118:117	119:117	121:117	114:113	115:113	116:113	118:117	119:117	121:117
Exosome complex component RRP40 OS=Mus musculus GN=Exosc3 PE=1 SV=3	Q7TQK4	0.00	4.40	4.44	51.82	1.13	0.98	1.13	1.09	1.11	1.09	0.00	5.28	5.28	51.09	1.58	2.07	1.38	1.53	1.61	1.27	1.34	1.43	1.25	1.29	1.34	1.17
DNA-directed RNA polymerase I subunit RPA2 OS=Mus musculus GN=Polr1b PE=2 SV=2	P70700	0.00	0.00	4.41	21.32	1.07	1.00	1.00	0.92	1.01	0.95	0.00	4.54	4.54	22.82	0.94	0.90	0.85	0.84	0.82	0.86	1.00	0.95	0.92	0.88	0.91	0.90
RNA-binding protein 42 OS=Mus musculus GN=Rbm42 PE=1 SV=1	Q91V81	0.00	0.00	4.47	25.11	0.86	0.90	0.91	0.99	1.02	1.10	0.00	0.00	4.99	29.11	0.79	0.99	0.72	0.94	1.03	1.22	0.82	0.95	0.81	0.96	1.02	1.16
Nuclear transcription factor Y subunit gamma OS=Mus musculus GN=Nfyc PE=2 SV=2	P70353	0.00	0.00	4.39	18.21	0.96	1.03	1.08	0.95	1.02	1.00	0.00	4.07	4.07	26.57	0.89	0.99	1.15	0.96	1.03	0.98	0.92	1.01	1.11	0.96	1.02	0.99
CCAAT/enhancer-binding protein beta OS=Mus musculus GN=Cebpb PE=1 SV=1	P28033	0.00	0.00	4.39	29.05	0.96	1.03	1.26	1.22	2.96	2.54	0.00	5.56	5.56	46.62	1.14	1.18	1.07	2.05	4.49	2.94	1.05	1.10	1.16	1.58	3.65	2.73
Small nuclear ribonucleoprotein F OS=Mus musculus GN=Snrpf PE=2 SV=1	P62307	0.00	0.00	4.35	59.30	0.97	0.99	1.29	1.33	1.49	1.31	0.00	5.45	5.45	63.95	0.90	1.27	1.11	0.90	1.17	1.14	0.93	1.12	1.20	1.09	1.32	1.22
Enhancer of rudimentary homolog OS=Mus musculus GN=Erh PE=1 SV=1	P84089	0.00	0.00	4.31	56.73	0.87	0.72	1.56	0.28	0.67	1.08	0.00	0.00	6.29	51.92	0.84	0.72	0.73	1.21	0.79	0.95	0.86	0.72	1.07	0.59	0.73	1.01
Microtubule-associated protein 4 OS=Mus musculus GN=Map4 PE=1 SV=3	P27546	0.00	4.30	4.35	17.78	1.06	1.07	0.97	0.97	0.97	0.87	0.14	0.00	2.01	16.62	1.10	0.90	1.04	0.97	1.10	0.91	1.08	0.98	1.00	0.97	1.03	0.89
PHD finger protein 14 OS=Mus musculus GN=Phf14 PE=1 SV=1	Q9D4H9	0.00	0.00	4.33	14.53	0.96	0.99	0.95	0.99	1.03	0.98	0.00	4.71	4.72	18.39	1.84	1.92	0.70	2.61	3.28	2.99	1.33	1.38	0.82	1.61	1.84	1.71
RNA-binding protein PNO1 OS=Mus musculus GN=Pno1 PE=2 SV=1	Q9CPS7	0.00	4.30	4.30	31.45	0.90	0.92	1.05	0.94	1.29	1.10	0.00	4.83	4.84	50.81	0.88	0.90	0.87	0.86	1.00	0.91	0.89	0.91	0.95	0.90	1.14	1.00
Leucine-rich repeat and calponin homology domain-containing protein 1 OS=Mus musculus GN=Lrch1 PE=1 SV=2	P62046	0.00	0.00	3.29	27.08	1.04	0.85	0.86	0.95	0.77	0.81	0.00	0.00	2.80	23.70	1.08	0.86	0.90	0.94	0.88	0.88	1.06	0.85	0.88	0.95	0.82	0.84
Symplekin OS=Mus musculus GN=Sympk PE=1 SV=1	Q80X82	0.00	0.00	4.37	24.69	0.87	0.88	0.83	0.92	0.86	0.90	0.00	0.00	4.17	28.58	0.79	0.58	0.60	0.82	0.93	0.79	0.83	0.71	0.71	0.87	0.89	0.84
Protein FAM172A OS=Mus musculus GN=Fam172a PE=2 SV=2	Q3TNH5	0.00	0.00	4.26	27.10	1.01	0.99	1.12	0.99	0.95	1.01	0.00	2.22	2.23	35.73	1.01	1.09	0.83	1.16	1.07	0.91	1.01	1.04	0.96	1.07	1.00	0.96
Putative uncharacterized protein OS=Mus musculus GN=Fam172a PE=2 SV=1	Q3V345	0.00	0.00	2.25	30.25	1.01	0.99	1.12	0.99	0.95	1.01	0.00	0.00	1.70	49.38	1.01	1.09	0.83	1.16	1.07	0.91	1.01	1.04	0.96	1.07	1.00	0.96
Protein Vezf1 (Fragment) OS=Mus musculus GN=Vezf1 PE=4 SV=1	Q5SXC3	0.00	0.00	4.03	18.15	0.95	1.13	0.53	1.09	1.57	1.75	0.00	0.00	2.42	20.54	1.09	1.43	1.20	0.92	0.85	0.92	1.01	1.27	0.80	1.00	1.15	1.27
F-actin-capping protein subunit alpha-2 OS=Mus musculus GN=Capza2 PE=1 SV=3	P47754	0.00	0.00	4.29	38.11	1.12	0.82	0.90	0.96	0.89	0.90	0.00	4.18	8.20	45.10	1.14	0.75	1.05	1.16	1.15	0.89	1.13	0.78	0.97	1.06	1.01	0.89
Serine/threonine-protein kinase TAO1 OS=Mus musculus GN=Taok1 PE=1 SV=1	Q5F2E8	0.00	0.00	8.99	26.67	0.92	0.97	0.99	1.05	1.09	1.09	0.00	2.27	5.41	33.07	0.90	0.90	1.00	0.96	0.95	0.95	0.91	0.94	1.00	1.00	1.01	1.01
Pyruvate kinase isozymes M1/M2 OS=Mus musculus GN=Pkm PE=1 SV=4	P52480	0.00	4.23	4.23	18.64	1.05	1.06	1.07	1.05	0.91	0.92	0.00	6.79	6.80	42.56	1.69	1.50	1.56	1.63	1.02	0.31	1.33	1.26	1.29	1.31	0.96	0.53
Death-inducer obliterator 1 OS=Mus musculus GN=Dido1 PE=1 SV=4	Q8C9B9	0.00	4.20	4.23	20.08	1.11	1.00	1.10	1.02	1.00	0.96	0.00	2.68	2.71	24.25	1.11	1.09	1.14	0.99	1.11	0.95	1.11	1.04	1.12	1.00	1.05	0.96
Smad nuclear-interacting protein 1 OS=Mus musculus GN=Snip1 PE=1 SV=1	Q8BIZ6	0.00	4.20	4.20	36.55	1.10	1.10	1.06	1.00	1.00	1.00	0.00	3.13	3.13	52.22	1.12	1.05	1.05	1.01	1.04	1.06	1.11	1.07	1.05	1.00	1.02	1.03
Mediator of RNA polymerase II transcription subunit 12 OS=Mus musculus GN=Med12 PE=2 SV=1	A2AGH6	0.00	0.00	4.39	14.11	1.19	0.91	1.03	1.05	0.96	0.95	0.00	0.00	4.31	18.95	1.01	0.98	1.01	0.86	0.97	0.79	1.10	0.95	1.02	0.95	0.97	0.87
Ribonuclease P protein subunit p30 OS=Mus musculus GN=Rpp30 PE=2 SV=1	O88796	0.00	0.00	4.19	32.09	0.71	1.06	1.13	1.42	1.66	2.21	0.00	3.02	3.02	47.01	0.56	0.95	0.83	0.93	1.45	0.81	0.63	1.00	0.97	1.15	1.55	1.34
DNA-directed RNA polymerase II subunit RPB7 OS=Mus musculus GN=Polr2g PE=2 SV=1	P62488	0.00	4.19	4.19	49.42	0.97	0.96	0.97	0.93	0.90	0.89	0.00	6.12	6.12	58.14	1.27	0.95	1.00	0.69	0.88	0.74	1.11	0.96	0.99	0.80	0.89	0.81
Integrator complex subunit 8 OS=Mus musculus GN=Ints8 PE=2 SV=1	Q80V86	0.00	4.17	4.23	21.31	0.94	0.95	0.91	1.00	0.98	0.99	0.00	4.01	4.05	20.10	0.81	0.97	1.03	0.95	1.03	0.80	0.87	0.96	0.97	0.98	1.00	0.89
Serine beta-lactamase-like protein LACTB, mitochondrial OS=Mus musculus GN=Lactb PE=1 SV=1	Q9EP89	0.00	0.00	4.17	17.79	0.96	0.81	0.83	0.77	0.47	0.44	0.13	2.00	2.01	21.96	0.94	0.92	0.82	0.89	0.78	0.74	0.95	0.86	0.83	0.83	0.61	0.57
Protein syndesmos OS=Mus musculus GN=Nudt16l1 PE=1 SV=2	Q8VHN8	0.00	4.17	4.17	32.23	0.90	1.11	0.96	0.96	1.09	1.10	0.00	6.47	6.47	43.13	0.97	1.05	0.99	1.13	1.06	0.95	0.94	1.08	0.98	1.04	1.07	1.02
Anaphase-promoting complex subunit 1 OS=Mus musculus GN=Anapc1 PE=1 SV=2	P53995	0.00	0.00	4.18	12.91	0.90	1.07	0.98	1.17	1.24	1.36	0.00	2.46	2.47	17.64	0.65	0.85	0.81	1.06	1.24	1.47	0.77	0.95	0.89	1.11	1.24	1.41
40S ribosomal protein S24 OS=Mus musculus GN=Rps24 PE=1 SV=1	P62849	0.00	0.00	4.17	24.06	1.00	0.85	0.97	1.07	1.27	0.94	0.00	0.00	4.00	32.33	1.12	1.08	1.33	1.06	0.77	1.20	1.06	0.95	1.14	1.06	0.99	1.06
DNA ligase 3 OS=Mus musculus GN=Lig3 PE=1 SV=2	P97386	0.00	0.00	4.16	14.68	1.15	0.96	1.15	1.43	1.27	1.45	0.00	0.00	4.86	20.79	0.99	1.13	1.24	1.06	0.98	0.96	1.07	1.04	1.19	1.23	1.12	1.18
Telomeric repeat-binding factor 2 OS=Mus musculus GN=Terf2 PE=1 SV=3	O35144	0.00	0.00	4.16	29.57	1.08	1.12	0.97	0.74	0.71	0.65	0.00	4.98	4.99	46.95	1.22	0.97	0.95	0.84	0.59	0.13	1.15	1.04	0.96	0.79	0.65	0.29
Serine/arginine-rich splicing factor 2 OS=Mus musculus GN=Srsf2 PE=1 SV=4	Q62093	0.00	0.00	4.15	57.01	0.94	0.91	0.79	1.32	1.43	0.82	0.00	0.00	5.40	66.52	1.07	1.08	1.10	1.18	1.09	0.93	1.00	0.99	0.93	1.25	1.25	0.87
Protein Sp140 OS=Mus musculus GN=Sp140 PE=2 SV=1	Q6NSQ5	0.00	4.14	8.72	28.09	1.14	0.98	1.19	1.46	0.84	1.28	0.00	2.64	10.97	36.52	0.94	1.22	0.94	1.04	0.86	0.86	1.03	1.10	1.06	1.23	0.85	1.05
Nuclear pore complex protein Nup50 OS=Mus musculus GN=Nup50 PE=1 SV=3	Q9JIH2	0.00	4.13	4.16	38.84	1.08	1.07	0.83	1.00	0.70	0.72	0.00	10.95	10.96	34.55	1.29	1.21	0.81	1.64	0.46	0.19	1.18	1.14	0.82	1.28	0.57	0.37
F-box-like/WD repeat-containing protein TBL1X OS=Mus musculus GN=Tbl1x PE=2 SV=2	Q9QXE7	0.00	4.12	4.76	28.46	0.94	1.00	0.96	0.89	0.93	0.97	0.00	4.92	6.93	29.60	1.06	1.03	1.13	1.04	0.87	0.92	1.00	1.01	1.04	0.96	0.90	0.95
Zinc finger MYM-type protein 4 OS=Mus musculus GN=Zmym4 PE=1 SV=1	A2A791	0.00	4.12	4.12	14.07	0.98	1.01	0.95	0.90	0.96	0.96	0.00	6.86	6.88	13.69	0.91	0.97	0.93	0.94	0.99	1.01	0.95	0.99	0.94	0.92	0.98	0.99
Splicing factor 3B subunit 5 OS=Mus musculus GN=Sf3b5 PE=2 SV=1	Q923D4	0.00	0.00	4.12	39.53	1.06	1.11	1.28	0.86	1.12	0.92	0.00	4.00	4.00	38.37	1.04	0.94	1.01	0.93	0.79	0.93	1.05	1.02	1.14	0.90	0.94	0.92

Protien identification and qunatitation results from ProteinPilot for all the analyzed samples

Name	Accession number	% FDR	Unused	Total	%Cov	114:113	115:113	116:113	118:117	119:117	121:117	% FDR	Unused	Total	%Cov	114:113	115:113	116:113	118:117	119:117	121:117	114:113	115:113	116:113	118:117	119:117	121:117
Serine/arginine repetitive matrix protein 2 OS=Mus musculus GN=Srrm2 PE=1 SV=3	Q8BTI8	0.00	4.11	4.16	40.36	0.91	0.89	0.90	1.54	1.24	1.38	0.00	2.64	2.66	45.58	1.27	1.02	1.21	0.93	1.20	1.15	1.08	0.95	1.04	1.20	1.22	1.26
TFIIH basal transcription factor complex helicase XPD subunit OS=Mus musculus GN=Ercc2 PE=2 SV=2	O08811	0.00	0.00	4.26	16.32	0.86	0.86	0.88	0.87	0.95	1.17	0.00	4.37	4.57	31.45	0.77	1.01	0.98	1.14	1.05	1.01	0.81	0.93	0.93	1.00	1.00	1.09
UAP56-interacting factor OS=Mus musculus GN=Fyttd1 PE=1 SV=1	Q91Z49	0.00	4.09	4.14	34.38	1.01	0.98	0.95	0.95	0.99	1.08	0.00	4.06	4.06	38.49	1.26	1.03	1.28	1.06	0.75	0.74	1.13	1.00	1.10	1.00	0.86	0.89
RNA polymerase II-associated factor 1 homolog OS=Mus musculus GN=Paf1 PE=2 SV=1	Q8K2T8	0.00	4.09	4.10	20.75	1.08	0.86	1.00	0.88	0.82	0.81	0.00	10.08	10.10	31.96	1.45	0.69	1.18	1.60	0.87	1.00	1.25	0.77	1.09	1.19	0.85	0.90
PR domain zinc finger protein 10 OS=Mus musculus GN=Prdm10 PE=1 SV=2	Q3UTQ7	0.00	4.08	4.18	14.19	1.00	1.04	1.07	0.91	1.00	1.04	0.00	0.00	2.29	15.37	1.15	1.18	0.93	0.95	1.12	1.17	1.07	1.11	1.00	0.93	1.06	1.10
60S ribosomal protein L35 OS=Mus musculus GN=Rpl35 PE=2 SV=1	Q6ZWV7	0.00	4.08	4.08	42.28	1.19	1.06	1.03	0.93	1.09	0.95	0.00	3.46	3.46	44.72	1.24	0.83	0.96	1.28	1.60	1.10	1.21	0.94	1.00	1.09	1.32	1.02
Myosin light polypeptide 6 OS=Mus musculus GN=Myl6 PE=1 SV=3	Q60605	0.00	0.00	4.08	48.34	1.06	0.77	0.86	0.60	0.60	0.59	0.00	0.00	4.00	33.11	0.66	0.38	0.52	0.42	0.38	0.26	0.84	0.54	0.66	0.50	0.48	0.39
CAPZB3 OS=Mus musculus GN=Capzb PE=2 SV=1	A2AMV7	0.00	4.08	4.08	15.95	1.18	0.49	0.72	0.99	0.70	0.66	0.00	6.87	6.87	32.89	1.21	0.45	0.63	0.97	0.72	0.37	1.20	0.47	0.67	0.98	0.71	0.49
Engulfment and cell motility protein 1 OS=Mus musculus GN=Elmo1 PE=1 SV=2	Q8BPU7	0.00	0.00	4.13	27.51	0.95	0.98	1.02	0.95	0.95	0.95	0.00	0.00	7.06	29.85	1.02	0.98	1.06	1.09	1.04	1.09	0.98	0.98	1.04	1.02	1.00	1.02
Small nuclear ribonucleoprotein E OS=Mus musculus GN=Snrpe PE=2 SV=1	P62305	0.00	4.07	4.07	50.00	0.92	0.78	0.93	1.11	1.02	1.09	0.00	6.00	6.00	38.04	0.84	0.86	0.90	0.95	1.03	1.01	0.88	0.82	0.92	1.02	1.02	1.05
DNA replication licensing factor MCM6 OS=Mus musculus GN=Mcm6 PE=1 SV=1	P97311	0.00	0.00	4.11	17.90	0.98	1.02	0.97	1.06	0.91	0.90	0.00	3.31	3.34	38.86	0.98	1.02	0.98	1.03	1.20	0.90	0.98	1.02	0.98	1.04	1.05	0.90
DNA-directed RNA polymerases I, II, and III subunit RPABC1 OS=Mus musculus GN=Polr2e PE=2 SV=1	Q80UW8	0.00	0.00	4.05	51.43	1.13	1.14	1.16	0.93	0.93	0.93	0.00	7.39	7.39	62.38	1.13	1.13	1.10	0.96	0.95	0.95	1.13	1.13	1.13	0.95	0.94	0.94
Transcription factor PU.1 OS=Mus musculus GN=Spi1 PE=1 SV=2	P17433	0.00	0.00	4.05	18.38	0.76	0.85	0.99	0.99	1.39	1.37	0.00	4.10	4.11	32.35	0.95	1.07	0.88	0.96	1.19	0.97	0.85	0.95	0.93	0.98	1.29	1.15
Serine/threonine-protein phosphatase PP1-beta catalytic subunit OS=Mus musculus GN=Ppp1cb PE=1 SV=3	P62141	0.00	4.04	14.87	40.37	0.96	0.95	0.90	1.05	1.03	0.95	0.00	4.18	16.94	51.68	0.57	0.50	0.70	1.18	1.10	0.45	0.74	0.69	0.80	1.11	1.06	0.65
Zinc finger protein 800 OS=Mus musculus GN=Znf800 PE=1 SV=1	Q0VEE6	0.00	0.00	4.13	22.05	0.94	0.95	0.93	1.13	0.93	1.19	0.00	4.03	4.12	30.06	0.93	0.90	1.02	1.17	1.00	1.51	0.93	0.92	0.97	1.15	0.96	1.34
Ubiquitin carboxyl-terminal hydrolase 7 OS=Mus musculus GN=Usp7 PE=1 SV=1	Q6A4J8	0.00	0.00	4.10	14.51	1.19	1.12	1.08	0.95	0.82	0.80	0.00	0.00	7.13	20.04	1.58	1.36	1.34	1.06	0.83	0.44	1.37	1.23	1.20	1.00	0.83	0.59
Lysine-specific demethylase PHF2 OS=Mus musculus GN=Phf2 PE=1 SV=2	Q9WTU0	0.00	4.04	4.05	13.32	0.98	1.07	0.97	0.88	1.00	0.93	0.00	4.61	4.62	21.99	0.95	1.04	0.95	0.92	1.00	0.88	0.96	1.05	0.96	0.90	1.00	0.90
Erythrocyte band 7 integral membrane protein OS=Mus musculus GN=Stom PE=1 SV=3	P54116	0.00	4.04	4.05	32.04	1.09	0.44	0.70	0.66	0.36	0.43	0.14	2.05	2.05	50.35	1.13	0.90	0.99	0.62	0.52	0.73	1.11	0.63	0.84	0.64	0.44	0.56
Steroid hormone receptor ERR1 OS=Mus musculus GN=Esrra PE=1 SV=4	O08580	0.00	4.03	4.10	32.70	0.53	0.68	0.69	0.93	0.88	0.88	0.14	2.02	2.04	30.33	1.28	1.04	0.92	0.94	1.02	1.05	0.82	0.84	0.79	0.93	0.95	0.96
Mediator of RNA polymerase II transcription subunit 23 OS=Mus musculus GN=Med23 PE=1 SV=2	Q80YQ2	0.00	0.00	4.07	15.29	0.91	0.88	0.94	0.98	1.03	1.06	0.15	0.00	2.19	20.92	1.11	0.95	1.12	0.80	1.00	1.26	1.00	0.91	1.02	0.89	1.01	1.15
Protein SEC13 homolog OS=Mus musculus GN=Sec13 PE=2 SV=3	Q9D1M0	0.00	4.03	4.03	12.73	1.19	0.77	0.94	0.70	0.88	0.70	0.00	4.75	4.78	20.19	1.13	0.98	1.09	0.96	0.97	0.92	1.16	0.87	1.01	0.82	0.92	0.80
Transcription factor Sp1 OS=Mus musculus GN=Sp1 PE=1 SV=2	O89090	0.00	0.00	4.06	11.61	1.15	0.99	0.86	1.02	0.84	1.17	0.13	0.00	2.00	10.59	0.91	1.05	0.79	0.37	1.03	0.72	1.02	1.02	0.82	0.61	0.93	0.92
Bromodomain adjacent to zinc finger domain protein 2A OS=Mus musculus GN=Baz2a PE=1 SV=2	Q91YE5	0.00	0.00	4.04	14.08	0.95	0.97	1.01	0.96	0.98	1.09	0.00	0.00	4.46	17.63	1.01	0.95	1.05	0.95	0.96	0.90	0.98	0.96	1.03	0.95	0.97	0.99
Mediator of RNA polymerase II transcription subunit 27 OS=Mus musculus GN=Med27 PE=2 SV=2	Q9DB40	0.00	4.02	4.03	40.51	0.86	0.88	1.13	0.67	1.03	0.68	0.31	1.73	1.73	30.23	0.68	0.94	1.12	0.78	0.86	0.95	0.77	0.91	1.12	0.72	0.94	0.80
Protein Pop1 OS=Mus musculus GN=Pop1 PE=2 SV=1	Q9D4G5	0.00	4.01	4.04	18.82	1.06	0.98	1.13	1.17	1.33	1.39	0.00	7.90	7.98	30.74	1.22	1.22	1.49	1.05	1.41	0.60	1.14	1.10	1.29	1.11	1.37	0.91
Protein FAM98B OS=Mus musculus GN=Fam98b PE=2 SV=1	Q80VD1	0.00	4.01	4.03	31.00	1.14	0.95	0.95	1.17	1.00	0.91	0.00	6.00	6.00	37.53	0.97	0.98	0.97	1.10	0.99	1.02	1.05	0.96	0.96	1.13	1.00	0.96
Chromatin modification-related protein MEAF6 OS=Mus musculus GN=Meaf6 PE=2 SV=1	Q2VPQ9	0.00	4.01	4.02	41.36	0.61	1.03	1.03	0.80	0.84	0.83	0.00	6.19	6.20	42.93	0.89	0.78	0.81	0.80	0.81	0.55	0.74	0.90	0.91	0.80	0.82	0.68
Ras GTPase-activating protein-binding protein 1 OS=Mus musculus GN=G3bp1 PE=1 SV=1	P97855	0.00	0.00	4.01	33.76	1.16	1.15	0.88	1.63	1.57	0.86	0.00	6.20	6.20	21.29	0.79	1.01	0.82	1.57	0.86	0.95	0.95	1.08	0.85	1.60	1.16	0.91
Serum albumin OS=Mus musculus GN=Alb PE=1 SV=3	P07724	0.00	0.00	4.01	18.26	1.09	1.00	0.89	1.50	0.71	0.87	0.00	4.94	4.94	23.52	1.24	1.18	1.36	0.85	0.81	1.28	1.16	1.09	1.10	1.13	0.76	1.06
39S ribosomal protein L39, mitochondrial OS=Mus musculus GN=Mrpl39 PE=2 SV=4	Q9JKF7	0.00	4.01	4.01	44.05	0.93	0.93	0.81	0.76	0.74	0.59	0.00	2.33	2.33	29.76	0.96	0.95	1.03	1.00	0.94	0.89	0.95	0.94	0.91	0.87	0.84	0.72
Pre-mRNA branch site protein p14 OS=Mus musculus GN=Sf3b14 PE=2 SV=1	P59708	0.00	4.01	4.01	56.00	0.53	0.89	0.82	1.02	0.99	1.46	0.00	4.32	4.32	60.80	1.32	0.56	1.01	1.04	0.33	0.52	0.84	0.70	0.91	1.03	0.57	0.87
Plectin OS=Mus musculus GN=Plec PE=4 SV=1	E9QMZ5	0.00	4.00	425.79	74.00	1.18	0.82	0.94	1.02	0.92	1.00	0.00	0.00	425.31	77.53	1.15	0.73	1.05	1.28	1.05	1.36	1.16	0.77	0.99	1.14	0.98	1.16
Protein Atad2b OS=Mus musculus GN=Atad2b PE=3 SV=1	E9Q166	0.00	4.00	8.28	23.77	1.08	1.11	0.98	0.94	1.01	0.98	0.00	7.82	13.01	30.96	1.00	1.02	1.08	0.93	1.10	1.07	1.04	1.06	1.03	0.93	1.05	1.02
Putative RNA-binding protein Luc7-like 1 OS=Mus musculus GN=Luc7l PE=2 SV=2	Q9CYI4	0.00	4.00	6.34	39.35	1.06	1.12	1.02	0.95	1.15	0.98	0.14	2.00	4.11	38.81	0.85	1.08	0.69	1.09	0.92	1.07	0.95	1.10	0.84	1.01	1.03	1.02
F-actin-capping protein subunit alpha-1 OS=Mus musculus GN=Capza1 PE=1 SV=4	P47753	0.00	0.00	2.26	24.83	1.09	0.39	0.61	0.89	0.72	0.55	0.00	0.00	9.17	43.36	0.96	0.27	0.52	1.54	0.85	1.38	1.02	0.32	0.56	1.17	0.78	0.87
Tropomyosin alpha-3 chain OS=Mus musculus GN=Tpm3 PE=1 SV=2	P21107	0.00	0.00	2.21	30.99	0.63	0.50	0.51	0.38	0.33	0.32	0.99	0.01	1.37	39.44	0.90	0.62	0.67	0.55	0.44	0.52	0.76	0.55	0.58	0.46	0.38	0.40
Oxysterol-binding protein OS=Mus musculus GN=Osbpl8 PE=3 SV=1	G3X9N6	0.00	4.00	4.06	22.08	0.77	0.42	0.55	1.39	0.87	0.97	0.00	2.33	2.36	23.97	0.82	0.25	0.57	0.94	1.20	0.24	0.79	0.33	0.56	1.14	1.02	0.48
Twinfilin-2 OS=Mus musculus GN=Twf2 PE=1 SV=1	Q9Z0P5	0.00	4.00	4.04	32.95	0.93	0.52	0.60	1.09	0.73	1.16	0.00	0.00	4.01	33.24	0.99	1.01	0.89	0.88	0.81	0.80	0.96	0.72	0.73	0.98	0.77	0.96

Protien identification and qunatitation results from ProteinPilot for all the analyzed samples

Name	Accession number	% FDR	Unused	Total	%Cov	114:113	115:113	116:113	118:117	119:117	121:117	% FDR	Unused	Total	%Cov	114:113	115:113	116:113	118:117	119:117	121:117	114:113	115:113	116:113	118:117	119:117	121:117
40S ribosomal protein SA OS=Mus musculus GN=Rpsa PE=1 SV=4	P14206	0.00	0.00	4.03	25.08	1.24	1.21	1.27	1.43	1.17	1.03	0.00	0.00	3.49	35.93	0.93	1.25	1.12	1.37	1.46	1.27	1.07	1.23	1.19	1.40	1.31	1.14
Zinc fingers and homeoboxes protein 1 OS=Mus musculus GN=Zhx1 PE=1 SV=2	P70121	0.00	0.00	4.03	14.89	1.04	1.03	0.97	0.89	1.00	0.86	0.00	4.00	4.02	13.97	0.82	0.88	0.93	1.02	1.03	1.27	0.92	0.95	0.95	0.95	1.01	1.05
Mediator of RNA polymerase II transcription subunit 24 OS=Mus musculus GN=Med24 PE=1 SV=1	Q99K74	0.00	0.00	4.03	11.45	1.04	0.89	0.91	0.98	0.93	0.93	0.00	0.00	2.25	16.82	0.95	1.22	0.90	1.12	0.66	0.03	0.99	1.04	0.91	1.05	0.78	0.16
Ras-related protein Rab-1B OS=Mus musculus GN=Rab1b PE=1 SV=1	Q9D1G1	0.00	0.00	4.00	18.41	0.94	0.90	0.97	0.90	0.96	0.99	0.00	4.12	4.12	25.37	0.99	0.80	0.82	0.99	0.87	1.10	0.96	0.85	0.89	0.95	0.92	1.04
Ras-related protein Rab-35 OS=Mus musculus GN=Rab35 PE=1 SV=1	Q6PHN9	0.00	0.00	4.00	22.89	0.94	0.90	0.97	0.90	0.96	0.99	0.00	0.01	4.01	37.31	0.99	0.80	0.82	0.99	0.87	1.10	0.96	0.85	0.89	0.95	0.92	1.04
Protein Rab1 OS=Mus musculus GN=Rab1 PE=4 SV=1	Q5SW88	0.00	0.00	4.00	18.81	0.94	0.90	0.97	0.90	0.96	0.99	0.00	0.01	4.01	18.81	0.99	0.80	0.82	0.99	0.87	1.10	0.96	0.85	0.89	0.95	0.92	1.04
Ras-related protein Rab-1A OS=Mus musculus GN=Rab1A PE=1 SV=3	P62821	0.00	0.00	4.00	18.54	0.94	0.90	0.97	0.90	0.96	0.99	0.00	0.01	4.01	18.54	0.99	0.80	0.82	0.99	0.87	1.10	0.96	0.85	0.89	0.95	0.92	1.04
Ras-related protein Rab-10 OS=Mus musculus GN=Rab10 PE=1 SV=1	P61027	0.00	0.00	4.03	28.00	0.94	0.90	0.97	0.90	0.96	0.99	0.00	0.00	4.02	37.00	0.99	0.80	0.82	0.99	0.87	1.10	0.96	0.85	0.89	0.95	0.92	1.04
Ras-related protein Rab-8A OS=Mus musculus GN=Rab8a PE=1 SV=2	P55258	0.00	0.00	4.00	17.87	0.94	0.90	0.97	0.90	0.96	0.99	0.00	0.00	4.01	38.16	0.99	0.80	0.82	0.99	0.87	1.10	0.96	0.85	0.89	0.95	0.92	1.04
Ras-related protein Rab-15 OS=Mus musculus GN=Rab15 PE=1 SV=1	Q8K386	0.00	0.00	4.00	25.47	0.94	0.90	0.97	0.90	0.96	0.99	0.00	0.00	4.00	38.68	0.99	0.80	0.82	0.99	0.87	1.10	0.96	0.85	0.89	0.95	0.92	1.04
Ras-related protein Rab-8B OS=Mus musculus GN=Rab8b PE=1 SV=1	P61028	0.00	0.00	4.00	36.23	0.94	0.90	0.97	0.90	0.96	0.99	0.00	0.00	4.00	21.26	0.99	0.80	0.82	0.99	0.87	1.10	0.96	0.85	0.89	0.95	0.92	1.04
DNA replication licensing factor MCM2 OS=Mus musculus GN=Mcm2 PE=1 SV=3	P97310	0.22	0.00	4.02	23.67	0.98	1.06	0.97	1.08	0.81	0.76	0.00	5.42	5.44	33.85	1.09	1.05	1.33	1.17	0.95	0.73	1.03	1.05	1.14	1.12	0.87	0.74
Protein Znf512b OS=Mus musculus GN=Znf512b PE=4 SV=1	B7ZCR6	0.22	0.00	4.02	16.34	1.20	1.07	1.03	0.79	0.84	0.74	0.14	0.00	2.05	14.50	1.00	1.16	1.34	1.02	1.03	1.10	1.10	1.11	1.17	0.90	0.93	0.90
Histidine--tRNA ligase, cytoplasmic OS=Mus musculus GN=Hars PE=2 SV=2	Q61035	0.22	0.00	4.01	33.79	0.72	1.13	0.80	1.26	1.19	0.83	0.00	2.52	2.54	22.20	1.00	1.18	1.07	1.24	1.24	1.16	0.85	1.15	0.92	1.25	1.21	0.98
DNA-directed RNA polymerase II subunit RPB11 OS=Mus musculus GN=Polr2j PE=2 SV=1	O08740	0.21	4.00	4.01	53.85	1.39	1.29	1.17	1.11	1.13	1.13	0.13	2.00	2.00	37.61	1.17	1.01	0.90	0.98	1.27	0.54	1.28	1.14	1.03	1.04	1.20	0.78
Exosome complex component CSL4 OS=Mus musculus GN=Exosc1 PE=2 SV=1	Q9DAA6	0.21	4.00	4.01	36.41	1.01	1.08	1.10	1.02	1.17	1.16	0.00	5.82	5.82	36.92	1.24	1.22	1.31	0.82	0.93	0.42	1.12	1.15	1.20	0.92	1.04	0.70
Eukaryotic translation initiation factor 5A-1 OS=Mus musculus GN=Eif5a PE=1 SV=2	P63242	0.21	4.00	4.01	28.57	0.91	0.82	0.87	1.12	0.90	0.79	0.00	3.53	3.54	35.06	1.06	1.10	0.95	1.15	1.04	0.64	0.98	0.95	0.91	1.13	0.97	0.71
Eukaryotic translation initiation factor 5A-2 OS=Mus musculus GN=Eif5a2 PE=2 SV=3	Q8BGY2	0.21	0.00	2.01	20.92	0.91	0.82	0.87	1.12	0.90	0.79	0.00	0.00	2.01	30.07	1.06	1.10	0.95	1.15	1.04	0.64	0.98	0.95	0.91	1.13	0.97	0.71
Neutrophil cytosol factor 1 OS=Mus musculus GN=Ncf1 PE=1 SV=3	Q09014	0.21	0.00	4.00	24.87	0.95	1.04	0.91	1.04	1.01	0.93	0.00	0.00	3.61	35.38	1.09	0.67	1.57	0.90	0.73	1.57	1.01	0.83	1.20	0.97	0.86	1.21
Beta-hexosaminidase subunit alpha OS=Mus musculus GN=Hexa PE=2 SV=2	P29416	0.21	0.00	4.00	14.58	0.87	0.96	0.89	0.99	0.90	0.88	0.00	0.00	4.04	20.08	0.81	0.90	0.89	1.21	0.96	1.00	0.84	0.93	0.89	1.10	0.93	0.94
DNA-directed RNA polymerase II subunit RPB3 OS=Mus musculus GN=Polr2c PE=2 SV=1	Q99M46	0.21	0.00	4.00	19.64	1.01	0.90	1.07	0.93	0.96	1.11	0.00	0.00	8.00	28.00	1.01	0.97	0.88	0.85	0.72	0.81	1.01	0.93	0.97	0.89	0.84	0.95
DNA-directed RNA polymerase I subunit RPA43 OS=Mus musculus GN=Twistnb PE=1 SV=1	Q78WZ7	0.21	0.00	4.00	17.58	1.07	1.03	1.04	0.95	0.90	0.93	0.00	6.77	6.77	25.45	1.00	1.06	0.96	0.97	1.00	0.89	1.03	1.04	1.00	0.96	0.95	0.91
60S acidic ribosomal protein P2 OS=Mus musculus GN=Rplp2 PE=1 SV=3	P99027	0.21	4.00	4.00	49.57	0.93	0.65	0.84	0.99	0.82	0.83	0.00	10.00	10.00	63.48	1.08	0.78	0.93	1.18	0.81	0.48	1.00	0.71	0.88	1.08	0.82	0.63
Histone H2A type 1-F OS=Mus musculus GN=Hist1h2af PE=1 SV=3	Q8CGP5	0.21	0.00	57.14	90.00	0.86	0.96	1.02	0.88	1.20	1.13	0.00	4.77	58.03	83.85	0.64	0.70	0.30	0.46	1.01	1.14	0.74	0.82	0.55	0.64	1.10	1.13
Histone H2A type 3 OS=Mus musculus GN=Hist3h2a PE=1 SV=3	Q8BFU2	0.21	0.00	58.45	88.46	0.86	0.96	1.02	0.88	1.20	1.13	0.00	0.00	59.52	85.38	0.64	0.70	0.30	0.46	1.01	1.14	0.74	0.82	0.55	0.64	1.10	1.13
Histone H2A type 1 OS=Mus musculus GN=Hist1h2ab PE=1 SV=3	P22752	0.21	0.00	58.45	93.08	0.86	0.96	1.02	0.88	1.20	1.13	0.00	0.00	59.49	83.85	0.64	0.70	0.30	0.46	1.01	1.14	0.74	0.82	0.55	0.64	1.10	1.13
Histone H2A type 1-H OS=Mus musculus GN=Hist1h2ah PE=1 SV=3	Q8CGP6	0.21	0.00	57.14	91.41	0.86	0.96	1.02	0.88	1.20	1.13	0.00	0.00	57.49	82.03	0.64	0.70	0.30	0.46	1.01	1.14	0.74	0.82	0.55	0.64	1.10	1.13
Histone H2A type 1-K OS=Mus musculus GN=Hist1h2ak PE=1 SV=3	Q8CGP7	0.21	0.00	56.56	85.38	0.86	0.96	1.02	0.88	1.20	1.13	0.00	0.00	55.70	79.23	0.64	0.70	0.30	0.46	1.01	1.14	0.74	0.82	0.55	0.64	1.10	1.13
Histone H2A OS=Mus musculus GN=Hist1h2aa PE=2 SV=1	Q8CGP4	0.21	0.00	45.76	61.24	0.86	0.96	1.02	0.88	1.20	1.13	0.00	0.00	45.47	79.84	0.64	0.70	0.30	0.46	1.01	1.14	0.74	0.82	0.55	0.64	1.10	1.13
Guanine nucleotide-binding protein subunit beta-2-like 1 OS=Mus musculus GN=Gnb2l1 PE=1 SV=3	P68040	0.21	3.91	3.91	23.66	1.05	0.85	1.12	1.71	1.15	0.88	0.00	5.12	5.14	36.28	1.21	1.34	1.20	1.37	0.90	0.63	1.13	1.07	1.16	1.53	1.01	0.74
Polynucleotide 5'-hydroxyl-kinase NOL9 OS=Mus musculus GN=Nol9 PE=1 SV=1	Q3TZX8	0.21	3.90	3.91	21.71	1.11	1.17	1.20	1.39	1.66	1.66	0.00	5.71	5.73	31.93	1.11	0.90	1.14	1.64	2.54	3.10	1.11	1.03	1.17	1.51	2.05	2.27
Nurim OS=Mus musculus GN=Nrm PE=2 SV=1	Q8VC65	0.21	3.88	3.88	20.99	0.74	0.82	0.96	0.81	0.97	1.08	0.00	5.82	5.82	26.34	0.82	0.95	0.80	0.84	0.93	1.20	0.78	0.89	0.88	0.82	0.95	1.14
Replication factor C subunit 5 OS=Mus musculus GN=Rfc5 PE=2 SV=1	Q9D0F6	0.21	0.00	3.87	33.63	1.00	0.95	1.01	0.96	0.86	0.82	0.00	5.82	5.82	55.75	1.17	1.07	0.95	0.80	0.92	0.76	1.08	1.00	0.98	0.88	0.89	0.79
Beta-catenin-like protein 1 OS=Mus musculus GN=Ctnnbl1 PE=1 SV=1	Q9CWL8	0.21	0.00	3.87	25.58	1.19	1.06	0.95	0.86	0.89	0.86	0.00	5.01	5.01	31.26	1.04	0.83	0.86	0.65	0.19	0.13	1.11	0.94	0.91	0.75	0.41	0.33
Forkhead box protein P1 OS=Mus musculus GN=Foxp1 PE=1 SV=1	P58462	0.21	0.00	3.70	22.70	0.88	0.91	1.04	1.12	1.60	1.72	0.00	0.00	9.04	32.20	1.21	1.11	1.49	0.74	1.14	1.34	1.03	1.00	1.24	0.91	1.35	1.52
Signal-transducing adaptor protein 1 OS=Mus musculus GN=Stap1 PE=1 SV=1	Q9JM90	0.21	3.84	3.84	19.87	0.91	1.08	1.14	0.94	1.14	1.26	0.98	1.33	1.34	23.57	1.07	0.88	0.64	0.89	1.43	1.19	0.99	0.97	0.86	0.91	1.28	1.22
Arginine and glutamate-rich protein 1 OS=Mus musculus GN=Arglu1 PE=1 SV=2	Q3UL36	0.21	3.83	5.35	56.46	1.47	1.00	1.20	0.94	0.48	0.50	0.00	6.00	6.11	49.45	1.16	0.82	1.28	0.94	1.00	0.87	1.31	0.91	1.24	0.94	0.70	0.66

Protien identification and qunatitation results from ProteinPilot for all the analyzed samples

Name	Accession number	% FDR	Unused	Total	%Cov	114:113	115:113	116:113	118:117	119:117	121:117	% FDR	Unused	Total	%Cov	114:113	115:113	116:113	118:117	119:117	121:117	114:113	115:113	116:113	118:117	119:117	121:117
Probable dimethyladenosine transferase OS=Mus musculus GN=Dimt1 PE=2 SV=1	Q9D0D4	0.21	3.82	3.83	39.62	0.63	0.64	0.85	0.95	1.27	0.15	0.00	7.92	7.93	57.19	0.97	0.91	1.03	0.74	1.03	0.33	0.78	0.76	0.93	0.84	1.14	0.22
Interferon-stimulated 20 kDa exonuclease-like 2 OS=Mus musculus GN=Isg20l2 PE=2 SV=2	Q3U1G5	0.21	3.82	3.82	26.36	0.98	1.04	1.18	0.68	0.90	0.78	0.00	5.06	5.07	50.27	0.95	1.09	0.95	0.95	1.07	0.93	0.97	1.06	1.06	0.81	0.98	0.85
Unconventional myosin-Ie OS=Mus musculus GN=Myo1e PE=1 SV=1	E9Q634	0.21	3.75	3.81	22.76	1.15	0.49	0.65	1.04	1.09	1.09	0.00	8.52	8.56	37.40	1.08	0.71	0.76	0.77	1.08	0.69	1.11	0.59	0.70	0.90	1.08	0.86
Myosin IF OS=Mus musculus GN=Myo1f PE=4 SV=1	Q8CG29	0.21	0.02	2.18	21.13	1.15	0.49	0.65	1.04	1.09	1.09	0.72	1.54	2.01	27.05	0.95	0.78	0.82	0.93	0.79	0.72	1.05	0.62	0.73	0.98	0.93	0.89
Echinoderm microtubule-associated protein-like 3 OS=Mus musculus GN=Eml3 PE=2 SV=1	Q8VC03	0.21	3.73	3.74	18.73	1.06	1.12	1.06	0.96	0.95	0.95	0.00	4.04	4.05	21.52	1.14	1.22	1.04	0.95	1.03	0.83	1.10	1.17	1.05	0.95	0.99	0.89
B-cell CLL/lymphoma 7 protein family member B OS=Mus musculus GN=Bcl7b PE=1 SV=1	Q921K9	0.21	0.00	3.73	27.23	0.93	1.03	1.05	1.08	1.20	1.20	0.00	4.13	4.14	40.59	0.79	0.87	0.95	0.93	0.64	1.01	0.86	0.95	1.00	1.00	0.88	1.10
ATP-dependent RNA helicase DDX1 OS=Mus musculus GN=Ddx1 PE=1 SV=1	Q91VR5	0.21	0.00	3.71	17.43	0.96	0.99	0.92	1.06	0.92	0.92	0.00	19.59	19.61	39.19	0.96	1.04	1.16	2.88	2.56	0.36	0.96	1.01	1.03	1.75	1.53	0.57
Cyclic AMP-dependent transcription factor ATF-3 OS=Mus musculus GN=Atf3 PE=2 SV=1	Q60765	0.21	0.00	3.84	35.91	0.82	0.87	0.95	1.14	1.34	2.54	0.15	2.16	2.17	34.25	1.85	1.20	0.86	0.83	1.00	2.31	1.23	1.02	0.90	0.97	1.16	2.42
H/ACA ribonucleoprotein complex subunit 3 OS=Mus musculus GN=Nop10 PE=3 SV=1	Q9CQS2	0.21	3.70	3.70	60.94	0.84	0.95	1.01	0.99	1.14	1.14	0.00	3.16	3.16	59.38	0.69	0.79	0.66	0.89	0.11	1.38	0.76	0.87	0.82	0.94	0.35	1.25
Nesprin-1 OS=Mus musculus GN=Syne1 PE=1 SV=2	Q6ZWR6	0.21	3.69	5.69	17.85	1.06	1.08	1.03	0.82	0.90	0.95	0.00	0.00	5.48	24.15	1.02	0.98	1.05	0.92	1.00	0.79	1.04	1.03	1.04	0.87	0.95	0.87
F-box only protein 28 OS=Mus musculus GN=Fbxo28 PE=2 SV=1	Q8BIG4	0.21	3.64	3.67	35.60	1.20	1.20	1.18	0.94	1.04	1.04	0.00	3.14	3.16	42.39	1.11	1.00	0.99	1.10	0.95	1.08	1.15	1.10	1.08	1.01	1.00	1.06
Protein dpy-30 homolog OS=Mus musculus GN=Dpy30 PE=1 SV=1	Q99LT0	0.21	3.62	3.63	27.27	1.03	0.98	1.08	0.90	0.95	0.89	0.14	2.01	2.02	44.44	0.99	0.91	1.00	1.06	1.09	0.94	1.01	0.95	1.04	0.98	1.01	0.91
U6 snRNA-associated Sm-like protein LSm6 OS=Mus musculus GN=Lsm6 PE=3 SV=1	P62313	0.21	0.00	3.61	45.00	0.98	0.94	0.98	0.87	1.01	1.03	0.00	3.09	3.10	56.25	1.08	1.01	1.05	1.00	1.02	1.04	1.03	0.97	1.01	0.93	1.01	1.03
Peptidyl-prolyl cis-trans isomerase E OS=Mus musculus GN=Ppie PE=2 SV=2	Q9QZH3	0.21	3.59	3.59	21.26	0.93	0.96	1.11	1.03	1.25	1.10	0.00	6.23	6.24	40.86	1.07	0.99	0.97	1.11	1.02	1.08	1.00	0.98	1.04	1.07	1.13	1.09
DNA helicase INO80 OS=Mus musculus GN=Ino80 PE=2 SV=2	Q6ZPV2	0.21	3.58	3.62	21.87	0.96	1.12	0.95	1.00	1.18	1.33	0.00	4.15	4.16	25.66	1.20	1.56	0.70	0.50	0.98	1.18	1.08	1.32	0.81	0.71	1.08	1.25
Elongation factor 1-delta OS=Mus musculus GN=Eef1d PE=1 SV=3	P57776	0.21	0.00	2.00	24.56	0.93	0.90	1.07	1.66	1.57	1.26	0.00	0.00	3.46	41.64	0.95	0.94	0.80	1.36	1.34	0.56	0.94	0.92	0.92	1.50	1.45	0.84
Zinc finger X-chromosomal protein OS=Mus musculus GN=Zfx PE=1 SV=2	P17012	0.21	0.00	3.52	8.13	1.01	1.01	1.04	0.89	0.92	0.89	0.00	2.24	2.24	14.39	0.93	1.02	0.98	0.99	1.07	1.09	0.97	1.01	1.01	0.94	0.99	0.98
Zinc finger autosomal protein OS=Mus musculus GN=Zfa PE=2 SV=1	P23607	0.20	0.00	3.52	7.95	1.01	1.01	1.04	0.89	0.92	0.89	0.00	0.00	2.24	13.48	0.93	1.02	0.98	0.99	1.07	1.09	0.97	1.01	1.01	0.94	0.99	0.98
Replication protein A 70 kDa DNA-binding subunit OS=Mus musculus GN=Rpa1 PE=2 SV=1	Q8VEE4	0.20	0.00	3.50	26.16	1.28	1.05	1.10	1.05	1.07	0.96	0.00	0.00	4.17	30.34	1.66	0.77	0.96	1.02	1.08	0.08	1.46	0.90	1.03	1.03	1.07	0.28
Malignant T-cell-amplified sequence 1 OS=Mus musculus GN=Mcts1 PE=2 SV=1	Q9DB27	0.20	3.42	3.44	22.65	1.11	1.00	1.19	0.80	0.72	0.78	0.00	4.14	4.14	47.51	1.00	0.90	0.83	0.82	0.62	0.79	1.05	0.95	1.00	0.81	0.67	0.79
DnaJ homolog subfamily A member 2 OS=Mus musculus GN=Dnaja2 PE=1 SV=1	Q9QYJ0	0.20	0.00	3.41	16.99	1.12	1.09	0.97	1.10	0.96	0.95	0.15	2.12	2.13	13.35	1.11	1.07	1.08	1.02	0.98	0.95	1.11	1.08	1.02	1.06	0.97	0.95
CGG triplet repeat-binding protein 1 OS=Mus musculus GN=Cggbp1 PE=2 SV=1	Q8BHG9	0.20	3.40	3.40	29.34	0.85	0.88	0.86	0.89	0.85	0.83	0.00	3.70	3.73	47.90	0.91	0.94	0.86	1.09	0.84	0.02	0.88	0.91	0.86	0.98	0.84	0.14
Integrator complex subunit 7 OS=Mus musculus GN=Ints7 PE=1 SV=1	Q7TQK1	0.20	3.39	3.45	25.57	1.05	0.87	0.88	0.95	0.86	0.91	0.00	14.38	14.40	34.99	0.97	0.95	1.00	0.96	0.95	0.99	1.01	0.91	0.94	0.96	0.91	0.95
Actin-related protein 6 OS=Mus musculus GN=Actr6 PE=2 SV=2	Q9D864	0.20	3.37	3.38	20.45	0.84	0.89	0.87	0.89	0.97	1.08	0.00	6.07	6.07	20.20	0.90	1.04	1.01	1.00	1.10	1.13	0.87	0.96	0.94	0.94	1.03	1.10
E3 ubiquitin-protein ligase RING2 OS=Mus musculus GN=Rnf2 PE=1 SV=1	Q9CQJ4	0.20	3.35	3.43	21.13	1.15	1.01	1.02	1.03	1.03	1.02	0.00	4.44	4.46	35.71	0.89	0.91	0.95	1.13	1.15	1.20	1.01	0.96	0.98	1.08	1.09	1.11
Keratin, type I cytoskeletal 10 OS=Mus musculus GN=Krt10 PE=1 SV=3	P02535	0.20	3.35	3.39	31.05	0.55	0.65	0.42	0.49	0.53	0.51	0.13	0.00	2.03	39.65	1.05	1.03	1.04	0.75	0.76	0.64	0.76	0.82	0.66	0.61	0.64	0.57
Cell growth-regulating nucleolar protein OS=Mus musculus GN=Lyar PE=1 SV=2	Q08288	0.20	3.34	3.52	23.20	1.24	1.13	0.99	0.90	0.82	0.86	0.00	2.22	2.39	28.09	1.02	1.08	1.01	1.00	1.08	1.10	1.12	1.10	1.00	0.95	0.94	0.97
Zinc finger CCCH domain-containing protein 18 OS=Mus musculus GN=Zc3h18 PE=1 SV=1	Q0P678	0.20	0.00	3.36	32.70	1.01	0.96	0.84	0.94	0.96	0.86	0.00	0.00	2.45	30.17	0.98	0.90	1.08	1.32	1.92	1.39	1.00	0.93	0.95	1.11	1.36	1.10
Transcription initiation factor TFIID subunit 9 OS=Mus musculus GN=Taf9 PE=2 SV=1	Q8VI33	0.27	3.33	3.34	50.76	1.20	1.05	1.10	0.71	0.86	0.74	0.14	2.04	2.19	38.64	1.07	0.87	1.15	0.96	0.83	0.71	1.13	0.95	1.12	0.83	0.84	0.72
Transcription initiation factor TFIID subunit 9B OS=Mus musculus GN=Taf9b PE=1 SV=2	Q6NZA9	0.27	0.00	2.01	24.10	1.20	1.05	1.10	0.71	0.86	0.74	0.14	0.00	2.15	35.34	1.07	0.87	1.15	0.96	0.83	0.71	1.13	0.95	1.12	0.83	0.84	0.72
KAT8 regulatory NSL complex subunit 3 OS=Mus musculus GN=Kansl3 PE=2 SV=1	A2RSY1	0.27	3.32	3.39	19.71	1.10	1.08	1.10	0.95	0.97	0.91	0.00	2.43	2.45	22.37	0.93	0.97	0.82	0.91	1.04	0.90	1.01	1.02	0.95	0.93	1.00	0.90
Eukaryotic translation initiation factor 2A OS=Mus musculus GN=Eif2a PE=2 SV=2	Q8BJW6	0.27	3.31	3.32	17.56	0.95	0.90	0.90	0.95	0.98	0.95	0.00	3.11	3.12	20.65	1.87	3.60	1.98	2.73	4.25	2.00	1.34	1.80	1.34	1.61	2.04	1.38
Origin recognition complex subunit 4 OS=Mus musculus GN=Orc4 PE=1 SV=2	O88708	0.27	0.00	3.35	24.94	1.32	1.22	1.14	0.90	0.87	0.79	0.00	2.69	2.72	38.11	1.06	0.96	0.99	1.01	1.03	0.78	1.18	1.09	1.06	0.95	0.95	0.79
40S ribosomal protein S5 OS=Mus musculus GN=Rps5 PE=2 SV=3	P97461	0.27	0.00	3.31	62.25	0.89	0.93	0.95	1.09	1.09	1.05	0.00	0.00	6.63	52.45	0.89	0.65	0.49	1.34	1.64	1.50	0.89	0.78	0.68	1.21	1.34	1.25
Lysozyme C-2 OS=Mus musculus GN=Lyz2 PE=1 SV=2	P08905	0.27	3.30	3.31	46.62	0.94	0.84	0.84	1.39	0.82	0.46	0.00	3.22	3.23	37.84	0.74	0.86	0.65	1.37	0.81	0.65	0.83	0.85	0.74	1.38	0.81	0.55
Nucleus accumbens-associated protein 1 OS=Mus musculus GN=Nacc1 PE=1 SV=1	Q7TSZ8	0.27	3.30	3.31	12.45	1.21	1.07	1.02	0.95	0.95	0.90	0.15	2.11	2.12	10.31	0.97	1.19	1.09	1.05	1.05	1.18	1.09	1.13	1.05	1.00	1.00	1.03
MAD2L1-binding protein OS=Mus musculus GN=Mad2l1bp PE=2 SV=2	Q9DCX1	0.27	0.00	3.27	18.84	0.88	0.96	0.92	1.12	0.99	1.04	0.15	0.00	2.13	25.72	1.07	1.17	1.09	0.99	1.01	0.96	0.97	1.06	1.00	1.05	1.00	1.00

Protien identification and qunatitation results from ProteinPilot for all the analyzed samples

Name	Accession number	% FDR	Unused	Total	%Cov	114:113	115:113	116:113	118:117	119:117	121:117	% FDR	Unused	Total	%Cov	114:113	115:113	116:113	118:117	119:117	121:117	114:113	115:113	116:113	118:117	119:117	121:117
Polyamine-modulated factor 1 OS=Mus musculus GN=Pmf1 PE=1 SV=1	Q9CPV5	0.27	3.23	3.23	16.34	0.92	1.06	1.08	0.92	0.90	0.88	0.98	1.31	1.31	42.08	0.84	0.93	0.70	0.89	1.06	1.08	0.88	0.99	0.87	0.90	0.98	0.97
Sorting nexin-8 OS=Mus musculus GN=Snx8 PE=2 SV=1	Q8CFD4	0.27	3.16	3.17	29.63	0.72	0.82	0.86	0.89	0.82	0.77	0.14	0.00	2.07	29.41	0.91	0.88	0.92	0.94	1.03	0.79	0.81	0.85	0.89	0.91	0.92	0.78
Kinetochore-associated protein DSN1 homolog OS=Mus musculus GN=Dsn1 PE=2 SV=1	Q9CYC5	0.27	3.16	3.17	28.16	0.93	1.07	1.07	0.94	0.98	0.90	0.00	2.95	2.95	33.62	1.00	1.03	1.03	1.01	0.79	0.82	0.96	1.05	1.05	0.97	0.88	0.86
Integrator complex subunit 11 OS=Mus musculus GN=Cpsf3l PE=2 SV=1	Q9CWS4	0.27	3.15	3.25	18.50	0.78	0.89	0.85	0.97	0.98	0.95	0.13	2.00	2.02	23.17	0.97	1.04	0.81	0.92	0.90	1.10	0.87	0.96	0.83	0.95	0.94	1.02
rRNA-processing protein FCF1 homolog OS=Mus musculus GN=Fcf1 PE=2 SV=2	Q9CTH6	0.27	0.00	3.16	23.23	0.80	0.91	0.89	0.97	1.14	1.24	0.00	0.00	4.80	28.79	0.73	0.70	0.74	1.25	1.27	1.66	0.77	0.80	0.81	1.10	1.20	1.43
Transcription elongation factor B polypeptide 2 OS=Mus musculus GN=Tceb2 PE=1 SV=1	P62869	0.26	3.15	3.15	36.44	1.19	0.92	1.09	0.93	1.08	1.02	0.00	0.00	4.11	33.90	1.36	0.78	1.15	1.13	1.22	0.58	1.27	0.85	1.12	1.02	1.15	0.77
Dual specificity protein kinase CLK3 OS=Mus musculus GN=Clk3 PE=1 SV=2	O35492	0.26	3.13	3.15	29.15	0.94	1.03	0.98	0.95	0.97	0.90	0.00	4.76	4.77	33.54	1.28	1.11	1.29	1.14	1.22	0.47	1.10	1.07	1.13	1.04	1.09	0.65
Kinesin-like protein KIF18B OS=Mus musculus GN=Kif18b PE=2 SV=2	Q6PFD6	0.26	3.12	3.16	11.63	1.05	1.11	1.07	0.90	0.97	1.01	0.00	4.47	4.52	20.14	1.03	0.96	1.07	0.74	0.79	0.85	1.04	1.03	1.07	0.82	0.88	0.92
Transcription initiation factor IIB OS=Mus musculus GN=Gtf2b PE=1 SV=1	P62915	0.26	0.00	3.11	22.78	0.94	0.95	0.90	0.82	0.91	0.84	0.00	2.45	2.45	44.94	1.31	0.98	1.07	1.03	1.05	0.81	1.11	0.97	0.98	0.92	0.98	0.82
Putative RNA-binding protein 3 OS=Mus musculus GN=Rbm3 PE=1 SV=1	O89086	0.26	0.00	3.11	53.59	0.78	1.02	1.32	1.38	1.49	0.45	0.00	0.00	4.00	71.24	0.59	0.74	0.33	1.05	0.31	0.68	0.68	0.87	0.66	1.20	0.68	0.55
DNA-directed RNA polymerases I, II, and III subunit RPABC3 OS=Mus musculus GN=Polr2h PE=2 SV=3	Q923G2	0.26	3.10	3.10	37.33	1.02	0.99	0.93	0.86	0.89	0.91	0.00	6.11	6.11	66.00	1.00	0.95	0.92	0.98	0.97	1.09	1.01	0.97	0.92	0.92	0.93	1.00
Mediator of RNA polymerase II transcription subunit 14 OS=Mus musculus GN=Med14 PE=1 SV=1	A2ABV5	0.26	3.05	3.28	19.40	1.04	1.19	1.00	0.80	0.91	0.71	0.71	1.45	1.72	25.98	0.49	0.72	1.24	1.20	0.93	2.70	0.71	0.93	1.11	0.98	0.92	1.39
Complement component 1 Q subcomponent-binding protein, mitochondrial OS=Mus musculus GN=C1qbp PE=2 SV=1	Q8R5L1	0.26	3.05	3.06	30.47	1.11	1.07	1.27	1.21	1.33	1.24	0.00	5.41	5.42	54.12	0.79	0.99	0.82	1.96	0.72	0.69	0.94	1.03	1.02	1.54	0.98	0.92
C-terminal-binding protein 2 OS=Mus musculus GN=Ctbp2 PE=1 SV=2	P56546	0.26	0.00	6.64	38.65	0.98	0.97	1.09	1.24	1.18	1.47	0.14	0.00	5.75	46.29	0.77	1.06	0.77	1.46	1.50	1.67	0.87	1.01	0.91	1.34	1.33	1.57
Nuclear pore complex protein Nup88 OS=Mus musculus GN=Nup88 PE=2 SV=1	Q8CEC0	0.26	3.04	3.09	29.08	1.03	0.96	1.00	0.99	0.94	0.90	0.00	5.82	5.91	25.10	0.90	0.91	0.90	1.01	1.04	0.98	0.96	0.94	0.95	1.00	0.99	0.94
DnaJ homolog subfamily A member 1 OS=Mus musculus GN=Dnaja1 PE=1 SV=1	P63037	0.26	0.00	3.04	25.19	0.94	0.93	0.95	1.10	1.14	1.10	0.00	3.16	3.17	24.94	1.84	1.32	1.82	1.61	1.47	1.04	1.31	1.11	1.31	1.33	1.29	1.07
Protein FRG1 OS=Mus musculus GN=Frg1 PE=1 SV=2	P97376	0.26	0.00	3.01	32.56	1.11	1.22	0.89	0.90	1.15	1.18	0.00	4.70	4.70	27.91	0.93	0.95	0.90	0.98	1.04	0.96	1.01	1.08	0.90	0.94	1.09	1.07
26S proteasome non-ATPase regulatory subunit 11 OS=Mus musculus GN=Psmd11 PE=1 SV=3	Q8BG32	0.26	0.00	3.00	36.97	0.97	0.59	0.96	0.58	1.12	1.47	0.15	2.10	2.11	30.33	0.95	1.05	1.10	0.97	1.04	1.20	0.96	0.78	1.03	0.75	1.08	1.33
C->U-editing enzyme APOBEC-1 OS=Mus musculus GN=Apobec1 PE=1 SV=1	P51908	0.26	0.00	2.97	21.40	0.82	0.91	1.10	1.29	0.85	0.78	0.00	6.00	6.00	31.88	0.90	0.86	0.75	1.41	0.91	0.04	0.86	0.88	0.91	1.35	0.88	0.19
SH3 and PX domain-containing protein 2B OS=Mus musculus GN=Sh3pxd2b PE=1 SV=1	A2AAY5	0.26	0.00	3.06	26.10	1.09	1.03	1.12	1.04	1.05	1.00	0.00	4.22	4.28	30.73	0.99	1.05	0.94	1.07	1.32	1.18	1.04	1.04	1.02	1.05	1.17	1.09
Condensin-2 complex subunit D3 OS=Mus musculus GN=Ncapd3 PE=1 SV=3	Q6ZQK0	0.26	0.00	3.06	16.73	0.93	0.87	1.09	1.01	0.95	0.90	0.00	2.22	2.25	18.53	1.10	1.01	0.99	0.96	0.91	0.90	1.01	0.94	1.04	0.99	0.93	0.90
Histone-lysine N-methyltransferase SUV39H1 OS=Mus musculus GN=Suv39h1 PE=1 SV=1	O54864	0.26	0.00	2.95	15.78	1.20	1.63	1.91	0.84	1.15	0.91	0.31	1.75	1.76	20.63	0.76	0.98	1.08	1.22	1.32	1.12	0.95	1.26	1.43	1.01	1.23	1.01
Anaphase-promoting complex subunit 2 OS=Mus musculus GN=Anapc2 PE=1 SV=2	Q8BZQ7	0.26	0.00	3.03	24.85	0.91	0.90	0.96	1.02	1.01	1.07	0.00	7.52	7.56	31.06	0.96	1.09	1.09	1.03	1.11	1.07	0.94	0.99	1.02	1.02	1.06	1.07
DNA-directed RNA polymerase I subunit RPA49 OS=Mus musculus GN=Polr1e PE=1 SV=2	Q8K202	0.26	2.90	2.93	28.01	0.83	0.98	0.86	0.97	0.95	0.97	0.00	8.02	8.04	39.42	0.85	1.01	0.90	1.01	0.94	0.95	0.84	1.00	0.87	0.99	0.94	0.96
60S ribosomal protein L26 OS=Mus musculus GN=Rpl26 PE=2 SV=1	P61255	0.26	0.00	2.88	45.52	1.00	0.87	1.25	1.24	1.46	1.57	0.00	0.00	6.30	42.07	1.08	0.92	0.90	1.57	1.75	1.94	1.04	0.90	1.06	1.39	1.60	1.75
Replication factor C subunit 1 OS=Mus musculus GN=Rfc1 PE=1 SV=2	P35601	0.26	0.00	2.90	20.07	0.84	1.01	0.66	0.67	0.57	0.61	0.00	0.00	2.23	15.21	1.32	1.10	1.47	0.89	0.82	0.63	1.05	1.05	0.99	0.77	0.68	0.62
Beta-hexosaminidase subunit beta OS=Mus musculus GN=Hexb PE=2 SV=2	P20060	0.26	0.00	2.84	25.00	1.05	1.06	1.06	1.04	1.10	1.00	0.00	5.20	5.20	29.66	1.05	0.97	0.87	1.15	0.95	0.90	1.05	1.01	0.96	1.09	1.02	0.95
N-glycosylase/DNA lyase OS=Mus musculus GN=Ogg1 PE=2 SV=2	O08760	0.26	0.00	2.81	24.06	0.97	1.04	0.91	0.89	0.92	1.03	0.49	1.70	1.71	29.28	1.00	0.97	0.98	0.85	0.83	0.91	0.99	1.00	0.95	0.87	0.87	0.97
Monoacylglycerol lipase ABHD12 OS=Mus musculus GN=Abhd12 PE=1 SV=2	Q99LR1	0.26	2.80	2.80	25.38	1.05	1.26	0.98	1.01	1.16	0.69	0.50	1.71	1.71	24.37	0.86	0.97	0.95	0.86	0.79	0.44	0.95	1.11	0.97	0.93	0.95	0.55
PHD finger protein 6 OS=Mus musculus GN=Phf6 PE=1 SV=1	Q9D4J7	0.26	2.77	2.77	16.21	0.90	0.88	0.87	0.81	0.86	0.88	0.00	3.87	3.88	23.90	1.03	1.07	1.16	0.96	1.01	0.37	0.96	0.97	1.00	0.88	0.93	0.57
Melanoma-associated antigen G1 OS=Mus musculus GN=Ndnl2 PE=1 SV=1	Q9CPR8	0.26	0.00	2.72	28.67	1.11	0.96	0.98	0.98	1.14	0.99	0.98	1.32	1.32	28.32	0.89	0.89	0.84	1.10	1.36	1.17	0.99	0.92	0.91	1.04	1.24	1.08
Baculoviral IAP repeat-containing protein 5 OS=Mus musculus GN=Birc5 PE=1 SV=1	O70201	0.26	0.00	2.70	32.86	1.39	1.21	0.84	0.83	0.79	0.98	0.00	3.95	3.95	41.43	1.21	0.68	1.26	0.82	0.79	0.93	1.30	0.91	1.03	0.82	0.79	0.95
Transcription initiation factor TFIID subunit 1 OS=Mus musculus GN=Taf1 PE=2 SV=2	Q80UV9	0.25	0.00	2.72	14.97	0.89	1.17	0.95	0.69	0.79	0.94	0.14	2.03	2.04	17.50	0.90	1.11	0.90	0.80	0.96	0.62	0.89	1.14	0.92	0.74	0.87	0.76
60S ribosomal protein L30 OS=Mus musculus GN=Rpl30 PE=2 SV=2	P62889	0.25	0.00	2.68	29.57	1.42	1.20	1.15	1.49	1.49	1.33	0.00	3.35	3.35	53.04	1.05	1.00	0.86	1.07	0.85	0.81	1.22	1.10	1.00	1.26	1.12	1.04
Mitotic spindle assembly checkpoint protein MAD2A OS=Mus musculus GN=Mad2l1 PE=2 SV=2	Q9Z1B5	0.25	0.00	2.66	40.49	1.14	1.10	1.26	0.90	0.85	0.95	0.00	3.62	3.63	35.12	0.76	0.89	0.92	0.86	0.95	1.03	0.93	0.99	1.08	0.88	0.90	0.99
Small nuclear ribonucleoprotein G OS=Mus musculus GN=Snrpg PE=1 SV=1	P62309	0.25	2.61	2.61	53.95	0.73	0.90	1.09	1.10	1.33	1.82	0.00	4.12	4.12	26.32	0.79	0.85	0.67	1.01	0.39	0.99	0.76	0.87	0.86	1.05	0.72	1.34

Protien identification and qunatitation results from ProteinPilot for all the analyzed samples

Name	Accession number	% FDR	Unused	Total	%Cov	114:113	115:113	116:113	118:117	119:117	121:117	% FDR	Unused	Total	%Cov	114:113	115:113	116:113	118:117	119:117	121:117	114:113	115:113	116:113	118:117	119:117	121:117
Histone-lysine N-methyltransferase SUV39H2 OS=Mus musculus GN=Suv39h2 PE=1 SV=1	Q9EQQ0	0.25	2.60	2.62	20.96	0.90	0.99	0.89	0.94	0.89	0.90	0.00	2.18	2.18	24.74	0.88	0.95	0.93	0.93	0.93	0.82	0.89	0.97	0.91	0.93	0.91	0.86
Prohibitin OS=Mus musculus GN=Phb PE=1 SV=1	P67778	0.25	2.60	2.61	50.37	0.90	0.93	1.02	1.15	1.25	1.13	0.13	2.00	2.00	33.09	1.04	1.11	1.16	1.19	1.15	0.93	0.96	1.01	1.09	1.17	1.20	1.02
Trifunctional enzyme subunit beta, mitochondrial OS=Mus musculus GN=Hadhb PE=1 SV=1	Q99JY0	0.25	2.60	2.60	15.16	1.00	1.03	0.86	0.87	0.91	0.97	0.00	2.18	2.18	14.11	1.22	0.90	1.00	1.18	1.15	1.00	1.11	0.96	0.93	1.01	1.02	0.99
Ras suppressor protein 1 OS=Mus musculus GN=Rsu1 PE=2 SV=3	Q01730	0.25	0.00	2.62	31.05	0.90	1.02	1.09	1.17	1.01	1.05	0.00	0.00	2.24	24.19	1.21	1.05	1.27	1.01	0.69	0.47	1.04	1.03	1.17	1.09	0.83	0.70
U6 snRNA-associated Sm-like protein LSm2 OS=Mus musculus GN=Lsm2 PE=3 SV=1	O35900	0.25	0.00	2.58	44.21	0.92	0.79	0.92	0.90	1.02	1.15	0.14	0.00	2.04	41.05	0.95	1.02	0.87	0.93	1.04	0.92	0.94	0.90	0.90	0.92	1.03	1.03
Trifunctional enzyme subunit alpha, mitochondrial OS=Mus musculus GN=Hadha PE=1 SV=1	Q8BMS1	0.25	2.57	2.58	23.59	0.90	0.86	0.95	0.98	1.00	0.94	0.00	2.46	2.50	25.16	0.98	0.95	0.90	0.81	0.85	0.95	0.94	0.90	0.92	0.89	0.92	0.95
Protein Btaf1 OS=Mus musculus GN=Btaf1 PE=4 SV=1	E9QAE3	0.25	0.00	2.75	20.24	0.94	1.00	0.93	0.79	0.91	0.82	0.00	2.55	2.69	19.10	0.95	0.98	0.83	0.87	1.02	0.90	0.94	0.99	0.88	0.83	0.96	0.86
Nucleolar protein 16 OS=Mus musculus GN=Nop16 PE=2 SV=1	Q9CPT5	0.25	0.00	2.52	38.20	0.96	0.97	0.96	0.96	1.02	1.01	0.00	0.00	3.16	41.01	0.94	0.98	0.89	1.02	1.17	1.21	0.95	0.98	0.92	0.99	1.09	1.11
Serine/Arginine-related protein 53 OS=Mus musculus GN=Rsrc1 PE=1 SV=1	Q9DBU6	0.25	0.00	2.51	39.82	0.90	0.95	0.90	0.86	0.84	0.97	0.00	5.07	5.08	51.50	0.86	0.94	1.08	0.91	0.91	0.79	0.88	0.94	0.99	0.89	0.87	0.88
Core-binding factor subunit beta OS=Mus musculus GN=Cbfb PE=1 SV=1	Q08024	0.25	2.50	2.50	40.11	0.93	1.00	1.01	1.14	1.06	1.04	0.00	0.00	2.75	52.94	0.90	0.97	0.92	1.08	1.04	1.04	0.91	0.99	0.96	1.11	1.05	1.04
Pericentrin OS=Mus musculus GN=Pcnt PE=1 SV=2	P48725	0.25	0.00	3.21	22.50	0.95	1.02	0.95	0.90	0.82	0.91	0.00	0.00	3.11	31.54	1.13	1.22	1.32	0.92	1.04	1.04	1.04	1.12	1.12	0.91	0.92	0.97
Protein lin-54 homolog OS=Mus musculus GN=Lin54 PE=2 SV=2	Q571G4	0.25	0.00	2.50	15.49	0.63	0.95	0.69	0.95	0.72	0.97	0.15	0.00	2.01	15.35	0.65	1.03	0.91	0.86	0.62	0.24	0.64	0.99	0.79	0.90	0.67	0.49
Peptidyl-prolyl cis-trans isomerase-like 2 OS=Mus musculus GN=Ppil2 PE=2 SV=2	Q9D787	0.25	0.00	2.49	19.58	1.00	1.03	1.08	1.06	1.05	1.15	0.00	2.24	2.24	20.92	0.97	1.14	0.97	1.17	0.85	1.51	0.99	1.08	1.02	1.11	0.94	1.32
Zinc finger MYND domain-containing protein 11 OS=Mus musculus GN=Zmynd11 PE=2 SV=2	Q8R5C8	0.25	2.48	2.54	19.27	1.12	1.19	1.04	0.94	0.91	0.95	0.15	0.00	2.08	27.58	1.08	1.11	1.13	0.82	0.80	0.82	1.10	1.15	1.08	0.87	0.86	0.89
RNA-binding protein 45 OS=Mus musculus GN=Rbm45 PE=2 SV=1	Q8BHN5	0.25	2.48	2.49	26.68	0.90	0.96	0.85	1.01	0.91	0.93	0.00	3.42	3.42	26.89	0.95	1.02	0.86	1.09	1.14	0.83	0.92	0.99	0.86	1.05	1.02	0.88
Nuclear respiratory factor 1 OS=Mus musculus GN=Nrf1 PE=2 SV=2	Q9WU00	0.25	0.00	2.46	15.90	0.90	0.97	0.93	0.91	0.91	0.90	0.00	0.00	3.70	16.30	0.81	1.42	1.14	0.83	0.90	1.03	0.85	1.17	1.03	0.87	0.90	0.96
60S ribosomal protein L31 OS=Mus musculus GN=Rpl31 PE=2 SV=1	P62900	0.25	0.00	2.46	33.60	1.71	1.42	1.53	1.96	2.15	1.69	0.13	0.00	1.99	28.80	1.20	1.05	0.95	1.25	1.26	0.98	1.43	1.22	1.21	1.56	1.64	1.29
Coronin-1B OS=Mus musculus GN=Coro1b PE=1 SV=1	Q9WUM3	0.25	0.00	4.47	24.38	1.00	0.70	0.82	0.94	0.72	0.84	0.15	2.12	3.54	34.92	1.11	0.79	0.84	0.86	0.75	0.69	1.05	0.74	0.83	0.90	0.73	0.76
Zinc finger transcription factor Trps1 OS=Mus musculus GN=Trps1 PE=1 SV=1	Q925H1	0.25	2.42	2.45	14.21	1.02	1.00	0.95	1.10	1.01	1.05	0.00	2.17	2.19	24.12	0.96	0.94	0.92	0.90	1.07	1.03	0.99	0.97	0.94	0.99	1.04	1.04
Peptidyl-prolyl cis-trans isomerase CWC27 homolog OS=Mus musculus GN=Cwc27 PE=1 SV=1	Q3TKY6	0.25	2.41	2.42	29.64	1.33	1.14	1.03	0.60	0.85	0.86	0.14	2.04	2.04	23.03	1.36	1.00	1.43	1.10	1.27	1.50	1.34	1.07	1.21	0.81	1.04	1.13
DNA repair protein XRCC1 OS=Mus musculus GN=Xrcc1 PE=1 SV=2	Q60596	0.43	0.00	2.43	18.07	1.02	1.08	1.15	0.86	0.89	0.90	0.00	6.21	6.21	27.58	1.42	2.25	1.69	1.47	1.42	1.06	1.20	1.56	1.39	1.12	1.12	0.98
Profilin-1 OS=Mus musculus GN=Pfn1 PE=1 SV=2	P62962	0.43	0.00	2.40	19.29	1.16	0.99	0.98	1.04	1.16	1.27	0.00	5.30	5.30	51.43	0.98	0.83	0.84	0.93	0.79	1.28	1.07	0.91	0.91	0.98	0.95	1.28
Apoptotic chromatin condensation inducer in the nucleus OS=Mus musculus GN=Acin1 PE=1 SV=3	Q9JIX8	0.43	0.00	21.34	34.45	1.02	1.03	1.01	0.94	1.03	1.02	0.00	0.00	25.70	42.15	1.04	0.76	0.89	1.05	0.77	0.61	1.03	0.88	0.95	0.99	0.89	0.79
Insulin-like growth factor 2 mRNA-binding protein 3 OS=Mus musculus GN=Igf2bp3 PE=1 SV=1	Q9CPN8	0.43	2.36	2.37	26.77	1.00	0.99	1.02	1.50	1.32	1.11	0.13	1.88	1.88	19.69	1.00	0.58	0.82	1.46	1.06	1.07	1.00	0.76	0.92	1.48	1.18	1.09
Breast cancer metastasis-suppressor 1-like protein OS=Mus musculus GN=Brms1l PE=2 SV=1	Q3U1T3	0.43	2.35	2.36	24.15	0.98	1.08	1.17	0.98	0.98	0.98	0.14	2.02	2.02	17.03	1.09	1.05	0.96	1.08	0.83	1.04	1.03	1.06	1.06	1.03	0.90	1.01
THAP domain-containing protein 11 OS=Mus musculus GN=Thap11 PE=1 SV=1	Q9JJD0	0.43	2.33	2.35	30.16	1.17	1.26	1.11	0.87	0.96	0.88	0.00	4.01	4.05	32.46	1.10	0.97	1.09	1.11	0.89	0.79	1.13	1.11	1.10	0.98	0.92	0.84
Protein timeless homolog OS=Mus musculus GN=Timeless PE=1 SV=3	Q9R1X4	0.43	2.32	2.38	17.54	1.02	0.98	1.02	0.94	0.78	0.77	0.49	1.64	1.68	26.40	1.10	1.03	1.04	0.83	0.76	0.67	1.06	1.00	1.03	0.88	0.77	0.72
Uncharacterized protein OS=Mus musculus GN=Gm10774 PE=3 SV=1	E9Q3B5	0.43	2.29	2.29	34.33	1.18	0.98	1.07	0.96	0.93	0.95	0.14	2.05	2.06	56.72	1.11	0.96	0.88	1.08	1.05	0.87	1.14	0.97	0.97	1.02	0.99	0.91
DNA-directed RNA polymerases I, II, and III subunit RPABC5 OS=Mus musculus GN=Polr2l PE=2 SV=1	P62876	0.43	0.00	2.29	34.33	1.18	0.98	1.07	0.96	0.93	0.95	0.14	0.00	2.06	56.72	1.11	0.96	0.88	1.08	1.05	0.87	1.14	0.97	0.97	1.02	0.99	0.91
Serine/arginine-rich splicing factor 5 OS=Mus musculus GN=Srsf5 PE=1 SV=2	O35326	0.43	2.28	4.07	59.85	1.12	1.29	1.07	1.03	1.20	0.89	0.00	0.00	8.23	70.00	0.97	1.13	0.97	1.28	1.41	0.61	1.04	1.21	1.02	1.15	1.30	0.73
Nucleoporin p58/p45 OS=Mus musculus GN=Nupl1 PE=1 SV=1	Q8R332	0.55	0.00	2.29	16.01	0.86	0.81	0.61	0.65	0.76	0.79	0.00	8.17	8.21	18.40	0.96	0.93	0.98	0.89	1.03	0.99	0.91	0.87	0.78	0.76	0.88	0.89
Vesicle-associated membrane protein-associated protein B OS=Mus musculus GN=Vapb PE=2 SV=3	Q9QY76	0.54	0.00	2.00	14.81	1.03	0.93	1.10	1.17	1.08	1.00	0.13	0.00	1.95	20.58	0.95	0.87	1.28	0.96	0.94	0.86	0.99	0.90	1.19	1.06	1.00	0.92
Vesicle-associated membrane protein-associated protein A OS=Mus musculus GN=Vapa PE=1 SV=2	Q9WV55	0.55	2.25	2.25	17.27	1.03	0.93	1.10	1.17	1.08	1.00	0.13	0.00	1.70	22.09	0.95	0.87	1.28	0.96	0.94	0.86	0.99	0.90	1.19	1.06	1.00	0.92
39S ribosomal protein L37, mitochondrial OS=Mus musculus GN=Mrpl37 PE=2 SV=1	Q921S7	0.54	2.24	2.25	43.03	0.77	0.83	0.78	0.78	0.95	0.76	0.00	4.60	4.60	42.79	0.85	0.79	0.79	0.90	0.88	0.73	0.81	0.81	0.78	0.84	0.91	0.74
Programmed cell death protein 7 OS=Mus musculus GN=Pdcd7 PE=2 SV=1	Q3U2X6	0.54	2.22	2.25	34.92	0.86	0.90	0.86	1.14	1.03	1.17	0.13	2.00	2.01	27.89	0.99	0.79	0.99	1.05	0.95	1.16	0.92	0.84	0.92	1.09	0.99	1.16
Vigilin OS=Mus musculus GN=Hdlbp PE=1 SV=1	Q8VDJ3	0.54	0.00	2.27	21.21	0.87	1.12	0.95	0.93	1.04	0.63	0.14	2.04	2.07	28.23	0.95	1.19	1.06	1.36	1.34	1.26	0.91	1.15	1.00	1.12	1.18	0.89
ETS-related transcription factor Elf-1 OS=Mus musculus GN=Elf1 PE=2 SV=1	Q60775	0.54	0.00	2.22	14.71	0.79	0.49	0.99	1.63	0.91	1.43	0.00	6.07	6.07	22.39	0.84	0.79	0.94	0.83	0.68	0.85	0.81	0.63	0.96	1.16	0.79	1.10
Formin-like protein 1 OS=Mus musculus GN=Fmnl1 PE=1 SV=1	Q9JL26	0.54	2.20	2.23	23.13	0.96	0.98	0.88	1.07	0.99	1.07	0.99	1.35	1.38	27.61	0.80	0.92	1.22	1.13	0.77	0.79	0.88	0.95	1.04	1.10	0.87	0.92

Protien identification and qunatitation results from ProteinPilot for all the analyzed samples

Name	Accession number	% FDR	Unused	Total	%Cov	114:113	115:113	116:113	118:117	119:117	121:117	% FDR	Unused	Total	%Cov	114:113	115:113	116:113	118:117	119:117	121:117	114:113	115:113	116:113	118:117	119:117	121:117
39S ribosomal protein L21, mitochondrial OS=Mus musculus GN=Mrpl21 PE=2 SV=1	Q9D1N9	0.54	2.20	2.21	22.97	1.06	0.99	0.97	0.83	0.95	0.77	0.15	2.07	2.07	38.76	0.90	0.90	0.91	0.90	0.96	0.89	0.97	0.94	0.94	0.86	0.96	0.82
Protein Krt78 OS=Mus musculus GN=Krt78 PE=4 SV=1	E9Q0F0	0.54	2.19	2.36	37.08	0.67	0.73	0.56	0.54	0.44	0.01	0.14	2.04	2.52	35.21	0.95	0.83	0.86	0.58	0.59	0.01	0.79	0.78	0.70	0.56	0.51	0.01
GTP-binding protein 8 OS=Mus musculus GN=Gtpbp8 PE=2 SV=1	Q9CY28	0.54	2.19	2.21	18.95	0.95	1.00	0.91	1.00	0.96	0.89	0.00	2.21	2.22	33.33	0.94	0.95	0.89	1.12	1.07	1.15	0.95	0.98	0.90	1.06	1.01	1.01
Protein Setd1a OS=Mus musculus GN=Setd1a PE=4 SV=1	E9PYH6	0.54	2.19	2.20	17.54	0.95	0.77	0.94	1.04	0.83	0.95	0.14	2.05	2.05	15.85	0.63	0.79	0.78	0.94	1.12	1.17	0.77	0.78	0.86	0.99	0.96	1.06
Cytosolic endo-beta-N-acetylglucosaminidase OS=Mus musculus GN=Engase PE=2 SV=1	Q8BX80	0.54	2.19	2.19	13.76	1.01	1.21	1.07	0.82	0.82	0.78	0.00	2.17	2.19	29.84	0.98	0.98	1.11	0.92	1.11	0.95	1.00	1.09	1.09	0.87	0.95	0.86
Actin-related protein 8 OS=Mus musculus GN=Actr8 PE=2 SV=1	Q8R2S9	0.54	2.19	2.19	11.54	0.79	0.97	0.85	0.91	0.88	0.96	0.00	2.23	2.25	27.88	0.83	0.90	0.90	0.99	1.07	0.80	0.81	0.94	0.87	0.95	0.97	0.88
Elongation factor 2 OS=Mus musculus GN=Eef2 PE=1 SV=2	P58252	0.60	0.00	4.19	16.43	1.05	0.93	0.98	1.01	1.16	1.15	0.00	2.24	4.24	19.23	1.50	0.73	1.47	0.85	0.77	0.62	1.25	0.82	1.20	0.92	0.95	0.84
Histone-lysine N-methyltransferase MLL4 OS=Mus musculus GN=Wbp7 PE=1 SV=3	O08550	0.65	0.00	2.60	20.27	1.07	0.90	1.12	0.94	0.90	0.90	0.00	0.00	2.55	25.14	1.22	1.67	1.20	1.03	0.84	0.86	1.14	1.23	1.16	0.98	0.87	0.88
ETS translocation variant 3 OS=Mus musculus GN=Etv3 PE=2 SV=2	Q8R4Z4	0.71	0.00	2.20	23.78	0.85	1.17	1.16	1.32	1.02	1.69	0.14	0.00	2.02	22.81	0.89	1.18	1.05	1.53	1.22	1.69	0.87	1.17	1.10	1.42	1.12	1.69
Dihydrolipoyllysine-residue acetyltransferase component of pyruvate dehydrogenase complex, mitochondrial OS=Mus musculus GN=Dlat PE=1 SV=2	Q8BMF4	0.71	2.18	2.19	27.10	0.98	0.79	0.90	1.06	0.93	0.89	0.00	9.70	9.71	30.06	0.82	0.58	0.51	1.14	0.94	0.14	0.90	0.67	0.68	1.10	0.93	0.35
MCG1618, isoform CRA_c OS=Mus musculus GN=Nsmce4a PE=4 SV=1	G3XA30	0.71	2.18	2.18	31.23	0.90	0.98	0.91	1.00	1.19	1.18	0.00	4.00	4.00	39.90	0.74	0.83	0.77	1.21	1.34	1.11	0.81	0.90	0.84	1.10	1.26	1.14
DNA-directed RNA polymerases I and III subunit RPAC1 OS=Mus musculus GN=Polr1c PE=1 SV=3	P52432	0.71	0.00	2.18	24.57	1.08	1.11	0.93	1.00	1.11	0.95	0.00	0.00	4.15	33.82	1.04	1.01	0.99	1.08	0.95	1.08	1.06	1.06	0.96	1.04	1.02	1.01
Cyclin-dependent kinase 2 OS=Mus musculus GN=Cdk2 PE=1 SV=2	P97377	0.71	0.00	4.19	24.28	1.15	1.13	1.07	0.93	0.86	0.84	0.00	5.09	7.11	33.82	1.20	1.06	0.89	0.67	0.70	0.52	1.17	1.09	0.97	0.79	0.78	0.66
Tripartite motif-containing protein 35 OS=Mus musculus GN=Trim35 PE=2 SV=2	Q8C006	0.71	2.16	2.16	21.36	1.21	1.09	1.13	0.91	0.95	1.10	0.00	2.20	2.20	26.75	1.19	1.09	1.25	1.03	1.03	1.06	1.20	1.09	1.19	0.97	0.99	1.08
Zinc finger protein 148 OS=Mus musculus GN=Znf148 PE=1 SV=2	Q61624	0.71	0.00	2.17	21.16	0.93	0.94	0.95	0.88	0.86	0.87	0.00	4.08	4.08	21.16	1.05	0.92	0.97	0.86	0.93	0.85	0.99	0.93	0.96	0.87	0.90	0.86
Zinc finger protein with KRAB and SCAN domains 3 OS=Mus musculus GN=Zkscan3 PE=2 SV=1	Q91VW9	0.71	2.15	2.17	21.16	0.94	0.95	1.05	1.01	0.94	1.00	0.00	0.00	3.55	26.22	1.10	0.95	1.19	0.88	0.86	0.78	1.01	0.95	1.12	0.94	0.90	0.88
Histone deacetylase complex subunit SAP130 OS=Mus musculus GN=Sap130 PE=1 SV=2	Q8BIH0	0.71	0.00	2.16	19.11	1.04	0.93	1.07	0.95	0.97	0.80	0.00	2.42	2.43	18.26	1.14	1.14	1.16	0.92	0.69	0.78	1.09	1.03	1.11	0.93	0.82	0.79
Protein Chd2 OS=Mus musculus GN=Chd2 PE=4 SV=1	E9PZM4	0.71	2.14	6.87	15.87	1.45	1.32	1.49	0.84	0.87	0.82	0.00	7.75	8.99	21.67	0.90	0.79	1.03	0.63	0.70	0.56	1.14	1.02	1.24	0.72	0.78	0.68
Enhancer of yellow 2 transcription factor homolog OS=Mus musculus GN=Eny2 PE=2 SV=1	Q9JIX0	0.70	2.14	2.15	43.56	1.19	1.31	1.09	1.08	1.10	1.39	0.00	4.00	4.01	59.41	1.61	0.84	1.54	0.83	0.47	0.14	1.39	1.05	1.29	0.95	0.72	0.45
Zinc finger matrin-type protein 2 OS=Mus musculus GN=Zmat2 PE=2 SV=1	Q9CPW7	0.70	2.14	2.14	26.13	1.17	0.98	0.86	0.86	0.94	0.79	0.00	2.18	2.18	32.16	1.49	0.90	1.09	1.09	0.85	0.71	1.32	0.94	0.96	0.96	0.89	0.75
U6 snRNA-associated Sm-like protein LSm7 OS=Mus musculus GN=Lsm7 PE=3 SV=1	Q9CQQ8	0.70	2.14	2.14	15.53	1.22	1.05	1.04	1.06	1.01	0.94	0.00	3.68	3.68	40.78	1.45	0.75	1.24	0.63	0.64	0.59	1.33	0.89	1.13	0.82	0.81	0.74
Bromodomain-containing protein 9 OS=Mus musculus GN=Brd9 PE=2 SV=1	Q3UQU0	0.70	2.13	2.14	12.42	1.13	0.98	0.88	0.87	0.86	1.01	0.00	2.45	2.45	16.28	1.08	0.99	0.82	0.72	0.88	0.53	1.10	0.99	0.85	0.79	0.87	0.73
A-kinase anchor protein 8 OS=Mus musculus GN=Akap8 PE=1 SV=1	Q9DBR0	0.70	0.00	2.13	20.52	1.16	1.10	1.12	0.98	0.95	1.12	0.00	4.59	4.62	28.68	1.12	1.25	1.29	1.10	1.02	1.26	1.14	1.17	1.20	1.04	0.98	1.19
Eukaryotic translation initiation factor 4H OS=Mus musculus GN=Eif4h PE=1 SV=3	Q9WUK2	0.70	0.00	2.12	56.05	1.17	1.33	1.29	1.14	1.24	0.86	0.14	2.01	2.01	43.15	0.95	1.05	1.06	1.20	1.17	1.05	1.05	1.18	1.17	1.17	1.20	0.95
Zinc finger protein 143 OS=Mus musculus GN=Znf143 PE=1 SV=2	O70230	0.75	2.11	2.12	15.36	0.90	0.97	0.92	1.03	0.98	1.08	0.00	4.00	4.00	14.73	0.98	0.95	1.12	0.91	0.90	0.95	0.94	0.96	1.01	0.97	0.94	1.01
Zinc finger protein 76 OS=Mus musculus GN=Znf76 PE=2 SV=1	Q8BMU0	0.81	0.00	2.00	10.92	0.90	0.97	0.92	1.03	0.98	1.08	0.00	0.00	2.00	10.04	0.98	0.95	1.12	0.91	0.90	0.95	0.94	0.96	1.01	0.97	0.94	1.01
Protein Zfp523 (Fragment) OS=Mus musculus GN=Zfp523 PE=4 SV=1	B2KF19	0.81	0.00	2.00	15.75	0.90	0.97	0.92	1.03	0.98	1.08	0.00	0.00	2.00	16.44	0.98	0.95	1.12	0.91	0.90	0.95	0.94	0.96	1.01	0.97	0.94	1.01
Interferon regulatory factor 5 OS=Mus musculus GN=Irf5 PE=1 SV=1	P56477	0.81	0.00	2.17	16.30	1.10	1.18	1.07	1.54	1.39	1.42	0.13	2.00	2.09	21.93	1.07	1.21	1.43	1.79	1.71	1.66	1.08	1.20	1.24	1.66	1.54	1.53
RNA binding protein fox-1 homolog 2 OS=Mus musculus GN=Rbfox2 PE=1 SV=2	Q8BP71	0.87	2.09	2.09	32.07	1.05	0.98	1.11	1.08	1.03	1.00	0.00	0.00	2.25	22.49	0.85	1.01	0.88	0.96	1.00	1.05	0.94	1.00	0.99	1.02	1.01	1.02
Lethal(3)malignant brain tumor-like protein 2 OS=Mus musculus GN=L3mbtl2 PE=1 SV=2	P59178	0.92	2.08	2.08	20.06	1.08	1.11	1.05	1.01	1.09	1.11	0.14	0.00	2.05	15.50	0.98	0.91	1.01	1.13	1.13	1.28	1.03	1.00	1.03	1.07	1.11	1.19
Transcription factor p65 OS=Mus musculus GN=Rela PE=1 SV=1	Q04207	0.98	0.00	2.08	17.67	1.36	1.84	1.89	1.20	1.01	1.16	0.13	2.00	2.00	23.13	1.04	1.38	1.33	1.45	0.93	1.46	1.19	1.59	1.58	1.32	0.97	1.30

Immunology and Cell Biology (2013) 91, 377–387

www.nature.com/icb

ORIGINAL ARTICLE

The synergy in cytokine production through MyD88-TRIF pathways is co-ordinated with ERK phosphorylation in macrophages

Rebecca Suet Ting Tan[1,7], Bin Lin[2,7,8], Qian Liu[2], Lisa Tucker-Kellogg[3,4], Bow Ho[5], Bernard PL Leung[6,9] and Jeak Ling Ding[1,2,9]

Although specific single Toll-like receptor (TLR) ligands are known to drive the development of Th1 or Th2 immunity, the outcome of different combinations of TLR ligands on innate immunity is not well defined. Spatiotemporal dynamics are critical in determining the specificity of the immune response, but the mechanisms underlying combinatorial TLR stimulation remain unclear. Here, we tested pairwise combinations of TLR ligands separated by different time intervals for their effect on cytokine production in macrophages. We observed that stimulation via a combination of MyD88- and TRIF-utilizing adaptors leads to a highly synergistic cytokine response. On a timescale of 4–24 h, macrophages pretreated with poly(I:C) (TLR3 ligand) are cross-primed to a second stimulation with R848 (TLR7 ligand) and vice versa, and each condition exhibits different optimal time windows of synergistic response for each cytokine. We show that the synergy resulting from combinatorial stimuli (poly(I:C) and R848 is also regulated by the order and dosage of the TLR agonists. Secondary response genes, which depend on new protein synthesis for transcription, show greater synergy than primary response genes, and such enhancement is abolished when new protein synthesis is inhibited. Synergistic cytokine production appears concordant with sustained ERK phosphorylation, suggesting that the *de novo* factors act via inhibition of ERK dephosphorylation, for example, by the downregulation of dual specificity phosphatase 6. Taken together, our findings illustrate a checkpoint in the innate immune system, where the synchronization of timing of both MyD88 and TRIF pathways is required for a maximal cytokine response and potential memory effect in macrophages.
Immunology and Cell Biology (2013) **91,** 377–387; doi:10.1038/icb.2013.13; published online 9 April 2013

Keywords: macrophage; pathogen recognition; signaling crosstalk; Toll-like receptor

The innate immune system possesses a range of receptors, which detect conserved microbial ligands called pathogen-associated molecular patterns (PAMPs).[1] In the mouse and human Toll-like receptor (TLR) system, a total of 13 different receptors are known, each of which recognizes distinct bacterial or viral PAMP such as single-stranded and double-stranded RNA (TLR7 and TLR3, respectively).[2] In spite of the recognition of a diverse range of PAMP, TLR signaling converges on only two adaptors, MyD88 and TRIF. All TLRs utilize MyD88 with the exception of TLR3, which depends exclusively on TRIF. TLR4 is unique as it signals via both MyD88 and TRIF.

Although TLRs make use of a shared set of signal transduction molecules downstream of these two adaptors, the biological effect of each TLR agonist can differ considerably. For example, *in vitro* stimulation of dendritic cells (DCs) with TLR5 agonist, flagellin, induces Th1 responses, whereas TLR2 agonist, Pam_3CSK_4, induces a Th2 response.[3] Further complexity occurs *in vivo* when immune cells encounter pathogens bearing multiple TLR ligands. The importance of this complexity is reflected in several studies,[4–10] which have noted that certain pairwise combinations of TLR ligands induce much higher cytokine production when administered simultaneously rather than individually, a phenomenon described as synergy. Most of these studies have focused on the synergistic induction of interleukin (IL)-12p70 by DC, which acts on adaptive immunity to drive Th1 responses.[4–8] However, the effect of combinatorial PAMP stimulation on macrophages, which are normally the first cells to encounter pathogens in host tissues and exert their

[1]NUS graduate School for Integrative Science and Engineering, National University of Singapore, Singapore; [2]Department of Biological Sciences, Faculty of Science, National University of Singapore, Singapore; [3]Computational and Systems Biology, Singapore-MIT Alliance, Singapore; [4]Mechanobiology Institute, National University of Singapore, Singapore; [5]Department of Microbiology, Yong Loo Lin School of Medicine, National University of Singapore, Singapore and [6]Department of Physiology, Yong Loo Lin School of Medicine, National University of Singapore, Singapore
Correspondence: Professor JL Ding, Department of Biological Sciences, Faculty of Science, National University of Singapore, 14 Science Drive 4, S1A #05-03, Singapore 117543, Singapore.
E-mail: dbsdjl@nus.edu.sg
[7]These two authors are first coauthors.
[8]Current address: Laboratory of Systems Biology, NIAID, NIH 9000 Rockville Pike Building 4, Room 228 Bethesda MD 20892.
[9]These two authors are senior coauthors.
Received 30 April 2012; revised 12 March 2013; accepted 12 March 2013; published online 9 April 2013

effect on innate rather than adaptive immunity,[9,10] remains relatively unexamined.

Although synergistic combinations of TLR agonists are known, the underlying logic governing TLR–TLR interaction and the resulting non-additive responses to complex stimuli remains unclear. The presence of multiple receptors and adaptors make it possible for crosstalk and nonlinear responses to occur, thus maintaining a more finely controlled, rapid and lower-energy system.[11] Both empirical and *in silico* data suggest that the temporal aspects of immune signaling can have profound effects on biological outcomes.[12,13] In adaptive immunity, the second response to a pathogen is much higher due to immunological memory of the first infection. However, this occurs on the timescale of several days to weeks, whereas innate immunity responds within hours. Our preliminary data showed that certain combinations of TLR ligands led to an enhanced cytokine response. We hypothesized that cells of the innate immune system could show either (1) an enhanced response to a second stimulation with a different TLR ligand (cross-priming) or (2) a reduced response to a second stimulation with the same TLR ligand (tolerance or antagonism), demonstrating a 'memory' of the first stimulation. Therefore, we examined the effect of dosage and temporal intervals between two TLR agonists known to induce synergistic cytokine production: poly(I:C) (TLR3 ligand) and R848 (TLR7 ligand) in macrophages. Our results show that appropriate timing and dosage of TLR agonists are critical parameters regulating the synergistic production of different cytokines, with variable optimal time windows for different classes of cytokines. In addition, we showed that while poly(I:C) dose-dependently enhances synergistic responses, R848 exhibits a threshold effect, suggesting two different mechanisms by which each signal contributes to synergy. We also demonstrate that synergy is dependent on new protein synthesis and is associated with enhanced and sustained ERK phosphorylation, which may be caused by the downregulation of dual specificity phosphatase 6 (DUSP6).

RESULTS

Combinatorial stimulation with poly(I:C) and R848 induces highest synergy in cytokine production

As a preliminary study, we stimulated RAW264.7 cells with pairwise combinations of TLR ligands for up to 24 h and measured a panel of 18 cytokines via a multiplex cytokine assay. We found that out of the

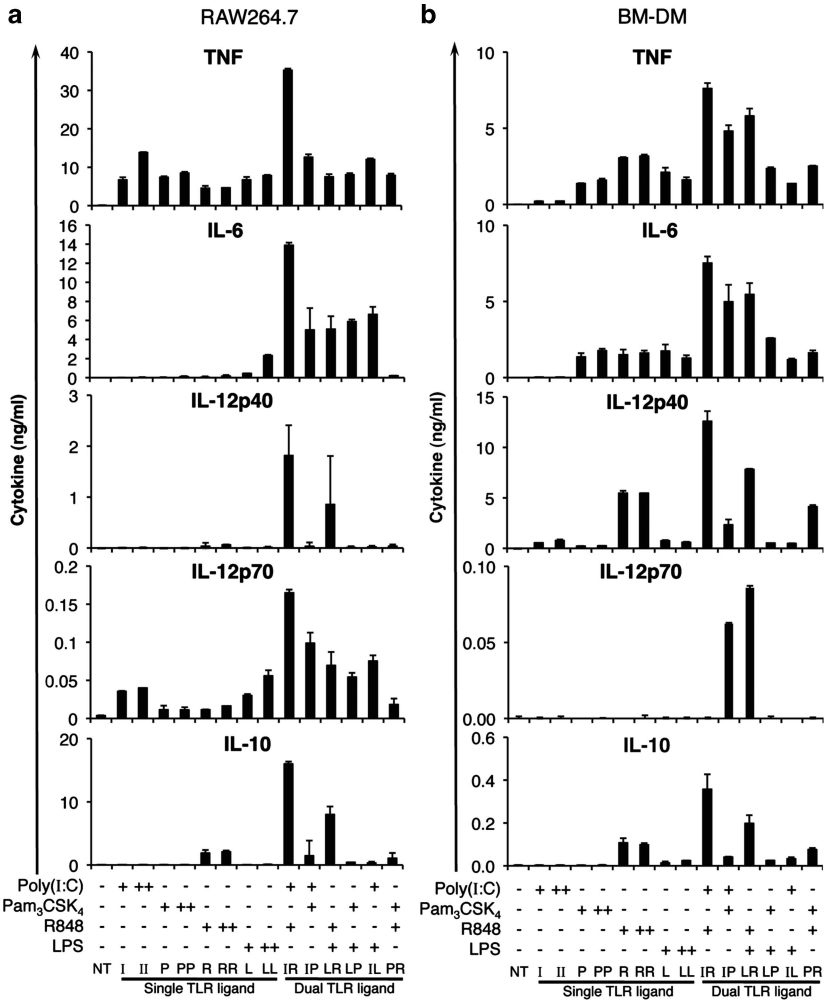

Figure 1 Multiplex cytokine assay of cells stimulated with various TLR ligand combinations. (**a**) RAW264.7 cells and (**b**) bone marrow-derived macrophages derived from BALB/c mice were stimulated with the indicated combinations of TLR ligands and cell culture supernatants were harvested after 24 h. The dosages of the TLR ligands were as follows: poly(I:C) 10 μg ml^{-1}, Pam_3CSK_4 10 ng ml^{-1}, R848 25 ng ml^{-1} and LPS 10 ng ml^{-1}. '+ +' Indicates a double dose of the same ligand. The profiles of a panel of five cytokines (TNF, IL-6, IL-12p40, IL-12p70 and IL-10) were analyzed by a multiplex cytokine bead array (Panomics) according to the manufacturer's instructions.

a

Ligand		Dose 1	2	3	4	5	6
Poly(I:C) (μg/ml)	I	10	20	40	80	160	320
LPS (ng/ml)	L	0.4	0.8	1.6	5	10	50
R848 (ng/ml)	R	1.25	2.5	5	10	20	40
Pam_3CSK_4 (ng/ml)	P	10	20	40	80	160	320

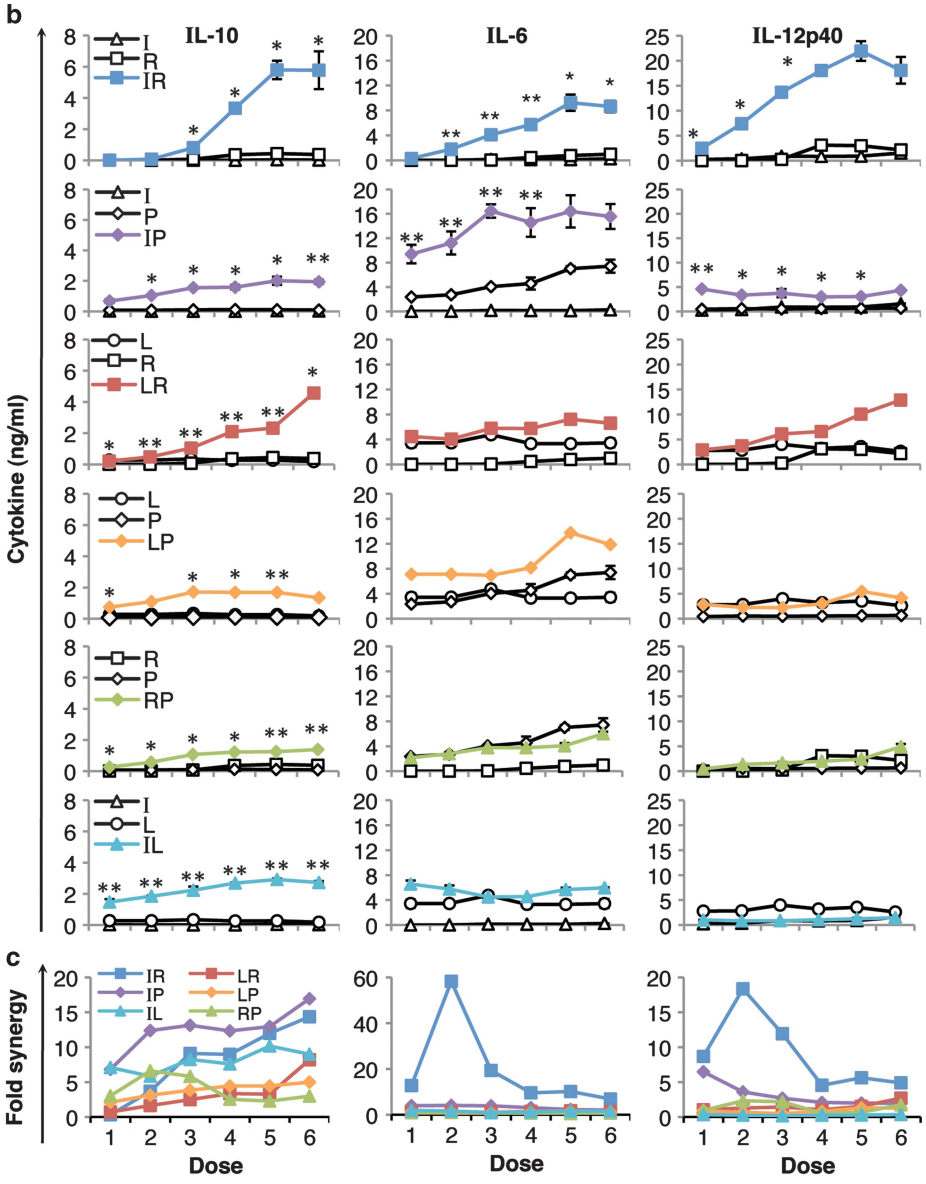

Figure 2 Combinatorial ligand stimulation of TRIF and MyD88 shows the greatest synergy in mouse macrophages. BALB/c bone marrow-derived macrophages (BM-DM) were stimulated with the indicated combinations and doses of TLR ligands as indicated in (**a**) for 24 h and cytokine concentration in cell-free supernatants were measured by ELISA. (**b**) Cytokine production and (**c**) fold synergy of IL-10, IL-6 and IL-12p40. Single TLR ligand stimulated values are indicated with open symbols and black lines: poly(I:C) (triangle), R848 (square), Pam_3CSK_4 (diamond) and LPS (circle). Combinatorial TLR ligand-stimulated values are indicated by filled and coloured symbols: poly(I:C) and R848 (blue square), poly(I:C) and Pam_3CSK_4 (purple diamond), LPS and R848 (red square), LPS and Pam_3CSK_4 (orange diamond), R848 and Pam_3CSK_4 (green diamond), or poly(I:C) and LPS (cyan triangle). Data shown are representative of three independent experiments. Student's *t-test* was performed to compare double TLR ligand stimulation (coloured lines) with the sum of single stimulations (white symbols, black lines) $^*P<0.05$, $^{**}P<0.01$.

18 cytokines measured, only tumor necrosis factor (TNF), IL-6, IL-10 and IL-12p40 were synergistically upregulated (Figure 1a). Based on this initial study, these four highly upregulated cytokines and IL-12p70 were further examined in BALB/c-derived bone-marrow macrophages (BM-DMs; Figure 1b). We observed comparable profiles of cytokine synergy in both the RAW 264.7 cell line and primary BM-DM cells derived from BALB/c mice, under similar conditions of TLR ligand stimulation (Figures 1a and b). Poly(I:C) was used as a TLR3 ligand, which signals exclusively via TRIF. Pam_3CSK_4 (TLR2 ligand) and R848 (TLR7 ligand) were used as MyD88-exclusive ligands, which signal via

the cell surface and endosomal compartments, respectively. Lipopolysaccharide (LPS) was included as a positive control that activates both the TRIF and MyD88 pathways. We found that simultaneous stimulation with two TLR ligands induced higher cytokines than double dose of a single TLR ligand (Figure 1, $++$) if the TLR ligands collectively activated both MyD88 and TRIF pathways.

In order to dissect the logic governing synergistic cytokine production in response to dual TLR ligand stimulation, we challenged BALB/c BM-DM with different pairwise combinations of MyD88- and TRIF-utilizing TLR ligands at increasing doses as indicated in Figure 2a, and cytokine production was measured 24 h later (Figure 2b). Using these different TLR ligands, we then tested the hypothesis that induction via MyD88 and TRIF combinations (poly(I:C) + R848/Pam_3CSK_4) would lead to synergistic cytokine production due to an interaction between the two pathways, whereas combinations of ligands inducing MyD88-MyD88

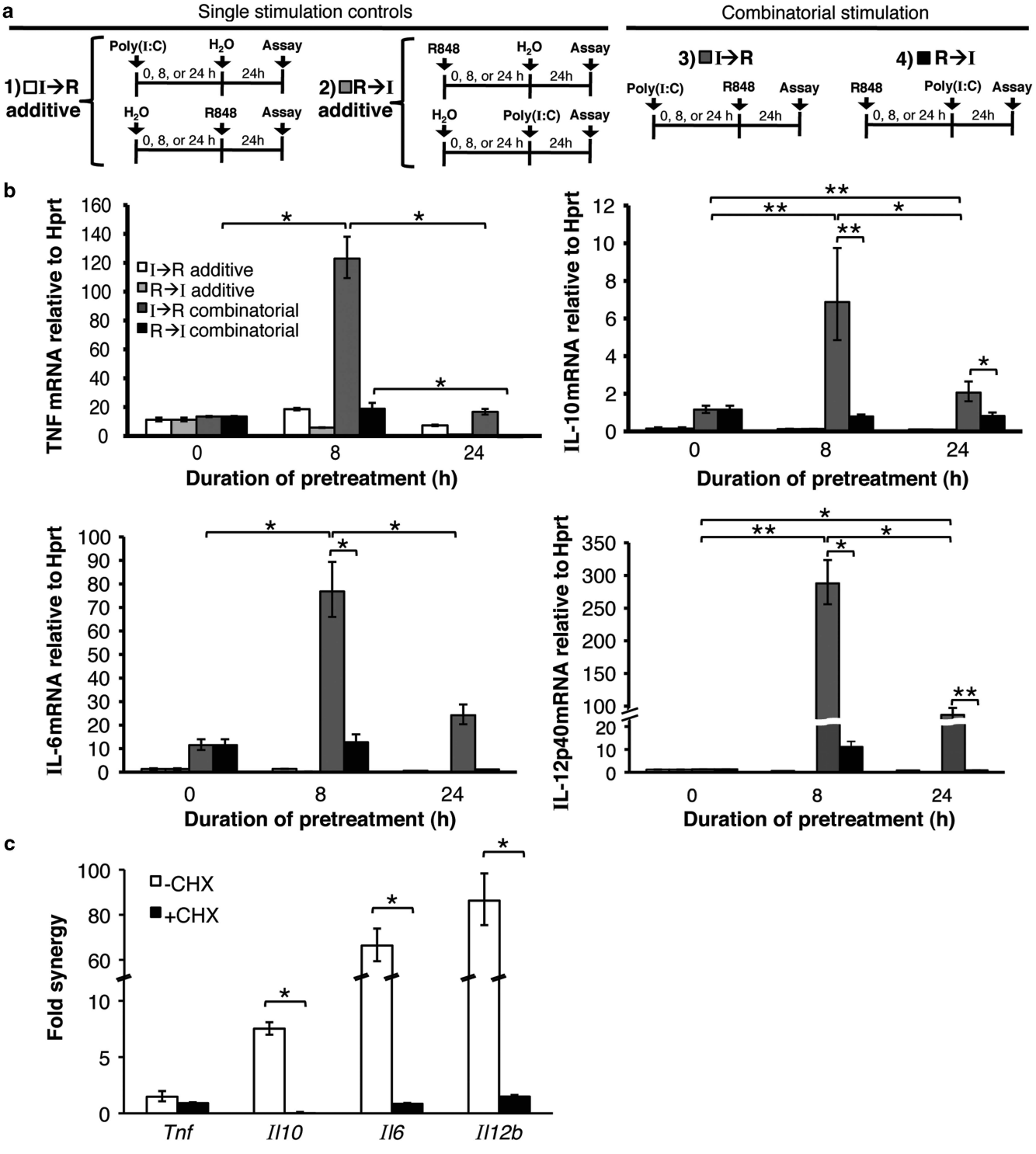

(R848 + Pam_3CSK_4) and TRIF-TRIF (poly(I:C) + LPS) would not. We observed that only low to moderate levels of both pro- and anti-inflammatory cytokines were produced when the BM-DM were challenged with single TLR ligands (Figure 2b, blank symbols), even at increasing doses. When challenged simultaneously with two TLR ligands, there was no significant increase in cytokine production if the two ligands activated the same signaling pathways (Figure 2b, green, R848 + Pam_3CSK_4; both engage only MyD88). However, when challenged with the combination of MyD88- and TRIF-utilizing ligands (Figure 2b, blue, poly(I:C) + R848; or purple, poly(I:C) + Pam_3CSK_4), the production of pro- and anti-inflammatory cytokines was much greater (Figure 2b, filled symbols) than that observed for single ligand stimulation (Figure 2b, open symbols). This was especially profound in the case where poly(I:C) (TRIF only) was paired with R848 or Pam_3CSK_4 (MyD88 only; Figure 2b, blue and purple, respectively). In an intermediate condition, where cells were challenged with LPS (MyD88 and TRIF ligand), further addition of MyD88-utilizing ligands, R848 or Pam_3CSK_4 (Figure 2b, LPS + R848, red; LPS + Pam_3CSK_4, orange), caused no synergy in the production of IL-6 and IL-12p40 (Figure 2b, red and green, respectively), although there was still synergistic production of IL-10.

To quantify the synergistic effect, the cytokine production under combinatorial stimulation was divided by the sum of the respective single stimulations to give a value we termed 'fold synergy' (Figure 2c). For the proinflammatory cytokines, IL-6 and IL-12p40, the levels produced by combinatorial stimulation is much greater than the single stimulated cells, with up to 20- to 60-fold synergy at low doses. However, as the dose increases, single stimulated cells also began to increase cytokine production, whereas the double stimulated cells approached saturation levels of cytokine production, causing the calculated fold synergy to drop. Interestingly, the anti-inflammatory cytokine, IL-10, shows a reverse trend, with synergy increasing as the dose increases (Figure 2c). This indicates that synergy affects different classes of cytokines in opposing ways, and that there is a negative feedback regulation limiting the amount of proinflammatory cytokines produced. Importantly, these patterns were reproduced in C57BL/6-derived primary macrophages (Supplementary Figure 1), showing that this was a general rather than strain-specific phenomenon.

Appropriate timing and order of TLR stimulation influence the optimal synergy

Following from the demonstration that the combination of different doses of poly(I:C) and R848 leads to synergy, we further investigated the kinetic effects with these two ligands. During the course of infection, macrophages may encounter different TLR ligands in a sequential manner. Thus, we tested the effect of both poly(I:C) followed by R848 [I→R combinatorial] and R848 followed by poly(I:C) [R→I combinatorial], measuring mRNA expression of TNF, IL-10, IL-6 and IL-12p40. Briefly, cells were pretreated with the first TLR ligand for 0, 8 or 24 h and then collected 8 h after stimulation with the second TLR ligand. To discriminate additive effects from potential synergy or antagonism, stimulations with single TLR agonists were included as controls (Figure 3a). The synergy of all cytokine mRNA was sensitive to the duration of pre-stimulation, with synergy increasing from 0 to 8 h and declining by 24 h (Figure 3b). Interestingly, the effect of the order of stimulation also strongly influenced the response where [I→R combinatorial, dark grey] led to much higher expression of cytokine mRNA than [R→I combinatorial, black] at the same time points. Importantly, our data show that priming by poly(I:C) is crucial for optimal synergy in cytokine gene expression in the macrophages, possibly via the action of synergy factor(s).

De novo protein synthesis is required for synergy effect on secondary response genes

To examine whether the 'synergy factor' is a newly synthesized or pre-existing protein, we used cycloheximide (CHX) to inhibit *de novo* protein synthesis in BM-DM and measured its effect on the cytokine transcripts. For IL-6 and IL-12p40, CHX treatment abrogated the synergy (Figure 3c), indicating a strong requirement for the newly synthesized protein. For TNF, there was only a low synergy of ~1.5-fold observed at the transcriptional level, which was slightly reduced by CHX treatment. It appears that synergy for the expression of secondary response genes (*Il6* and *Il12b*) mainly occurs at the transcriptional level and is highly dependent on new protein synthesis. In contrast, the synergy of primary response genes (*Tnf* and *Il10*) more likely occurs at the post-transcriptional level, and may not require new protein synthesis. Our observation is consistent with previous reports that LPS induction of secondary response genes but not primary response genes requires new protein synthesis.[14]

Both timing and dose of stimulation affects cytokine protein production

Next, we extended our study to the protein level using both BM-DM and RAW cells, as there is no apparent difference in the cytokine expression profiles for the primary cells and cell line (Figures 1a and b and Supplementary Figure 2). Briefly, BM-DM were stimulated with

Figure 3 Synergy in mRNA expression is dependent on *de novo* protein synthesis. (**a**) Graphical summary of experimental design. Bone marrow-derived macrophages (BM-DMs) were treated with either poly(I:C) followed by R848 [I→R combinatorial, dark grey] or R848 followed by poly(I:C) [R→I combinatorial, black]. Assuming a purely additive effect of two TLR stimulations, the single stimulation control for I→R [I→R additive, white] was taken to be the sum of cytokines produced by cells stimulated first with poly(I:C) for 0, 8 or 24 h followed by a mock stimulation with water for 8 h, and cells which were mock stimulated first with water for 0, 8 or 24 h followed by R848 stimulation for 8 h. Similarly, the single stimulation control for R→I [R→I additive, light grey] was the sum of cytokines produced by cells stimulated with R848 for 0, 8 or 24 h followed by water for 8 h and cells stimulated with water for 0, 4, 8, 16 or 24 h followed by poly(I:C) for 8 h. (**b**) BM-DM were pretreated with one TLR ligand for 0, 8 or 24 h, followed by a second TLR ligand for another 8 h. 0 h pretreatment denotes simultaneous stimulation. [I→R] (dark grey) symbolizes poly(I:C) as the first TLR ligand, followed by R848 as the second TLR ligand. [R→I] (black) indicates the same stimulations in reverse order. The single stimulation controls are computed for [I→R] (white) and [R→I] (light grey) as described in **a**. IL-10, TNF, IL-6 and IL-12p40 mRNA were measured by real-time PCR using Taqman probes specific to each cytokine. Similar results were obtained in two other independent experiments. Data represent means ± s.d. of triplicate measurements in a representative experiment. Student's *t*-tests were performed from the data of all three independent experiments (* = $P<0.05$, ** = $P<0.01$). (**c**) BM-DM were pretreated with poly(I:C) for 8 h, followed by R848 for another 4 h in the absence (white bars) or presence (black bars) of 10 μg ml^{-1} CHX for 15 min. Fold synergy was calculated by dividing the experimental group by the control group data. Similar results were obtained in two other independent experiments. Data represent means ± s.d. of triplicate measurements in a representative experiment. Student's *t*-tests were performed from the data of all three independent experiments (* = $P<0.05$).

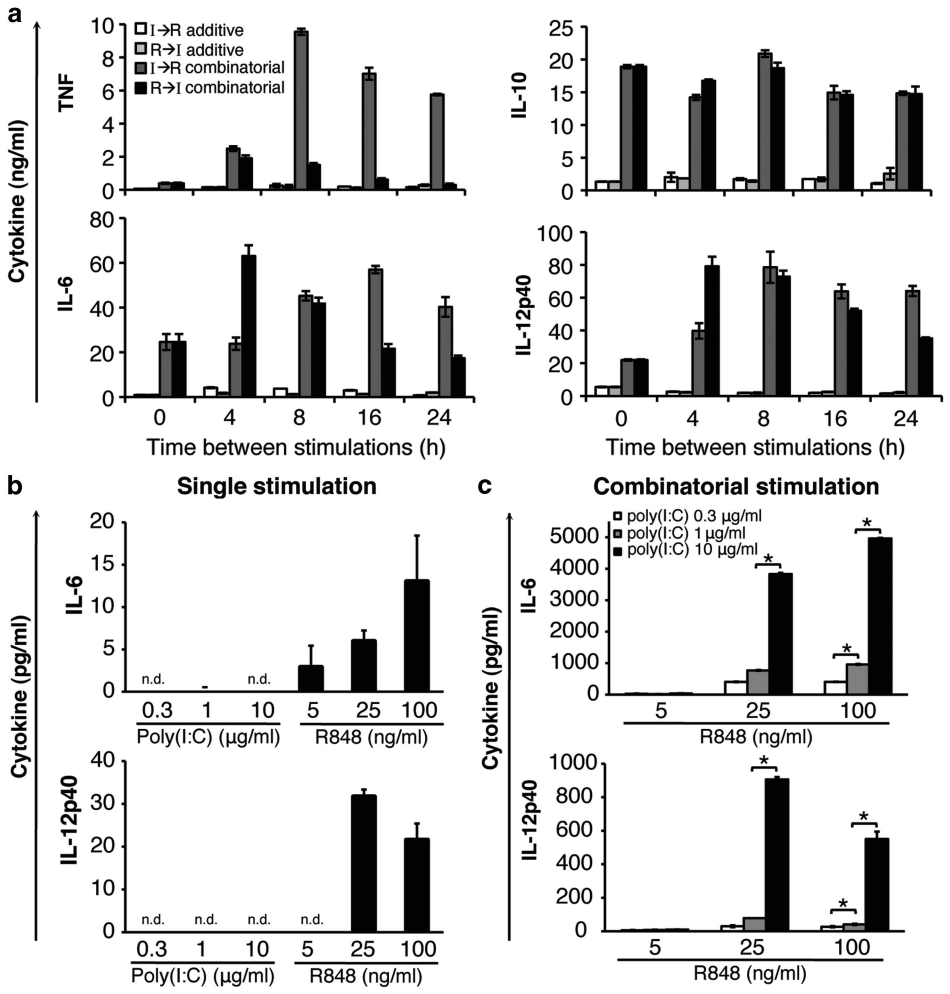

Figure 4 Time and dosage of TLR ligands induce synergy in cytokine production. (**a**) Pattern of cytokine protein production induced by different time intervals between poly(I:C) and R848 stimulation. Bone marrow-derived macrophages were pretreated with one TLR agonist for 0, 4, 8, 16 or 24 h (0 h pre-stimulation denotes simultaneous stimulation), followed by a second TLR agonist for 24 h. [I→R combinatorial] (dark grey) symbolizes 10 μg ml^{-1} of poly(I:C) as the first TLR agonist, followed by 25 ng ml^{-1} of R848 as second TLR agonist. [R→I combinatorial] (black) indicates the same stimulations in reverse order. The hypothetical additive effects are computed for [I→R additive] (white) and [R→I additive] (light grey). IL-10, TNF, IL-6 and IL-12p40 in cell-free supernatants were measured by ELISA. Data are means ± s.d. of triplicate measurements in a representative experiment. Similar results were obtained in two other independent experiments. (**b**) In RAW264.7 cells, stimulation with single TLR agonists results in low levels of cytokine production. (**c**) Poly(I:C) dose-dependently enhances R848-induced IL-6 production when both TLR ligands were applied simultaneously to RAW264.7 cells (upper panel). Stimulation with poly(I:C) for 8 h before R848 also shows dose-dependent effect on IL-12p40 production (lower panel). Cell-free supernatants were collected 24 h after the second stimulation. IL-6 and IL-12p40 concentrations were measured by ELISA. ND describes 'not detectable' within the limits of assay (lower limit of detection, 5 ng ml^{-1}). Data represent means ± s.d. of triplicate measurements in a representative experiment. Similar results were obtained in two other independent experiments. Student's *t*-tests were performed from the data of all three independent experiments (*$P<0.05$).

poly(I:C) for 0–24 h followed by R848 for 24 h [I→R] or R848 for 0–24 h followed by poly(I:C) [R→I]. At these time points, combinatorial cells were still healthy, showing a level of apoptosis similar to that of untreated cells (Supplementary Figures 2a and b). Similar to our previous findings, stimulation with single TLR ligands led to only a low level of response (Figure 4a, white and light gray bars). However, double TLR ligand stimulation led to a high and synergistic response for all cytokines tested and at all time intervals, as indicated by the difference between the white and dark grey bars or the light grey and black bars (Figure 4a). This enhancement of cytokine production was also seen by intracellular cytokine staining for IL-6 and IL-12p40 (Supplementary Figure 2c) Interestingly, each of the cytokines showed differential sensitivity to the order and timing of the second TLR stimulation. First, the anti-inflammatory cytokine, IL-10, was produced at a high and synergistic level (Figure 4a) regardless of the timing of the second TLR stimulation. In stark contrast, proinflammatory TNF was produced at a much higher level under [I→R] stimulation than [R→I] when the time interval between stimulations was 8 h or more. At 8 h interval, the difference in the order of stimulation was the most apparent, where [R→I] showed 9.5 ng ml^{-1} TNF production, whereas [I→R] only showed six times less TNF production (1.5 ng ml^{-1}, Figure 4a). This suggests that there are different mechanisms of synergy depending on the order of stimulation, where the synergy is greatest for R848-primed cells at 4 h after first stimulation and was sustained over longer time. In contrast, poly(I:C)-pretreated cells remain highly cross-primed to second stimulation with R848 from 8 to 24 h after pre-stimulation. The [R→I] stimulation induced a pattern of production of IL-6 and IL-12p40 similar to TNF, where 4 h pre-stimulation with R848 followed by poly(I:C) led to the highest cytokine production (Figure 4a).

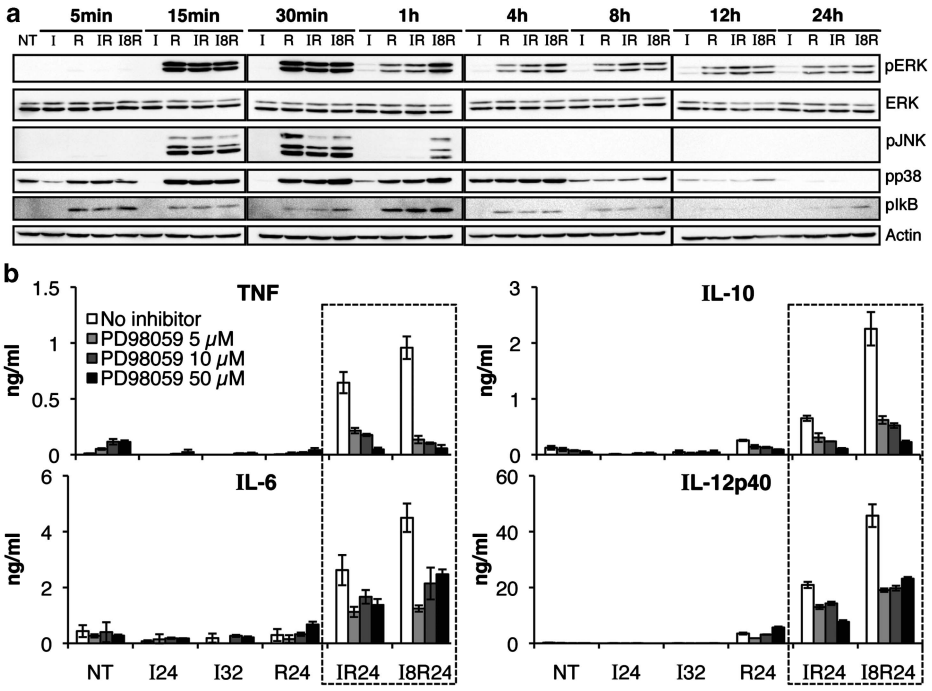

Figure 5 Synergy in cytokine expression is associated with sustained ERK phosphorylation. (**a**) Bone marrow-derived macrophages were treated with either 10 μg ml^{-1} poly(I:C) or 25 ng ml^{-1} R848 alone, poly(I:C) and R848 together simultaneously (IR) or pretreated with poly(I:C) for 8 h followed by a second stimulation of R848 (I8R). After second PAMP stimulation, cells were harvested at the indicated time points. Cell lysates were resolved on SDS-polyacrylamide gel electrophoresis gel, transferred to poly(vinylidene fluoride) membrane and probed with anti-phospho-ERK, anti-total-ERK, anti-phospho-p38, anti-phospho-JNK, anti-phospho-IkB and anti-actin. (**b**) ERK inhibition reduces but does not completely abolish synergistic cytokine production (boxed). Cells were left untreated (NT) or stimulated with 10 μg ml^{-1} poly(I:C) for 24 h (I24) or 32 h (I32), 25 ng ml^{-1} R848 for 24 h (R24), poly(I:C) and R848 simultaneously for 24 h (IR24), or pretreated with poly(I:C) for 8 h followed by R848 for 24 h (I8R24), in the presence or absence of increasing doses ERK inhibitor, PD98059 (5 μM, 10 μM or 50 μM). TNF, IL-10, IL-6 and IL-12p40 in cell-free supernatants were measured by ELISA.

Longer intervals (8–24 h) between the first and second stimulations remained synergistic, but the fold synergy declines as the interval increases. This suggests that priming with poly(I:C) induced a factor which is maximally active 4 h after R848 stimulation. In contrast, longer pre-stimulation with poly(I:C) from 8 to 16 h led to the maximal production of IL-6 and IL-12p40 under [I→R] stimulation. Thus, poly(I:C) may be acting via a mechanism that is most active 8–16 h after poly(I:C) stimulation. Taken together, our results show that crosstalk between signaling pathways induced by poly(I:C) and R848 must be synchronized for maximal cytokine production, with different time windows for different classes of cytokines.

Poly(I:C) strongly enhances R848-induced cytokine production although it is a weak inducer by itself

The requirement for signaling synchronization prompted us to examine the respective roles of poly(I:C) and R848 in signaling crosstalk. Similar to others,[4–6] we observed that R848 alone induced a basal level of IL-6 and IL-12p40 production, whereas poly(I:C) alone induced a low or undetectable amount of cytokines (Figure 4b). However, we observed that poly(I:C) strongly enhanced R848-induced cytokine production at the mRNA level (Figure 3). To substantiate this finding, we tested whether poly(I:C) and R848 would contribute to the synergy in a dose-dependent manner by using three doses each of poly(I:C) (0.3, 1 and 10 μg ml^{-1}) followed by R848 (5, 25 and 100 ng ml^{-1}; Figure 4c). By testing all nine possible combinations of poly(I:C) and R848 with various doses each, and measuring IL-6 and IL-12p40 production 24 h after the second TLR stimulation, we observed no significant synergy at 5 ng ml^{-1} of R848, even when the dose of poly(I:C) was as high as 10 μg ml^{-1}. Increasing the dosage of R848 to 25 ng ml^{-1} led to significant synergy, but no further enhancement was observed at 100 ng ml^{-1} (Figure 4c). Taken together, these results further support the notion that R848 alone is not able to induce a high level of cytokine production even at increasing dosage, although it contributes a basal level of induction. In contrast, under 25 and 100 ng ml^{-1} of R848, poly(I:C) enhanced IL-6 production dose dependently (Figure 4c), although on its own, poly(I:C) did not induce detectable amounts of IL-6 (Figure 4b). These data suggest that poly(I:C) contributes to synergy via induction of 'synergy factors' rather than a direct induction of IL-6. Similar observations were made for IL-12p40 (Figure 4c, lower panel). Collectively, these results support our observation that R848 stimulates basal levels of cytokine production, whereas poly(I:C) dose-dependently induces 'synergy factors', which seemed to greatly enhance the R848-induced cytokine production. Although blocking the type I interferon receptor slightly reduced the amount of cytokines produced (Supplementary Figure 3a), suggesting that the 'synergy' factor might be a type I interferon, addition of exogenous IFN-β failed to induce high levels of cytokine synergy compared with poly(I:C) pretreatment for 8 h (I8R) (Supplementary Figure 3b). The priming effect of poly(I:C) is robust as a low concentration (0.3 μg ml^{-1}) was sufficient to synergize with R848 for effective cytokine induction. Our results also underscore the concept that the innate immune system elicits a *memory* response after the first encounter with a PAMP, and it is able to adjust the level of synergy according to the dose and timing/order of infection.

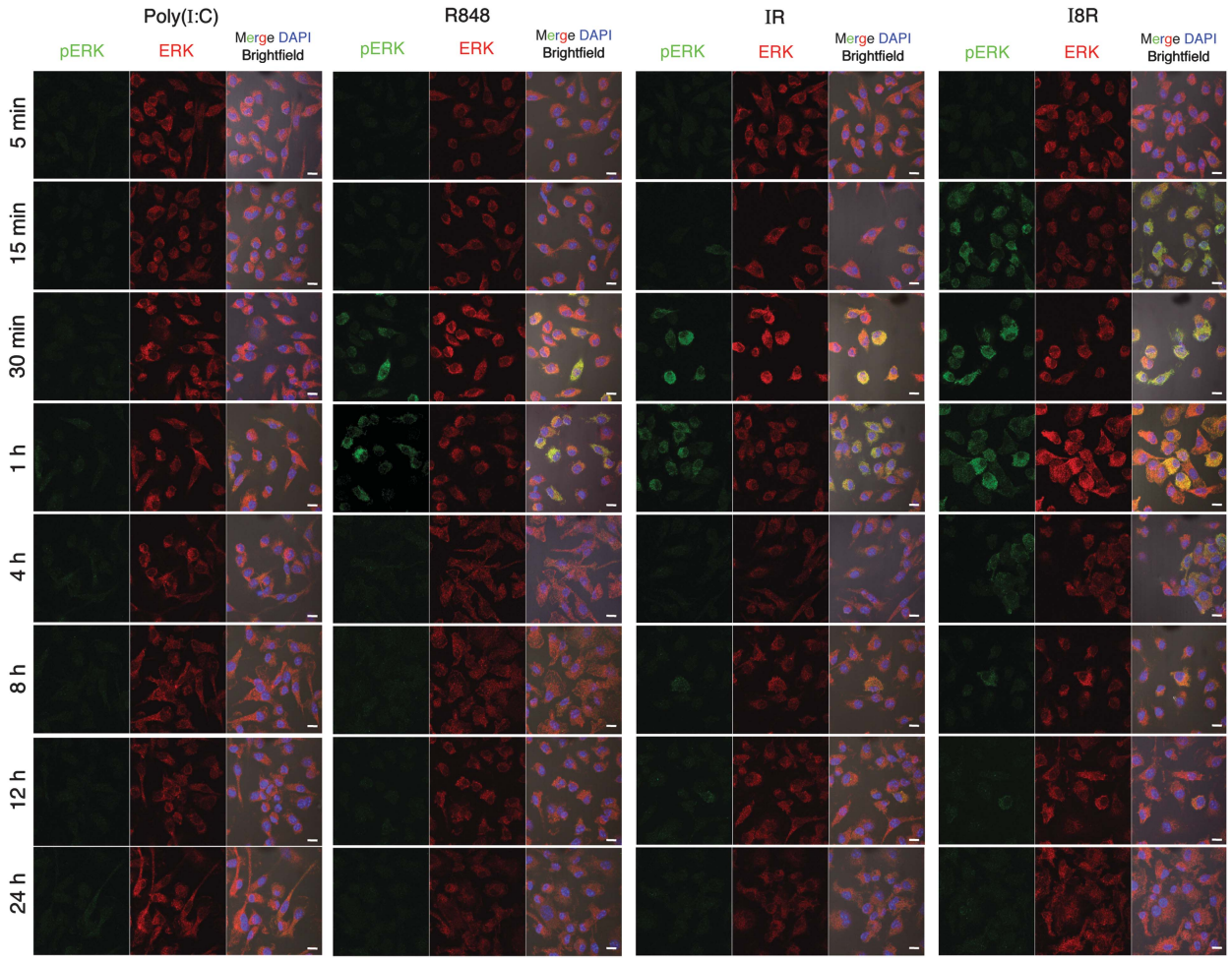

Figure 6 Phospho-ERK is localized to the cytoplasm following TLR stimulation. Bone marrow-derived macrophages were treated with either 10 μg ml^{-1} poly(I:C) or 25 ng ml^{-1} R848 alone, poly(I:C) and R848 together simultaneously (IR) or poly(I:C) for 8 h followed by R848. Cells were fixed at the indicated time points with 4% paraformaldehyde in phosphate-buffered saline (PBS), permeabilized with 0.1% Triton X-100 PBS and stained overnight at 4 °C, for phospho-ERK and total ERK, using antibodies raised in rabbit and mouse, respectively. Cells were washed in PBS and then stained with goat anti-rabbit Alexa-488 and donkey anti-mouse Alexa-546 for 1 h at room temperature. Nuclei are stained (blue) with 4′-6-diamidino-2-phenylindole. Images were taken on LSM510 confocal microscope (Zeiss). Scale bar indicated is 10 μm.

Synergy is associated with sustained cytoplasmic ERK phosphorylation

Next, we investigated the involvement of signaling molecules in the synergy resulting from combinatorial TLR stimulation of BM-DM. Single TLR stimulation is known to result in transient mitogen-activated protein kinase (MAPK) activation, upstream of cytokine expression. In human DCs, synergistic induction of IL-12p70 is known to be associated with sustained c-Jun phosphorylation.[4,15] Thus, we measured the phosphorylation of three key components of the MAPK pathway, extracellular signal-regulated kinase (ERK), p38 and c-Jun N-terminal kinase (JNK), as well as phosphorylated IκBα, in macrophages over time. We found that while single stimulations with either poly(I:C) or R848 led to similar profiles of p38, JNK and IκBα phosphorylation, simultaneous stimulation with both poly(I:C) and R848 (IR) enhanced ERK phosphorylation, which was sustained up to 8 h (Figure 5a). This result suggests that strong and sustained ERK phosphorylation might have a role in enhancing cytokine production observed when poly(I:C) and R848 are simultaneously encountered by the macrophages. Interestingly, this effect is even more pronounced when cells were pretreated with poly(I:C) for 8 h (Figure 5a, I8R). In this experiment, cells were either pretreated with or without poly(I:C) for the first 8 h, then stimulated with R848 and collected at the indicated time points. Our data show that although there is no direct phosphorylation caused by poly(I:C) from 4 h onwards, poly(I:C) pre-stimulation led to a much stronger phosphorylation of ERK upon second challenge with R848 (Figure 5a).

To confirm the role of sustained ERK signaling in synergy, we investigated the effect of PD98059, a chemical inhibitor of MEKs upstream of ERK. We found that inhibition of ERK reduced the production of all cytokines tested (Figure 5b), showing that sustained ERK phosphorylation is a possible mechanism of cytokine synergy.

Localization of ERK in synergy

ERK signaling regulates a vast number of cellular processes, from development to proliferation and apoptosis, sometimes in opposing ways. Other than the strength and duration of the ERK signal, specificity in response might also be determined by the subcellular localization of activated ERK, which determines substrate specificity. Cytoplasmic ERK is known to be associated with the cytoskeleton and activates various substrates such as Raf-1[16] and epidermal growth factor receptor[17], whereas nuclear-localized ERK activates transcription factors such as Elk-1[18] and c-Jun.[19] Thus, we sought to

determine the subcellular localization of phosphorylated ERK under dual TLR ligand stimulation. Consistent with the western blot data, single stimulation with either poly(I:C) or R848 led to a transient phosphorylation of ERK with a peak of 30–60 min, whereas dual TLR ligand stimulation (IR or I8R) led to sustained ERK phosphorylation up to 12 h post-stimulation (Figure 6). In either single or dual TLR stimulation, phosphorylated ERK was cytoplasmically distributed, suggesting that synergy might be mediated by a cytoplasmic target of ERK.

To further investigate the mechanism by which phosphorylated ERK was being retained in the cytoplasm, we examined the mRNA levels of DUSPs by real-time PCR. DUSPs are involved in the negative regulation of MAPK signaling, acting by dephosphorylating and thus inactivating their substrates.[20] We hypothesized that if sustained ERK signaling is the cause of synergy, we would see a reduction of DUSP under synergistic conditions. ERK is known to be a substrate of DUSPs 1–9 and 14. The mRNAs of DUSPs 3, 4, 5, 7, 8, 9 and 14 were not detected by reverse transcription PCR in untreated or stimulated samples. We were, however, able to detect transcripts of DUSP1, 2 and 6 (Figure 7). Interestingly, DUSP2 is known to be localized to the nucleus[21], whereas DUSP6 is localized in the cytoplasm.[22] Our data show that although DUSP1 and DUSP2 are upregulated upon synergistic stimulation, DUSP6 is downregulated (Figure 7). This suggests that the sustained ERK signaling responsible for synergistic cytokine production is plausibly due to a downregulation of DUSP6.

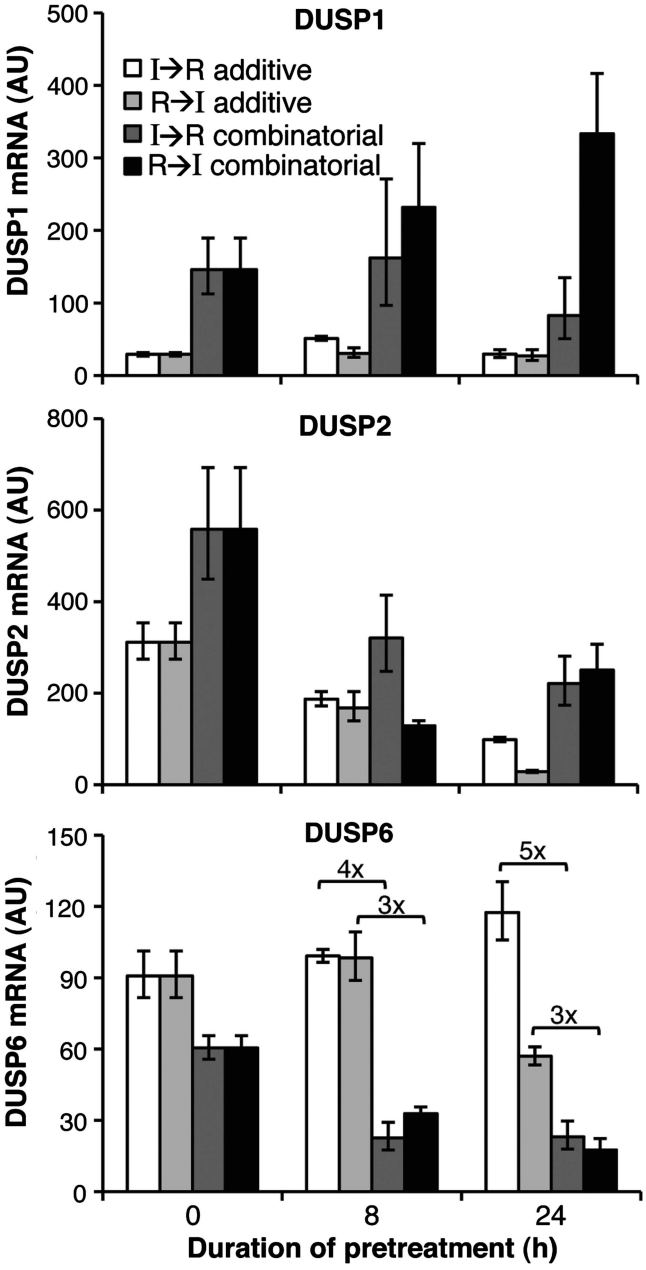

Figure 7 DUSP 1, 2 and 6 mRNA expression under synergistic conditions. Bone-marrow derived macrophages were pretreated with a first TLR ligand for 0, 8 or 24 h, followed by a second TLR ligand for another 8 h. 0 h pre-stimulation denotes simultaneous stimulation. [I→R combinatorial, dark grey] symbolizes poly(I:C) as the first TLR ligand, followed by R848 as second TLR ligand. [R→I combinatorial, black] indicates the same stimulations in reverse order. The hypothetical additive effects were computed for [I→R additive, white] and [R→I additive, light grey]. DUSP1, DUSP2 and DUSP6 mRNAs were measured by real-time PCR in the SYBR green format using primers specific to each mRNA. Data represent means ± s.d. of a representative experiment. The fold downregulation of DUSP6 mRNA for each of the combinatorial stimulations compared with their respective controls are as labeled.

DISCUSSION

We have shown that innate immune response to complex stimuli is determined not only by the combination of TLR ligands, but also by the timing, order and dosage of TLR agonists. The requirement for optimal timing and order indicates that signaling pathways elicited by the two TLR agonists (double-stranded RNA poly(I:C) and single-stranded RNA R848) must be synchronized for optimal induction of the respective cytokines. Our results recapitulate the concept that the immune system is able to adjust the level of synergy according to the dose and timing/order of infection. Therefore, it is important to consider the context of infection when studying immune-signaling crosstalk. In addition, we have narrowed down the range of possible synergy factors to newly synthesized protein(s), which appear(s) to sustain ERK phosphorylation and cytoplasmic localization, facilitating future identification and characterization.

Synergistic cytokine induction has been extensively studied in DC, with a focus on IL-12p70 production and subsequent Th1 adaptive immune responses.[4–8] In contrast, macrophages are known to produce much lower levels of IL-12p70 in a non-synergistic manner.[15] This is unsurprising, given that macrophages function primarily in innate rather than adaptive immunity. Indeed, DC and macrophages are known to produce different cytokine profiles in response to the same pathogen, with DC secreting higher amounts of IL-12p70 in response to *Mycobacterium tuberculosis*, compared with that of macrophages.[23] We have shown, however, that macrophages are able to synergistically secrete high amounts of IL-12p40, one of the subunits of IL-12p70. Nevertheless under the same conditions, only low amounts of IL-12p70 and IL-23 were secreted (Supplementary Figure 4), raising the possibility that macrophages produce large amounts of IL-12p40 as a monomer or homodimer (p80). In this form, IL-12p40 can act as a macrophage chemoattractant, and it has shown to be involved in the recruitment of macrophages to the lung in response to Sendai virus infection in mice, conferring resistance to lethality.[24] It is noteworthy that Sendai virus is a single-stranded RNA virus, which undergoes a double-stranded RNA phase during genomic replication in the host cell, and thus contains both TLR3 and TLR7 ligands similar to those used in our study. Therefore, synergistic levels of production of IL-12p40 by macrophages may promote innate immunity by increasing the

number of immune cells at the site of infection, rather than combining with IL-12p35 to form IL-12p70 and drive Th1 responses. These cell type-specific differences may be attributed to differential usage of TLRs,[23] or differential chromatin status (the IL-6 promoter is constitutively open in fibroblasts but closed in macrophages),[25] or cell type-specific synergy factors.

Although there are differences in IL-12p70 secretion, both macrophages and DC synergistically produce IL-6 and TNF in response to combinatorial stimulation by poly(I:C) and R848.[4] This is consistent with the idea that the activation of both MyD88- and TRIF-mediated pathways is required for synergy.[8,9] From our data, poly(I:C) was unable to induce IL-6 or IL-12p40 production (Figure 4c) and yet it boosted the fold synergy of these two cytokines in a dose-dependent manner. It is likely that R848 elicits a basal level of cytokine induction (Figure 4c), which was enhanced by poly(I:C) signaling through a protein synthesis-dependent mechanism (Figure 3c). This possibility is supported by our study of signaling molecules, which shows that poly(I:C) is a weaker inducer than R848 alone, but has a modulating effect when simultaneously administered with R848, prolonging and enhancing the ERK phosphorylation signal (Figures 5 and 6). However, these results do not rule out the possible involvement of other signaling pathways such as the interferon regulatory factors. An alternative explanation could be that poly(I:C) causes synergy with R848 through chromatin modifications, a mechanism that has been demonstrated in other studies.[26–29] Taken together, our results show that a first encounter with poly(I:C) seems to imprint a memory effect, which cross-primes the macrophages for a more rapid, higher and sustained immune response to the second PAMP challenge with R848.

Previous microarray studies have found that DUSP genes are synergistically upregulated under combinatorial TLR stimulation.[4,30] Our study is the first to implicate the downregulation DUSP proteins in the regulation of synergistic cytokine production, linking DUSP6 downregulation to the sustained phosphorylation of ERK. Regulation of the phosphoproteome is a key mechanism regulating innate immunity,[31] and our findings suggest that dephosphorylation events are just as important as kinase activity in modulating the magnitude of the response.

Our results showed that secondary response genes such as *Il6* and *Il12b* elicited a greater extent of synergy (70- to 90-fold) at the mRNA level than primary response genes such as *Tnf* (1- to 2-fold; Figure 3b, white bars) in response to poly(I:C) and R848. Our observation is consistent with previous reports that secondary response gene (for example, *Il6*, *Il12b*) production in response to LPS strictly requires both MyD88 and TRIF signaling, whereas primary response genes (for example, *Tnf*, *Il10*) still have residual production in the absence of either MyD88 or TRIF, and this is probably regulated by a newly synthesized protein.[14] Interestingly, we found that the fold synergy of secondary response genes is highly dependent on new protein synthesis (Figure 3c), whereas the primary response genes are not affected. Considering the importance of *trans*-regulatory elements[13] and chromosome remodeling[14,25,32] in gene regulation, the newly synthesized proteins are plausibly enhancer-binding proteins or proteins which may influence chromatin remodeling. Identification of these 'synergy-inducing proteins' is warranted in future studies to further understand the mechanism of signaling crosstalk and regulation of secondary response genes in *innate immune memory*.

METHODS

Materials

Media and supplements were purchased from Gibco, Life Technologies (Carlsbad, CA, USA). Fetal bovine serum was purchased from Hyclone, Thermofischer Scientific (Waltham, MA, USA). Recombinant mouse macrophage colony stimulating factor (M-CSF) was purchased from Ebioscience (San Diego, CA, USA). TLR ligands R848 and low-molecular-weight poly(I:C) were from Invivogen (San Diego, CA, USA), Pam_3CSK_4 from Calbiochem, EMD Biochemicals (Darmstadt, Germany) and *Escherichia coli* 055:B55 LPS from Sigma-Aldrich (St Louis, MO, USA). Maxisorp microtitre 96-well plates were obtained from Nunc (Roskilde, Denmark). Rabbit monoclonal antibodies against phospho-p38 (#4511), phospho-ERK1/2 (#4370) and phospho-JNK (#4668) were obtained from Cell Signaling Technologies (Boston, MA, USA). Rabbit monoclonal antibody to β-actin and goat polyclonal horse radish peroxidase (HRP)-conjugated secondary antibodies to rabbit IgG were from Sigma-Aldrich. Alexa Fluor-488 secondary goat anti-rabbit (H + L) highly cross-absorbed was from Molecular Probes, Invitrogen (Carlsbad, CA, USA).

Animals

Mouse BM-DM were prepared as described previously.[33] Briefly, femurs were isolated from 8-week-old female BALB/c mice, and the resulting bone-marrow cells were resuspended in Dulbecco's modified Eagle's medium containing 10% (v/v) fetal bovine serum, 100 U ml^{-1} penicillin, 100 mg ml^{-1} streptomycin and 100 U ml^{-1} recombinant M-CSF at a density of 4×10^6 cells per ml. On day 3 post harvest, additional M-CSF media was supplied and cells were cultured for another 4 days before plating. Experiments on mice were performed according to the guidelines and regulations of the Institutional Animal Care and Use Committee (IACUC protocol number: 049-11).

Cell culture

Primary BM-DM and mouse macrophage cell line RAW 264.7 were cultured in Dulbecco's modified Eagle's medium with 10% fetal bovine serum. Cells were stimulated 24 h after plating with 1 ml of fresh medium per well with the respective TLR ligands. At indicated time intervals, the second PAMP or pyrogen-free water (mock) was applied to the cells as second stimulation. The final concentrations of TLR ligands in the culture were 25 ng ml^{-1} of R848, 10 μg ml^{-1} of poly(I:C), 10 ng ml^{-1} Pam_3CSK_4 or 10 ng ml^{-1} *E. coli* 055:B55 LPS.

CHX treatment

BM-DM at a density of 1×10^6 cells per ml in 0.5 ml was plated per well into 24-well plates. At 24 h after plating, the cells were pre-treated with 10 μg ml^{-1} of CHX (Sigma, St Louis, MO, USA) for 15 min, and then 2 μl of poly(I:C) at 2.5 μg ml^{-1} or pyrogen-free water was applied as first stimulation. This was followed 8 h later by a second stimulation with 2 μl of R848 at 6.25 ng ml^{-1} or pyrogen-free water.

Measurement of cytokine production

Culture supernatants were collected at 24 h after the second stimulation and stored at −80 °C. The levels of IL-12p40, IL-6, IL-10, TNF (BD Biosciences Inc.) were measured according to the manufacturer's instructions. For the multiplex cytokine assay, a luminex kit (Panomics/Affymetrix, Freemont, CA, USA) was used according to the manufacturer's instructions. The lower limit of detection was 2.5 pg ml^{-1} for all cytokines tested. Student's *t*-tests were performed from the data of three independent experiments and $P < 0.05$ were considered significant. For CHX treatment, BM-DM were pretreated with 10 mg ml^{-1} of CHX from Sigma-Aldrich for 15 min before stimulation.

Real-time PCR

Cells were harvested with Trizol (Invitrogen) and frozen at −80 °C until mRNA extraction. cDNAs were synthesized with Superscript III reverse transcriptase (Invitrogen). All real-time PCR were carried out with Light cycler 480 (Roche, Penzburg, Germany). Lightcycler 480 probes master mix (Roche) were used for the Taqman assays, and pre-designed TaqMan Gene Expression Assays (Life Technologies) Mm00446190_m1, Mm00434174_m1, Mm01290062_m1 Mm00446968_m1 were used for the detection of *Il6*, *Il12b*, *Il10, Tnf and Hprt* mRNA, respectively. The PCR cycles constituted 1 cycle of 95 °C for 10 min, followed by 40 cycles of 95 °C for 10 s, 60 °C for 20 s. The mRNA levels were normalized to that of *Hprt* and expressed as relative amount

to *Hprt*. DUSP1, DUSP2 and DUSP6 mRNAs were detected with SYBR Green method by using Lightcycler 480 SYBR Green I Master Mix (Roche), and the mRNA levels were normalized to that of β-actin. Forward primer: 5′-CACCCGCGAGCACAGCTTCT-3′ and reverse primer: 5′-TGCTCTGG GCCTCGTCACCC-3′ was used for detection of β-actin mRNA. Forward primer 5′-TTCGCTTTCAACGCCGGCCA-3′ and reverse primer 5′-AGCTC AGGGCAGGAAGCCGA-3′ was used for DUSP1 mRNA detection. Forward primer 5′-CCGTGTGCTTCTTGCGAGGC-3′ and reverse primer 5′-TTG GGGCAGCTGGCAGAGACA-3′ was used for DUSP2 mRNA detection. Forward primer 5′-ACCGCTTTACCAGGCGCTGC-3′ and reverse primer 5′-TCGCAGTGCAGGGCGAACTC-3′ was used for DUSP6 mRNA detection. All primers were designed to amplify intron spanning cDNA products, thereby excluding the amplification of genomic DNA. The PCR reaction conditions were 95 °C for 10 min, followed by 40 cycles of 95 °C for 10 s, 62 °C for 10 s and 72 °C for 15 s.

Western blot analysis

Cells were lysed in RIPA buffer in the presence of protease and phosphatase inhibitor cocktail from Roche. A measure of 10 μg total protein was separated on 10% SDS-polyacrylamide gel electrophoresis and electrotransferred to a poly(vinylidene fluoride) membrane. Transblots were washed three times in Tris buffered saline with Tween-20 (TBST) (50 mM Tris-base, 150 mM NaCl, 0.01% Tween-20, pH 7.6) before blocking with 5% skimmed milk in TBST for 1 h. Primary antibodies diluted in 5% bovine serum albumin TBST and incubated with the membranes overnight at 4 °C with gentle agitation. Following incubation with primary antibodies, membranes were washed three times with TBST. Protein detection was carried out by incubating blots with respective HRP-conjugated secondary antibodies (1:5000) for 1 h. Molecular weights were calibrated in proportion to the running distance of Precision Plus dual colour protein standards from Bio-Rad (Richmond, CA, USA). The immunodetected bands were visualized on Kodak film using an ECL system from Pierce, Thermofischer Scientific.

Immunofluorescence microscopy

BALB/c derived BM-DM were cultured on glass coverslips in 24-well tissue culture plates overnight, followed by stimulation with poly(I:C) or R848 or both. After the indicated time points, cells were fixed in 4% paraformaldehyde in phosphate-buffered saline for 15 min, then permeabilized with 5% bovine serum albumin/phosphate-buffered saline with 0.1% Triton X-100 for 15 min. Cells were then stained with rabbit anti-phospho-ERK (1:250) and mouse anti-total ERK (1:250) followed by Alexa Fluor-488 secondary goat anti-rabbit (1:500) and Alexa Fluor-546 secondary donkey anti-mouse (1:500). Nuclei were stained with 4′-6-diamidino-2-phenylindole in ProLong Gold antifade reagent. Images were obtained on a Carl Zeiss LSM 510 Meta microscope.

1 Ishii KJ, Koyama S, Nakagawa A, Coban C, Akira S. Host innate immune receptors and beyond: making sense of microbial infections. *Cell Host Microbe* 2008; **3:** 352–363.
2 Akira S, Uematsu S, Takeuchi O. Pathogen recognition and innate immunity. *Cell* 2006; **124:** 783–801.
3 Agrawal S, Agrawal A, Doughty B, Gerwitz A, Blenis J, Van Dyke T *et al.* Cutting edge: different Toll-like receptor agonists instruct dendritic cells to induce distinct Th responses via differential modulation of extracellular signal-regulated kinase-mitogen-activated protein kinase and c-Fos. *J Immunol* 2003; **171:** 4984–4989.
4 Napolitani G, Rinaldi A, Bertoni F, Sallusto F, Lanzavecchia A. Selected Toll-like receptor agonist combinations synergistically trigger a T helper type 1-polarizing program in dendritic cells. *Nat Immunol* 2005; **6:** 769–776.
5 Theiner G, Rössner S, Dalpke A, Bode K, Berger T, Gessner A *et al.* TLR9 cooperates with TLR4 to increase IL-12 release by murine dendritic cells. *Mol Immunol* 2008; **45:** 244–252.
6 Zhu Q, Egelston C, Vivekanandhan A, Uematsu S, Akira S, Klinman DM *et al.* Toll-like receptor ligands synergize through distinct dendritic cell pathways to induce T cell responses: implications for vaccines. *Proc Natl Acad Sci USA* 2008; **105:** 16260–16265.
7 Bohnenkamp HR, Papazisis KT, Burchell JM, Taylor-Papadimitriou J. Synergism of Toll-like receptor-induced interleukin-12p70 secretion by monocyte-derived dendritic cells is mediated through p38 MAPK and lowers the threshold of T-helper cell type 1 responses. *Cell Immunol* 2007; **247:** 72–84.
8 Krummen M, Balkow S, Shen L, Heinz S, Loquai C, Probst HC *et al.* Release of IL-12 by dendritic cells activated by TLR ligation is dependent on MyD88 signaling, whereas TRIF signaling is indispensable for TLR synergy. *J Leukoc Biol* 2010; **88:** 189–199.
9 Bagchi A, Herrup EA, Warren HS, Trigilio J, Shin HS, Valentine C *et al.* MyD88-dependent and MyD88-independent pathways in synergy, priming, and tolerance between TLR agonists. *J Immunol* 2007; **178:** 1164–1171.
10 De Nardo D, De Nardo CM, Nguyen T, Hamilton JA, Scholz GM. Signaling crosstalk during sequential TLR4 and TLR9 activation amplifies the inflammatory response of mouse macrophages. *J Immunol* 2009; **183:** 8110–8118.
11 Macagno A, Napolitani G, Lanzavecchia A, Sallusto F. Duration, combination and timing: the signal integration model of dendritic cell activation. *Trends Immunol* 2007; **28:** 227–233.
12 Alon U. Network motifs: theory and experimental approaches. *Nat Rev Genet* 2007; **8:** 450–461.
13 Litvak V, Ramsey SA, Rust AG, Zak DE, Kennedy KA, Lampano AE *et al.* Function of C/EBPdelta in a regulatory circuit that discriminates between transient and persistent TLR4-induced signals. *Nat Immunol* 2009; **10:** 437–443.
14 Kayama H, Ramirez-Carrozzi VR, Yamamoto M, Mizutani T, Kuwata H, Iba H *et al.* Class-specific regulation of pro-inflammatory genes by MyD88 pathways and IkappaB-zeta. *J Biol Chem* 2008; **283:** 12468–12477.
15 Mäkelä SM, Strengell M, Pietilä TE, Osterlund P, Julkunen I. Multiple signaling pathways contribute to synergistic TLR ligand-dependent cytokine gene expression in human monocyte-derived macrophages and dendritic cells. *J Leukoc Biol* 2009; **85:** 664–672.
16 Anderson NG, Li P, Marsden LA, Williams N, Roberts TM, Sturgill TW. Raf-1 is a potential substrate for mitogen-activated protein kinase *in vivo*. *Biochem J* 1991; **277** (Pt 2), 573–576.
17 Northwood IC, Gonzalez FA, Wartmann M, Raden DL, Davis RJ. Isolation and characterization of two growth factor-stimulated protein kinases that phosphorylate the epidermal growth factor receptor at threonine 669. *J Biol Chem* 1991; **266:** 15266–15276.
18 Marais R, Wynne J, Treisman R. The SRF accessory protein Elk-1 contains a growth factor-regulated transcriptional activation domain. *Cell* 1993; **73:** 381–393.
19 Pulverer BJ, Kyriakis JM, Avruch J, Nikolakaki E, Woodgett JR. Phosphorylation of c-jun mediated by MAP kinases. *Nature* 1991; **353:** 670–674.
20 Lang R, Hammer M, Mages J. DUSP meet immunology: dual specificity MAPK phosphatases in control of the inflammatory response. *J Immunol* 2006; **177:** 7497–7504.
21 Rohan PJ, Davis P, Moskaluk CA, Kearns M, Krutzsch H, Siebenlist U *et al.* PAC-1: a mitogen-induced nuclear protein tyrosine phosphatase. *Science* 1993; **259:** 1763–1766.
22 Mourey RJ, Vega QC, Campbell JS, Wenderoth MP, Hauschka SD, Krebs EG *et al.* A novel cytoplasmic dual specificity protein tyrosine phosphatase implicated in muscle and neuronal differentiation. *J Biol Chem* 1996; **271:** 3795–3802.
23 Pompei L, Jang S, Zamlynny B, Ravikumar S, McBride A, Hickman SP *et al.* Disparity in IL-12 release in dendritic cells and macrophages in response to Mycobacterium tuberculosis is due to use of distinct TLRs. *J Immunol* 2007; **178:** 5192–5199.
24 Gunsten S, Mikols CL, Grayson MH, Schwendener RA, Agapov E, Tidwell RM *et al.* IL-12 p80-dependent macrophage recruitment primes the host for increased survival following a lethal respiratory viral infection. *Immunology* 2009; **126:** 500–513.
25 Ramirez-Carrozzi VR, Braas D, Bhatt DM, Cheng CS, Hong C, Doty KR *et al.* A unifying model for the selective regulation of inducible transcription by CpG islands and nucleosome remodeling. *Cell* 2009; **138:** 114–128.
26 Foster SL, Hargreaves DC, Medzhitov R. Gene-specific control of inflammation by TLR-induced chromatin modifications. *Nature* 2007; **447:** 972–978.
27 Park SH, Park-Min KH, Chen J, Hu X, Ivashkiv LB. Tumor necrosis factor induces GSK3 kinase-mediated cross-tolerance to endotoxin in macrophages. *Nat Immunol* 2011; **12:** 607–615.
28 Kleinnijenhuis J, Quintin J, Preijers F, Joosten LA, Ifrim DC, Saeed S *et al.* Bacille Calmette-Guerin induces NOD2-dependent nonspecific protection from reinfection via epigenetic reprogramming of monocytes. *Proc Natl Acad Sci USA* 2012; **109:** 17537–17542.
29 Quintin J, Saeed S, Martens JH, Giamarellos-Bourboulis EJ, Ifrim DC, Logie C *et al.* Candida albicans infection affords protection against reinfection via functional reprogramming of monocytes. *Cell Host Microbe* 2012; **12:** 223–232.
30 Tross D, Petrenko L, Klaschik S, Zhu Q, Klinman DM. Global changes in gene expression and synergistic interactions induced by TLR9 and TLR3. *Mol Immunol* 2009; **46:** 2557–2564.
31 Weintz G, Olsen JV, Frühauf K, Niedzielska M, Amit I, Jantsch J *et al.* The phosphoproteome of toll-like receptor-activated macrophages. *Molecular systems biology* 2010; **6:** 371.
32 Ramirez-Carrozzi VR, Nazarian AA, Li CC, Gore SL, Sridharan R, Imbalzano AN *et al.* Selective and antagonistic functions of SWI/SNF and Mi-2beta nucleosome remodeling complexes during an inflammatory response. *Genes Dev* 2006; **20:** 282–296.
33 Zhang X, Goncalves R, Mosser DM. The isolation and characterization of murine macrophages. *Curr Protoc Immunol* 2008, Chapter 14 (Unit 14), 11.

The Supplementary Information that accompanies this paper is available on the Immunology and Cell Biology website (http://www.nature.com/icb)

Synchronization of IRF1, JunB and C/EBPβ activities during TLR3-TLR7 crosstalk orchestrates timely cytokine synergy in proinflammatory response[1]

Qian Liu*,[2], Yong Zhu*,[2], Wai Khang Yong*, Newman Siu Kwan Sze†, Nguan Soon Tan† and Jeak Ling Ding*,[3]

*Department of Biological Sciences, Faculty of Science, National University of Singapore, Singapore, 117543.

†School of Biological Sciences, Nanyang Technological University, 60 Nanyang Drive, Singapore 637511.

Running title: Mechanism of proinflammatory cytokine synergy

[1] This work was supported by grants from the A*STAR Biomedical Research Council (BMRC 10/1/21/19/658) and National Medical Research Council (NMRC/CBRG/0055/2014).

[2] Equal first authors

[3] Correspondence: Email: dbsdjl@nus.edu.sg; Tel: 65-6516 2776; Fax: 65-6779 2486.

Abstract

Multiple PAMP[4]-induced TLR-pathway crosstalk provokes proinflammatory cytokine synergy in macrophages, which is important for pathogen resistance and immune homeostasis. But the detailed mechanisms are unclear. Here, we demonstrate viral RNA-analogue induced transcription synergy of *Il6* and *Il12b* via IRF1 (TLR3-TRIF-responsive), C/EBPβ (TLR7-MyD88-responsive) and JunB (all-responsive). Co-activation of TLR3 and TLR7 pathways synchronizes the interaction of IRF1, JunB and C/EBPβ with the *Il6* and *Il12b* promoters, facilitating maximal gene expression. MyD88 pathway-activation suppresses TRIF-induced IRF1 in a delayed mode, thus controlling the magnitude and timing of cytokine expression. Our findings provide novel mechanisms of cooperation of different TLR pathways to achieve optimal immune responses, with potentials for immunomodulatory strategies.

[4] Abbreviations: IRF, interferon regulatory factor ; iTRAQ, Isobaric tag for relative and absolute quantitation; MyD88, myeloid differentiation primary-response protein 88; NE, nuclear extract; PAMP, pathogen-associated molecular pattern; TRIF, TIR domain-containing adaptor including IFN-β; R, R848; I, poly(I:C); NT, non-treated; TF, transcription factor; GO, Gene Ontology.

Introduction

Tissue-resident macrophages are deployed in frontline immunity, providing surveillance on invading pathogens. Macrophages use TLRs as central sensors of pathogens (1) to recognize pathogen-associated molecular patterns (PAMPs) unique to the microbes, for example, viral single-stranded (ss) and double-stranded (ds) RNAs. Activated resident macrophages produce cytokines to recruit and communicate with other immune cells. Effective and coordinated cytokine production contributes to elimination of the infectious agents, builds up memory and repairs tissues without compromising homeostasis. Any imbalance or imprecision in cytokine production could either reduce resistance to pathogen infection or cause a fatal cytokine storm and chronic inflammatory diseases (2-4).

Production of cytokines induced by PAMP-activated TLRs mainly occur through the recruitment of two adaptors, MyD88 and TRIF (5). MyD88, used by all TLRs except TLR3, activates NFκB, which is a core transcription factor (TF) for pro-inflammatory cytokines. In contrast, TRIF, the adaptor for TLR3 and TLR4 (1), activates interferon regulatory factor 3 (IRF3), a master transcription controller of antiviral responses. In addition, both MyD88 and TRIF activate MAPK pathway (6). Invading pathogens are likely to interact with multiple TLRs and the magnitude and timing of cytokine production, which determines the quality of immune response, are dependent on the coordinated sum of the signals induced by these different TLRs. Co-stimulation with MyD88- and TRIF-activating TLR ligands has been observed to synergize cytokine production in innate immune cells (7-9), indicating crosstalk between MyD88 and TRIF pathways. By co-stimulation of mouse macrophages with R848 (R) (an ssRNA analogue, recognized by TLR7) and poly(I:C) (I) (a dsRNA analogue, recognized by TLR3), we demonstrate that TLR3-TRIF and TLR7-MyD88 pathways

collaborate to induce synergistic and timely expression of pro-inflammatory cytokines through coordinated actions of transcription factors JunB, C/EBPβ and IRF1.

Materials and Methods

All experiments were carried out in compliance with the Institutional Animal Care and Use guidelines (IACUC Protocol Ref: 049/11).

Reagents and assays

QuantiGene plex 2.0 (Affymetrix) was used to profile cytokine expressions in murine BMDM. TaqMan Gene Expression Assays (Life Technologies) Mm00446190_m1, Mm00434174_m1, and Mm00446968_m1 were used for quantifying expression of *Il6* and *Il12b* relative to *Hprt*. In knockdown experiments, IL6 and IL12p40 were measured using ELISA kits (BD OptEIA™). Scramble control or ON-TARGETplus SMARTpool siRNA (Darmacon) against mouse *Junb*, *Irf1* or/and *Cebpb* (at 50 nM each), were transfected into J774 macrophages using X-tremeGENE HP DNA Transfection Reagent (Roche). Antibody against JunB (sc73), RelB (sc226), IRF1 (sc640), IRF8 (sc6058) and GAPDH (sc32233) are from Santacruz; RelA (ab7970), TBP (ab818) and IRF3 (ab25950) from Abcam; C/EBP beta (MA1-827) from Thermo; NFκB p50 (14-6732-63) and cREL (14-6111-82) from eBiosciences.

Macrophages and stimulations

BMDM was isolated as described previously (10). Isolated BMDM or mouse macrophage J774 cell line were cultured and stimulated singly with 10 μg/ml of poly(I:C) (I) or 25 ng/ml of R848 (R), or simultaneously co-stimulated (IR) as described previously (9).

Chromatin binding protein extraction and iTRAQ analysis

Chromatin binding proteins were purified and analyzed by iTRAQ (11).

Nuclear extract (NE), promoter cloning and 3'-end biotin labeling, and pull down assay

Details of *Il6* and *Il12b* promoter cloning and 3'-end biotin labeling are described in the legend to supplemental figure 2A. NE was prepared from J774 treated with I, R or IR for 5 h as described previously(12) with modification (pelleting nuclei by a 14,000 ×g pulse spin for 15s). 100 fmol Biotin labeled promoters were incubated with 25 μg NE in 100 μl binding mixture of 10 mM Tris-HCl, pH 7.5, 50 mM KCl, 1 mM DTT, 12.5 % glycerol, 0.05 % NP-40, 5 μg polydI:dC (Sigma) at 25 °C for 25-30 min. Biotin labeled promoters were then pulled down from the binding mixture with streptavidin-conjugated magnetic Dynabeads M-280 (Life Technologies Inc.) at 4°C for 3 h with agitation.

Results

Co-stimulation of TLR7 and TLR3 induces transcriptional synergy of *Il6* and *Il12b*.

To investigate whether cytokine synergy is a prevalent event in the activated macrophages (9), we compared the fold synergy of macrophage-specific major chemokines and cytokines, in mouse BMDM. Fold-synergy was evaluated as described in the legend to figure 1. Proinflammatory cytokines (*Il6* and *Il12b*) *and* anti-inflammatory *Il10*, elicited the highest synergy of >5-fold (**Figure 1**). This study focused on proinflammatory cytokines. The synergistic expression of *Il6* and *Il12b* is neither attributable to chromatin remodeling (**Figure S1A**) nor to enhanced mRNA stability (**Figure S1B**), indicating elevated transcriptional activity under co-stimulation.

Proteomic analysis revealed potential synergy factors

Next, we searched for newly synthesized/activated TFs, which may play a role in the observed synergy. We compared the profiles of chromatin binding proteins from differently stimulated macrophages on the basis that transcriptional synergy might be facilitated by the collaboration of R-induced and I-induced TFs, or by co-stimulation (IR)-activated TFs. J774, which exhibits synergy consistent with that of primary BMDM (**Figure S1C**), was used for this study. iTRAQ (13) analysis of chromatin binding proteins from two biological replicates, identified proteomes of ~1100 proteins with false discovery rates of <1%. As anticipated, the majority is nucleic acid binding proteins and TFs (**Figure S1D**). The enriched functional clusters within the proteins perturbed were sorted (**Figure S1E, F**). Interestingly, the GO (gene ontology) functional annotation cluster of the “regulation of transcription” was enriched in the proteins upregulated by 5 h co-stimulation but not other treatments. We listed the IR5

upregulated proteins from the "regulation of transcription" cluster and their iTRAQ ratios under different treatments in **Table 1**, with potential synergy factors earmarked. C/EBPβ and NFκB-p105 were more responsive to R stimulation, while interferon activated protein 204 (Ifi204) responded to I only. JunB and ATF3 are more upregulated after co-stimulation than single stimulation, indicating synergistic actions of two distinct pathways. As a negative regulator of cytokines (14), ATF3 was not further studied here. Being relatively uncharacterized, Ifi204 was also excluded. Western blot of NFκBp105, JunB and C/EBPβ (**Figure S1G, H)** validated their changes in expression detected by iTRAQ, and they are shortlisted as potential synergy factors.

JunB, C/EBPβ and IRF1 are the core interaction partners of *Il6* and *Il12b* promoters

By promoter affinity pulldown of nuclear extracts, we examined the direct or indirect involvement of TFs in the regulation of *Il6* and *Il12b* transcription. Candidates shortlisted by iTRAQ and other low abundance cytokine regulatory factors, which might have been missed in iTRAQ analysis, were analyzed. In total, we examined: (1) JunB, (2) C/EBPβ, (3) NFκB family members (RelA, RelB and c-Rel, NFκBp50), and (4) IRF1, IRF3, and IRF8, that are known to be downstream of the TRIF signaling pathway and are involved in the production of type I interferon. We observed consistent association of JunB, IRF1 and C/EBPβ to both *Il6* and *Il12b* promoters (**Figure 2A**), compared to controls (**Figure S2A**). The intensities of the detection signal appeared roughly proportional to their respective levels in the nuclear extract, suggesting that these TFs associate with the respective promoter independently of each other. Notably, the dominant upper band of JunB was dose-dependently sensitive to phosphatase treatment (**Figure S2B**), indicating that JunB was extensively phosphorylated upon induction. Surprisingly, Rel proteins were not significantly associated with either *Il12b* or *Il6* promoter,

although NFκB is functionally important for pro-inflammatory responses, and there is a characterized κB binding element in *Il12b* (15) and *Il6* promoters (16).

Co-stimulation synchronizes the activation of C/EBPβ, IRF1 and JunB.

The IRF1 and C/EBPβ were strongly induced by I and R, respectively (see nuclear extracts, Figure 2), and no additive effect was observed with co-stimulation by IR. This suggests that IRF1 and C/EBPβ are separately regulated under TRIF- and MyD88- signaling pathways, respectively. In contrast, JunB expression, which was induced weakly by I but strongly by R, was substantially higher in co-stimulation.

Next, we examined the dynamic profile of IRF1, C/EBPβ and JunB under different treatments (**Figure 3**). C/EBPβ responded mainly to R stimulation. IRF1 was upregulated and sustained by I, but transiently (1 h) upregulated by R, likely due to the rapid primary activation of NFκB, which is known to be required for IRF1 expression (17). However, R-induced MyD88 pathway activation apparently represses the I-induced expression of IRF1 in a delayed mode. The IRF1 returned to a low basal level at 12 h post co-stimulation, correlating with subdued cytokine gene transcriptions. In contrast, JunB was rapidly upregulated within 1 h, by all stimulations. Notably, over 4-8 h, R induced a stronger JunB response than I. By 12 h, both I and R induced comparable levels of JunB, indicating equally limited potentials in single stimulations. Nevertheless, in co-stimulated macrophages, JunB expression was sustained and accumulated over 8-24 h. Taken together, the coincidence of the levels of IRF1, C/EBPβ and JunB in the 4-12 h post-combinatorial stimulation and the obvious correlation with the mRNA peaks of *Il6* and *Il12b* (Figure S1C), strongly indicate their co-operation in synergistic transcription.

TRIF- and MyD88- signaling pathways collaborate to synergize IL6 and IL12p40 expression through synchronized IRF1 and C/EBPβ activities

The functional cooperation between TRIF-responsive IRF1 and MyD88-responsive C/EBPβ in macrophages was examined using single and double knockdown with gene-specific siRNAs of *Irf1* and *Cebpb* (**Figure S2C**). *Irf1* and/or *Cebpβ* knockdown significantly attenuated both the mRNA and protein levels of *Il6* and *Il12b* in R- and IR- stimulated cells (**Figure 4A and 4B**). In I-stimulated cells, the *Il6* and *Il12b* mRNA levels remained basal. In IR-stimulated cells, the effect of single knockdown was only incremental, while double knockdown further reduced *Il6* and *Il12b* (IL12p40: ~50% by si*Irf1*+si*Cebpb*; IL6: ~75% by si*Irf1*+si*Cebpb*). This indicates that co-stimulation of TLR3 and TLR7 significantly induced expression of *Il6* and *Il12b*, and the co-presence of a certain level of IRF1 and C/EBPβ is necessary and sufficient for the optimal transcription of *Il6* and *Il12b*.

TRIF- and MyD88- signaling pathways collaborate to synergize cytokine expression through enhancing JunB production and synchronizing IRF-JunB activation.

To functionally characterize JunB-mediated regulation of expression of *Il6* and *Il12b* and its potential cooperation with IRF1, we knocked down *Junb* alone or both *Junb and Irf1* (**Figure S2D**). Significant reduction in R- or IR- induced *Il6* and *Il12b* was observed in *Junb* knockdown cells (**Figure 5A and 5B**) at both the mRNA and protein levels. With I-stimulation, both *Il6* or *Il12b* mRNAs remained extremely low, similar to non-treated cells (Figure 4A and 4B), thus the impact of *JunB* knockdown on I-induced cytokine expression was not further assessed. The drastic difference in the induction of cytokines between single and co-stimulation, compared to the smaller difference caused by *Junb* knockdown, clearly indicates the involvement of additional critical cofactors induced by TRIF-pathway, which is necessary for the synergistic transactivation of *Il6* and *Il12b*. This is supported by the double

knockdown of *Junb* and *Irf1,* which yielded more pronounced attenuation of *Il6* and *Il12b* (IL12p40: ~75% by si*Junb*+si*Irf1*; IL6: ~80% by si*Irf1*+si*Junb*) at both mRNA and protein levels (Figure 5A and 5B) compared to single knockdown. Thus co-stimulation mediated enhancement of JunB itself promoted cytokine expression and at the same time, Junb collaborates with TRIF-responsive IRF1 to augment cytokine production.

Taken together, R strongly upregulates and sustains MyD88-responsive JunB and C/EBPβ but R only transiently activates IRF1, resulting in mild transcription activation of *Il6* and *Il12b*. In contrast, I induces a high level of TRIF-responsive IRF1 but only minimally of JunB and C/EBPβ. On its own, IRF1 appeared insufficient to drive the basal transcription. However, co-stimulation synchronized the activation of IRF1, JunB and C/EBPβ for up to 8-12 h, where these TFs probably worked in concert to achieve optimal cytokine expression.

Discussion

Thus far, the precise molecular mechanisms governing the expression of individual cytokine genes are only poorly investigated, although NFκB, AP1 and/or IRFs activities are known to be involved. Also, how cytokine synergy is induced by TRIF- and MyD88- coupled TLR signaling pathways remains unknown. Our findings demonstrated that the TRIF- and MyD88- signaling pathways synergize directly at the transcription of *Il6* and *Il12b*, although the activation of NF-κB members and chromatin remodeling appeared redundantly or additively induced by PAMP stimulations. Of particular significance is our identification of the critical active core transcription complex of *Il6* and *Il12b* - **IRF1**, **C/EBPβ** and **JunB**. IRF1 and C/EBPβ are respectively responsive to TLR3/TRIF- and TLR7/MyD88-activation, while JunB is responsive to both TLR3/TRIF- and TLR7/MyD88- activation, but preferentially more responsive to and sustained by TLR7-MyD88 signaling, and enhanced by co-stimulation. siRNA knockdown further demonstrated that all these TFs are crucial for optimal transcription of *Il6 and Il12b*. Thus, we propose that TLR3/TRIF- and TLR7/MyD88-signaling pathways synergize the transcription of *Il6* and *Il12b* through contributing distinct newly synthesized TFs as the core components of optimal transcriptional complexes (**Figure S2E**). However, we cannot preclude other yet to be defined "transcriptional synergy factors" (X), which may be the products of cooperation of distinct pathways in co-stimulation (18). Thus, both mechanisms (1. TLR3/TRIF and TLR7/MyD88 each contribute newly synthesized TFs to cooperate in cytokine regulation, or 2. TLR3/TRIF and TLR7/MyD88 cooperate to produce a new transcription factor which is not present under single stimulation but has a regulatory role on cytokine production) could participate in a network to regulate *Il6* and *Il12b* expression *in vivo*.

While IRF1 is known to be strongly induced in macrophages by IFN-γ, the detailed functional role and the mechanisms of IRF1 in regulating immune responses are poorly understood (19). IRF1 plays a major role in the transcriptional regulation of the *Il12a* but not *Il12b* (20), although an IRF1-binding element was characterized in the *Il12b* promoter (21). Current investigation revealed that IRF1 is the principle TF induced by the TLR3-TRIF signaling pathway and it binds both *Il6* and *Il12b* promoters. As IRF1 has not been reported to bind mouse *Il6* promoter before, we employed EMSA and identified a 142 bp region (-344 to -203) in the mouse *Il6* promoter to bind IRF1 (Figure S2F, G). Binding of JunB and C/EBPβ to both the mouse *Il6* and *Il12b* promoters has been reported previously (22-24). An earlier investigation using *Il12b*-promoter reporter assay demonstrated the cooperation between AP1-binding site and the adjacent C/EBPs-binding site (24). However, we found that IRF1 is required to achieve optimal transcription of both *Il6* and *Il12b*. Surprisingly, we did not detect significant association of the well-recognized master regulator, NFκB, to either *Il6* or *Il12b* promoter. Plausibly, as a primary response regulator, NFκB members function at the outset of the assembly of pre-initiation transcriptional complex for *Il6* and *Il12b (14)*. The promoter-binding of NFκB could be transient and highly dynamic, and thus not captured by pulldown.

In summary, we show, for the first time that the pro-inflammatory cytokine genes, *Il6* and *Il12b*, share a similar core configuration of transcriptional complex (including IRF1, C/EBPβ and JunB), which facilitates an optimal and timely expression of IL6 and IL12p40 in macrophages, to precisely respond to viral signals of infection. The delayed inhibition of IRF1 expression by TLR7-MyD88 signaling correlates with the progressive waning of *Il6 and Il12b* transcription. Thus, the crosstalk of TLR3-TRIF and TLR-MyD88 signaling pathways probably controls the timing and magnitude of IL6 and IL12p40 production, through down-regulating IRF1, a critical event that warrants future investigation. A comparison of *Il6* and

Il12b transcriptional proteome would provide information on additional regulatory factors, specific to either *Il6* or *Il12b* or both, which are anticipated to exist *in vivo*. These factors could fine-tune the regulation leading to specific outcome of each cytokine expression. Such insights on how cytokine synergy is orchestrated will help us develop novel strategies to resolve immune over-activation and regain homeostasis. Furthermore, knowledge on cytokine synergy could be beneficially employed in the design of improved vaccines and immunotherapeutics (25).

Disclosures

The authors declare no competing financial interests.

References

1. Ishii, K. J., S. Koyama, A. Nakagawa, C. Coban, and S. Akira. 2008. Host innate immune receptors and beyond: making sense of microbial infections. *Cell Host Microbe* 3: 352-363.

2. Berg, D. J., N. Davidson, R. Kuhn, W. Muller, S. Menon, G. Holland, L. Thompson-Snipes, M. W. Leach, and D. Rennick. 1996. Enterocolitis and colon cancer in interleukin-10-deficient mice are associated with aberrant cytokine production and CD4(+) TH1-like responses. *J Clin Invest* 98: 1010-1020.

3. Parrillo, J. E. 1993. Pathogenetic mechanisms of septic shock. *The New England journal of medicine* 328: 1471-1477.

4. Medzhitov, R. 2008. Origin and physiological roles of inflammation. *Nature* 454: 428-435.

5. Kawai, T., and S. Akira. 2010. The role of pattern-recognition receptors in innate immunity: update on Toll-like receptors. *Nature immunology* 11: 373-384.

6. Honda, K., and T. Taniguchi. 2006. IRFs: master regulators of signalling by Toll-like receptors and cytosolic pattern-recognition receptors. *Nature reviews. Immunology* 6: 644-658.

7. Whitmore, M. M., M. J. DeVeer, A. Edling, R. K. Oates, B. Simons, D. Lindner, and B. R. Williams. 2004. Synergistic activation of innate immunity by double-stranded RNA and CpG DNA promotes enhanced antitumor activity. *Cancer research* 64: 5850-5860.

8. Napolitani, G., A. Rinaldi, F. Bertoni, F. Sallusto, and A. Lanzavecchia. 2005. Selected Toll-like receptor agonist combinations synergistically trigger a T helper type 1-polarizing program in dendritic cells. *Nature immunology* 6: 769-776.

9. Suet Ting Tan, R., B. Lin, Q. Liu, L. Tucker-Kellogg, B. Ho, B. P. Leung, and J. Ling Ding. 2013. The synergy in cytokine production through MyD88-TRIF pathways is co-ordinated with ERK phosphorylation in macrophages. *Immunol Cell Biol* 91: 377-387.

10. Iglesias, M. J., S. J. Reilly, O. Emanuelsson, B. Sennblad, M. Pirmoradian Najafabadi, L. Folkersen, A. Malarstig, J. Lagergren, P. Eriksson, A. Hamsten, and J. Odeberg. Combined chromatin and expression analysis reveals specific regulatory mechanisms within cytokine genes in the macrophage early immune response. *PLoS One* 7: e32306.

11. Dutta, B., S. S. Adav, C. G. Koh, S. K. Lim, E. Meshorer, and S. K. Sze. 2012. Elucidating the temporal dynamics of chromatin-associated protein release upon DNA digestion by quantitative proteomic approach. *Journal of proteomics* 75: 5493-5506.

12. Birbach, A., P. Gold, B. R. Binder, E. Hofer, R. de Martin, and J. A. Schmid. 2002. Signaling molecules of the NF-kappa B pathway shuttle constitutively between cytoplasm and nucleus. ***The Journal of biological chemistry*** **277: 10842-10851.**

13. Zieske, L. R. 2006. A perspective on the use of iTRAQ reagent technology for protein complex and profiling studies. ***Journal of experimental botany*** **57: 1501-1508.**

14. Gilchrist, M., V. Thorsson, B. Li, A. G. Rust, M. Korb, J. C. Roach, K. Kennedy, T. Hai, H. Bolouri, and A. Aderem. 2006. Systems biology approaches identify ATF3 as a negative regulator of Toll-like receptor 4. ***Nature*** **441: 173-178.**

15. Murphy, T. L., M. G. Cleveland, P. Kulesza, J. Magram, and K. M. Murphy. 1995. Regulation of interleukin 12 p40 expression through an NF-kappa B half-site. ***Mol Cell Biol*** **15: 5258-5267.**

16. Libermann, T. A., and D. Baltimore. 1990. Activation of interleukin-6 gene expression through the NF-kappa B transcription factor. ***Mol Cell Biol*** **10: 2327-2334.**

17. Su, R. C., A. Sivro, J. Kimani, W. Jaoko, F. A. Plummer, and T. B. Ball. 2011. Epigenetic control of IRF1 responses in HIV-exposed seronegative versus HIV-susceptible individuals. ***Blood*** **117: 2649-2657.**

18. Kayama, H., V. R. Ramirez-Carrozzi, M. Yamamoto, T. Mizutani, H. Kuwata, H. Iba, M. Matsumoto, K. Honda, S. T. Smale, and K. Takeda. 2008. Class-specific regulation of pro-inflammatory genes by MyD88 pathways and IkappaBzeta. ***The Journal of biological chemistry*** **283: 12468-12477.**

19. Ikushima, H., H. Negishi, and T. Taniguchi. The IRF Family Transcription Factors at the Interface of Innate and Adaptive Immune Responses. ***Cold Spring Harb Symp Quant Biol.***

20. Liu, J., S. Cao, L. M. Herman, and X. Ma. 2003. Differential regulation of interleukin (IL)-12 p35 and p40 gene expression and interferon (IFN)-gamma-primed IL-12 production by IFN regulatory factor 1. *The Journal of experimental medicine* 198: 1265-1276.

21. Maruyama, S., K. Sumita, H. Shen, M. Kanoh, X. Xu, M. Sato, M. Matsumoto, H. Shinomiya, and Y. Asano. 2003. Identification of IFN regulatory factor-1 binding site in IL-12 p40 gene promoter. *J Immunol* 170: 997-1001.

22. Plevy, S. E., J. H. Gemberling, S. Hsu, A. J. Dorner, and S. T. Smale. 1997. Multiple control elements mediate activation of the murine and human interleukin 12 p40 promoters: evidence of functional synergy between C/EBP and Rel proteins. *Mol Cell Biol* 17: 4572-4588.

23. Baccam, M., S. Y. Woo, C. Vinson, and G. A. Bishop. 2003. CD40-mediated transcriptional regulation of the IL-6 gene in B lymphocytes: involvement of NF-kappa B, AP-1, and C/EBP. *J Immunol* 170: 3099-3108.

24. Zhu, C., K. Gagnidze, J. H. Gemberling, and S. E. Plevy. 2001. Characterization of an activation protein-1-binding site in the murine interleukin-12 p40 promoter. Demonstration of novel functional elements by a reductionist approach. *The Journal of biological chemistry* 276: 18519-18528.

25. Trinchieri, G., and A. Sher. 2007. Cooperation of Toll-like receptor signals in innate immune defence. *Nature reviews. Immunology* 7: 179-190.

Figure legend

Figure 1. Transcriptional synergy of *Il6* and *Il12b* under TLR7-TLR3 co-stimulation. BMDMs were treated with I and/or R for 8 h followed by QuantiGene analysis. Fold-synergy was obtained by: $\text{Fold synergy} = \frac{\text{mRNA induced by IR}}{\text{mRNA induced by I} + \text{mRNA induced by R}}$. Proinflammatory cytokine genes with fold synergy above 5 (red line), eg, *Il6* and *Il12b* (red box) were further studied.

Figure 2. C/EBPβ, IRF1 and JunB bind to *Il6* and *Il12b* promoter. Cells were stimulated with I, R or IR for 5 h followed by nuclear extraction. Control cells were non-treated (NT). Biotin labeled *Il6* and *Il12b* promoters were separately incubated with nuclear extracts to pulldown transcription factors. Pulldown samples were then subjected to Western blot analysis. The data shown are representative of three independent experiments.

Figure 3. Co-stimulation synchronizes C/EBPβ, IRF1 and JunB. J774 cells were stimulated with I, R, IR or non-treated control (NT), for 5, 30 min, 1, 4, 8, 12, 24 h. Whole cell lysates were collected to check the dynamic profiles of C/EBPβ, JunB and IRF1 by Western blot immunodetection using the respective antibodies. The detected protein bands were densitometrically quantified relative to GAPDH. The data are representative of three independent experiments.

Figure 4. IRF1 and C/EBPβ collaborate to synergize IL6 and IL12p40 production. J774 cells were transfected with sequence-specific siRNA targeting *Irf1* or *Cebpb*, singly or doubly, or transfected with a non-targeting scramble siRNA control for 24 h. Cells were then

stimulated with I, R, IR or no treatment (NT) for: (A) 8 h to test for cytokine mRNA or (B) 12 h to measure cytokine protein. Data are presented as means ± SEM of three independent experiments. * P <0.05, ** P < 0.01 (two tail student's *t*-test).

Figure 5. IRF1 and JunB collaborate to synergize IL6 and IL12p40 production. J774 cells were transfected with sequence-specific siRNA targeting *Irf1* or *Junb* singly or doubly or transfected with a non-targeting scramble siRNA control for 24 h. Cells were then stimulated with I, R, IR or no stimulation (NT) for: (A) 8 h to test for cytokine mRNA or (B) 12 h to measure cytokine protein. Data are presented as means ± SEM of three independent experiments. * P <0.05, ** P < 0.01 (two tail student's *t*-test).

Figure 1

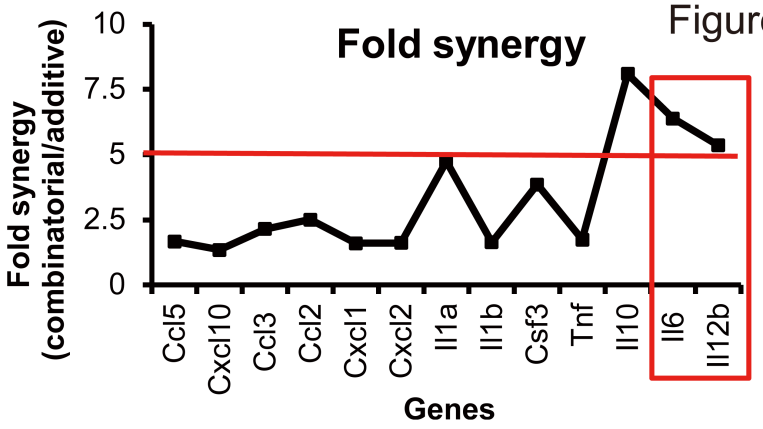

Figure 2

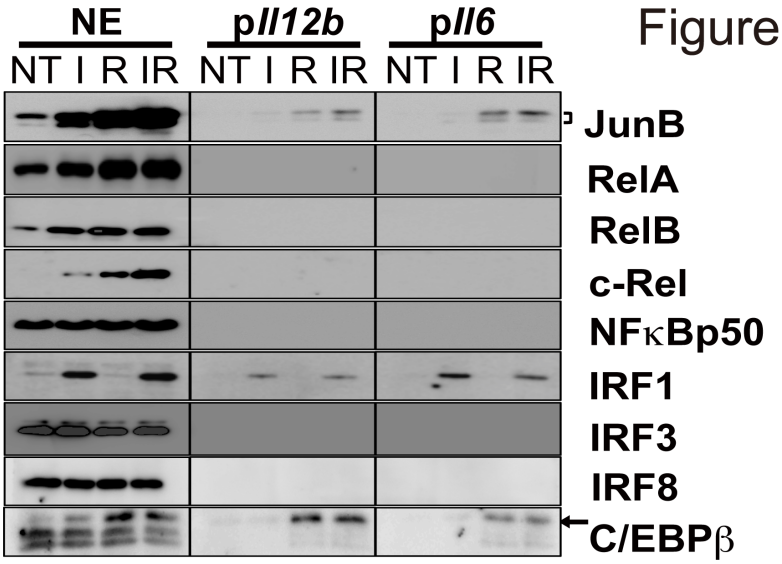

Figure 3

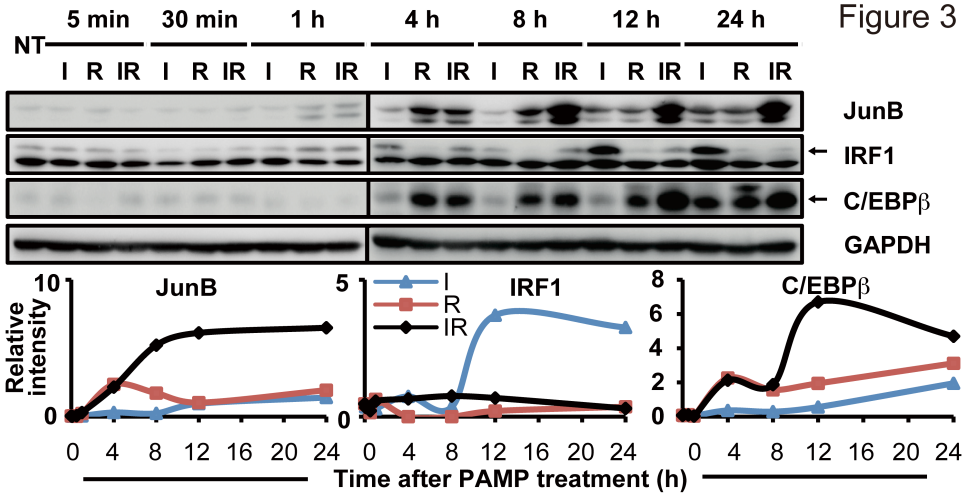

Figure 4

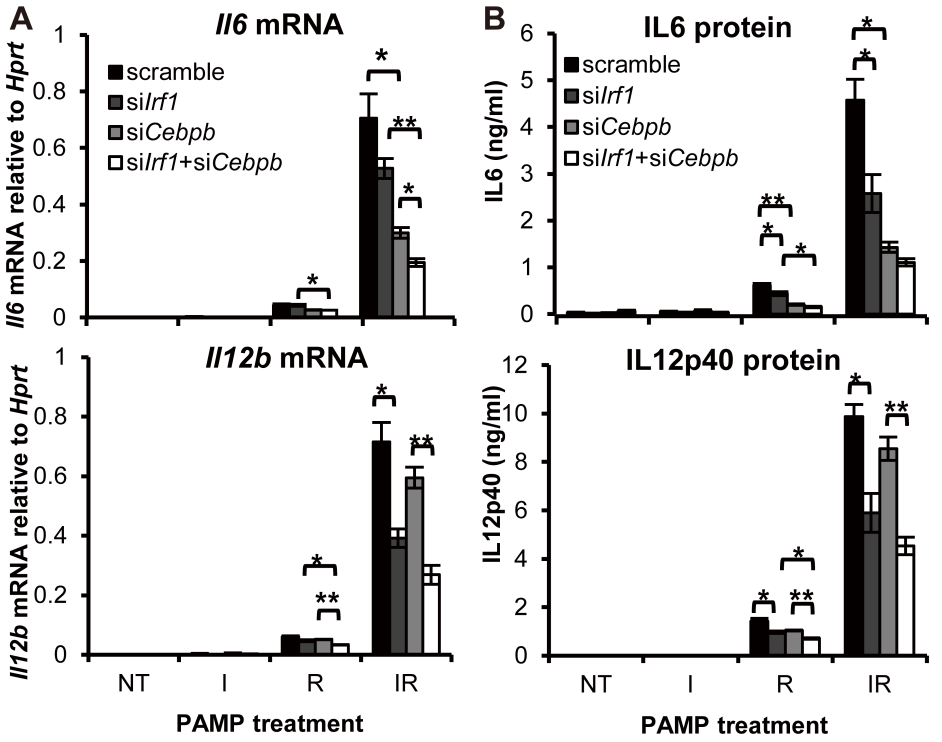

Figure 5

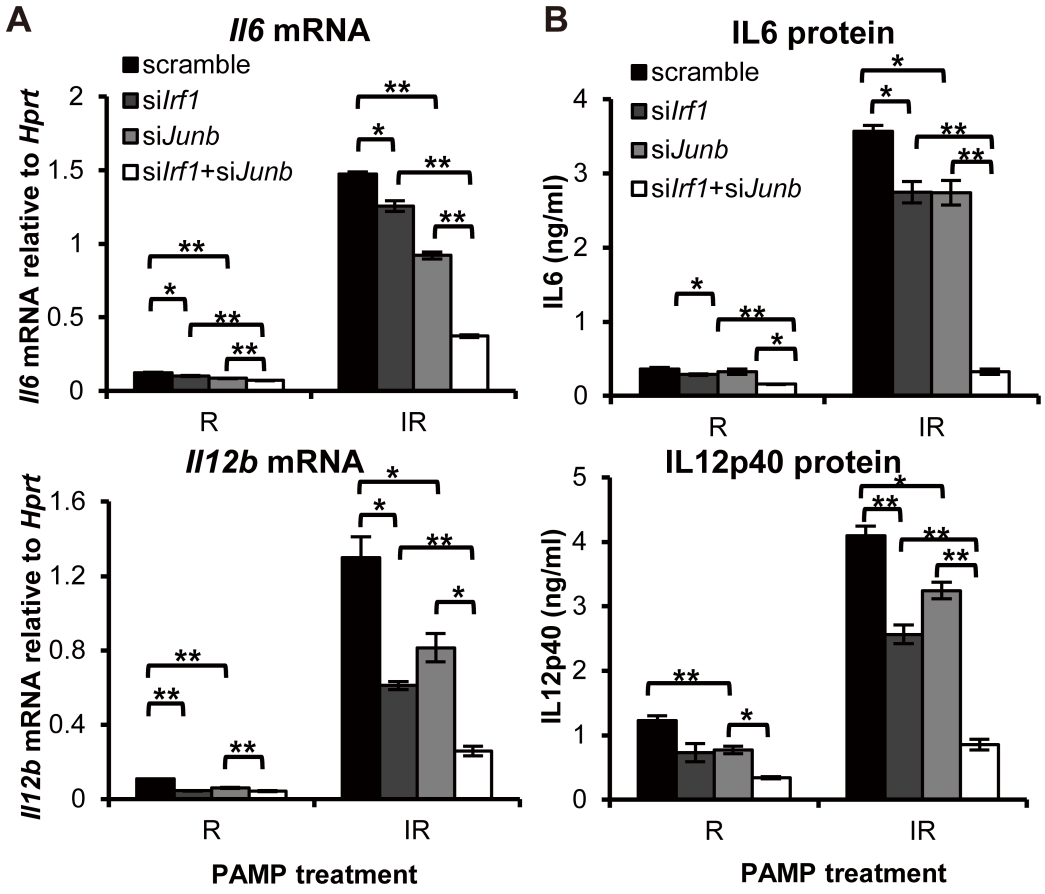

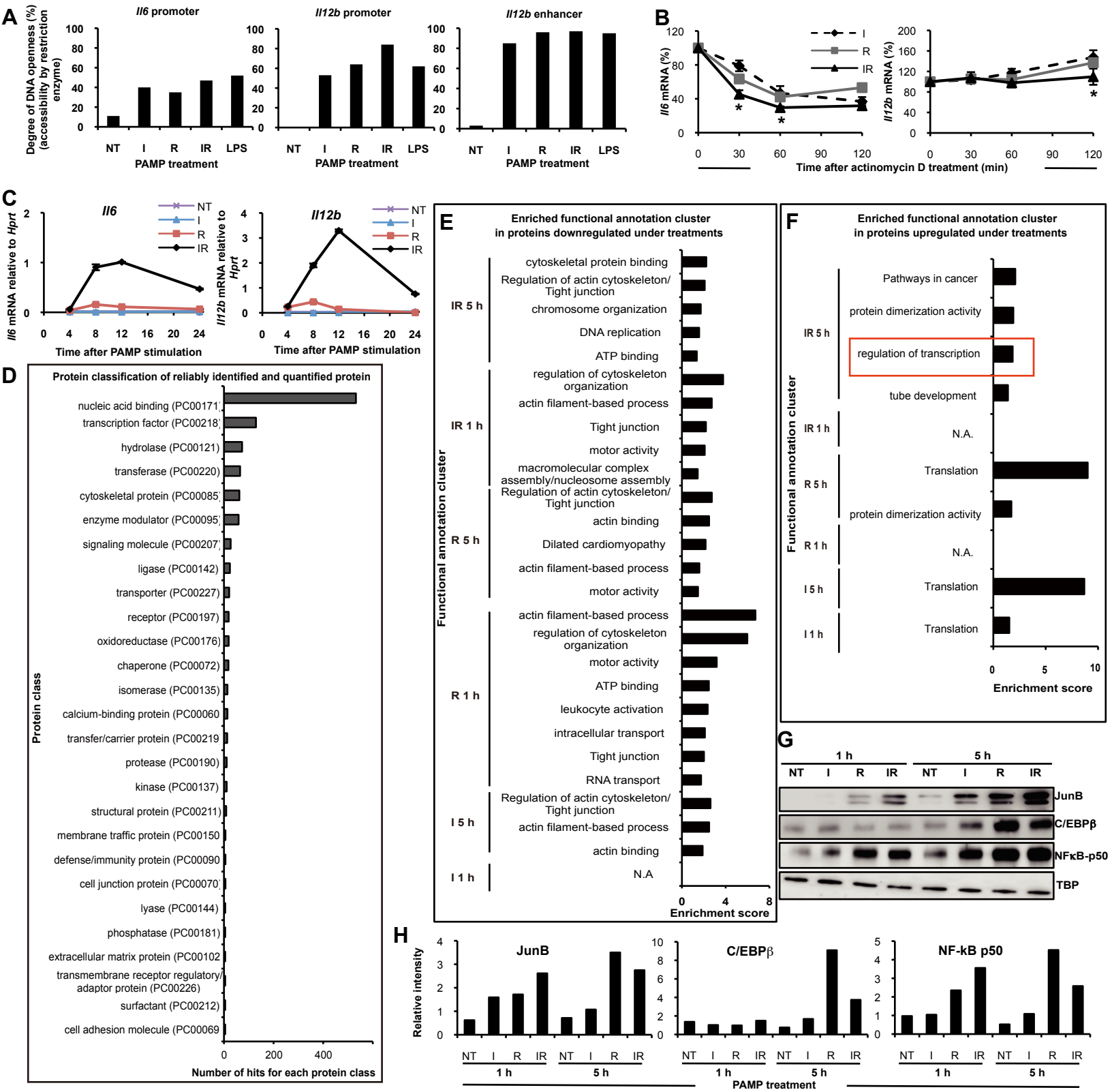

Supplemental figure 1.

(A) Restriction enzyme accessibility assay of murine *Il6* promoter, and both the promoter and enhancer of *Il12b* to check for chromatin remodeling upon immune-stimulation. J774 cells were treated with I and/or R, or LPS for 5 h before collection of cells for nuclei extraction. Enzymes was added to nuclei (AflII for IL6 promoter analysis, SpeI for both promoter and enhancer of Il12b) for 1 h at 37°C. Genomic DNAs were extracted with TRizol reagent (Invitrogen). The percentage of DNA digested at the restriction site was determined by SYBR Green RT-PCR (LightCycler® 480 Roche). A series of diluted genomic DNA, which were not digested with the restriction enzymes, were amplified (together with those test samples mentioned above), to create standard curves for both target region and a control region nearby without targeted restriction site (to be used as internal calibrator for quantification). The percentage of DNA digested was calculated by subtracting the relative ratio of "apparent template" covering the restriction site (amplifiable) to that of non-digested control region. The primers for *Il6* promoter are 5'-cccatcaagacatgctcaagtg-3' (forward) and 5'-gcacaatgtgacgtcgtttagc-3' (reverse). The primers for *Il12b* promoter are 5'-tctgtatgatagatgcactcagg-3' (forward) and 5'- ggaaacccaaagtagaaactgac -3' (reverse). The primers for *Il12b* enhancer region are 5'- agtttcaccagtgactccagca -3' (forward) and 5'- acagtctcaaaggaccatggct -3' (reverse). Primers for control region are 5'-gaggcagagagccagcattg-3' (forward) and 5'-aagggaaaaccggcaagtgag-3' (reverse). Data are representative of two independent experiments.

(B) BMDMs were incubated for 4 h with I (dashed line) or R (solid grey line) or IR (solid black line). The *Il6*, *Il12b* and *Hprt* mRNA levels were determined by real-time PCR in samples collected before (0 min) and 30, 60, 120 min after the addition of actinomycin D (5 μg/ml), which halts synthesis of new mRNAs. The amounts of *Il6* and *Il12b* mRNAs after actinomycin D treatment are shown as a percentage of the levels in the cells at the start, time 0. Data are presented as means ± SEM of three independent experiments. * P <0.05 (one tail student's t-test).

(C) J774 cells were stimulated simultaneously by adding I and R for 4, 8, 16 and 24 h (indicated as "IR" with black line), control for IR is the levels of cytokine produced by I single treatment (blue line) and R single treatment (red line), each for 4, 8, 16 and 24 h. No treatment control was indicated as NT (purple line). Cytokine mRNA relative to *Hprt* were measured by Taqman Realtime PCR. Data are means and SEM of three independent experiments.

(D) PANTHER(Protein ANalysis THrough Evolutionary Relationships)-classification of proteins reliably identified by iTRAQ.

(E) Functional annotation clusters enriched in proteins down-regulated (with arbitrary threshold of fold difference ≤0.67) under different treatment (analyses using the Database for Annotation, Visualization and Integrated Discovery (DAVID) v6.7). There was no functional annotation cluster enriched in proteins down-regulated by I for 1 h (indicated as N.A, not applicable).

(F) Functional annotation clusters enriched in proteins up-regulated (with arbitrary threshold of fold difference ≥1.5) under different treatments. Annotation cluster of "regulation of trasncription" (indicated in red box) was exclusively enriched in 5 h combinatorial stimulation. There was no functional annotation cluster enriched in proteins up-regulated by IR or R for 1h (indicated as N.A, not applicable).

(G) Validation of iTRAQ ratio of potential synergy factors by Western blot analysis. Data are representative of two biological replicates.

(H) Densitometric quantification of the Western blot bands shown in G. Bands of JunB, C/EBPβ and NFkB-p50 are quantified relative to TBP. The data are representative of two biological replicates.

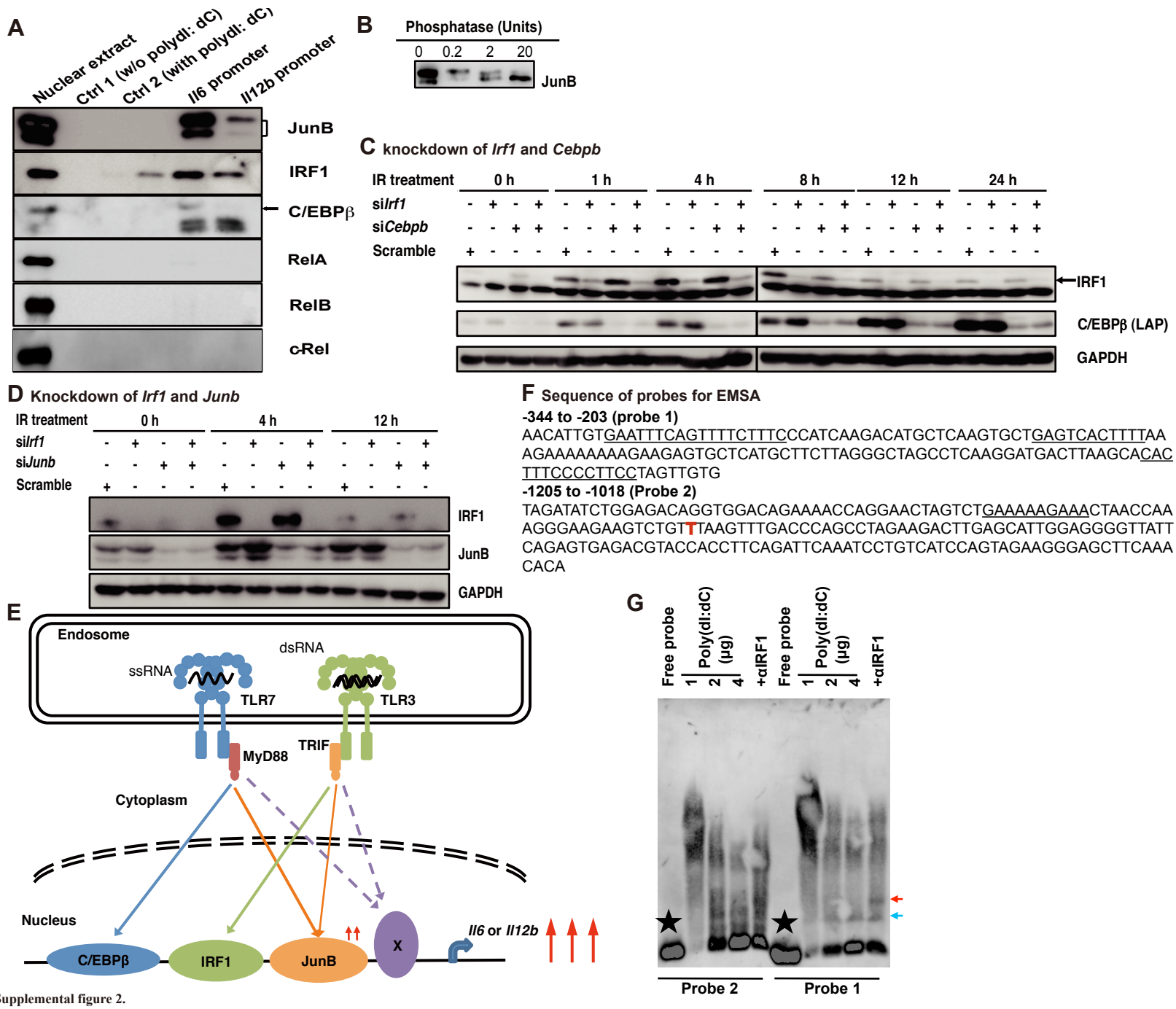

Supplemental figure 2.

(A) *In vitro* promoter-affinity pulldown of TFs from nuclear extracts of macrophages was not due to non-specific binding by the empty beads. Nuclear extracts (NE) were prepared from J774 cells stimulated by IR for 5 h. The *Il12b* promoter region, -640 to +17, was amplified using primers: 5'-agttcatgctgctatcaatcca-3' and 5'-cacccactgttccttctgct-3', and cloned into pGEM-T easy vector (Promega). Plasmid construct was double-restriction digested with ApaI&SacI to release the promoter fragment. The *Il6* promoter region, -1578 to +31, was amplified by primers: 5'-attctcgagatttaatctactctaatcgcctgt-3' and 5'–cccaagcttagcggtttctggaattgactat-3' using genomic DNA as template and cloned into pGL2 promoter vector (Promega). The *Il6* promoter fragment was released from the plasmid DNAs by PstI&HindIII double digestion. The purified promoter DNAs were labeled with biotin using 3' end DNA labeling kit (Thermo Fisher Scientific, Waltham, MA, USA, No. 89818), according to manufacturer's instruction. Labeled DNAs were further purified using Wizard SV Gel and PCR clean-up kit (Promega). Biotin labeled probes were then incubated with NE followed by streptavidin-conjugated beads pull down as described in materials and methods. As a negative control, nuclear extracts were incubated in the binding mixture without probe (ctrl 1 and ctrl 2). In the binding reaction, polydI:dC was added for all conditions except ctrl 1. After probes were pulled down by beads, the beads were re-suspended in SDS-PAGE sample buffer and boiled at 100 °C for 5 min. Protein samples derived from 10% binding reaction (10 fmol DNA: 4 μg nuclear proteins) each were then analyzed by Western blot. All the targets, except IRF1, showed only specific binding to the promoters. The non-specific binding of IRF1 to empty beads was not significant compared with the bands from samples with promoter pull down. Data are representative of two independent experiments.

(B) Characterization of the two bands of JunB indicated that the upper band is a highly phosphorylated form. 5 μg nuclear extract from J774 cells treated with IR for 5 h were incubated with 0, 0.2, 2, 20 U phosphatase (CIAP, Promega) for 1 h at 37 °C and then analyzed by Western blot. Data are representative of two independent experiments.

(C) *Irf1* and *Cebpb* were successfully knocked down by siRNA. J774 cells were transfected with sequence-specific siRNA targeting *Irf1* or *Cebpb*, singly or doubly, or transfected with a non-targeting scramble siRNA control, for 24 h. Cells were then stimulated with IR for 0, 1, 4, 8, 12, 24 h to test knockdown efficiency. Data are representative of three independent experiments.

(D) *Irf1* and/or *Junb* was successfully knocked down by siRNA. J774 cells were transfected with sequence-specific siRNA targeting *Irf1* or *Junb* singly or doubly or transfected with a non-targeting scramble siRNA control for 24 h. Cells were then stimulated with IR for 0, 1, 4, 8, 12, 24 h to test knockdown efficiency. Data are representative of three independent experiments.

(E) A schematic model of TLR3-TLR7 signaling crosstalk, which induces cytokine transcriptional synergy after co-activation with poly(I:C) and R848. Under co-activation of TLR3 and 7, the induction of JunB is enhanced (small red arrows), and IRF1 and C/EBPβ were, respectively, induced by TRIF and MyD88 pathways (solid lines), which synergize *Il6* and *Il12b* production (big red arrows). Yet to be identified transcription factor (X) might also contribute to cytokine synergy (dashed lines).

(F) Sequence of probe 1 and 2 (from mouse *Il6* promoter) for EMSA. Putative IRF1 binding element(s) were predicted using LASAGNA2.0. A region (-344 to -203) that contains putative IRF1 binding sites (underlined text) was chosen as probe 1. Probe 1 was amplified by PCR using a 5'-end biotin-labeled forward primer: 5'-/Biotin-TEG/AACATTGTGAATTTCAGTTTTCTTTCC-3' and a reverse primer: 5'-CACAACTAGGAAGGGGAAAGTG-3'. In addition, a distal region (-1205 to -1018) containing: (i) the assay site (-1128, **T**) of a pre-designed and validated anti-IRF1 ChIP-qPCR Primer Assay for mouse *Il6*, GPM1036981(-)02A from QIAGEN, and (ii) a visually spotted minimal potential binding site (underlined text), was chosen as Probe 2. Probe 2 was obtained by digesting the *Il6* promoter mentioned in Figure S2A, with BmtI, which flanked probe 2. Then probe 2 was biotin-labeled at the 3'-protruding ends produced by BmtI restriction digestion.

(G) IRF1 and IRF2 binding site(s) are located within -344 to -203 of the *Il6* promoter. 20 μl binding reactions containing 5 fmol probe 1 (-344 to -203) or 10 fmol probe 2 (-1205 to -1018), 2.5 μl nuclear extract (~ 4 μg protein from J774 treated with IR for 5 h), 1.25 μg poly(dI:dC), 10 mM Tris-HCl (pH 7.5), 50 mM KCl, 1 mM DTT, 0.05% NP-40, and 10 % glycerol were incubated for 30 min at 25 °C. For supershift, rabbit polyclonal antibodies (1 μg each in a 20 μl binding mixture) were included, the DNA probes were added after 1 h incubation of antibody with nuclear extract in ice-bath. The binding mixtures were resolved in 1.5 % agarose in 0.25× TBE followed by wet transfer to a positively charged nitrocellulose membrane. After UV-crosslinking and washing with 5 % SDS in PBS (PBSS), the blot was incubated in 1:7,500 diluted Streptavidin-conjugated HRP (Thermo) in PBSS for 10-15 min. After washing (3×10 min, with PBS-T (0.05% Tween), the biotin signal was detected using ECL. Probe 1 but not probe 2 exhibits IRF1-specific binding. While a prevalent non-specific binding smear became rather distinct specific binding pattern (blue arrow) with increasing concentration of poly(dI:dC), especially in probe 1, anti-IRF1 caused the appearance of super-shift (red arrow). The black star represents free probes.

TLR3-TLR7 pathway crosstalk confers innate immune memory and homeostasis

Bing Liu[1,†], Qian Liu[2,†], Sucheendra Kumar Palaniappan[3], Ivet Bahar[1], P. S. Thiagarajan[3,*], Jeak Ling Ding[2,*]

[1]Department of Computational & Systems Biology, School of Medicine, University of Pittsburgh, United States; [2]Department of Biological Sciences, Faculty of Science, and [3]Department of Computer Science School of Computing, National University of Singapore, Singapore.

[†]Equal first authors

[*]Co-correspondents:

P. S. Thiagarajan, email: thiagu@comp.nus.edu.sg, tel: 65-65167998.

Jeak Ling Ding, email: dbsdjl@nus.edu.sg, tel: 65-65162776

Running title: Modeling TLR3-TLR7 crosstalk

Characters count (60,000 chars): 51,000

Abstract

Toll-like receptor (TLR) pathways recognize pathogen-associated molecular patterns (PAMPs) and trigger innate immune response by producing cytokines. The innate immune response is highly dependent on the timing of encountering PAMPS, suggestive of a short-term 'memory' that primes the cell for enhanced/modified immune response once it has been triggered by a first stimulus. In particular, TLR3 activation appears to prime macrophages for a subsequent TLR7 activation, leading to synergistic production of cytokines. However, the detailed mechanism governing this synergy is unclear. Here, by developing the first calibrated mathematical model for the kinetics of TLR3 and TLR7 pathways and their crosstalk, followed by experimental validation, we demonstrate the involvement of JAK-STAT pathway in controlling the induction of cytokine synergy. This pathway plays a dual role: it mediates cytokine synergy thus boosting the immune response, while maintaining homeostasis to avoid excessive inflammatory response. Thus our results suggest a 'cytokine rheostat' mechanism regulated by the JAK-STAT1 pathway, which enables macrophages to fine tune their response to multiple, temporally-separated infection events involving the TLR3-TLR7 pathways.

Keywords (five): Toll-like receptors / cytokine homeostasis / incoherent feedforward loops / mathematical model / Statistical modeling checking

Subject Categories: Quantitative Biology & Dynamical Systems; Immunology

Introduction

As front-line innate immune defense cells, macrophages distinguish foreign microbial organisms by recognizing their unique structures known as pathogen-associated molecular patterns, PAMPs (Gubler et al, 1984). PAMPS are recognized by pattern recognition receptors (PRRs) on host cells, which signal the onset of the immune response. Toll-like receptors (TLRs) are the best characterized PRRs. They are evolutionarily conserved type I transmembrane proteins that are localized on the cell surface as well as the membranes of intracellular vesicles such as endosomes, lysosomes and endolysosomes (Takeuchi & Akira, 2010); (Kawai & Akira, 2010). TLR signaling triggers different biological responses depending on the adaptor proteins involved, e.g. myeloid differentiation primary-response gene 88 (MyD88) and/or TIR-domain-containing adapter-inducing interferon-β (TRIF). MyD88 is recruited by all the TLRs except TLR3, and it activates NF-κB and mitogen-activated protein kinases (MAPKs) to produce mainly inflammatory cytokines. On the other hand, TRIF is exclusively recruited by TLR3 and TLR4 to activate interferon regulatory factor (IRF) family members and NF-κB, which then leads to the induction of type I interferons (IFNs) as well as inflammatory cytokines (Takeuchi & Akira, 2010).

As the 'lingua franca' used by both innate and adaptive immune cells, cytokines exert various local and distal effects including the recruitment and activation of leukocytes. The invading pathogens often contain multiple PAMPs and hence it is highly likely that they interact with various TLRs simultaneously or at different stages of the infection (Tan et al, 2014). It has been reported that combinatorial TLR activations can alter the levels of cytokine production, and in some cases, induce synergistic levels of cytokines (Bagchi et al, 2007; Bohnenkamp et al, 2007; De Nardo et al, 2009; Krummen et al, 2010; Makela et al, 2009; Napolitani et al, 2005; Zhou et al, 2007). The magnitude and timing of cytokine production by the innate immune cells significantly affect subsequent events. Deficient or excessive cytokine production may either cause an ineffective immune protection or disrupt immune homeostasis. It is therefore crucial to understand how the TLR pathways communicate with each other to modulate the levels of cytokines, which may otherwise manifest in disorders such as acute and chronic inflammation.

Recent evidence indicated that synergistic production of cytokines depends on the order and timing of TLR stimulations. Specifically, the activation of TRIF followed by the activation of MyD88 pathways in macrophages generates a significantly stronger immune response compared to that triggered when the reverse order of the two activations (Tan et al, 2013; Zhou et al, 2007; Zhu et al, 2008). This observation suggests that the activation of the TRIF pathway could create a certain short-term innate immune 'memory' which could prime the cell for enhanced response to a subsequent PAMP challenge. However, the mechanistic basis of this immune memory is unclear. It is also uncertain how host cells restore homeostasis after the cytokine 'storm' resulting from combinatorial

stimulations. Therefore, there is a need for a systems-level understanding of the time-dependent mechanism of crosstalk between TLR signaling pathways.

Previous efforts using systemic approaches for studying TLR networks (see a recent review, (Vandenbon et al, 2012)) made it possible to construct a comprehensive map of the TLR signaling network using existing data in the literature (Oda & Kitano, 2006). However, this provided a static visualization of the protein-protein interaction network implicated in TLR signaling. To assess the dynamics of this network, the TLR map has been reformulated to enable a steady-state based flux balance analysis (Li et al, 2009). However, the lack of detailed information on the reaction kinetics hindered the use of the map for further quantitative studies. Earlier efforts on quantitative modeling of specific TLR pathways have focused on the TLR3 (Helmy et al, 2009) and TLR4 pathways, with special emphasis on the NF-κB signaling module (Basak et al, 2007; Cheong et al, 2008; Covert et al, 2005; Gutierrez et al, 2010; Litvak et al, 2009; Selvarajoo et al, 2008; Shih et al, 2009; Werner et al, 2005). While these models elucidated various aspects of TLR signaling, their utilities have been limited by the over-simplification by imposing linear dynamics (Helmy et al, 2009; Selvarajoo et al, 2008), the lack of model calibration (Gutierrez et al, 2010), or the exclusion of key interactions such as the AP-1 activation branch and cytokine production (Basak et al, 2007; Cheong et al, 2008; Covert et al, 2005; Litvak et al, 2009; Shih et al, 2009; Werner et al, 2005). More importantly, none of these models took into account of the dynamic crosstalk between the different TLR pathways, which appears to be crucial for understanding the regulation of cytokine synergy.

Here, we focus on the interplay between the TLR3 and TLR7 pathways towards uncovering the main mechanisms responsible for the creation of an immune system memory and synergistic production of cytokines while maintaining homeostasis. An important first step towards this goal is the construction of a computational model containing the necessary components and the determination of the model parameters. To this aim we used both existing data in the literature and new data from our own experiments, and determined the unknown parameters by an optimal fit to 136 data points used for model training via a statistical logic-based computing framework that we developed recently (Palaniappan et al, 2013). The calibrated model was verified to reproduce the dependence of the synergistic production of cytokines on the time interval and order of stimuli. For example, an 8 h time lag between TLR3 and TLR7 activations would lead to maximal synergy. The same model was further observed to successfully reproduce 30 additional data points reserved for model testing. Having established the model and parameters, we proceeded to a sensitivity analysis which pointed to the crucial role of type I IFN, MAPK and STAT pathways in regulating cytokine synergy. Simulations with different sequential orders and time intervals of stimuli further showed that the production of type I IFN is mainly due to TLR3 activation, which explained the order-dependency of cytokine production. Both *in silico* simulations and experimental analyses consistently revealed the distinct roles of MAPKs in regulating cytokine production. In particular, JNK was found to upregulate cytokine synergy, while ERK and p38 would mainly downregulate the synergy, possibly through an

anti-inflammatory cytokine, IL-10. Among the possible crosstalk mechanisms, we determined that JAK-STAT pathway was responsible for time-dependent synergy of antiviral immune response. We also found that cytokine response to STAT1 was biphasic due to the dual opposing effects of STAT1 on cytokine production and the ensuing formation of an incoherent feed-forward loop (I1-FFL; a network motif noted by (Hart & Alon, 2013)). STAT1 appears to be indispensable for creating an immune memory that may boost the cytokine levels and even lead to a cytokine 'storm' in response to a succeeding PAMP challenge; while it also helps restore homeostasis by downregulating cytokine production, possibly through enhancing IL-10 production.

Results

Cytokine synergy is dependent on the order of TLR3 and TLR7 activations, and on the intervening time between the two stimuli.

Combinatorial activations of TLR3 and TLR7 by a simultaneous challenge with their respective ligands, poly(I:C) (double-stranded RNA analogue) and R848 (single-stranded RNA analogue) (Zhou et al, 2007), can lead to significant upregulation of the proinflammatory cytokine genes e.g. interleukin-6 gene (*Il6*) and interleukin-12 gene (*Il12b*) (Liu et al; Zhou et al, 2007). To understand the underlying mechanism, we first examined the time-dependent expression profiles of *Il6* and *Il12b* transcripts after poly (I:C) (denoted as **I**) and R848 (denoted as **R**) treatments (**Figure 1A**). To this end, bone marrow derived macrophages (BMDMs) were treated with both **I** and **R**, but in different orders (1st PAMP (**I**) followed by 2nd (**R**) or *vice versa*) and with different time intervals (Δt = 0, 8 and 24 h) between the two treatments. Cells were collected for real time quantitative PCR analysis at 4, 8, 16 or 24 h after the second PAMP stimulation. For example, in the case of **I** followed by **R**, the cells were first treated with poly (I:C) for 0, 8 or 24 h, and then with R848 for another 4, 8, 16 or 24 h. The control for combinatorial stimulation was single stimulation with either **I** or **R**.

Cytokine expression was observed to be upregulated after combinatorial stimulation regardless of the time intervals and sequence of the two PAMP treatments (**Figure 1B**). However, the upregulation was significantly more pronounced when cells were treated with **I** first followed by **R** rather than the converse regime, indicating that the treatment order had a significant effect on cytokine synergy (**Figure 1B**). Furthermore, different time intervals between **I** and **R** treatments also affected the level of synergy: in particular a pretreatment of 8 hours with **I** elicited the strongest cytokine synergy in response to the 2nd treatment (by **R**) (**Figure 1B** *upper left* and **C**).

Kinetic model for TLR3 and TLR7 signaling network

In order to understand the potential mechanisms governing the cytokine synergy observed under combinatorial stimulations, we built a computational model that includes known signaling cascades as well as the interactions potentially enabling the crosstalk between the TLR3 and TLR7 pathways (**Figure 2**). Here we briefly depict the main features of the TLR3 and TLR7 pathways followed by a description of the potential crosstalk mechanisms. Supplementary **Table S1** lists all acronyms used below, as well as the initial concentrations adopted in our simulations.

TLR3 pathway. In our model, the TLR3 signaling (Takeuchi & Akira, 2010) is initiated by the sensing of poly(I:C) by TLR3. This in turn activates the adaptor protein, TRIF, which then recruits TRAF6, TRADD, FADD and RIP1 to form a multi-protein complex. The latter activates the TAK1 complex, which, in turn, simultaneously activates the IKK complex and the MAPKs (i.e. ERK, p38

and JNK), which drive the translocation of NF-κB to the nucleus and the activation of AP-1 transcription factor, respectively, to end up inducing the transcription and translation of inflammatory cytokines. Simultaneously, the TRIF-dependent pathway also activates the interferon-regulatory factor IRF3 via a TRAF3-dependent pathway, which leads to subsequent type I IFN production. In summary, TLR3 induces antiviral immune response by promoting the production of type I IFNs predominantly, and cytokines (e.g. IL-6 and IL-12) to a lesser extent.

TLR7 pathway. In contrast to the TLR3 pathway, the TLR7 pathway is initiated by the sensing of R848 (Kawai & Akira, 2010; Takeuchi & Akira, 2010). The activated TLR7 in turn activates MyD88, which recruits and activates the IL-1 receptor associated kinases, IRAK4, IRAK1, IRAK2 and IRAK-M. The activated IRAK complex interacts with TRAF6 and activates the TAK1 complex. At this point, the TLR3 and TLR7 pathways merge, leading to the above mentioned activation of AP-1 and NF-κB and production of cytokines. These constitute the predominant signaling events in the TLR7 pathway. To a lesser extent, the TLR7 pathway also activates the transcription factor IRF7, which then translocates into the nucleus and promotes the production of type I IFNs.

Potential crosstalk mechanisms. Our data in **Figure 1B** show that R848-stimulated TLR7-MyD88 pathway induces cytokine production mildly. Also, the poly(I:C)-stimulated-TLR3-TRIF pathway alone produces only marginal levels of cytokines, but it greatly enhanced TLR7-MyD88 induced cytokine expression, indicating that downstream components activated specifically by TLR3-TRIF might cooperatively interact with TLR7-MyD88 pathway (Tan et al, 2013) to boost cytokine expression.

The key downstream events in TLR3-TRIF pathway which distinguish it from the MyD88 pathway are the activation of IRF3 and the associated production of type I IFN (Doyle et al, 2002; Kawai & Akira, 2010) (**Figure 2**). Our model includes the following IRF3- and type I IFN-mediated mechanisms: **(i)** Activated IRF3 is known to bind to NF-κB and AP-1 to form an enhanceosome in the nucleus (Oeckinghaus et al, 2011) to boost the transcription of *Il6* and *Il12b*. In addition, IRF3 can bind to the Interferon-Stimulated Response Element (ISRE) of the gene promoter and induce cytokine regulatory genes (Doyle et al, 2002). **(ii)** Secreted type I IFNs are recognized by the interferon-associated receptors 1 and 2, IFNAR1 and IFNAR2 on the cell surface, which, in turn, activate the Janus activated kinases (JAKs) tyrosine kinase 2 (TYK2) and JAK1. Activation of JAKs leads to the tyrosine phosphorylation of STAT2 and STAT1, inducing the formation of the STAT1–STAT2–IRF9 complex, also known as ISGF3 (IFN-stimulated gene factor 3) complex. This complex translocates to the nucleus and initiates the transcription of genes at the ISREs. Genes activated by ISGF3, such as IRF1, might be involved in cytokine synergy (Platanias, 2005). **(iii)** Secreted type I IFN can also activate NF-κB p52 through NF-κB inducing kinase (NIK) and the tumor necrosis factor receptor-associated factor-2 (TRAF2), which may regulate cytokine expression (Yang et al, 2005). **(iv)** Type I

IFN in the nucleus can also activate PI3K-AKT pathway, leading to the activation of NF-κB (Yang et al, 2001). **(v)** We also modeled the anti-inflammatory cytokine, IL-10-mediated feedback. Activated ERK and p38 phosphorylate mitogen- and stress- activated protein kinase-1/2 (MSK1/2), which promotes the transcription of *Il10* (Newton & Dixit, 2012). STAT1 target genes may also upregulate *Il10* expression (Pattison et al, 2012). Secreted IL-10 then inhibits proinflammatory cytokine production via a JAK-STAT3-dependent pathway (Murray, 2006).

The reaction network of our model is summarized in **Figure S1** and the corresponding set of kinetic equations (ODEs) is presented in **Text S1**. Protein associations, degradations and translocations are described by mass-action kinetics while activation and inhibition reactions were modeled with Michaelis-Menten kinetics. Gene transcription was modeled using the equation proposed by (Kuttykrishnan et al, 2010). The resulting mathematical model consists of 97 molecules or molecular complexes, 126 reactions and 143 parameters. The parameter selection and evaluation is described next.

The descriptive and predictive powers of the calibrated model

The values of 27 rate constants for the reactions associated with the NF-κB pathway were adopted from the literature (Lipniacki et al, 2004). To estimate the remaining 116 unknown parameters, we utilized our experimental data on the time courses of *Il6* and *Il12b* mRNAs (**Figure 1B**) measured under the following conditions: (1) single poly(I:C) stimulation (**I**), (2) single R848 stimulation (**R**), (3) simultaneous poly(I:C) and R848 stimulation (**IR**), (4) poly(I:C) stimulation followed by R848 stimulation with an 8-hour interval between the two treatments ($\mathbf{I_8R}$), (5) poly(I:C) stimulation followed by R848 stimulation with a 24-hour interval ($\mathbf{I_{24}R}$), (6) R848 stimulation followed by poly (I:C) stimulation with an 8-hour interval ($\mathbf{R_8I}$), and (7) R848 stimulation followed by poly (I:C) stimulation after an 24-hour interval ($\mathbf{R_{24}I}$). The expression levels of *Il6* and *Il12b* were measured at 10 time points (0, 4, 8, 12, 16, 24, 28, 32, 40, 48 h) under conditions of **R** or **I** single treatment, and at 4 h, 8 h, 16 h and 24 h after second stimulation (**IR**, $\mathbf{I_8R}$, $\mathbf{I_{24}R}$, $\mathbf{R_8I}$ and $\mathbf{R_{24}I}$). In addition to these newly generated data, we also used our published data (Tan et al, 2013) on the expression levels of several major players in cytokine regulation, including phosphorylated ERK, p38, JNK and IκBα. The concentrations of these signaling molecules were measured at 7 time points (5, 15, 30 min, 1, 4, 8, 12 h) under the conditions of **R**, **I**, **IR**, $\mathbf{I_8R}$ and $\mathbf{I_{24}R}$. We reserved the *Il6* and *Il12b* time course under $\mathbf{I_{24}R}$, $\mathbf{R_8I}$, and $\mathbf{R_{24}I}$ conditions as the test dataset and used the remaining data to train/calibrate the model parameters (unknown rate constants) by using a statistical logic-based framework developed recently (Palaniappan et al, 2013) (see *Materials and Methods*). The initial concentrations of proteins were allowed to vary 5% around their nominal values in order to account for cellular heterogeneities. The resulting kinetic parameters are shown in Supplementary **Table S2**.

Figure 3A shows the profiles generated by our simulations using the optimized set of parameters (*blue curves*) in comparison to experimental data (*red dots*). The simulation curves broadly capture the experimentally observed qualitative trends and reproduce the two rounds of activation behaviors of IκBα. **Figure 3B** shows the comparison of the *Il12b* and *Il6* expression data (*left*) with the simulated profiles (*right*) for different conditions. The model successfully reproduced the time- and order-dependent synergy of cytokine production and its predictions matched not only the training data (**R**, **I**, **IR**, $\mathbf{I_8R}$) but also the test data ($\mathbf{I_{24}R}$, $\mathbf{R_8I}$, $\mathbf{R_{24}I}$). Both the predicted and test data consistently showed early and massive surge in the cytokine expression under $\mathbf{I_8R}$ stimulation, and a delayed and diminished response under $\mathbf{I_{24}R}$ stimulation, which support of the significance of the timing of PAMP treatments. This validated model was used next to perform a variety of *in silico* experiments.

Sensitivity analysis identified key components and reactions controlling cytokine synergy

To identify the components and reactions that are essential to inducing a synergistic cytokine production, we conducted an extensive sensitivity analysis, using logic-based statistical model checking (SMC) technique (Palaniappan et al, 2013).

We first carried out control coefficients-based sensitivity analysis for initial concentrations of major species in the model. The model output was defined as the integrated *Il12b* and *Il6* expression in response to the five conditions (**R**, **I**, **IR**, $\mathbf{I_8R}$, $\mathbf{I_{24}R}$). The computed normalized local sensitivities are summarized in **Figure 4A**.

The results for single stimulation conditions show that TLR7 and directly downstream components along TLR7 pathway are more sensitive to **R** stimulation than TLR3 pathway, and its downstream components are more sensitive to **I** stimulation (*lower* portion). TLR3-mediated cytokine production is mainly regulated by IκBα-NF-κB (indicated by an arrow), which exhibits high sensitivities under all five conditions. In contrast, AP-1, another key transcription factor that regulates cytokine production, is sensitive only under conditions that involve TLR7 activation (**R**, **IR**, $\mathbf{I_8R}$, $\mathbf{I_{24}R}$). MKK1/2, MKK3/6, MKK/4/7, ERK, p38, and JNK display sensitivity patterns similar to the downstream AP-1, suggesting that the MAPK signaling cascades (*Core* box in **Figure S1**) play crucial roles in coupling the upstream TLR3 and TLR7 signaling modules to the downstream transcription module, especially under combinatorial stimulation conditions. Although the three MAPK cascades (involving JNK, ERK and p38) can activate AP-1 in parallel, the components on the JNK signaling cascade exhibit positive sensitivities, while those of the ERK and p38 cascades show negative sensitivities. This draws attention to the distinct roles of JNK, ERK and p38 in regulating cytokine synergy. The highly negative sensitivities displayed by MSK1/2 and STAT3 suggest the potential importance of IL-10 induced STAT3 activation in inhibiting cytokine production and maintaining homeostasis. Interestingly, TYK2-JAK1 and STAT1-STAT2 had very strong controls over the system response while the influences of proteins on the AKT and NIK pathways were low,

which implies the importance of JAK-STAT1/2 pathway among all the potential crosstalk mechanisms.

We next computed the global sensitivities of the model to kinetic parameters using a multi-parametric sensitivity analysis (MPSA) method (see details in Materials and Methods) based on our SMC approach. The model output is defined as integrated *Il12b* and *Il6* expression under $\mathbf{I_8R}$ stimulation. The results are presented in **Figure 4B**. 32 kinetic parameters (rate constants) are distinguished by their strong effects on cytokine production (global sensitivities > 0.1, colored *blue*). The corresponding reactions are indicated by *red arrows* in **Figure S1**. These are classified into seven functional groups (**Figure 4C)**: the production of *Il12b, Il6* and type I IFN, JAK-STAT1/2 signaling cascade, IL-10-STAT3 signaling cascade, and the three MAPK signaling cascades (ERK, p38 and JNK) also noted above. The two rate constants (k_{72} and k_{73}) that give rise to the highest sensitivities are associated with the transcription and degradation of *Il12b* and *Il6* mRNA, respectively. This is not surprising as these two parameters directly determine the production and level of *Il12b* and *Il6* mRNAs. Seven rate constants associated with reactions along the JNK pathway, which leads to the activation of AP-1, also exert strong controls. This result is consistent with the local sensitivity analysis, which suggests the dominant role of JNK pathway in activating AP-1 over the ERK and p38 pathways. In addition, the analysis highlights the important inhibitory role of the reactions associated with IL-10-STAT3 pathway, compared to other inhibitory interactions in the system, such as A20 (**Figure S1**). Additionally, many critical reactions are involved in type I IFN transcription and the activation of JAK1-STAT1/2 pathway, which can be connected by our hypothesized pathway Type I IFN → STAT1/2 → cytokines. Thus, a crucial insight that emerges from these findings is that the time-dependent cytokine synergy we observed experimentally may be induced by a STAT1/2-mediated crosstalk mechanism, in addition to the regulatory feedback of MAPK signaling cascades.

The time interval between TLR3- and TLR7-stimulations influences cytokine synergy but not type I IFN production

In addition to the crucial components and reactions we identified in the previous section, the overall expressions of both *Il6* and *Il12b* genes are also highly sensitive to the time interval, Δt, between the two PAMP treatments, as illustrated in **Figure 1C**. Here we simulated the model behavior by varying Δt between TLR3 and TLR7 activations from 0 h to 48 h in order to explore the dependency of the immune response in the timing of combined stimulations. The predicted effects in terms of *Il6* and *Il12b* expression levels are shown in **Figure 5A**. We calculated the peak amplitudes and peak time (starting from **R** stimulation) of each response curve in Figure 5A and plotted them as functions of Δt (**Figure 5B**). With increasing Δt, the peak amplitudes of *Il6* and *Il12b* first increased until maximal values were reached, and then dropped. Maximal amplitudes were reached around Δt = 7 h for both *Il6* and *Il12b* production. This is consistent with our experimental data shown in Figure 1C, which

indicated that the optimal Δt was 8 h (among the measurements made at concrete intervals). On the other hand, the duration required to reach the response peaks was robustly found to be around 4 h for both *Il12b* and *Il6*.

We also simulated the time profiles of type I IFN for different values of Δt under sequential treatments (**Figure 5C**): poly(I:C) followed by R848 (**I→R**) (*left panel*), and R848 followed by poly(I:C) (**R→I**) (*right panel*). The effects of Δt on type I IFN production is negligible in the former case. In contrast, for R→I stimulation, the production curve significantly shifted along with the starting time point of I stimulation, and maintained a constant peak amplitude.

Taken together, these results imply that the type I IFN production is predominantly governed by the application time of the first stimulus (**I**), or by the activation of the TLR3 signaling pathway (**Figure 5C**), whereas cytokine production is regulated by both TLR3 and TLR7 pathways or their crosstalk. Importantly, although type I IFN is implicated in most of the putative crosstalk pathways between TLR3 and TLR7 pathways, it is not sufficient *per se* to account for the dependency of cytokine production (or synergy) on the time interval, Δt, between the two consecutive stimuli.

In silico knockdown of MAPKs revealed the distinct effects of JNK, ERK and p38 on cytokine production, confirmed by experiments

The sensitivity analysis presented in **Figure 4** drew attention to the significant role of MAPKs in modulating cytokine synergy. As shown in **Figure S1**, TAK1 complex activated the ERK, JNK and p38 signaling cascades in parallel, and either of these cascades was capable of triggering the activation of AP-1 and promoting the production of *Il12b* and *Il6* mRNA. At the same time, ERK and p38 also induced the production of anti-inflammatory cytokine IL-10, which led to the suppression of IL-12p40 and IL-6 production through STAT3-dependent pathway. This forms the incoherent type 1 feed-forward loops (I1-FFL), a circuit in which a regulator X activates Z, and X also activates Y which in turn inhibits Z.

To assess the effects of different MAPK pathways on cytokine synergy, we performed *in silico* knockout experiments, by eliminating the phosphorylation reactions along each of the three MAPK cascades. The predicted time profiles of *Il12b* and *Il6* mRNA for Δt in the range [0 - 48 h] are shown in **Figure 6A-C**. Knocking down 90% of activated JNK significantly decreased the cytokine production, indicating its dominant upregulating role amongst the three cascades. In contrast, the knockdown of activated ERK increased cytokine production under various conditions (e.g. **IR**, $\mathbf{I_8R}$, $\mathbf{I_{24}R}$), indicating that the inhibitory effect of ERK mediated by IL-10 and STAT3 are stronger than enhancing effect mediated by AP-1. Hence ERK acts as an overall negative modulator (or suppressor) of cytokine production. p38 also downregulated cytokine production under combinatorial treatment, although the effect was relatively small (if not negligible) compared to ERK.

To experimentally verify the model predictions, we perturbed the initial amount of JNK, ERK and p38 by incubating BMDM cells with the inhibitors SP600125 (JNK inhibitor), U0126 (ERK inhibitor) and SB203580 (p38 inhibitor) for 50 min. BMDMs were then treated first with poly(I:C) for 0, 8 or 24 h followed by R848 for 8 h before RT-PCR. As can be seen in **Figure 6D**, for all the three conditions, JNK inhibition caused a decrease in the cytokine production, while low ERK levels increased cytokine production (consistent with its negative regulation that has been removed upon its inhibition). Finally, p38 inhibition slightly increased cytokine production in general. These observations are consistent with the simulation results shown in **Figure 6A-C,** and confirm the distinctive effect of each MAPK signaling cascade on the (synergistic) production of cytokine.

JAK-STAT1/2 pathway is the main mechanism responsible for induction of cytokine synergy

The sensitivity analysis results (**Figure 4**) implied that JAK-STAT1/2 pathway is a major determinant of cytokine synergy. To confirm this, we carried out *in silico* knockout experiments where the four putative mechanisms discussed earlier were inactivated; namely (i) transcriptional activation of type 1 IFNs and other target genes by IRF3 (downstream of TLR3), (ii) core reactions induced by Akt activation and (iii) those induced by NIK activation (both Akt and NIK being activated via secreted type 1 IFN), and (iv) JAK-STAT1/2 mechanism potentially establishing crosstalks relevant to cytokine synergy were turned off by knocking out IRF3, Akt, NIK or JAK-STAT1/2, and the time evolution of cytokine levels under each of the four knockout conditions were examined, subject to different combinatorial stimulation protocols. The results from simulations for *Il12b* mRNA levels are presented in **Figure 7**, and their counterparts for *Il6* mRNA levels in the **Figure S2**. The data clearly show that the knockout of STAT1-STAT2 almost completely abrogates the synergistic production of cytokines, irrespective of the time interval between the two stimuli, whereas the other three have no detectable effect. We also performed *in silico* knockouts for different combinations of the putative mechanisms (**Figure S3**), which invariably confirmed the essential role of JAK-STAT1/2 pathway in mediating the cytokine synergy, consistent with the parameter sensitivity results.

In silico and experimental knockdown of STAT1 highlighted the complex regulatory role of the incoherent feedforward loop

Similar to the ERK and p38 signaling events, the JAK-STAT1/2 pathway mediates an I1-FFL since its target genes not only directly regulate the production of IL-12p40 and IL-6 but also enhance the production of IL-10 which inhibits IL-12p40 and IL-6. In the previous section, we showed that knockout of STAT1 would lead to a significant decrease in cytokine synergy (**Figure 7D**). However, the negative local sensitivity values associated with STAT1-STAT2 complex (**Figure 4A**) suggest that a mild decrease in STAT1 initial concentration might induce cytokine production. The opposing roles of STAT1 in cytokine synergy imply that the STAT1-mediated I1-FFL (**Figure 8A**) might lead

to the generation of non-monotonic input-output relation, i.e. *biphasic response* (Hart & Alon, 2013; Kim et al, 2008). To verify this, we evaluated the *Il12b* mRNA levels 8 h after the second PAMP challenge under **IR**, $\mathbf{I_8R}$ and $\mathbf{I_{24}R}$ conditions with the STAT1 initial concentration ranging from 0.01 to 10 nM. The results summarized in **Figure 8B** show that a biphasic response occurred under $\mathbf{I_8R}$ and $\mathbf{I_{24}R}$ (but not **IR**) conditions. Reducing STAT1 concentration starting from physiological concentration (2.3 nM; indicated as 'normal') led to an increase and then a decrease in the cytokine production in both time-delayed combinatorial stimuli.

To confirm the role of STAT1 predicted by our model, we performed *in vitro* STAT1 knockdown experiments with mouse macrophage cell line, J744 cells. Cells were transfected with *Stat1* sequence-specific siRNA or non-target control siRNA. **Figure 8C** shows substantial knockdown of STAT1 at 24 h, after which the cells were stimulated with **IR**, $\mathbf{I_8R}$ or $\mathbf{I_{24}R}$ for 8 h. As shown in **Figure 8D**, STAT1 knockdown resulted in the enhancement of *Il6* and *Il12b* mRNA expression in cells stimulated with **IR**, $\mathbf{I_8R}$ and $\mathbf{I_{24}R}$. These observations agree well with the *in silico* model predictions, in support of the biphasic response inducible by STAT1-mediated I1-FFL.

Discussion

TLR signaling pathways protect the host against a broad range of microbial pathogens. Here, our empirical and computational analyses identified how two key TLR pathways coordinate an optimal innate immune response in macrophages. Specifically, when TLR3 is activated, it primarily leads to the production of type I IFNs via TRIF-dependent pathway. This initial response primes the host cell for a more effective immune response (in terms of the MyD88-mediated production of proinflammatory cytokines) to a subsequent TLR7-specific PAMP challenge, by creating a form of an immunological memory. This synergy effect is highly time-dependent, and an optimal immune response requires a proper synchronization of events downstream of TLR3 and TLR7 pathways. In the present study, we found that the time-dependent synergistic cytokine production predominantly controlled by the JAK-STAT1/2 pathway, triggered by the autocrine type I IFNs, upregulated by the TLR3 signaling cascade. Through a combination of efforts in experimental and computational approaches, we revealed the dual opposing roles of JAK-STAT pathway: knocking down STAT1 led to a decrease in cytokine gene expression via transcription factors such as IRF1 (unpublished data), as well as an increase of cytokine production via its target, anti-inflammatory cytokine, e.g. IL-10. The overall cytokine production depends on a subtle time-dependent coordination of those factors. Thus, STAT1 is not only an essential mediator for generating the cytokine synergy to boost immune response, but also a modulator for avoiding excessive immune responses. The study further highlighted the effects of MAPK signaling cascades, revealing the opposite effects of JNK (an enhancer of cytokine production) and ERK (a suppressor of cytokine production), predicted by the model and simulations, and confirmed by experiments.

In the past two decades, intense research has identified and characterized hundreds of components and interactions implicated in TLR signaling. Various systems biology approaches have been used for improving our understanding of TLR-mediated innate immune responses (Vandenbon et al, 2012). However, an accurate and validated mathematical model of TLR signaling network, taking into account of the dynamic crosstalk between various TLR pathways has been hitherto lacking (Basak et al, 2007; Cheong et al, 2008; Covert et al, 2005; Hoffmann et al, 2002; Li et al, 2011; Longo et al, 2013; O'Dea et al, 2007; Oda & Kitano, 2006; Shih et al, 2009; Shinohara et al, 2014; Tay et al, 2010; Werner et al, 2005). In the present study, we have developed a first calibrated ODE-based kinetic model for the time-dependent coupling between two specific TLR pathways and its complex implications. Furthermore, a novel JAK-STAT-mediated synergistic mechanism and the complex role of STAT1 is suggested by our study, which could guide future experimental investigations on discovering unidentified components and their interactions in the TLR signaling network. As new data become available our model can be refined and extended to help gain more insights.

The innate immune system must be tightly regulated so as to amplify the appropriate level of protective responses during infection, attenuate the damage inflicted by inflammation, as well as to

maintain or restore homeostasis. For example, complement pathways can crosstalk to enhance antibacterial activities under inflammatory conditions and simultaneously establish tight surveillance (Liu et al, 2011). In this context, 'priming' and 'tolerance' are important concepts that have emerged from accumulating evidence (Biswas & Lopez-Collazo, 2009; Shnyra et al, 1998). For example, it has been reported that a low dose of lipopolysaccharide (LPS), an inducer of TLR4 signaling, could prime macrophages and amplify cytokine production in response to a subsequent high dose-LPS stimulation; whereas, preconditioning macrophages with a high dose of LPS renders the cells much less responsive to a subsequent high dose-LPS stimulation (Fu et al, 2012a). Basic mechanisms underlying these priming and tolerance phenomena have been predicted in a recent work (Fu et al, 2012a), which computationally enumerated all possible topologies of an essential network with three abstract nodes. A follow-up study (Fu et al, 2012b) further hypothesized that IFNs and STAT1 might contribute to LPS-mediated priming in macrophages. Our study clearly demonstrates that IFN and STAT1 play a key role in priming the cell for subsequent challenges, and as such, it validates the hypothesis made by Xing and coworkers for TLR4, since TLR4 signaling itself is mediated by both MyD88 and TRIF.

The biphasic modulation of cytokine production through an incoherent type 1 feedforward loop (I1-FFL) deserves further attention. I1-FFL is one of the most frequently observed network motifs in biological networks. It appears hundreds of times in bacteria (Alon, 2007), yeast (Milo et al, 2002), and animals (Boyer et al, 2005; Milo et al, 2002). It has been reported (Hart & Alon, 2013) that the roles of I1-FFL include: (i) shortening of gene-circuit response time, (ii) generation of gene expression pulses (Hart & Alon, 2013), (iii) distinguishing time-varying inputs, (iv) filtering out noise, (v) detecting fold change of input signal, and (vi) generating non-monotonic input-output relations (Hart & Alon, 2013). There exist three I1-FFLs in our model, mediated by ERK, p38 and STAT1 respectively. Among them, we found that the STAT1-dependent I1-FFL, inducing a biphasic response, is crucial to both amplifying the antiviral response and avoiding excessive inflammatory response. The I1-FFL mediated by p38 has minimal effect on cytokine production, but that of ERK is also shown to induce a strong (suppressive) effect. At the gene transcription level, Litvak et al (2009) identified a coherent type 1 feedforward loop (C1-FFL) formed by NF-κB, ATF3 and C/EBPδ, which discriminates between transient and persistent TLR4-induced signal. As a future direction, it might be interesting to explore the role of the gene transcription circuit downstream of TLR3-TLR7 signaling, and examine how different network motifs (e.g. I1-FFL, C1-FFL) cooperate to determine the immune response.

A large number of previous modeling efforts have been focused on the NF-κB signaling module, which constitutes a core component downstream of all TLR pathways (Cheong et al, 2008; Covert et al, 2005; Hoffmann et al, 2002; Shinohara et al, 2014; Tay et al, 2010; Werner et al, 2005). An important finding indicates that a strong negative feedback loop mediated by IκBα can result in the oscillatory behavior of NF-κB level upon tumor necrosis factor-α (TNFα) stimulation (Hoffmann et al, 2002; Werner et al, 2005). Interestingly, when cells are stimulated by LPS that initiates TLR4

signaling, activated NF-κB exhibits sustained behavior (Covert et al, 2005). It has been shown that the stability of LPS-induced NF-κB activation is achieved by two rounds of NF-κB activation: (i) an early NF-κB response via MyD88-dependent pathway, and (ii) a late NF-κB response via TRIF-dependent pathway, which first activates IRF3, leading to the expression of TNFα, and then triggering the TNFR pathway with a time delay of 30 min (Covert et al, 2005). We have included the IκBα-mediated negative feedback loop in our model and observed a dampened oscillatory behavior of activated NF-κB under single poly(I:C) stimulation (**Figure S4**). Upon combinatorial stimulation with poly(I:C) and R848, the NF-κB activity was significantly increased and the oscillation behavior disappeared (**Figure S5**). Thus, there is an analogy between the TLR4-dependent two-round NF-κB activation mechanism identified by Covert et al (Covert et al, 2005) and the TLR3-TLR7-dependent synergistic cytokine production mechanism identified here. Both mechanisms are controlled by MyD88-TRIF pathways and are mediated by IRF3-induced expression of autocrine signaling molecules. Since similar signaling network structures evolve to achieve modular dynamic functions (Purvis & Lahav, 2013) it might be interesting to see if the MyD88-TRIF-IRF3 mediated crosstalk mechanisms are present in other TLR pathways.

Apart from TLRs, other pattern recognition receptors (PPRs) including retinoic acid-inducible gene 1 (RIG-I)-like receptors (RLRs), C-type lectin receptors, NOD-like receptors, also contribute to PAMP recognition and the regulation of innate immunity (Kawai & Akira, 2011). As pathogens often contain various PAMPs activating multiple PRRs, TLRs in crosstalk with other PRRs, orchestrate both host innate and adaptive immune responses to combat infections (Kawai & Akira, 2011). For instance, hepatitis C virus (HCV) is recognized by both TLR3 and RIG-I. The HCV RNA delivered from infected hepatocytes can also trigger the activation of the TLR7 pathway (Takahashi et al, 2010). PRR crosstalk can either positively or negatively regulate the eventual immune responses. Different types of collaborative responses have been reviewed by (Tan et al, 2014). Thus, it is important to understand how immune responses are coordinated and regulated by different PRRs. In this context, an important future direction will be the extension of the current model to non-TLR-PRR pathways as well as different cell types.

Turning to computational methods, our study demonstrated that statistical model checking (SMC)-based framework (Palaniappan et al, 2013) can be advantageously applied to noisy cell-population data to obtain good estimates for hundreds of unknown parameters. Furthermore, we also showed that this framework enables the computation of global sensitivities of parameters for a large signaling network. To cope with even larger networks in the future, we plan to refine this method by exploiting the inherent massive parallelism in numerical simulation and develop a platform-aware GPU-based implementation using the strategy proposed recently (Hagiescu et al, 2013; Liu et al, 2012).

In summary, our experimental and computational modeling analyses revealed how macrophages create ‘innate immune memory’ by activating TLR3 pathway and augmenting immune response to a

subsequent PAMP challenge. We have obtained novel insights regarding the crosstalk mechanisms between two major TLR pathways that help achieve this innate immune memory-based responses to time-dependent multiple infections. The model also provides a potential platform for designing and testing pharmaceutical strategies for immunotherapy.

Material and Methods

Mathematical modeling

Our model consists of multiple modules **(Figure S1**) the time evolution of which is described by a system of ODEs corresponding to each reaction/interaction schematically shown in **Figure S1**. Each molecular species (or model component) x_i is associated with an equation of the form, $\frac{dx_i}{dt} = f_i(\mathbf{x}, \boldsymbol{\Theta})$, where the function f_i describes the kinetics of the reactions that produce or deplete x_i, $\mathbf{x}$ is a vector that denotes the instantaneous concentration $x_i(t)$ of *all* components involved in this reaction, and the vector $\boldsymbol{\Theta}$ denotes the rate constants governing this reaction. The reaction rates for assembly/binding, catalysis and transcription are described using mass action kinetics, Michaelis-Menten kinetics, or the equations developed by Kuttykrishnan et al (Kuttykrishnan et al, 2010). We assume that $x_i(t)$ takes on values in the interval, $[L_i, U_i]$, where L_i and U_i are non-negative rational numbers with $L_i < U_i$. We address cell-to-cell variability explicitly by using probability distributions over the initial concentrations and rate constants (**Table S2**). The text files corresponding to the system of 97 ODEs are available in the supplementary information.

Statistical model checking (SMC)

SMC is a scalable computational technique for verifying whether a probabilistic dynamical system satisfies properties encoded as temporal logic formulas (Younes et al, 2004). We employed a recently developed SMC-based technique (Palaniappan et al, 2013) where we specified qualitative or quantitative properties of interest using a mildly strengthened bounded linear temporal logic (BLTL). Our BLTL is defined over a finite set of atomic propositions (*APs*), which is of the form (i, l, u) with $L_i \leq I < u \leq U_i$, meaning "the current concentration level of x_i falls in the interval [l, u].". The logic operators consist of $\wedge$ (and), $\vee$ (or), $\neg$ (negation), and time bounded **U** (until), **G** (global) and **F** (future). We define the BLTL formulas as: (i) every *AP* and the constants *true* and *false* are BLTL formulas; (ii) if ψ , ψ' are BLTL formulas then $\neg\psi$, $\psi \wedge \psi'$ and $\psi \vee \psi'$ are BLTL formulas; (iii) if

ψ , ψ' are BLTL formulas and $t \le T$ is a positive integer then $\psi \mathbf{U}^{\le t} \psi'$, $\psi \mathbf{U}^{t} \psi'$, $\mathbf{F}^{\le t} \psi$ and $\mathbf{G}^{\le t} \psi$ are BLTL formulas.

Since experimental data were available at a finite number of time points, we applied the SMC method to the discrete time points, $\mathbf{T} = \{0,1,\ldots,T\}$. A *trajectory* in our model is a solution (up to time, T) to the ODE system. The notion of a trajectory σ satisfying a BLTL specified property φ at time point $t \in \mathbf{T}$ is written as $\sigma, t \models \phi$ and is defined as follows: (i) σ,t|=(i,l,u) iff $l \le \sigma(t)(i) \le u$, where $\sigma(t)(i)$ is the i^{th} component of vector $\sigma(t)$; (ii) ∧ , ∨ , and ¬ are interpreted in the usual way; (iii) $\sigma, t \models \psi \mathbf{U}^{\le k} \psi'$ iff there exists k' such that $k' \le k$, $t + k' \le T$ and $\sigma, t + k' \models \psi'$. $\sigma, t + k'' \models \psi$ for every $0 \le k'' < k'$; (iv) $\sigma, t \models \psi \mathbf{U}^{k} \psi'$ iff $t + k \le T$ and $\sigma, t + k \models \psi'$. $\sigma, t + k' \models \psi$ for every $0 \le k' < k$. (v) $\sigma, t \models \mathbf{F}^{\le k} \psi$ iff $\sigma, t \models true \mathbf{U}^{\le k} \psi$. (vi) $\sigma, t \models \mathbf{G}^{\le k} \psi$ iff $\sigma, t \models \neg \mathbf{F}^{\le k} \neg \psi$.

Let $\mathbf{B}$ represent the set of all trajectories of our ODE system, starting from an initial state, (the set of all initial concentrations defined in **Table S1)**. We note that the set of trajectories satisfying a BLTL formula ψ , denoted as $B(\psi) = \{\sigma \mid \sigma, 0 \models \psi, \sigma \in \mathbf{B}\}$ can be identified by the corresponding set of initial states, denoted as $I(\psi) \subseteq \mathbf{I}$. Thus, we define probabilistic BLTL formulas in the form of $\Pr_{\ge \theta}(\psi)$, where $\theta \in (0,1]$, meaning the probability that a trajectory in $\mathbf{B}$ belongs to $B(\psi)$ is at least θ . We then use $M \models \Pr_{\ge \theta}(\psi)$ to denote that *M*, the systems of ODEs, meets the specification ψ with a probability of at least θ .

Using SMC, properties can be verified and/or assigned confidence levels and error bounds. Specifically, we verified each property using a sequential hypothesis test between the null hypothesis H0: $p \ge \theta + \delta$ and the alternative hypothesis H1: $p \le \theta - \delta$, where p is the probability of *M* satisfying ψ and δ specifies the indifference region. The strength of the test is determined by the parameter α and β which bound the type-I and type II errors, respectively. The test proceeds by generating a sequence of sample trajectories, $\sigma_1, \sigma_2 \ldots$ A corresponding sequence of Bernoulli random variables $x_1, x_2, \ldots$ is assumed, where x_k = 1 if $\sigma, 0 \models \psi$, and zero otherwise. For each generated sample, we update the score ω_n using the function

$$\omega_n = \frac{(\theta - \delta)^{\sum_{i=1}^{n} x_i} (1 - (\theta - \delta))^{(m - \sum_{i=1}^{n} x_i)}}{(\theta + \delta)^{\sum_{i=1}^{n} x_i} (1 - (\theta + \delta))^{(m - \sum_{i=1}^{n} x_i)}}$$

where n is the number of generated samples. We accept hypothesis H0 if $\omega_n \geq (1-\beta)/\alpha$, and hypothesis H1 if $\omega_n \leq \beta/(1-\alpha)$; otherwise, we draw another sample. Our implementation of this scheme is available at our website (http://www.comp.nus.edu.sg/~rpsysbio/smc). It is written in MATLAB and C++, and employs the SUNDIALS CVODE package (Hindmarsh et al, 2005) to solve the ODE system.

Parameter estimation

Unknown parameters were estimated using an SMC-based approach. We encoded the training data in terms of time series of experimental data as well as qualitative dynamic trends, defined by the respective BLTL formulas ψ_{exp} and ψ_{qlty}. For each estimate **w** of unknown parameters, we assumed a prior distribution as **w** ~ U(0.95**w**, 1.05**w**) so as to take into account the cellular stochasticity. We ran our SMC procedure to evaluate the goodness of **w,** in terms of fitting the training data, by verifying $\Pr_{\geq 0.9}(\psi_{\text{exp}} \wedge \psi_{qlty})$ with strength of statistical test (α=0.05, β=0.05). Specifically, we quantified the goodness of **w** using the following objective function:

$$F(\mathrm{w}) = J^{+}_{qlty}(\mathrm{w}) + \sum_{i \in 0} \frac{J^{i,+}_{\text{exp}}(\mathrm{w})}{J^{i}_{\text{exp}}}$$

where J^{i}_{exp} is the number of conjuncts in ψ^{i}_{exp}, $J^{i,+}_{\text{exp}}(\mathbf{w})$ is the number of formulas of the form ψ^{t}_{i} (a conjunct in ψ^{i}_{exp}) where $\Pr_{\geq 0.9}(\psi^{t}_{i})$ holds with the statistical strength of (α/J ,β)(J being defined as $J = \sum_{i \in O} J^{i}_{\text{exp}} + J_{qlty}$) and $J^{+}_{qlty}(\mathbf{w})$ is the number of conjuncts in ψ_{qlty} where $P_{r \geq 0.9}\left(\psi_{l.qlty}\right)$ holds with the strength (α/J ,β). We implemented the stochastic ranking evolutionary strategy (SRES) (Runarsson & Yao, 2000) to evolve candidate parameters in order to search for the **w** values with global minimum objective value $F(\mathbf{w})$ in the parameter solution space. The resulting list of parameter is presented in **Table S2**.

Sensitivity analysis

Local sensitivity analysis was performed using the standard approach (Liu & Thiagarajan, 2012). Global sensitivity analysis was performed using an SMC-based multi-parametric sensitivity analysis (MPSA) method (Cho et al, 2003). We encoded the time profile of *Il12b* (the model output) as a BLTL formula, ψ_{IL12}. The MPSA procedure involves drawing a representative set of samples from the parameter space. For each sampled combination of parameter values **w**, we compute the objective

value $F(\mathbf{w})$ with respect to the ψ_{IL12}. The sampled parameter sets were classified into two classes using a threshold objective value. The sensitivities were then evaluated as Kolmogorov-Smirnov cumulative frequencies associated with the two classes.

Preparation of bone marrow-derived macrophages (BMDMs)

BMDMs were extracted from the tibia and femur of 8-week old female balb/c mice. Bone marrow cells were harvested and cultured in Dulbecco's modified Eagle's medium (DMEM) (Gibco, Life Technologies, Carlsbad, CA, USA), supplemented with 10% (v/v) fetal bovine serum (FBS) (Hyclone, Thermo Fischer Scientific, Waltham, MA, USA), 100 U/ml recombinant M-CSF (Ebioscience, San Diego, CA, USA), 100 U/ml penicillin and 100 μg/ml streptomycin (Gibco, Life Technologies, Carlsbad, CA, USA) at a density of $1.5x10^6$ cells/ml. Additional complete medium with M-CSF was added three days after plating. Then cells were cultured for another four days before harvesting the adherent macrophages. Mouse work was under the guidance and regulation of Institutional Animal Care and Use Committee (IACUC protocol number: 049-11).

Cell culture and PAMP treatments

BMDMs and J774 cells were cultured in DMEM supplemented with 10% (v/v) FBS in 37°C incubator with 5% CO_2 and 95% air supply. BMDM cells were plated at a density of $1x10^6$/ml and J774 were plated at $0.4x10^6$ cells/ml. The final concentration of PAMP treatment is 10 μg/ml and 25 ng/ml for poly(I:C) and R848 (InvivoGen, SD, CA, USA).

Western blot experiments

Cells were lysed with Radioimmunoprecipitation assay (RIPA) buffer supplemented with proteinase- and phosphatase-inhibitor cocktail (Roche). 15 μg of total protein were resolved in a reducing SDS-PAGE (10%) and electrotransferred to polyvinyldifluoride membranes. Blots were subsequently blocked with 5% dry, skimmed milk in TBST (50 mM Tris-base, 150 mM NaCl, 0.01% Tween-20, pH 7.6) and probed with specific antibodies: Rabbit polyclonal antibodies against STAT1 (#9172) were obtained from Cell Signaling Technologies (Boston, MA, USA). Mouse monoclonal anti-GAPDH (sc-32233) was purchased from Santa Cruz Biotechnologies. Blots were then incubated with HRP-conjugated rabbit or mouse secondary antibodies (Sigma) and visualized with Western Bright ECL (Advansta, Menlo Park, CA, US) and ImageQuant LAS4000 mini system (GE, Fairfield, CT, US).

siRNA transfections

For RNAi experiments, cells were transfected with a scramble control (Darmacon) or ON-TARGETplus SMARTpool siRNA (Darmacon) against mouse *Stat1* (50 nM) with X-tremeGENE HP DNA Transfection Reagent (Roche) for 24 h until subsequent PAMP stimulation.

MAPK inhibitor treatment

Inhibitors for JNK (SP600125), ERK (U0126) and p38 (SB203580) were purchased from Cell Signaling Technology (Boston, MA, USA). Cells were first treated with 10 μM inhibitors for 50 min, followed by corresponding PAMP stimulation. Media were not changed after inhibitor treatment.

Real-time quantitative PCR

Total RNA from cells was extracted with Trizol (Invitrogen). cDNAs were synthesized with Superscript III reverse transcriptase (Invitrogen). Lightcycler 480 master probes master (Roche) were used for the Taqman assays, and pre-designed TaqMan Gene Expression Assays (Life Technologies) Mm00446190_m1, Mm00434174_m1, Mm00446968_m1 were used for the detection of *Il6*, *Il12b*, and *Hprt* mRNA, respectively. Real-time PCR was carried out with Light cycler 480 system (Roche). The PCR cycles were: 1 cycle of 95°C for 10 min, 40 cycles of 95°C for 10 s, 60°C for 20 s. The mRNA levels of *Il6* and *Il12b* were normalized with respect to the amount of *Hprt*.

Calculation of "fold-synergy" for cytokine production

To quantify the synergistic effect, the cytokine production under combinatorial stimulation was divided by the sum of the respective single stimulations. This ratio was termed "fold synergy".

Statistical analysis

Data are represented as mean values and standard deviations based on at least three independent experiments. Statistically significant differences between treatments were analyzed with one-tailed Student's t-test. A value of $p < 0.05$ was considered significant (*) and $p < 0.01$ very significant (**).

Acknowledgments

This work was supported by a grant from the National Medical Research Council (NMRC/CBRG/0055/2014), Singapore. This study was also partially supported by the Singapore MOE ARC grant MOE2011-T2-2-012. Support by the National Institutes of Health awards P41-GM103712 and U19-AI068021 is gratefully acknowledged by IB.

Author Contributions

BL, QL, SP, PST, and JLD conceived and designed research; BL, QL, and SP performed the *in silico* modeling and experiments; BL, QL, SP, IB, PST, and JLD analyzed the results; BL, QL, SP, IB, PST, and JLD wrote the paper.

Conflict of Interest

The authors declare that they have no conflict of interest.

References

Alon U (2007) Network motifs: theory and experimental approaches. *Nat Rev Genet* **8:** 450-461

Bagchi A, Herrup EA, Warren HS, Trigilio J, Shin HS, Valentine C, Hellman J (2007) MyD88-dependent and MyD88-independent pathways in synergy, priming, and tolerance between TLR agonists. *J Immunol* **178:** 1164-1171

Basak S, Kim H, Kearns JD, Tergaonkar V, O'Dea E, Werner SL, Benedict CA, Ware CF, Ghosh G, Verma IM, Hoffmann A (2007) A fourth IkappaB protein within the NF-kappaB signaling module. *Cell* **128:** 369-381

Biswas SK, Lopez-Collazo E (2009) Endotoxin tolerance: new mechanisms, molecules and clinical significance. *Trends Immunol* **30:** 475-487

Bohnenkamp HR, Papazisis KT, Burchell JM, Taylor-Papadimitriou J (2007) Synergism of Toll-like receptor-induced interleukin-12p70 secretion by monocyte-derived dendritic cells is mediated through p38 MAPK and lowers the threshold of T-helper cell type 1 responses. *Cell Immunol* **247:** 72-84

Boyer LA, Lee TI, Cole MF, Johnstone SE, Levine SS, Zucker JP, Guenther MG, Kumar RM, Murray HL, Jenner RG, Gifford DK, Melton DA, Jaenisch R, Young RA (2005) Core transcriptional regulatory circuitry in human embryonic stem cells. *Cell* **122:** 947-956

Cheong R, Hoffmann A, Levchenko A (2008) Understanding NF-kappaB signaling via mathematical modeling. *Mol Syst Biol* **4:** 192

Cho KH, Shin SY, Kolch W, Wolkenhauer O (2003) Experimental design in systems biology, based on parameter sensitivity analysis using a Monte Carlo method: A case study for the TNF alpha-mediated NF-kappa B signal transduction pathway. *Simulation-Transactions of the Society for Modeling and Simulation International* **79:** 726-739

Covert MW, Leung TH, Gaston JE, Baltimore D (2005) Achieving stability of lipopolysaccharide-induced NF-kappaB activation. *Science* **309:** 1854-1857

De Nardo D, De Nardo CM, Nguyen T, Hamilton JA, Scholz GM (2009) Signaling crosstalk during sequential TLR4 and TLR9 activation amplifies the inflammatory response of mouse macrophages. *J Immunol* **183:** 8110-8118

Doyle S, Vaidya S, O'Connell R, Dadgostar H, Dempsey P, Wu T, Rao G, Sun R, Haberland M, Modlin R, Cheng G (2002) IRF3 mediates a TLR3/TLR4-specific antiviral gene program. *Immunity* **17:** 251-263

Fu Y, Glaros T, Zhu M, Wang P, Wu Z, Tyson JJ, Li L, Xing J (2012a) Network topologies and dynamics leading to endotoxin tolerance and priming in innate immune cells. *PLoS Comput Biol* **8:** e1002526

Fu Y, Jiang X, Zhang H, Xing J (2012b) A strategy to study pathway cross-talks of cells under repetitive exposure to stimuli. *BMC Syst Biol* **6 Suppl 3:** S6

Gubler U, Chua AO, Hoffman BJ, Collier KJ, Eng J (1984) Cloned cDNA to cholecystokinin mRNA predicts an identical preprocholecystokinin in pig brain and gut. *Proc Natl Acad Sci U S A* **81:** 4307-4310

Gutierrez J, St Laurent G, 3rd, Urcuqui-Inchima S (2010) Propagation of kinetic uncertainties through a canonical topology of the TLR4 signaling network in different regions of biochemical reaction space. *Theor Biol Med Model* **7:** 7

Hagiescu A, Liu B, Ramanathan R, Palaniappan SK, Cui Z, Chattopadhyay B, Thiagarajan PS, Wong WF (2013) GPU code generation for ODE-based applications with phased shared-data access patterns. *ACM T Archit Code Op* **10:** 5501-5519

Hart Y, Alon U (2013) The utility of paradoxical components in biological circuits. *Mol Cell* **49:** 213-221

Helmy M, Gohda J, Inoue J, Tomita M, Tsuchiya M, Selvarajoo K (2009) Predicting novel features of toll-like receptor 3 signaling in macrophages. *PLoS One* **4:** e4661

Hindmarsh AC, Brown PN, Grant KE, Lee SL, Serban R, Shumaker DE, Woodward CS (2005) SUNDIALS: Suite of nonlinear and differential/algebraic equation solvers. *Acm Transactions on Mathematical Software* **31:** 363-396

Hoffmann A, Levchenko A, Scott ML, Baltimore D (2002) The IkappaB-NF-kappaB signaling module: temporal control and selective gene activation. *Science* **298:** 1241-1245

Kawai T, Akira S (2010) The role of pattern-recognition receptors in innate immunity: update on Toll-like receptors. *Nat Immunol* **11:** 373-384

Kawai T, Akira S (2011) Toll-like receptors and their crosstalk with other innate receptors in infection and immunity. *Immunity* **34:** 637-650

Kim D, Kwon YK, Cho KH (2008) The biphasic behavior of incoherent feed-forward loops in biomolecular regulatory networks. *Bioessays* **30:** 1204-1211

Krummen M, Balkow S, Shen L, Heinz S, Loquai C, Probst HC, Grabbe S (2010) Release of IL-12 by dendritic cells activated by TLR ligation is dependent on MyD88 signaling, whereas TRIF signaling is indispensable for TLR synergy. *J Leukoc Biol* **88:** 189-199

Kuttykrishnan S, Sabina J, Langton LL, Johnston M, Brent MR (2010) A quantitative model of glucose signaling in yeast reveals an incoherent feed forward loop leading to a specific, transient pulse of transcription. *Proc Natl Acad Sci U S A* **107:** 16743-16748

Li F, Thiele I, Jamshidi N, Palsson BO (2009) Identification of potential pathway mediation targets in Toll-like receptor signaling. *PLoS Comput Biol* **5:** e1000292

Li S, Wang L, Berman M, Kong YY, Dorf ME (2011) Mapping a dynamic innate immunity protein interaction network regulating type I interferon production. *Immunity* **35:** 426-440

Lipniacki T, Paszek P, Brasier AR, Luxon B, Kimmel M (2004) Mathematical model of NF-kappaB regulatory module. *J Theor Biol* **228:** 195-215

Litvak V, Ramsey SA, Rust AG, Zak DE, Kennedy KA, Lampano AE, Nykter M, Shmulevich I, Aderem A (2009) Function of C/EBPdelta in a regulatory circuit that discriminates between transient and persistent TLR4-induced signals. *Nat Immunol* **10:** 437-443

Liu B, Hagiescu A, Palaniappan SK, Chattopadhyay B, Cui Z, Wong WF, Thiagarajan PS (2012) Approximate probabilistic analysis of biopathway dynamics. *Bioinformatics* **28:** 1508-1516

Liu B, Thiagarajan PS (2012) Modeling and analysis of biopathways dynamics. *J Bioinform Comput Biol* **10:** 1231001

Liu B, Zhang J, Tan PY, Hsu D, Blom AM, Leong B, Sethi S, Ho B, Ding JL, Thiagarajan PS (2011) A computational and experimental study of the regulatory mechanisms of the complement system. *PLoS Comput Biol* **7:** e1001059

Liu Q, Yong Z, Wai KY, Newman SKS, Nguan ST, Ding JL (2015) Synchronization of IRF1, JunB and C/EBPβ activities during TLR3-TLR7 crosstalk orchestrates timely cytokine synergy in proinflammatory response. *under review*

Longo DM, Selimkhanov J, Kearns JD, Hasty J, Hoffmann A, Tsimring LS (2013) Dual delayed feedback provides sensitivity and robustness to the NF-kappaB signaling module. *PLoS Comput Biol* **9:** e1003112

Makela SM, Strengell M, Pietila TE, Osterlund P, Julkunen I (2009) Multiple signaling pathways contribute to synergistic TLR ligand-dependent cytokine gene expression in human monocyte-derived macrophages and dendritic cells. *J Leukoc Biol* **85:** 664-672

Milo R, Shen-Orr S, Itzkovitz S, Kashtan N, Chklovskii D, Alon U (2002) Network motifs: simple building blocks of complex networks. *Science* **298:** 824-827

Murray PJ (2006) Understanding and exploiting the endogenous interleukin-10/STAT3-mediated anti-inflammatory response. *Curr Opin Pharmacol* **6:** 379-386

Napolitani G, Rinaldi A, Bertoni F, Sallusto F, Lanzavecchia A (2005) Selected Toll-like receptor agonist combinations synergistically trigger a T helper type 1-polarizing program in dendritic cells. *Nat Immunol* **6:** 769-776

Newton K, Dixit VM (2012) Signaling in innate immunity and inflammation. *Cold Spring Harb Perspect Biol* **4**

O'Dea EL, Barken D, Peralta RQ, Tran KT, Werner SL, Kearns JD, Levchenko A, Hoffmann A (2007) A homeostatic model of IkappaB metabolism to control constitutive NF-kappaB activity. *Mol Syst Biol* **3:** 111

Oda K, Kitano H (2006) A comprehensive map of the toll-like receptor signaling network. *Mol Syst Biol* **2:** 2006 0015

Oeckinghaus A, Hayden MS, Ghosh S (2011) Crosstalk in NF-kappaB signaling pathways. *Nat Immunol* **12:** 695-708

Palaniappan S, Gyori B, Liu B, Hsu D, Thiagarajan PS (2013) Statistical model checking based calibration and analysis of bio-pathway models. *Let Notes Comput Sc* **8130:** 120-134

Pattison MJ, Mackenzie KF, Arthur JS (2012) Inhibition of JAKs in macrophages increases lipopolysaccharide-induced cytokine production by blocking IL-10-mediated feedback. *J Immunol* **189:** 2784-2792

Platanias LC (2005) Mechanisms of type-I- and type-II-interferon-mediated signalling. *Nat Rev Immunol* **5:** 375-386

Purvis JE, Lahav G (2013) Encoding and decoding cellular information through signaling dynamics. *Cell* **152:** 945-956

Runarsson TP, Yao X (2000) Stochastic ranking for constrained evolutionary optimization. *IEEE T Evolut Comput* **4:** 284-294

Selvarajoo K, Takada Y, Gohda J, Helmy M, Akira S, Tomita M, Tsuchiya M, Inoue J, Matsuo K (2008) Signaling flux redistribution at toll-like receptor pathway junctions. *PLoS One* **3:** e3430

Shih VF, Kearns JD, Basak S, Savinova OV, Ghosh G, Hoffmann A (2009) Kinetic control of negative feedback regulators of NF-kappaB/RelA determines their pathogen- and cytokine-receptor signaling specificity. *Proc Natl Acad Sci U S A* **106:** 9619-9624

Shinohara H, Behar M, Inoue K, Hiroshima M, Yasuda T, Nagashima T, Kimura S, Sanjo H, Maeda S, Yumoto N, Ki S, Akira S, Sako Y, Hoffmann A, Kurosaki T, Okada-Hatakeyama M (2014) Positive feedback within a kinase signaling complex functions as a switch mechanism for NF-kappaB activation. *Science* **344:** 760-764

Shnyra A, Brewington R, Alipio A, Amura C, Morrison DC (1998) Reprogramming of lipopolysaccharide-primed macrophages is controlled by a counterbalanced production of IL-10 and IL-12. *J Immunol* **160:** 3729-3736

Takahashi K, Asabe S, Wieland S, Garaigorta U, Gastaminza P, Isogawa M, Chisari FV (2010) Plasmacytoid dendritic cells sense hepatitis C virus-infected cells, produce interferon, and inhibit infection. *Proc Natl Acad Sci U S A* **107:** 7431-7436

Takeuchi O, Akira S (2010) Pattern recognition receptors and inflammation. *Cell* **140:** 805-820

Tan RS, Ho B, Leung BP, Ding JL (2014) TLR Cross-talk Confers Specificity to Innate Immunity. *Int Rev Immunol*

Tan RS, Lin B, Liu Q, Tucker-Kellogg L, Ho B, Leung BP, Ding JL (2013) The synergy in cytokine production through MyD88-TRIF pathways is co-ordinated with ERK phosphorylation in macrophages. *Immunol Cell Biol* **91:** 377-387

Tay S, Hughey JJ, Lee TK, Lipniacki T, Quake SR, Covert MW (2010) Single-cell NF-kappaB dynamics reveal digital activation and analogue information processing. *Nature* **466:** 267-271

Vandenbon A, Teraguchi S, Akira S, Takeda K, Standley DM (2012) Systems biology approaches to toll-like receptor signaling. *Wiley Interdiscip Rev Syst Biol Med* **4:** 497-507

Werner SL, Barken D, Hoffmann A (2005) Stimulus specificity of gene expression programs determined by temporal control of IKK activity. *Science* **309:** 1857-1861

Yang CH, Murti A, Pfeffer LM (2005) Interferon induces NF-kappa B-inducing kinase/tumor necrosis factor receptor-associated factor-dependent NF-kappa B activation to promote cell survival. *J Biol Chem* **280:** 31530-31536

Yang CH, Murti A, Pfeffer SR, Kim JG, Donner DB, Pfeffer LM (2001) Interferon alpha /beta promotes cell survival by activating nuclear factor kappa B through phosphatidylinositol 3-kinase and Akt. *J Biol Chem* **276:** 13756-13761

Younes HLS, Kwiatkowska M, Norman G, Parker D (2004) Numerical vs. statistical probabilistic model checking: An empirical study. *Tools and Algorithms for the Construction and Analysis of Systems, Proceedings* **2988:** 46-60

Zhou L, Nazarian AA, Xu J, Tantin D, Corcoran LM, Smale ST (2007) An inducible enhancer required for Il12b promoter activity in an insulated chromatin environment. *Mol Cell Biol* **27:** 2698-2712

Zhu Q, Egelston C, Vivekanandhan A, Uematsu S, Akira S, Klinman DM, Belyakov IM, Berzofsky JA (2008) Toll-like receptor ligands synergize through distinct dendritic cell pathways to induce T cell responses: implications for vaccines. *Proc Natl Acad Sci U S A* **105:** 16260-16265

Figure Legends

Figure 1. Characterization of *Il6* and *Il12b* expression profiles after TLR3 and TLR7 co-activation. A. Experimental design. Bone marrow-derived macrophages (BMDMs) were treated with 1st PAMP for 0, 8, 24 h followed by 2nd PAMP for 4, 8, 16, 24 h. The control for the combinatorial stimulation is the single PAMP stimulation. Taking I_8R_{16} as an example, the single control for it are poly (I:C) stimulation for 8 h or R848 stimulation for 16 h. **B.** *Il6* and *Il12b* mRNA levels detected by real-time (RT)-PCR, under different treatment protocols. BMDMs were treated with 10 μg/ml poly(I:C) followed by 25 ng/ml R848 (*left*), or with R848 followed by poly(I:C) (*middle*), or single stimulation for 4, 8, 12, 16, 24, 28, 32, 40, 48 h as control (*right*; NT stands for no treatment). Time intervals between poly(I:C) and R848 treatments were 0 (■), 8 (×), 24 (Δ) h. Results are normalized with respect to hypoxanthine guanine phosphoribosyl transferase (*Hprt*). Solid *red* curves refer to combinatorial stimulation, dashed *blue* curves indicate additive control for combinatorial stimulation as described in **A**. Data are representative of three independent experiments. **C.** *Il6* and *Il12b* mRNA levels for BMDMs treated with 10 μg/ml poly(I:C) for 0, 4, 8, 12, 16, 24 h followed by 25 ng/ml R848 stimulation for 8 h. Data are presented as means ± SEM of three individual experiments.

Figure 2. Schematic representation of TLR3 and TLR7 signaling network of interactions. TLR3 recognizes dsRNA (and analogues such as poly(I:C)) derived from viruses or virus-infected cells and induces antiviral immune response by promoting the expression of type I IFNs and inflammatory cytokines (e.g. IL-6 and IL-12p40), via the TRIF-dependent pathway. TLR7 recognizes ssRNA (and analogues such as R848) and induces the production of type I IFNs and cytokines via the MyD88-dependent pathway. IRF3 and IRF7 activated by TLR3 and TLR7 pathways respectively lead to the production of type I IFNs. NF-κB and AP-1 activated by both pathways lead to the production of inflammatory cytokines. The detailed reaction schema is shown in **Figure S1**..

Figure 3. Model predictions and experimental validation. A. Experimental and simulated protein dynamics of the TLR3-TLR7 pathway. The time profiles of activated ERK, p38, JNK, and IkBα under the following four conditions were simulated using estimated parameters and compared against the experimental data: R848 single stimulation, poly(I:C) single stimulation, poly(I:C) and R848 combinatorial stimulation with 0 h time interval, poly(I:C) and R848 combinatorial stimulation with 8 h time interval. *Blue curves* depict the model simulation results and *red dots* display experimental data. **B**. Model predictions and experimental validation of the synergistic cytokine production. The simulated time profiles of *Il6* and *Il12b* expression levels under various conditions (*right* panels) reconcile the observed (*left* panel) time-dependent synergistic effect induced by the combinatorial TLR3-TLR7 activation. On the *left panels*, the experimental data are connected by lines to guide the eye.

Figure 4. Sensitivity analysis. A. Local sensitivities (control coefficients) of the initial protein concentrations (listed along the ordinate) to the integrated response of the *Il12b* production under **R**, **I**, **IR**, $\mathbf{I_8R}$ and $\mathbf{I_{24}R}$ conditions. The heat map is color-coded from *red* (high positive sensitivity) to *blue* (high negative sensitivity). The former group refers to compounds whose *increase* in initial concentration would enhance cytokine production, and the latter to those whose *decrease* in initial concentration might enhance cytokine production. Components whose initial concentrations have little or no effect on the system dynamics are shown in *light colors* or *white*. **B.** Global sensitivities calculated according to the SMC-MPSA method. Sensitive parameters (that strongly influence the observed behavior) are shown by the peaks, colored *dark blue*. Robust parameters (the variations of

which have little effect of the model dynamics) are colored *purple*. The highest peaks refer to *Il6* and *Il12b* transcription or degradation rate constants. **C.** Functional classification of 33 kinetic parameters that led to the highest sensitivity peaks (above the *dotted* threshold line in panel **B**). The corresponding reactions are indicated by *red arrows* in **Figure S1**.

Figure 5. Dependency of the immune response on the time interval Δt between the two stimuli. **A**. Predicted time evolutions of the *Il6* and *Il12b* mRNA expression levels in response to various combinatorial stimulations with a time interval Δt (between the first (**I**) and second (**R**) stimulus) varying from 0 h to 48 h. The series of dotted curves represent results for successive Δt values, the ordinate referring to the time elapsed with respect to the application of the first stimulus. Highest cytokine production occurs when the time interval between the two stimuli is $\Delta t \approx 7$ h. The results for $\Delta t = 0$ (*blue*), 8 h (*magenta*), and 24 h (*dark green*) are shown by the *thick colored* curves. **B**. Peak amplitude and peak time derived from curves in (**A**). **C**. Predicted expression profiles for type I IFN produced in response to the combinatorial I→R (*left* panel) or R→I (*right* panel) stimuli with Δt ranging from 0 h to 48 h.

Figure 6. Effect of JNK, ERK and p38 inhibition on cytokine production. A-C Time evolution of *Il12b* mRNA (*left*) and *Il6* mRNA (*right*) levels in the absence of JNK (**A**), ERK (**B**) and p38 (**C**) activation. The series of curves refer to different time intervals between the two stimuli (similar to **Figure 5A**). JNK and ERK have opposite effects, i.e. upregulation and downregulation of cytokines, as can be seen from the comparison of the computationally predicted curves for $\Delta t = 0$, 8 and 24 (*colored, thick*) with those deduced from control simulations (*thick, gray curves*). The inhibition of p38 has relatively small effects, if any, on cytokine production. **D**. Experimental verification of computational predictions. BMDMs were treated with 10μM MAPK inhibitors for 50 min followed by **IR, I_8R** or **$I_{24}R$** stimulation. After 8 h of R848 stimulation, *Il6* and *Il12b* mRNA were then measured with RT-PCR normalized with *Hprt*. Data are presented as mean values and SEMs obtained from three independent experiments.

Figure 7. Knockout simulations highlight the significance of JAK-STAT pathway in triggering synergistic cytokine production. Simulation profiles of *Il12b* mRNA (**A**) in the absence of Akt activation reaction, **(B)** without crosstalk mechanism induced by IRF3, (**C)** in the absence of NIK activation, and (**D)** in the absence of STAT1-STAT2 activation.

Figure 8. *In silico* and empirical knockdown of STAT1 revealed a complex regulatory role of an incoherent feedforward loop. A. A STAT1-mediated incoherent type 1 feedforward loop. **B.** Simulated STAT1 initial concentration-cytokine production response curves under IR, I_8R, and $I_{24}R$ conditions. **C.** Knockdown efficiency of *Stat1*. J774 cells were transfected with either anti-*Stat1* siRNA or control scramble siRNA for 24. Cell lysates were collected for Western analysis. Data are representative of two independent experiments. **D.** *Stat1* knockdown enhanced cytokine production. 24 h after either anti-*Stat1* siRNA or control siRNA transfection, cells were stimulated with IR, I_8R, $I_{24}R$ for 8 h. Then expression of *Il6* and *Il12b* mRNAs were analyzed by real-time PCR. Data are presented as means ± SEM of three individual experiments.

Fig. 1

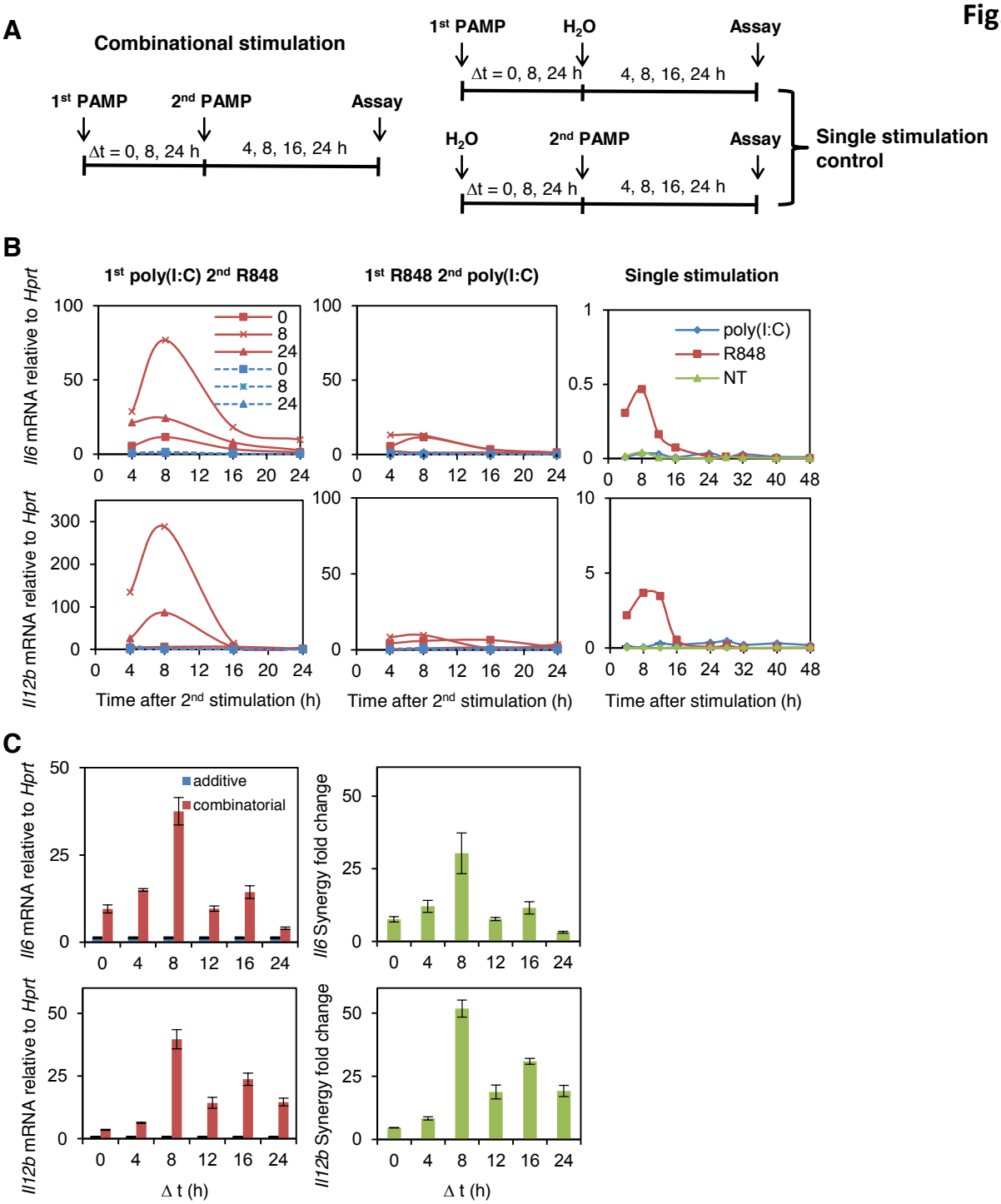
A
Combinational stimulation
1st PAMP
2nd PAMP
Assay
Δt = 0, 8, 24 h
4, 8, 16, 24 h
1st PAMP
H2O
Assay
Δt = 0, 8, 24 h
4, 8, 16, 24 h
H2O
2nd PAMP
Assay
Δt = 0, 8, 24 h
4, 8, 16, 24 h
Single stimulation control
B
1st poly(I:C) 2nd R848
1st R848 2nd poly(I:C)
Single stimulation
Il6 mRNA relative to Hprt
Il12b mRNA relative to Hprt
0
8
24
0
8
24
poly(I:C)
R848
NT
Time after 2nd stimulation (h)
Time after 2nd stimulation (h)
Time after stimulation (h)
C
additive
combinatorial
Il6 mRNA relative to Hprt
Il12b mRNA relative to Hprt
Il6 Synergy fold change
Il12b Synergy fold change
Δ t (h)
Δ t (h)

Fig. 2

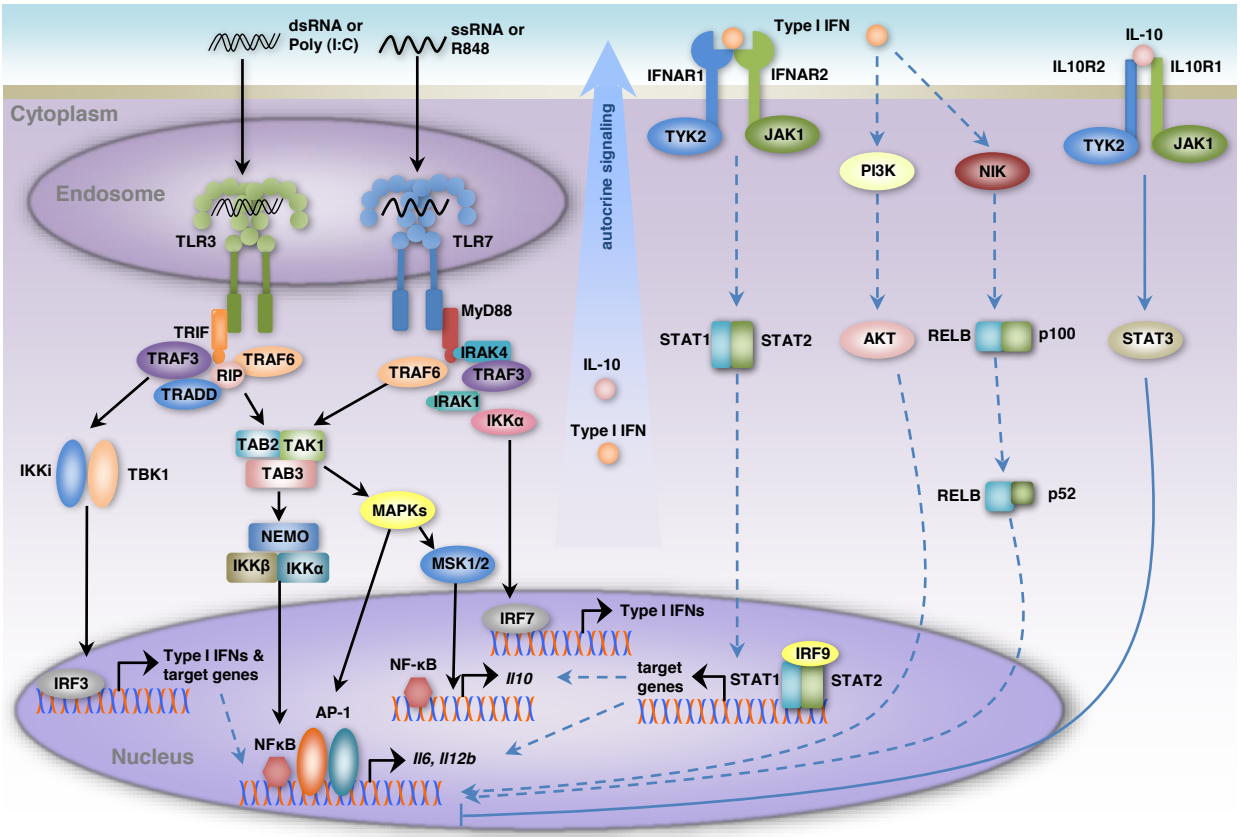
dsRNA or Poly (I:C)
ssRNA or R848
Cytoplasm
Endosome
TLR3
TLR7
TRIF
TRAF3
TRAF6
RIP
TRADD
MyD88
IRAK4
TRAF6
TRAF3
IRAK1
IKKα
TAB2
TAK1
TAB3
IKKi
TBK1
MAPKs
NEMO
IKKβ
IKKα
MSK1/2
IRF3
Type I IFNs & target genes
AP-1
NF-κB
Il10
NFκB
Il6, Il12b
Nucleus
IRF7
Type I IFNs
target genes
IRF9
STAT1
STAT2
autocrine signaling
IL-10
Type I IFN
IFNAR1
IFNAR2
TYK2
JAK1
PI3K
AKT
NIK
RELB
p100
p52
IL10R2
IL10R1
STAT3

Fig. 3

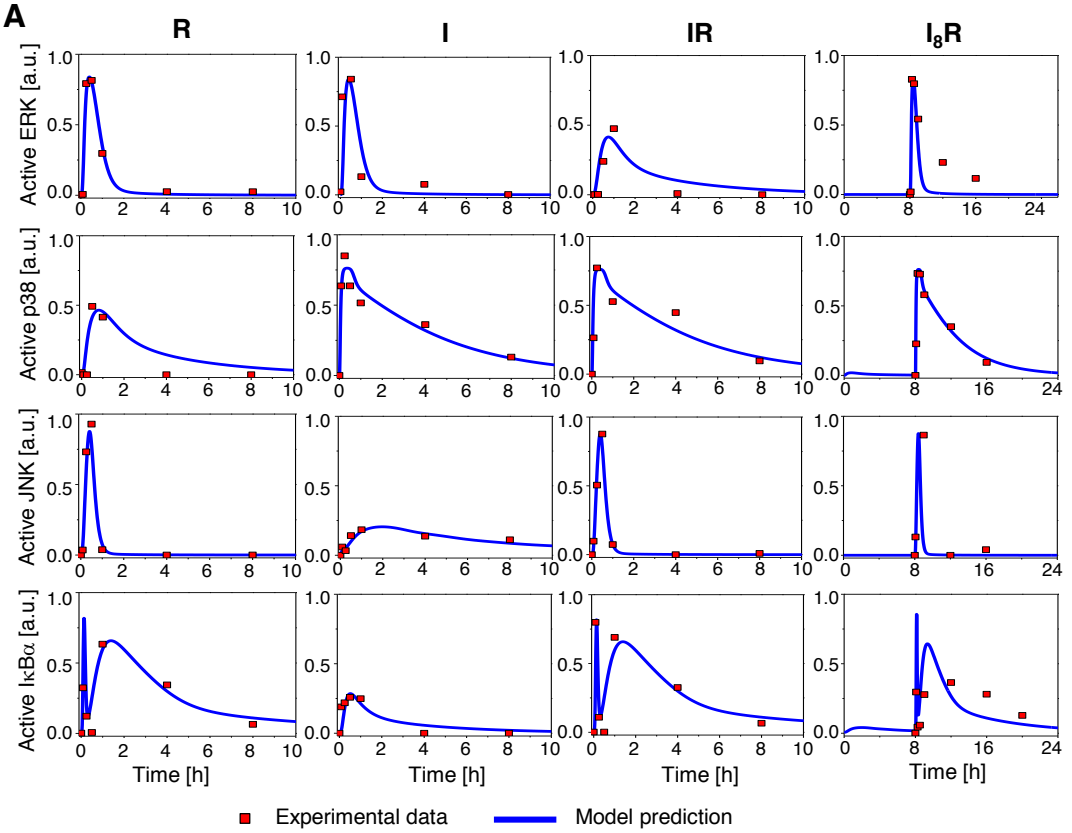
A
R
I
IR
I8R
Active ERK [a.u.]
Active p38 [a.u.]
Active JNK [a.u.]
Active IκBα [a.u.]
Time [h]
Experimental data
Model prediction

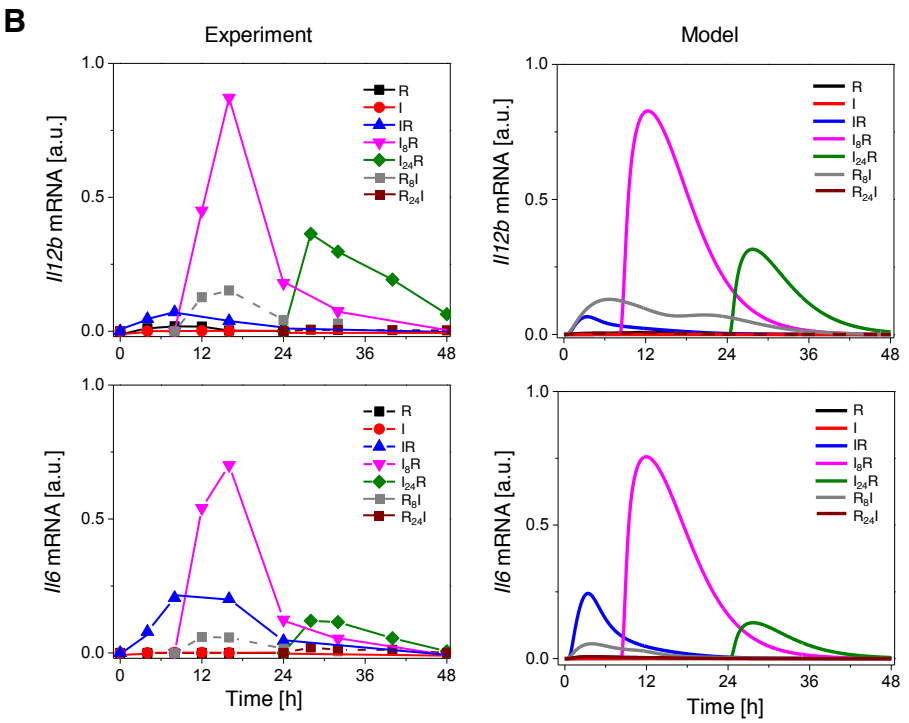
B
Experiment
Model
Il12b mRNA [a.u.]
Il6 mRNA [a.u.]
Time [h]
R
I
IR
I8R
I24R
R8I
R24I

A

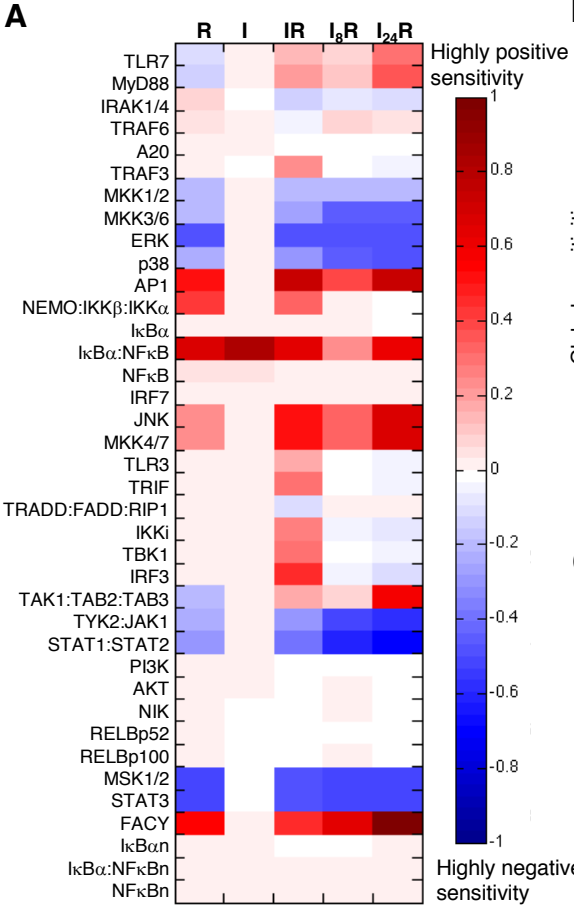

B

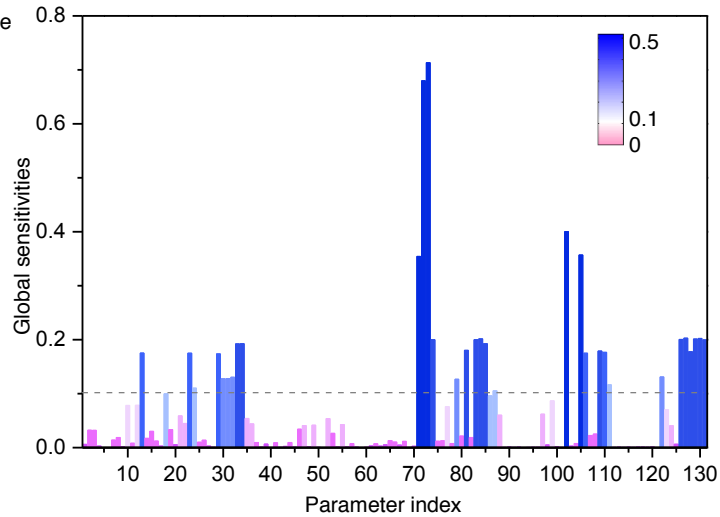

C

Sensitive kinetic parameters	Functional group
k_{71}, k_{72}, k_{73}, k_{74}, k_{102}, k_{105}	*Il6*/*Il12b* transcription/degradation
k_{83}, k_{84}, k_{85}, k_{87}, k_{111}, k_{128}	JAK-STAT1/2 signaling cascade
k_{122}, k_{126}, k_{127}, k_{129}, k_{130}, k_{131}	IL-10-STAT3 signaling cascade
k_{81}, k_{106}, k_{109}, k_{110}	Type I IFN transcription/degradation
k_{31}, k_{30}, k_{31}, k_{32}, k_{33}, k_{34}, k_{79}	JNK signaling cascade
k_{13}, k_{23}	p38 signaling cascade
k_{18}, k_{24}	ERK signaling cascade

Fig. 5

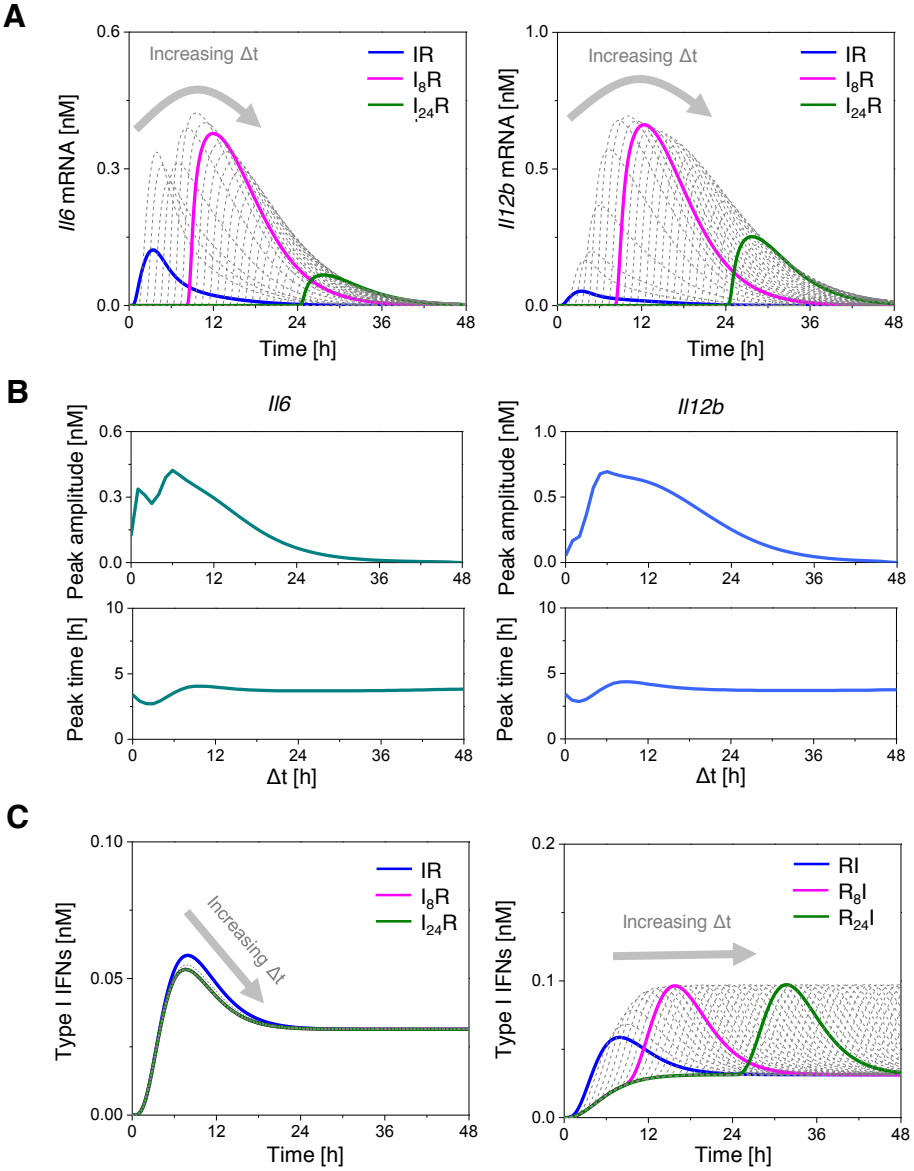
A
Increasing Δt
IR
I8R
I24R
Il6 mRNA [nM]
Il12b mRNA [nM]
Time [h]
B
Il6
Il12b
Peak amplitude [nM]
Peak time [h]
Δt [h]
C
Type I IFNs [nM]
RI
R8I
R24I
Time [h]

Fig. 6

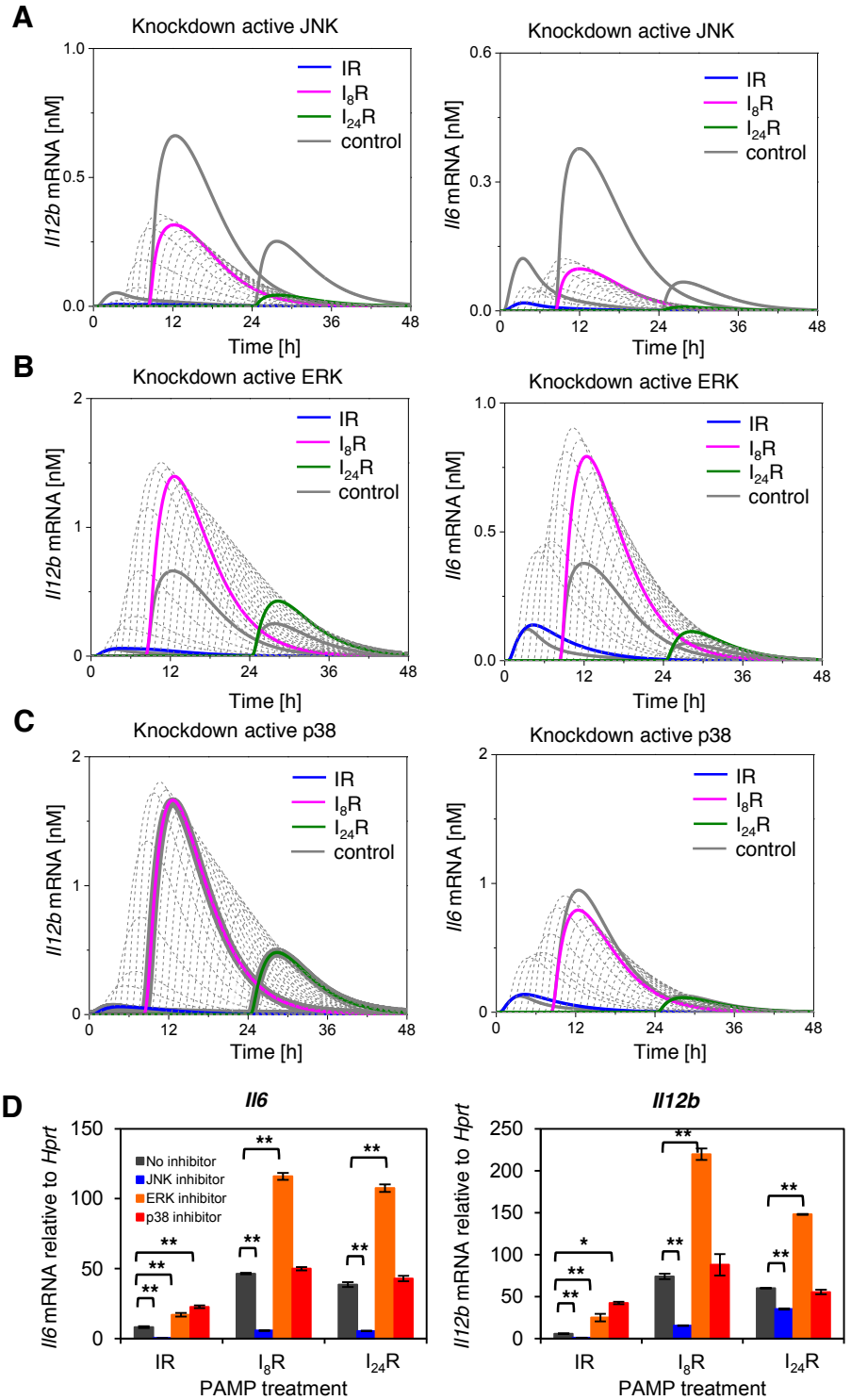
A
Knockdown active JNK
Il12b mRNA [nM]
Time [h]
IR
I8R
I24R
control
Knockdown active JNK
Il6 mRNA [nM]
Time [h]
B
Knockdown active ERK
Il12b mRNA [nM]
Time [h]
Knockdown active ERK
Il6 mRNA [nM]
Time [h]
C
Knockdown active p38
Il12b mRNA [nM]
Time [h]
Knockdown active p38
Il6 mRNA [nM]
Time [h]
D
Il6
Il6 mRNA relative to Hprt
No inhibitor
JNK inhibitor
ERK inhibitor
p38 inhibitor
PAMP treatment
Il12b
Il12b mRNA relative to Hprt
PAMP treatment

Fig. 7

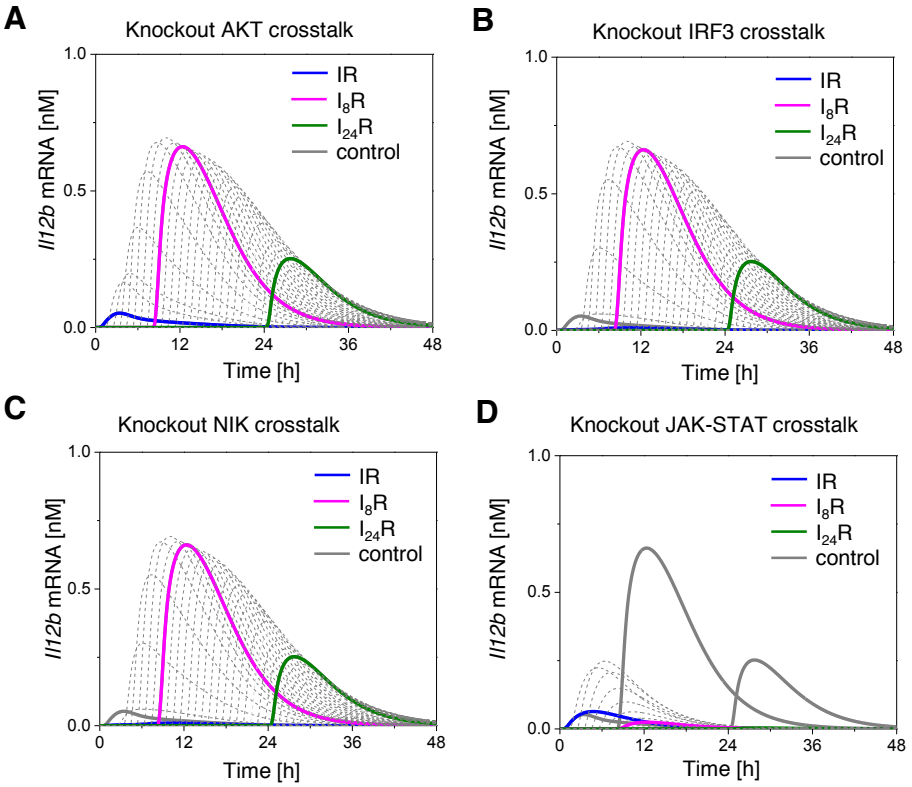
A
Knockout AKT crosstalk
B
Knockout IRF3 crosstalk
C
Knockout NIK crosstalk
D
Knockout JAK-STAT crosstalk
Il12b mRNA [nM]
Time [h]
IR
I8R
I24R
control
0.0
0.5
1.0
0
12
24
36
48

Fig. 8

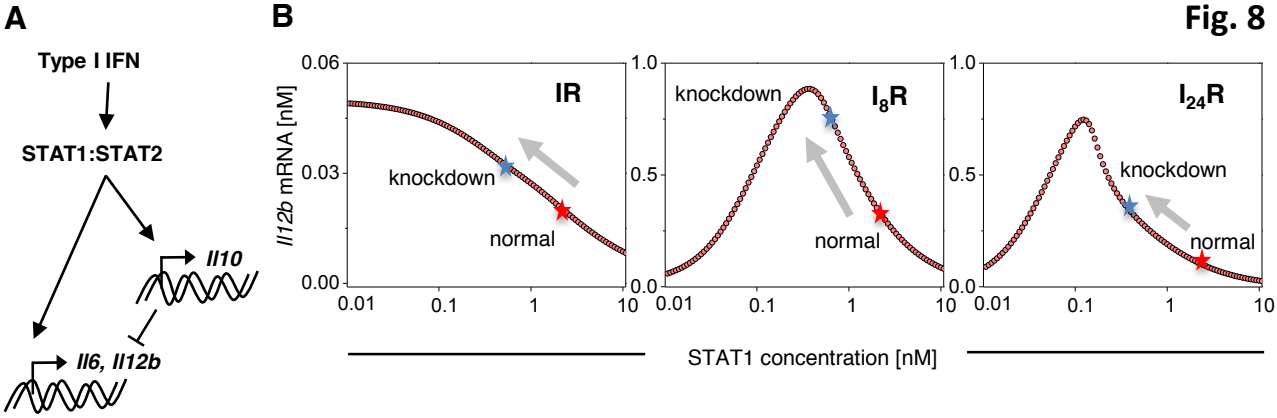
A
Type I IFN
STAT1:STAT2
Il10
Il6, Il12b
B
Il12b mRNA [nM]
IR
knockdown
normal
I8R
I24R
STAT1 concentration [nM]

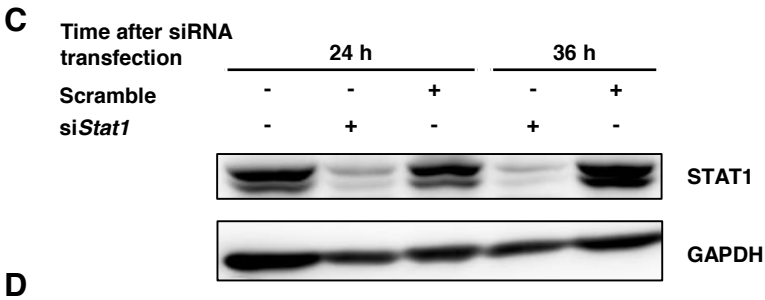
C
Time after siRNA transfection
24 h
36 h
Scramble
siStat1
STAT1
GAPDH

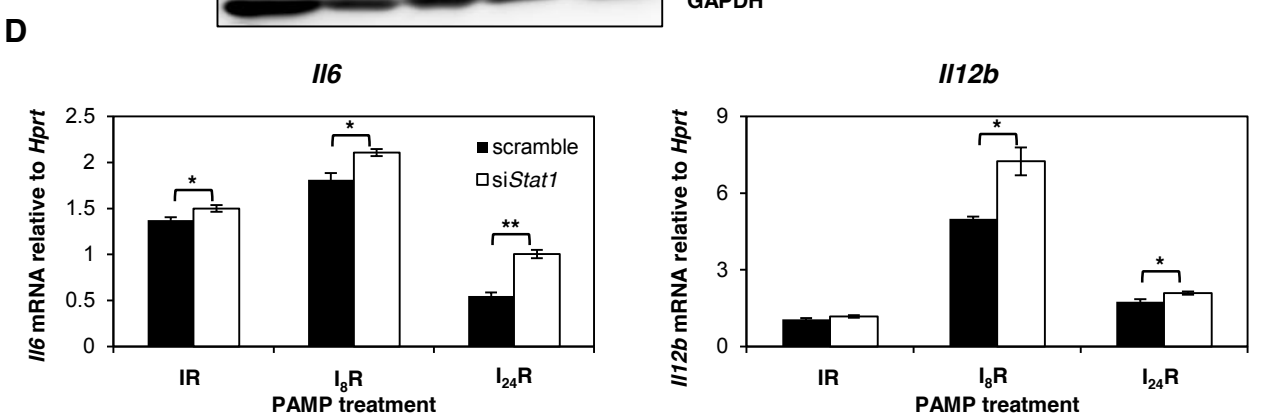
D
Il6
Il12b
Il6 mRNA relative to Hprt
Il12b mRNA relative to Hprt
scramble
siStat1
IR
I8R
I24R
PAMP treatment

Supplementary Information

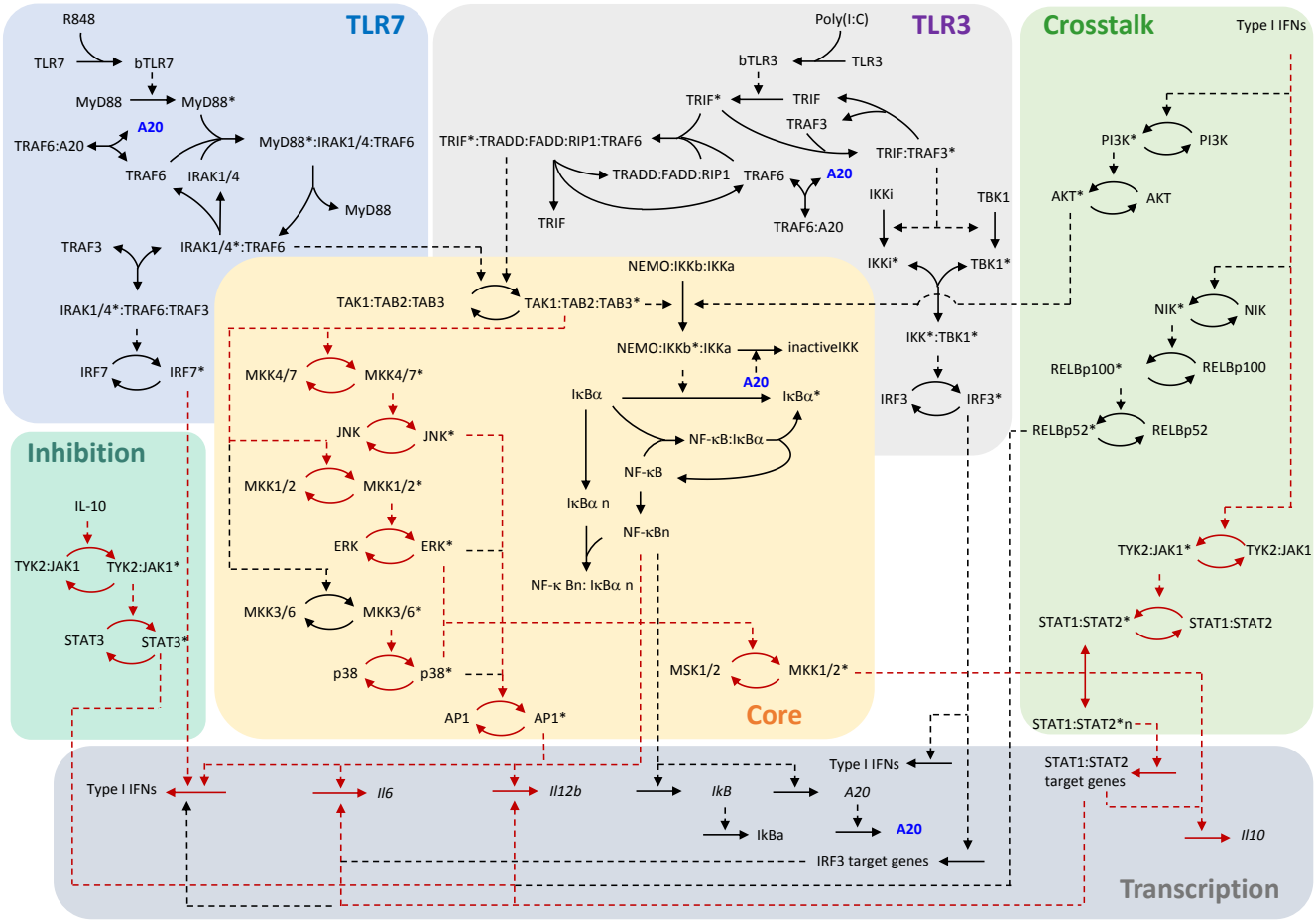

Figure S1: Reaction schema for the same signaling network organized by different modules, designated as TLR7-, TLR3-, and core-interactions, inhibition and transcription events, and TLR3-TLR7 cross-talk. Complexes are denoted by the names of their components, separated by a ":". Single-headed solid arrows designate irreversible reactions and double-headed arrows, reversible reactions. Dotted arrows represent enzymatic reactions. The corresponding kinetic equations are presented in the supplementary information. The reactions with high global sensitivities, identified from sensitivity analysis, are labeled in *red*.

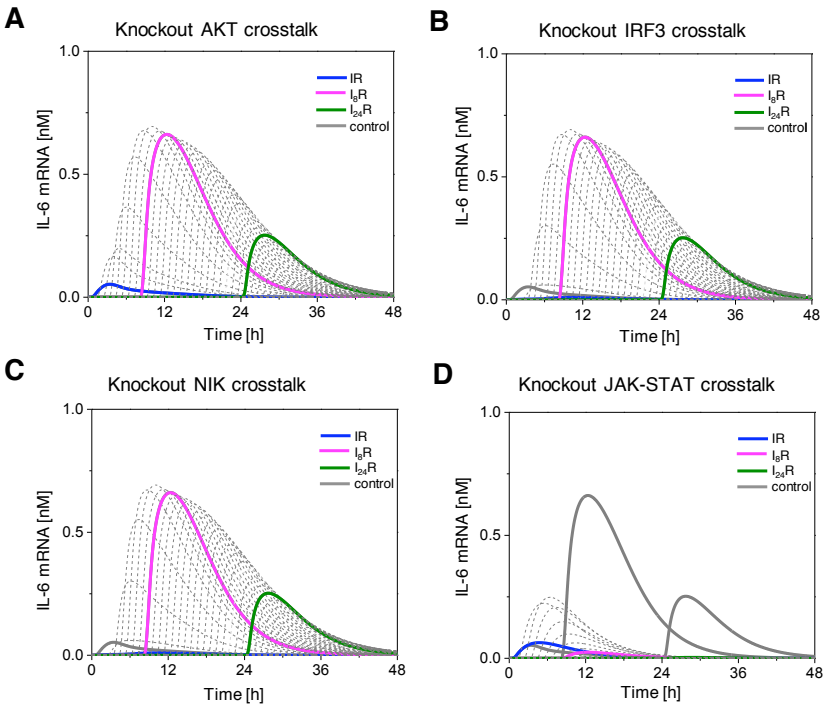

Figure S2: Knockdown simulation results (the counterpart of these data for *Il12b* mRNA is presented in **Figure 7**). A. Simulation profiles of *Il6* mRNA without AKT activation reaction. B. Simulation profiles of *Il6* mRNA without crosstalk mechanism induced by IRF3. C. Simulation profiles of *Il6* mRNA without NIK activation reaction. D. Simulation profiles of *Il6* mRNA without STAT1-STAT2 activation reaction.

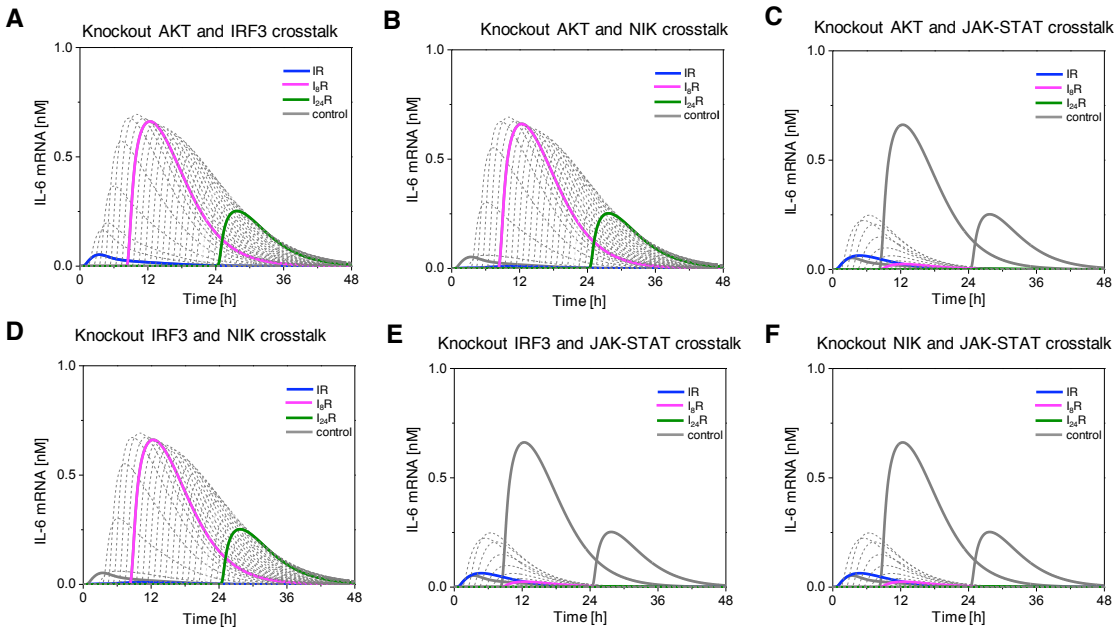

Figure S3: Combinational knockdown simulation results. A. Simulation profiles of *IL6* mRNA without AKT activation reaction and crosstalk mechanism induced by IRF3. B. Simulation profiles of *IL6* mRNA without AKT activation reaction and NIK activation reaction. C. Simulation profiles of *IL6* mRNA without AKT activation reaction and STAT1-STAT2 activation reaction. D. Simulation profiles of *IL6* mRNA without crosstalk mechanism induced by IRF3 and NIK activation reaction. E. Simulation profiles of *IL6* mRNA without crosstalk mechanism induced by IRF3 and STAT1-STAT2 activation reaction. F. Simulation profiles of *IL6* mRNA without STAT1-STAT2 activation reaction and NIK activation reaction.

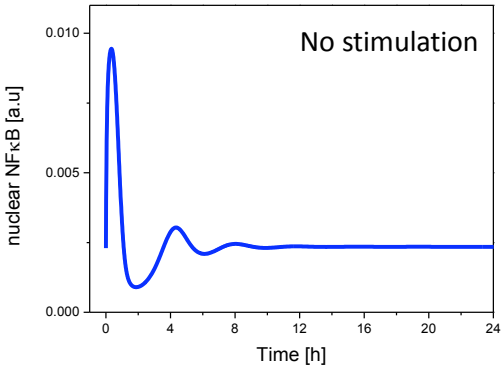

Figure S4: Nuclear NFκB profile under no-stimulation condition.

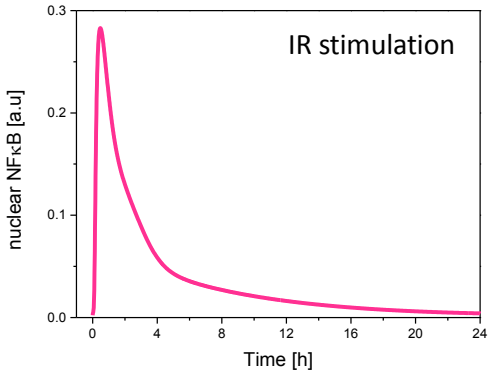

Figure S5: Nuclear NFκB profile under IR-stimulation condition.

Text S1: Incoherent Type 1 Feed-Forward Loop (I1-FFL)

Feed-forward loop (FFL) is one of the most common network motifs in biomolecular regulatory networks [9, 1]. For instance, transcription factor X regulates transcription factor Y, and both X and Y regulate target gene Z. Thus, the X, Y and Z form a FFL. Since each of the three transcriptional interactions in a FFL can be either positive (activation) or negative (inhibition), there are eight possible combinations of positive or negative interactions, which have been named as coherent/incoherent type 1-4 FFLs (see below). The abundance and functionality of different FFLs have been studied and discussed in [7]. Of particular interest in our context is the inherent type 1 FFL (I1-FFL), a circuit in which X activates Z and Y, and Y inhibit Z. It has been reviewed in [4] that the roles of I1-FFL include: (i) shortening of gene-circuit response time [8], (ii) generation of gene expression pulses [2], (iii) distinguishing time-varying inputs, (iv) filtering out noise [10], (v) detecting fold change of input signal [3], and (vi) generating nonmonotonic input-output relations [5]. The behavior resulted from (vi) is also called *biphasic response*, which can be time-dependent: as time evolves the output response initially increases but subsequently decreases, even if the input is sustained; or dose-dependent: over a certain range of input dose, the output response increases but subsequent decreases. It has been shown that the parameters inducing biphasic responses are highly limited [6]. In the signaling network studied in this work, we showed that the I1-FFLs mediated by STAT1 induces a dose-dependent biphasic response, which is crucial to both amplifying antiviral response and avoiding excessive inflammatory response.

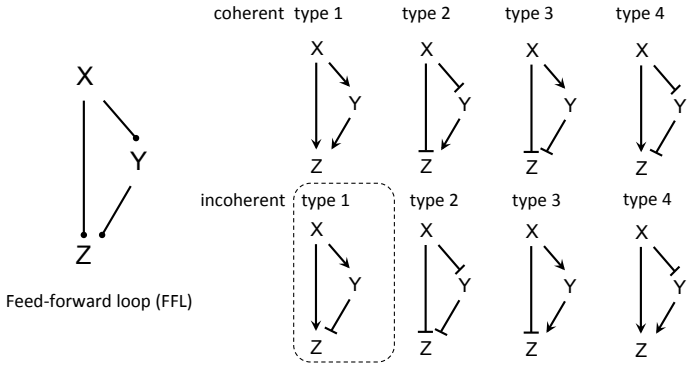

Table S1: List of species and their initial concentrations[1]

Name	**Initial State (nM)**	**Description**
TLR7	0.53 ± 0.027	Toll-like receptor 7
MyD88	0.87 ± 0.044	Myeloid differentiation primary response 88
IRAK1/4	0.13 ± 0.0064	Interleukin-1 receptor-associated kinase 1/4
TRAF6	1.0 ± 0.05	TNF receptor-associated factor 6
A20	0.0048 ± 0.00024	Zinc finger protein A20
TRAF3	0.2 ± 0.01	TNF receptor-associated factor 3
Mkk1/2	0.99 ± 0.05	Mitogen-activated protein kinase kinase 1/2
Mkk3/6	0.00018 ± 8.86e-06	Mitogen-activated protein kinase kinase 3/6
ERK	0.076 ± 0.0038	Extracellular signal-regulated kinase
p38	0.46 ± 0.023	p38 mitogen-activated protein kinase
AP1	0.2 ± 0.01	AP-1 transcription factor
NEMO:IKKb:IKKa	0.2 ± 0.01	A complex of NF-kappa-B essential modulator, inhibitor of nuclear factor kappa-B kinase subunit beta, and inhibitor of nuclear factor kappa-B kinase subunit alpha
IκBα	0.0025 ± 0.00013	Nuclear factor of kappa light polypeptide gene enhancer in B-cells inhibitor, alpha
NFκB	0.003 ± 0.00015	Nuclear factor kappa-light-chain-enhancer of activated B cells
IκBα:NFkB	0.06 ± 0.003	A complex of NFkB and IκBα
IRF7	0.2 ± 0.01	Interferon regulatory factor 7
JNK	0.32 ± 0.016	c-Jun N-terminal kinases
Mkk4/7	0.0064 ± 0.00032	Mitogen-activated protein kinase kinase 4/7
TLR3	0.22 ± 0.011	Toll-like receptor 3
TRIF	0.2 ± 0.01	TIR-domain-containing adapter-inducing interferon-beta
TRADD:FADD:RIP1	0.2 ± 0.01	A complex of TNFRSF1A-associated via death domain protien, Fas-Associated protein with death domain protien, and Receptor-interacting serine/threonine-protein kinase 1
IKKi	0.2 ± 0.01	Inhibitor of nuclear factor kappa-B kinase subunit epsilon
TBK1	0.18 ± 0.0088	TANK-binding kinase 1
IRF3	0.18 ± 0.0092	Interferon regulatory factor 3
Tak1:Tab2:Tab3	1.0 ± 0.05	A complex of Transforming growth factor beta activated kinase-1, Tak1 binding protien 2, and Tak1 binding protien 3
Tyk2:Jak1	0.26 ± 0.013	A complex of Tyrosine kinase 2 and Janus kinase 1
Stat1:Stat2	1 ± 0.05	A complex of Signal transducer and activator of transcription 1 and 2
PI3K	0.62 ± 0.031	Phosphoinositide 3-kinase
Akt	0.25 ± 0.012	Protein kinase B
NIK	0.01 ± 0.0005	NF-kappa-B-inducing kinase
RelBp52	0.01 ± 0.0005	NF-kappaB Rel-like domain-containing protein/p52 heterodimer

Continued on next page

Table S1 – continued from previous page

Name	Initial State	Description
RelBp100	0.01 ± 0.0005	NF-kappaB Rel-like domain-containing protein/p100 heterodimer
MSK1/2	1 ± 0.05	Mitogen- and stress-activated protein kinase 1/2
STAT3	10 ± 0.5	Signal transducer and activator of transcription 3
FacY	1 ± 0.05	Stat1:Stat2 target factors (e.g. IRF1)
IκBαn	0.0034 ± 0.00017	nuclear IκBα
IκBα:NFkBn	0.0001 ± 0.000005	nuclear IκBα-NFkB complex
NFκBn	0.0023 ± 0.00012	nuclear NFκB
R848	0.08 ± 0.004	Resiquimod
Poly(I:C)	0.015 ± 0.00074	Polyinosinic:polycytidylic acid
IFN	0 ± 0	Type 1 interferon

[1]Species with prefix "b" denotes its binding form. Species with suffix "*" denotes its activated form. Species with suffix "n" denotes its localization is nucleus.

Table S2: List of parameters and their values.

Parameter	**Value**
k_1	4.31
k_2	62.1
k_3	79.7
k_4	18.3
k_5	0.401
k_6	0.555
k_7	0.455
k_8	10.2
k_9	0.115
k_{10}	49.6
k_{11}	93.7
k_{12}	11.6
k_{13}	83.0
k_{14}	0.001
k_{15}	60
k_{16}	0.15
k_{17}	30
k_{18}	0.066
k_{19}	0.498
k_{20}	0.001
k_{21}	0.0015
k_{22}	0.48
k_{23}	0.337
k_{24}	0.093
k_{25}	0.0325
k_{26}	0.285
k_{27}	0.000000019
k_{28}	0.446
k_{29}	0.05
k_{30}	53.2
k_{31}	64.1
k_{32}	0.85
k_{33}	0.128
k_{34}	0.128

Continued on next page

Table S2 – continued from previous page

Parameter	Value
k_{35}	30
k_{36}	0.024
k_{37}	0.018
k_{38}	0.0012
k_{39}	12
k_{40}	6
k_{41}	0.09
k_{42}	30
k_{43}	0.6
k_{44}	0.085
k_{45}	0.04
k_{46}	0.024
k_{47}	30
k_{48}	0.006
k_{49}	0.0075
k_{50}	0.0075
k_{51}	0.0075
k_{52}	0.00003
k_{53}	6
k_{54}	6
k_{55}	0.00003
k_{56}	1
k_{57}	0.666
k_{58}	0.938
k_{59}	0.0197
k_{60}	1
k_{61}	0.00616
k_{62}	0.884
k_{63}	1
k_{64}	0.994
k_{65}	0.818
k_{66}	0.24
k_{67}	0.0409
k_{68}	0.0189
k_{69}	0.0122

Continued on next page

Table S2 – continued from previous page

Parameter	Value
k_{70}	1
k_{71}	0.055
k_{72}	0.00453
k_{73}	0.0045
k_{74}	0.347
k_{75}	4.18
k_{76}	0.011
k_{77}	7712
k_{78}	2.35
k_{79}	19992
k_{80}	0.112
k_{81}	20
k_{82}	0.5
k_{83}	0.00181
k_{84}	0.372
k_{85}	0.0407
k_{86}	0.0169
k_{87}	0.0387
k_{88}	0.0132
k_{89}	3.68E-08
k_{90}	0.00104
k_{91}	0.000000006
k_{92}	0.835
k_{93}	0.162
k_{94}	0.954
k_{95}	0.622
k_{96}	18.6
k_{97}	83.8
k_{98}	0.000129
k_{99}	449
k_{100}	0.183
k_{101}	7.29
k_{102}	55.1
k_{103}	1
k_{104}	0.01

Continued on next page

Table S2 – continued from previous page

Parameter	Value
k_{105}	0.421
k_{106}	0.122
k_{107}	0.00797
k_{108}	0.00692
k_{109}	0.00817
k_{110}	0.83
k_{111}	0.002
k_{112}	0.001
k_{113}	0.001
k_{114}	0.001
k_{115}	0.001
k_{116}	0.001
k_{117}	0.001
k_{118}	0.000001
k_{119}	0.000001
k_{120}	0.000001
k_{121}	0.000001
k_{122}	600
k_{123}	600
k_{124}	1
k_{125}	0.1
k_{126}	0.5
k_{127}	0.01
k_{128}	0.05
k_{129}	0.1
k_{130}	0.1
k_{131}	0.1
k_{132}	0.393
k_{133}	0.0001
k_{134}	0.0001
k_{135}	0.0001
k_{136}	0.0001
k_{137}	0.0001
k_{138}	0.0001
k_{139}	0.0001

Continued on next page

Table S2 – continued from previous page

Parameter	Value
k_{140}	0.0001
k_{141}	0.0001
k_{142}	0.393
$V_{Nucleus}$	0.2

Text S1: The ODE Model

$$
\begin{aligned}
\frac{\mathrm{d}\,([\mathrm{TLR7}])}{\mathrm{d}t} &= -\,(\mathrm{k}_1 \cdot [\mathrm{R848}] \cdot [\mathrm{TLR7}]) \\
\frac{\mathrm{d}\,([\mathrm{bTLR7}])}{\mathrm{d}t} &= -\,(\mathrm{k}_2 \cdot [\mathrm{bTLR7}]) \\
&\quad +\,(\mathrm{k}_1 \cdot [\mathrm{R848}] \cdot [\mathrm{TLR7}]) \\
\frac{\mathrm{d}\,([\mathrm{MyD88}*])}{\mathrm{d}t} &= +\,(\mathrm{k}_3 \cdot [\mathrm{bTLR7}] \cdot [\mathrm{MyD88}]) \\
&\quad -\,(\mathrm{k}_4 \cdot [\mathrm{MyD88}*] \cdot [\mathrm{IRAK1/4}] \cdot [\mathrm{TRAF6}]) \\
\frac{\mathrm{d}\,([\mathrm{MyD88}])}{\mathrm{d}t} &= -\,(\mathrm{k}_3 \cdot [\mathrm{bTLR7}] \cdot [\mathrm{MyD88}]) \\
&\quad +\,(\mathrm{k}_7 \cdot [\mathrm{MyD88}* : \mathrm{IRAK1/4} : \mathrm{TRAF6}]) \\
\frac{\mathrm{d}\,([\mathrm{IRAK1/4}])}{\mathrm{d}t} &= -\,(\mathrm{k}_4 \cdot [\mathrm{MyD88}*] \cdot [\mathrm{IRAK1/4}] \cdot [\mathrm{TRAF6}]) \\
&\quad +\,(\mathrm{k}_{19} \cdot [\mathrm{IRAK1/4}* : \mathrm{TRAF6}]) \\
\frac{\mathrm{d}\,([\mathrm{TRAF6}])}{\mathrm{d}t} &= -\,(\mathrm{k}_{60} \cdot [\mathrm{TRIF}*] \cdot [\mathrm{TRADD} : \mathrm{FADD} : \mathrm{RIP1}] \cdot [\mathrm{TRAF6}]) \\
&\quad +\,(\mathrm{k}_{70} \cdot [\mathrm{TRIF}* : \mathrm{TRADD} : \mathrm{FADD} : \mathrm{RIP1} : \mathrm{TRAF6}]) \\
&\quad -\,(\mathrm{k}_4 \cdot [\mathrm{MyD88}*] \cdot [\mathrm{IRAK1/4}] \cdot [\mathrm{TRAF6}]) \\
&\quad -\,((\mathrm{k}_{26} \cdot [\mathrm{TRAF6}] \cdot [\mathrm{A20}] - \mathrm{k}_{27} \cdot [\mathrm{TRAF6} : \mathrm{A20}])) \\
&\quad +\,(\mathrm{k}_{19} \cdot [\mathrm{IRAK1/4}* : \mathrm{TRAF6}]) \\
\frac{\mathrm{d}\,([\mathrm{MyD88}* : \mathrm{IRAK1/4} : \mathrm{TRAF6}])}{\mathrm{d}t} &= +\,(\mathrm{k}_4 \cdot [\mathrm{MyD88}*] \cdot [\mathrm{IRAK1/4}] \cdot [\mathrm{TRAF6}]) \\
&\quad -\,(\mathrm{k}_7 \cdot [\mathrm{MyD88}* : \mathrm{IRAK1/4} : \mathrm{TRAF6}]) \\
\frac{\mathrm{d}\,([\mathrm{A20}])}{\mathrm{d}t} &= +\,(\mathrm{k}_{35} \cdot [\mathrm{A20mRNA}]) \\
&\quad -\,(\mathrm{k}_{37} \cdot [\mathrm{A20}]) \\
&\quad -\,((\mathrm{k}_{26} \cdot [\mathrm{TRAF6}] \cdot [\mathrm{A20}] - \mathrm{k}_{27} \cdot [\mathrm{TRAF6} : \mathrm{A20}])) \\
\frac{\mathrm{d}\,([\mathrm{TRAF6} : \mathrm{A20}])}{\mathrm{d}t} &= +\,((\mathrm{k}_{26} \cdot [\mathrm{TRAF6}] \cdot [\mathrm{A20}] - \mathrm{k}_{27} \cdot [\mathrm{TRAF6} : \mathrm{A20}])) \\
\frac{\mathrm{d}\,([\mathrm{IRAK1/4}* : \mathrm{TRAF6}])}{\mathrm{d}t} &= +\,(\mathrm{k}_7 \cdot [\mathrm{MyD88}* : \mathrm{IRAK1/4} : \mathrm{TRAF6}]) \\
&\quad -\,((\mathrm{k}_9 \cdot [\mathrm{IRAK1/4}* : \mathrm{TRAF6}] \cdot [\mathrm{TRAF3}] - \mathrm{k}_{28} \cdot [\mathrm{IRAK1/4}* : \mathrm{TRAF6} : \mathrm{TRAF3}])) \\
&\quad -\,(\mathrm{k}_{19} \cdot [\mathrm{IRAK1/4}* : \mathrm{TRAF6}]) \\
\frac{\mathrm{d}\,([\mathrm{TRAF3}])}{\mathrm{d}t} &= -\,((\mathrm{k}_{58} \cdot [\mathrm{TRIF}*] \cdot [\mathrm{TRAF3}] - \mathrm{k}_{59} \cdot [\mathrm{TRIF}* : \mathrm{TRAF3}])) \\
&\quad +\,(\mathrm{k}_{69} \cdot [\mathrm{TRIF}* : \mathrm{TRAF3}]) \\
&\quad -\,((\mathrm{k}_9 \cdot [\mathrm{IRAK1/4}* : \mathrm{TRAF6}] \cdot [\mathrm{TRAF3}] - \mathrm{k}_{28} \cdot [\mathrm{IRAK1/4}* : \mathrm{TRAF6} : \mathrm{TRAF3}])) \\
\frac{\mathrm{d}\,([\mathrm{Mkk1/2}])}{\mathrm{d}t} &= -\left(\frac{\mathrm{k}_{10} \cdot [\mathrm{Tak1} : \mathrm{Tab2} : \mathrm{Tab3}*] \cdot [\mathrm{Mkk1/2}]}{\mathrm{k}_{77} + [\mathrm{Mkk1/2}]}\right) \\
&\quad +\,(\mathrm{k}_{24} \cdot [\mathrm{Mkk1/2}*]) \\
\frac{\mathrm{d}\,([\mathrm{Mkk3/6}])}{\mathrm{d}t} &= -\left(\frac{\mathrm{k}_{11} \cdot [\mathrm{Tak1} : \mathrm{Tab2} : \mathrm{Tab3}*] \cdot [\mathrm{Mkk3/6}]}{\mathrm{k}_{78} + [\mathrm{Mkk3/6}]}\right) \\
&\quad +\,(\mathrm{k}_{25} \cdot [\mathrm{Mkk3/6}*]) \\
\frac{\mathrm{d}\,([\mathrm{ERK}])}{\mathrm{d}t} &= -\,(\mathrm{k}_{12} \cdot [\mathrm{ERK}] \cdot [\mathrm{Mkk1/2}*]) \\
&\quad +\,(\mathrm{k}_{18} \cdot [\mathrm{ERK}*]) \\
\frac{\mathrm{d}\,([\mathrm{ERK}*])}{\mathrm{d}t} &= +\,(\mathrm{k}_{12} \cdot [\mathrm{ERK}] \cdot [\mathrm{Mkk1/2}*]) \\
&\quad -\,(\mathrm{k}_{18} \cdot [\mathrm{ERK}*]) \\
\frac{\mathrm{d}\,([\mathrm{Mkk1/2}*])}{\mathrm{d}t} &= +\left(\frac{\mathrm{k}_{10} \cdot [\mathrm{Tak1} : \mathrm{Tab2} : \mathrm{Tab3}*] \cdot [\mathrm{Mkk1/2}]}{\mathrm{k}_{77} + [\mathrm{Mkk1/2}]}\right) \\
&\quad -\,(\mathrm{k}_{24} \cdot [\mathrm{Mkk1/2}*]) \\
\frac{\mathrm{d}\,([\mathrm{Mkk3/6}*])}{\mathrm{d}t} &= +\left(\frac{\mathrm{k}_{11} \cdot [\mathrm{Tak1} : \mathrm{Tab2} : \mathrm{Tab3}*] \cdot [\mathrm{Mkk3/6}]}{\mathrm{k}_{78} + [\mathrm{Mkk3/6}]}\right) \\
&\quad -\,(\mathrm{k}_{25} \cdot [\mathrm{Mkk3/6}*]) \\
\frac{\mathrm{d}\,([\mathrm{p38}*])}{\mathrm{d}t} &= +\,(\mathrm{k}_{13} \cdot [\mathrm{p38}] \cdot [\mathrm{Mkk3/6}*]) \\
&\quad -\,(\mathrm{k}_{23} \cdot [\mathrm{p38}*])
\end{aligned}
$$

$$
\begin{aligned}
\frac{\mathrm{d}\left([\mathrm{p38}]\right)}{\mathrm{d}t} &= -\left(\mathrm{k}_{13} \cdot [\mathrm{p38}] \cdot [\mathrm{Mkk3/6*}]\right) \\
&\quad + \left(\mathrm{k}_{23} \cdot [\mathrm{p38*}]\right) \\
\frac{\mathrm{d}\left([\mathrm{AP1}]\right)}{\mathrm{d}t} &= -\left(\mathrm{k}_{32} \cdot [\mathrm{JNK*}] \cdot [\mathrm{AP1}]\right) \\
&\quad - \left(\mathrm{k}_{20} \cdot [\mathrm{ERK*}] \cdot [\mathrm{AP1}]\right) \\
&\quad - \left(\mathrm{k}_{14} \cdot [\mathrm{p38*}] \cdot [\mathrm{AP1}]\right) \\
&\quad + \left(\mathrm{k}_{29} \cdot [\mathrm{AP1*}]\right) \\
\frac{\mathrm{d}\left([\mathrm{NEMO} : \mathrm{IKKb} : \mathrm{IKKa}]\right)}{\mathrm{d}t} &= +\left(\mathrm{k}_{21}\right) \\
&\quad - \left(\mathrm{k}_{49} \cdot [\mathrm{NEMO} : \mathrm{IKKb} : \mathrm{IKKa}]\right) \\
&\quad - \left(\mathrm{k}_{94} \cdot [\mathrm{Akt*}] \cdot [\mathrm{NEMO} : \mathrm{IKKb} : \mathrm{IKKa}]\right) \\
&\quad - \left(\mathrm{k}_{75} \cdot [\mathrm{NEMO} : \mathrm{IKKb} : \mathrm{IKKa}] \cdot [\mathrm{Tak1} : \mathrm{Tab2} : \mathrm{Tab3*}]\right) \\
\frac{\mathrm{d}\left([\mathrm{NEMO} : \mathrm{IKKb*} : \mathrm{IKKa}]\right)}{\mathrm{d}t} &= +\left(\mathrm{k}_{54} \cdot [\mathrm{NEMO} : \mathrm{IKKb*} : \mathrm{IKKa} : \mathrm{NF}\kappa\mathrm{B} : \mathrm{I}\kappa\mathrm{B}\alpha]\right) \\
&\quad - \left(\mathrm{k}_{39} \cdot [\mathrm{NEMO} : \mathrm{IKKb*} : \mathrm{IKKa}] \cdot [\mathrm{I}\kappa\mathrm{B}\alpha]\right) \\
&\quad + \left(\mathrm{k}_{40} \cdot [\mathrm{NEMO} : \mathrm{IKKb*} : \mathrm{IKKa} : \mathrm{I}\kappa\mathrm{B}\alpha]\right) \\
&\quad - \left(\mathrm{k}_{41} \cdot [\mathrm{NEMO} : \mathrm{IKKb*} : \mathrm{IKKa}]\right) \\
&\quad - \left(\mathrm{k}_{50} \cdot [\mathrm{NEMO} : \mathrm{IKKb*} : \mathrm{IKKa}]\right) \\
&\quad - \left(\mathrm{k}_{53} \cdot [\mathrm{NEMO} : \mathrm{IKKb*} : \mathrm{IKKa}] \cdot [\mathrm{A20}]\right) \\
&\quad + \left(\mathrm{k}_{76} \cdot [\mathrm{NEMO} : \mathrm{IKKb} : \mathrm{IKK} : \mathrm{Tak1} : \mathrm{Tab2} : \mathrm{Tab3*}]\right) \\
&\quad + \left(\mathrm{k}_{94} \cdot [\mathrm{Akt*}] \cdot [\mathrm{NEMO} : \mathrm{IKKb} : \mathrm{IKKa}]\right) \\
&\quad - \left(\mathrm{k}_{15} \cdot [\mathrm{NEMO} : \mathrm{IKKb*} : \mathrm{IKKa}] \cdot [\mathrm{NF}\kappa\mathrm{B} : \mathrm{I}\kappa\mathrm{B}\alpha]\right) \\
\frac{\mathrm{d}\left([\mathrm{I}\kappa\mathrm{B}\alpha]\right)}{\mathrm{d}t} &= +\left(\mathrm{k}_{47} \cdot [\mathrm{I}\kappa\mathrm{B}\alpha\mathrm{mRNA}]\right) \\
&\quad - \left(\mathrm{k}_{48} \cdot [\mathrm{I}\kappa\mathrm{B}\alpha]\right) \\
&\quad - \left(\mathrm{k}_{39} \cdot [\mathrm{NEMO} : \mathrm{IKKb*} : \mathrm{IKKa}] \cdot [\mathrm{I}\kappa\mathrm{B}\alpha]\right) \\
&\quad - \left(\left(\mathrm{k}_{44} \cdot [\mathrm{I}\kappa\mathrm{B}\alpha] - \mathrm{k}_{45} \cdot [\mathrm{I}\kappa\mathrm{B}\alpha\mathrm{n}]\right)\right) \\
&\quad - \left(\mathrm{k}_{17} \cdot [\mathrm{NF}\kappa\mathrm{B}] \cdot [\mathrm{I}\kappa\mathrm{B}\alpha]\right) \\
\frac{\mathrm{d}\left([\mathrm{NF}\kappa\mathrm{B} : \mathrm{I}\kappa\mathrm{B}\alpha]\right)}{\mathrm{d}t} &= -\left(\mathrm{k}_{38} \cdot [\mathrm{NF}\kappa\mathrm{B} : \mathrm{I}\kappa\mathrm{B}\alpha]\right) \\
&\quad + \left(\mathrm{k}_{43} \cdot [\mathrm{I}\kappa\mathrm{B}\alpha\mathrm{n} : \mathrm{NF}\kappa\mathrm{Bn}]\right) \\
&\quad - \left(\mathrm{k}_{15} \cdot [\mathrm{NEMO} : \mathrm{IKKb*} : \mathrm{IKKa}] \cdot [\mathrm{NF}\kappa\mathrm{B} : \mathrm{I}\kappa\mathrm{B}\alpha]\right) \\
&\quad + \left(\mathrm{k}_{17} \cdot [\mathrm{NF}\kappa\mathrm{B}] \cdot [\mathrm{I}\kappa\mathrm{B}\alpha]\right) \\
\frac{\mathrm{d}\left([\mathrm{NF}\kappa\mathrm{B}]\right)}{\mathrm{d}t} &= +\left(\mathrm{k}_{38} \cdot [\mathrm{NF}\kappa\mathrm{B} : \mathrm{I}\kappa\mathrm{B}\alpha]\right) \\
&\quad + \left(\mathrm{k}_{54} \cdot [\mathrm{NEMO} : \mathrm{IKKb*} : \mathrm{IKKa} : \mathrm{NF}\kappa\mathrm{B} : \mathrm{I}\kappa\mathrm{B}\alpha]\right) \\
&\quad - \left(\mathrm{k}_{17} \cdot [\mathrm{NF}\kappa\mathrm{B}] \cdot [\mathrm{I}\kappa\mathrm{B}\alpha]\right) \\
&\quad - \left(\mathrm{k}_{16} \cdot [\mathrm{NF}\kappa\mathrm{B}]\right) \\
\frac{\mathrm{d}\left([\mathrm{A20mRNA}]\right)}{\mathrm{d}t} &= -\left(\mathrm{k}_{36} \cdot [\mathrm{A20mRNA}]\right) \\
&\quad + \left(\mathrm{k}_{52} \cdot [\mathrm{NF}\kappa\mathrm{Bn}]\right) \\
\frac{\mathrm{d}\left([\mathrm{I}\kappa\mathrm{B}\alpha\mathrm{mRNA}]\right)}{\mathrm{d}t} &= -\left(\mathrm{k}_{46} \cdot [\mathrm{I}\kappa\mathrm{B}\alpha\mathrm{mRNA}]\right) \\
&\quad + \left(\mathrm{k}_{55} \cdot [\mathrm{NF}\kappa\mathrm{Bn}]\right) \\
\frac{\mathrm{d}\left([\mathrm{IRF7}]\right)}{\mathrm{d}t} &= -\left(\mathrm{k}_{5} \cdot [\mathrm{IRAK1/4*} : \mathrm{TRAF6} : \mathrm{TRAF3}] \cdot [\mathrm{IRF7}]\right) \\
&\quad + \left(\mathrm{k}_{6} \cdot [\mathrm{IRF7*}]\right) \\
\frac{\mathrm{d}\left([\mathrm{JNK}]\right)}{\mathrm{d}t} &= +\left(\mathrm{k}_{33} \cdot [\mathrm{JNK*}]\right) \\
&\quad - \left(\mathrm{k}_{30} \cdot [\mathrm{JNK}] \cdot [\mathrm{Mkk4/7*}]\right) \\
\frac{\mathrm{d}\left([\mathrm{Mkk4/7*}]\right)}{\mathrm{d}t} &= -\left(\mathrm{k}_{34} \cdot [\mathrm{Mkk4/7*}]\right) \\
&\quad + \left(\frac{\mathrm{k}_{31} \cdot [\mathrm{Tak1} : \mathrm{Tab2} : \mathrm{Tab3*}] \cdot [\mathrm{Mkk4/7}]}{\mathrm{k}_{79} + [\mathrm{Mkk4/7}]}\right) \\
\frac{\mathrm{d}\left([\mathrm{JNK*}]\right)}{\mathrm{d}t} &= -\left(\mathrm{k}_{33} \cdot [\mathrm{JNK*}]\right) \\
&\quad + \left(\mathrm{k}_{30} \cdot [\mathrm{JNK}] \cdot [\mathrm{Mkk4/7*}]\right) \\
\frac{\mathrm{d}\left([\mathrm{Mkk4/7}]\right)}{\mathrm{d}t} &= +\left(\mathrm{k}_{34} \cdot [\mathrm{Mkk4/7*}]\right) \\
&\quad - \left(\frac{\mathrm{k}_{31} \cdot [\mathrm{Tak1} : \mathrm{Tab2} : \mathrm{Tab3*}] \cdot [\mathrm{Mkk4/7}]}{\mathrm{k}_{79} + [\mathrm{Mkk4/7}]}\right)
\end{aligned}
$$

$$
\begin{aligned}
\frac{\mathrm{d}\left([\mathrm{IRAK1/4*} : \mathrm{TRAF6} : \mathrm{TRAF3}]\right)}{\mathrm{d}t} &= +\left((\mathrm{k_9} \cdot [\mathrm{IRAK1/4*} : \mathrm{TRAF6}] \cdot [\mathrm{TRAF3}] - \mathrm{k_{28}} \cdot [\mathrm{IRAK1/4*} : \mathrm{TRAF6} : \mathrm{TRAF3}]\right)\\
\frac{\mathrm{d}\left([\mathrm{I\kappa B\alpha *}]\right)}{\mathrm{d}t} &= -\left(\mathrm{k_{144}} \cdot [\mathrm{I\kappa B\alpha *}]\right)\\
&\quad +\left(\mathrm{k_{38}} \cdot [\mathrm{NF\kappa B} : \mathrm{I\kappa B\alpha}]\right)\\
&\quad +\left(\mathrm{k_{54}} \cdot [\mathrm{NEMO} : \mathrm{IKKb*} : \mathrm{IKKa} : \mathrm{NF\kappa B} : \mathrm{I\kappa B\alpha}]\right)\\
&\quad +\left(\mathrm{k_{40}} \cdot [\mathrm{NEMO} : \mathrm{IKKb*} : \mathrm{IKKa} : \mathrm{I\kappa B\alpha}]\right)\\
\frac{\mathrm{d}\left([\mathrm{NEMO} : \mathrm{IKKb*} : \mathrm{IKKa} : \mathrm{NF\kappa B} : \mathrm{I\kappa B\alpha}]\right)}{\mathrm{d}t} &= -\left(\mathrm{k_{54}} \cdot [\mathrm{NEMO} : \mathrm{IKKb*} : \mathrm{IKKa} : \mathrm{NF\kappa B} : \mathrm{I\kappa B\alpha}]\right)\\
&\quad +\left(\mathrm{k_{15}} \cdot [\mathrm{NEMO} : \mathrm{IKKb*} : \mathrm{IKKa}] \cdot [\mathrm{NF\kappa B} : \mathrm{IkBa}]\right)\\
\frac{\mathrm{d}\left([\mathrm{NEMO} : \mathrm{IKKb*} : \mathrm{IKKa} : \mathrm{I\kappa B\alpha}]\right)}{\mathrm{d}t} &= +\left(\mathrm{k_{39}} \cdot [\mathrm{NEMO} : \mathrm{IKKb*} : \mathrm{IKKa}] \cdot [\mathrm{I\kappa B\alpha}]\right)\\
&\quad -\left(\mathrm{k_{40}} \cdot [\mathrm{NEMO} : \mathrm{IKKb*} : \mathrm{IKKa} : \mathrm{I\kappa B\alpha}]\right)\\
\frac{\mathrm{d}\left([\mathrm{inactiveIKK}]\right)}{\mathrm{d}t} &= +\left(\mathrm{k_{41}} \cdot [\mathrm{NEMO} : \mathrm{IKKb*} : \mathrm{IKKa}]\right)\\
&\quad -\left(\mathrm{k_{51}} \cdot [\mathrm{inactiveIKK}]\right)\\
&\quad +\left(\mathrm{k_{53}} \cdot [\mathrm{NEMO} : \mathrm{IKKb*} : \mathrm{IKKa}] \cdot [\mathrm{A20}]\right)\\
\frac{\mathrm{d}\left([\mathrm{TLR3}]\right)}{\mathrm{d}t} &= -\left(\mathrm{k_{56}} \cdot [\mathrm{Poly(I:C)}] \cdot [\mathrm{TLR3}]\right)\\
\frac{\mathrm{d}\left([\mathrm{bTLR3}]\right)}{\mathrm{d}t} &= +\left(\mathrm{k_{56}} \cdot [\mathrm{Poly(I:C)}] \cdot [\mathrm{TLR3}]\right)\\
&\quad -\left(\mathrm{k_{67}} \cdot [\mathrm{bTLR3}]\right)\\
\frac{\mathrm{d}\left([\mathrm{TRIF}]\right)}{\mathrm{d}t} &= -\left(\mathrm{k_{57}} \cdot [\mathrm{bTLR3}] \cdot [\mathrm{TRIF}]\right)\\
&\quad +\left(\mathrm{k_{69}} \cdot [\mathrm{TRIF*} : \mathrm{TRAF3}]\right)\\
&\quad +\left(\mathrm{k_{70}} \cdot [\mathrm{TRIF*} : \mathrm{TRADD} : \mathrm{FADD} : \mathrm{RIP1} : \mathrm{TRAF6}]\right)\\
\frac{\mathrm{d}\left([\mathrm{TRIF*}]\right)}{\mathrm{d}t} &= +\left(\mathrm{k_{57}} \cdot [\mathrm{bTLR3}] \cdot [\mathrm{TRIF}]\right)\\
&\quad -\left((\mathrm{k_{58}} \cdot [\mathrm{TRIF*}] \cdot [\mathrm{TRAF3}] - \mathrm{k_{59}} \cdot [\mathrm{TRIF*} : \mathrm{TRAF3}]\right))\\
&\quad -\left(\mathrm{k_{60}} \cdot [\mathrm{TRIF*}] \cdot [\mathrm{TRADD} : \mathrm{FADD} : \mathrm{RIP1}] \cdot [\mathrm{TRAF6}]\right)\\
\frac{\mathrm{d}\left([\mathrm{TRIF*} : \mathrm{TRAF3}]\right)}{\mathrm{d}t} &= +\left((\mathrm{k_{58}} \cdot [\mathrm{TRIF*}] \cdot [\mathrm{TRAF3}] - \mathrm{k_{59}} \cdot [\mathrm{TRIF*} : \mathrm{TRAF3}]\right))\\
&\quad -\left(\mathrm{k_{69}} \cdot [\mathrm{TRIF*} : \mathrm{TRAF3}]\right)\\
\frac{\mathrm{d}\left([\mathrm{TRADD} : \mathrm{FADD} : \mathrm{RIP1}]\right)}{\mathrm{d}t} &= -\left(\mathrm{k_{60}} \cdot [\mathrm{TRIF*}] \cdot [\mathrm{TRADD} : \mathrm{FADD} : \mathrm{RIP1}] \cdot [\mathrm{TRAF6}]\right)\\
&\quad +\left(\mathrm{k_{70}} \cdot [\mathrm{TRIF*} : \mathrm{TRADD} : \mathrm{FADD} : \mathrm{RIP1} : \mathrm{TRAF6}]\right)\\
\frac{\mathrm{d}\left([\mathrm{TRIF*} : \mathrm{TRADD} : \mathrm{FADD} : \mathrm{RIP1} : \mathrm{TRAF6}]\right)}{\mathrm{d}t} &= +\left(\mathrm{k_{60}} \cdot [\mathrm{TRIF*}] \cdot [\mathrm{TRADD} : \mathrm{FADD} : \mathrm{RIP1}] \cdot [\mathrm{TRAF6}]\right)\\
&\quad -\left(\mathrm{k_{70}} \cdot [\mathrm{TRIF*} : \mathrm{TRADD} : \mathrm{FADD} : \mathrm{RIP1} : \mathrm{TRAF6}]\right)\\
\frac{\mathrm{d}\left([\mathrm{IKKi}]\right)}{\mathrm{d}t} &= -\left(\mathrm{k_{62}} \cdot [\mathrm{TRIF*} : \mathrm{TRAF3}] \cdot [\mathrm{IKKi}]\right)\\
&\quad +\left(\mathrm{k_{66}} \cdot [\mathrm{IKKi} : \mathrm{TBK1*}]\right)\\
\frac{\mathrm{d}\left([\mathrm{IKKi*}]\right)}{\mathrm{d}t} &= +\left(\mathrm{k_{62}} \cdot [\mathrm{TRIF*} : \mathrm{TRAF3}] \cdot [\mathrm{IKKi}]\right)\\
&\quad -\left(\mathrm{k_{64}} \cdot [\mathrm{TBK1*}] \cdot [\mathrm{IKKi*}]\right)\\
\frac{\mathrm{d}\left([\mathrm{TBK1}]\right)}{\mathrm{d}t} &= -\left(\mathrm{k_{63}} \cdot [\mathrm{TRIF*} : \mathrm{TRAF3}] \cdot [\mathrm{TBK1}]\right)\\
&\quad +\left(\mathrm{k_{66}} \cdot [\mathrm{IKKi} : \mathrm{TBK1*}]\right)\\
\frac{\mathrm{d}\left([\mathrm{TBK1*}]\right)}{\mathrm{d}t} &= +\left(\mathrm{k_{63}} \cdot [\mathrm{TRIF*} : \mathrm{TRAF3}] \cdot [\mathrm{TBK1}]\right)\\
&\quad -\left(\mathrm{k_{64}} \cdot [\mathrm{TBK1*}] \cdot [\mathrm{IKKi*}]\right)\\
\frac{\mathrm{d}\left([\mathrm{IKKi} : \mathrm{TBK1*}]\right)}{\mathrm{d}t} &= +\left(\mathrm{k_{64}} \cdot [\mathrm{TBK1*}] \cdot [\mathrm{IKKi*}]\right)\\
&\quad -\left(\mathrm{k_{66}} \cdot [\mathrm{IKKi} : \mathrm{TBK1*}]\right)\\
\frac{\mathrm{d}\left([\mathrm{IRF3}]\right)}{\mathrm{d}t} &= -\left(\mathrm{k_{65}} \cdot [\mathrm{IKKi} : \mathrm{TBK1*}] \cdot [\mathrm{IRF3}]\right)\\
&\quad +\left(\mathrm{k_{68}} \cdot [\mathrm{IRF3*}]\right)
\end{aligned}
$$

$$
\begin{aligned}
\frac{\mathrm{d}\left([\mathrm{A}]\right)}{\mathrm{d}t} &= -\left(\mathrm{k}_{105}\cdot[\mathrm{A}]\right)\\
&\quad -\left(\mathrm{k}_{71}\cdot[\mathrm{A}]\right)\\
&\quad +\left(\mathrm{k}_{118}\cdot\left(0.0001+0.9999\cdot\left(1-\frac{1}{1+\mathrm{k}_{120}\cdot[\mathrm{RelBp52}]}\right)\right)\right)\\
&\quad +\left(\mathrm{k}_{102}\cdot\left(1-\frac{1}{1+\mathrm{k}_{98}\cdot[\mathrm{NF\kappa Bn}]}\right.\right.\\
&\quad \cdot\frac{1}{1+\mathrm{k}_{97}\cdot[\mathrm{NF\kappa Bn}]\cdot[\mathrm{AP1}*]\cdot[\mathrm{FacY}*]^{1.5}}\cdot\frac{1}{1+\mathrm{k}_{100}\cdot[\mathrm{AP1}*]}\\
&\quad \left.\left.\cdot\frac{1}{1+\mathrm{k}_{96}\cdot[\mathrm{factX}]\cdot[\mathrm{NF\kappa Bn}]\cdot[\mathrm{AP1}*]}\right)\right)\\
\frac{\mathrm{d}\left([\mathrm{A2}]\right)}{\mathrm{d}t} &= +\left(\mathrm{k}_{71}\cdot[\mathrm{A}]\right)\\
&\quad -\left(\mathrm{k}_{72}\cdot[\mathrm{A2}]\right)\\
\frac{\mathrm{d}\left([\mathrm{A3}]\right)}{\mathrm{d}t} &= +\left(\mathrm{k}_{72}\cdot[\mathrm{A2}]\right)\\
&\quad -\left(\mathrm{k}_{73}\cdot[\mathrm{A3}]\right)\\
\frac{\mathrm{d}\left([\mathrm{IL6mRNA}]\right)}{\mathrm{d}t} &= +\left(\mathrm{k}_{73}\cdot[\mathrm{A3}]\right)\\
&\quad -\left(\mathrm{k}_{74}\cdot[\mathrm{IL6mRNA}]\right)\\
&\quad -\left(\mathrm{k}_{123}\cdot[\mathrm{IL6mRNA}]\cdot[\mathrm{STAT3}*]\right)\\
\frac{\mathrm{d}\left([\mathrm{Tak1:Tab2:Tab3}]\right)}{\mathrm{d}t} &= -\left(\mathrm{k}_{61}\cdot[\mathrm{TRIF}*:\mathrm{TRADD:FADD:RIP1:TRAF6}]\cdot[\mathrm{Tak1:Tab2:Tab3}]\right)\\
&\quad +\left(\mathrm{k}_{22}\cdot[\mathrm{Tak1:Tab2:Tab3}*]\right)\\
&\quad -\left(\mathrm{k}_{8}\cdot[\mathrm{IRAK1/4}*:\mathrm{TRAF6}]\cdot[\mathrm{Tak1:Tab2:Tab3}]\right)\\
\frac{\mathrm{d}\left([\mathrm{NEMO:IKKb:IKK:Tak1:Tab2:Tab3}*]\right)}{\mathrm{d}t} &= -\left(\mathrm{k}_{76}\cdot[\mathrm{NEMO:IKKb:IKK:Tak1:Tab2:Tab3}*]\right)\\
&\quad +\left(\mathrm{k}_{75}\cdot[\mathrm{NEMO:IKKb:IKKa}]\cdot[\mathrm{Tak1:Tab2:Tab3}*]\right)\\
\frac{\mathrm{d}\left([\mathrm{Tak1:Tab2:Tab3}*]\right)}{\mathrm{d}t} &= +\left(\mathrm{k}_{61}\cdot[\mathrm{TRIF}*:\mathrm{TRADD:FADD:RIP1:TRAF6}]\cdot[\mathrm{Tak1:Tab2:Tab3}]\right)\\
&\quad -\left(\mathrm{k}_{22}\cdot[\mathrm{Tak1:Tab2:Tab3}*]\right)\\
&\quad +\left(\mathrm{k}_{76}\cdot[\mathrm{NEMO:IKKb:IKK:Tak1:Tab2:Tab3}*]\right)\\
&\quad +\left(\mathrm{k}_{8}\cdot[\mathrm{IRAK1/4}*:\mathrm{TRAF6}]\cdot[\mathrm{Tak1:Tab2:Tab3}]\right)\\
&\quad -\left(\mathrm{k}_{75}\cdot[\mathrm{NEMO:IKKb:IKKa}]\cdot[\mathrm{Tak1:Tab2:Tab3}*]\right)\\
\frac{\mathrm{d}\left([\mathrm{B}]\right)}{\mathrm{d}t} &= -\left(\mathrm{k}_{71}\cdot[\mathrm{B}]\right)\\
&\quad +\left(\mathrm{k}_{102}\cdot\left(1-\frac{1}{1+\mathrm{k}_{98}\cdot[\mathrm{NF\kappa Bn}]}\right.\right.\\
&\quad \cdot\frac{1}{1+\mathrm{k}_{99}\cdot[\mathrm{NF\kappa Bn}]\cdot[\mathrm{AP1}*]\cdot[\mathrm{FacY}*]^{1.5}}\cdot\frac{1}{1+\mathrm{k}_{100}\cdot[\mathrm{AP1}*]}\\
&\quad \left.\left.\cdot\frac{1}{1+\mathrm{k}_{101}\cdot[\mathrm{factX}]\cdot[\mathrm{NF\kappa Bn}]\cdot[\mathrm{AP1}*]}\right)\right)\\
&\quad -\left(\mathrm{k}_{105}\cdot[\mathrm{B}]\right)\\
&\quad +\left(\mathrm{k}_{119}\cdot\left(0.0001+0.9999\cdot\left(1-\frac{1}{1+\mathrm{k}_{121}\cdot[\mathrm{RelBp52}]}\right)\right)\right)\\
\frac{\mathrm{d}\left([\mathrm{B2}]\right)}{\mathrm{d}t} &= +\left(\mathrm{k}_{71}\cdot[\mathrm{B}]\right)\\
&\quad -\left(\mathrm{k}_{72}\cdot[\mathrm{B2}]\right)\\
\frac{\mathrm{d}\left([\mathrm{B3}]\right)}{\mathrm{d}t} &= +\left(\mathrm{k}_{72}\cdot[\mathrm{B2}]\right)\\
&\quad -\left(\mathrm{k}_{73}\cdot[\mathrm{B3}]\right)\\
\frac{\mathrm{d}\left([\mathrm{IL12mRNA}]\right)}{\mathrm{d}t} &= +\left(\mathrm{k}_{73}\cdot[\mathrm{B3}]\right)\\
&\quad -\left(\mathrm{k}_{74}\cdot[\mathrm{IL12mRNA}]\right)\\
&\quad -\left(\mathrm{k}_{122}\cdot[\mathrm{IL12mRNA}]\cdot[\mathrm{STAT3}*]\right)
\end{aligned}
$$

$$
\begin{aligned}
\frac{\mathrm{d}\left([\mathrm{C}]\right)}{\mathrm{d}t} &= +\left(\mathrm{k}_{80} \cdot \left(0.0001 + 0.9999 \cdot \left(1 - \frac{1}{1 + \mathrm{k}_{82} \cdot [\mathrm{IRF3}*]}\right.\right.\right. \\
&\quad \left.\left.\left. \cdot \frac{1}{1 + \mathrm{k}_{133} \cdot [\mathrm{AP1}*] \cdot [\mathrm{IRF3}*] \cdot [\mathrm{NF}\kappa\mathrm{Bn}]}\right)\right)\right) \\
&\quad - (\mathrm{k}_{106} \cdot [\mathrm{C}]) \\
&\quad - (\mathrm{k}_{110} \cdot [\mathrm{C}]) \\
&\quad + \left(\mathrm{k}_{81} \cdot \left(0.0001 + 0.9999 \cdot \left(1 - \frac{1}{1 + \mathrm{k}_{134} \cdot [\mathrm{IRF7}*]}\right)\right)\right) \\
\frac{\mathrm{d}\left([\mathrm{C2}]\right)}{\mathrm{d}t} &= +(\mathrm{k}_{106} \cdot [\mathrm{C}]) \\
&\quad - (\mathrm{k}_{107} \cdot [\mathrm{C2}]) \\
\frac{\mathrm{d}\left([\mathrm{C3}]\right)}{\mathrm{d}t} &= +(\mathrm{k}_{107} \cdot [\mathrm{C2}]) \\
&\quad - (\mathrm{k}_{108} \cdot [\mathrm{C3}]) \\
\frac{\mathrm{d}\left([\mathrm{Type1IFN}]\right)}{\mathrm{d}t} &= +(\mathrm{k}_{108} \cdot [\mathrm{C3}]) \\
&\quad - (\mathrm{k}_{109} \cdot [\mathrm{Type1IFN}]) \\
&\quad + \left(\mathrm{k}_{89} \cdot \left(0.0001 + 0.9999 \cdot \left(1 - \frac{1}{1 + \mathrm{k}_{90} \cdot [\mathrm{Stat1} : \mathrm{Stat2} * \mathrm{n}]}\right)\right)\right) \\
\frac{\mathrm{d}\left([\mathrm{Tyk2} : \mathrm{Jak1}]\right)}{\mathrm{d}t} &= -(\mathrm{k}_{83} \cdot [\mathrm{Type1IFN}] \cdot [\mathrm{Tyk2} : \mathrm{Jak1}]) \\
&\quad + (\mathrm{k}_{85} \cdot [\mathrm{Tyk2} : \mathrm{Jak1}*]) \\
&\quad - (\mathrm{k}_{135} \cdot [\mathrm{IL10}] \cdot [\mathrm{Tyk2} : \mathrm{Jak1}]) \\
\frac{\mathrm{d}\left([\mathrm{Tyk2} : \mathrm{Jak1}*]\right)}{\mathrm{d}t} &= +(\mathrm{k}_{83} \cdot [\mathrm{Type1IFN}] \cdot [\mathrm{Tyk2} : \mathrm{Jak1}]) \\
&\quad - (\mathrm{k}_{85} \cdot [\mathrm{Tyk2} : \mathrm{Jak1}*]) \\
&\quad + (\mathrm{k}_{135} \cdot [\mathrm{IL10}] \cdot [\mathrm{Tyk2} : \mathrm{Jak1}]) \\
\frac{\mathrm{d}\left([\mathrm{Stat1} : \mathrm{Stat2}]\right)}{\mathrm{d}t} &= -(\mathrm{k}_{84} \cdot [\mathrm{Tyk2} : \mathrm{Jak1}*] \cdot [\mathrm{Stat1} : \mathrm{Stat2}]) \\
&\quad + (\mathrm{k}_{86} \cdot [\mathrm{Stat1} : \mathrm{Stat2}*]) \\
\frac{\mathrm{d}\left([\mathrm{Stat1} : \mathrm{Stat2}*]\right)}{\mathrm{d}t} &= +(\mathrm{k}_{84} \cdot [\mathrm{Tyk2} : \mathrm{Jak1}*] \cdot [\mathrm{Stat1} : \mathrm{Stat2}]) \\
&\quad - (\mathrm{k}_{86} \cdot [\mathrm{Stat1} : \mathrm{Stat2}*]) \\
&\quad - ((\mathrm{k}_{87} \cdot [\mathrm{Stat1} : \mathrm{Stat2}*] - \mathrm{k}_{88} \cdot [\mathrm{Stat1} : \mathrm{Stat2} * \mathrm{n}])) \\
\frac{\mathrm{d}\left([\mathrm{PI3k}]\right)}{\mathrm{d}t} &= -(\mathrm{k}_{91} \cdot [\mathrm{Type1IFN}] \cdot [\mathrm{PI3k}]) \\
&\quad + (\mathrm{k}_{93} \cdot [\mathrm{PI3K}*]) \\
\frac{\mathrm{d}\left([\mathrm{PI3K}*]\right)}{\mathrm{d}t} &= +(\mathrm{k}_{91} \cdot [\mathrm{Type1IFN}] \cdot [\mathrm{PI3k}]) \\
&\quad - (\mathrm{k}_{93} \cdot [\mathrm{PI3K}*]) \\
\frac{\mathrm{d}\left([\mathrm{Akt}]\right)}{\mathrm{d}t} &= -(\mathrm{k}_{92} \cdot [\mathrm{PI3K}*] \cdot [\mathrm{Akt}]) \\
&\quad + (\mathrm{k}_{95} \cdot [\mathrm{Akt}*]) \\
\frac{\mathrm{d}\left([\mathrm{Akt}*]\right)}{\mathrm{d}t} &= +(\mathrm{k}_{92} \cdot [\mathrm{PI3K}*] \cdot [\mathrm{Akt}]) \\
&\quad - (\mathrm{k}_{95} \cdot [\mathrm{Akt}*]) \\
\frac{\mathrm{d}\left([\mathrm{NIK}]\right)}{\mathrm{d}t} &= -(\mathrm{k}_{112} \cdot [\mathrm{Type1IFN}] \cdot [\mathrm{NIK}]) \\
&\quad + (\mathrm{k}_{113} \cdot [\mathrm{NIK}*]) \\
\frac{\mathrm{d}\left([\mathrm{NIK}*]\right)}{\mathrm{d}t} &= +(\mathrm{k}_{112} \cdot [\mathrm{Type1IFN}] \cdot [\mathrm{NIK}]) \\
&\quad - (\mathrm{k}_{113} \cdot [\mathrm{NIK}*]) \\
\frac{\mathrm{d}\left([\mathrm{RelBp52}]\right)}{\mathrm{d}t} &= -(\mathrm{k}_{116} \cdot [\mathrm{RelBp100}*] \cdot [\mathrm{RelBp52}]) \\
&\quad + (\mathrm{k}_{117} \cdot [\mathrm{RelBp52}*]) \\
\frac{\mathrm{d}\left([\mathrm{RelBp100}]\right)}{\mathrm{d}t} &= -(\mathrm{k}_{114} \cdot [\mathrm{NIK}*] \cdot [\mathrm{RelBp100}]) \\
&\quad + (\mathrm{k}_{115} \cdot [\mathrm{RelBp100}*]) \\
\frac{\mathrm{d}\left([\mathrm{RelBp100}*]\right)}{\mathrm{d}t} &= +(\mathrm{k}_{114} \cdot [\mathrm{NIK}*] \cdot [\mathrm{RelBp100}]) \\
&\quad - (\mathrm{k}_{115} \cdot [\mathrm{RelBp100}*])
\end{aligned}
$$

$$
\begin{aligned}
\frac{\mathrm{d}\left([\mathrm{RelBp52}*]\right)}{\mathrm{d}t} &= +\left(\mathrm{k}_{116} \cdot [\mathrm{RelBp100}*] \cdot [\mathrm{RelBp52}]\right) \\
&\quad -\left(\mathrm{k}_{117} \cdot [\mathrm{RelBp52}*]\right) \\
\frac{\mathrm{d}\left([\mathrm{IL10}]\right)}{\mathrm{d}t} &= +\left(\mathrm{k}_{136} \cdot [\mathrm{MSK1/2}*]\right) \\
&\quad -\left(\mathrm{k}_{127} \cdot [\mathrm{IL10}]\right) \\
&\quad +\left(\mathrm{k}_{137} \cdot [\mathrm{Stat1} : \mathrm{Stat2} * \mathrm{n}]\right) \\
&\quad +\left(\mathrm{k}_{130} \cdot [\mathrm{MSK1/2}*] \cdot [\mathrm{Stat1} : \mathrm{Stat2} * \mathrm{n}]\right) \\
\frac{\mathrm{d}\left([\mathrm{MSK1/2}]\right)}{\mathrm{d}t} &= -\left(\mathrm{k}_{143} \cdot [\mathrm{MSK1/2}] \cdot [\mathrm{ERK}*]\right) \\
&\quad -\left(\mathrm{k}_{138} \cdot [\mathrm{MSK1/2}] \cdot [\mathrm{p38}*]\right) \\
&\quad +\left(\mathrm{k}_{139} \cdot [\mathrm{MSK1/2}*]\right) \\
&\quad -\left(\mathrm{k}_{140} \cdot [\mathrm{MSK1/2}] \cdot [\mathrm{ERK}*] \cdot [\mathrm{p38}*]\right) \\
\frac{\mathrm{d}\left([\mathrm{MSK1/2}*]\right)}{\mathrm{d}t} &= +\left(\mathrm{k}_{143} \cdot [\mathrm{MSK1/2}] \cdot [\mathrm{ERK}*]\right) \\
&\quad +\left(\mathrm{k}_{138} \cdot [\mathrm{MSK1/2}] \cdot [\mathrm{p38}*]\right) \\
&\quad -\left(\mathrm{k}_{139} \cdot [\mathrm{MSK1/2}*]\right) \\
&\quad +\left(\mathrm{k}_{140} \cdot [\mathrm{MSK1/2}] \cdot [\mathrm{ERK}*] \cdot [\mathrm{p38}*]\right) \\
\frac{\mathrm{d}\left([\mathrm{STAT3}]\right)}{\mathrm{d}t} &= -\left(\mathrm{k}_{141} \cdot [\mathrm{STAT3}] \cdot [\mathrm{Tyk2} : \mathrm{Jak1}*]\right) \\
&\quad +\left(\mathrm{k}_{142} \cdot [\mathrm{STAT3}*]\right) \\
&\quad -\left(\mathrm{k}_{129} \cdot [\mathrm{STAT3}] \cdot [\mathrm{IL10}]\right) \\
\frac{\mathrm{d}\left([\mathrm{STAT3}*]\right)}{\mathrm{d}t} &= +\left(\mathrm{k}_{141} \cdot [\mathrm{STAT3}] \cdot [\mathrm{Tyk2} : \mathrm{Jak1}*]\right) \\
&\quad -\left(\mathrm{k}_{142} \cdot [\mathrm{STAT3}*]\right) \\
&\quad +\left(\mathrm{k}_{129} \cdot [\mathrm{STAT3}] \cdot [\mathrm{IL10}]\right) \\
\frac{\mathrm{d}\left([\mathrm{FacY}]\right)}{\mathrm{d}t} &= -\left(\frac{k_{(\mathrm{CT_JAK_STAT_6})} \cdot [\mathrm{Stat1} : \mathrm{Stat2} * \mathrm{n}] \cdot [\mathrm{FacY}]}{\mathrm{k2}_{(\mathrm{CT_JAK_STAT_6})} + [\mathrm{FacY}]}\right) \\
\frac{\mathrm{d}\left([\mathrm{I}\kappa\mathrm{B}\alpha\mathrm{n}]\right)}{\mathrm{d}t} &= -V_{\mathrm{Nuclues}} \cdot \left(\mathrm{k}_{42} \cdot [\mathrm{NF}\kappa\mathrm{Bn}] \cdot [\mathrm{I}\kappa\mathrm{B}\alpha\mathrm{n}]\right) \\
&\quad +\left((\mathrm{k}_{44} \cdot [\mathrm{I}\kappa\mathrm{B}\alpha] - \mathrm{k}_{45} \cdot [\mathrm{I}\kappa\mathrm{B}\alpha\mathrm{n}])\right) \\
\frac{\mathrm{d}\left([\mathrm{I}\kappa\mathrm{B}\alpha\mathrm{n} : \mathrm{NF}\kappa\mathrm{Bn}]\right)}{\mathrm{d}t} &= +V_{\mathrm{Nuclues}} \cdot \left(\mathrm{k}_{42} \cdot [\mathrm{NF}\kappa\mathrm{Bn}] \cdot [\mathrm{I}\kappa\mathrm{B}\alpha\mathrm{n}]\right) \\
&\quad -\left(\mathrm{k}_{43} \cdot [\mathrm{I}\kappa\mathrm{B}\alpha\mathrm{n} : \mathrm{NF}\kappa\mathrm{Bn}]\right) \\
\frac{\mathrm{d}\left([\mathrm{NF}\kappa\mathrm{Bn}]\right)}{\mathrm{d}t} &= -V_{\mathrm{Nuclues}} \cdot \left(\mathrm{k}_{42} \cdot [\mathrm{NF}\kappa\mathrm{Bn}] \cdot [\mathrm{I}\kappa\mathrm{B}\alpha\mathrm{n}]\right) \\
&\quad +\left(\mathrm{k}_{16} \cdot [\mathrm{NF}\kappa\mathrm{B}]\right) \\
\frac{\mathrm{d}\left([\mathrm{AP1}*]\right)}{\mathrm{d}t} &= +\left(\mathrm{k}_{32} \cdot [\mathrm{JNK}*] \cdot [\mathrm{AP1}]\right) \\
&\quad +\left(\mathrm{k}_{20} \cdot [\mathrm{ERK}*] \cdot [\mathrm{AP1}]\right) \\
&\quad +\left(\mathrm{k}_{14} \cdot [\mathrm{p38}*] \cdot [\mathrm{AP1}]\right) \\
&\quad -\left(\mathrm{k}_{29} \cdot [\mathrm{AP1}*]\right) \\
\frac{\mathrm{d}\left([\mathrm{Stat1} : \mathrm{Stat2} * \mathrm{n}]\right)}{\mathrm{d}t} &= +\left((\mathrm{k}_{87} \cdot [\mathrm{Stat1} : \mathrm{Stat2}*] - \mathrm{k}_{88} \cdot [\mathrm{Stat1} : \mathrm{Stat2} * \mathrm{n}])\right) \\
&\quad -V_{\mathrm{Nuclues}} \cdot \left(\mathrm{k}_{128} \cdot [\mathrm{Stat1} : \mathrm{Stat2} * \mathrm{n}]\right) \\
\frac{\mathrm{d}\left([\mathrm{factX}]\right)}{\mathrm{d}t} &= +V_{\mathrm{Nuclues}} \cdot \left(\mathrm{k}_{103} \cdot [\mathrm{IRF3}*]\right) \\
&\quad -V_{\mathrm{Nuclues}} \cdot \left(\mathrm{k}_{104} \cdot [\mathrm{factX}]\right) \\
\frac{\mathrm{d}\left([\mathrm{FacY}*]\right)}{\mathrm{d}t} &= +\left(\frac{k_{124} \cdot [\mathrm{Stat1} : \mathrm{Stat2} * \mathrm{n}] \cdot [\mathrm{FacY}]}{\mathrm{k}_{125} + [\mathrm{FacY}]}\right) \\
&\quad -V_{\mathrm{Nuclues}} \cdot \left(\mathrm{k}_{111} \cdot [\mathrm{FacY}*]\right) \\
\frac{\mathrm{d}\left([\mathrm{IRF3}*]\right)}{\mathrm{d}t} &= +\left(\mathrm{k}_{65} \cdot [\mathrm{IKKi} : \mathrm{TBK1}*] \cdot [\mathrm{IRF3}]\right) \\
&\quad -\left(\mathrm{k}_{68} \cdot [\mathrm{IRF3}*]\right) \\
\frac{\mathrm{d}\left([\mathrm{IRF7}*]\right)}{\mathrm{d}t} &= +\left(\mathrm{k}_{5} \cdot [\mathrm{IRAK1/4}* : \mathrm{TRAF6} : \mathrm{TRAF3}] \cdot [\mathrm{IRF7}]\right) \\
&\quad -\left(\mathrm{k}_{6} \cdot [\mathrm{IRF7}*]\right)
\end{aligned}
$$

References

[1] U. Alon. Network motifs: theory and experimental approaches. *Nat Rev Genet*, 8(6):450–461, 2007.

[2] S. Basu, R. Mehreja, S. Thiberge, M.-T. Chen, and R. Weiss. Spatiotemporal control of gene expression with pulse-generating networks. *Proc Natl Acad Sci*, 101(17):6355–6360, 2004.

[3] L. Goentoro, O. Shoval, M. W. Kirschner, and U. Alon. The incoherent feedforward loop can provide fold-change detection in gene regulation. *Mol Cell*, 36(5):894–899, 2009.

[4] Y. Hart and U. Alon. The utility of paradoxical components in biological circuits. *Mol Cell*, 49(2):213–221, 2013.

[5] S. Kaplan, A. Bren, E. Dekel, and U. Alon. The incoherent feed-forward loop can generate non-monotonic input functions for genes. *Mol Syst Biol*, 4(1), 2008.

[6] D. Kim, Y.-K. Kwon, and K.-H. Cho. The biphasic behavior of incoherent feed-forward loops in biomolecular regulatory networks. *Bioessays*, 30(11-12):1204–1211, 2008.

[7] S. Mangan and U. Alon. Structure and function of the feed-forward loop network motif. *Proc Natl Acad Sci*, 100(21):11980–11985, 2003.

[8] S. Mangan, S. Itzkovitz, A. Zaslaver, and U. Alon. The incoherent feed-forward loop accelerates the response-time of the gal system of escherichia coli. *J Mol Biol*, 356(5):1073–1081, 2006.

[9] R. Milo, S. Shen-Orr, S. Itzkovitz, N. Kashtan, D. Chklovskii, and U. Alon. Network motifs: simple building blocks of complex networks. *Science*, 298(5594):824–827, 2002.

[10] M. Osella, C. Bosia, D. Corá, and M. Caselle. The role of incoherent microrna-mediated feedforward loops in noise buffering. *PLoS Comput Biol*, 7(3):e1001101, 2011.

IUIS international union of immunological societies

Immunology Without Borders

15th ICI

IMMUNITAS VIS NATURAE

MILAN 2013

15TH INTERNATIONAL CONGRESS OF IMMUNOLOGY

MILAN, ITALY / AUGUST 22-27 / 2013

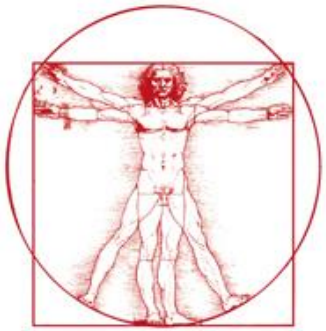

SIICA Società Italiana di Immunologia Immunologia Clinica e Allergologia

CERTIFICATE OF ATTENDANCE

WE HEREWITH CERTIFY THAT

QIAN LIU

has attended the

15th International Congress of Immunology – ICI 2013
held in Milan, August 22-27, 2013

Luciano Adorini
President of ICI

Luciano Adorini

Copyright Clearance Center

Confirmation Number: 11287560
Order Date: 01/04/2015

Customer Information

Customer: Qian Liu
Account Number: 3000875447
Organization: Qian Liu
Email: shaniaqliu@gmail.com
Phone: +65 90371126
Payment Method: Invoice

This is not an invoice

Order Details

Nature Reviews Immunology

Billing Status: **N/A**

Order detail ID: 65996898
ISSN: 1474-1741
Publication Type: e-Journal
Volume:
Issue:
Start page:
Publisher: NATURE PUBLISHING GROUP

Permission Status: **Granted**
Permission type: Republish or display content
Type of use: Republish in a thesis/dissertation
Order License Id: 3541781285774

Requestor type	Academic institution
Format	Print, Electronic
Portion	chart/graph/table/figure
Number of charts/graphs/tables/figures	1
Title or numeric reference of the portion(s)	Figure 1, Schematic representation of the structure...inducing IFNÎ²; SYK, spleen tyrosine kinase.
Title of the article or chapter the portion is from	Cooperation of Toll-like receptor signals in innate immune defence
Editor of portion(s)	N/A
Author of portion(s)	Giorgio Trinchieri and Alan Sher
Volume of serial or monograph	7
Page range of portion	180
Publication date of portion	March 2007
Rights for	Main product
Duration of use	Life of current edition
Creation of copies for the disabled	no
With minor editing privileges	yes
For distribution to	Worldwide
In the following language(s)	Original language of publication
With incidental	no

promotional use	
Lifetime unit quantity of new product	Up to 499
Made available in the following markets	education
The requesting person/organization	Liu Qian
Order reference number	
Author/Editor	Liu Qian
The standard identifier	NUS thesis database
Title	The mechanism of cytokine synergy
Publisher	National University of Singapore
Expected publication date	Jun 2015
Estimated size (pages)	150

Note: This item was invoiced separately through our **RightsLink service.** More info **$ 0.00**

Total order items: 1 **Order Total: $0.00**